

# EMERGING INFECTIOUS DISEASES<sup>®</sup>



Zoonotic Infections

August 2022



Umberto Boccioni (1882–1916), *Elasticity*, 1912. Oil on canvas 39.3 in x 39.3 in/100.06 cm x 100.06 cm. Museo del Novecento, Milano, Italy. Digital image from Art Resource, New York, New York, USA.

# EMERGING INFECTIOUS DISEASES®

EDITOR-IN-CHIEF

D. Peter Drotman

## ASSOCIATE EDITORS

Charles Ben Beard, Fort Collins, Colorado, USA  
 Ermias Belay, Atlanta, Georgia, USA  
 Sharon Bloom, Atlanta, Georgia, USA  
 Richard Bradbury, Melbourne, Australia  
 Corrie Brown, Athens, Georgia, USA  
 Benjamin J. Cowling, Hong Kong, China  
 Michel Drancourt, Marseille, France  
 Paul V. Effler, Perth, Australia  
 Anthony Fiore, Atlanta, Georgia, USA  
 David O. Freedman, Birmingham, Alabama, USA  
 Peter Gerner-Smidt, Atlanta, Georgia, USA  
 Stephen Hadler, Atlanta, Georgia, USA  
 Nina Marano, Atlanta, Georgia, USA  
 Martin I. Meltzer, Atlanta, Georgia, USA  
 David Morens, Bethesda, Maryland, USA  
 J. Glenn Morris, Jr., Gainesville, Florida, USA  
 Patrice Nordmann, Fribourg, Switzerland  
 Johann D.D. Pitout, Calgary, Alberta, Canada  
 Ann Powers, Fort Collins, Colorado, USA  
 Didier Raoult, Marseille, France  
 Pierre E. Rollin, Atlanta, Georgia, USA  
 Frederic E. Shaw, Atlanta, Georgia, USA  
 David H. Walker, Galveston, Texas, USA  
 J. Scott Weese, Guelph, Ontario, Canada

### Deputy Editor-in-Chief

Matthew J. Kuehnert, Westfield, New Jersey, USA

### Managing Editor

Byron Breedlove, Atlanta, Georgia, USA

### Technical Writer-Editors Shannon O'Connor, Team Lead;

Dana Dolan, Thomas Gryczan, Amy Guinn,  
 Tony Pearson-Clarke, Jill Russell, Jude Rutledge,  
 Cheryl Salerno, P. Lynne Stockton, Susan Zunino

### Production, Graphics, and Information Technology Staff

Reginald Tucker, Team Lead; William Hale, Barbara Segal

### Journal Administrators J. McLean Boggess, Susan Richardson

**Editorial Assistants** Letitia Carelock, Alexandria Myrick

**Communications/Social Media** Sarah Logan Gregory,  
 Team Lead; Heidi Floyd

### Associate Editor Emeritus

Charles H. Calisher, Fort Collins, Colorado, USA

### Founding Editor

Joseph E. McDade, Rome, Georgia, USA

## EDITORIAL BOARD

Barry J. Beaty, Fort Collins, Colorado, USA  
 David M. Bell, Atlanta, Georgia, USA  
 Martin J. Blaser, New York, New York, USA  
 Andrea Boggild, Toronto, Ontario, Canada  
 Christopher Braden, Atlanta, Georgia, USA  
 Arturo Casadevall, New York, New York, USA  
 Kenneth G. Castro, Atlanta, Georgia, USA  
 Christian Drosten, Charité Berlin, Germany  
 Clare A. Dykewicz, Atlanta, Georgia, USA  
 Isaac Chun-Hai Fung, Statesboro, Georgia, USA  
 Kathleen Gensheimer, College Park, Maryland, USA  
 Rachel Gorwitz, Atlanta, Georgia, USA  
 Duane J. Gubler, Singapore  
 Scott Halstead, Westwood, Massachusetts, USA  
 Thomas W. Hennessy, Anchorage, Alaska, USA  
 David L. Heymann, London, UK  
 Keith Klugman, Seattle, Washington, USA  
 S.K. Lam, Kuala Lumpur, Malaysia  
 Shawn Lockhart, Atlanta, Georgia, USA  
 John S. Mackenzie, Perth, Western Australia, Australia  
 Jennifer H. McQuiston, Atlanta, Georgia, USA  
 Nkuchia M. M'ikanatha, Harrisburg, Pennsylvania, USA  
 Frederick A. Murphy, Bethesda, Maryland, USA  
 Barbara E. Murray, Houston, Texas, USA  
 Stephen M. Ostroff, Silver Spring, Maryland, USA  
 W. Clyde Partin, Jr., Atlanta, Georgia, USA  
 Mario Raviglione, Milan, Italy, and Geneva, Switzerland  
 David Relman, Palo Alto, California, USA  
 Connie Schmaljohn, Frederick, Maryland, USA  
 Tom Schwan, Hamilton, Montana, USA  
 Rosemary Soave, New York, New York, USA  
 Robert Swanepoel, Pretoria, South Africa  
 David E. Swayne, Athens, Georgia, USA  
 Kathrine R. Tan, Atlanta, Georgia, USA  
 Phillip Tarr, St. Louis, Missouri, USA  
 Neil M. Vora, New York, New York, USA  
 Duc Vugia, Richmond, California, USA  
 J. Todd Weber, Atlanta, Georgia, USA  
 Mary Edythe Wilson, Iowa City, Iowa, USA

Emerging Infectious Diseases is published monthly by the Centers for Disease Control and Prevention, 1600 Clifton Rd NE, Mailstop H16-2, Atlanta, GA 30329-4027, USA. Telephone 404-639-1960; email, [eideditor@cdc.gov](mailto:eideditor@cdc.gov)

The conclusions, findings, and opinions expressed by authors contributing to this journal do not necessarily reflect the official position of the U.S. Department of Health and Human Services, the Public Health Service, the Centers for Disease Control and Prevention, or the authors' affiliated institutions. Use of trade names is for identification only and does not imply endorsement by any of the groups named above.

All material published in *Emerging Infectious Diseases* is in the public domain and may be used and reprinted without special permission; proper citation, however, is required.

Use of trade names is for identification only and does not imply endorsement by the Public Health Service or by the U.S. Department of Health and Human Services.

EMERGING INFECTIOUS DISEASES is a registered service mark of the U.S. Department of Health & Human Services (HHS).

# EMERGING INFECTIOUS DISEASES®

Zoonotic infections

August 2022



## On the Cover

Umberto Boccioni (1882–1916), *Elasticity*, 1912. Oil on Canvas 39.3 x 39.3 in/100.06 x 100.06 cm. Museo del Novecento, Milano, Italy. Digital image from Art Resource, New York, New York, USA.

About the Cover p. 1741

Medscape  
EDUCATION  
ACTIVITY

## Lack of Evidence for Ribavirin Treatment of Lassa Fever in Systematic Review of Published and Unpublished Studies

These reports provide little support for ribavirin in patients with confirmed Lassa fever.

H.-Y. Yuan et al.

1559

## Research

### Transmissibility of SARS-CoV-2 B.1.1.214 and Alpha Variants during 4 COVID-19 Waves, Kyoto, Japan, January 2020–June 2021

Y. Matsumura et al.

1569

### Dominant Carbapenemase-Encoding Plasmids in Clinical Enterobacteriales Isolates and Hypervirulent *Klebsiella pneumoniae*, Singapore

M. Yong et al.

1578

### Increasing and More Commonly Refractory *Mycobacterium avium* Pulmonary Disease, Toronto, Ontario, Canada

D. Raats et al.

1589

### Dog Ownership and Risk for Alveolar Echinococcosis, Germany

J. Schmidberger et al.

1597

### Characterization of Emerging Serotype 19A Pneumococcal Strains in Invasive Disease and Carriage, Belgium

S. Desmet et al.

1606

### Invasive Pneumococcal Disease and Long-Term Mortality Rates in Adults, Alberta, Canada

K.A. Versluys et al.

1615

### COVID-19 Symptoms and Deaths among Healthcare Workers, United States

S. Lin et al.

1624

## Synopses

### Incidence of Nontuberculous Mycobacterial Pulmonary Infection, by Ethnic Group, Hawaii, USA, 2005–2019

R.A. Blakney et al.

1543

### Investigation of COVID-19 Outbreak among Wildland Firefighters during Wildfire Response, Colorado, USA, 2020

A.R. Metz et al.

1551

**Factors Associated with Delayed or Missed Second-Dose mRNA COVID-19 Vaccination among Persons ≥12 Years of Age, United States**  
L. Meng et al. 1633

**COVID-19 Vaccination Intent and Belief that Vaccination Will End the Pandemic**  
M. de Vries et al. 1642

**Association of Environmental Factors with Seasonal Intensity of *Erysipelothrix rhusiopathiae* Seropositivity among Arctic Caribou**  
O.A. Aleuy et al. 1650

## Dispatches

**Culling of Urban Norway Rats and Carriage of *Bartonella* spp. Bacteria, Vancouver, British Columbia, Canada**  
K.A. Byers et al. 1659

**Zoonotic Threat of G4 Genotype Eurasian Avian-Like Swine Influenza A(H1N1) Viruses, China, 2020**  
M. Gu et al. 1664

**Increased Incidence of Invasive Pneumococcal Disease among Children after COVID-19 Pandemic, England**  
M. Bertran et al. 1669

**Novel Chronic Anaplasmosis in Splenectomized Patient, Amazon Rainforest**  
O. Duron et al. 1673

**Anthelmintic Baiting of Foxes against *Echinococcus multilocularis* in Small Public Area, Japan**  
K. Uruguchi et al. 1677

***Spiroplasma ixodetis* Infections in Immunocompetent and Immunosuppressed Patients after Tick Exposure, Sweden**  
J. Eimer et al. 1681

**Toxigenic *Corynebacterium diphtheriae* Infection in Cat, Texas**  
R. Tyler Jr, et al. 1686

**Child Melioidosis Deaths Caused by *Burkholderia pseudomallei*-Contaminated Borehole Water, Vietnam, 2019**  
Q.T.L. Tran et al. 1689

**Association of Phylogenomic Relatedness among *Neisseria gonorrhoeae* Strains with Antimicrobial Resistance, Austria, 2016–2020**  
J. Schaeffer et al. 1694

**Serial Intervals for SARS-CoV-2 Omicron and Delta Variants, Belgium, November 19–December 31, 2021**  
C. Kremer et al. 1699

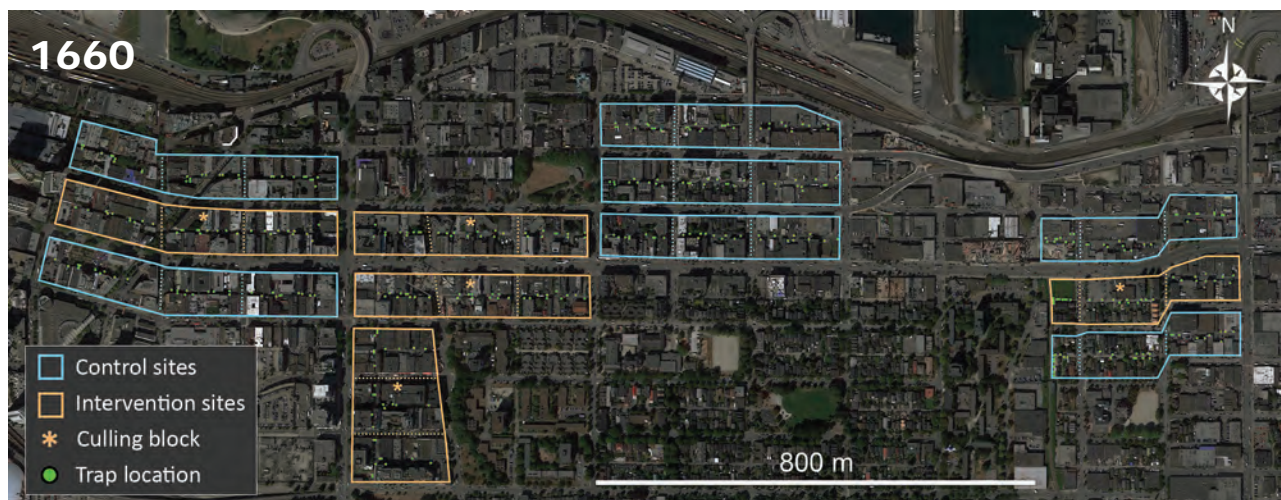
**Novel Reassortant Avian Influenza A(H5N6) Virus, China, 2021**  
J. Chen et al. 1703

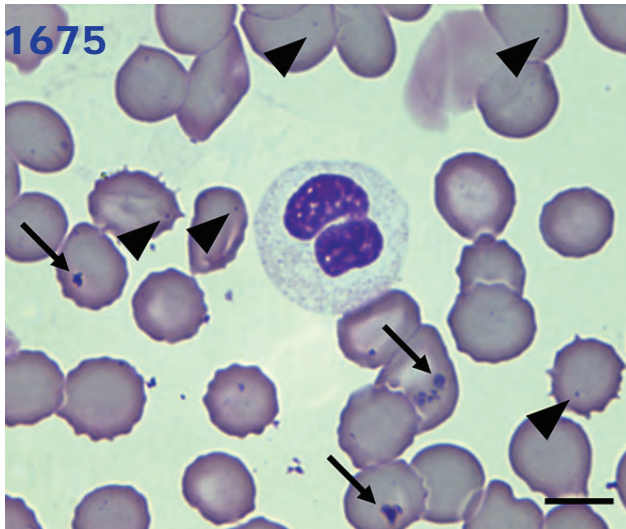
**Effectiveness of Naturally Acquired and Vaccine-Induced Immune Responses to SARS-CoV-2 Mu Variant**  
E.F. de Oliveira-Filho et al. 1708

## Research Letters

**Lymphocytic Choriomeningitis Virus Infection, Australia**  
L. Caly et al. 1713

**Public Health Risk of Foodborne Pathogens in Edible African Land Snails, Cameroon**  
M.N. Tanyitiku et al. 1715





***Bacillus subtilis* Variant *natto* Bacteremia of Gastrointestinal Origin, Japan**

I. Tanaka et al. 1718

**Invasive *Streptococcus oralis* Expressing Serotype 3 Pneumococcal Capsule, Japan**

B. Chang et al. 1720

**Hepatitis E Virus Outbreak among Tigray War Refugees from Ethiopia, Sudan**

A. Ahmed et al. 1722

**Emergence of Dengue Virus Serotype 2 Cosmopolitan Genotype, Brazil**

M. Giovanetti et al. 1725

**Early SARS-CoV-2 Reinfections within 60 Days and Implications for Retesting Policies**

L. Nevejan et al. 1729

**Household Secondary Attack Rates of SARS-CoV-2 Omicron Variant, South Korea, February 2022**

D.S. Lim et al. 1731

**Estimating COVID-19 Vaccine Effectiveness for Skilled Nursing Facility Healthcare Personnel, California, USA**

M. Magro et al. 1734



# EMERGING INFECTIOUS DISEASES®

August 2022

## Comment Letters

**Seroprevalence of Chikungunya Virus, Jamaica, and New Tools for Surveillance**

A.R.R. Freitas et al. 1736

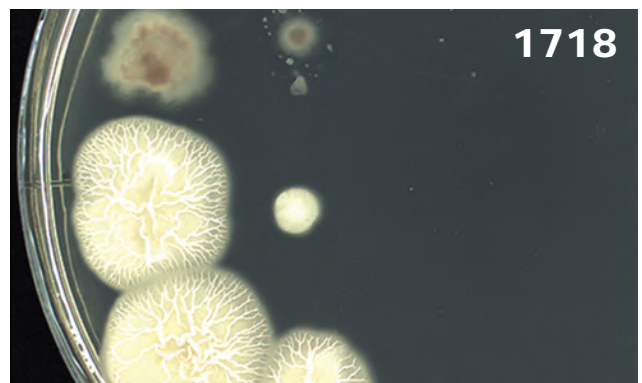
**Imported Monkeypox from International Traveler, Maryland, USA, 2021**

F.S. Minhaj et al. 1738

## In Memoriam

**Karen Foster (1955–2022)**

B. Breedlove 1740



## About the Cover

**“A Great Synthesis of Labor, Light, and Movement”**

B. Breedlove 1741

## Etymologia

***Dermatophilus congolensis***

R.D. Ollhoff et al. 1663

***Anopheles culicifacies***

G. Kumar 1728

## Online Report

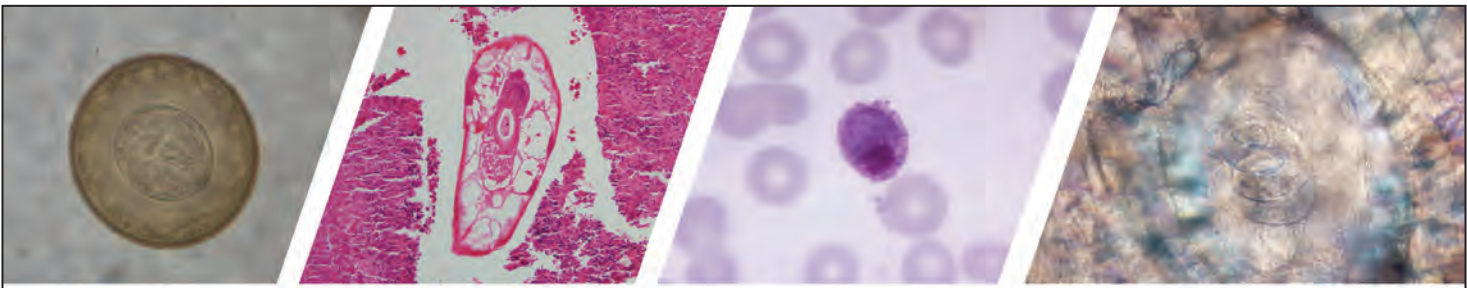


**Weighing Potential Benefits and Harms of *Mycoplasma genitalium* Testing and Treatment Approaches**

This systematic review demonstrates increasing antimicrobial resistance and incomplete understanding of the bacterium’s natural history.

L.E. Manhart et al.

[https://wwwnc.cdc.gov/eid/article/28/8/22-0094\\_article](https://wwwnc.cdc.gov/eid/article/28/8/22-0094_article)



# Diagnostic Assistance and Training in Laboratory Identification of Parasites

A free service of CDC available to laboratorians, pathologists, and other health professionals in the United States and abroad



Diagnosis from photographs of worms, histological sections, fecal, blood, and other specimen types



Expert diagnostic review



Formal diagnostic laboratory report



Submission of samples via secure file share

Visit the DPDx website for information on laboratory diagnosis, geographic distribution, clinical features, parasite life cycles, and training via Monthly Case Studies of parasitic diseases.

[www.cdc.gov/dpdx](http://www.cdc.gov/dpdx)  
[dpdx@cdc.gov](mailto:dpdx@cdc.gov)



U.S. Department of  
Health and Human Services  
Centers for Disease  
Control and Prevention

# Incidence of Nontuberculous Mycobacterial Pulmonary Infection, by Ethnic Group, Hawaii, USA, 2005–2019

Rebekah A. Blakney, Emily E. Ricotta, Timothy B. Frankland, Stacey Honda, Adrian Zelazny, Katrin D. Mayer-Barber, Samantha G. Dean,<sup>1</sup> Dean Follmann, Kenneth N. Olivier, Yihe G. Daida, D. Rebecca Prevots

To further clarify differences in the risk for nontuberculous mycobacterial pulmonary infection (NTM-PI) among ethnic populations in Hawaii, USA, we conducted a retrospective cohort study among beneficiaries of Kaiser Permanente Hawaii (KPH). We abstracted demographic, socioeconomic, clinical, and microbiological data from KPH electronic health records for 2005–2019. An NTM-PI case-patient was defined as a person from whom  $\geq 1$  NTM pulmonary isolate was obtained. We performed Cox proportional hazards regression to estimate incidence of NTM-PI while controlling for confounders. Across ethnic groups, risk for NTM-PI was higher among persons who were underweight (body mass index [BMI]  $< 18.5$  kg/m<sup>2</sup>). Among beneficiaries who self-identified as any Asian ethnicity, risk for incident NTM-PI was increased by 30%. Low BMI may increase susceptibility to NTM-PI, and risk may be higher for persons who self-identify as Asian, independent of BMI.

In the United States, studies have indicated that risk for nontuberculous mycobacterial pulmonary disease (NTM-PD) differs by geographic location and ethnic group (1). Nontuberculous mycobacteria are environmental bacteria that are widespread in soil and water and can be acquired through the natural or built environment (2). Nationally, disease prevalence is highest in the southeastern United States and Hawaii (1,3), and disease is associated with selected environmental conditions (2), as well as with higher mycobacterial abundance in

household plumbing (4). However, independent of geographic region, estimated prevalence is 2-fold higher among persons who self-identify as Asian/Pacific Islander than among those who self-identify as White (1). The incidence and prevalence of NTM infection and disease are increasing in the United States (5), and testing and positivity rates are highest among persons who self-identify as Asian (6); prevalence is also increasing in Hawaii (7) and the US-affiliated Pacific Islands (8).

Persons classified as Asian/Pacific Islander represent diverse populations, and aggregating these subpopulations may mask substantial heterogeneity (9). In a prior study in Hawaii, we identified substantial disparities in NTM pulmonary infection (NTM-PI) risk within Asian and Native Hawaiian and Other Pacific Islander (NHOPI) populations (7). To clarify ethnic disparities in NTM-PI risk, and particularly the role of BMI and other potential confounding factors among Asian/Pacific Islander populations, we conducted a retrospective cohort study among Kaiser Permanente Hawaii (KPH) beneficiaries. This research was approved by the KPH Institutional Review Board and was classified as nonhuman subjects research by the National Institutes of Health Office of Human Subjects Research Protection.

## Methods

### Study Population

We abstracted demographic, clinical, and microbiological data from KPH electronic health records (EHRs) for the years 2005–2019. We included beneficiaries for each year in which they were enrolled

Author affiliations: National Institutes of Health, Bethesda, Maryland, USA (R.A. Blakney, E.E. Ricotta, A. Zelazny, K.D. Mayer-Barber, S.G. Dean, D. Follmann, K.N. Olivier, D.R. Prevots); Kaiser Permanente Hawaii, Honolulu, Hawaii, USA (T.B. Frankland, S. Honda, Y.G. Daida)

DOI: <https://doi.org/10.3201/eid2808.212375>

<sup>1</sup>Current affiliation: Yale University, New Haven, Connecticut, USA

for  $\geq 9$  months; we excluded persons  $\geq 90$  years of age according to limited dataset regulations. Longitudinal demographic data included age on July 1 for each study year, sex, postal code, and census tract-level socioeconomic measures (median household income, neighborhood deprivation index, percentage graduated from high school). The neighborhood deprivation index is a measure of neighborhood-level socioeconomic status calculated by Kaiser Permanente (10). The index captures census tract-level measures of income, education, employment, housing, and occupation; higher scores indicate higher deprivation.

Demographic data included self-reported ethnicity; the standard KPH beneficiary enrollment form enables identification with  $\geq 1$  of 28 ethnic groups (Table 1). Additional health variables abstracted included height, weight, BMI, and smoking status. We searched EHRs for a set of prespecified codes from the International Classification of Disease, 9th and 10th revisions (ICD-9/10), for relevant underlying conditions ever coded. Although KPH does not serve the entire population of Hawaii, comparison with census data indicates that the KPH beneficiary population is generally representative of Hawaii residents with respect to age, ethnicity, and socioeconomic status (Appendix Table 2, <https://wwwnc.cdc.gov/EID/article/28/8/21-2375-App1.pdf>) (11,12).

### Microbiology and Case Definitions

We queried the KPH EHRs to identify beneficiaries who had undergone mycobacterial testing and had positive NTM culture results. Mycobacterial testing was conducted in a KPH Clinical Laboratory Improvement Amendments–certified laboratory; no methods were changed during the study period. We identified *Mycobacterium avium* complex by using commercially available probes and sent other isolates to Associated Regional and University Pathologists Laboratories (Salt Lake City, UT, USA) for speciation.

We defined cases by using the 2020 American Thoracic Society (ATS) microbiological criteria (13). A confirmed case of NTM-PI was defined as either  $\geq 2$  sputum cultures positive for the same pathogenic NTM species or  $\geq 1$  bronchoalveolar lavage, lung biopsy, or pleural fluid cultures positive for the same NTM species. Probable NTM-PI was defined as a single positive sputum culture. We excluded samples from nonpulmonary body sites, *Mycobacterium gordonae*, and samples not identified to complex or species. We included only cultures from beneficiaries who were residents of Hawaii (as determined by 2010 census postal code tabulation areas) for  $\geq 1$  year before

the year of culture collection and residents of Hawaii during the year in which the culture was collected.

### Analyses

We included beneficiaries who were  $\geq 18$  years of age at study entry, defined as the first year during the study period when the person had been a KPH beneficiary for  $\geq 9$  months. In addition, we included only beneficiaries who were Hawaii residents for  $> 2$  years during the study period. Self-reported ethnic group was termed “only” when a participant reported identification with either Asian, White, or NHOPI groups exclusively and “any” when a participant reported identification with any of those 3 ethnic groups (Table 1). For analysis of BMI, beneficiaries were categorized as underweight ( $< 18.5$  kg/m<sup>2</sup>), normal weight (18.5 to  $< 25$  kg/m<sup>2</sup>), or overweight ( $\geq 25$  kg/m<sup>2</sup>) according to their first available BMI score during the study period within 2 years of study entry.

An incident NTM-PI case-patient was defined as a person with an eligible culture and no respiratory cultures positive for NTM (excluding *M. gordonae*) in the prior year. We estimated NTM-PI incidence and compared it across ethnic groups. We described concurrent conditions of interest, including pulmonary conditions and immune disorders, by NTM-PI status and ethnicity. We calculated BMI distribution by ethnic group as well as NTM-PI incidence by BMI and ethnicity. We further described NTM species distribution for persons with confirmed and probable incident NTM-PI.

Our primary analysis was time to incident NTM-PI. We modeled NTM-PI incidence by using multivariable Cox proportional hazards regression. We used patient age as the time scale (14), starting with patient’s age at study entry and ending with age in 2019 or the last year in which the person was a KPH beneficiary during the study period. We used 2 approaches to categorize ethnic identification for the purpose of comparison across groups and for modeling disease incidence. For our first approach, we restricted models to beneficiaries self-identifying as only Asian, only White, and only NHOPI. We then modeled ethnic group as a categorical variable with 3 levels (only Asian, only White, or only NHOPI). For our second approach, we restricted the model to beneficiaries who reported ethnicity and modeled self-identifying as Asian by using a single referent group: any Asian versus non-Asian. We modeled Asian subgroups where sample size permitted; Japanese, Chinese, South Korean, and Filipino were modeled as any identification versus no identification. We did not further disaggregate NHOPI subgroups because of small sample size.

**Table 1.** NTM-PI incidence among Kaiser Permanente Hawaii beneficiaries, by ethnic group, Hawaii, USA, 2005–2019\*

| Ethnicity†                           | Beneficiaries, % | No. cases | Incidence, cases/100,000 person-years | Incidence rate ratio (95% CI)‡ |
|--------------------------------------|------------------|-----------|---------------------------------------|--------------------------------|
| All reporting ethnicity              | 255,605          | 733       | 36                                    | 1 (0.9–1.2)                    |
| White                                |                  |           |                                       |                                |
| Any White                            | 111,583 (44)     | 299       | 35                                    | Referent                       |
| Only White                           | 74,289 (29)      | 209       | 38                                    | 1.1 (0.9–1.3)                  |
| Black                                | 4,925 (2)        | 5         | ND                                    | ND                             |
| American Indian, Aleutian, or Eskimo | 5,383 (2)        | 4         | ND                                    | ND                             |
| Asian                                |                  |           |                                       |                                |
| Only Asian                           | 85,676 (34)      | 328       | 46                                    | 1.3 (1.1–1.5)                  |
| Any Asian                            | 123,187 (48)     | 423       | 41                                    | 1.2 (1–1.4)                    |
| Filipino                             | 49,869 (20)      | 155       | 39                                    | 1.1 (0.9–1.4)                  |
| Japanese                             | 32,238 (13)      | 137       | 46                                    | 1.3 (1.1–1.6)                  |
| Chinese                              | 17,987 (7)       | 68        | 43                                    | 1.2 (0.9–1.6)                  |
| Korean                               | 5,157 (2)        | 25        | 63                                    | 1.8 (1.2–2.7)                  |
| Other Asian                          | 4,463 (2)        | 7         | ND                                    | ND                             |
| Vietnamese                           | 1,893 (1)        | 9         | ND                                    | ND                             |
| NHOPI                                |                  |           |                                       |                                |
| Only NHOPI                           | 27,003 (11)      | 36        | 17                                    | 0.5 (0.3–0.7)                  |
| Any NHOPI                            | 66,120 (26)      | 140       | 27                                    | 0.8 (0.6–0.9)                  |
| Pacific Islander                     | 51,861 (20)      | 114       | 28                                    | 0.8 (0.6–1)                    |
| Hawaiian                             | 41,853 (16)      | 115       | 32                                    | 0.9 (0.7–1.1)                  |
| Samoan                               | 5,642 (2)        | 9         | ND                                    | ND                             |
| Other                                | 18,830 (7)       | 34        | 25                                    | 0.7 (0.5–1)                    |

\*ND, calculation not done because numbers of cases and follow-up times were too low to estimate incidence; NHOPI, Native Hawaiian and Other Pacific Islander; NTM-PI, nontuberculous mycobacterial pulmonary infection.

†Ethnic groups are not mutually exclusive except noted by "only." Ethnicity not reported by 43,218 (14%), single ethnicity reported by 177,016 (69%), multiple ethnicities reported by 78,589 (31%). Only ethnicities for which NTM-PI prevalence was >1% are shown. Asian not presented: Laotian, Asian Indian or Pakistani, Hmong, Kampuchean, Thai; NHOPI not presented: Fiji Islander, Micronesian, Chamorro, Guamanian, Polynesian, Tahitian, Tongan, Melanesian, New Guinean.

‡Incidence rate ratio only calculated for ethnic groups with >10 NTM-PI cases.

We first evaluated univariable models with factors known to be associated with NTM, including sex, BMI, concurrent conditions, and socioeconomic status. We excluded beneficiaries who did not have a BMI measurement within 2 years from the start of follow-up or who did not report ethnicity. On the basis of statistical significance in univariable models and judgment of clinically important confounders, we then constructed a multivariable base model encompassing sex, BMI, pulmonary conditions (modeled as a single binary variable indicating the presence of chronic obstructive pulmonary disease, emphysema, chronic asthma, chronic bronchitis, idiopathic pulmonary fibrosis, hypersensitivity pneumonia, or other unspecified lung diseases, because of high levels of concurrence), immune mechanism disorders, and lung cancer.

We investigated potential interactions between sex and covariates included in the base model and identified a statistically significant interaction between BMI score and sex; for this reason, we then added an interaction term for BMI and sex to the model. We evaluated ethnicity in univariable models and found that ethnic group was associated with NTM risk. When added to the multivariable base model, ethnic group improved model fit as evaluated by likelihood ratio tests. We also evaluated interactions between covariates and ethnicity by constructing

a model with interaction terms for ethnicity (only Asian, only White, only NHOPI) and all covariates and compared with likelihood ratio tests for the nested model. We found no statistically significant interactions by ethnicity.

## Results

A total of 298,823 KPH beneficiaries met our analysis inclusion criteria and were considered our population at risk (Table 2). Of those, 739 were classified as NTM-PI case-patients, of which 456 (62%) were confirmed case-patients, resulting in a cumulative incidence of 247 cases/100,000 beneficiaries. The average annual NTM-PI incidence was 44.8 cases/100,000 beneficiaries.

The most commonly reported ethnicity was Asian (123,187 [48%]), followed by White (111,583 [44%]) and NHOPI (66,120 [26%]) (Table 1). Overall, 31% of beneficiaries reported identification with >1 ethnic group. The highest incidence of NTM-PI was 46 cases/100,000 person-years among beneficiaries who self-identified with only the 11 Asian ethnic groups; within the Asian category, the highest incidence was among beneficiaries who self-identified as South Korean (63/100,000 person-years) or Japanese (46/100,000 person-years). The lowest incidence of 17/100,000 person-years was observed among beneficiaries who reported only NHOPI identification, and incidence was similar among NHOPI subgroups.

We compared the demographic and ethnic distribution across categories of probable and confirmed cases (Table 2). Median age was similar across case categories: 61 (interquartile range [IQR] 51–71) years for probable case-patients and 63 (IQR 55–71) years for confirmed case-patients. The distribution of probable and confirmed case-patients was similar across ethnic groups. The census tract median household income was similar for the any White and any NHOPI groups but was somewhat higher for the any Asian group (Table 3). However, the deprivation index was higher for the any NHOPI group compared with the any Asian or any White groups. With respect to underlying conditions, the proportion of beneficiaries with diabetes was highest (24%) among any NHOPI compared with 21% among any Asian and 13% among any White. Prevalence of other concurrent conditions was low; overall rates were similar among the ethnic groups. Median age varied by ethnic group; the NHOPI population was younger on average (median age 37 years) relative to the Asian population (median age 42 years) and the White population (median age 45 years).

Few KPH beneficiaries were categorized as underweight (5,027 [2%]); most were in the overweight/obese clinical category (149,970 [62%]). BMI varied by ethnic group; the highest proportion of persons with normal or underweight BMI scores was among persons self-identifying as Asian (44,552 [43%]), and a lower proportion of persons with normal or underweight BMI scores was among persons who identified as NHOPI (11,168 [20%]) (Table 3). In contrast, among NTM-PI case-patients, 45 (6.3%) were underweight, 324 (45.4%) were normal weight, and 345 (48.3%) were overweight/obese. Across all ethnic groups, the pattern of increasing NTM-PI incidence with decreasing BMI was similar (Figure);

compared with beneficiaries who were normal weight, beneficiaries who were underweight had a 1.4- to 2.5-fold increased risk for NTM-PI. The NTM-PI risk among beneficiaries who were normal weight compared with those who were overweight was also 1.4- to 1.8-fold higher.

To assess the effect of BMI change on NTM-PI risk, we evaluated change in weight among NTM-PI case-patients and non-NTM-PI controls. In the 2-year period ( $\pm 6$  months) before incident culture collection, the weight of NTM-PI case-patients decreased; median change was  $-1.9\%$  (IQR  $-6.7\%$  to  $1.5\%$ ). A convenience sample of non-NTM-PI controls included beneficiaries  $>53$  years of age (the first quartile age of NTM-PI case-patients), whose first and last weight measurements were 2 years ( $\pm 6$  months) apart. Median weight change for controls was generally stable, showing a slight decrease of  $-0.25\%$  (IQR  $-4.2\%$  to  $3.3\%$ ).

When we evaluated the frequency of microbiological follow-up among case-patients, the median number of acid-fast bacteria cultures performed during the study period was 4 (IQR 3–7); range was 1–43. The median follow-up time was 6 years (IQR 3–12 years). Most case-patients had only 1 incident NTM-PI (608 [82%]), but 131 (18%) had  $\geq 2$  incident infections. The most common NTM species isolated was *M. avium* complex (69%), followed by *M. fortuitum* group (24%) and *M. abscessus* (21%) (Appendix Table 2). We found little difference in *Mycobacterium* spp. distribution among ethnic groups (Appendix Table 3). We further evaluated our microbiological case definition relative to the ICD-9/10 code for NTM-PD (ICD-9, 031.0; ICD-10, A31.0) and found 69% sensitivity for confirmed cases, 25% sensitivity for probable cases,  $>99\%$  specificity, and a positive predictive value of 73%.

In models in which ethnicity was a mutually exclusive categorical variable with only White as the

**Table 2.** Demographic characteristics for Kaiser Permanente Hawaii beneficiaries, by nontuberculous mycobacterial pulmonary infection status, Hawaii, USA, 2005–2019\*

| Variable | All, no. (%) or median (IQR) | Probable cases, no. (%) or median (IQR) | Confirmed cases, no. (%) or median (IQR) | Confirmed and probable cases, no. (%) or median (IQR) |
|----------|------------------------------|---|--|---|
| Total    | 298,823                      | 283                                     | 456                                      | 739   |
| Age, y   | 42 (30–55)                   | 61 (51–71)                              | 63 (55–71)                               | 63 (54–71)  |
| Sex      |                              |   |  |   |
| F        | 148,328 (50)                 | 145 (51)                                | 251 (55)                                 | 396 (54)  |
| M        | 150,495 (50)                 | 138 (49)                                | 205 (45)                                 | 343 (46)  |
| Asian    |                              |   |  |   |
| Any      | 123,187 (48)                 | 150 (54)                                | 273 (60)                                 | 423 (58)  |
| Only     | 85,676 (34)                  | 116 (42)                                | 212 (47)                                 | 328 (45)  |
| White    |                              |   |  |   |
| Any      | 111,583 (44)                 | 114 (41)                                | 185 (41)                                 | 299 (41)  |
| Only     | 74,289 (29)                  | 81 (29)                                 | 128 (28)                                 | 209 (29)  |
| NHOPI    |                              |   |  |   |
| Any      | 66,120 (26)                  | 62 (22)                                 | 78 (17)                                  | 140 (19)  |
| Only     | 27,003 (11)                  | 18 (6)                                  | 18 (4)                                   | 36 (5)  |

\*IQR, interquartile range; NHOPI, Native Hawaiian and Other Pacific Islander.

reference group, the risk for incident NTM-PI was increased for the only Asian group (30%) (adjusted hazard ratio [aHR] 1.3, 95% CI 1.1–1.6). For the only NHOPI group relative to the only White group, the aHR for NTM-PI did not differ significantly (aHR 0.92, 95% CI 0.63–1.3) (Table 4). The aHR was similar when ethnicity was modeled as a binary variable indicating whether the beneficiary self-identified as any Asian or no Asian; risk for NTM-PI was increased 30% for those with identification as any Asian relative to no Asian (aHR 1.3, 95% CI 1.1–1.5). Analysis of Asian subgroups indicated a stronger association for Filipinos; NTM-PI risk was higher among those self-identifying as Filipino versus not Filipino than among those in the broader any Asian category. The association between BMI and NTM-PI incidence varied by sex. Decreasing BMI was associated with a higher NTM-PI risk for women than for men. In multivariable models that also included concurrent conditions and ethnicity and were controlled for age, each 1 kg/m<sup>2</sup> increase in BMI decreased the risk for infection by 9% for women and 4% for men.

## Discussion

We found that within the state of Hawaii, risk for NTM-PI was increased among persons who self-identified with any Asian ethnicity, even after we controlled for demographic and clinical risk factors. In contrast, after adjusting for these same demographic and clinical risk factors, risk was similar for persons who self-identified as any NHOPI compared with persons who self-identified as any White. A unique aspect of our study is that we have detailed information on Asian subgroups; the group categorized in Hawaii as Asian represents populations originating in several countries, primarily Japan, China, South Korea, and the Philippines. The higher risk for NTM-PI among persons identifying with Asian subgroups in our study is consistent with available data from countries in northeast Asia. Those data indicate generally higher disease burdens in Japan, South Korea, and Taiwan compared with estimates from Europe and other parts of the United States (15). Limited to no data are available from the Philippines or other countries in Southeast Asia.

A recent population-based study from South Korea estimated an age-adjusted incidence of 17.9 cases/100,000 persons and prevalence of 33.3 cases/100,000 persons for 2016 (16). In Japan, a hospital survey-based NTM-PD estimate was 15 cases/100,000 persons in 2015 (17). In the US-Affiliated Pacific Islands, a laboratory-based study estimated an NTM-PI prevalence of 48 cases/100,000 persons

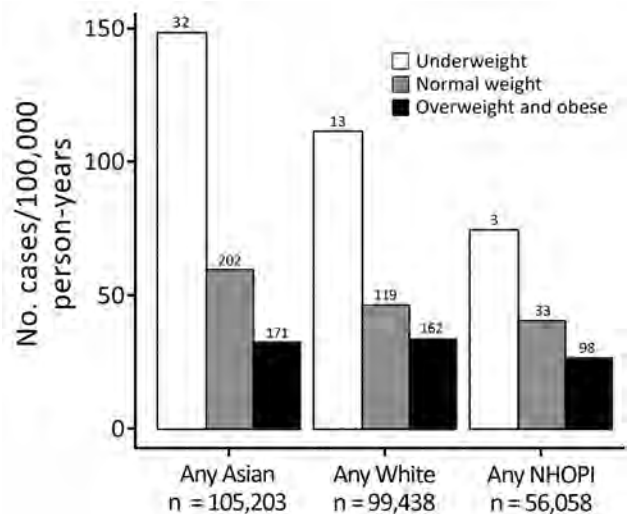


**Figure.** Nontuberculous mycobacterial pulmonary infection incidence among Kaiser Permanente Hawaii beneficiaries, by ethnicity and body mass index category, Hawaii, USA, 2005–2019. Numbers above bars indicate incidence (cases/100,000 person-years) by BMI category. Underweight, <18.5 kg/m<sup>2</sup>; normal weight, 18.5 to <25 kg/m<sup>2</sup>; overweight/obese, ≥25 kg/m<sup>2</sup>. NHOPI, Native Hawaiian and Other Pacific Islander.

in 2011; prevalence increased during 2007–2011 (8), similar to the average annual NTM-PI incidence of 44.8 cases/100,000 beneficiaries estimated in our study. Average annual NTM-PI incidence in our study is probably higher than that estimated in Japan and South Korea because of their more specific case criteria, which are based on full ATS NTM-PD diagnosis guidelines.

The reasons for the increased risk for Asian populations, those resident in Hawaii as well as in Asian countries, are not clear. Higher risk associated with self-described ethnicity may represent a mix of genetic ancestry, behavioral, or environmental factors. Because we did not measure specific behaviors or exposures and do not have any precise measures of genetic admixtures, we cannot estimate the relative contribution of these factors to our findings. Findings from a multiethnic cohort study (a large, ongoing, prospective study of diet, lifestyle, and genetic risks) suggests a role for differences in susceptibility among populations identifying with East Asian and Native Hawaiian ethnicity, even after lifestyle factors were accounted for (18).

Because exposure to nontuberculous mycobacteria is common, particularly in a high-risk geographic area such as Hawaii (19), but disease is still relatively rare, host susceptibility with involvement of multiple genes and pathways probably plays a

**Table 3.** Clinical and demographic features for Kaiser Permanente Hawaii beneficiaries, by ethnic group, Hawaii, USA, 2005–2019\*

| Variable                                      | Any Asian, no. (%) or median (IQR) | Any White, no. (%) or median (IQR) | Any NHOPI, no. (%) or median (IQR) |
|---|------------------------------------|------------------------------------|------------------------------------|
| Age, y  | 42 (30–56)                         | 45 (32–57)                         | 37 (27–50)                         |
| Ever smoked                                   | 32,375 (28)                        | 32,577 (31)                        | 22,612 (37)                        |
| Census-tract socioeconomic measures           |                                    |                                    |                                    |
| Household income, USD                         | 72,634 (58,184–88,143)             | 68,359 (58,295–83,750)             | 68,359 (54,470–81,464)             |
| Neighborhood deprivation index                | –0.23 (–0.62 to 0.28)              | –0.33 (–0.65 to 0.07)              | –0.08 (–0.48 to 0.51)              |
| Graduation from high school                   | 90 (84–94)                         | 92 (88–95)                         | 90 (85–93)                         |
| BMI   |                                    |                                    |                                    |
| BMI, kg/m <sup>2</sup>                        | 25.9 (22.7–30)                     | 26.6 (23.3–31)                     | 30.5 (25.9–35.9)                   |
| Underweight, <18.5 kg/m <sup>2</sup>          | 2,853 (3)                          | 1,725 (2)                          | 531 (1)                            |
| Normal weight, 18.5 to <25, kg/m <sup>2</sup> | 41,699 (40)                        | 35,606 (36)                        | 10,637 (19)                        |
| Overweight or obese, ≥25 kg/m <sup>2</sup>    | 60,551 (58)                        | 62,107 (62)                        | 44,890 (80)                        |
| Concurrent conditions                         |                                    |                                    |                                    |
| Diabetes                                      | 25,676 (21)                        | 14,385 (13)                        | 15,543 (24)                        |
| Lung cancer                                   | 1,083 (1)                          | 1,099 (1)                          | 582 (1)                            |
| Bronchiectasis                                | 842 (1)                            | 518 (<1)                           | 293 (<1)                           |
| Chronic asthma                                | 2,726 (2)                          | 2,795 (3)                          | 2,044 (3)                          |
| Chronic obstructive pulmonary disease         | 4,788 (4)                          | 5,709 (5)                          | 3,004 (5)                          |
| Emphysema                                     | 1,093 (1)                          | 1,357 (1)                          | 630 (1)                            |
| Chronic bronchitis                            | 1,993 (2)                          | 2,323 (2)                          | 1,436 (2)                          |
| Other pulmonary disease                       | 3,099 (3)                          | 3,319 (3)                          | 1,747 (3)                          |
| Immune mechanism disease                      | 457 (<1)                           | 586 (1)                            | 225 (<1)                           |

\*BMI, body mass index; IQR, interquartile range; NHOPI, Native Hawaiian and Other Pacific Islander.

role in pathogenesis (20). Several studies have evaluated the role of genetics among persons of various ethnic groups and used a variety of approaches, including candidate gene approaches (21), whole-exome sequencing (22), and genome-wide association studies (23,24). Most recently, genome-wide association studies in Japan and South Korea have identified single-nucleotide polymorphisms (SNPs) associated with disease susceptibility. However, the relative prevalence of some of those SNPs in different populations remain unknown, and further studies are needed to compare the prevalence of these SNPs across populations.

We found an inverse relationship between BMI and NTM risk. Risk was highest for clinically underweight beneficiaries compared with those with BMIs categorized as normal or overweight/obese. These findings of an increased risk for incident NTM with

decreasing BMI is consistent with findings of other studies showing not only the role of low BMI in disease progression (25,26) but also in susceptibility to infection or disease. A recent study that used South Korea national insurance data and prospectively ascertained BMI and NTM-PD over 9 years (27) found that lower BMI at baseline as well as weight loss during the study period were associated with higher NTM-PD risk. Proposed mechanisms for increased risk among persons with low BMI include fat loss with changes in adipokines (e.g., as leptin, resistin, and adiponectin) (28). Studies of mice have shown that experimental fat ablation can contribute to increased lung disease during mycobacterial infection (29). Leptin levels decreased with lower BMI, and pulmonary bacterial loads after *Mycobacterium tuberculosis* infection in mice that were genetically deficient in leptin were higher (30). Nevertheless,

**Table 4.** Cox proportional hazards regression of risk for NTM-PI among Kaiser Permanente Hawaii beneficiaries, Hawaii, USA, 2005–2019\*

| Category  | Only White reference, aHR (95% CI)† | Only Asian reference, aHR (95% CI)† | Not Asian reference, aHR (95% CI)‡ |
|---|-------------------------------------|-------------------------------------|------------------------------------|
| Body mass index§                                |                                     |                                     |                                    |
| M   | 0.96 (0.94–0.99)                    | 0.96 (0.94–0.99)                    | 0.97 (0.95–0.99)                   |
| F   | 0.91 (0.89–0.93)                    | 0.91 (0.89–0.93)                    | 0.91 (0.89–0.93)                   |
| Ethnicity                                       |                                     |                                     |                                    |
| Only White                                      | Referent                            | 0.77 (0.64–0.92)                    | NA                                 |
| Only Native Hawaiian and Other Pacific Islander | 0.9 (0.62–1.3)                      | 0.69 (0.48–1)                       | NA                                 |
| Only Asian                                      | 1.3 (1.1–1.6)                       | Reference                           | NA                                 |
| Any Asian                                       | NA                                  | NA                                  | 1.3 (1.1–1.5)                      |

\*Models adjusted for pulmonary condition (chronic obstructive pulmonary disease, chronic asthma, emphysema, chronic bronchitis, idiopathic pulmonary fibrosis, hypersensitivity pneumonia, other unclassified lung diseases); malignant neoplasm of trachea, bronchus, and lung; disorders involving the immune mechanism. aHR, adjusted hazard ratio; NA, not applicable; NTM-PI, nontuberculous mycobacterial pulmonary infections.

†No. modeled = 161,465; no. NTM-PI cases = 554.

‡No. modeled = 220,493; no. NTM-PI cases = 709.

§No. missing: only Asian and only White reference = 25,503; not Asian reference = 35,112.

the specific effects of individual adipokines on host resistance to mycobacterial NTM in human infection remain unknown (28). The association between BMI and NTM-PI depended on sex in our study population, in which decreasing BMI was associated with proportionally higher risk among women than men. It is hypothesized that estrogen, leptin, and adiponectin may play an additional role in susceptibility to NTM-PI in older women (31).

A strength of our study is the large sample size that included persons of diverse Asian and Pacific Islander ethnicities in a single geographic area where risk for NTM infection is high. Among the limitations of our study was our reliance on the microbiological component of the ATS case criteria because we did not have radiographic or symptom data (13); however, other studies indicate that the microbiological component predictive value for true cases is high. In a similar retrospective study at an integrated health-care system, among persons from whom  $\geq 1$  NTM isolate was obtained, 69.5% had nodules, bronchiectasis, or cavities compatible with NTM disease (32). Moreover, the finding that the 69% of those with confirmed cases and the 25% of those with probable cases had ICD-9/10 codes, with an overall positive predictive value of 73%, suggests that we are identifying a high proportion of true disease, particularly among persons with confirmed cases.

A second limitation is that follow-up was not standardized in this beneficiary population, and therefore the availability of BMI measurements was associated with healthcare use. Overall, 33,269 (11%) beneficiaries did not have a BMI measurement available; those who did not have a BMI measurement were more likely to be younger and to not have any underlying conditions. However, we have no evidence that these missing data influenced the patterns by ethnic group. Use of BMI score as a measurement of body composition is itself a limitation because it does not distinguish fat mass from muscle mass. Last, ethnicity groupings are artificial, given that populations in Hawaii are highly heterogeneous and 31% of beneficiaries reported  $>1$  ethnicity. In addition, Asian and NHOPI identification is defined broadly and includes diverse subpopulations. Caution should be taken when generalizing these findings to ethnic populations outside of Hawaii (9).

In conclusion, we found that lower BMI was associated with increased risk for NTM-PI and that self-identifying as Asian, independent of other ethnic identification, was associated with a higher risk for NTM-PI. Whereas risk for NTM-PI seemed to be

lower for the NHOPI population, our findings suggest that after confounders were controlled for, the risk is similar to that for beneficiaries self-identifying as White.

This work was supported in part by the Intramural Research Program of the National Institute of Allergy and Infectious Diseases.

### About the Author

Ms. Blakney is a research analyst in the Epidemiology and Population Studies Unit, Laboratory of Clinical Immunology and Microbiology, Division of Intramural Research, National Institute of Allergy and Infectious Diseases, National Institutes of Health. Her research focuses on the epidemiology of infectious diseases, including healthcare-associated infections, invasive fungal infections, and NTM infections.

### References

- Adjemian J, Olivier KN, Seitz AE, Holland SM, Prevots DR. Prevalence of nontuberculous mycobacterial lung disease in U.S. Medicare beneficiaries. *Am J Respir Crit Care Med*. 2012;185:881–6. <https://doi.org/10.1164/rccm.201111-2016OC>
- Adjemian J, Daniel-Wayman S, Ricotta E, Prevots DR. Epidemiology of nontuberculous mycobacteriosis. *Semin Respir Crit Care Med*. 2018;39:325–35. <https://doi.org/10.1055/s-0038-1651491>
- Strollo SE, Adjemian J, Adjemian MK, Prevots DR. The burden of pulmonary nontuberculous mycobacterial disease in the United States. *Ann Am Thorac Soc*. 2015;12:1458–64. <https://doi.org/10.1513/AnnalsATS.201503-173OC>
- Gebert MJ, Delgado-Baquerizo M, Oliverio AM, Webster TM, Nichols LM, Honda JR, et al. Ecological analyses of mycobacteria in showerhead biofilms and their relevance to human health. *MBio*. 2018;9:e01614-18. <https://doi.org/10.1128/mBio.01614-18>
- Winthrop KL, Marras TK, Adjemian J, Zhang H, Wang P, Zhang Q. Incidence and prevalence of nontuberculous mycobacterial lung disease in a large U.S. managed care health plan, 2008–2015. *Ann Am Thorac Soc*. 2020;17:178–85. <https://doi.org/10.1513/AnnalsATS.201804-236OC>
- Dean SG, Ricotta EE, Fintzi J, Lai YL, Kadri SS, Olivier KN, et al. Mycobacterial testing trends, United States, 2009–2015. *Emerg Infect Dis*. 2020;26:2243–6. <https://doi.org/10.3201/eid2609.200749>
- Adjemian J, Frankland TB, Daida YG, Honda JR, Olivier KN, Zelazny A, et al. Epidemiology of nontuberculous mycobacterial lung disease and tuberculosis, Hawaii, USA. *Emerg Infect Dis*. 2017;23:439–47. <https://doi.org/10.3201/eid2303.161827>
- Lin C, Russell C, Soll B, Chow D, Bamrah S, Brostrom R, et al. Increasing prevalence of nontuberculous mycobacteria in respiratory specimens from US-Affiliated Pacific Island jurisdictions. *Emerg Infect Dis*. 2018;24:485–91. <https://doi.org/10.3201/eid2403.171301>
- Holland AT, Palaniappan LP. Problems with the collection and interpretation of Asian-American health data: omission, aggregation, and extrapolation. *Ann Epidemiol*. 2012;22:397–405. <https://doi.org/10.1016/j.annepidem.2012.04.001>

10. Messer LC, Laraia BA, Kaufman JS, Eyster J, Holzman C, Culhane J, et al. The development of a standardized neighborhood deprivation index. *J Urban Health*. 2006;83:1041–62. <https://doi.org/10.1007/s11524-006-9094-x>
11. US Census. QuickFacts Hawaii [cited 2021 Nov 18]. <https://www.census.gov/quickfacts/HI>
12. US Census. 2019 Population estimates by age, sex, race, and Hispanic origin [cited 2021 Oct 5]. <https://www.census.gov/newsroom/press-kits/2020/population-estimates-detailed.html>
13. Daley CL, Iaccarino JM, Lange C, Cambau E, Wallace RJ Jr, Andrejak C, et al. Treatment of nontuberculous mycobacterial pulmonary disease: an official ATS/ERS/ESCMID/IDSA Clinical Practice Guideline. *Clin Infect Dis*. 2020;71:905–13. <https://doi.org/10.1093/cid/ciaa1125>
14. Korn EL, Graubard BI, Midthune D. Time-to-event analysis of longitudinal follow-up of a survey: choice of the time-scale. *Am J Epidemiol*. 1997;145:72–80. <https://doi.org/10.1093/oxfordjournals.aje.a009034>
15. Prevots DR, Marras TK. Epidemiology of human pulmonary infection with nontuberculous mycobacteria: a review. *Clin Chest Med*. 2015;36:13–34. <https://doi.org/10.1016/j.ccm.2014.10.002>
16. Park SC, Kang MJ, Han CH, Lee SM, Kim CJ, Lee JM, et al. Prevalence, incidence, and mortality of nontuberculous mycobacterial infection in Korea: a nationwide population-based study. *BMC Pulm Med*. 2019;19:140. <https://doi.org/10.1186/s12890-019-0901-z>
17. Namkoong H, Kurashima A, Morimoto K, Hoshino Y, Hasegawa N, Ato M, et al. Epidemiology of pulmonary nontuberculous mycobacterial disease, Japan. *Emerg Infect Dis*. 2016;22:1116–7. <https://doi.org/10.3201/eid2206.151086>
18. Maskarinec G, Jacobs S, Morimoto Y, Chock M, Grandinetti A, Kolonel LN. Disparity in diabetes risk across Native Hawaiians and different Asian groups: the multiethnic cohort. *Asia Pac J Public Health*. 2015;27:375–84. <https://doi.org/10.1177/1010539514548757>
19. Nelson ST, Robinson S, Rey K, Brown L, Jones N, Dawrs SN, et al. Exposure pathways of nontuberculous mycobacteria through soil, streams, and groundwater, Hawai'i, USA. *Geohealth*. 2021;5:e2020GH000350.
20. Wu UI, Holland SM. Host susceptibility to non-tuberculous mycobacterial infections. *Lancet Infect Dis*. 2015;15:968–80. [https://doi.org/10.1016/S1473-3099\(15\)00089-4](https://doi.org/10.1016/S1473-3099(15)00089-4)
21. Szymanski EP, Leung JM, Fowler CJ, Haney C, Hsu AP, Chen F, et al. Pulmonary nontuberculous mycobacterial infection. a multisystem, multigenic disease. *Am J Respir Crit Care Med*. 2015;192:618–28. <https://doi.org/10.1164/rccm.201502-0387OC>
22. Chen F, Szymanski EP, Olivier KN, Liu X, Tettelin H, Holland SM, et al. Whole-exome sequencing identifies the 6q12-q16 linkage region and a candidate gene, TTK, for pulmonary nontuberculous mycobacterial disease. *Am J Respir Crit Care Med*. 2017;196:1599–604. <https://doi.org/10.1164/rccm.201612-2479OC>
23. Namkoong H, Omae Y, Asakura T, Ishii M, Suzuki S, Morimoto K, et al.; Nontuberculous Mycobacteriosis and Bronchiectasis–Japan Research Consortium (NTM-JRC). Genome-wide association study in patients with pulmonary *Mycobacterium avium* complex disease. *Eur Respir J*. 2021;58:1902269. <https://doi.org/10.1183/13993003.02269-2019>
24. Cho J, Park K, Choi SM, Lee J, Lee CH, Lee JK, et al. Genome-wide association study of non-tuberculous mycobacterial pulmonary disease. *Thorax*. 2021;76:169–77. <https://doi.org/10.1136/thoraxjnl-2019-214430>
25. Hachisu Y, Murata K, Takei K, Tsuchiya T, Tsurumaki H, Koga Y, et al. Prognostic nutritional index as a predictor of mortality in nontuberculous mycobacterial lung disease. *J Thorac Dis*. 2020;12:3101–9. <https://doi.org/10.21037/jtd-20-803>
26. Fujiwara K, Furuuchi K, Aono A, Uesugi F, Shirai T, Nakamoto K, et al. Clinical risk factors related to treatment failure in *Mycobacterium abscessus* lung disease. *Eur J Clin Microbiol Infect Dis*. 2020;40:247–54.
27. Song JH, Kim BS, Kwak N, Han K, Yim JJ. Impact of body mass index on development of nontuberculous mycobacterial pulmonary disease. *Eur Respir J*. 2021;57:2000454. <https://doi.org/10.1183/13993003.00454-2020>
28. Chan ED, Iseman MD. Underlying host risk factors for nontuberculous mycobacterial lung disease. *Semin Respir Crit Care Med*. 2013;34:110–23. <https://doi.org/10.1055/s-0033-1333573>
29. Ayyappan JP, Ganapathi U, Lizardo K, Vinnard C, Subbian S, Perlin DS, et al. Adipose tissue regulates pulmonary pathology during TB infection. *MBio*. 2019;10:e02771-18. <https://doi.org/10.1128/mBio.02771-18>
30. Wieland CW, Florquin S, Chan ED, Leemans JC, Weijer S, Verbon A, et al. Pulmonary *Mycobacterium tuberculosis* infection in leptin-deficient ob/ob mice. *Int Immunol*. 2005;17:1399–408. <https://doi.org/10.1093/intimm/dxh317>
31. Chan ED, Iseman MD. Slender, older women appear to be more susceptible to nontuberculous mycobacterial lung disease. *Genet Med*. 2010;7:5–18. <https://doi.org/10.1016/j.genm.2010.01.005>
32. Prevots DR, Shaw PA, Strickland D, Jackson LA, Raebel MA, Blosky MA, et al. Nontuberculous mycobacterial lung disease prevalence at four integrated health care delivery systems. *Am J Respir Crit Care Med*. 2010;182:970–6. <https://doi.org/10.1164/rccm.201002-0310OC>

---

Address for correspondence: D. Rebecca Prevots, NIAID, NIH, Rm 7D10, 5601 Fishers Ln, Rockville, MD 20892, USA; email: [rprevots@niaid.nih.gov](mailto:rprevots@niaid.nih.gov)

---

# Investigation of COVID-19 Outbreak among Wildland Firefighters during Wildfire Response, Colorado, USA, 2020

Amanda Reiff Metz, Matthew Bauer, Chelsey Epperly, Ginger Stringer, Kristen E. Marshall, Lindsey Martin Webb, Molly Hetherington-Rauth, Shannon R. Matzinger, Sarah Elizabeth Totten, Emily A. Travanty, Kristen M. Good, Alexis Burakoff

A COVID-19 outbreak occurred among Cameron Peak Fire responders in Colorado, USA, during August 2020–January 2021. The Cameron Peak Fire was the largest recorded wildfire in Colorado history, lasting August–December 2020. At least 6,123 responders were involved, including 1,260 firefighters in 63 crews who mobilized to the fire camps. A total of 79 COVID-19 cases were identified among responders, and 273 close contacts were quarantined. State and local public health investigated the outbreak and coordinated with wildfire management teams to prevent disease spread. We performed whole-genome sequencing and applied social network analysis to visualize clusters and transmission dynamics. Phylogenetic analysis identified 8 lineages among sequenced specimens, implying multiple introductions. Social network analysis identified spread between and within crews. Strategies such as implementing symptom screening and testing of arriving responders, educating responders about overlapping symptoms of smoke inhalation and COVID-19, improving physical distancing of crews, and encouraging vaccinations are recommended.

The Cameron Peak Fire in Colorado, USA, began on August 13, 2020. Because of the magnitude of this wildfire, the response was coordinated by various Incident Management Teams (IMT); wildfire

responders included Colorado wildland firefighter crews as well as crews from around the country deployed to Colorado for the response. On August 25, 2020, the Larimer County Department of Health and Environment (LCDHE) and the Colorado Department of Public Health and Environment (CDPHE) received notification of a wildland firefighter responding to the Cameron Peak Fire who tested positive for SARS-CoV-2, the virus that causes COVID-19. This firefighter initially reported difficulty breathing and was transported to the local emergency department, then released. The next day, he was admitted to the hospital for continuing symptoms and tested positive for SARS-CoV-2 by reverse transcription PCR (RT-PCR). LCDHE, in partnership with the IMT, began contact tracing on the basis of the Centers for Disease Control and Prevention (CDC) definition of someone who was within 6 feet of an infected person for a cumulative 15 minutes or more over a 24-hour period (1). Two persons working on the same crew and 5 additional responders at the camp were identified as close contacts and quarantined. During contact interviews, it was reported that 2 crew members of the index case-patient were experiencing cough and headaches; both subsequently tested positive for SARS-CoV-2. An outbreak was declared and reported on September 2, 2020.

Wildfire response personnel operating across the state were in contact with CDPHE throughout the wildfire season regarding COVID-19 prevention and response plans. In July 2020, before the Cameron Peak Fire, CDPHE released public guidance documents addressing best practices for mitigating COVID-19 risks at wildfire camps (2). This document supplemented best practice guidance available from other sources

---

Author affiliations: Colorado Department of Public Health and Environment, Denver, Colorado, USA (A.R. Metz, C. Epperly, G. Stringer, K.E. Marshall, L.M. Webb, M. Hetherington-Rauth, S.R. Matzinger, S.E. Totten, E.A. Travanty, K.M. Good, A. Burakoff); Larimer County Department of Health and Environment, Fort Collins, Colorado, USA (M. Bauer); Centers for Disease Control and Prevention, Atlanta, Georgia, USA (K.E. Marshall)

DOI: <https://doi.org/10.3201/eid2808.220310>

such as CDC (3), United States Forest Service (USFS) (4), the Fire Management Board (5), and United States Department of the Interior (6). At the time that the Cameron Peak Fire started, a CDPHE occupational health epidemiologist regularly attended a morning safety briefing call organized by the USFS, in which incident management team representatives from all active fires in Colorado called in with updates on safety concerns including COVID-19.

## Methods

### Case Investigations

LCDHE and the Cameron Peak IMT collaborated to conduct case investigations and contact tracing activities. An outbreak case was defined as confirmed or probable COVID-19 (determined using the Council of State and Territorial Epidemiologists' 2020 Interim COVID-19 Case Definition) (7) in a responder who was onsite at the Cameron Peak Fire within 14 days of symptom onset or positive test. Close contacts were identified on the basis of the CDC definition and quarantined. CDPHE and local hospital laboratories conducted SARS-CoV-2 RT-PCR testing using various platforms.

Outbreak response consultation calls among CDPHE, LCDHE, and IMT were held to provide recommendations for isolation of cases, quarantine of close contacts, and prevention practices such as improving physical distancing. CDPHE's Rapid

Response Team hosted a testing event for Cameron Peak Fire responders before the first positive case was identified; surveillance and outbreak screening testing was offered to all Cameron Peak Fire responders starting August 24. Once the outbreak was identified, widespread testing was conducted 11 more times during August 26–October 25, 2020. After the fire, the USFS conducted a Facilitated Learning Analysis to identify lessons learned from the outbreak response (8).

### Whole-Genome Sequencing

CDPHE performed tiled amplicon whole-genome sequencing (WGS) on 40 (51%) available specimens from wildfire responders (Appendix, <https://wwwnc.cdc.gov/EID/article/28/8/22-0310-App1.pdf>); the remainder of the specimens were unavailable for sequencing because they were not sent to the CDPHE laboratory. We assembled sequencing data by using the Monroe workflow and CDPHE's publicly available Nanopore data workflow (<https://github.com/CDPHE>).

Of the specimens available for WGS, 24 resulted in sequence determination; we used those sequences to construct a focal phylogenetic tree of the Cameron Peak Fire outbreak (Figure 1). In addition, to investigate the potential for multistate lineage introduction or community transmission, we constructed a contextual phylogenetic tree by using the 24 whole-genome sequences of the Cameron Peak Fire specimens and additional

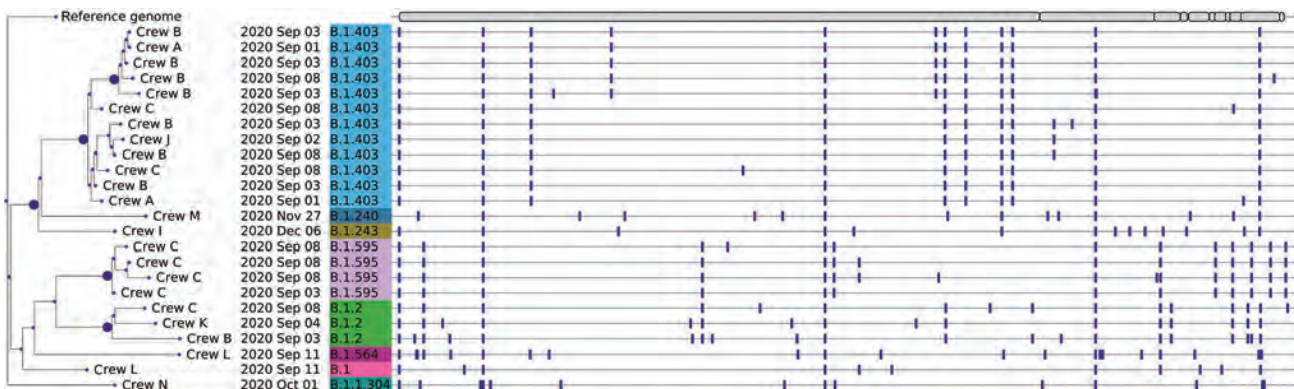


**Figure 1.** Phylogenetic tree of SARS-CoV-2 consensus whole-genome sequences from 24 of 42 positive specimens from Cameron Peak firefighters available at the Colorado State Public Health Lab with  $\geq 89\%$  genome coverage. Nodes with at least 95% ultrafast bootstrap support are labeled. Firefighter crew, sample collection date, and lineage are displayed at the tips. A visualization of the reference genome is depicted at the top of the phylogeny. Vertical bars shown across each consensus sequence indicate positions of nucleotide changes relative to the reference genome. High-quality consensus sequences were defined as sequences with  $\geq 89\%$  genome coverage ( $10\times$  sequence coverage depth for Illumina [<https://www.illumina.com>] and  $20\times$  for Oxford Nanopore [<https://nanoporetech.com>]) and minimum base quality of 20. Prior to phylogenetic inference, consensus sequences were aligned to the reference genome (Genbank accession no. NC\_045512.2), and insertions were removed so that all sequences were 29,903 nt in length. Phylogenetic inference of the consensus sequences was performed using IQTree version 2.0.3 (<http://www.iqtree.org>) with 1,000 ultrafast bootstrap replicates and phylogenetic tree visualization was performed using the python module ete3 version 3.1.2 (<https://pypi.org/project/ete3>). Pangolin v.2.4.2<sup>5</sup> (9) and Nextstrain's Nextclade tools (10) were used to assign lineage and clade designations to each assembled genome.

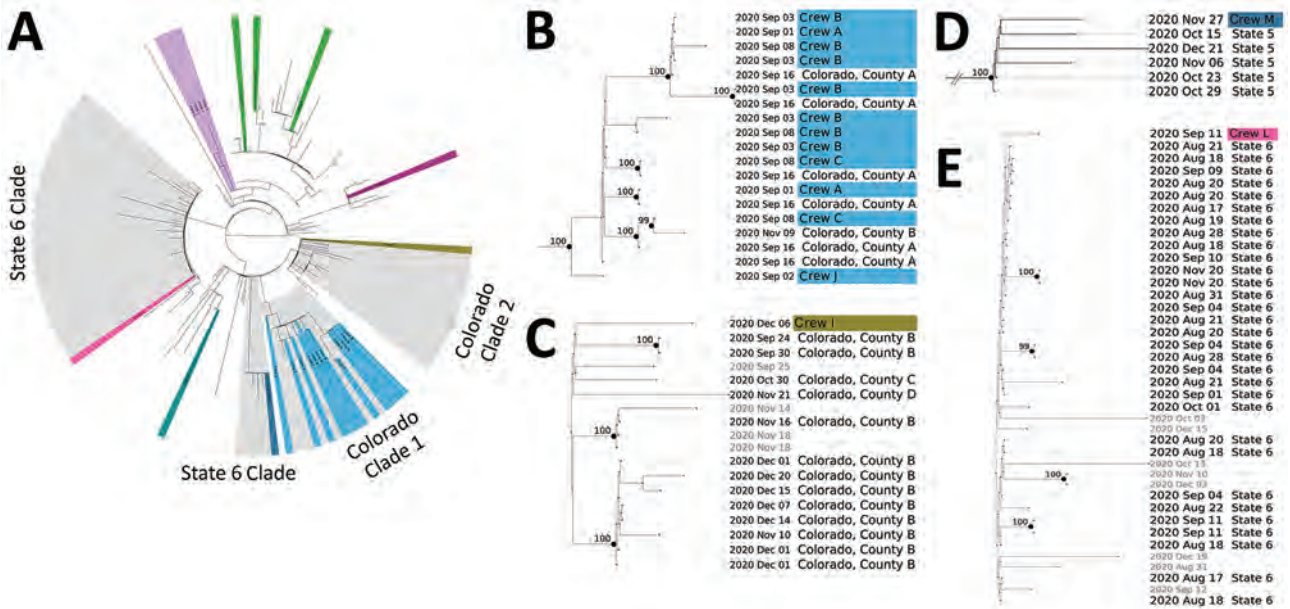


**Figure 2.** Contextual phylogenetic tree and enlarged clades showing genetic relatedness of the Cameron Peak firefighter sequences to sequences of SARS-CoV-2 collected within the United States during September–December 2020. A) Full contextual tree constructed using 754 contextual sequences subsampled from GISAID (<https://www.gisaid.org>) plus 24 Cameron Peak firefighter consensus sequences. The phylogeny has been pruned to display 164 contextual sequences and Cameron Peak firefighter sequences. Cameron Peak sequences are highlighted in color according to their lineage assignment. Clades highlighted in gray represent potential community and interstate transmission events. Cameron Peak sequences assigned to lineage B.1.2 (green) do not cluster together on the contextual phylogeny to form a monophyletic group, suggesting that they are genetically divergent from one another and likely do not represent a single transmission event, despite belonging to the same lineage. Mutation differences among these sequences are shown in detail in Figure 1. B) Colorado clade 1. Twelve Cameron Peak firefighters formed a monophyletic group with sequences from 2 Colorado counties. C) Colorado clade 2. A single Cameron Peak firefighter sequence formed a clade with sequences collected from 3 Colorado counties and additional sequences collected from outside of Colorado (not labeled). Low support values for this clade may be expected because of low sequence diversity. D) State 5 clade. The Cameron Peak firefighter sequence formed a monophyletic clade with sequences collected from his or her state of deployment (State 5). E) State 6 clade. The Cameron Peak firefighter sequence formed a clade with sequences collected from his or her state of deployment (state 6) and additional sequences collected from outside of Colorado and not from his or her state of deployment (not labeled). Low support values for this clade may be caused by low sequence diversity. For panels B–E, all sequences within a clade are assigned the same lineage. Collection dates are labeled for all tips. Cameron Peak firefighter sequences are highlighted according to their lineage and labeled with crew. Nodes with at least 95% ultrafast bootstrap support values are labeled. Additional information is available in the Appendix (<https://wwwnc.cdc.gov/EID/article/28/8/22-0310-App1.pdf>).

whole-genome sequences that were either publicly available or additionally sequenced at the CDPHE State Public Health Laboratory (Figure 2; Appendix).

**Social Network Analysis**

We conducted social network analysis of all SARS-CoV-2–positive responders by using R Studio version 1.2.5033 (<https://www.rstudio.com>) and Gephi Graph Visualization and Manipulation software version 0.9.2 (<https://gephi.org>). We applied this analysis to WGS results to visualize clusters and transmission dynamics among Cameron Peak Fire crews (11). We assumed epidemiologic links of exposure between responders belonging to the same crew for network construction. Data showing potential exposure outside of crew assignments (i.e., socializing with members of other crews) were not available. This

activity was reviewed by CDC and was conducted consistent with applicable federal law and CDC policy (45 C.F.R. part 46, 21 C.F.R. part 56; 42 U.S.C. Sect. 241(d); 5 U.S.C. Sect. 552a; 44 U.S.C. Sect. 3501 et seq).

**Results**

The outbreak among wildfire responders occurred during August 25, 2020–January 8, 2021. (In Colorado, an outbreak is considered resolved 28 days after symptom onset of the last case.) A total of 6,123 responders were involved in the response. We identified 79 cases (78 confirmed and 1 probable); 73 of these were confirmed to be firefighters from 1 of the 63 crews, for an attack rate of 5.8% among 1,260 firefighters who were deployed full-time to the incident (Figure 3). The remainder of responder case-patients were persons from IMT, equipment operators, and

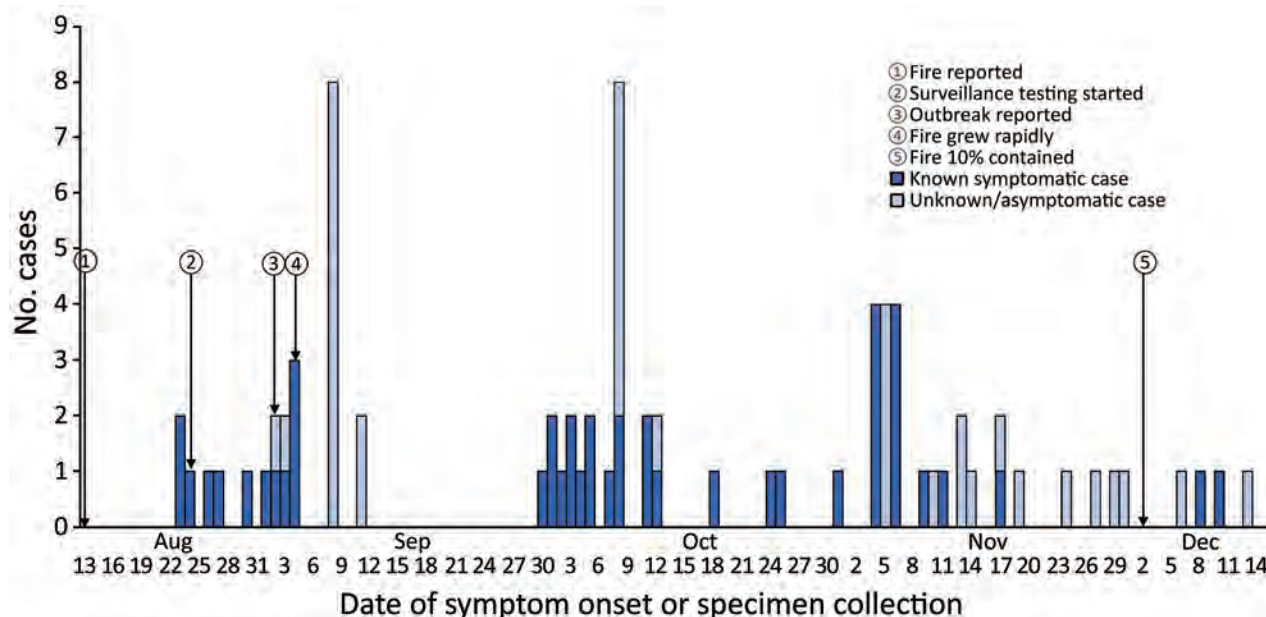


(Figure 2, panel A). The analysis revealed 4 clades that provided evidence of possible intrastate and interstate transmission (Figure 2, panels B–E). Twelve Cameron Peak Fire sequences formed a monophyletic clade with sequences collected from 2 Colorado counties with high support values (ultrafast bootstrap support >95% for nodes; Figure 2, panel B). Another sequence from a Cameron Peak Fire responder formed a clade with sequences collected from 3 Colorado counties and additional sequences collected from outside of Colorado but with low support values (ultrafast bootstrap support <95% for nodes; Figure 2, panel C). In addition, in 2 cases, sequences from 2 different responders formed a clade with contextual sequences collected from their state of deployment; 1 clade was supported with high support values but the other was not (Figure 2, panels D and E). Although not all clades were supported with high bootstrap values, low support values might be expected if sequence diversity is insufficient, which could result from either low diversity of SARS-CoV-2 circulating in the United States at the time, or low diversity among samples that were able to be sequenced and deposited in public repositories. Short branch lengths as observed on the tree are indicative of low divergence among sequences (12).

Social network analysis showed the 79 responders with COVID-19 clustered into 26 crews deploying from 17 states (Figure 4). Nine crews with responders from 10 states experienced  $\geq 3$  cases. We observed multiple lineages within single crews, suggesting multiple points of introduction, probable crew intermingling, and possible lapses in prevention measures such as social distancing.

**Discussion**

The Cameron Peak Fire was the largest recorded wildfire in Colorado’s history, burning 208,913 acres. A total of 79 cases of COVID-19 were identified among Cameron Peak Fire responders deployed from 17 states. Multiple points of SARS-CoV-2 introduction were likely because of frequent crew turnover as the wildfire grew, as suggested by WGS and social network analysis results.

Balancing management of a large-scale wildfire and control of COVID-19 among responders created several challenges for disease prevention and mitigation. Frequent responder turnover because of 2- to 3-week deployments, combined with the length of the fire, resulted in continuous opportunities for introduction of COVID-19 into wildfire camps (13). COVID-19 testing was available for incoming responders, but no testing or quarantine was required upon arrival, and no surveillance testing was required during the deployment period. In addition, turnover of responders resulted in several instances in which case-patients in isolation or contacts in quarantine were demobilized back to their home states or deployed to other wildfire responses before case investigation and contact tracing could be completed. In these situations, CDPHE notified the states to which responders were demobilized, and LCDHE coordinated with Cameron Peak IMT to ensure these responders were immediately notified and given instructions to proceed home immediately, avoiding contact with others and stops in indoor public settings during their travel. However, the potential for multistate spread was a major concern when responders were demobilized and sent home or to other responses.

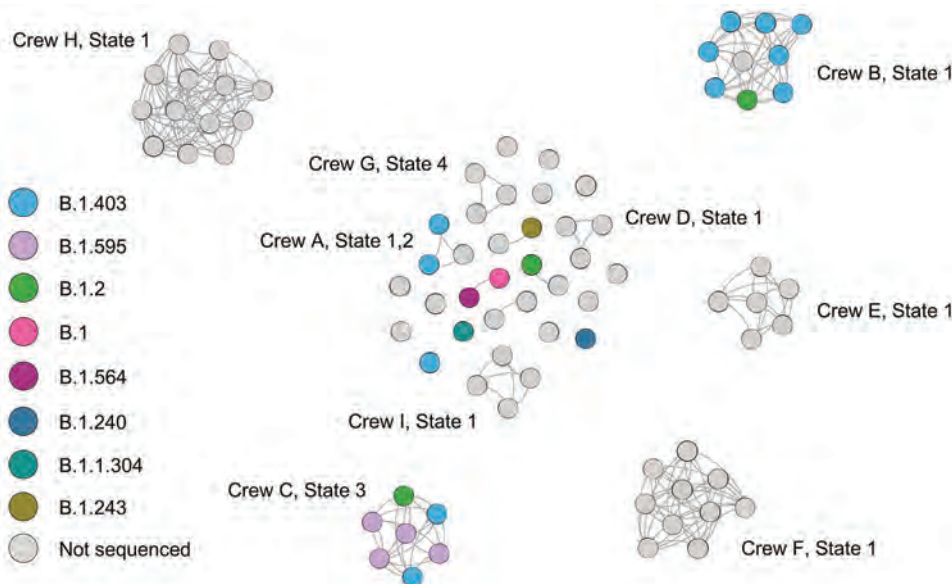


**Figure 4.** Social network analysis of Cameron Peak firefighter crews with COVID-19, Colorado, USA, August–December 2020. All responders testing positive for SARS-CoV-2 (nodes) are included in this figure to show contact within crews (edges). Crews with  $\geq 3$  firefighters positive with SARS-CoV-2 are labeled.

The difficulty of screening responders for COVID-19 symptoms was compounded by challenges differentiating the effects of smoke and high altitude from symptoms of COVID-19. Smoke inhalation can cause several respiratory symptoms that are similar to COVID-19, including coughing, shortness of breath, sore throat, and chest pain (14). Altitude sickness symptoms also overlap with COVID-19 symptoms and can include headaches, fatigue, nausea, and vomiting, as well as, in more severe cases, shortness of breath, weakness, and cough (15). Symptoms of acute and chronic smoke exposure overlap with and can worsen COVID-19 symptoms, complicating symptom-based identification of COVID-19 (13,16). Elevations in the fire-affected area ranged from  $\approx$ 5,200 feet to >10,000 feet, resulting in the potential for altitude sickness for crews, particularly those coming to Colorado from states at lower elevations.

Often, responders continued to work while they were symptomatic and infectious and did not report symptoms until their illness became severe or they experienced a distinguishing symptom, such as loss of taste or smell. COVID-19 mitigation was further challenged by how fire camps were set up, potentially increasing exposure opportunities. Crews often camped together or worked geographically closely before implementation of mitigation and quarantine measures, potentially increasing exposure opportunities. Furthermore, because these camps were often located in areas with limited cell service, Wi-Fi hotspots provided relatively small areas where responders could access Wi-Fi, creating additional opportunities for exposure when responders gathered closely together in areas where Wi-Fi was available (9). Other barriers to the public health response included some responders' distrust of their positive SARS-CoV-2 test results because of lack of symptoms or overlap with smoke inhalation symptoms. Further, many responders were employed as contractors and were not provided paid sick leave to cover quarantine or isolation. Fire response coordinators and commanders indicated that some crew members might have been hesitant to report symptoms or get tested because of concerns over having to quarantine or isolate without pay. Challenges in gathering complete symptom information could be caused by responders' reluctance to be pulled from their crew, which could further strain resources during the response. Contact tracing was challenging early in the investigation because case-patients were unable to identify their close contacts or unwilling to provide names of close contacts to avoid quarantine. Further, responders and response commanders were resistant to implementing full

quarantines because staffing needs were strained by the severity of the Cameron Peak Fire and other wildfires happening concurrently in the region. Critical infrastructure-modified quarantine and testing-based strategies were used when full quarantines were not feasible, including release from quarantine after a negative RT-PCR result from a specimen collected 7 days after exposure (which was not a recommended practice under standard quarantine guidance at that time) or monitoring responders for symptoms while allowing them to continue working during quarantine (17).

The results of WGS and social network analysis suggest multiple SARS-CoV-2 introduction events throughout the wildfire response, as well as spread both between and within crews. The presence of sequences from a single lineage in >1 crew combined with near-identical nucleotide changes observed among these sequences suggest intercrew transmission or transmission between fire crews and nearby communities (Figure 2, panel B). Contextual analysis suggests possible transmission events linked to Cameron Peak Fire responders from both outside and within the state of Colorado; in a few instances, analysis suggested transmission from the state from which an individual was deployed and in other instances from surrounding counties within the state of Colorado. One state deployment introduction (state 5) and 1 Colorado county introduction (Colorado county A) are well supported by bootstrapping, but in the other 2 instances, support was weak. This result of low sequence diversity across many states present in sequences available in public repositories from this time period.

The first limitation of our study is that COVID-19 cases were likely underreported because of insufficient testing and lack of reporting of symptoms by responders. Surveillance testing was optional and the overlap between COVID-19 symptoms and symptoms associated with smoke inhalation and altitude sickness might have led some persons not to get tested when symptomatic. Second, only 51% of outbreak-related specimens were available for WGS because not all specimens were sent to the CDPHE laboratory, including those collected through the local hospital; therefore, results might not be complete. Finally, social network analysis epidemiologic links were assumed for responders on the same crew but lacked more robust data showing intercrew mingling during and outside of response activities.

Many lessons were learned in this COVID-19 outbreak during a wildfire response. Open communication between fire response agencies and public health agencies enabled enhanced prevention strategies. Fire

response agencies should consider symptom screening and testing of all arriving responders to limit introduction of SARS-CoV-2 into fire camps; educating responders about potentially overlapping symptoms of smoke inhalation, COVID-19, and altitude (when relevant); and improving physical distancing of crews onsite. Surveillance testing offers the ability to detect cases early and to prevent transmission before an outbreak occurs (18). Rapid testing options, such as the use of rapid antigen tests, can provide many benefits in wildfire response and other emergency management settings, including quick turnaround of results, which can minimize the need to quarantine critical responders while awaiting results; encouraging action in response to mild symptoms that might otherwise be dismissed as the result of smoke or altitude, because it is a quick and easy option to differentiate symptoms; and ease of implementation in remote and nonmedical settings, not requiring transport of persons off-site or coordination with nearby medical facilities. Response agencies should work with jurisdictional public health agencies at the beginning of each response to determine what testing options are currently available and how best to implement testing of responders. Rapidly identifying cases would lead to timely case investigations and contact tracing activities that could help mitigate spread of disease by enabling timely isolation of case-patients and quarantine of close contacts. Policies to compensate responders for time spent in isolation or quarantine could improve compliance with testing and screening procedures. During the response, fire response agencies recommended mask use, especially when other social distancing measures were difficult to maintain. Continuing the use of masks in indoor settings or close interactions with others could be considered in areas of high transmission even in the absence of local public health requirements. In current and future fire seasons, we encourage COVID-19 vaccination and surveillance testing, particularly given the challenges of implementing other mitigation techniques in resource-constrained fire responses. Response agencies should consider collaborating with public health agencies to ensure that appropriate disease control measures are put in place when COVID-19 has been identified among responders, including encouraging cooperation of persons who are identified as case-patients or close contacts to prevent the spread of disease. The lessons learned during this outbreak can contribute to developing best practices for managing wildfire response and outbreaks of COVID-19 and other communicable diseases among responders to large-scale emergency events.

## Acknowledgments

We thank the CDPHE Rapid Response Testing Teams responding to the COVID-19 outbreak at the Cameron Peak Fire Incident.

## About the Author

Ms. Metz works at the Colorado Department of Public Health and Environment as a COVID-19 Epi Response Team Unit Manager for metropolitan area counties in Colorado. Her research interests include infectious disease epidemiology and outbreak investigations.

## References

- Centers for Disease Control and Prevention. Interim guidance on developing a COVID-19 case investigation & contact tracing plan. Appendix A: glossary of key terms. Close contact [cited 2021 Aug 9]. <https://www.cdc.gov/coronavirus/2019-ncov/php/contact-tracing/contact-tracing-plan/appendix.html#contact>
- Colorado Department of Public Health and Environment. Best practices for managing the risks of COVID-19 and wildfires. 2020 Aug 24 [cited 2021 Jun 15]. <https://covid19.colorado.gov/covid-19-and-wildfires>
- Centers for Disease Control and Prevention. FAQs and communication resources for wildland firefighters. 2021 [cited 2021 Jun 15]. <https://www.cdc.gov/coronavirus/2019-ncov/community/wildland-firefighters-faq.html>
- United States Department of Agriculture. Wildfire smoke and COVID-19: frequently asked questions [cited 2021 Jun 15]. [https://www.nifc.gov/sites/default/files/pio/documents/Smoke\\_COVID19\\_FS\\_FactSheet.pdf](https://www.nifc.gov/sites/default/files/pio/documents/Smoke_COVID19_FS_FactSheet.pdf)
- National Wildfire Coordinating Group. Fire management board—COVID-19 information [cited 2021 Jul 30]. <https://www.nwcg.gov/partners/fmb/covid-19>
- US Department of Interior Office of Wildland Fire. Wildfires and COVID-19 [cited 2021 Jul 30]. <https://www.doi.gov/wildlandfire/wildfires-covid-19>
- Centers for Disease Control and Prevention. Coronavirus disease 2019 (COVID-19) 2020 interim case definition, approved April 5, 2020 [cited 2021 Feb 1]. <https://www.cdc.gov/nndss/conditions/coronavirus-disease-2019-covid-19/case-definition/2020/08/05/>
- Petersen A, Dearing F, Nordgren B. Managing a COVID-19 worst-case scenario: the Cameron Peak Fire story [cited 2021 May 19]. [https://experience.arcgis.com/experience/0d12d48a842745868c1cef3b7b99cd83/page/page\\_0/](https://experience.arcgis.com/experience/0d12d48a842745868c1cef3b7b99cd83/page/page_0/)
- Rambaut A, Holmes EC, O'Toole Á, Hill V, McCrone JT, Ruis C, et al. A dynamic nomenclature proposal for SARS-CoV-2 lineages to assist genomic epidemiology. *Nat Microbiol.* 2020;5:1403–7. <https://doi.org/10.1038/s41564-020-0770-5>
- Hadfield J, Megill C, Bell SM, Huddleston J, Potter B, Callender C, et al. Nextstrain: real-time tracking of pathogen evolution. *Bioinformatics.* 2018;34:4121–3. <https://doi.org/10.1093/bioinformatics/bty407>
- Kirbyuk U, Binder AM, Ghinai I, Zawitz C, Levin R, Samala U, et al. Network characteristics and visualization of COVID-19 outbreak in a large detention facility in the United States—Cook County, Illinois, 2020. *MMWR Morb Mortal Wkly Rep.* 2020;69:1625–30. <https://doi.org/10.15585/mmwr.mm6944a3>

## SYNOPSIS

12. Guindon S, Dufayard J-F, Lefort V, Anisimova M, Hordijk W, Gascuel O. New algorithms and methods to estimate maximum-likelihood phylogenies: assessing the performance of PhyML 3.0. *Syst Biol*. 2010;59:307–21. <https://doi.org/10.1093/sysbio/syq010>
13. Navarro KM, Clark KA, Hardt DJ, Reid CE, Lahm PW, Domitrovich JW, et al. Wildland firefighter exposure to smoke and COVID-19: a new risk on the fire line. *Sci Total Environ*. 2021;760:144296. <https://doi.org/10.1016/j.scitotenv.2020.144296>
14. Centers for Disease Control and Prevention. Wildfire smoke [cited 2021 Aug 9]. <https://www.cdc.gov/disasters/wildfires/smoke.html>
15. Centers for Disease Control and Prevention. Travel to high altitudes [cited 2021 Aug 9]. <https://wwwnc.cdc.gov/travel/page/travel-to-high-altitudes>
16. Henderson SB. The COVID-19 pandemic and wildfire smoke: potentially concomitant disasters. *Am J Public Health*. 2020;110:1140–2. <https://doi.org/10.2105/AJPH.2020.305744>
17. Centers for Disease Control and Prevention. Testing strategy for coronavirus (COVID-19) in high-density critical infrastructure workplaces after a COVID-19 case is identified [cited 2021 Jun 15]. <https://www.cdc.gov/coronavirus/2019-ncov/community/worker-safety-support/hd-testing.html>
18. Brook CE, Northrup GR, Ehrenberg AJ, Doudna JA, Boots M; IGI SARS-CoV-2 Testing Consortium. Optimizing COVID-19 control with asymptomatic surveillance testing in a university environment. *Epidemics*. 2021;37:100527. <https://doi.org/10.1016/j.epidem.2021.100527>

Address for correspondence: Amanda Metz, Colorado Department of Public Health and Environment, 4300 Cherry Creek Dr S, Denver, CO 80246, USA; email: [amanda.metz@state.co.us](mailto:amanda.metz@state.co.us)



Want to stay updated on the latest news in *Emerging Infectious Diseases*? Let us connect you to the world of global health. Discover groundbreaking research studies, pictures, podcasts, and more by following us on Twitter at @CDC\_EIDjournal.

# Lack of Evidence for Ribavirin Treatment of Lassa Fever in Systematic Review of Published and Unpublished Studies<sup>1</sup>

Hung-Yuan Cheng, Clare E. French, Alex P. Salam, Sarah Dawson, Alexandra McAleenan, Luke A. McGuinness, Jelena Savović, Peter W. Horby, Jonathan A.C. Sterne



In support of improving patient care, this activity has been planned and implemented by Medscape, LLC and Emerging Infectious Diseases. Medscape, LLC is jointly accredited by the Accreditation Council for Continuing Medical Education (ACCME), the Accreditation Council for Pharmacy Education (ACPE), and the American Nurses Credentialing Center (ANCC), to provide continuing education for the healthcare team.

Medscape, LLC designates this Journal-based CME activity for a maximum of 1.00 **AMA PRA Category 1 Credit(s)**<sup>TM</sup>. Physicians should claim only the credit commensurate with the extent of their participation in the activity.

Successful completion of this CME activity, which includes participation in the evaluation component, enables the participant to earn up to 1.0 MOC points in the American Board of Internal Medicine's (ABIM) Maintenance of Certification (MOC) program. Participants will earn MOC points equivalent to the amount of CME credits claimed for the activity. It is the CME activity provider's responsibility to submit participant completion information to ACCME for the purpose of granting ABIM MOC credit.

All other clinicians completing this activity will be issued a certificate of participation. To participate in this journal CME activity: (1) review the learning objectives and author disclosures; (2) study the education content; (3) take the post-test with a 75% minimum passing score and complete the evaluation at <http://www.medscape.org/journal/eid>; and (4) view/print certificate. For CME questions, see page 1744.

**Release date: July 22, 2022; Expiration date: July 22, 2023**

## Learning Objectives

Upon completion of this activity, participants will be able to:

- Describe the overall effectiveness of ribavirin for treatment of Lassa fever, according to a systematic review of published literature and unpublished study results
- Determine the effectiveness of ribavirin for treatment of Lassa fever in subgroups, according to a systematic review of published literature and unpublished study results
- Identify clinical implications of the effectiveness of ribavirin for treatment of Lassa fever, according to a systematic review of published literature and unpublished study results

## CME Editor

**Jude Rutledge, BA**, Technical Writer/Editor, Emerging Infectious Diseases. *Disclosure: Jude Rutledge has disclosed no relevant financial relationships.*

## CME Author

**Laurie Barclay, MD**, freelance writer and reviewer, Medscape, LLC. *Disclosure: Laurie Barclay, MD, has the following relevant financial relationships: formerly owned stocks in AbbVie Inc.*

## Authors

**Hung-Yuan Cheng, DPhil; Clare E. French, PhD; Alex P. Salam, DPhil; Sarah Dawson, MSc; Alexandra McAleenan, PhD; Luke A. McGuinness, PhD; Jelena Savović, PhD; Peter W. Horby, MD, PhD; and Jonathan A.C. Sterne, PhD.**

Author affiliations: Population Health Sciences, University of Bristol, Bristol, UK (H.-Y. Cheng, C.E. French, S. Dawson, A. McAleenan, L.A. McGuinness, J. Savović, J.A.C. Sterne); National Institute for Health and Care Research (NIHR) Health Protection Research Unit in Behavioural Science and Evaluation, University of Bristol, Bristol (C.E. French); United Kingdom Public Health Rapid Support Team, London, UK (A.P. Salam); Pandemic Sciences Centre, University of Oxford, Oxford, UK (A.P. Salam, P.W. Horby); NIHR Applied Research Collaboration West, Bristol (J. Savović); International Severe Acute Respiratory and Emerging Infections Consortium, Oxford (P. Horby); NIHR Bristol Biomedical Research Centre, Bristol (J.A.C. Sterne); Health Data Research UK South West, Bristol (J.A.C. Sterne)

DOI: <https://doi.org/10.3201/eid2808.211787>

<sup>1</sup>Preliminary results from this study were presented at the World Health Organization Emergency Program on December 21, 2019.

Ribavirin has been used widely to treat Lassa fever in West Africa since the 1980s. However, few studies have systematically appraised the evidence for its use. We conducted a systematic review of published and unpublished literature retrieved from electronic databases and gray literature from inception to March 8, 2022. We identified 13 studies of the comparative effectiveness of ribavirin versus no ribavirin treatment on mortality outcomes, including unpublished data from a study in Sierra Leone provided through a US Freedom of Information Act request. Although ribavirin was associated with decreased mortality rates, results of these studies were at critical or serious risk for bias when appraised using the ROBINS-I tool. Important risks for bias related to lack of control for confounders, immortal time bias, and missing outcome data. Robust evidence supporting the use of ribavirin in Lassa fever is lacking. Well-conducted clinical trials to elucidate the effectiveness of ribavirin for Lassa fever are needed.

Lassa virus infection, first described in 1962, is a viral hemorrhagic fever (1). It is a substantial public health burden, causing an estimated 100,000–200,000 cases each year, mainly in West Africa (2,3). Many cases are mild or asymptomatic and are not formally diagnosed (4). The nonspecific clinical manifestation makes Lassa fever difficult to recognize on clinical grounds alone, especially in the early phases. The case-fatality rate is estimated to be 10%–20% in hospitalized patients (5,6) but increases sharply during outbreaks (7). No vaccine is available, but studies examining recombinant vaccinia virus in animals have entered the preclinical phase, and a DNA vaccine has entered a phase I trial in humans (8–10). Lassa virus is part of the US Centers for Disease Control and Prevention's list of category A Select Agents and is considered a priority pathogen by the World Health Organization (WHO) because of its epidemic potential, its severity, lack of available vaccines, and, most important, limited therapeutic options.

The most influential study of the efficacy of ribavirin in treatment of Lassa fever, published in 1986, reported that administration of intravenous ribavirin within the first 6 days of illness decreased mortality rates from severe Lassa fever from 55% to 5% (11). These findings have underpinned the widespread use of, and unequivocal recommendations for, ribavirin for treatment of Lassa fever. Several retrospective observational studies document the use of ribavirin and describe lower case-fatality rates in patients treated with ribavirin (12–17). However, potential biases in those results make it difficult to evaluate the effectiveness of ribavirin in clinical practice. Recent unpublished results obtained through the US Freedom of Information Act, and

secondary analysis of these results, weaken the case for use of ribavirin (18). Therefore, we undertook a systematic review of published and unpublished study results, which we appraised by using a state-of-the-art risk for bias tool (19), to evaluate ribavirin for treating Lassa fever.

## Methods

This review follows the guidelines of Preferred Reporting Items for Systematic Reviews and Meta-Analyses (PRISMA) (20) (Appendix Table 1, <https://wwwnc.cdc.gov/EID/article/28/8/21-1787-App1.pdf>). A protocol is registered on the International Prospective Register of Systematic Reviews (PROSPERO 2019 CRD42019141818) (<https://www.crd.york.ac.uk/prospero>).

We conducted a comprehensive search of multiple bibliographic databases from inception to March 8, 2022: Ovid Medline, Ovid Embase, Central Register of Controlled Trials, BIOSIS, WHO Global Index Medicus, and Web of Science (including Science Citation Index Expanded and Conference Proceedings Citation Index-Science). We also searched the WHO International Clinical Trials Registry Platform, ClinicalTrials.gov, and Pan African Clinical Trial Registry databases to identify relevant reports. We searched the keywords “Lassa” and “ribavirin” within Google.com and the WHO website to retrieve gray literature on March 8, 2022. We developed search strings for each database (Appendix). To identify further relevant studies, we checked reference lists of included studies and papers, citing them using the Web of Science database. We also contacted authors for clarification and supplementary information. We applied no restriction in language, publication type, study design, or date in the searches.

We also included unpublished results from a study that included the data reported by McCormick et al. (11). The unpublished results (Birch & Davis Associates and Sherikon Inc., US Army Medical Research and Development Command, unpub. data, [https://media.tghn.org/medialibrary/2019/03/Responsive\\_Documents\\_of\\_Peter\\_Horby.pdf.pdf](https://media.tghn.org/medialibrary/2019/03/Responsive_Documents_of_Peter_Horby.pdf.pdf); G.V. Ludwig, pers. comm., 2019 March 4, [https://media.tghn.org/medialibrary/2019/03/Dr.\\_Ludwig\\_memo.pdf](https://media.tghn.org/medialibrary/2019/03/Dr._Ludwig_memo.pdf)) were requested by P.W.H. through the US Freedom of Information Act. We refer to this study as IND 16666, its Food and Drug Administration Investigational New Drug application number.

## Study Selection

We included randomized controlled trials (RCTs), controlled trials, cohort and case-control studies

comparing ribavirin treatment with no ribavirin (e.g., supportive treatment) in patients having either or both confirmed and suspected Lassa fever that reported mortality (number of deaths or case-fatality rate). No study reported prespecified secondary outcomes or adverse events, except McCormick et al. (11). Therefore, we focused only on mortality in this review.

Two authors independently screened titles and abstracts of retrieved records by using Rayyan (21). All records were screened twice, once by the first author (H.C.) and then by 1 of the co-authors (C.E.F., S.D., A.M., and A.P.S.). For records that were potentially eligible, we retrieved and screened the full-text articles, using Excel (Microsoft, <https://www.microsoft.com>) to record inclusion decisions and manage the workflow. Full-text articles were reviewed independently (H.C. paired with C.E.F. or A.P.S.) to assess the eligibility. We resolved any discrepancies between authors by discussion between the paired assessors. Two authors independently extracted data compiled by 2 authors (H.C. paired with C.E.F. or A.P.S.) by using a prepiloted data extraction form in an Excel spreadsheet.

### Risk for Bias Assessment

Three authors (C.E.F., L.A.M., and H.C.) independently assessed risk for bias for each study by using the ROBINS-I tool (19). The tool consists of 7 domains containing a series of signaling questions to judge risk for bias as low, moderate, serious, or critical. For the first domain, we determined bias attributable to confounding or potential confounding factors through a literature review and expert opinion (A.P.S. and P.W.H.). We identified 3 key confounding factors: age, pregnancy status, and indicators of disease severity. For the third domain, bias in classification of interventions, we included assessment of immortal time bias (22). We provide support for judgments in individual results (Appendix Table 2).

### Data Analysis and Presentation

As described by Salam et al. (18), we used data reported in tables and an appendix within the IND 16666 report to derive aggregated datasets containing the number of deaths according to treatment groups and individual characteristics. On the basis of these datasets, we estimated mortality odds ratios (ORs) comparing ribavirin with no treatment, overall and within subgroups defined by patient characteristics (aminotransferase [AST] level and whether pregnant) in the IND 16666 report. We also extracted results from a logistic regression analysis in the IND 16666

report in which the effect of ribavirin compared with no treatment was adjusted for patient characteristics (age, sex, time to admission, time to treatment, length of stay, and log transformed AST level).

The various reports used different criteria and diagnostic tests to define confirmed Lassa fever cases. Only 1 study, Shaffer et al. (12,15), provided raw data reporting confirmed Lassa fever according to different case definitions: based on antigen, IgM, and IgG. In this study, we used positive antigen solely as the criteria for the confirmed case because it was consistently reported in the dataset (15). We also conducted a sensitivity analyses estimating ORs on the basis of other case definitions.

We estimated overall ORs and, when available, ORs in subgroups defined by timing of treatment (starting <7 and  $\geq$ 7 days after disease onset). We did not conduct meta-analyses because most results were rated as at critical overall risk for bias (19). We displayed ORs and 95% CIs for the association of ribavirin with no treatment in forest plots by using Stata 15 MP (StataCorp LLC, <https://www.stata.com>).

### Results

We retrieved 2,232 unique records, of which we excluded 2,162 on the basis of titles and abstracts. We retrieved full-text articles for the remaining 70 records for eligibility assessment, after which we excluded 55 further records (Figure 1). One study met the inclusion criteria but was excluded because it reported aggregated outcome data that included unknown treatment status (23). Other studies did not report outcome data according to treatment status (24–28). We contacted the authors for further information but received no responses. We extracted results from 13 eligible studies described in 15 published and unpublished reports and assessed the risk for bias in these results.

### Study Characteristics

We summarized the characteristics of the included studies (Appendix Table 3). All studies were from West Africa (6 from Nigeria and 7 from Sierra Leone) (11,12,14,15,17,29–36; Birch & Davis Associates and Sherikon Inc., US Army Medical Research and Development Command, unpub. data, [https://media.tghn.org/medialibrary/2019/03/Responsive\\_Documents\\_of\\_Peter\\_Horby.pdf.pdf](https://media.tghn.org/medialibrary/2019/03/Responsive_Documents_of_Peter_Horby.pdf.pdf); G.V. Ludwig, pers. comm., 2019 March 4, [https://media.tghn.org/medialibrary/2019/03/Dr.\\_Ludwig\\_memo.pdf](https://media.tghn.org/medialibrary/2019/03/Dr._Ludwig_memo.pdf); M.-L. Orji et al., unpub. data, <https://doi.org/10.20944/preprints202005.0269.v1>). McCormick et al. (11) and its additional data reported in IND 16666 were

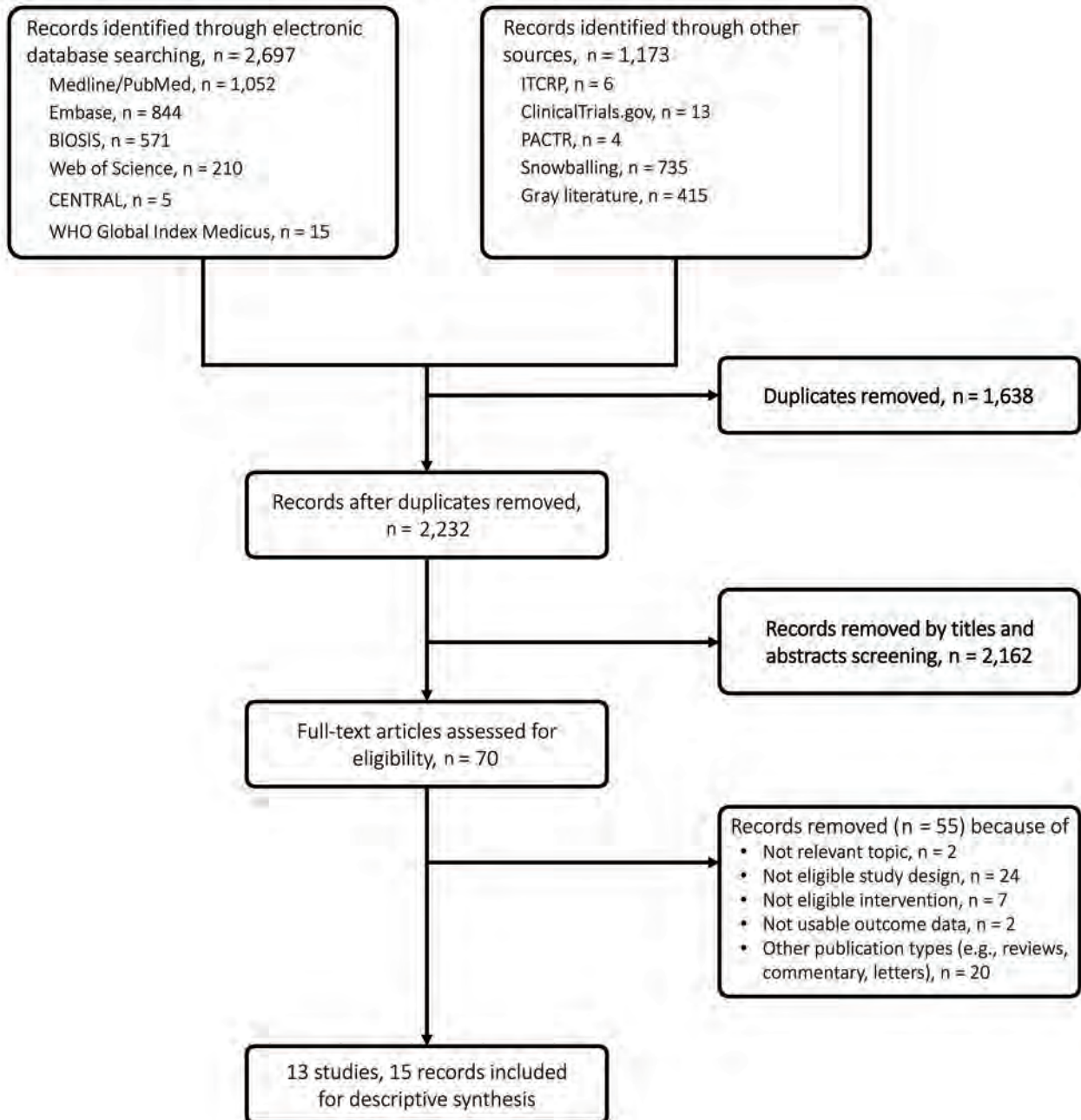


**Figure 1.** Study selection flowchart for a systematic review of published and unpublished studies for evidence for ribavirin treatment of Lassa fever. ITCRP, World Health Organization International Clinical Trials Registry Platform; PACTR, Pan African Clinical Trial Registry.

described as clinical trials, but we concluded that all studies were observational cohorts, because they did not compare treatment groups that were assigned using randomization. The year of publication ranged from 1986 to 2020. The length of follow up ranged from 1 month to 15 years.

The studies ranged in size from 10 to 1,850 confirmed cases. Most included both child and adult patients, although 2 did not report the characteristics

of patients comprehensively (11,34). Price et al. (34) included pregnant women only. Dahmane et al. (14) recruited children and women with obstetric conditions. Samuels et al. (35) and Orji et al. (M.-L. Orji et al., unpub. data) included children only. Nine of 13 studies were funded by internal or not-for-profit research funders.

Criteria for confirming Lassa fever varied between studies (Appendix Table 4). Real-time PCR

was the most common diagnostic test used, followed by virus isolation and Lassa IgM. In IND 16666, the criterion for the no treatment group was either or both bring febrile and having positive Lassa IgG whereas to receive ribavirin participants had to meet 1 of 3 specified diagnostic criteria (Appendix Table 3).

Only 4 studies reported details of ribavirin treatment regimens (11,14,38; Birch & Davis Associates and Sherikon Inc., US Army Medical Research and Development Command, unpub. data, [https://media.tghn.org/medialibrary/2019/03/Responsive\\_Documents\\_of\\_Peter\\_Horby.pdf.pdf](https://media.tghn.org/medialibrary/2019/03/Responsive_Documents_of_Peter_Horby.pdf.pdf); G.V. Ludwig, pers. comm., 2019 March 4, [https://media.tghn.org/medialibrary/2019/03/Dr\\_Ludwig\\_memo.pdf](https://media.tghn.org/medialibrary/2019/03/Dr_Ludwig_memo.pdf)) (Appendix Table 4). McCormick et al. (11) reported 3 ribavirin regimens: 1 oral and 2 intravenous. Dahmane et al. (14) reported 1 intravenous ribavirin regimen according to an international guideline. Although 7 ribavirin regimens were reported in IND 16666, the treatment durations and administration routes were not clear. In all studies except Samuels et al. (35), detailed information regarding the supportive treatment used was lacking. Three studies reported malaria screening and the use of antimalarial drugs and antibiotics before Lassa fever confirmation (14,34,36).

We assessed risk for bias in 14 results from 13 studies comparing the effects of ribavirin treatment

with no ribavirin treatment on overall mortality outcomes, including 2 results with and without logistic regression adjustment from IND 16666 (Figure 2). The overall risk for bias was rated critical for all results, except for the logistic regression result from IND 16666, which was rated serious.

**Estimated Effects of Ribavirin Treatment on Mortality, Overall and in Subgroups**

In the McCormick et al. (11) study, for which additional data was reported by IND 16666, ribavirin treatment was associated with higher overall mortality rates in confirmed Lassa fever patients, compared with no ribavirin treatment (Figure 3). However, the IND 16666 study found that, after adjusting for confounding factors using logistic regression, ribavirin was associated with lower overall mortality rates (OR 0.88 [95% CI 0.81–0.95]). We noted that the CI for this logistic regression result appeared too narrow when compared with the unadjusted result derived from the reported numbers of patients and deaths, which was most likely caused by an error in the statistical analysis but could not be checked further.

When results of those studies were stratified by AST levels, ribavirin treatment was associated with lower mortality rates in patients with AST  $\geq 150$  IU/L (OR 0.18 [0.08–0.39] in McCormick et al. [11] and OR



**Figure 2.** Summary of risk for bias assessment for a systematic review of published and unpublished studies for evidence for ribavirin treatment of Lassa fever. Bias categories: D1, bias due to confounding; D2, bias in selection of participants into the study; D3, bias in classification of interventions; D4, bias due to deviations from intended interventions; D5, bias due to missing data; D6, bias in measurement of outcomes; D7, bias in selection of the reported result. \*IND 16666, unpublished study requested by P.W.H. through the US Freedom of Information Act (Birch & Davis Associates and Sherikon Inc., US Army Medical Research and Development Command, unpub. data, [https://media.tghn.org/medialibrary/2019/03/Responsive\\_Documents\\_of\\_Peter\\_Horby.pdf.pdf](https://media.tghn.org/medialibrary/2019/03/Responsive_Documents_of_Peter_Horby.pdf.pdf); G.V. Ludwig, pers. comm., 2019 March 4, [https://media.tghn.org/medialibrary/2019/03/Dr\\_Ludwig\\_memo.pdf](https://media.tghn.org/medialibrary/2019/03/Dr_Ludwig_memo.pdf)). †M.-L. Orji et al., unpub. data, <https://doi.org/10.20944/preprints202005.0269.v1>.

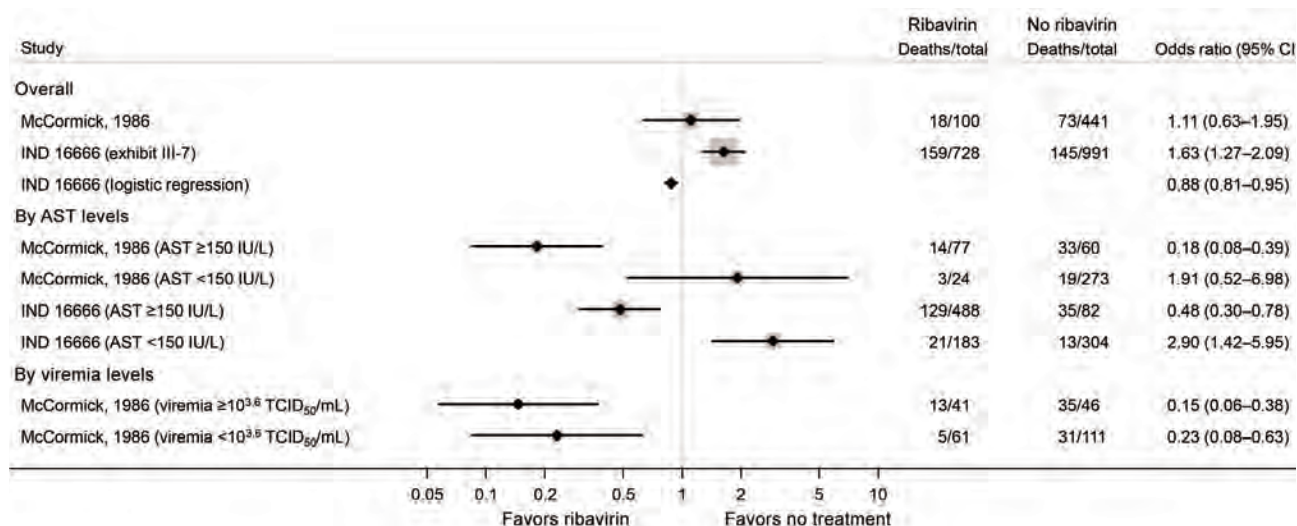


**Figure 3.** Estimated effects of ribavirin compared with no treatment on mortality outcomes from the McCormick (11) and IND 16666 (Birch & Davis Associates and Sherikon Inc., US Army Medical Research and Development Command, unpub. data, [https://media.tghn.org/medialibrary/2019/03/Responsive\\_Documents\\_of\\_Peter\\_Horby.pdf.pdf](https://media.tghn.org/medialibrary/2019/03/Responsive_Documents_of_Peter_Horby.pdf.pdf); G.V. Ludwig, pers. comm., 2019 March 4, [https://media.tghn.org/medialibrary/2019/03/Dr\\_Ludwig\\_memo.pdf](https://media.tghn.org/medialibrary/2019/03/Dr_Ludwig_memo.pdf)) studies in a systematic review of published and unpublished studies for evidence for ribavirin treatment of Lassa fever. A horizontal line represents the 95% CI of a study result, with each end of the line representing the boundaries. A point estimate of the study result is represented by a black diamond. A gray box gives a representation of the size of a study compared with all studies in the figure.

0.48 [0.30–0.78] in IND 16666). By contrast, in patients with AST <150 IU/L, ribavirin was associated with higher mortality rates (OR 1.91 [0.52–6.98] in McCormick et al. [11] and OR 2.90 [1.42–5.95] in IND 16666 study). In patients with measurable viremia, ribavirin use was associated with lower mortality rates. However, those results should be interpreted with caution because AST or viremia levels were reported to be

missing or not measurable in 20%–40% of patients in each study.

The other studies mostly found that ribavirin was associated with lower overall mortality rates compared with no ribavirin treatment (Figure 4). However, most of these results were rated as being at critical risk for bias because of lack of adjustment for confounding, immortal time bias, or both (14,17,32; M.-L. Orji et al.,

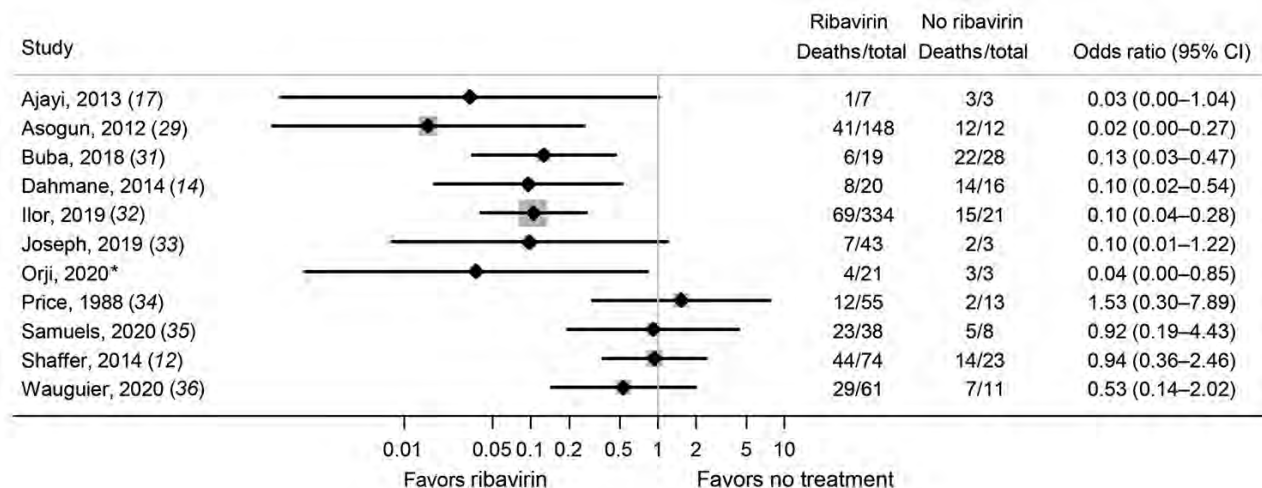


**Figure 4.** Estimated effects of ribavirin compared with no treatment on mortality outcomes from studies other than McCormick (11) and IND 16666 (Birch & Davis Associates and Sherikon Inc., US Army Medical Research and Development Command, unpub. data, [https://media.tghn.org/medialibrary/2019/03/Responsive\\_Documents\\_of\\_Peter\\_Horby.pdf.pdf](https://media.tghn.org/medialibrary/2019/03/Responsive_Documents_of_Peter_Horby.pdf.pdf); G.V. Ludwig, pers. comm., 2019 March 4, [https://media.tghn.org/medialibrary/2019/03/Dr\\_Ludwig\\_memo.pdf](https://media.tghn.org/medialibrary/2019/03/Dr_Ludwig_memo.pdf)) studies in a systematic review of published and unpublished studies for evidence for ribavirin treatment of Lassa fever. \*M.-L. Orji et al., unpub. data, <https://doi.org/10.20944/preprints202005.0269.v1>. A horizontal line represents the 95% CI of a study result, with each end of the line representing the boundaries. A point estimate of the study result is represented by a black diamond. A gray box gives a representation of the size of a study compared with all studies in the figure.

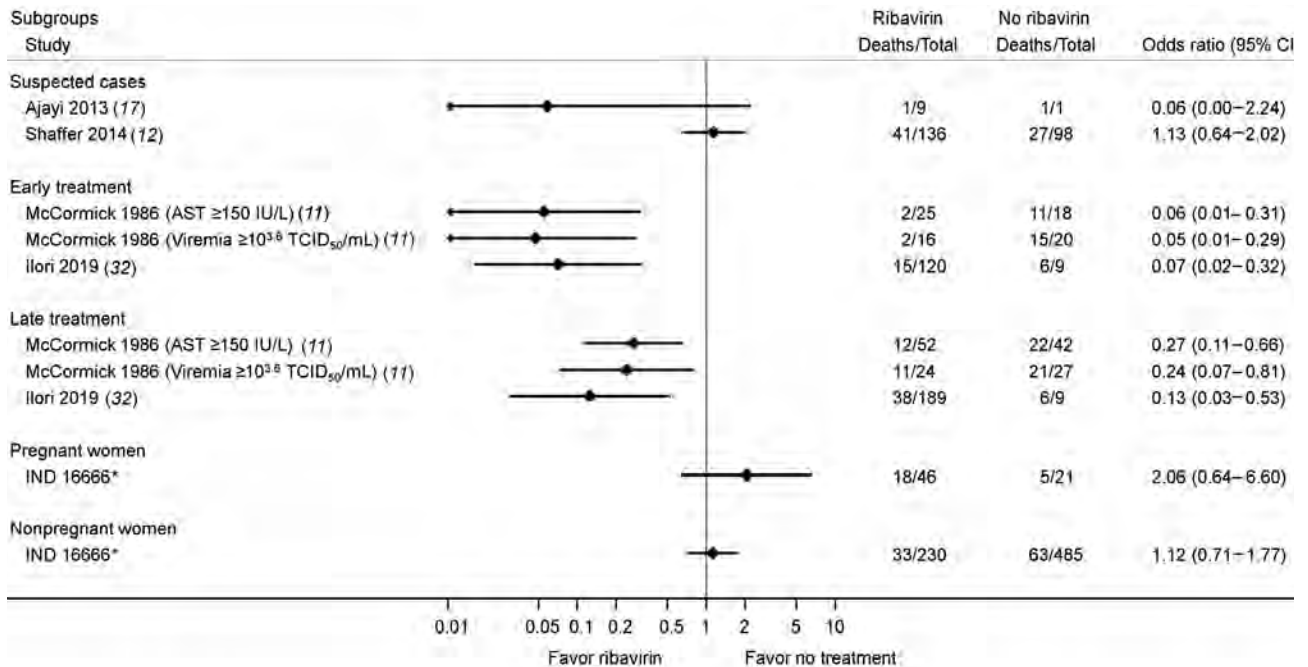


**Figure 5.** Estimated effects of ribavirin compared with no treatment on mortality outcomes within patient subgroups in a systematic review of published and unpublished studies for evidence for ribavirin treatment of Lassa fever. \*IND 16666, unpublished study requested by P.W.H. through the US Freedom of Information Act (Birch & Davis Associates and Sherikon Inc., US Army Medical Research and Development Command, unpub. data, [https://media.tghn.org/medialibrary/2019/03/Responsive\\_Documents\\_of\\_Peter\\_Horby.pdf](https://media.tghn.org/medialibrary/2019/03/Responsive_Documents_of_Peter_Horby.pdf); G.V. Ludwig, pers. comm., 2019 March 4, [https://media.tghn.org/medialibrary/2019/03/Dr\\_Ludwig\\_memo.pdf](https://media.tghn.org/medialibrary/2019/03/Dr_Ludwig_memo.pdf)).

unpub. data), which arose because some patients did not receive their intended ribavirin treatment because they died before treatment could be started and were then analyzed in the no treatment group.

Estimated associations of ribavirin treatment with mortality rates within patient subgroups are reported in the included studies (Figure 5). Many studies included suspected Lassa fever cases, but only 2 studies provided usable data for estimating associations of ribavirin treatment with deaths in suspected cases. Results were discordant; the estimated ORs were 0.06 (95% CI 0.00–2.24) in Ajayi et al. (17) and 1.13 (0.64–2.02) in Shaffer et al. (12,15). We calculated case-fatality rates and ORs from Shaffer et al. (12,15) on the basis of different case definitions (Appendix Table 5).

Two studies investigated the effects of early versus late ribavirin treatment after disease onset (11,32). McCormick et al. (11) found that in the subgroups AST  $\geq 150$  IU/L and viremia  $\geq 10^{3.6}$  median tissue culture infectious dose/mL, the association of ribavirin treatment with a lower mortality rate was more pronounced for treatment within 7 days (early) than at  $\geq 7$  days (late) after disease onset (11). Similar results were noted in Ilori et al. (32); the ORs were 0.07 (95% CI 0.02–0.32) for early treatment (within 7 days of disease onset) and 0.13 (95% CI 0.03–0.53) for late treatment ( $\geq 7$  days after disease onset).

Only 1 study provided a result of subgroup analysis to compare pregnant women with nonpregnant women. The IND 16666 study reported separate results for pregnant women (OR 2.06 [95% CI 0.64–6.60]) and nonpregnant women (OR 1.12 [95% CI 0.71–1.77]).

## Discussion

This systematic review summarizes associations of ribavirin treatment, compared with no ribavirin treatment, with overall mortality outcomes in confirmed Lassa fever, using both published and unpublished study results. Although ribavirin treatment was generally associated with lower mortality rates, almost all results were rated as being at critical risk for bias. In the single adjusted result from the IND 16666 study, ribavirin was associated with modestly lower mortality rates. However, that result was assessed as being at serious risk for bias, and the CI appeared too narrow compared with the CI derived from the numbers of patients and deaths. Although ribavirin was reported to be associated with lower mortality rates in certain subgroups, including patients with AST  $\geq 150$  IU/L and measurable viremia, missing data and the post-hoc nature of the analyses limit the credibility of these findings. By contrast, ribavirin was reported to be associated with higher mortality rates than

ribavirin treatment in other subgroups, such as patients with AST <150 IU/L. In summary, it is uncertain based on the available literature whether ribavirin reduces mortality rates in Lassa fever patients.

For decades, ribavirin has been used to treat Lassa fever, supported in particular by the results of the McCormick study (11). However, treatment guidelines generally do not highlight the weakness of the primary evidence, nor do they distinguish patient subgroups (e.g., patients with AST <150 IU/L) where benefit has not been demonstrated and, in fact, there may be hazard from using ribavirin (37,38). Because ribavirin causes adverse events and is expensive (up to 5,000€/patient) (14,37), it is important to justify its use in treating Lassa fever, especially in low- and middle-income countries where healthcare resources are limited. Although such uncertainty exists in the efficacy and safety of ribavirin, we believe that it is important to firmly establish evidence of efficacy and safety by conducting randomized controlled clinical trials. For example, WHO has identified the need for a multicenter phase 2b/3 RCT with 2 possible designs: a 4-arm factorial design with ribavirin and best supportive care and a 3-arm RCT with ribavirin, best supportive care, and another drug (39). In line with this approach, a combination of ribavirin and favipiravir treatment has been proposed by Raabe et al. (40)

Our findings agree with those of a previous systematic review (41). Both reviews identified a need to reevaluate the safety and efficacy of ribavirin for Lassa fever. In comparison with the prior review (which included studies published up to March 2019), our study included 6 additional studies, presented more detailed results (including secondary analyses), and provided a more detailed evaluation of the potential biases in study results.

Our review was conducted using state-of-the-art systematic review methodology. We conducted comprehensive literature searches, including a range of electronic databases and gray literature, without date, language, or study design restrictions. We used the ROBINS-I tool (19) for risk for bias assessments; this tool is the most comprehensive and widely used tool for assessing risk for bias in the results of non-randomized studies of interventions. Our review incorporated recent changes to ROBINS-I that address immortal time bias; evidence of such bias was identified in several of the included studies.

We conducted secondary analyses of the related McCormick (11) and IND 16666 studies. To estimate overall associations of ribavirin treatment with mortality outcomes, we grouped different ribavirin treatment regimens and routes of administration. Treatment

efficacies might differ between these regimens, but it was challenging to distinguish the ribavirin regimens used in these studies because their details were not fully described. There may have been differences in the care given to the no ribavirin treatment groups across studies; such care could be no medical support, minimal medical support, or supportive treatment, and the type of care is likely to have varied over time, by country and by setting. We did not perform subgroup analyses, investigating the implications of different criteria used to define Lassa fever, because except for Shaffer et al. (12,15), no studies provided data that could be used for subgroup analyses. We only identified studies conducted in Nigeria and Sierra Leone, but Lassa fever is endemic in several other countries in West Africa.

These findings have important implications for both clinical practice and research. The serious limitations of the available evidence means that although the studies we reviewed suggest an association of ribavirin treatment for Lassa fever with decreased mortality rates, this conclusion must be viewed with limited confidence. Evidence from high-quality randomized trials is urgently required, and clinical and research communities should work collaboratively to address and overcome ethics and resource issues to fund and conduct such trials in West Africa.

### Acknowledgments

The authors thank the study authors and experts who took time to reply to our requests and provided suggestions.

This review was supported by the World Health Organization (reference no. 2019/890244-1). H.C., S.D., J.S., and J.A.C.S. received financial support. The funder played no role in the conduct of this review. L.A.M. is supported by an NIHR Doctoral Research Fellowship (DRF-2018-11-ST2-048). C.E.F. is supported by the NIHR Health Protection Research Unit in Behavioural Science and Evaluation at the University of Bristol in partnership with the UK Health Security Agency. J.S. is partly supported by the NIHR Applied Research Collaboration West. The UK Public Health Rapid Support Team (A.P.S.) is funded by UK Aid from the Department of Health and Social Care and is jointly run by UK Health Security Agency and the London School of Hygiene & Tropical Medicine. P.W.H. is supported by the Wellcome Trust (grant no. 215091/Z/18/Z), the Bill and Melinda Gates Foundation (grant no. OPP1209135), and the EDCTP2 Programme supported by the European Union (ALERRT: RIA2016E-1612). J.A.C.S. is supported by the NIHR Bristol Biomedical Research Centre and by Health Data Research UK South West.

Author contributions: H.C., S.D., C.E.F., A.M., A.P.S., and J.S. performed screening for the review. SD designed, managed, and conducted electronic database searches. H.C. conducted gray literature searches. H.C., C.E.F., and A.P.S. conducted data extraction. H.C., C.E.F., J.S., and J.A.C. conceived the risk of bias assessment tool while A.S. and P.W.H. acted as field experts, providing clinical inputs. H.C., C.E.F., A.M., L.A.M. and A.S. assessed risk of bias in the included studies. H.C. drafted the manuscript, designed screening, data collection tools, performed data analysis, and manage the review. P.H. initiated the collaboration with J.S. and J.A.C.S. to conceptualize the review and oversee the review project together. All authors revised the draft paper and provided comments and declarations. All authors read and approved the final manuscript. All authors declare that there is no conflict of interest regarding the publication of this manuscript. Data and materials are available from the corresponding author upon request. The views expressed in this article are those of the authors and do not necessarily reflect the opinions of the National Health Service, the National Institute for Health Research, or the Department of Health and Social Care.

## About the Author

Dr. Cheng is a research fellow in the Bristol Medical School, University of Bristol, and a practicing pharmacist. His research interests include high-consequence infectious disease and clinical pharmacology and pharmacotherapy in infectious diseases.

## References

1. Frame JD, Baldwin JM Jr, Gocke DJ, Troup JM. Lassa fever, a new virus disease of man from West Africa. I. Clinical description and pathological findings. *Am J Trop Med Hyg.* 1970;19:670–6. <https://doi.org/10.4269/ajtmh.1970.19.670>
2. Ogbu O, Ajuluchukwu E, Uneke CJ. Lassa fever in West African sub-region: an overview. *J Vector Borne Dis.* 2007;44:1–11.
3. McCormick JB, Fisher-Hoch SP. Lassa fever. *Curr Top Microbiol Immunol.* 2002;262:75–109. [https://doi.org/10.1007/978-3-642-56029-3\\_4](https://doi.org/10.1007/978-3-642-56029-3_4)
4. World Health Organization. Lassa fever. 2021 [cited 2022 Mar 22]. <https://www.who.int/health-topics/lassa-fever>
5. McCormick JB, King IJ, Webb PA, Johnson KM, O'Sullivan R, Smith ES, et al. A case-control study of the clinical diagnosis and course of Lassa fever. *J Infect Dis.* 1987;155:445–55. <https://doi.org/10.1093/infdis/155.3.445>
6. McCormick JB, Webb PA, Krebs JW, Johnson KM, Smith ES. A prospective study of the epidemiology and ecology of Lassa fever. *J Infect Dis.* 1987;155:437–44. <https://doi.org/10.1093/infdis/155.3.437>
7. Fisher-Hoch SP, Tomori O, Nasidi A, Perez-Oronoz GI, Fakile Y, Hutwagner L, et al. Review of cases of nosocomial Lassa fever in Nigeria: the high price of poor medical practice. *BMJ.* 1995;311:857–9. <https://doi.org/10.1136/bmj.311.7009.857>
8. Fisher-Hoch SP, McCormick JB, Auperin D, Brown BG, Castor M, Perez G, et al. Protection of rhesus monkeys from fatal Lassa fever by vaccination with a recombinant vaccinia virus containing the Lassa virus glycoprotein gene. *Proc Natl Acad Sci U S A.* 1989;86:317–21. <https://doi.org/10.1073/pnas.86.1.317>
9. Lukashevich IS, Carrion R Jr, Salvato MS, Mansfield K, Brasky K, Zapata J, et al. Safety, immunogenicity, and efficacy of the ML29 reassortant vaccine for Lassa fever in small non-human primates. *Vaccine.* 2008;26:5246–54. <https://doi.org/10.1016/j.vaccine.2008.07.057>
10. CEPI Press Office. CEPI partner INOVIO launches Lassa vaccine phase I trial in West Africa. 2021 Feb 23 [cited 2022 Mar 22]. [https://cepi.net/news\\_cepi/cepi-partner-inovio-launches-lassa-vaccine-phase-i-trial-in-west-africa](https://cepi.net/news_cepi/cepi-partner-inovio-launches-lassa-vaccine-phase-i-trial-in-west-africa)
11. McCormick JB, King IJ, Webb PA, Scribner CL, Craven RB, Johnson KM, et al. Lassa fever. Effective therapy with ribavirin. *N Engl J Med.* 1986;314:20–6. <https://doi.org/10.1056/NEJM198601023140104>
12. Shaffer JG, Grant DS, Schieffelin JS, Boisen ML, Goba A, Hartnett JN, et al.; Viral Hemorrhagic Fever Consortium. Lassa fever in post-conflict sierra leone. *PLoS Negl Trop Dis.* 2014;8:e2748. <https://doi.org/10.1371/journal.pntd.0002748>
13. Okokhere P, Colubri A, Azubike C, Iruolagbe C, Osazuwa O, Tabrizi S, et al. Clinical and laboratory predictors of Lassa fever outcome in a dedicated treatment facility in Nigeria: a retrospective, observational cohort study. *Lancet Infect Dis.* 2018;18:684–95. [https://doi.org/10.1016/S1473-3099\(18\)30121-X](https://doi.org/10.1016/S1473-3099(18)30121-X)
14. Dahmane A, van Griensven J, Van Herp M, Van den Bergh R, Nzomukunda Y, Prior J, et al. Constraints in the diagnosis and treatment of Lassa Fever and the effect on mortality in hospitalized children and women with obstetric conditions in a rural district hospital in Sierra Leone. *Trans R Soc Trop Med Hyg.* 2014;108:126–32. <https://doi.org/10.1093/trstmh/tru009>
15. Shaffer JG, Schieffelin JS, Grant DS, Goba A, Momoh M, Kanneh L, et al.; Viral Hemorrhagic Fever Consortium. Data set on Lassa fever in post-conflict Sierra Leone. *Data Brief.* 2019;23:103673. <https://doi.org/10.1016/j.dib.2019.01.021>
16. Inegbenebor U, Okosun J, Inegbenebor J. Prevention of lassa fever in Nigeria. *Trans R Soc Trop Med Hyg.* 2010;104:51–4. <https://doi.org/10.1016/j.trstmh.2009.07.008>
17. Ajayi NA, Nwigwe CG, Azuogu BN, Onyire BN, Nwonwu EU, Ogbonnaya LU, et al. Containing a Lassa fever epidemic in a resource-limited setting: outbreak description and lessons learned from Abakaliki, Nigeria (January-March 2012). *Int J Infect Dis.* 2013;17:e1011–6. <https://doi.org/10.1016/j.ijid.2013.05.015>
18. Salam AP, Cheng V, Edwards T, Olliaro P, Sterne J, Horby P. Time to reconsider the role of ribavirin in Lassa fever. *PLoS Negl Trop Dis.* 2021;15:e0009522. <https://doi.org/10.1371/journal.pntd.0009522>
19. Sterne JA, Hernán MA, Reeves BC, Savović J, Berkman ND, Viswanathan M, et al. ROBINS-I: a tool for assessing risk of bias in non-randomised studies of interventions. *BMJ.* 2016;355:i4919. <https://doi.org/10.1136/bmj.i4919>
20. Moher D, Liberati A, Tetzlaff J, Altman DG; PRISMA Group. Preferred reporting items for systematic reviews and meta-analyses: the PRISMA statement. *BMJ.* 2009;339(jul21 1):b2535. <https://doi.org/10.1136/bmj.b2535>
21. Ouzzani M, Hammady H, Fedorowicz Z, Elmagarmid A. Rayyan-a web and mobile app for systematic reviews. *Syst Rev.* 2016;5:210. <https://doi.org/10.1186/s13643-016-0384-4>
22. Hernán MA, Sauer BC, Hernández-Díaz S, Platt R, Shrier I. Specifying a target trial prevents immortal time bias and

- other self-inflicted injuries in observational analyses. *J Clin Epidemiol*. 2016;79:70–5. <https://doi.org/10.1016/j.jclinepi.2016.04.014>
23. Hamblion EL, Raftery P, Wendland A, Dweh E, Williams GS, George RNC, et al. The challenges of detecting and responding to a Lassa fever outbreak in an Ebola-affected setting. *Int J Infect Dis*. 2018;66:65–73. <https://doi.org/10.1016/j.ijid.2017.11.007>
  24. Allan R, Mardell S, Ladbury R, Pearce E, Skinner K, Saluzzo JF, et al. The progression from endemic to epidemic Lassa fever in war-torn West Africa. In: Saluzzo JF, Dodet B, editors. *Emergence and control of rodent-borne viral diseases: hantaviral and arenaviral diseases: congrès, Annecy, 28–31 Octobre 1998*. 1st edition. Paris: Elsevier; 1999. p. 197–205.
  25. Ehichioya D, Asogun D, Hass M, Becker-Ziaja B, Gunther S, Omilabu S. A retrospective laboratory analysis of clinically diagnosed Lassa fever cases in a tertiary hospital in Nigeria. *Int J Infect Dis*. 2010;1:e209–10. <https://doi.org/10.1016/j.ijid.2010.02.1953>
  26. Fisher-Hoch SP, Gborie S, Parker L, Huggins J. Unexpected adverse reactions during a clinical trial in rural west Africa. *Antiviral Res*. 1992;19:139–47. [https://doi.org/10.1016/0166-3542\(92\)90073-E](https://doi.org/10.1016/0166-3542(92)90073-E)
  27. Riner A, Chan-Tack KM, Murray JS. Original research: Intravenous ribavirin—review of the FDA’s Emergency Investigational New Drug Database (1997–2008) and literature review. *Postgrad Med*. 2009;121:139–46. <https://doi.org/10.3810/pgm.2009.05.2014>
  28. Ilesanmi O, Ayodeji O, Abejegah C. Mortality among confirmed Lassa fever cases during the 2017–2019 outbreak in Ondo State, Nigeria [abstract]. *Trans R Soc Trop Med Hyg*. 2019;113(Suppl 1):S89.
  29. Asogun DA, Adomeh DI, Ehimuan J, Odia I, Hass M, Gabriel M, et al. Molecular diagnostics for lassa fever at Irrua specialist teaching hospital, Nigeria: lessons learnt from two years of laboratory operation. *PLoS Negl Trop Dis*. 2012;6:e1839. <https://doi.org/10.1371/journal.pntd.0001839>
  30. Bouree P. Les parasitoses intestinales sont encore fréquentes. *Med Sante Trop*. 2015;25:130. <https://doi.org/10.1684/mst.2015.0459>
  31. Buba MI, Dalhat MM, Nguku PM, Waziri N, Mohammad JO, Bomoi IM, et al. Mortality among confirmed Lassa fever cases during the 2015–2016 outbreak in Nigeria. *Am J Public Health*. 2018;108:262–4. <https://doi.org/10.2105/AJPH.2017.304186>
  32. Ilori EA, Furuse Y, Ipadeola OB, Dan-Nwafor CC, Abubakar A, Womi-Eteng OE, et al.; Nigeria Lassa Fever National Response Team. Epidemiologic and clinical features of Lassa fever outbreak in Nigeria, January 1–May 6, 2018. *Emerg Infect Dis*. 2019;25:1066–74. <https://doi.org/10.3201/eid2506.181035>
  33. Joseph A, Robinson O, Justus E, Matthew N, Chukwuemeka U. Clinical profile of Lassa fever patients in Abakaliki, south-eastern Nigeria, January–March 2018. *Ann Med Health Sci Res*. 2019;9:598–602.
  34. Price ME, Fisher-Hoch SP, Craven RB, McCormick JB. A prospective study of maternal and fetal outcome in acute Lassa fever infection during pregnancy. *BMJ*. 1988;297:584–7. <https://doi.org/10.1136/bmj.297.6648.584>
  35. Samuels RJ, Moon TD, Starnes JR, Alhasan F, Gbakie M, Goba A, et al. Lassa fever among children in Eastern Province, Sierra Leone: a 7-year retrospective analysis (2012–2018). *Am J Trop Med Hyg*. 2020;104:585–92. <https://doi.org/10.4269/ajtmh.20-0773>
  36. Wauquier N, Couffignal C, Manchon P, Smith E, Lungay V, Coomber M, et al. High heart rate at admission as a predictive factor of mortality in hospitalized patients with Lassa fever: An observational cohort study in Sierra Leone. *J Infect*. 2020;80:671–93. <https://doi.org/10.1016/j.jinf.2020.01.021>
  37. Bausch DG, Hadi CM, Khan SH, Lertora JJ. Review of the literature and proposed guidelines for the use of oral ribavirin as postexposure prophylaxis for Lassa fever. *Clin Infect Dis*. 2010;51:1435–41. <https://doi.org/10.1086/657315>
  38. World Health Organization. Clinical management of patients with viral haemorrhagic fever: a pocket guide for front-line health workers: interim emergency guidance for country adaptation. 2016 Feb [cited 2022 Mar 22]. [https://apps.who.int/iris/bitstream/handle/10665/205570/9789241549608\\_eng.pdf](https://apps.who.int/iris/bitstream/handle/10665/205570/9789241549608_eng.pdf)
  39. World Health Organization. WHO R&D blueprint. “Efficacy trials of Lassa therapeutics: endpoints, trial design, site selection” WHO workshop – final report. 2018 Apr 25 [cited 2022 Mar 22]. [https://www.who.int/blueprint/what/norms-standards/LassaTxeval\\_FinalmeetingReport.pdf](https://www.who.int/blueprint/what/norms-standards/LassaTxeval_FinalmeetingReport.pdf)
  40. Raabe VN, Kann G, Ribner BS, Morales A, Varkey JB, Mehta AK, et al.; Emory Serious Communicable Diseases Unit. Favipiravir and ribavirin treatment of epidemiologically linked cases of Lassa fever. *Clin Infect Dis*. 2017;65:855–9. <https://doi.org/10.1093/cid/cix406>
  41. Eberhardt KA, Mischlinger J, Jordan S, Groger M, Günther S, Ramharter M. Ribavirin for the treatment of Lassa fever: A systematic review and meta-analysis. *Int J Infect Dis*. 2019;87:15–20. <https://doi.org/10.1016/j.ijid.2019.07.015>

---

Address for correspondence: Jonathan A.C. Sterne, Department of Population Health Sciences, Bristol Medical School, Oakfield House, Oakfield Grove, Bristol BS8 2BN, UK; email: jonathan.sterne@bristol.ac.uk

# Transmissibility of SARS-CoV-2 B.1.1.214 and Alpha Variants during 4 COVID-19 Waves, Kyoto, Japan, January 2020–June 2021

Yasufumi Matsumura, Miki Nagao, Masaki Yamamoto, Yasuhiro Tsuchido, Taro Noguchi, Koh Shinohara, Satomi Yukawa, Hiromi Inoue, Takeshi Ikeda

Household transmission is a primary source of SARS-CoV-2 spread. We used COVID-19 epidemiologic investigation data and viral genome analysis data collected in the city of Kyoto, Japan, during January 2020–June 2021 to evaluate the effects of different settings and viral strains on SARS-CoV-2 transmission. Epidemiologic investigations of 5,061 COVID-19 cases found that the most common category for close contact was within households (35.3%); this category also had the highest reverse transcription PCR positivity. The prevalent viral lineage shifted from B.1.1.214 in the third wave to the Alpha variant in the fourth wave. The proportion of secondary cases associated with households also increased from the third to fourth waves (27% vs. 29%). Among 564 contacts from 206 households, Alpha variant was significantly associated with household transmission (odds ratio 1.52, 95% CI 1.06–2.18) compared with B.1.1.214. Public health interventions targeting household contacts and specific variants could help control SARS-CoV-2 transmission.

**R**obust testing, isolation, and epidemiologic investigations of patients and their close contacts by local public health authorities are key strategies for containing SARS-CoV-2 transmission (1). In response to the COVID-19 pandemic, the Ministry of Health, Labour and Welfare in Japan, according to law, implemented an all-case tracing approach that included mandatory reporting of laboratory-confirmed COVID-19 cases, case investigations, and contact tracing. In Japan, after outbreaks on cruise ships and identification of imported cases,

COVID-19 clusters were reported in healthcare and long-term care facilities (LTCFs), restaurants, workplaces, and events, and those became the main target of COVID-19 interventions (2,3). Households have become the main venue for community transmission (4,5), and household contacts have a higher risk for secondary infection than nonhousehold contacts (6). Moreover, household transmission could be increasingly relevant during periods of social distancing and stay-at-home orders (7).

Specific SARS-CoV-2 variants, namely, those designated variants of concern (VOCs), generally have higher transmissibility than non-VOCs. The Alpha VOC was estimated to have a reproduction number 43%–90% higher than previous variants and has spread worldwide, including throughout Japan (8).

Kyoto, an ancient capital city of Japan, has a population of  $\approx$ 1 million and is known as a tourist destination. By June 2021, Kyoto had experienced 4 waves of COVID-19. In response to these waves, the Health and Welfare Bureau of Kyoto City and a tertiary referral hospital of Kyoto University Hospital, which has infectious disease and clinical laboratory specialists, collaborated to perform epidemiologic investigations, establish interventions for cluster-associated cases, and conduct molecular epidemiologic surveillance. We describe COVID-19 epidemiology in Kyoto and focus on the effects of cluster and household transmission of different SARS-CoV-2 variants.

## Materials and Methods

### Active Epidemiologic Investigations

The Health and Welfare Bureau of Kyoto performed active epidemiologic investigations of all laboratory-confirmed COVID-19 cases in the city according to the guidelines of the National Institute of Infectious

Author affiliations: Kyoto University Graduate School of Medicine, Kyoto, Japan (Y. Matsumura, M. Nagao, M. Yamamoto, Y. Tsuchido, T. Noguchi, K. Shinohara, S. Yukawa); Health and Welfare Bureau of Kyoto City, Kyoto (H. Inoue, T. Ikeda)

DOI: <https://doi.org/10.3201/eid2808.220420>

Diseases, Japan (9). These investigations collected the clinical data of COVID-19 patients, behavioral histories for 14 days before symptom onset or diagnosis, and detailed activity histories for 2 days before symptom onset or diagnosis. On the basis of those data, the bureau conducted contact tracing by identifying potential sources of infection and close contacts. The epidemiologic study was determined to be public health surveillance as defined in Article 15 of the Act on the Prevention of Infectious Diseases and Medical Care for Patients with Infectious Diseases (1999); thus, informed consent was not required.

The bureau defined close contacts as persons who lived with a COVID-19 patient or who had been <2 m from a patient for >15 min without using necessary preventive measures, such as personal protective equipment, within 2 days before the COVID-19 patient's symptom onset or diagnosis (9). All household members of COVID-19 patients were considered close contacts (9). The bureau requested that close contacts quarantine for at least 14 days and get 1 reverse transcription PCR (RT-PCR) test at the beginning of the quarantine regardless of symptoms.

We defined a cluster as identification of >5 cases at the same facility or among a group of contacts within 14 days of symptom onset or diagnosis for any patient, excluding household contacts. For clusters and cases that occurred in high-risk settings such as healthcare facilities, non-close contacts who shared a space with COVID-19 case-patients, such as in a workplace, also underwent RT-PCR testing to identify asymptomatic cases.

We obtained epidemiologic data from existing local databases, and we determined the RT-PCR test positivity of close contacts according to the source of infection. We compared the number of household transmissions and the number of clusters between the third and fourth COVID-19 waves in Kyoto and between SARS-CoV-2 variants.

### Epidemiologic Data

We obtained data on the number of COVID-19 cases in Kyoto and in Japan during January 2020–June 2021 from official websites for Kyoto City and the Ministry of Health, Labour and Welfare, Japan (10,11). We also obtained data from these websites on the number of persons who received RT-PCR testing at the official laboratories of Kyoto City or Kyoto Prefecture and commercial laboratories.

### Clinical Samples

Respiratory tract samples that tested positive by RT-PCR were sent to the reference laboratory at

Kyoto University and subjected to genome analysis. The samples were obtained from RT-PCR testing sites, acute-care hospitals, close contacts found by active epidemiologic investigations, and mass PCR testing for residents and workers of adult daycare and LTCFs.

### Genome Analysis

We prepared a genome library by using an amplicon-based next-generation sequencing assay, the research-use-only COVIDSeq Test (RUO Version; Illumina, <https://www.illumina.com>), and sequenced samples by using the NovaSeq6000, NextSeq1000, NextSeq550, or MiniSeq platforms (Illumina). We processed the data by using DRAGEN COVID Lineage App version 3.5.3 (Illumina), and generated consensus sequences by using the SARS-CoV-2 reference genome (GenBank accession no. NC\_045512). Using Pangolin version 3.1.20 (12), we assigned lineages to sequenced genomes that had >90% breadth of coverage of the reference genome and for genome data from Japan obtained from the GISAID database (<https://www.gisaid.org>) on July 13, 2021. We defined VOCs according to the World Health Organization designations as of June 22, 2021 (13). We used IQ-TREE multicore version 2.1.2 COVID-edition (<http://www.iqtree.org>) for phylogenetic analysis. We submitted SARS-CoV-2 sequences obtained in this study to GISAID (Appendix 1, <https://wwwnc.cdc.gov/EID/article/28/8/22-0420-App1.xlsx>).

### Statistical Analysis

We calculated the secondary attack rate (SAR) by dividing the number of secondary cases within 14 days of the index case-patients' positive RT-PCR test date by the total number of household contacts. We defined the index case as the first laboratory-confirmed case in the household. We excluded households in which coprimary cases had the same symptom onset date or same diagnosis date as primary cases. To analyze the association between SARS-CoV-2 variant and household transmission and to predict SAR, we used a generalized linear mixed-effects logistic regression model. In this model, we used random intercepts to account for clustering by household, the dependent variable of SARS-CoV-2 infection of contacts, and the predictors of the age of the index case-patient, the age of the contact, the presence of symptoms in the index case-patient, the household size, and the SARS-CoV-2 lineage, as previously described (14).

We used Fisher exact test to compare the categorical variable sex and Mann-Whitney U test to compare the continuous variable age. We considered  $p < 0.05$

statistically significant. We conducted statistical analyses by using R version 4.1.3 (R Foundation for Statistical Computing, <https://www.r-project.org>). The Ethics Committee of Kyoto University Graduate School and the Faculty of Medicine approved this study (approval no. R2379) and waived the need to obtain informed consent from study subjects.

## Results

During January 2020–June 2021, Japan had a total of 792,256 reported COVID-19 cases, among which 11,477 cases were reported in Kyoto (Figure 1). Japan and the city of Kyoto experienced 4 COVID-19 waves during that period. The third (December 2020–February 2021) and fourth (April 2021–June 2021) waves were larger than the first (April 2020–May 2020) and second (July 2020–September 2020) waves (Figure 1).

We performed genomic analysis on a total of 2,600 nonduplicate samples, representing 22.7% of COVID-19 cases in Kyoto. We determined pangolin lineages for 2,318 samples, the median coverage of which was 99.7% (interquartile range [IQR] 99.1%–99.8%) of the reference genome. The primary lineage responsible for each wave in Kyoto shifted during the 4 waves, from B.1 (47.1%) during the first wave to B.1.1.284 (88.6%) in the second, B.1.1.214 (85.4%) in the third, and B.1.1.7 (Alpha; 93.4%) in the fourth (Figure 2, panel A). During March 2021, between the third and fourth waves, R.1 was the most common (53.8%) lineage. We noted 2 VOCs: Alpha lineages B.1.1.7 and Q.1 ( $n = 998$ ) during January 2021–June

2021 and Delta B.1.617.2-like ( $n = 9$ ) during July 2021. The prevalent lineages in the 4 COVID-19 waves in Kyoto were the same as the rest of the country, except Japan had B.1.1 dominance during the first wave (Figure 2, panel B).

Active epidemiologic investigation of 5,061 COVID-19 cases in Kyoto identified 13,562 close contacts during November 2020–March 2021. The most common contact categories were household contacts (35.3%) and family living separately (10.4%), followed by workplace (staff 17.6% and user 8.2%), school (12.9%), and friend contacts (11.5%). Of close contacts, 11,813 (87.1%) had RT-PCR tests and 15.1% tested positive (Table 1). Test positivity was the highest among household contacts (24.9%) and friend contacts (16.4%). The test positivity rate among the general population during the same period was 5.9%.

We assessed the association of COVID-19 cases with household transmission events and clusters during the third and fourth waves in Kyoto (Table 2). Compared with cases in the third wave, the mean number of cases per day was higher during the fourth wave (51.0 vs. 68.5), as was the percentage of household cases among all cases (26.7% vs. 28.9%). The percentage of cluster-associated cases among all cases was higher during the third wave than during the fourth wave (15.4% vs. 10.7%), as was the median number of cases associated with each cluster (11 vs. 7), but the mean number of clusters per day was higher during the fourth wave than the third wave (0.70 vs. 0.44). The most common settings for clusters

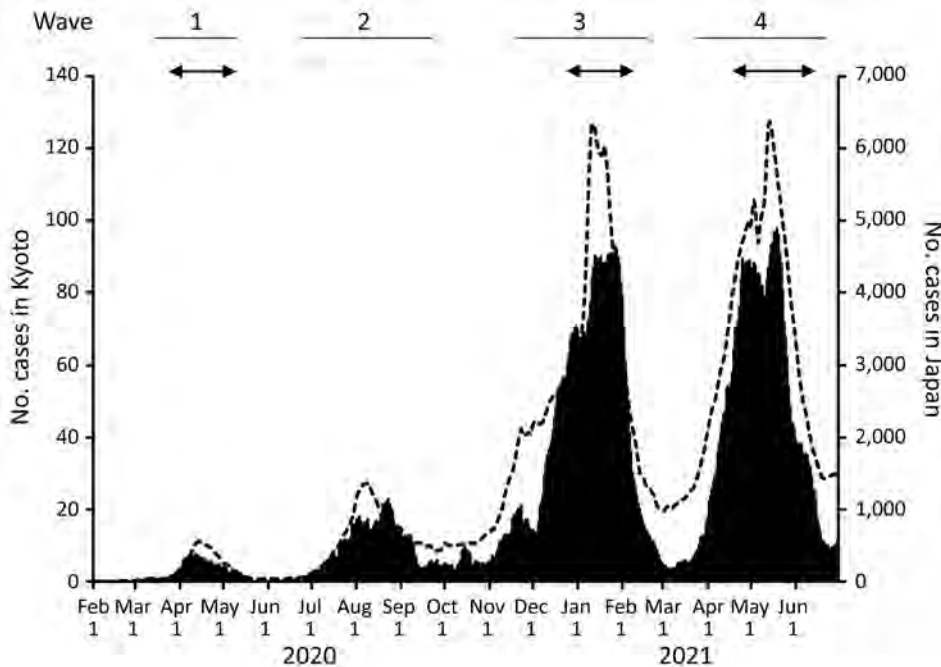
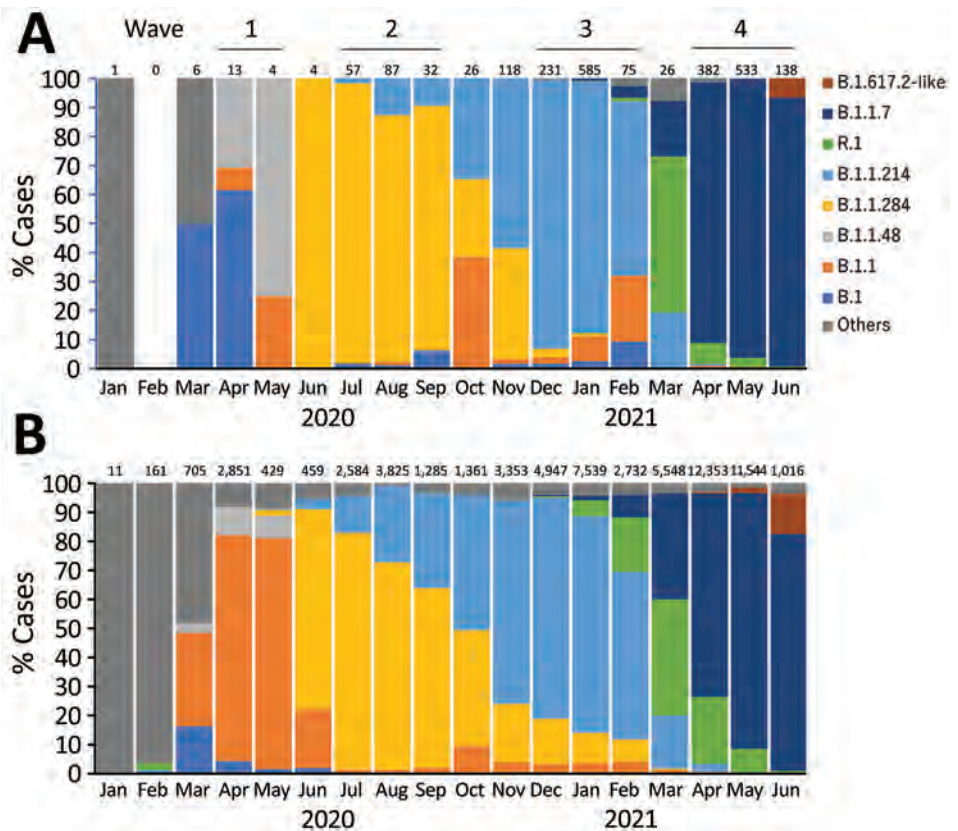


**Figure 1.** Seven-day moving average of cases during 4 COVID-19 waves, Kyoto, Japan, January 2020–June 2021. Solid black represents averages in Kyoto City and dashed lines represent averages in Japan. Arrows indicate the state of emergency designation in Kyoto Prefecture, in which Kyoto is located. Scales for the y-axes differ substantially to underscore patterns but do not permit direct comparisons.

**Figure 2.** Prevalence of major SARS-CoV-2 viral lineages detected among respiratory tract specimens collected during 4 COVID-19 waves in Japan, January 2020–June 2021. A) Lineages detected in Kyoto City. B) Lineages detected from 62,703 genomes obtained in Japan and downloaded from the GISAID database (<https://www.gisaid.org>). Number of available genomes analyzed per month is shown above each bar. The most common lineages during each wave in Kyoto were B.1 (n = 8, 47.1%) during the first wave; B.1.1.284 (n = 156, 88.6%) during the second; B.1.1.214 (n = 766, 86.0%) during the third; and B.1.1.7 (Alpha; n = 983, 93.4%) during the fourth. B.1.48 was the second most common lineage during the first wave (n = 7, 41.2%) and R.1 was the most common lineage during March 2021 (n = 14, 53.8%), between the third and fourth waves. The most common lineages during each wave in Japan were B.1.1 (n = 2,561, 78.1%) during the first wave; B.1.1.284 (n = 5,641, 73.3%) during the second; B.1.1.214 (n = 10,970, 72.1%) during the third; and B.1.1.7 (Alpha; n = 19,630, 78.8%) during the fourth. B.1.48 was the second most common lineage during the first wave (n = 313, 9.5%) and R.1 was the second most common lineage during March 2021 (n = 2,217, 40.0%).



during the third wave were welfare facilities (60.0%) and hospitals (25.0%), but during the fourth wave, offices (30.2%) and adult daycare and LTCFs (16.3%) were the most common settings (Appendix 2 Table, <https://wwwnc.cdc.gov/EID/article/28/8/22-0420-App2.pdf>).

Because Alpha was the main variant during the fourth wave, we compared the household transmission rates associated with the Alpha VOC and the non-VOC B.1.1.214. We investigated 310 households in which ≥1 member was infected with SARS-CoV-2 during November 2020–May 2021, regardless of symptoms, and for which all members had RT-PCR

testing. We noted 245 households in which ≥1 household member was infected with Alpha or B.1.1.214 SARS-CoV-2 lineages. We excluded 29 households with incomplete demographic data, 9 households with >1 index case, and 1 household with a contact infected >14 days after the symptom onset or diagnosis of the index case. Thus, we found 206 households eligible for comparison, 106 with Alpha infections and 100 with B.1.1.214 infections (Table 3).

Of the households with Alpha infections, we noted 106 index cases and 282 contacts; the median household size was 3 persons. Of 100 households with B.1.1.214 infections, we noted 100 index cases and 282 contacts,

**Table 1.** Reverse transcription PCR test positivity for close contacts of 5,061 COVID-19 case-patients, Kyoto, Japan, November 2020–March 2021

| Contact category                  | No. identified | No. (%) tested       | No. (%) positive    |
|-----------------------------------|----------------|----------------------|---------------------|
| Household members living together | 4,789          | 4,523 (94.4)         | 1,128 (24.9)        |
| Family living separately          | 1,415          | 1,038 (73.4)         | 150 (14.5)          |
| School, including nursery         | 1,755          | 1,696 (96.6)         | 38 (2.2)            |
| Workplace, working staff          | 2,384          | 1,966 (82.5)         | 169 (8.6)           |
| Workplace, user                   | 1,114          | 1,030 (92.5)         | 67 (6.5)            |
| Friend                            | 1,566          | 1,174 (75.0)         | 193 (16.4)          |
| Others                            | 539            | 386 (71.6)           | 39 (10.1)           |
| <b>Total</b>                      | <b>13,562</b>  | <b>11,813 (87.1)</b> | <b>1,784 (15.1)</b> |

**Table 2.** COVID-19 cases associated with households or clusters during the third and fourth disease waves, Kyoto, Japan\*

| Variables   | Third wave        |  | Fourth wave    |
|---|-------------------|--|----------------|
|   | 2020 Dec–2021 Feb |  | 2021 Apr–May   |
| Total no. cases (mean no./d)                        | 4,592 (51.0)      |  | 4,181 (68.5)   |
| Total no. (%) secondary cases among households      | 1,228 (26.7)      |  | 1,208 (28.9)   |
| Total no. (%) cases associated with clusters        | 849 (18.5)        |  | 449 (10.7)     |
| Median no. cases associated with each cluster (IQR) | 11 (9–20.5)       |  | 7 (6–9)        |
| Total no. clusters (mean no./day)                   | 50 (0.56)         |  | 43 (0.70)      |
| Median test positivity of each cluster, % (IQR)†    | 18 (9.7–37)       |  | 34 (15.6–66.3) |

\*IQR, interquartile range.

†Calculated by using epidemiologic data available for 48 clusters in the third wave and 35 clusters in the fourth wave.

and the median household size was 4 persons. Contacts had RT-PCR testing a median of 6 (IQR 4–7) days after the index case was tested. Comparing lineages, we did not note statistically significant differences in the household size, age, or sex of the index cases and their contacts. We were able to determine lineages for 63 households with  $\geq 2$  (maximum of 5) members, and the lineages among each member were concordant in all households. The observed SAR in households with Alpha (62.4%) was higher than in households with B.1.1.214 (53.9%) (Table 4). In addition to differences between lineages, the observed SAR in each category was higher among adult (persons 19–59 years of age) index case-patients, elderly (persons  $\geq 60$  years of age) contacts, symptomatic index cases, and small household sizes (2–3 members) (Table 4). A risk factor analysis conducted by using a generalized linear mixed-effects model found that index case symptoms (adjusted odds ratio [aOR] 2.84, 95% CI 1.49–5.42;  $p < 0.01$ ) and Alpha lineage (aOR 1.52, 95% CI 1.06–2.18;  $p = 0.02$ ) were significantly associated with household transmission (Table 4). Persons living in households of  $\geq 4$  members were at a lower risk for transmission. All model-predicted SARs were similar to the observed SARs, indicating the model was valid.

We performed a phylogenetic analysis of 135 Alpha and 143 B.1.1.214 genomes obtained from all 206 households (Appendix 2 Figure). Among these genomes, 127 were obtained from  $\geq 2$  household members. The average number of single-nucleotide polymorphism (SNP) differences among genomes from each household was smaller than SNP differences among other genomes in the corresponding lineage. B.1.1.214 genomes had a median of 0 (range 0–10) SNP differences among household members versus 14.3 SNPs from genomes outside the household, and B.1.1.7 genomes had a median of 0.7 (range 0–5) SNP differences within households versus 6.6 SNPs from genomes outside the household.

## Discussion

Kyoto and Japan experienced 4 waves of COVID-19 and the prevalent lineages in Kyoto's 4 waves were

similar to those in Japan (Figure 2). Before the first wave (January–March 2020), SARS-CoV-2 lineages A and B, which caused the initial outbreak in China, were introduced to Japan, then lineage B.1 or B.1.1 was introduced from Europe (15). The B.1 derivatives have a spike protein D614G mutation, resulting in increased transmissibility (16); this mutation subsequently resulted in worldwide spread and replacement of other existing lineages (17). The first wave in Japan was characterized by B.1/B.1.1 and its derivatives, which evolved and spread domestically (15). Among these lineages, B.1.48 was a domestic lineage that has not been reported outside Japan. The B.1.48 lineage was the second most common lineage in Kyoto and had a higher prevalence in that city than in Japan overall. This finding suggests a local outbreak, although the sample size during the first wave in Kyoto was limited. The second and third waves were caused by 2 domestic B.1 derivatives, B.1.1.284 in the second wave and B.1.1.214 in the third wave (18). These lineages did not harbor mutations in the spike protein, and explanations for lineage replacement are lacking.

**Table 3.** Characteristics of 206 households whose members were infected with SARS-CoV-2 B.1.1.214 or Alpha variants, Kyoto, Japan, November 2020–May 2021\*

| Variables              | Alpha      | Non-VOC    | p value |
|------------------------|------------|------------|---------|
| No. households         | 106        | 100        |         |
| Median household size  | 3          | 4          |         |
| IQR                    | 3–4        | 3–4        | 0.19    |
| Range                  | 2–10       | 2–9        |         |
| No. index cases        | 106        | 100        |         |
| Median age, y          | 38         | 47.5       |         |
| IQR                    | 23–56      | 27.75–58   | 0.12    |
| Range                  | 5–93       | 7–91       |         |
| Sex, no. (%)           |            |            |         |
| M                      | 73 (68.9)  | 70 (70.0)  | 0.95    |
| F                      | 33 (31.1)  | 30 (30.0)  |         |
| No. household contacts | 282        | 282        |         |
| Median age, y          | 35.5       | 35.5       |         |
| IQR                    | 13–53      | 16–52      | 0.96    |
| Range                  | 0–90       | 1–95       |         |
| Sex, no. (%)           |            |            |         |
| M                      | 129 (45.7) | 130 (46.1) | 0.90    |
| F                      | 153 (54.3) | 152 (53.9) |         |

\*Alpha variant B.1.1.7 or non-VOC B.1.1.214. IQR, interquartile range; VOC, variant of concern.

**Table 4.** Secondary attack rates and risk factors for SARS-CoV-2 infection in 206 households whose members were infected with SARS-CoV-2 B.1.1.214 or Alpha variants, Kyoto, Japan, November 2020–May 2021\*

| Variables               | No. contacts | No. infected | Secondary attack rate, % |                  | Adjusted odds ratio (95% CI)† | p value† |
|-------------------------|--------------|--------------|--------------------------|------------------|-------------------------------|----------|
|                         |              |              | Observed                 | Predicted (IQR)† |                               |          |
| Overall                 | 564          | 328          | 58.2                     | 58.1 (46.5–71.1) | NA                            | NA       |
| Index case age group, y |              |              |                          |                  |                               |          |
| ≤18                     | 57           | 23           | 40.4                     | 40.4 (28.3–49.8) | 0.67 (0.35–1.28)              | 0.22     |
| 19–59                   | 419          | 256          | 61.1                     | 61.1 (51.7–70.9) | Referent                      |          |
| ≥60                     | 88           | 49           | 55.7                     | 55.5 (44.9–64.0) | 0.73 (0.44–1.22)              | 0.23     |
| Contacts age group, y   |              |              |                          |                  |                               |          |
| ≤18                     | 167          | 82           | 49.1                     | 49.1 (37.3–61.9) | 0.72 (0.48–1.07)              | 0.10     |
| 19–59                   | 344          | 208          | 60.5                     | 60.4 (52.7–70.9) | Referent                      |          |
| ≥60                     | 53           | 38           | 71.7                     | 71.9 (66.0–81.0) | 1.75 (0.89–3.42)              | 0.10     |
| Index case symptoms     |              |              |                          |                  |                               |          |
| Asymptomatic            | 58           | 19           | 32.8                     | 32.7 (24.1–43.4) | Referent                      |          |
| Symptomatic             | 506          | 309          | 61.1                     | 61.1 (51.7–70.9) | 2.84 (1.49–5.42)              | <0.01    |
| Household size          |              |              |                          |                  |                               |          |
| 2–3                     | 171          | 123          | 71.9                     | 71.9 (70.9–78.7) | Referent                      |          |
| 4                       | 189          | 112          | 59.3                     | 59.3 (52.0–69.3) | 0.61 (0.38–0.97)              | 0.04     |
| 5                       | 100          | 43           | 43.0                     | 42.9 (37.3–47.5) | 0.34 (0.20–0.58)              | <0.01    |
| ≥6                      | 104          | 50           | 48.1                     | 48.0 (44.4–55.3) | 0.46 (0.26–0.79)              | <0.01    |
| SARS-CoV-2 lineage      |              |              |                          |                  |                               |          |
| Non-VOC, B.1.1.214      | 282          | 152          | 53.9                     | 54.0 (44.9–64.0) | Referent                      |          |
| Alpha, B.1.1.7          | 282          | 176          | 62.4                     | 62.3 (55.3–72.7) | 1.52 (1.06–2.18)              | 0.02     |

\*IQR, interquartile range; NA, not applicable; VOC, variant of concern.

†Calculated by using a generalized linear mixed-effects logistic regression model.

Between the third and fourth waves, during March 2021, the R.1 lineage, which was predominantly found in the United States, replaced B.1.1.214 in Kyoto and in Japan. R.1 harbors the spike protein mutation E484K, which is associated with immune escape and an increased reproduction number (19). The global origin of R.1 currently is unknown, but it was possibly imported from a country where the presumptive ancestor of B.1.1.316 was circulating (18). R.1 was replaced by the Alpha variant, which was responsible for the fourth COVID-19 wave in Japan. The Alpha variant was first detected in England and caused a global pandemic because of its higher transmissibility (8,20).

Genomic sequencing to detect variants has been performed worldwide at an unprecedented rate, but the coverage of samples is still biased toward regions and countries with high testing and sequencing capacity (21). In Japan, genome sequencing is performed under governmental leadership in national or regional infectious disease laboratories or large-scale private laboratories. By June 28, 2021, ≈7% of SARS-CoV-2–positive samples had been analyzed (22). We determined the genomes of 20% of cases in Kyoto through a collaboration between the local health department and a university hospital. In addition to genomic surveillance, the collaboration included mass PCR testing needed for epidemiologic investigations, mass screening for SARS-CoV-2 antibodies among essential workers, and establishing COVID-19 infection control programs targeting

small-scale hospitals and facilities for elderly or disabled persons.

With the all-case investigation strategy, we were able to test 87.1% of case-contacts. By contrast, data from US public health authorities reported that 59% of US cases had been investigated, 71% of contacts were notified, and only 14.1%–54.7% of contacts had been tested (23). We found the RT-PCR test positivity rate of contacts in Kyoto was the highest among household members (24.9%). In addition, the positivity rate among family members living separately was 14.5%, which was similar to the average in the general population (15.1%), indicating that households were the main transmission venues during the third COVID-19 wave in Kyoto (Table 1). The importance of RT-PCR testing of close contacts was confirmed by the higher test positivity rate (15.1%) among close contacts than among the general population (5.9%).

The incidence of clusters was higher during the fourth wave than the third wave in Kyoto (Table 2). However, the frequency of cluster-associated cases and the number of cases per cluster was lower in the fourth wave. Clusters occurred in hospitals and LTCFs and were related to inappropriate use of personal protective equipment (3). Clusters also were reported from other congregate settings, such as house parties, homeless shelters, and food processing facilities (24). As described, we interceded in hospitals and adult daycare and LTCFs to improve infection prevention measures, which might have contributed to

the decreased incidence of clusters and numbers of cases per cluster in those settings.

Two doses of a COVID-19 vaccine (BNT162b2 [Pfizer-BioNTech, <https://www.pfizer.com>] or mRNA-1273 [Moderna, <https://www.moderna.com>]) are highly effective against the Alpha variant and non-VOCs (25). Japan designated healthcare workers as a vaccine priority group and began a vaccination program for them on May 2021; vaccination for residents of LTCFs began in March 2021. By the end of May 2021, 12.2% of Kyoto citizens had received  $\geq 1$  dose of a vaccine, and 3.2% had received 2 doses. These vaccination data suggest that vaccination might be associated with the reduction in cluster-associated cases but might not be associated with the number of overall cases during the fourth wave.

Household secondary cases accounted for 26.7%–28.9% of all COVID-19 cases in Kyoto, and these rates increased during the fourth wave compared with the third wave. Similarly, a study conducted in Canada at the beginning of the pandemic (January–July 2020) reported a 20.5% rate of household secondary cases (5). During the third and fourth COVID-19 waves in Kyoto, the city declared a state of emergency and residents were advised to stay at home. This stay-at-home recommendation might have contributed to the suppression of community spread but also might be associated with the increased rates of household transmission. A modeling study in China estimated that 51.5% of infections occurred in households during the first outbreak, and this number increased to 69.8% after quarantine (7). During lockdown in the United States, household transmission was estimated to increase 25%–50% (26).

The SARs we found in Kyoto were higher than other reported SARs, probably reflecting differences in lineages, transmission opportunities, and case investigation strategies. We assumed a very low possibility of transmission from outside the household during quarantine because public health centers issued a strong request for citizens to stay home. Data from 10 prefectures of Japan, not including Kyoto, reported a 19.0% SAR during the first wave, in which imported and cluster-associated cases were the main sources of transmission, but we noted a 53.9% SAR for B.1.1.214 in this study (Table 4). Those data were mostly generated from cases during the third wave, during which household transmission increased because of the state of emergency and prevalence of different lineages with potentially superior transmissibility. A meta-analysis of worldwide data estimated that SARs increased over time from 13.4%

during January–February 2020 to 31.1% during July 2020–March 2021 and that these increases might be associated with the spread of variants with increased transmissibility (27). That report also noted SARs as high as 24.5% (range 10.9%–46.2%) for Alpha variants (27). In our cohort, household infection with Alpha clearly was associated with an increased SAR of 62.4% and a higher risk for transmission with an aOR of 1.52 (Table 4), which probably contributed to the larger number of household secondary cases during the fourth wave (Table 2). Delta variants are associated with a higher risk for household transmission than Alpha variants and have an aOR of 1.70 (28), which implies a further increase in SAR and effects of household transmission. Vaccination lowers the risk for household transmission of VOCs and can be a vital strategy for reducing infections (28,29). However, the Delta and Omicron VOCs that emerged after Alpha have the potential for immune escape; observational studies suggest that vaccine effectiveness against Delta was lower than for Alpha (30) and that effectiveness against Omicron is further lower than that for Delta (31). In addition, postvaccine immunity could wane over time (25,31). Proposed booster doses could improve vaccine effectiveness, even against Delta and Omicron variants (25,32). Improved vaccination programs that include booster doses and evaluation studies of vaccine effectiveness in households could help reduce household transmissions.

In addition to VOCs, the risk factors for household transmission include age, fewer household members, contact frequency, and symptomatic index cases (5,14,33–35). Our results are consistent with previous reports that show a lower risk for persons  $\leq 18$  years of age to be index cases and higher risk for transmission among adult contacts, small households, and symptomatic index cases (5,14,33–35) (Table 4). In an outbreak in China, interventions targeting households, mass isolation of patients, quarantine of household contacts, and movement restriction policies succeeded in reducing the reproduction number of index cases by 52% and secondary cases by 63% (35). Public health interventions targeting households, such as public health messaging, self-quarantine at home (35), and promoting isolation facility use (5), appear to be effective strategies for reducing the number of COVID-19 cases.

The strengths of this study include a high coverage of epidemiologic investigations, which were supported by a high proportion of testing among close contacts and cluster-associated contacts, as well as genomic surveillance. The first limitation of

the study is that differences among the study periods in the analyses of the cases and contacts (Tables 1–4) should be noted when interpreting and generalizing the results in combination. Second, we could not perform risk factor analyses for RT-PCR test positivity among close contacts and those of the cluster-associated cases because of the absence of detailed epidemiologic data, including clinical symptoms, vaccination status, infection prevention measures, and RT-PCR testing delays. Thus, the effects of different variants on close contact categories other than households and on cluster-associated cases were not elucidated.

In conclusion, this study elucidates the epidemiologic characteristics of COVID-19 patients and their contacts in Kyoto, Japan, and highlights the role of household transmission, as enhanced by the Alpha variant, by using viral genomic analysis. In addition to current epidemiologic investigation efforts, including contact tracing, strengthening interventions that target household are needed for infection control. Continued collaboration between public health departments and academia can accurately illuminate the epidemiology of COVID-19 and whether emerging VOCs have higher transmissibility.

### Acknowledgments

We thank Kaori Ishizaki, Kazuki Kitamura, Shoichi Nakai, Eiki Kure, Yosuke Kumano, and Mizuki Mori for their technical assistance.

This research was supported by the COVID-19 Private Fund to the Shinya Yamanaka laboratory, CiRA, Kyoto University.

Y.M. is the guarantor of this work and, as such, had full access to all the data in the study and takes responsibility for the integrity of the data and the accuracy of the data analysis. Y.M. and M.N. conceived and designed the study. All authors contributed materials and data collection. Y.M. performed the experiments and analyzed the data. Y.M. and M.N. drafted the manuscript, and all authors reviewed and approved the final version of the manuscript.

### About the Author

Dr. Matsumura is an associate professor at the Department of Clinical Laboratory Medicine, Kyoto University Graduate School of Medicine, Kyoto, Japan. His main research interests include molecular diagnostics for SARS-CoV-2 and clinical treatment for and molecular epidemiology of antimicrobial drug resistance mechanisms among gram-negative bacteria.

### References

1. World Health Organization. Contact tracing in the context of COVID-19: interim guidance, 1 February 2021 [cited 2022 Feb 21]. <https://apps.who.int/iris/handle/10665/339128>
2. Oshitani H; Expert Members of The National COVID-19 Cluster Taskforce at The Ministry of Health, Labour and Welfare, Japan. Cluster-based approach to coronavirus disease 2019 (COVID-19) response in Japan, from February to April 2020. *Jpn J Infect Dis.* 2020;73:491–3. <https://doi.org/10.7883/yoken.JJID.2020.363>
3. Furuse Y, Sando E, Tsuchiya N, Miyahara R, Yasuda I, Ko YK, et al. Clusters of coronavirus disease in communities, Japan, January–April 2020. *Emerg Infect Dis.* 2020;26:2176–9. <https://doi.org/10.3201/eid2609.202272>
4. World Health Organization. Report of the WHO–China joint mission on coronavirus disease 2019 (COVID-19) [cited 2022 Feb 21]. [https://www.who.int/publications/i/item/report-of-the-who-china-joint-mission-on-coronavirus-disease-2019-\(covid-19\)](https://www.who.int/publications/i/item/report-of-the-who-china-joint-mission-on-coronavirus-disease-2019-(covid-19))
5. Paul LA, Daneman N, Schwartz KL, Science M, Brown KA, Whelan M, et al. Association of age and pediatric household transmission of SARS-CoV-2 infection. *JAMA Pediatr.* 2021;175:1151–8. <https://doi.org/10.1001/jamapediatrics.2021.2770>
6. Madewell ZJ, Yang Y, Longini IM Jr, Halloran ME, Dean NE. Household transmission of SARS-CoV-2: a systematic review and meta-analysis. *JAMA Netw Open.* 2020;3:e2031756. <https://doi.org/10.1001/jamanetworkopen.2020.31756>
7. Shen M, Peng Z, Guo Y, Rong L, Li Y, Xiao Y, et al. Assessing the effects of metropolitan-wide quarantine on the spread of COVID-19 in public space and households. *Int J Infect Dis.* 2020;96:503–5. <https://doi.org/10.1016/j.ijid.2020.05.019>
8. Davies NG, Abbott S, Barnard RC, Jarvis CI, Kucharski AJ, Munday JD, et al.; CMMID COVID-19 Working Group; COVID-19 Genomics UK (COG-UK) Consortium. Estimated transmissibility and impact of SARS-CoV-2 lineage B.1.1.7 in England. *Science.* 2021;372:eabg3055. <https://doi.org/10.1126/science.abg3055>
9. National Institute of Infectious Diseases. Manual for active epidemiological surveillance of patients with novel coronavirus infection (provisional version) [cited 2022 Apr 11]. <https://www.niid.go.jp/niid/images/epi/corona/2019nCoV-02-200227-en.pdf>
10. Kyoto City. COVID-19 latest information [in Japanese] [cited 2022 Apr 11]. <https://www.city.kyoto.lg.jp/hokenfukushi/page/0000268303.html>
11. Ministry of Health, Labour and Welfare. Situation report on COVID-19 [cited 2022 Apr 11]. [https://www.mhlw.go.jp/stf/covid-19/kokunainohasseijoukyou\\_00006.html](https://www.mhlw.go.jp/stf/covid-19/kokunainohasseijoukyou_00006.html)
12. Rambaut A, Holmes EC, O’Toole Á, Hill V, McCrone JT, Ruis C, et al. A dynamic nomenclature proposal for SARS-CoV-2 lineages to assist genomic epidemiology. *Nat Microbiol.* 2020;5:1403–7. <https://doi.org/10.1038/s41564-020-0770-5>
13. World Health Organization. Tracking SARS-CoV-2 variants [cited 2022 Apr 11]. <https://www.who.int/en/activities/tracking-SARS-CoV-2-variants>
14. Stich M, Elling R, Renk H, Janda A, Garbade SF, Müller B, et al. Transmission of severe acute respiratory syndrome coronavirus 2 in households with children, southwest Germany, May–August 2020. *Emerg Infect Dis.* 2021;27:3009–19. <https://doi.org/10.3201/eid2712.210978>
15. Sekizuka T, Itokawa K, Hashino M, Kawano-Sugaya T, Tanaka R, Yatsu K, et al. A genome epidemiological study of SARS-CoV-2 introduction into Japan. *MSphere.* 2020;5:e00786–20. <https://doi.org/10.1128/mSphere.00786-20>

16. Zhou B, Thao TTN, Hoffmann D, Taddeo A, Ebert N, Labrousseau F, et al. SARS-CoV-2 spike D614G change enhances replication and transmission. *Nature*. 2021;592:122–7. <https://doi.org/10.1038/s41586-021-03361-1>
17. Chen Z, Chong KC, Wong MCS, Boon SS, Huang J, Wang MH, et al. A global analysis of replacement of genetic variants of SARS-CoV-2 in association with containment capacity and changes in disease severity. *Clin Microbiol Infect*. 2021;27:750–7. <https://doi.org/10.1016/j.cmi.2021.01.018>
18. Sekizuka T, Itokawa K, Hashino M, Okubo K, Ohnishi A, Goto K, et al.; Virus Diagnosis Group (NIID Toyama); COVID-19 Genomic Surveillance Network in Japan (COG-JP). A discernable increase in the severe acute respiratory syndrome coronavirus 2 R.1 lineage carrying an E484K spike protein mutation in Japan. *Infect Genet Evol*. 2021;94:105013. <https://doi.org/10.1016/j.meegid.2021.105013>
19. Ito K, Piantam C, Nishiura H. Predicted dominance of variant Delta of SARS-CoV-2 before Tokyo Olympic Games, Japan, July 2021. *Euro Surveill*. 2021;26:2100570. <https://doi.org/10.2807/1560-7917.ES.2021.26.27.2100570>
20. Campbell F, Archer B, Laurenson-Schafer H, Jinnai Y, Konings F, Batra N, et al. Increased transmissibility and global spread of SARS-CoV-2 variants of concern as at June 2021. *Euro Surveill*. 2021;26:2100509. <https://doi.org/10.2807/1560-7917.ES.2021.26.24.2100509>
21. Oude Munnink BB, Worp N, Nieuwenhuijse DF, Sikkema RS, Haagmans B, Fouchier RAM, et al. The next phase of SARS-CoV-2 surveillance: real-time molecular epidemiology. *Nat Med*. 2021;27:1518–24. <https://doi.org/10.1038/s41591-021-01472-w>
22. Ministry of Health, Labour and Welfare. Materials of COVID-19 measures advisory board [in Japanese]. [https://www.mhlw.go.jp/stf/seisakunitsuite/bunya/0000121431\\_00256.html](https://www.mhlw.go.jp/stf/seisakunitsuite/bunya/0000121431_00256.html)
23. Lash RR, Moonan PK, Byers BL, Bonacci RA, Bonner KE, Donahue M, et al.; COVID-19 Contact Tracing Assessment Team. COVID-19 case investigation and contact tracing in the US, 2020. *JAMA Netw Open*. 2021;4:e2115850. <https://doi.org/10.1001/jamanetworkopen.2021.15850>
24. Liu T, Gong D, Xiao J, Hu J, He G, Rong Z, et al. Cluster infections play important roles in the rapid evolution of COVID-19 transmission: a systematic review. *Int J Infect Dis*. 2020;99:374–80. <https://doi.org/10.1016/j.ijid.2020.07.073>
25. Fiolet T, Kherabi Y, MacDonald CJ, Ghosn J, Peiffer-Smadja N. Comparing COVID-19 vaccines for their characteristics, efficacy and effectiveness against SARS-CoV-2 and variants of concern: a narrative review. *Clin Microbiol Infect*. 2022;28:202–21. <https://doi.org/10.1016/j.cmi.2021.10.005>
26. Curmei M, Ilyas A, Evans O, Steinhart J. Constructing and adjusting estimates for household transmission of SARS-CoV-2 from prior studies, widespread-testing and contact-tracing data. *Int J Epidemiol*. 2021;50:1444–57. <https://doi.org/10.1093/ije/dyab108>
27. Madewell ZJ, Yang Y, Longini IM Jr, Halloran ME, Dean NE. Factors associated with household transmission of SARS-CoV-2: an updated systematic review and meta-analysis. *JAMA Netw Open*. 2021;4:e2122240. <https://doi.org/10.1001/jamanetworkopen.2021.22240>
28. Allen H, Vusirikala A, Flannagan J, Twohig KA, Zaidi A, Chudasama D, et al.; COVID-19 Genomics UK (COG-UK Consortium). Household transmission of COVID-19 cases associated with SARS-CoV-2 delta variant (B.1.617.2): national case-control study. *Lancet Reg Health Eur*. 2022;12:100252. <https://doi.org/10.1016/j.lanpe.2021.100252>
29. Harris RJ, Hall JA, Zaidi A, Andrews NJ, Dunbar JK, Dabrera G. Effect of vaccination on household transmission of SARS-CoV-2 in England. *N Engl J Med*. 2021;385:759–60. <https://doi.org/10.1056/NEJMc2107717>
30. Lopez Bernal J, Andrews N, Gower C, Gallagher E, Simmons R, Thelwall S, et al. Effectiveness of Covid-19 vaccines against the B.1.617.2 (Delta) variant. *N Engl J Med*. 2021;385:585–94. <https://doi.org/10.1056/NEJMoa2108891>
31. Tseng HF, Ackerson BK, Luo Y, Sy LS, Talarico CA, Tian Y, et al. Effectiveness of mRNA-1273 against SARS-CoV-2 Omicron and Delta variants. *Nat Med*. 2022;28:1063–71. <https://doi.org/10.1038/s41591-022-01753-y>
32. Accorsi EK, Britton A, Fleming-Dutra KE, Smith ZR, Shang N, Derado G, et al. Association between 3 doses of mRNA COVID-19 vaccine and symptomatic infection caused by the SARS-CoV-2 Omicron and Delta variants. *JAMA*. 2022;327:639–51. <https://doi.org/10.1001/jama.2022.0470>
33. Rosenberg ES, Dufort EM, Blog DS, Hall EW, Hoefler D, Backenson BP, et al.; New York State Coronavirus 2019 Response Team. COVID-19 testing, epidemic features, hospital outcomes, and household prevalence, New York State – March 2020. *Clin Infect Dis*. 2020;71:1953–9. <https://doi.org/10.1093/cid/ciaa549>
34. Wu J, Huang Y, Tu C, Bi C, Chen Z, Luo L, et al. Household transmission of SARS-CoV-2, Zhuhai, China, 2020. *Clin Infect Dis*. 2020;71:2099–108. <https://doi.org/10.1093/cid/ciaa557>
35. Li F, Li YY, Liu MJ, Fang LQ, Dean NE, Wong GWK, et al. Household transmission of SARS-CoV-2 and risk factors for susceptibility and infectivity in Wuhan: a retrospective observational study. *Lancet Infect Dis*. 2021;21:617–28. [https://doi.org/10.1016/S1473-3099\(20\)30981-6](https://doi.org/10.1016/S1473-3099(20)30981-6)

---

Address for correspondence: Yasufumi Matsumura, Department of Clinical Laboratory Medicine, Kyoto University Graduate School of Medicine, 54 Shogoin-Kawahara-cho, Sakyo-ku, Kyoto 606-8507, Japan; email: yazblood@kuhp.kyoto-u.ac.jp

# Dominant Carbapenemase-Encoding Plasmids in Clinical Enterobacterales Isolates and Hypervirulent *Klebsiella pneumoniae*, Singapore

Melvin Yong, Yahua Chen, Guodong Oo, Kai Ching Chang, Wilson H.W. Chu, Jeanette Teo, Indumathi Venkatachalam, Natascha May Thevasagayam, Prakki S. Rama Sridatta, Vanessa Koh, Andrés E. Marcoleta, Hanrong Chen, Niranjan Nagarajan, Marimuthu Kalisvar, Oon Tek Ng, Yunn-Hwen Gan

Dissemination of carbapenemase-encoding plasmids by horizontal gene transfer in multidrug-resistant bacteria is the major driver of rising carbapenem-resistance, but the conjugative mechanics and evolution of clinically relevant plasmids are not yet clear. We performed whole-genome sequencing on 1,215 clinical Enterobacterales isolates collected in Singapore during 2010–2015. We identified 1,126 carbapenemase-encoding plasmids and discovered pKPC2 is becoming the dominant plasmid in Singapore, overtaking an earlier dominant plasmid, pNDM1. pKPC2 frequently conjugates with many Enterobacterales species, including hypervirulent *Klebsiella pneumoniae*, and maintains stability in vitro without selection pressure and minimal adaptive sequence changes. Furthermore, capsule and decreasing taxonomic relatedness between donor and recipient pairs are greater conjugation barriers for pNDM1 than pKPC2. The low fitness costs pKPC2 exerts in Enterobacterales species indicate previously undetected carriage selection in other ecological settings. The ease of conjugation and stability of pKPC2 in hypervirulent *K. pneumoniae* could fuel spread into the community.

Author affiliations: National University of Singapore, Singapore (M. Yong, Y. Chen, G. Oo, K.C. Chang, W.H.W. Chu, N. Nagarajan, M. Kalisvar, Y.-H. Gan); National University Hospital, Singapore (J. Teo); Singapore General Hospital, Singapore (I. Venkatachalam); National Centre for Infectious Diseases, Singapore (N.M. Thevasagayam, P.S.R. Sridatta, V. Koh, M. Kalisvar, O.T. Ng); Tan Tock Seng Hospital, Singapore (V. Koh, M. Kalisvar, O.T. Ng); Universidad de Chile, Santiago, Chile (A.E. Marcoleta); Genome Institute of Singapore, Singapore (H. Chen, N. Nagarajan); Nanyang Technological University, Singapore (O.T. Ng)

DOI: <https://doi.org/10.3201/eid2808.212542>

The global rise of carbapenem-resistant Enterobacterales (CRE) infections is posing a grave challenge to hospital systems worldwide (1). Carbapenemase genes usually are located on plasmids that can transmit vertically along clonal lineages and horizontally between different strains and species (2). However, the principles governing the transmission of carbapenemase-encoding plasmids in clinically relevant settings are complex and dynamic. Plasmid properties, donor, recipient, and ecologic factors all affect transmission (3,4).

Previously, we found a 71,861-bp pKPC2 plasmid, pKPC2\_sg1 (GenBank accession no. MN542377), in all 18 carbapenem-resistant hypervirulent *Klebsiella pneumoniae* isolates available in the Carbapenemase-Producing Enterobacteriaceae in Singapore (CaPES) collection (5,6). (Enterobacteriaceae is the former name of Enterobacterales.) The plasmid sequence was stable and unchanged after moving into different bacterial hosts or when maintained in human hosts for >200 days. This discovery prompted questions about the extent of pKPC2\_sg1 dominance in clinical settings in Singapore, and its transmissibility and stability in hypervirulent *K. pneumoniae*. Using >1,000 CRE isolates collected from the 6 public hospitals in Singapore during 2010–2015, a subset of which was previously described (6), we examined the distribution of different carbapenem-encoding plasmids to investigate the dynamics and dominance of pKPC2.

## Materials and Methods

### Bacterial Strains, Growth Conditions, and Plasmids

We analyzed 1,215 CRE isolates for carbapenemase plasmids distribution (Appendix 1 Table,

<https://wwwnc.cdc.gov/EID/article/28/8/21-2542-App1.xlsx>). We have included information on modified and unmodified plasmids, bacterial mutant generation and the Enterobacterales strains (Appendix 2, <https://wwwnc.cdc.gov/EID/article/28/8/21-2542-App2.pdf>). Unless otherwise specified, we grew strains on Lennox L Agar lysogeny agar (LA) (Invitrogen-ThermoFisher, <https://www.thermo-fisher.com>) at 37°C overnight before the assays.

### Whole-Genome Sequencing

We performed whole-genome sequencing (WGS) by using the MiSeq platform (Illumina, <https://www.illumina.com>) and the GridION X5 system (Oxford Nanopore Technologies, <https://nanoporetech.com>). To assemble genomes, we used SPAdes Genome Assembler version 3.11.1 (7) and Unicycler version 0.4.8 (8). For bacterial species assignment, we performed multilocus sequence typing (MLST) by using Bacterial Isolate Genome Sequence Database version 2.8 (9) or the Center for Genomic Epidemiology Bacterial Analysis Pipeline (<https://www.genomepidemiology.org>) and Kraken (10). We identified antimicrobial resistance genes in CRE isolates by using Abricate version 1.0.1 (11) and the National Center for Biotechnology Information (NCBI) Bacterial Antimicrobial Resistance Reference Gene Database (12). We identified virulence genes by using the Virulence Factor Database (13) (Appendix 2).

### Plasmid Annotation and Analysis

We analyzed the pKPC2 sequence (GenBank accession no. MN542377) by using GeneMarkS (14) to acquire a list of predicted protein sequences and subjected sequences to blastp (14). We used blastp results to annotate genes on the plasmid, which we drew by using the BLAST Ring Image Generator (15). We also analyzed the plasmid sequence by using Plasmid-Finder version 2.1 (16,17).

### Replicon Analysis

We used *EcoRI* and *BamHI* restriction enzymes to double digest pKPC2 DNA for 1 hour at 37°C, then ligated the fragments to the pR6K plasmid by using T4 DNA Ligase (Promega, <https://www.promega.com>). We then used *Escherichia coli* Stellar HST08 Competent Cells (TaKaRa Bio, Inc., <http://www.takara-bio.com>) to introduce fragments through heat shock, and selected the transformants on LA with kanamycin (50 µg/mL). However, pR6K cannot replicate in HST08 cells because the R6K replicon protein must be provided in trans via lambda *pir*. Only pR6K with ligated fragments carrying a functional replicon can replicate.

We harvested plasmids from the selected clones and submitted these to 1st BASE (<https://base-asia.com>) for Sanger sequencing to determine the inserts. We performed phylogenetic analysis on the identified *trfA* replicon by using ClustalW (<https://www.clustal.org>) and the maximum-likelihood method in MEGA-X version 10.2.6 (18).

### Bacterial Growth Assay

We streaked bacterial strains on LA containing antimicrobial drugs for various plasmids: 256 µg/mL erythromycin for pKPC2; 0.5 µg/mL meropenem for pNDM1; and 50 µg/mL kanamycin for pKPC2<sup>KmR</sup> or pNDM1<sup>KmR</sup>. We incubated plates at 37°C overnight, then inoculated colonies into Lennox L Broth Base lysogeny broth (LB; Invitrogen-ThermoFisher) containing the same antimicrobial drugs and placed in a shaking incubator set at 37°C and 150 rpm overnight. We measured the optical density at 600 nm (optical density 600) of overnight bacterial culture and recorded the reading before diluting it to 0.001. We added 200 µL of diluted cultures to a 96-well plate and placed these on a Synergy H1 plate reader (BioTek, <https://www.biotek.com>) at 37°C. We measured absorbance at optical density 600 hourly for 24 hours.

### Conjugation Experiments

We performed conjugation on 0.22 µm Cellulose Nitrate Filter (Sartorius, <https://www.sartorius.com>) nitrocellulose membranes using a 1:1 ratio of donor to recipient strains on LA. We measured plasmid transfer kinetics from *E. coli* MG1655 at various timepoints up to 4 hours at 37°C. We selected recipient strains on LA; *E. coli* SLC-568 with 50 µg/mL kanamycin or *K. pneumoniae* SGH10 with 40 µg/mL fosfomycin. We used the same antimicrobial drugs to select transconjugants on LA plus 256 µg/mL erythromycin for pKPC2 or 0.5 µg/mL meropenem for pNDM1. For conjugation assays of pKPC2<sup>KmR</sup> and pNDM1<sup>KmR</sup>, recipients carried pACYC184<sup>CmR</sup> for selection. We selected transconjugants on LA with 50 µg/mL chloramphenicol and 50 µg/mL kanamycin and selected recipients without kanamycin. For conjugation into hypervirulent *K. pneumoniae* recipients, we replaced chloramphenicol with 40 µg/mL fosfomycin. We measured conjugation frequency by dividing the number of transconjugants by the number of recipients.

### Plasmid Stability Assessment

We cultured strains in LB and 50 µg/mL kanamycin overnight, then subcultured every day by inoculating 4.88 µL of the culture into 5 mL of antimicrobial-free LB, as described (19). At generations 0, 30, 60, and 90,

we serially diluted bacterial cultures and plated on LA with and without 50 µg/mL kanamycin. We further subcultured selected bacterial strains to 300 generations and plated at generation 100, 200, and 300. We calculated plasmid stability as the number of antimicrobial-resistant bacteria per total bacterial count.

To test for plasmid incompatibility, we measured the stability of pKPC2<sup>KmR</sup> in *E. coli* MG1655 harboring both pKPC2<sup>KmR</sup> and pRK2-AraE as described (20), except we first grew the strain in LB with both 35 µg/mL gentamicin and 50 µg/mL kanamycin before subculturing for 100 generations in LB with 35 µg/mL gentamicin to select for pRK2-AraE. At every 10th generation, we plated the cultures on LA with 35 µg/mL gentamicin, and LA with 35 µg/mL gentamicin and 50 µg/mL kanamycin.

### Regression Analysis

To study the effect of taxonomic relatedness on pKPC2 and pNDM1 conjugation frequencies, we

applied a survival-analysis approach (21). We modeled the donor-recipient pair as a random effect to account for unobserved heterogeneity specific to each pair (Appendix 2).

### Results

#### Dominant Carbapenemase-Encoding Plasmid

From 1,312 CRE isolates (817 unique patients) submitted during September 2010–April 2015 as part of mandatory reporting to the National Public Health Laboratory, we successfully cultured, performed WGS on, and assembled genomes for 1,302 (99.2%) isolates. Of those, 1,251 (96.1%) identified bacterial species and carbapenemase genes were concordant with laboratory data (MIC >1 mg/L or disc diffusion zone diameter <23 mm for imipenem and meropenem) (6). We excluded 36 isolates because patient or date of culture information was missing; thus, we analyzed 1,215 (93.3%) isolates (Figure 1; Appendix

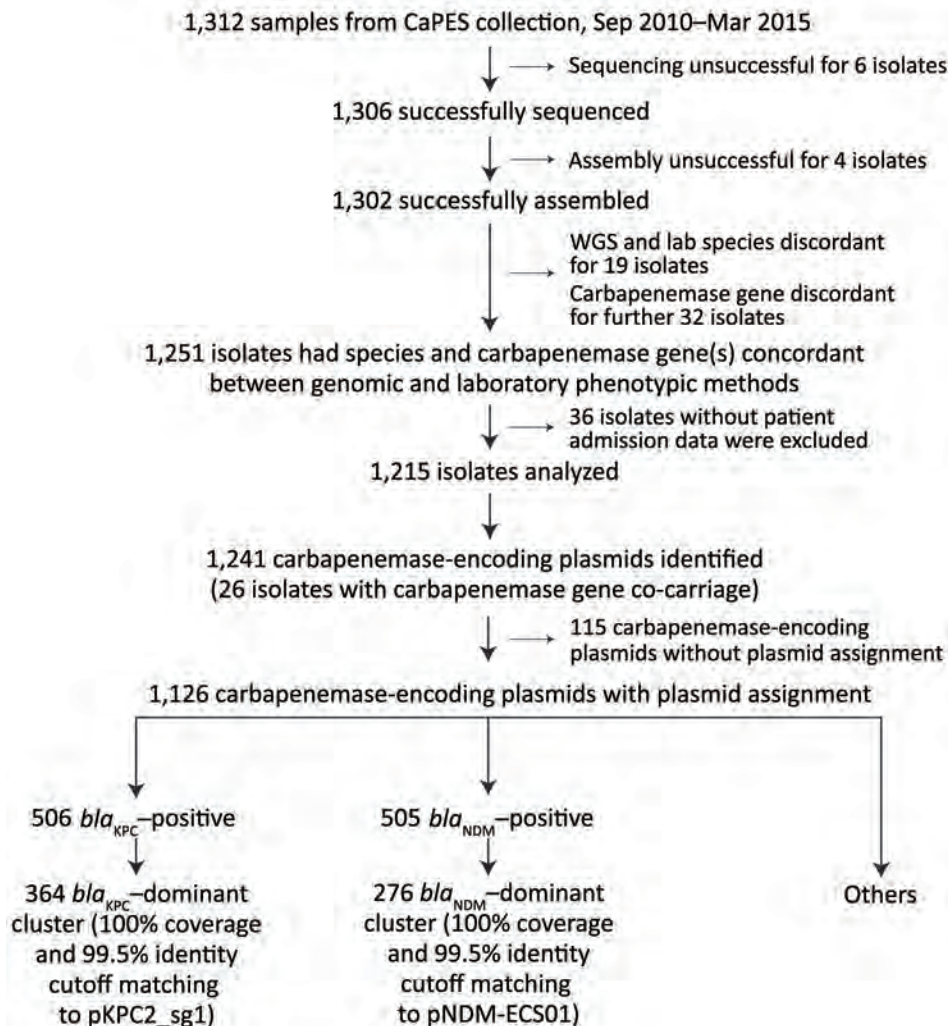


**Figure 1.** Flowchart of steps used for identifying dominant carbapenemase-encoding plasmids in clinical Enterobacteriales isolates and hypervirulent *Klebsiella pneumoniae*, Singapore. We collected 1,312 samples available in the CaPES collection and analyzed 1,215 whole-genome sequenced samples. We identified 2 dominant clusters with large numbers of carbapenemase-encoding plasmids; the *bla*<sub>KPC</sub>-dominant cluster comprised pKPC2 plasmids and the *bla*<sub>NDM</sub>-dominant cluster comprised pNDM1 plasmids. CaPES, Carbapenemase-Producing Enterobacteriaceae in Singapore (CaPES) (Enterobacteriaceae is the former name of Enterobacteriales); WGS, whole-genome sequencing.

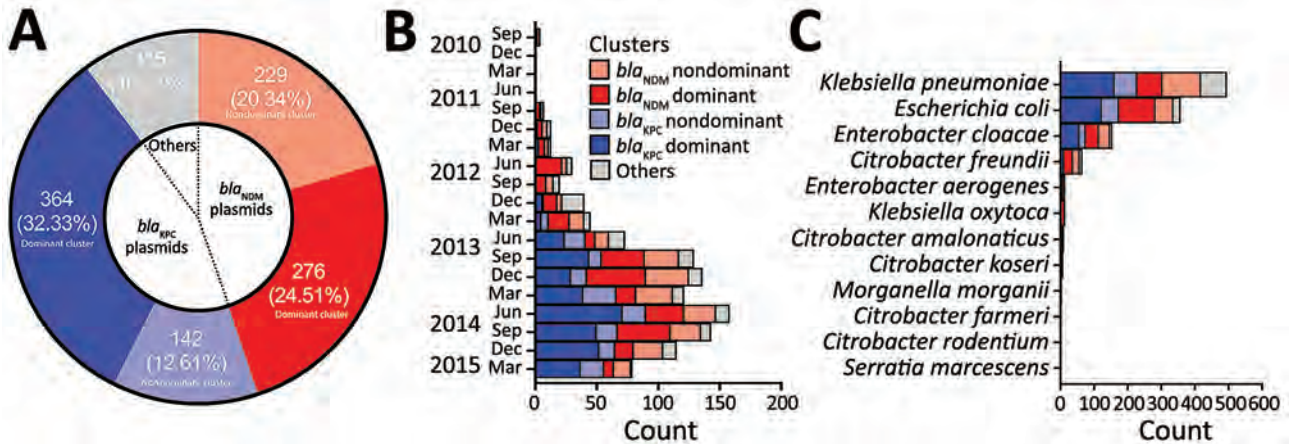


**Figure 2.** Percentage and distribution of dominant carbapenemase-encoding plasmids in clinical Enterobacteriales isolates and hypervirulent *Klebsiella pneumoniae*, Singapore. A) Percentage distribution of the total carbapenemase-encoding plasmids identified. The *bla*<sub>KPC</sub> dominant cluster refers to those harboring pKPC2 plasmid; *bla*<sub>NDM</sub> dominant cluster refers to those harboring pNDM1 plasmid. Others indicate carbapenemase-encoding plasmids that do not carry *bla*<sub>KPC</sub> or *bla*<sub>NDM</sub>. B, C) Distribution of carbapenemase-encoding plasmids identified among Carbapenemase-Producing Enterobacteriaceae in Singapore (CaPES) (Enterobacteriaceae is the former name of Enterobacteriales) samples collected during September 2010–March 2015 (B) and among Enterobacteriales isolates (C). Nondominant cluster refers to other plasmids carrying *bla*<sub>KPC</sub> or *bla*<sub>NDM</sub>. We found that pKPC2 was the most dominant carbapenemase-encoding plasmid in Singapore during 2010–2015.

1). We successfully identified 1,126 carbapenemase-encoding plasmids with assignments from the 1,215 isolates. We found 2 dominant carbapenemase-encoding plasmids: *bla*<sub>KPC</sub> ( $n = 506$ ; 44.94%) and *bla*<sub>NDM</sub> ( $n = 505$ ; 44.85%) (Figure 2, panel A). Among the 506 *bla*<sub>KPC</sub> plasmids, 364 (32.33%) were pKPC2 plasmids, which we termed the *bla*<sub>KPC</sub>-dominant cluster. Among the 505 *bla*<sub>NDM</sub> plasmids, 276 (24.51%) were pNDM1 plasmids, which we termed the *bla*<sub>NDM</sub>-dominant cluster. Nondominant plasmids included other *bla*<sub>KPC</sub> or *bla*<sub>NDM</sub> plasmids that did not fall into the pKPC2 or pNDM1 dominant clusters.

During 2010–2012, pNDM1 was predominant but pKPC2 subsequently caught up during 2013–2015 (Figure 2, panel B; Appendix 2 Figure 1, panel A). Those plasmids were largely found in 3 species: *K. pneumoniae* (43.96%), *E. coli* (31.71%), and *Enterobacter cloacae* (13.68%) (Figure 2, panel C). Bacterial sequence type (ST) distribution among *bla*<sub>KPC</sub>-positive and *bla*<sub>NDM</sub>-positive isolates showed that both *bla*<sub>KPC</sub> and *bla*<sub>NDM</sub> plasmids were widely distributed across numerous STs, particularly in *K. pneumoniae* (Appendix 2 Figure 1, panel B), indicating that widespread distribution is unlikely due to selective clonal expansion events. The *bla*<sub>KPC</sub>-dominant cluster also had more unique isolates than the other clusters, suggesting wider *bla*<sub>KPC</sub> transmission (Figure 3).

### Evolution of pKPC2 Features

Annotated features on the pKPC2 plasmid map show conjugative genes from the *tra* and *trb* operons and

complete conjugative machinery (Figure 4, panel A). A comparison against the GenBank database for similar plasmids revealed pKPC2 is a hybrid of pSA20021456.2-like plasmids (GenBank accession no. CP030221), with 74% coverage and 99.60% identity, and pKPCAPSS-like plasmids (GenBank accession no. KP008371), with 34% coverage and 99.99% identity (Figure 4, panel A). The conjugative and

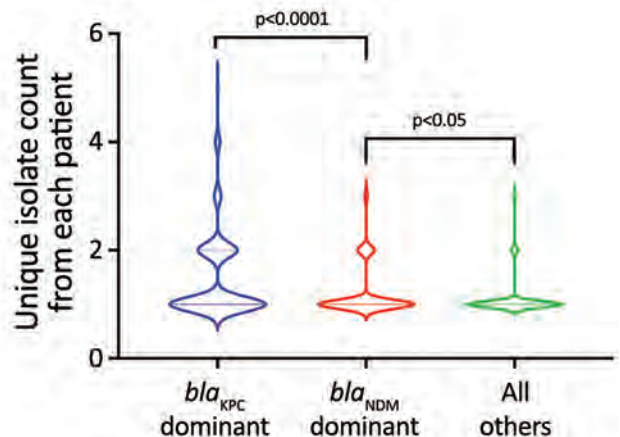


**Figure 3.** Violin plots showing the unique isolate counts from each patient in a study of dominant carbapenemase-encoding plasmids in clinical Enterobacteriales isolates and hypervirulent *Klebsiella pneumoniae*, Singapore. Unique isolates were defined as different species or different sequence types from same species. We separated unique isolates into 3 groups: *bla*<sub>KPC</sub> dominant ( $n = 196$ ), *bla*<sub>NDM</sub> dominant ( $n = 203$ ), and all others ( $n = 504$ ), which included *bla*<sub>KPC</sub> nondominant, *bla*<sub>NDM</sub> nondominant, and others. Brackets indicate p values for nonparametric Mann-Whitney tests between groups.

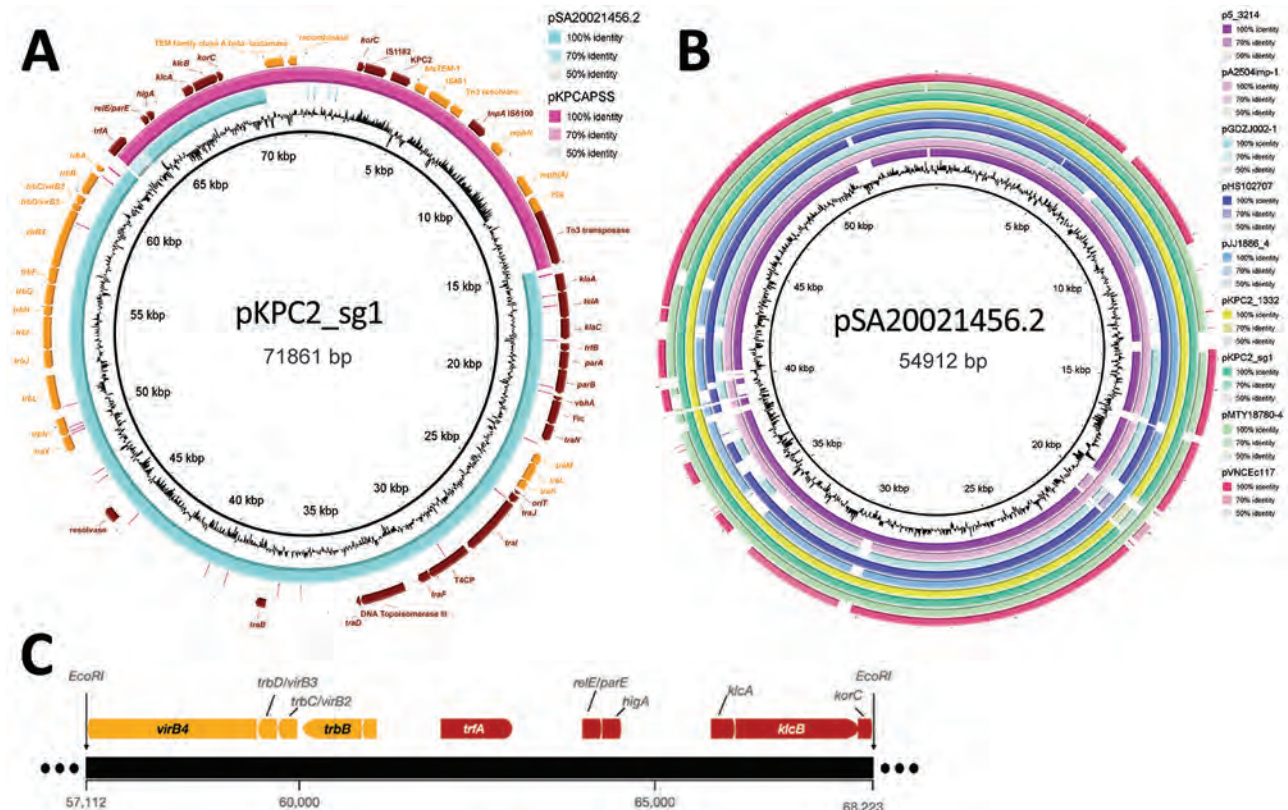


**Figure 4.** Annotated plasmid maps of the dominant carbapenemase-encoding plasmid in clinical Enterobacteriales isolates and hypervirulent *Klebsiella pneumoniae*, Singapore. A) Annotated plasmid map of pKPC2\_sg1 (GenBank accession no. MN542377), including the complete conjugative machinery (*oriT*, relaxase, T4CP, and T4SS) and the resistance genes, *bla*<sub>KPC-2</sub>, *bla*<sub>TEM-1</sub>, *mph(A)*, and TEM family class A  $\beta$ -lactamase (TEM-1). The region of pKPC2\_sg1 encoding the resistance genes was found in another plasmid called pKPCAPSS (GenBank accession no. KP008371), but the region encoding the conjugative machinery was highly similar to the sequence of pSA20021456.2 (GenBank accession no. CP030221). B) Plasmid alignment map showing other environmental or clinical plasmids with similar backbone, the pSA20021456.2 backbone, as pKPC2. C) Graphical representation of *EcoRI/BamHI* digested pKPC2 region containing replicon.

plasmid maintenance genes in pKPC2 are encoded in the pSA20021456.2-like backbone, which also is found in several other plasmids carried by environmental or clinical isolates (Figure 4, panel B). The region with resistance genes matches part of pKPCAPSS, which might have originated from Southeast Asia (22). Using PlasmidFinder 2.1 (16), we were unable to find any replicon on pKPC2. To determine the potential origin of replication (*oriV*), we used restriction enzyme digestion to identify the gene fragment in pKPC2 capable of replication (23,24). We cloned the fragments into the lambda *pir*-dependent vector of pR6K. We successfully selected *E. coli* colonies with pR6K containing an 11,111-bp fragment with the *trfA* gene (Figure 4, panel C), which is the prototypical protein essential for replication of incompatibility group P (IncP) plasmids with *oriV* consisting of 5 17-bp tandem repeats (25). We detected 9 similar, but not identical, 17-bp tandem repeats immediately downstream of *trfA* (Appendix 2 Figure 2). We cloned the *trfA* and *oriV* region into

pR6K and were able to successfully transform and replicate this region in *E. coli*, demonstrating that the *trfA* and *oriV* region is the minimal sequence required for replication (Appendix 2 Figure 3).

To further examine whether the *trfA* replicon in pKPC2 belongs to the IncP family, we measured the plasmid stability of pKPC2 in presence of another IncP plasmid, pRK2. Plasmids that belong to the same incompatibility group cannot coexist stably in the same host because they have similar replicons (26). In *E. coli* MG1655 harboring both plasmids, pKPC2 was gradually lost when pRK2 was under selection (Figure 5, panel A). Moreover, phylogenetic analysis revealed that pKPC2's *trfA* is related to the IncP family, but it does not belong to any existing subgroup and is more closely related to the IncP- $\epsilon$  subgroup, with some divergence (Figure 5, panel B). Analysis of pKPC2's conjugative *tra* and *trb* operons also revealed the gene arrangement typical in IncP *tra1* and *tra2* cores (Appendix 2 Figure 4) (27).

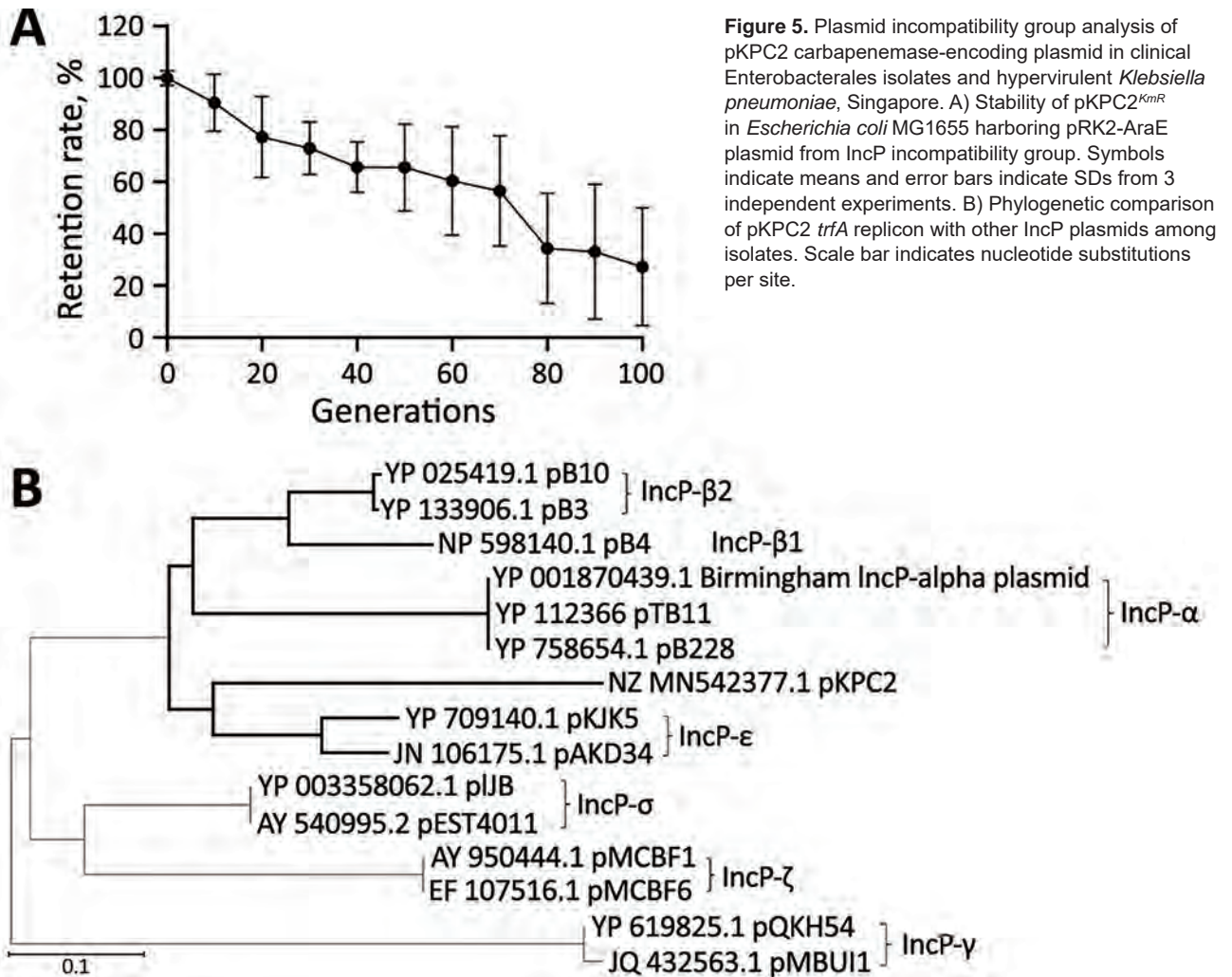


**Figure 5.** Plasmid incompatibility group analysis of pKPC2 carbapenemase-encoding plasmid in clinical Enterobacteriales isolates and hypervirulent *Klebsiella pneumoniae*, Singapore. A) Stability of pKPC2<sup>KmR</sup> in *Escherichia coli* MG1655 harboring pRK2-AraE plasmid from IncP incompatibility group. Symbols indicate means and error bars indicate SDs from 3 independent experiments. B) Phylogenetic comparison of pKPC2 *trfA* replicon with other IncP plasmids among isolates. Scale bar indicates nucleotide substitutions per site.

### Stability and Genetic Adaptation of pKPC2 In Vitro

pKPC2 exhibited faster conjugation kinetics, reaching nearly  $10^0$  after 2–3 hours, than did pNDM1 (GenBank accession no. JADPQD010000004), which took 3–4 hours to reach  $10^0$  (Figure 6, panel A). With hypervirulent *K. pneumoniae* SGH10 as the recipient, the conjugation frequency remained higher for pKPC2 than for pNDM1 (Figure 6, panel B).

To determine whether those plasmids exert any fitness cost on host strains, we measured the growth rate of host strains in presence or absence of the plasmids. We included plasmids tagged with kanamycin resistance, pKPC2<sup>KmR</sup> and pNDM1<sup>KmR</sup>, because they were used for subsequent experiments with kanamycin as a robust selection marker. We found no significant difference in growth rate for *E. coli* MG1655 or *K. pneumoniae* SGH10 (Figure 6, panels C, D). To simulate a nutrient-poor condition, we tested growth rates in minimal media, which also showed

no significant growth differences (Appendix 2 Figure 5). Furthermore, both plasmids remained stable for up to 300 generations without selection pressure (Figure 6, panels E, F). We compared the sequences of the 9 pKPC2<sup>KmR</sup> plasmids from the 300th generation (pKPC2<sup>KmR</sup>\_Gen300) *K. pneumoniae* SGH10 isolates to the original pKPC2<sup>KmR</sup> plasmid using in vitro plasmid evolution experiments and noted no major changes in the plasmid sequence (Appendix 2 Figure 6). Among the nine 300th-generation plasmids, 6 had 2 or 4 nucleotide mismatches on  $\beta$ -lactamase genes. However, sequence comparison of the pKPC2 and pKPC2<sup>KmR</sup> used in this study to the pKPC2\_sg1 from the clinical isolate *K. pneumoniae* ENT494 (GenBank accession no. MN542377) shows the same nucleotide polymorphism in the same genes (Appendix 2 Figure 7), indicating that these are likely the only bona fide evolved adaptations of the plasmid. Because host bacteria can also evolve to adapt to plasmid car-

riage (28), we compared the genomic sequences of nine 300th-generation *K. pneumoniae* SGH10 isolates carrying pKPC2 and nine 300th-generation isolates without pKPC2. We hypothesized that host adaptation would lead to an increased number of non-synonymous mutations in the strains carrying the plasmid versus the plasmid-null strains, leading to changes in protein function. However, our results indicated similar numbers of synonymous, non-synonymous, and total nucleotide polymorphism differences in both groups.

### pKPC2 Conjugation Frequency and Stability in Enterobacteriales Species

We hypothesize that the predominance of pKPC2 in our clinical isolates is due to its high conjugation frequency to different Enterobacteriales species. The conjugation frequency of pKPC2<sup>KmR</sup> from MG1655 to other *E. coli* or *E. cloacae* recipient strains were remarkably high, ranging from 10<sup>-1</sup> to 10<sup>0</sup> (Appendix 2 Figure 8, panel A). We observed the same

conjugation frequency for several clinical *Klebsiella* strains, such as *K. pneumoniae* NUH29, *K. quasipneumoniae* TTSH4, *K. oxytoca* 8071169380, and *K. varicola* NUH59. However, some *Klebsiella* recipient strains exhibited lower conjugation frequency, in the 10<sup>-3</sup> to 10<sup>-1</sup> range. For pNDM1<sup>KmR</sup>, the conjugation frequency was ≈10–100-fold lower than for pKPC2<sup>KmR</sup> for most pairs. When we used *K. pneumoniae* SGH10 as the donor to the same panel of Enterobacteriales recipients, the conjugation frequency of both plasmids was 10–100-fold lower than when *E. coli* MG1655 was the donor (Appendix 2 Figure 8, panel B). We then swapped the donor-recipient pairs by using the panel of Enterobacteriales strains as donors and *K. pneumoniae* SGH10 as the recipient (Appendix 2 Figure 8, panel C). Overall, the conjugation frequency for pKPC2<sup>KmR</sup> remained higher than the frequency for pNDM1<sup>KmR</sup> in most donor-recipient pairs. However, the conjugation frequency of the swapped donor-recipient pairs was not the same as the original pairs, indicating the effects of

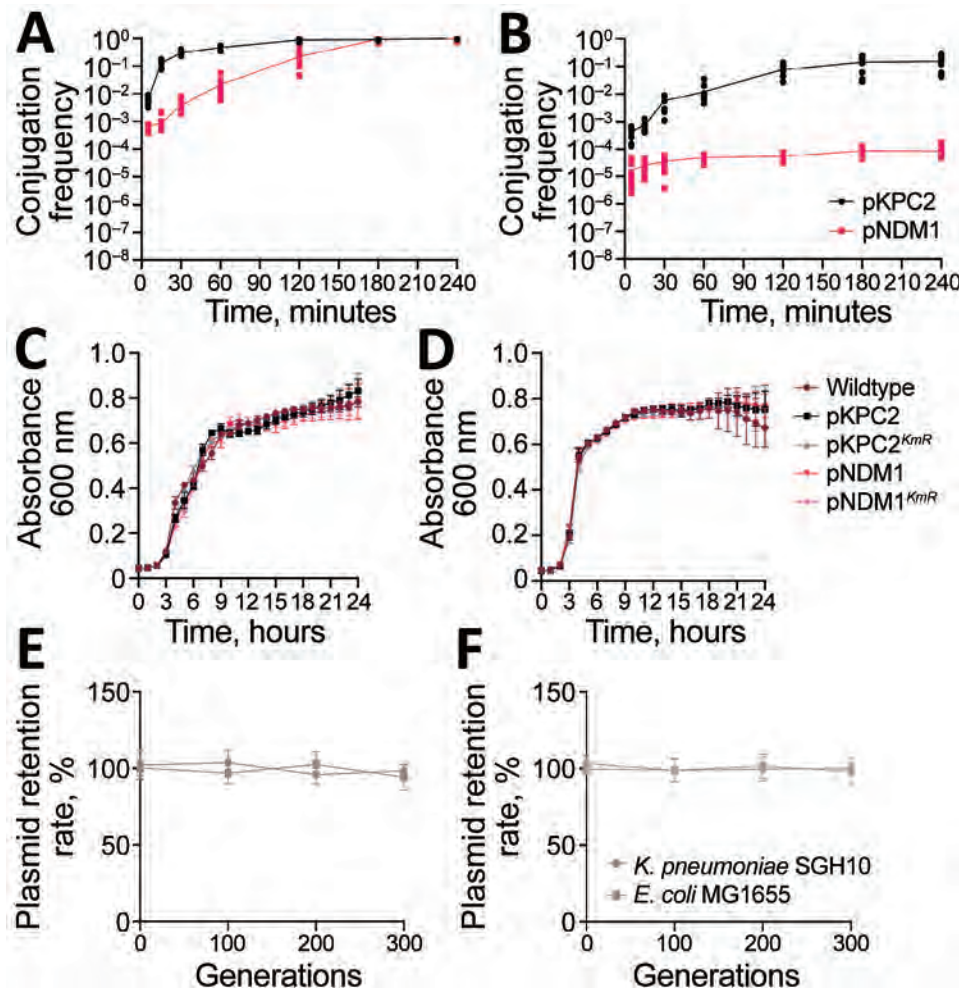


**Figure 6.** Characterization of pKPC2 carbapenemase-encoding plasmid in clinical Enterobacteriales isolates and hypervirulent *Klebsiella pneumoniae*, Singapore. A, B) Conjugation kinetics of pKPC2 and pNDM1 from *Escherichia coli* MG1655 (donor) to *E. coli* SLC-568 (recipient) (A) or to *K. pneumoniae* SGH10 (recipient) (B). The donor-recipient pairs were mixed in 1:1 ratio and conjugated for 4 hours at 37°C using filter matings. The number of transconjugant and recipient pairs were enumerated by plating. Results from 3 independent experiments were plotted as the conjugation frequency (transconjugant/recipient) over time (minutes). Error bars indicate SDs from 3 independent experiments. C, D) Representative growth curve of *E. coli* MG1655 (C) or *K. pneumoniae* SGH10 (D) with or without plasmids pKPC2, pKPC2<sup>KmR</sup>, pNDM1, pNDM1<sup>KmR</sup> grown in LB media at 37°C for 24 h. E, F) Stability of pKPC2<sup>KmR</sup> (E) and pNDM1<sup>KmR</sup> (F) in *K. pneumoniae* SGH10 and *E. coli* MG1655 grown in LB up to generation 300. Symbols indicate means and error bars indicate SDs from 3 independent experiments. LB, lysogeny broth.

donor and recipient factors. Both plasmids within the Enterobacterales strains were stable for up to 90 generations, except for *E. coli* UTI89, which failed to retain the pKPC2<sup>KmR</sup> plasmid (Appendix 2 Figure 8, panels D, E). These results align with clinical data showing the persistence of the pKPC2 plasmid over several months in patients without antimicrobial drug exposure (5).

### Conjugation Frequency and Stability of pKPC2 in Hypervirulent *K. pneumoniae*

Because pKPC2 was previously found in 18 local clinical hypervirulent *K. pneumoniae* isolates of K1, K2, and K20 capsular serotypes (5), we hypothesize that the plasmid does not face constraints in transmission to hypervirulent *K. pneumoniae*. Those isolates were loosely defined as hypervirulent *K. pneumoniae* based on occurrence of  $\geq 2$  virulence genes, such as *iro* and *rmpA* (Appendix 2 Table 1). Indeed, we observed high conjugation frequency for K1 strains (Appendix 2 Figure 9, panel A). On the other hand, K2 and K5 strains exhibited heterogeneity in their plasmid acceptance. However, plasmid conjugation success was independent of capsular types because we observed low conjugation frequency in 2 STs, K2/ST2039 and K5/ST60, whereas other STs of the same capsular type exhibited markedly higher conjugation frequency. Compared with pNDM1<sup>KmR</sup> (Appendix 2 Figure 9, panel B), the conjugation frequency of pKPC2<sup>KmR</sup> was  $\approx 10$ –100-fold higher. In fact, K2/ST2039 and K5/ST60 strains were low conjugators for both plasmids. Despite the low conjugation frequency, the plasmids maintained stability over 90 generations (Appendix 2 Figure 10).

### Effects of Taxonomic Factors on pNDM1 Conjugation

To examine the influence of taxonomic factors on pKPC2 and pNDM1 conjugation frequencies, we performed statistical analyses on available datasets (Appendix 2 Figures 8, 9) by using a survival-analysis approach (21). Comparing the baseline conjugation frequency between the same strain, we noted a statistically significant decrease in pKPC2 transfer between the same species (24.0-fold) or same genus (10.2-fold) but no statistically significant decrease between different genera (Table 1). On the other hand, we noted a statistically significant decrease in pNDM1 transfer between the same species (36.3-fold), same genus (123.0-fold), and different genera (87.1-fold). These results suggest that taxonomic factors have a higher influence on pNDM1 than pKPC2, which is especially notable for transfer between the same genus or different genera.

### Effect of Bacterial Capsule on Plasmid Conjugation

We examined a panel of isogenic deletion mutants of *K. pneumoniae* SGH10 as recipients that could affect donor-recipient pair mating dynamics. Conjugation frequency was enhanced in  $\Delta rmpA$  and  $\Delta ICEp10$  recipients, but the greatest impediment to plasmid conjugation was the capsule (Appendix 2 Figure 9, panel C). The  $\Delta wcaJ$  recipient exhibited conjugation efficiency approaching  $10^0$  for both plasmids (Appendix 2 Figure 9, panel D). Similarly, capsule absence increased the conjugation frequency of both plasmids from *E. coli* MG1655 to capsule-null mutants of the low conjugating hypervirulent *K. pneumoniae* isolates (Appendix 2 Figure 11). However, the increases in conjugation frequency of pNDM1<sup>KmR</sup> in  $\Delta wcaJ$  suggests that capsule is not as much of a barrier to pKPC2 as it is to pNDM1.

### Discussion

The spread of carbapenemase-encoding plasmids via horizontal gene transfer poses a major challenge to treatment against multidrug-resistant gram-negative bacteria because carbapenems are often antimicrobial agents of last resort. However, the dynamics and factors enabling the spread of these clinically significant plasmids have not been well studied. Previously, we found that pKPC2 is the only carbapenemase-encoding plasmid harbored by all the carbapenemase-resistant hypervirulent *K. pneumoniae* identified (5). Hypervirulent *K. pneumoniae* can cause *Klebsiella*-induced liver abscess, a community-acquired infection endemic in Asia-Pacific regions (29); the K1/ST23 lineage is predominantly responsible and causes 80% of these abscesses (30). Hypervirulent *K. pneumoniae* evolved through separate lineages from classical strains that typically cause multidrug-resistant nosocomial infections (30). Because hypervirulent *K. pneumoniae* is thought to be less receptive to horizontal gene transfer, pKPC2 in these strains could indicate that this plasmid has high transmission potential.

Our results showed that pKPC2 was the most prevalent carbapenemase-encoding plasmid among the clinical Enterobacterales isolates in CaPES. These plasmids are largely found in *K. pneumoniae*, *E. coli*, and *E. cloacae*, which also were the most prevalent carbapenemase-encoding plasmid-harboring species reported in other surveillance studies (31,32), showing that those are major reservoirs. Although KPC-2 has been documented on diverse plasmids and is known to undergo frequent recombination events (33), we uncovered a single plasmid that moves as a discrete and intact unit among diverse strains and species. One limitation of our epidemiologic study is

**Table.** Regression coefficients for pKPC2 and pNDM1 plasmid conjugation frequencies between donor-recipient pairs in a study of carbapenemase-encoding plasmids in clinical Enterobacteriales isolates and hypervirulent *Klebsiella pneumoniae*, Singapore\*

| Taxonomic relatedness (model parameter) | pKPC2 |                   | pNDM1 |                  |
|---|-------|-------------------|-------|------------------|
|   | Mean  | Bootstrap 95% CI  | Mean  | Bootstrap 95% CI |
| Same strain ( $\beta_0$ )               | -1.73 | -1.824 to -1.610  | -2.31 | -2.405 to -2.212 |
| Same species ( $\beta_1$ )              | -1.38 | -1.599 to -1.147  | -1.56 | -1.771 to -1.317 |
| Same genus ( $\beta_2$ )                | -1.01 | -1.162 to -0.866  | -2.09 | -2.258 to -1.907 |
| Different genus ( $\beta_3$ )           | 0.04  | -0.1165 to 0.1988 | -1.94 | -2.086 to -1.808 |

\*log base 10 conjugation frequencies and their bootstrap 95% CI as described in for the regression equation and fitting procedure are shown.

that we do not yet know whether the same trend in plasmid transfer persisted after 2015.

Several factors revealed by our in vitro data potentially explain the high prevalence and dominance of pKPC2 in clinical isolates. First, pKPC2 conjugates with fast kinetics and has high transmissibility among various host-recipient pairs. Although taxonomic relatedness is known to affect conjugation frequency (21), pNDM1 is more strongly affected by this relatedness than pKPC2, especially for transfer within same and other genera. This finding likely accounts for the success of pKPC2 as the dominant carbapenemase-encoding plasmid among Enterobacteriales clinical isolates. Second, pKPC2 has low fitness costs and is highly adapted to host species. The persistence of plasmids in bacterial populations over an extended period has long been regarded as an evolutionary dilemma (34). Although compensatory mechanisms could account for plasmid persistence within a community with a high conjugation rate, offsetting the disadvantage incurred by high fitness cost in the absence of selection pressure (35), another study reported that the key factor for the persistence of the pOXA48\_K8 plasmid is its low fitness costs across many clinical Enterobacteriaceae hosts in the gut, rather than its high conjugation frequency (36,37). We found that pKPC2 imposes low fitness cost and had high conjugation frequency across several Enterobacteriales isolates and a remarkable retention rate, even in low conjugating strains. pKPC2 exhibited no mutations after in vitro evolution experiments and almost no changes compared with original clinical isolates.

We noted that both the conjugative machinery and plasmid maintenance genes in pKPC2 are encoded by the pSA20021456.2-like backbone. Several plasmids with a similar backbone have been described (Figure 4, panel B), including the multidrug-resistant pHS102707 and the pJJ1886\_4 plasmids found in clinical *E. coli* strains (38,39). This finding raises the concern that plasmids with this backbone might have similar dissemination potential or be able to recombine with plasmid fragments bearing multidrug-resistant genes and a suitable oriV to become dominant under antimicrobial drug selection pressure. Although we might never know the origins and the evolutionary

steps taken by pKPC2, one clue is its phylogenetic relatedness to IncP- $\epsilon$  plasmids, which have been observed to be vectors in the spread of antimicrobial drug resistance in agricultural systems (40).

The high transmissibility of pKPC2 was also seen in hypervirulent *K. pneumoniae* clinical isolates. Hypervirulent *K. pneumoniae* is thought to face constraints in horizontal gene transfer, and its low gene content diversity further supported the idea that the thick capsular polysaccharide is a barrier to transfer (41). Reports of  $\Delta wcaJ$  in 4 different strains of *K. pneumoniae* showed an 8–20-fold increase in plasmid conjugation over 1 hour (42). Capsule deletion increased conjugation frequency by 10–100-fold in pNDM1 compared with pKPC2. This increase shows the capsule is more of a hindrance to pNDM1 than to pKPC2, suggesting that pKPC2 has a competitive advantage over pNDM1 in its transmission to encapsulated strains. This finding might explain why pKPC2 is the only carbapenemase-encoding plasmid among all the hypervirulent/carbapenem-resistant *K. pneumoniae* isolates we discovered (5). The high transmissibility of pKPC2 to the antimicrobial-sensitive, community-acquired hypervirulent *K. pneumoniae* strains suggests that pKPC2 or its predecessors might have undergone carriage selection for high transmissibility and persistence in isolates from ecologic settings that harbor similar features to hypervirulent *K. pneumoniae*. Although our mechanistic studies of plasmid transmission are limited to in vitro experiments, these studies provide insights and potential explanations on the pattern of transmission observed clinically.

In summary, this study underscores the need to track the spread and dominance of clinically relevant carbapenemase-encoding plasmids in health-care settings and examine transmission characteristics. Our findings reveal increasing dominance of pKPC2 over other carbapenemase-encoding plasmids during a 5-year period. pKPC2 appears to be a highly adapted hybrid plasmid exhibiting increased transmissibility and persistence among Enterobacteriales and hypervirulent *K. pneumoniae* strains. These highly evolved and adapted plasmids act as agents that move easily between various hosts and exert negligible fitness costs, facilitating their long-

term carriage even without selection pressure. We propose that the pKPC2 plasmid has already undergone carriage adaptation and been in circulation for some time. Insights gained on the transmission potential of pKPC2 and other similarly evolved plasmids could translate into better infection prevention measures or improved surveillance.

### Acknowledgments

We thank Swaine Chen for the gift of bacterial strains. We also thank the CaPES study group for their support; this group included Benjamin Cherng, Deepak Rama Narayana, Douglas Chan Su Gin, De Partha Pratim, Hsu Li Yang, Indumathi Venkatachalam, Jeanette Teo, Michelle Ang, Kalisvar Marimuthu, Koh Tse Hsien, Nancy Tee, Nares Smitasin, Ng Oon Tek, Ooi Say Tat, Raymond Fong, Raymond Lin Tzer Pin, Surinder Kaur Pada, Tan Thean Yen, and Thoon Koh Cheng.

N.M.T., P.S.R.S., K.M., V. K., and O.T.N. were supported by the Singapore Ministry of Health's National Medical Research Council (NMRC) under its collaborative grants, including Collaborative Solutions Targeting Antimicrobial Resistance Threats in Health Systems (CoSTAR-HS) (grant no. NMRC CGAug16C005), NMRC Clinician Scientist Award (grant no. MOH-000276), and NMRC Clinician Scientist Individual Research Grant (no. MOH-CIRG18nov-0006); the National Centre for Infectious Diseases under its NCID Catalyst Grant (no. FY202013VKHQ); and the German Federal Ministry of Health COVID-19 research and development funding to the World Health Organization (award no. 70826). A.E.M. was supported by Grant FONDECYT (no. 11181135), from Agencia Nacional de Investigación y Desarrollo, Chile. This research was also supported by NMRC grant nos. OFIRG20NOV-0045 and MOE2018-T3-1-03 to Y.H.G.

### About the Author

Mr. Yong is a doctoral student at the Department of Biochemistry, Infectious Diseases Translational Research Program, Yong Loo Lin School of Medicine, National University of Singapore. His main research interest is plasmid transmission and the development of novel antimicrobial drugs.

### References

- World Health Organization. Global priority list of antibiotic-resistant bacteria to guide research, discovery, and development of new antibiotics. Geneva: The Organization; 2017.
- Yang X, Dong N, Chan EW, Zhang R, Chen S. Carbapenem resistance-encoding and virulence-encoding conjugative plasmids in *Klebsiella pneumoniae*. Trends Microbiol. 2021;29:65–83. <https://doi.org/10.1016/j.tim.2020.04.012>
- Benz F, Huisman JS, Bakkeren E, Herter JA, Stadler T, Ackermann M, et al. Plasmid- and strain-specific factors drive variation in ESBL-plasmid spread in vitro and in vivo. ISME J. 2021;15:862–78. <https://doi.org/10.1038/s41396-020-00819-4>
- Rodríguez-Beltrán J, DelaFuente J, León-Sampedro R, MacLean RC, San Millán Á. Beyond horizontal gene transfer: the role of plasmids in bacterial evolution. Nat Rev Microbiol. 2021;19:347–59. <https://doi.org/10.1038/s41579-020-00497-1>
- Chen Y, Marimuthu K, Teo J, Venkatachalam I, Cherng BPZ, De Wang L, et al. Acquisition of plasmid with carbapenem-resistance gene *bla*<sub>KPC2</sub> in hypervirulent *Klebsiella pneumoniae*, Singapore. Emerg Infect Dis. 2020;26:549–59. <https://doi.org/10.3201/eid2603.191230>
- Marimuthu K, Venkatachalam I, Khong WX, Koh TH, Cherng BPZ, Van La M, et al.; Carbapenemase-Producing Enterobacteriaceae in Singapore (CaPES) Study Group. Clinical and molecular epidemiology of carbapenem-resistant Enterobacteriaceae among adult inpatients in Singapore. Clin Infect Dis. 2017;64:S68–75. <https://doi.org/10.1093/cid/cix113>
- Bankovich A, Nurk S, Antipov D, Gurevich AA, Dvorkin M, Kulikov AS, et al. SPAdes: a new genome assembly algorithm and its applications to single-cell sequencing. J Comput Biol. 2012;19:455–77. <https://doi.org/10.1089/cmb.2012.0021>
- Wick RR, Judd LM, Gorrie CL, Holt KE. Unicycler: resolving bacterial genome assemblies from short and long sequencing reads. PLOS Comput Biol. 2017;13:e1005595. <https://doi.org/10.1371/journal.pcbi.1005595>
- Jolley KA, Maiden MC. BIGSdb: Scalable analysis of bacterial genome variation at the population level. BMC Bioinformatics. 2010;11:595. <https://doi.org/10.1186/1471-2105-11-595>
- Wood DE, Salzberg SL. Kraken: ultrafast metagenomic sequence classification using exact alignments. Genome Biol. 2014;15:R46. <https://doi.org/10.1186/gb-2014-15-3-r46>
- Seemann T. Abricate [cited 2021 Aug 5]. <https://github.com/tseemann/abricate>
- Feldgarden M, Brover V, Haft DH, Prasad AB, Slotta DJ, Tolstoy I, et al. Validating the AMRFinder tool and resistance gene database by using antimicrobial resistance genotype-phenotype correlations in a collection of isolates. Antimicrob Agents Chemother. 2019;63:e00483-19. <https://doi.org/10.1128/AAC.00483-19>
- Chen L, Zheng D, Liu B, Yang J, Jin Q. VFDB 2016: hierarchical and refined dataset for big data analysis – 10 years on. Nucleic Acids Res. 2016;44:D694–7. <https://doi.org/10.1093/nar/gkv1239>
- Besemer J, Lomsadze A, Borodovsky M. GeneMarkS: a self-training method for prediction of gene starts in microbial genomes. Implications for finding sequence motifs in regulatory regions. Nucleic Acids Res. 2001;29:2607–18. <https://doi.org/10.1093/nar/29.12.2607>
- Alikhan NF, Petty NK, Ben Zakour NL, Beatson SA. BLAST Ring Image Generator (BRIG): simple prokaryote genome comparisons. BMC Genomics. 2011;12:402. <https://doi.org/10.1186/1471-2164-12-402>
- Carattoli A, Zankari E, García-Fernández A, Voldby Larsen M, Lund O, Villa L, et al. In silico detection and typing of plasmids using PlasmidFinder and plasmid multilocus sequence typing. Antimicrob Agents Chemother. 2014;58:3895–903. <https://doi.org/10.1128/AAC.02412-14>
- Robertson J, Nash JHE. MOB-suite: software tools for clustering, reconstruction and typing of plasmids from draft assemblies. Microb Genom. 2018;4. <https://doi.org/10.1099/mgen.0.000206>

18. Kumar S, Stecher G, Li M, Knyaz C, Tamura K. MEGA X: Molecular Evolutionary Genetics Analysis across computing platforms. *Mol Biol Evol.* 2018;35:1547–9. <https://doi.org/10.1093/molbev/msy096>
19. De Gelder L, Ponciano JM, Joyce P, Top EM. Stability of a promiscuous plasmid in different hosts: no guarantee for a long-term relationship. *Microbiology (Reading).* 2007;153:452–63. <https://doi.org/10.1099/mic.0.2006/001784-0>
20. Cook TB, Rand JM, Nurani W, Courtney DK, Liu SA, Pfeiffer BF. Genetic tools for reliable gene expression and recombineering in *Pseudomonas putida*. *J Ind Microbiol Biotechnol.* 2018;45:517–27. <https://doi.org/10.1007/s10295-017-2001-5>
21. Alderliesten JB, Duxbury SJN, Zwart MP, de Visser JAGM, Stegeman A, Fischer EAJ. Effect of donor-recipient relatedness on the plasmid conjugation frequency: a meta-analysis. *BMC Microbiol.* 2020;20:135. <https://doi.org/10.1186/s12866-020-01825-4>
22. Ageevets V, Sopova J, Lazareva I, Malakhova M, Ilina E, Kostryukova E, et al. Genetic environment of the *bla*<sub>KPC-2</sub> Gene in a *Klebsiella pneumoniae* isolate that may have been imported to Russia from Southeast Asia. *Antimicrob Agents Chemother.* 2017;61:e01856-16. <https://doi.org/10.1128/AAC.01856-16>
23. Miki T, Easton AM, Rownd RH. Cloning of replication, incompatibility, and stability functions of R plasmid NRI. *J Bacteriol.* 1980;141:87–99. <https://doi.org/10.1128/jb.141.1.87-99.1980>
24. Lovett MA, Helinski DR. Method for the isolation of the replication region of a bacterial replicon: construction of a mini-F<sup>+</sup> plasmid. *J Bacteriol.* 1976;127:982–7. <https://doi.org/10.1128/jb.127.2.982-987.1976>
25. Thomas CM, Smith CA. Incompatibility group P plasmids: genetics, evolution, and use in genetic manipulation. *Annu Rev Microbiol.* 1987;41:77–101. <https://doi.org/10.1146/annurev.mi.41.100187.000453>
26. Novick RP. Plasmid incompatibility. *Microbiol Rev.* 1987;51:381–95. <https://doi.org/10.1128/mr.51.4.381-395.1987>
27. Pansegrau W, Lanka E, Barth PT, Figurski DH, Guiney DG, Haas D, et al. Complete nucleotide sequence of Birmingham IncP alpha plasmids. Compilation and comparative analysis. *J Mol Biol.* 1994;239:623–63. <https://doi.org/10.1006/jmbi.1994.1404>
28. Stalder T, Rogers LM, Renfrow C, Yano H, Smith Z, Top EM. Emerging patterns of plasmid-host coevolution that stabilize antibiotic resistance. *Sci Rep.* 2017;7:4853. <https://doi.org/10.1038/s41598-017-04662-0>
29. Lee CR, Lee JH, Park KS, Jeon JH, Kim YB, Cha CJ, et al. Antimicrobial resistance of hypervirulent *Klebsiella pneumoniae*: epidemiology, hypervirulence-associated determinants, and resistance mechanisms. *Front Cell Infect Microbiol.* 2017;7:483. <https://doi.org/10.3389/fcimb.2017.00483>
30. Lam MMC, Wyres KL, Duchène S, Wick RR, Judd LM, Gan YH, et al. Population genomics of hypervirulent *Klebsiella pneumoniae* clonal-group 23 reveals early emergence and rapid global dissemination. *Nat Commun.* 2018;9:2703. <https://doi.org/10.1038/s41467-018-05114-7>
31. Sugawara Y, Hagiya H, Akeda Y, Aye MM, Myo Win HP, Sakamoto N, et al. Dissemination of carbapenemase-producing Enterobacteriaceae harbouring *bla*<sub>NDM</sub> or *bla*<sub>IMI</sub> in local market foods of Yangon, Myanmar. *Sci Rep.* 2019;9:14455. <https://doi.org/10.1038/s41598-019-51002-5>
32. Miltgen G, Cholley P, Martak D, Thouverez M, Seraphin P, Leclaire A, et al. Carbapenemase-producing Enterobacteriaceae circulating in the Reunion Island, a French territory in the Southwest Indian Ocean. *Antimicrob Resist Infect Control.* 2020;9:36. <https://doi.org/10.1186/s13756-020-0703-3>
33. David S, Cohen V, Reuter S, Sheppard AE, Giani T, Parkhill J, et al.; European Survey of Carbapenemase-Producing Enterobacteriaceae (EuSCAPE) Working Group; ESCMID Study Group for Epidemiological Markers (ESGEM). Integrated chromosomal and plasmid sequence analyses reveal diverse modes of carbapenemase gene spread among *Klebsiella pneumoniae*. *Proc Natl Acad Sci U S A.* 2020;117:25043–54. <https://doi.org/10.1073/pnas.2003407117>
34. Harrison E, Brockhurst MA. Plasmid-mediated horizontal gene transfer is a coevolutionary process. *Trends Microbiol.* 2012;20:262–7. <https://doi.org/10.1016/j.tim.2012.04.003>
35. Lopatkin AJ, Meredith HR, Srimani JK, Pfeiffer C, Durrett R, You L. Persistence and reversal of plasmid-mediated antibiotic resistance. *Nat Commun.* 2017;8:1689. <https://doi.org/10.1038/s41467-017-01532-1>
36. Alonso-del Valle A, León-Sampedro R, Rodríguez-Beltrán J, DelaFuente J, Hernández-García M, Ruiz-Garbayosa P, et al. Viability of plasmid fitness effects contributes to plasmid persistence in bacterial communities. *Nat Commun.* 2021;12:2653. <https://doi.org/10.1038/s41467-021-22849-y>
37. León-Sampedro R, DelaFuente J, Díaz-Agero C, Crellen T, Musicha P, Rodríguez-Beltrán J, et al.; R-GNOSIS WP5 Study Group. Pervasive transmission of a carbapenem resistance plasmid in the gut microbiota of hospitalized patients. *Nat Microbiol.* 2021;6:606–16. <https://doi.org/10.1038/s41564-021-00879-y>
38. Li G, Zhang Y, Bi D, Shen P, Ai F, Liu H, et al. First report of a clinical, multidrug-resistant *Enterobacteriaceae* isolate coharboring fosfomycin resistance gene *fosA3* and carbapenemase gene *bla*<sub>KPC-2</sub> on the same transposon, Tn1721. *Antimicrob Agents Chemother.* 2015;59:338–43. <https://doi.org/10.1128/AAC.03061-14>
39. Andersen PS, Stegger M, Aziz M, Contente-Cuomo T, Gibbons HS, Keim P, et al. Complete genome sequence of the epidemic and highly virulent CTX-M-15-producing H30-Rx subclone of *Escherichia coli* ST131. *Genome Announc.* 2013;1:e00988-13. <https://doi.org/10.1128/genomeA.00988-13>
40. Heuer H, Binh CT, Jechalke S, Kopmann C, Zimmerling U, Krögerrecklenfort E, et al. IncP-1ε plasmids are important vectors of antibiotic resistance genes in agricultural systems: diversification driven by class 1 integron gene cassettes. *Front Microbiol.* 2012;3:2. <https://doi.org/10.3389/fmicb.2012.00002>
41. Wyres KL, Wick RR, Judd LM, Froumine R, Tokolyi A, Gorrie CL, et al. Distinct evolutionary dynamics of horizontal gene transfer in drug resistant and virulent clones of *Klebsiella pneumoniae*. *PLoS Genet.* 2019;15:e1008114. <https://doi.org/10.1371/journal.pgen.1008114>
42. Haudiquet M, Buffet A, Rendueles O, Rocha EPC. Interplay between the cell envelope and mobile genetic elements shapes gene flow in populations of the nosocomial pathogen *Klebsiella pneumoniae*. *PLoS Biol.* 2021;19:e3001276. <https://doi.org/10.1371/journal.pbio.3001276>

Address for correspondence: Yunn-Hwen Gan, Infectious Diseases Translational Research Program, National University Singapore Yong Loo Lin School of Medicine, Biochemistry MD7, 8 Medical Dr, Singapore 117596, Singapore; email: bchganyh@nus.edu.sg

# Increasing and More Commonly Refractory *Mycobacterium avium* Pulmonary Disease, Toronto, Ontario, Canada

Daan Raats,<sup>1</sup> Sarah K. Brode, Mahtab Mehrabi, Theodore K. Marras

In mid-2014, Public Health Ontario Laboratories identified coincident increasing *Mycobacterium avium* isolation and falling *M. xenopi* isolation in the Toronto, Ontario, Canada, area. We performed a retrospective cohort of all patients in a Toronto clinic who began treatment for either *M. avium* or *M. xenopi* pulmonary disease during 2009–2012 (early period) or 2015–2018 (late period), studying their relative proportions and sputum culture conversion. We conducted a subgroup analysis among patients who lived in the Toronto-York region. The proportion of patients with *M. avium* was higher in the late period (138/146 [94.5%] vs. 82/106 [77.4%];  $p < 0.001$ ). Among *M. avium* patients, conversion was lower in the late period (26.1% vs. 39.0%;  $p = 0.05$ ). The increase in the proportion of patients with *M. avium* pulmonary disease and the reduction in the frequency of sputum culture conversion is unexplained but could suggest an increase in environmental *M. avium* exposure.

**P**ulmonary infection with nontuberculous mycobacteria (NTM) is a chronic, often progressive, debilitating disease. Most published data show that the frequency of NTM pulmonary disease (NTM-PD) is increasing worldwide (1–6), as are its substantial medical costs (7,8). The cause of this rise has not yet been elucidated. NTM are widespread in the environment but disease is uncommon, suggesting that host susceptibility is critical, although exposure magnitude is also likely key (9–11). Some observations indicate that the *Mycobacterium avium* complex

(MAC) might be a main driver for the increased occurrence of NTM-PD (2,5,12).

In Ontario, Canada, a rising prevalence of NTM-PD has been demonstrated previously, and, in the most recent years that have been studied, that increase was driven largely by an increase in MAC (2). More recently, in the spring of 2014, the Public Health Ontario Laboratory (PHOL) observed a sustained increase of >50% in the total number of *M. avium* isolates from pulmonary samples and persons with positive cultures for *M. avium* (13). A coincident reduction in *M. xenopi* isolates occurred without change in other NTM species. Curiously, this occurrence was only observed in the city of Toronto and the region immediately north (Regional Municipality of York), located between Lake Ontario and Lake Simcoe, which together encompass an area of 2,392 km<sup>2</sup> and had ≈4.1 million inhabitants as of 2018. In Ontario, at least 95% of NTM isolates are identified at the PHOL (14), permitting population-based study. Laboratory techniques at PHOL did not change at the time of increased isolation. Although the sudden increase in isolation frequency could suggest increased environmental exposure, the reason remains unclear.

Whether and how those changes relate to treatment outcomes of patients with NTM-PD caused by *M. avium* and *M. xenopi* has not been evaluated. In recent years, we observed that patients with *M. avium* pulmonary disease (Mav-PD) more often had microbiologically refractory disease and that we were encountering fewer patients with *M. xenopi* pulmonary disease (Mx-PD). On the basis of those observations, we studied relative proportions, culture conversion, culture reversion, and clinical treatment success of patients with Mav-PD and Mx-PD before and after 2014.

Author affiliations: Toronto Western Hospital, University Health Network, Toronto, Ontario, Canada (D. Raats, S.K. Brode, M. Mehrabi, T.K. Marras); West Park Health Care Centre, Toronto (S.K. Brode); University of Toronto, Toronto (S.K. Brode, T.K. Marras)

<sup>1</sup>Current affiliation: Ziekenhuis Oost-Limburg, Genk, Belgium.

DOI: <https://doi.org/10.3201/eid2808.220464>

## Methods

We designed this retrospective cohort study to compare patients with Mav-PD and Mx-PD treated before and after 2014. All patients assessed at the Toronto Western Hospital outpatient NTM clinic during July 1, 2003–December 31, 2019, were evaluated for eligibility. The NTM clinic is a tertiary care clinic, usually seeing patients after referral from infectious disease or pulmonary specialists. To be eligible for the study, patients were required to meet the American Thoracic Society/Infectious Diseases Society of America criteria for Mav-PD or Mx-PD (15) and to have begun treatment for NTM-PD during January 1, 2009–December 31, 2012, or January 1, 2015–December 31, 2018. These 4-year periods were selected to fall before and after the local surge in *M. avium* isolation and to permit adequate treatment follow-up among all patients in the early period, before the increase in *M. avium* isolation occurred. To be eligible, patients also were required to have been treated for  $\geq 6$  months with  $\geq 2$  antimycobacterial drugs (significant treatment). Patients with non-*M. avium* MAC species or those with confirmed macrolide resistance were excluded. Patients with multiple NTM species meeting the microbiologic criterion (15) over their clinical course were included, as long as they did not meet the criteria for both Mav-PD and Mx-PD at the start of their treatment. Patients previously treated for NTM-PD with a start date outside of the specified periods were also included, but a 6-month treatment-free interval was required for inclusion. Patients included in the first period were excluded from the second. The study was approved by the University Health Network Research Ethics Board; the need for informed consent was waived.

We collected demographic, clinical, microbiologic, and radiologic data until the first-occurring event of death, loss to follow up, or end of follow-up period. Patients started on treatment during 2009–2012 (early period) were followed until December 31, 2013. Patients started on treatment during 2015–2018 (late period) were followed until December 31, 2019. Follow-up time was measured from treatment initiation to death, loss to follow up, or follow-up end date. Treatment initiation and regimen were decided by the attending physician on the basis of contemporary guidelines.

Baseline clinical characteristics were age, sex, smoking history, comorbidities, body mass index, pulmonary function, corticosteroid use, current or recent chemotherapy, housing, and previous treatment for NTM-PD. Baseline data consisted of recorded observations preceding and closest available to the

start of treatment. Significant oral corticosteroid use was use of  $\geq 7.5$  mg prednisone (or equivalent) daily, for  $\geq 30$  days, within the 180 days before the baseline visit (16). The predominant radiologic pattern was nodular-bronchiectatic, fibrocavitary, or other, on the basis of computed tomography (CT) results obtained closest to treatment start (17). Antibiotics were listed only if prescribed for  $\geq 3$  months for oral or inhaled antibiotics, and only if prescribed for  $\geq 1$  month for intravenous antibiotics, to exclude antibiotics given for concurrent infections or discontinued early because of intolerance.

We assessed treatment outcomes by bacterial species (*M. avium* or *M. xenopi*), comparing patients who started NTM-PD treatment in the early period to those who started in the late period. Culture conversion within 12 months was the primary outcome, defined as  $\geq 3$  consecutive negative mycobacterial cultures collected  $\geq 4$  weeks apart (18). We considered the date of the first negative sample to be the date of culture conversion. We assessed the difference in culture conversion rate within and outside of the Toronto-York region in predefined subgroups on the basis of patients' residential postal codes. Culture reversion was defined as reappearance of the causative species in  $\geq 2$  samples in a patient still receiving treatment who had previously achieved culture conversion. Radiologic evolution was graded as improvement, stability, or progression on the basis of the radiologist's interpretation and was subsequently used to determine clinical treatment success. We considered patients with symptomatic improvement and at least radiologic stability or patients with radiologic improvement and at least symptomatic stability as demonstrating clinical treatment success. We evaluated that status on the basis of first available data 12 months after treatment initiation. For patients whose treatment was interrupted or incomplete, we used the last available data, but only if they were recorded after  $\geq 6$  months of treatment.

Continuous data were tested for normality through visual inspection and the Shapiro-Wilk test. Most continuous data were not normally distributed, and so we presented all data as medians with interquartile ranges (IQRs) for uniformity. We tested differences between groups by using Fisher exact tests or Mann-Whitney U tests as appropriate and used  $\chi^2$  tests for larger contingency tables. We excluded missing baseline data from respective analyses. We regarded patients with missing data for one of the outcomes as if they had not reached the respective outcome, so that if any bias would be introduced by including these outcomes, it would

be bias toward the null. We performed all statistical analyses using GraphPad Prism version 8.4 (<https://www.graphpad.com>).

## Results

During the study period, 984 patients were assessed in the NTM clinic; MAC or *M. xenopi* were isolated in 880 patients at some point. Significant NTM-PD treatment was started in the specified periods in 301 patients. We excluded 6 patients for not meeting American Thoracic Society/Infectious Diseases Society of America criteria (15), 36 patients for having non-*M. avium* MAC-PD, 1 patient for potentially having both Mav-PD and Mx-PD, 5 patients because of macrolide resistance, and 1 patient in whom outcomes could not be assessed. A total of 252 patients were eligible.

Among eligible patients, the relative proportion with Mav-PD was higher in the late period (138/146 patients [94.5%]) than in the early period (82/106 patients [77.4%];  $p < 0.001$ ). The proportion excluded for non-*M. avium* MAC-PD remained constant over both periods (data not shown).

We compared the general and NTM disease characteristics of the eligible patients (Tables 1, 2). Among patients with Mav-PD, comorbidities, lung function, and CT pattern were similar between periods. Inhaled corticosteroids were used more often in the early period than the late period (47.6% of patients vs. 26.2%), but this difference was not statistically significant ( $p = 0.12$ ). Patients in the early period were less likely to have had a positive smear for acid-fast bacilli (64.6% vs. 81.2%;  $p = 0.01$ ). Patients with

**Table 1.** Baseline characteristics of patients with *Mycobacterium avium* and *M. xenopi* pulmonary disease, Toronto, Ontario, Canada\*

| Characteristic                      | <i>Mycobacterium avium</i> |                         |           | <i>Mycobacterium xenopi</i> |                       |             |
|-------------------------------------|----------------------------|-------------------------|-----------|-----------------------------|-----------------------|-------------|
|                                     | Early period,<br>n = 82    | Late period,<br>n = 138 | p value   | Early period,<br>n = 24     | Late period,<br>n = 8 | p value     |
| Median age, y (IQR)                 | 66.3 (59.5–72.7)           | 68.8 (59.1–76.0)        | 0.16      | 57.4 (47.4–72.5)            | 61.7 (58.2–68.5)      | 0.51        |
| Sex                                 |                            |                         |           |                             |                       |             |
| F                                   | 54 (65.9)                  | 82 (59.4)               | 0.39      | 14 (58.3)                   | 5 (62.5)              | Referent    |
| M                                   | 28 (34.1)                  | 56 (40.6)               |           | 10 (41.7)                   | 3 (37.5)              |             |
| Race                                |                            |                         |           |                             |                       |             |
| White                               | 57 (69.5)                  | 95 (68.8)               | Referent† | 20 (83.3)                   | 8 (100)               | 0.55†       |
| East Asian                          | 22 (26.8)                  | 28 (20.3)               |           | 3 (12.5)                    | 0                     |             |
| South Asian                         | 2 (2.4)                    | 12 (8.7)                |           | 1 (4.2)                     | 0                     |             |
| Black                               | 1 (1.2)                    | 3 (2.2)                 |           | 0                           | 0                     |             |
| Smoking history                     |                            |                         |           |                             |                       |             |
| Never                               | 46 (56.1)                  | 72 (52.2)               | 0.56†     | 8 (33.3)                    | 1 (12.5)              | 0.39†       |
| Prior                               | 26 (31.7)                  | 53 (38.4)               |           | 12 (50.0)                   | 3 (37.5)              |             |
| Current                             | 10 (12.2)                  | 13 (9.4)                |           | 4 (16.7)                    | 4 (50.0)              |             |
| Median BMI, kg/m <sup>2</sup> (IQR) | 21.1 (18.5–23.2)           | 21.4 (19.1–24.3)        | 0.40      | 21.3 (19.4–24.3)            | 21.5 (20.7–25.2)      | 0.35        |
| % Predicted FEV <sub>1</sub> (IQR)  | 64.0 (46.5–75.0)           | 64.0 (46.3–79.8)        | 0.88      | 64.0 (45.5–75.5)            | 80.5 (43.0–95.0)      | 0.32        |
| % Predicted FVC (IQR)               | 80.0 (64.8–93.0)           | 78.0 (65.3–94.0)        | 0.98      | 83.0 (68.0–91.0)            | 101.0 (87.3–109.0)    | <b>0.03</b> |
| Comorbidities                       |                            |                         |           |                             |                       |             |
| COPD                                | 22 (26.8)                  | 46 (33.3)               | 0.37      | 12 (50.0)                   | 4 (50.0)              | Referent    |
| Asthma                              | 13 (15.9)                  | 18 (13.0)               | 0.56      | 5 (20.8)                    | 3 (37.5)              | 0.38        |
| Interstitial lung disease           | 2 (2.4)                    | 6 (4.4)                 | 0.71      | 0                           | 0                     | NA          |
| Previous tuberculosis               | 9 (11.0)                   | 11 (8.0)                | 0.47      | 3 (12.5)                    | 0                     | 0.55        |
| Cystic fibrosis or PCD              | 1 (1.2)                    | 3 (2.2)                 | Referent  | 0                           | 0                     | NA          |
| Previous chest radiotherapy         | 5 (6.1)                    | 14 (10.1)               | 0.33      | 4 (16.7)                    | 0                     | 0.55        |
| Autoimmune disease                  | 14 (17.1)                  | 24 (17.4)               | Referent  | 0                           | 0                     | NA          |
| GERD                                | 16 (19.5)                  | 38 (27.5)               | 0.20      | 6 (25.0)                    | 2 (25.0)              | Referent    |
| Aspiration                          | 5 (6.1)                    | 8 (5.8)                 | Referent  | 2 (8.3)                     | 0                     | Referent    |
| Medication use                      |                            |                         |           |                             |                       |             |
| Inhaled corticosteroids             | 39 (47.6)                  | 50 (26.2)               | 0.12      | 12 (50.0)                   | 4 (50.0)              | Referent    |
| Oral corticosteroids                | 4 (4.9)                    | 9 (6.5)                 | 0.77      | 0                           | 1 (12.5)              | 0.25        |
| Current or recent chemotherapy‡     | 1 (1.2)                    | 5 (3.6)                 | 0.42      | 1 (4.2)                     | 0                     | Referent    |
| Housing§                            |                            |                         |           |                             |                       |             |
| Detached single-family              | 33 (40.2)                  | 52 (37.7)               | 0.55      | 12 (50.0)                   | 5 (62.5)              | 0.53        |
| Attached single-family              | 16 (19.5)                  | 22 (15.9)               |           | 1 (4.2)                     | 1 (12.5)              |             |
| Low-rise multi-family               | 10 (12.2)                  | 12 (8.7)                |           | 4 (16.7)                    | 0                     |             |
| High-rise multi-family¶             | 23 (28.0)                  | 50 (36.2)               |           | 7 (29.2)                    | 2 (25.0)              |             |

\*Values are no. (%) except as indicated. Bold indicates significance. BMI, body mass index; COPD, chronic obstructive pulmonary disease; FEV<sub>1</sub>, forced expiratory volume in 1 s; FVC, forced vital capacity; GERD, gastroesophageal reflux disease; IQR, interquartile range; PCD, primary ciliary dyskinesia.

†Fisher exact tests comparing White and non-White persons and persons who have ever smoked with persons who have not.

‡Recent chemotherapy was defined as within 2 years of treatment initiation.

§Missing data for 2 *M. avium* patients in the late period.

¶Buildings with  $\geq 5$  stories were classified as high-rise.

RESEARCH

**Table 2.** NTM disease characteristics of patients with *Mycobacterium avium* and *M. xenopi* pulmonary disease, Toronto, Ontario, Canada\*

| Characteristic   | <i>M. avium</i>      |                      |             | <i>M. xenopi</i>     |                    |          |
|--|----------------------|----------------------|-------------|----------------------|--------------------|----------|
|  | Early period, n = 82 | Late period, n = 138 | p value     | Early period, n = 24 | Late period, n = 8 | p value  |
| Previous NTM treatment†  |                      |                      |             |                      |                    |          |
| Same species   | 10 (12.2)            | 23 (16.7)            | 0.47        | 2 (8.3)              | 1 (12.5)           | Referent |
| Any species  | 12 (14.6)            | 27 (19.6)            |             | 5 (20.8)             | 2 (25.0)           |          |
| History of positive AFB smear                                    | 53 (64.6)            | 112 (81.2)           | <b>0.01</b> | 13 (54.2)            | 5 (62.5)           | Referent |
| CT pattern   |                      |                      |             |                      |                    |          |
| Nodular-bronchiectatic   | 60 (73.2)            | 89 (64.5)            | 0.33        | 7 (29.2)             | 1 (12.5)           | 0.07     |
| Fibrocavitary  | 17 (20.7)            | 34 (24.6)            |             | 16 (66.7)            | 4 (50.0)           |          |
| Other  | 5 (6.1)              | 15 (10.9)            |             | 1 (4.2)              | 3 (37.5)           |          |
| CT cavitation, any size  | 33 (40.2)            | 57 (41.3)            | 0.89        | 18 (75.0)            | 4 (50.0)           | 0.22     |
| Median time from initial visit to treatment initiation, mo (IQR) | 1.5 (–15.3 to 17.5)  | 0.0 (–5.0 to 9.0)    | 0.39        | 0.5 (–8.5 to 17.3)   | 0.5 (–1.0 to 3.75) | 0.91     |

\*Values are no. (%) except as indicated. Bold indicates significance. AFB, acid-fast bacilli; CT, computed tomography; IQR, interquartile range; NTM, nontuberculous mycobacteria.

†All except 1 *M. avium* patient with previous treatment history had a record of a single previous treatment episode; all *M. xenopi* patients with previous treatment history had a record of a single previous treatment episode. P values compare previous treatment for any species

Mav-PD were older than patients with Mx-PD (median age 67.6 [IQR 59.2–74.9] vs. 57.4 [IQR 51.8–70.1] years;  $p = 0.03$ ), had COPD less frequently (68/220 [30.9%] vs. 16/32 [50.0%];  $p = 0.04$ ), and less frequently had fibrocavitary disease (51/220 [23.2%] vs. 20/32 [62.5%];  $p < 0.001$ ).

Patients were followed for an average of 40.1 months. Ten patients with Mav-PD left follow up within 12 months of treatment initiation; of those, 8 were treated in the late period. Four patients with Mx-PD left follow up within 12 months of treatment initiation; 3 of those were treated in the early period.

Antibiotic treatment differed somewhat between periods among patients with Mav-PD (Table 3).

Rifamycins were used more often in the late period than in the early period (79.0% vs. 62.2%;  $p = 0.008$ ); fluoroquinolones were used less often in the late period than the early period (13.0% vs. 56.1%;  $p < 0.001$ ). In the late period, 23 patients (16.7%) were started on treatment with 2 drugs, compared with just 2 patients (2.4%) in the early period, but this factor did not result in more frequent treatment changes later. The type of treatment used for Mx-PD was similar in both periods. Treatment duration in the early and late period was comparable for Mav-PD and Mx-PD.

Culture conversion among patients with Mav-PD was less frequent in the late period than the early period (26.1% vs. 39.0%;  $p = 0.05$ ) (Table 4). Culture

**Table 3.** Antibiotic treatment in early and late period used for patients with *Mycobacterium avium* and *M. xenopi* pulmonary disease, Toronto, Ontario, Canada\*

| Treatment                       | <i>M. avium</i>      |                      |                  | <i>M. xenopi</i>     |                    |          |
|---------------------------------|----------------------|----------------------|------------------|----------------------|--------------------|----------|
|                                 | Early period, n = 82 | Late period, n = 138 | p value          | Early period, n = 24 | Late period, n = 8 | p value  |
| Initial treatment               |                      |                      |                  |                      |                    |          |
| Macrolide                       | 82 (100)             | 138 (100)            | Referent         | 23 (95.8)            | 8 (100)            | Referent |
| Ethambutol                      | 78 (95.1)            | 126 (91.3)           | 0.42             | 21 (87.5)            | 8 (100)            | 0.55     |
| Rifamycin                       | 51 (62.2)            | 109 (79.0)           | <b>0.008</b>     | 14 (58.3)            | 6 (75.0)           | 0.68     |
| Fluoroquinolone                 | 46 (56.1)            | 18 (13.0)            | <b>&lt;0.001</b> | 9 (37.5)             | 3 (37.5)           | Referent |
| IV amikacin                     | 1 (1.2)              | 2 (1.5)              | Referent         | 1 (4.2)              | 0                  | Referent |
| Other                           | 0                    | 2 (1.5)†             | 0.53             | 2 (8.3)‡             | 0                  | Referent |
| Total initial drugs             |                      |                      |                  |                      |                    |          |
| 2 drugs                         | 2 (2.4)              | 23 (16.7)            | <b>0.001</b>     | 5 (20.8)             | 1 (12.5)           | 0.66     |
| 3 drugs                         | 67 (81.7)            | 111 (80.4)           |                  | 16 (66.7)            | 5 (62.5)           |          |
| >3 drugs                        | 13 (15.9)            | 4 (2.9)              |                  | 3 (12.5)             | 2 (25.0)           |          |
| Amikacin added                  |                      |                      |                  |                      |                    |          |
| IV                              | 20 (24.4)            | 23 (16.7)            | 0.62             | 7 (29.2)             | 1 (12.5)           | 0.68     |
| Inhaled only                    | 1 (1.2)              | 7 (5.1)              |                  | 2 (8.3)              | 1 (12.5)           |          |
| Treatment adapted               | 16 (19.5)            | 36 (26.1)            | 0.33             | 11 (45.8)            | 3 (37.5)           | Referent |
| Treatment intensified           | 7 (8.5)              | 15 (10.9)            | 0.65             | 9 (37.5)             | 2 (25.0)           | 0.68     |
| Median total duration, mo (IQR) | 21 (13.3–31.5)       | 18 (13.0–28.8)       | 0.38             | 15.5 (10.8–26.0)     | 18 (10.8–20.5)     | Referent |

\*Values are no. (%) except as indicated. Bold indicates significance. Drugs were counted toward initial treatment if started within the first 3 months of treatment. Changes in treatment were regarded as treatment adaptations if they took place after the first 3 months of treatment. Treatment adaptations were considered intensification if they resulted in a higher number of drugs used. IV, intravenous.

†Clofazimine in 1 patient, inhaled amikacin in 1 patient.

‡Clofazimine in 1 patient, linezolid in 1 patient.

**Table 4.** Outcomes of treatment in patients with *Mycobacterium avium* and *M. xenopi* pulmonary disease, Toronto, Ontario, Canada\*

| Outcome   | <i>M. avium</i>         |                         |             | <i>M. xenopi</i>        |                       |          |
|---|-------------------------|-------------------------|-------------|-------------------------|-----------------------|----------|
|   | Early period,<br>n = 82 | Late period,<br>n = 138 | p value     | Early period,<br>n = 24 | Late period,<br>n = 8 | p value  |
| Mean duration of follow up after treatment initiation, mo (IQR) | 31.0 (19.3–44.0)        | 31.0 (18.3–39.0)        | 0.23        | 28.0 (14.8–53.0)        | 18.5 (12.8–25.8)      | 0.32     |
| Culture conversion†   | 32 (39.0)               | 36 (26.1)               | <b>0.05</b> | 16 (66.7)               | 5 (62.5)              | Referent |
| Toronto-York region‡  | 29/68 (42.6)            | 26/109 (23.9)           | <b>0.01</b> | 14/19 (73.7)            | 5/6 (83.3)            | Referent |
| Outside Toronto-York region                                     | 3/14 (21.4)             | 10/29 (34.5)            | 0.49        | 2/5 (40.0)              | 0/2                   | Referent |
| Culture reversion   | 4 (12.5)                | 11 (30.6)               | 0.09        | 1/16 (6.25)             | 0/5                   | Referent |
| Clinical treatment success§                                     | 56 (68.3)               | 88 (63.8)               | 0.47        | 15 (62.5)               | 5 (62.5)              | Referent |

\*Values are no. (%) except as indicated. Bold indicates significance. Culture reversion is presented as no. (%) of patients out of those who had culture conversion). Patients with insufficient samples submitted for evaluation of culture conversion were deemed not converted. Patients with missing follow up computed tomography results were considered not clinically successful.

†Overall insufficient samples: *M. avium* early period, 19 (23.2%); *M. avium* late period, 23 (16.7%); *M. xenopi* early period, 4 (16.7%); *M. xenopi* late period, 2 (25%).

‡Insufficient samples among Toronto-York region patients: *M. avium* early period, 12 (17.6%); *M. avium* late period, 16 (14.7%); *M. xenopi* early period, 3 (15.8%); *M. xenopi* late period, 0.

§Missing computed tomography results: *M. avium* early period, 4 (5.0%); *M. avium* late period, 9 (6.5%); *M. xenopi* early period, 1 (4.2%); *M. xenopi* late period, 1 (12.5%).

reversion to positive after conversion to negative was numerically higher in the late period (30.6% vs. 12.5%;  $p = 0.09$ ). Culture conversion among patients with Mx-PD was stable between the 2 periods and much higher (21/32 patients [65.6%]) than conversion among patients with Mav-PD (68/220 patients [30.9%];  $p < 0.001$ ). Although we assumed a failure to culture convert if inadequate samples were submitted, recalculating after excluding patients with incomplete data did not change our comparative outcomes. Clinical treatment success was fairly consistent between periods and species.

## Discussion

After the increase in isolation frequency of *M. avium* in Toronto and the Regional Municipality of York, we observed a rise in the relative proportion of patients treated for Mav-PD at our center. The patients with Mav-PD who were treated after this increase occurred achieved culture conversion less often and had a numerically (but not statistically) higher risk for culture reversion, although their baseline characteristics were comparable and clinical treatment success did not differ.

A sudden population-based increase in the frequency of *M. avium* isolation, as was recently observed in parts of Ontario, has not been reported elsewhere. Meanwhile, we observed a relative increase in treated NTM-PD caused by *M. avium* but not NTM-PD caused by *M. intracellulare*. The increase in *M. avium* isolation is broadly consistent with previous observations in Ontario (14), parts of the United Kingdom (12), Catalonia (19) and Hawaii, USA (increased MAC isolation) (20), and more specifically in the Netherlands (increased *M. avium* isolation) (21). In Queensland, Australia, the magnitude of increase in *M. intracellulare* exceeded that of *M. avium* (1). In

Madrid, Spain, the isolation rate of *M. avium* was stable, whereas in Belgium the rate of *M. intracellulare* increased and the rate of *M. xenopi* decreased (22,23). The frequency of NTM-PD and MAC-PD in Denmark was relatively stable during 1997–2008 (24), but the prevalence of NTM-PD in Hawaii doubled from 2005 to 2013 (20). In addition, in the United States, substantial increases in NTM-PD overall have been identified in Medicare beneficiaries during 1997–2007 (25) and in both commercial managed care and Medicare settings during 2008–2015 (26). Species-level population-based data for Japan are unavailable, but regional data demonstrated that increases in MAC-PD consisted of increases caused by *M. avium* and *M. intracellulare* in both Nagasaki prefecture (27) and Kyoto (28).

Although the increase in isolation of *M. avium* observed in Ontario was temporally associated with a higher frequency of Mav-PD in our cohort, this association alone does not demonstrate causality. The lack of changes at the laboratory level suggests a change either in the number of persons with *M. avium* isolation or higher clinician awareness and more investigations (sputum sampling and CT scans). However, no coinciding proportional increase in sputum submission to the PHOL occurred during the increase in *M. avium* isolation (13). Although an increase in use of chest CT has been described in Ontario, the increase was nearly linear during 2007–2016 (29). Given the lack of obvious detection bias, the abrupt rise in pulmonary *M. avium* isolation is likely reflective of a population-based phenomenon of more persons with *M. avium*-positive sputum, which in turn led to the changes observed in the clinic. However, the evidence remains circumstantial.

For patients with Mav-PD in our cohort, culture conversion in the early period (39%) was lower than the ~60% that would be expected on the basis of a

meta-analysis from 2017 (30). Although this difference might be accounted for by the setting and severity of disease, culture conversion in the late period was even lower, occurring in only 26% of patients. In our secondary analysis, we included only patients living in the Toronto and York regions, which resulted in an even more substantial decrease in culture conversion over time. In addition, in the early period, we observed a frequency of culture reversion that was comparable to a large retrospective series (14% microbiologic recurrence on treatment, similar to the definition of reversion used in our study) (31), whereas reversion seemed to be more frequent in the late period.

The reduction in culture conversion between periods could be related to treatment regimens. Even though a third drug was more often omitted in the late period, this omission was mostly because of less frequent use of fluoroquinolones, and their effectiveness in treating *M. avium* is debatable (32). In addition, rifampin was used more often in the late period, making 3-drug treatment more often in line with current guidelines. Our low overall proportion of culture conversion could be seen as surprising. Accordingly, factors influencing culture conversion, despite not being the primary focus of this study, merited further consideration. In light of the large proportion of patients with cavitation on their CT results, the paucity of injectable amikacin therapy in the initial regimen might suggest inadequate treatment. We generally initiate oral therapy first and allow time for the patient to acclimate and for adjustment of drugs and doses before adding amikacin, which is usually added after  $\approx 12$  weeks and thus not classified in our initial 12-week regimen. In addition, we did not employ a minimum-size criterion for cavitation, so a large proportion of patients classified as such likely had small cavities ( $\leq 2$  cm), which might represent foci of bronchiectasis without substantial extrabronchial parenchymal destruction, for which parenteral therapy might not be required. The proportion of patients with Mx-PD who received amikacin was lower still. The reasons for this difference are unclear, although anecdotally, a substantially larger proportion of patients with *M. xenopi* might have declined the recommendation for peripherally inserted central catheter placement and intravenous therapy. On the other hand, acquiring new strains after treatment has begun might explain sputum culture reversion after successful conversion (33). Exposure to new strains because of higher levels of exposure might also be a factor in both the overall low conversion rate and the further reduction in the late period.

Because *M. avium* is acquired from the environment, probably more likely from water aerosols

than from soil (9–11,34), and higher levels of exposure have been linked with more frequent NTM-PD (10,35), increased exposure is a plausible mechanism for the changes that were observed in Ontario. Host susceptibility also plays a role in acquiring disease (6,36) but would be expected to change only gradually over time. Alterations in behavior, such as increased shower use (10) or climate changes leading to different surface water microbiome or higher atmospheric water content (9), could increase exposure but would not be restricted to such a narrowly defined region. *M. avium* colonizing municipal water and household plumbing might be a substantial source of Mav-PD (34). Also, all of the drinking water for Toronto and a large proportion of drinking water for the York region is sourced from Lake Ontario and treated in 1 of 4 water treatment plants, all of which use the same protocols for filtration and disinfection, before the water is pumped northward to consumers in Toronto and much of the York region. Although definitive proof is lacking, changes in the municipal water or its complex distribution system could potentially be causes of increased exposure. This serious public health issue needs additional research, ideally including evaluation of water samples at different sites. Toronto Public Health did not find geographic clustering within Toronto, but whether water testing was performed is unclear (13), and Ontario drinking water regulations do not mandate testing for NTM. Other potential confounding factors could not be evaluated in this study.

The consistent clinical treatment success for Mav-PD between periods, despite microbiologic outcomes, is encouraging. It appears that clinical results of treatment in our setting are not exclusively dependent upon culture conversion. For example, patients with more extensive disease at start of treatment might have lower chances of conversion but could still have a good clinical result, presumably associated with a reduction in burden of the organism. We lacked detailed data regarding the burden of organism (i.e., colony counts on solid media) and tried to remediate this shortcoming by looking at sputum smear conversion, but not enough useful data were available. In addition, the possibility of acquisition of new strains of *M. avium* during treatment could not be addressed.

A strength of our study is that comparing outcomes of patients before and after the increase in *M. avium* isolation at the largest NTM referral clinic within the area of increase provides data on a large sample of relevant patients divided over distinct time periods. In addition, by applying broad selection criteria, we were able to include most patients that were

treated for NTM-PD caused by *M. avium* or *M. xenopi* at our center, and the number of patients who did not complete follow up was low.

The first limitation of our study is that several patients in the late period were likely infected before the increase in *M. avium* isolation was observed, because NTM-PD is a chronic disease and treatment initiation might not accurately represent timing of infection. Nevertheless, treatment initiation is undoubtedly related to the infection progressing, which in turn could be influenced by increased exposure, so this approach was most suited to our objectives. Second, patients that were previously treated could have lower conversion rates. Because we excluded patients from the late period who were included in the early period, we expected previous treatment to be more frequent in the early period, and this factor could have reduced the likelihood of detecting a difference in outcomes. However, both Mav-PD groups had comparable levels of previous treatment, so the effect on our results was likely not substantial. Third, we would ideally have studied only patients living in Toronto and the York region, but because we only possessed patients' addresses at the time of data collection and patients could have moved in or out of the area during treatment, we had to limit this evaluation to a secondary analysis. Last, because sputum samples were collected at the discretion of the treating physician and according to patients' willingness, the timing and number of samples varied considerably between patients. However, we could not discern any sort of sampling bias that could have influenced the outcomes. We assumed a failure to culture convert if inadequate samples were submitted, but recalculating conversion frequencies after excluding patients with incomplete data did not change our comparative outcomes.

The increased isolation of *M. avium* in Ontario was temporally associated with a higher relative number of patients with Mav-PD, less frequent culture conversion, and a trend toward more frequent culture reversion in Mav-PD patients in our NTM clinic in Toronto. Our findings suggest the presence of a causal relationship between the increased frequency of *M. avium* isolation and clinical events, and by extension, the importance of investigations into the cause and public health consequences of the higher number of *M. avium* isolates.

### About the Author

Dr. Raats studied medicine in Belgium at the University of Leuven and trained at the University Hospital in Leuven to become a pulmonologist. After finishing his training, he did a fellowship in tuberculosis and nontuberculous

mycobacteria at the University of Toronto under supervision of Dr. Marras and Dr. Brode, where most of this work was done. He works at the Ziekenhuis Oost-Limburg in Genk, Belgium as a general pulmonologist with special interest in mycobacterial diseases.

### References

1. Thomson RM; NTM working group at Queensland TB Control Centre and Queensland Mycobacterial Reference Laboratory. Changing epidemiology of pulmonary nontuberculous mycobacteria infections. *Emerg Infect Dis.* 2010;16:1576–83. <https://doi.org/10.3201/eid1610.091201>
2. Marras TK, Mendelson D, Marchand-Austin A, May K, Jamieson FB. Pulmonary nontuberculous mycobacterial disease, Ontario, Canada, 1998–2010. *Emerg Infect Dis.* 2013;19:1889–91. <https://doi.org/10.3201/eid1911.130737>
3. Prevots DR, Shaw PA, Strickland D, Jackson LA, Raebel MA, Blosky MA, et al. Nontuberculous mycobacterial lung disease prevalence at four integrated health care delivery systems. *Am J Respir Crit Care Med.* 2010;182:970–6. <https://doi.org/10.1164/rccm.201002-0310OC>
4. McCallum AD, Watkin SW, Faccenda JF. Non-tuberculous mycobacterial infections in the Scottish Borders: identification, management and treatment outcomes – a retrospective review. *J R Coll Physicians Edinb.* 2011;41:294–303. <https://doi.org/10.4997/JRCPE.2011.403>
5. Namkoong H, Kurashima A, Morimoto K, Hoshino Y, Hasegawa N, Ato M, et al. Epidemiology of pulmonary nontuberculous mycobacterial disease, Japan. *Emerg Infect Dis.* 2016;22:1116–7. <https://doi.org/10.3201/eid2206.151086>
6. Prevots DR, Marras TK. Epidemiology of human pulmonary infection with nontuberculous mycobacteria: a review. *Clin Chest Med.* 2015;36:13–34. <https://doi.org/10.1016/j.ccm.2014.10.002>
7. Marras TK, Mirsaeidi M, Chou E, Eagle G, Zhang R, Leuchars M, et al. Health care utilization and expenditures following diagnosis of nontuberculous mycobacterial lung disease in the United States. *J Manag Care Spec Pharm.* 2018;24:964–74. <https://doi.org/10.18553/jmcp.2018.18122>
8. Ramsay LC, Shing E, Wang J, Marras TK, Kwong JC, Brode SK, et al. Costs associated with nontuberculous mycobacteria infection, Ontario, Canada, 2001–2012. *Emerg Infect Dis.* 2020;26:2097–107. <https://doi.org/10.3201/eid2609.190524>
9. Adjemian J, Olivier KN, Prevots DR. Nontuberculous mycobacteria among patients with cystic fibrosis in the United States: screening practices and environmental risk. *Am J Respir Crit Care Med.* 2014;190:581–6. <https://doi.org/10.1164/rccm.201405-0884OC>
10. Tzou CL, Dirac MA, Becker AL, Beck NK, Weigel KM, Meschke JS, et al. Association between *Mycobacterium avium* complex pulmonary disease and mycobacteria in home water and soil. *Ann Am Thorac Soc.* 2020;17:57–62. <https://doi.org/10.1513/AnnalsATS.201812-915OC>
11. Maekawa K, Ito Y, Hirai T, Kubo T, Imai S, Tatsumi S, et al. Environmental risk factors for pulmonary *Mycobacterium avium*-intracellulare complex disease. *Chest.* 2011;140:723–9. <https://doi.org/10.1378/chest.10-2315>
12. Shah NM, Davidson JA, Anderson LF, Lalor MK, Kim J, Thomas HL, et al. Pulmonary *Mycobacterium avium*-intracellulare is the main driver of the rise in non-tuberculous mycobacteria incidence in England, Wales and Northern Ireland, 2007–2012. *BMC Infect Dis.* 2016;16:195. <https://doi.org/10.1186/s12879-016-1521-3>

13. Boyle T. Public health vexed by bacterium. *The Toronto Star*. 2015 Nov 17.
14. Al Houqani M, Jamieson F, Chedore P, Mehta M, May K, Marras TK. Isolation prevalence of pulmonary nontuberculous mycobacteria in Ontario in 2007. *Can Respir J*. 2011;18:19–24. <https://doi.org/10.1155/2011/865831>
15. Griffith DE, Aksamit T, Brown-Elliott BA, Catanzaro A, Daley C, Gordin F, et al.; ATS Mycobacterial Diseases Subcommittee; American Thoracic Society; Infectious Disease Society of America. An official ATS/IDSA statement: diagnosis, treatment, and prevention of nontuberculous mycobacterial diseases. *Am J Respir Crit Care Med*. 2007;175:367–416. <https://doi.org/10.1164/rccm.200604-571ST>
16. Jick SS, Lieberman ES, Rahman MU, Choi HK. Glucocorticoid use, other associated factors, and the risk of tuberculosis. *Arthritis Rheum*. 2006;55:19–26. <https://doi.org/10.1002/art.21705>
17. Carrillo MC, Patsios D, Wagnetz U, Jamieson F, Marras TK. Comparison of the spectrum of radiologic and clinical manifestations of pulmonary disease caused by *Mycobacterium avium* complex and *Mycobacterium xenopi*. *Can Assoc Radiol J*. 2014;65:207–13. <https://doi.org/10.1016/j.carj.2013.05.006>
18. van Ingen J, Aksamit T, Andrejak C, Böttger EC, Cambau E, Daley CL, et al.; for NTM-NET. Treatment outcome definitions in nontuberculous mycobacterial pulmonary disease: an NTM-NET consensus statement. *Eur Respir J*. 2018;51:1800170. <https://doi.org/10.1183/13993003.00170-2018>
19. Santin M, Barrabeig I, Malchair P, Gonzalez-Luquero L, Benitez MA, Sabria J, et al. Pulmonary infections with nontuberculous mycobacteria, Catalonia, Spain, 1994–2014. *Emerg Infect Dis*. 2018;24:1091–4. <https://doi.org/10.3201/eid2406.172095>
20. Adjemian J, Frankland TB, Daida YG, Honda JR, Olivier KN, Zelazny A, et al. Epidemiology of nontuberculous mycobacterial lung disease and tuberculosis, Hawaii, USA. *Emerg Infect Dis* 2017;23:439–47.
21. van Ingen J, Hoefsloot W, Dekhuijzen PN, Boeree MJ, van Soolingen D. The changing pattern of clinical *Mycobacterium avium* isolation in the Netherlands. *Int J Tuberc Lung Dis*. 2010;14:1176–80.
22. Soetaert K, Subissi L, Ceysens PJ, Vanfleteren B, Chantrenne M, Asikainen T, et al. Strong increase of true and false positive mycobacterial cultures sent to the National Reference Centre in Belgium, 2007 to 2016. *Euro Surveill*. 2019;24:1800205. <https://doi.org/10.2807/1560-7917.ES.2019.24.11.1800205>
23. López-Roa P, Aznar E, Cacho J, Cogollos-Agruña R, Domingo D, García-Arata MI, et al. Epidemiology of non-tuberculous mycobacteria isolated from clinical specimens in Madrid, Spain, from 2013 to 2017. *Eur J Clin Microbiol Infect Dis*. 2020;39:1089–94. <https://doi.org/10.1007/s10096-020-03826-7>
24. Andrejak C, Thomsen VØ, Johansen IS, Riis A, Benfield TL, Duhaut P, et al. Nontuberculous pulmonary mycobacteriosis in Denmark: incidence and prognostic factors. *Am J Respir Crit Care Med*. 2010;181:514–21. <https://doi.org/10.1164/rccm.200905-0778OC>
25. Adjemian J, Olivier KN, Seitz AE, Holland SM, Prevots DR. Prevalence of nontuberculous mycobacterial lung disease in U.S. Medicare beneficiaries. *Am J Respir Crit Care Med*. 2012;185:881–6. <https://doi.org/10.1164/rccm.201111-2016OC>
26. Winthrop KL, Marras TK, Adjemian J, Zhang H, Wang P, Zhang Q. Incidence and prevalence of nontuberculous mycobacterial lung disease in a large U.S. managed care health plan, 2008–2015. *Ann Am Thorac Soc*. 2020;17:178–85. <https://doi.org/10.1513/AnnalsATS.201804-236OC>
27. Ide S, Nakamura S, Yamamoto Y, Kohno Y, Fukuda Y, Ikeda H, et al. Epidemiology and clinical features of pulmonary nontuberculous mycobacteriosis in Nagasaki, Japan. *PLoS One*. 2015;10:e0128304. <https://doi.org/10.1371/journal.pone.0128304>
28. Ito Y, Hirai T, Fujita K, Maekawa K, Niimi A, Ichiyama S, et al. Increasing patients with pulmonary *Mycobacterium avium* complex disease and associated underlying diseases in Japan. *J Infect Chemother*. 2015;21:352–6.
29. Smith-Bindman R, Kwan ML, Marlow EC, Theis MK, Bolch W, Cheng SY, et al. Trends in use of medical imaging in US health care systems and in Ontario, Canada, 2000–2016. *JAMA*. 2019;322:843–56. <https://doi.org/10.1001/jama.2019.11456>
30. Kwak N, Park J, Kim E, Lee CH, Han SK, Yim JJ. Treatment outcomes of *Mycobacterium avium* complex lung disease: a systematic review and meta-analysis. *Clin Infect Dis*. 2017;65:1077–84. <https://doi.org/10.1093/cid/cix517>
31. Wallace RJ Jr, Brown-Elliott BA, McNulty S, Philley JV, Killingley J, Wilson RW, et al. Macrolide/azalide therapy for nodular/bronchiectatic *Mycobacterium avium* complex lung disease. *Chest*. 2014;146:276–82. <https://doi.org/10.1378/chest.13-2538>
32. Daley CL, Iaccarino JM, Lange C, Cambau E, Wallace RJ Jr, Andrejak C, et al. Treatment of nontuberculous mycobacterial pulmonary disease: an official ATS/ERS/ESCMID/IDSA clinical practice guideline. *Eur Respir J*. 2020;56:2000535. <https://doi.org/10.1183/13993003.00535-2020>
33. Jhun BW, Kim S-Y, Moon SM, Jeon K, Kwon OJ, Huh HJ, et al. Development of macrolide resistance and reinfection in refractory *Mycobacterium avium* complex lung disease. *Am J Respir Crit Care Med*. 2018;198:1322–30. <https://doi.org/10.1164/rccm.201802-0321OC>
34. Lande L, Alexander DC, Wallace RJ Jr, Kwait R, Iakhiaeva E, Williams M, et al. *Mycobacterium avium* in community and household water, suburban Philadelphia, Pennsylvania, USA, 2010–2012. *Emerg Infect Dis*. 2019;25:473–81. <https://doi.org/10.3201/eid2503.180336>
35. Gebert MJ, Delgado-Baquerizo M, Oliverio AM, Webster TM, Nichols LM, Honda JR, et al. Ecological analyses of mycobacteria in showerhead biofilms and their relevance to human health. *MBio*. 2018;9:e01614–8. <https://doi.org/10.1128/mBio.01614-18>
36. Dirac MA, Horan KL, Doody DR, Meschke JS, Park DR, Jackson LA, et al. Environment or host? A case-control study of risk factors for *Mycobacterium avium* complex lung disease. *Am J Respir Crit Care Med*. 2012;186:684–91. <https://doi.org/10.1164/rccm.201205-0825OC>

---

Address for correspondence: Daan Raats, Ziekenhuis Oost-Limburg, Department of Respiratory Medicine, Schiepse Bos 5, 3600 Genk, Belgium; email: daan.raats@zol.be

# Dog Ownership and Risk for Alveolar Echinococcosis, Germany

Julian Schmidberger,<sup>1</sup> Janne Uhlenbruck,<sup>1</sup> Patrycja Schlingeloff,  
Pavlo Maksimov, Franz J. Conraths, Benjamin Mayer, Wolfgang Kratzer

Human alveolar echinococcosis is caused by the parasite *Echinococcus multilocularis*, and dog ownership has been identified as a risk factor. We sought to specify the factors of dog ownership underlying this risk by conducting a case–control study among dog owners in Germany. The analysis revealed an increased odds ratio of  $\approx 7$ -fold for dog owners whose dogs roam unattended in fields, 13-fold for dog owners who feed their dogs organic waste daily, 4-fold for dog owners who take their dog to a veterinarian only in case of illness, and 10-fold for dog owners who have never been informed by a veterinarian about the risk for infection. The results highlight the risk for infection associated with various factors of dog ownership and the value of veterinarians informing owners about prevention.

Human alveolar echinococcosis is a rare disease that can be caused by the parasite *Echinococcus multilocularis* (1,2). The pathogen *E. multilocularis* and human cases of the disease are predominantly distributed in the northern hemisphere (3,4). The most heavily affected countries in central Europe include Germany, France, Switzerland, and Austria (1,5), but large parts of Russia and China are also affected (1,5). Approximately 70%–80% of human cases in Germany are distributed in the main *E. multilocularis*-endemic areas of Baden-Württemberg and Bavaria. High-risk areas are found in the area of the Swabian Alb, the Alps, and the Alpine foothills (6). The prevalence of *E. multilocularis* infections in foxes in those areas is 40%–60% (7).

The life and development cycle of *E. multilocularis* parasites involves definitive and intermediate hosts.

---

Author affiliations: University Hospital Ulm, Ulm, Germany (J. Schmidberger, J. Uhlenbruck, P. Schlingeloff, W. Kratzer); Friedrich-Loeffler-Institute, Federal Research Institute for Animal Health, Greifswald-Insel Riems, Germany (P. Maksimov, F.J. Conraths); Institute for Epidemiology and Medical Biometry, Ulm (B. Mayer)

DOI: <https://doi.org/10.3201/eid2808.212514>

Adult *E. multilocularis* parasites usually colonize the small intestine of carnivores, mostly red foxes (*Vulpes vulpes*), dogs, and cats (2,8,9). These hosts excrete infectious worm eggs into the environment in their feces, through which small mammals, such as field mice (*Microtus arvalis*), voles (Arvicolinae), bank voles (*Myodes glareolus*), and other species can become infected. In the intermediate hosts, larval *E. multilocularis* stages (metacestodes) usually grow in the liver, where they cause alveolar echinococcosis and travel with the blood or lymph to other organs, behaving similarly to malignant tumors. In this process, the parasite can irreversibly damage the organs of the intermediate host, which can lead to death (1,8,9). A diseased intermediate host represents easier prey for the final host, because of its disease manifestations and symptoms, closing the development cycle. Humans can be terminal intermediate hosts who, similar to other intermediate hosts, inadvertently ingest worm eggs (fecal–oral route) and produce metacestodes. In >98% of cases of human infection, the liver is the primary organ affected (2).

Risk factors for human alveolar echinococcosis have so far been incompletely investigated. The currently available case–control studies of risk factors are relatively old or cannot be applied to the situation in Germany (10–13). Studies in France, Austria, and Alaska (USA), suggest that dog ownership is one of the most significant risk factors for infection with *E. multilocularis* and development of alveolar echinococcosis (11–13). A case–control study conducted in Germany in 2004, involving 40 patients and 120 controls, found increased odds ratios (ORs) for owners of dogs that poach and run unattended outdoors; persons who live close to fields, live in a farmhouse, farm, chew grass, and gather wood; and cat owners (10). To date, factors that could not be confirmed as significant include eating unwashed strawberries, picking berries far from the ground, and collecting mushrooms. A meta-analysis

---

<sup>1</sup>These authors contributed equally to this article.

considered those risk factors, including dog ownership (14). A systematic review and meta-analysis, in which 28 cross-sectional studies and 14 case-control studies were analyzed, also showed strong evidence for transmission by direct contact with dogs (15).

Data from the National Echinococcosis Registry Germany (<https://www.fuchsbandwurm.eu>), based on 673 patients with alveolar echinococcosis recorded during 1992–2018, show that 60%–75% of recorded patients own, have owned, or have had regular contact with >1 dogs. In Germany, according to a joint survey by the Central Association of Pet Owners (Zentralverband Zoologischer Fachbetrieb, <https://www.zzf.de>) and the Pet Supplies Industry Association (Industrieverband Heimtierbedarf, <https://www.ivh-online.de>), an estimated 9.4 million dogs lived in 19% of households in 2018. This estimate represents an increase of 2 million dogs since 2011 (16,17). Our aim with this case-control study was to further specify and examine in more detail the factors of dog ownership that are potential risk factors for human alveolar echinococcosis.

## Methods

### Study Design

For this case-control study, we recruited patients with alveolar echinococcosis from the National Echinococcosis Registry Germany and recruited healthy

volunteers from veterinary and veterinary medical facilities listed in the Veterinary Online Directory Germany (Figures 1, 2). We conducted a written survey of case-patients and controls during January 2019–February 2020 by using a questionnaire with 45 questions with dichotomous expressions and a 3–5-point Likert scale prepared for this purpose. The questionnaire included general questions about the dog (e.g., breed, coat length, sex) and its dietary behavior, deworming, grooming, and cleaning, as well as human dog-ownership habits.

### Alveolar Echinococcosis Case-Patients

The National Echinococcosis Registry Germany is a national disease registry that is part of a Deutsche Forschungsgemeinschaft-funded project in cooperation with the Robert Koch Institute (6). The registry records on a voluntary basis all cases of the disease diagnosed in Germany since 1992 ( $n = 626$  as of December 31, 2018). Compared with the cases reportable to the Robert Koch Institute within the framework of the reporting obligation according to the Infection Protection Act (<https://www.gesetze-im-internet.de>), cases in the National Echinococcosis Registry Germany include extensive information on epidemiology, risk factors, diagnostics, treatments, and patient care. In accordance with the study design, we selected cases from Baden-Württemberg, an area in southern Germany where alveolar echinococcosis is highly endemic.

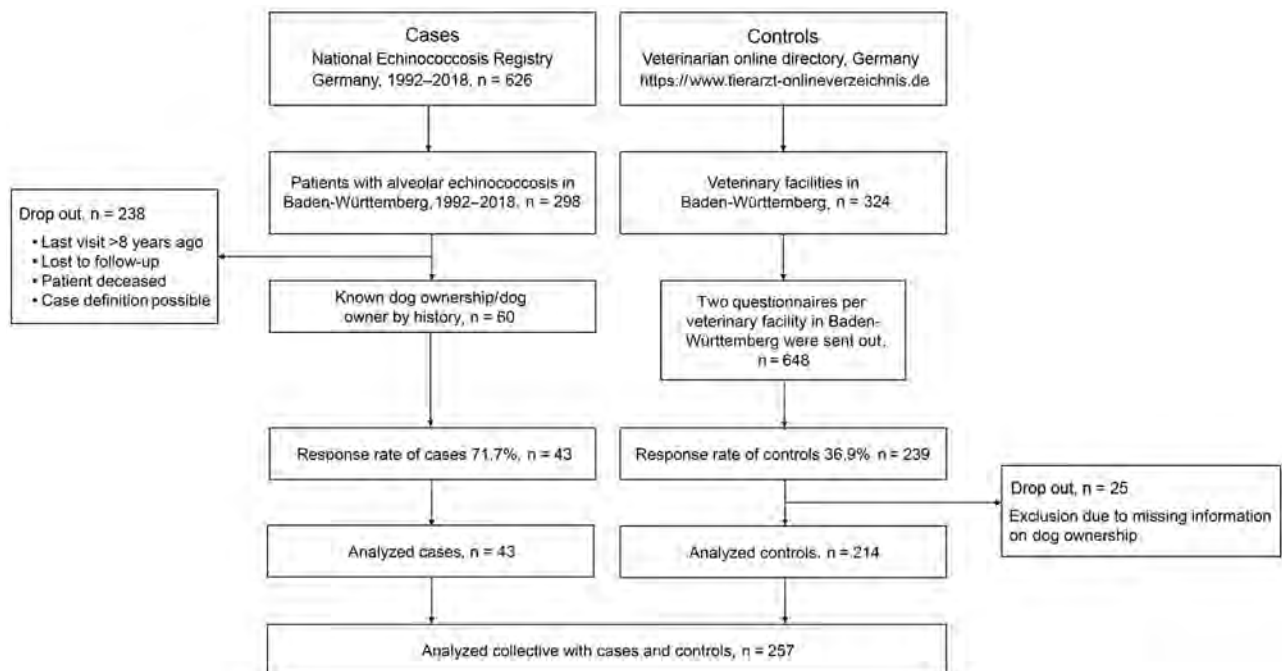


**Figure 1.** Inclusion and exclusion process for 43 case-patients and 214 controls in case-control study of dog ownership and human risk for alveolar echinococcosis, Baden-Württemberg, Germany, January 2019–February 2020.

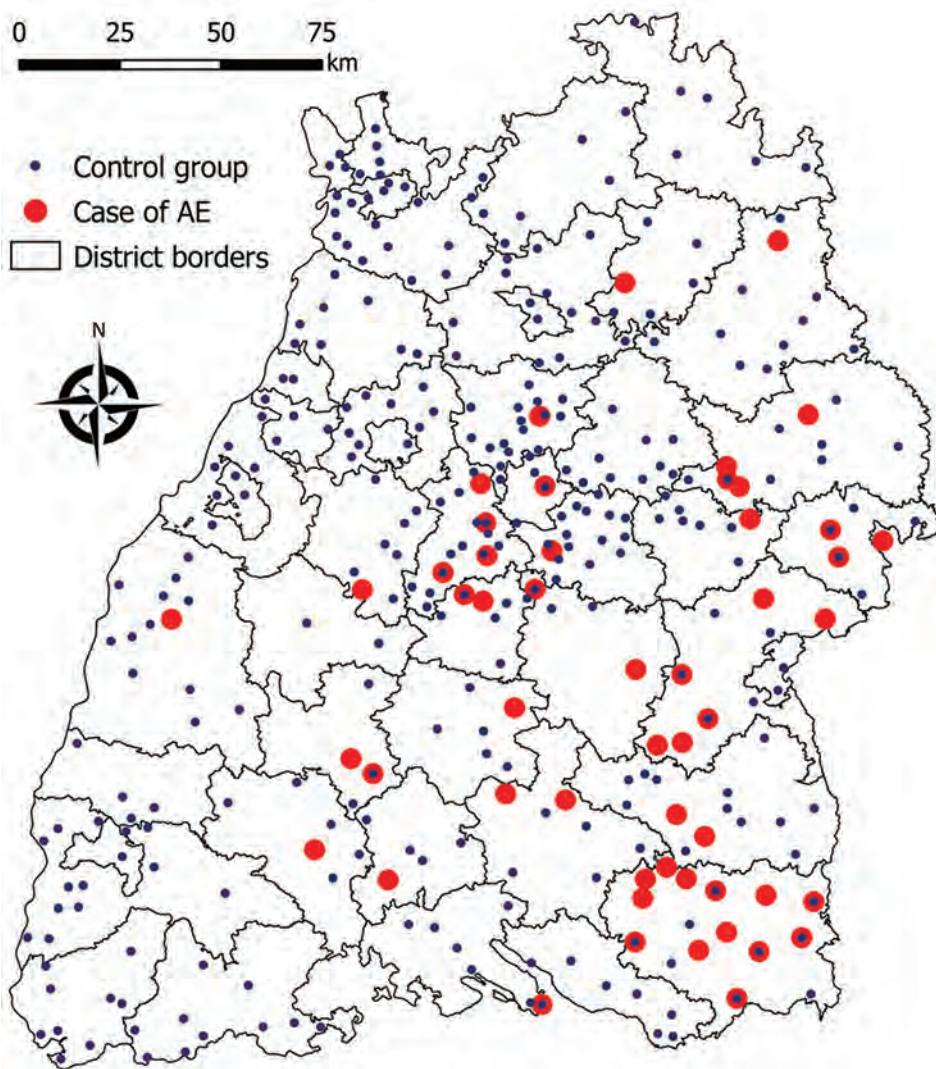


**Figure 2.** Distribution of 60 alveolar echinococcosis case-patients and 324 controls, Baden-Württemberg, Germany, January 2019–February 2020.

During 1992–2018, a total of 298 case-patients residing in Baden-Württemberg were registered in the national disease registry. Of these, we recruited 60 case-patients who, according to their medical history, owned dogs. Case-patients were excluded if their last visit to the hospital was >8 years earlier, if they had died, or if their case definition was only possible according to World Health Organization–Informal Working Group on Echinococcosis criteria (2) or no information on dog ownership was available ( $n = 238$  excluded patients). From the 60 contacted case-patients, we received 43 completed questionnaires from 43 dog owners with alveolar echinococcosis, resulting in a response rate of 71.7% (Figure 3, panel A).

#### Control Group

The Veterinary Online Directory Germany (<https://www.tierarzt-onlineverzeichnis.de>) includes all

veterinary facilities in Germany registered on a voluntary basis. We identified 324 veterinary facilities for Baden-Württemberg. We sent 2 questionnaires to each veterinary facility in Baden-Württemberg ( $n = 648$ ) and distributed them to dog owners without known alveolar echinococcosis. We received completed questionnaires back from 239 dog owners, resulting in a response rate of 36.9%. Of these questionnaires, we used 214 in the final analysis (Figure 3, panel B) and excluded 25 because of missing information about dog ownership.

#### Statistical Analyses

For statistical analyses, we used SAS version 9.4 (<https://www.sas.com>). We initially analyzed the data descriptively. We determined mean values  $\pm$ SDs and median, minimum, and maximum values and presented them as absolute or relative

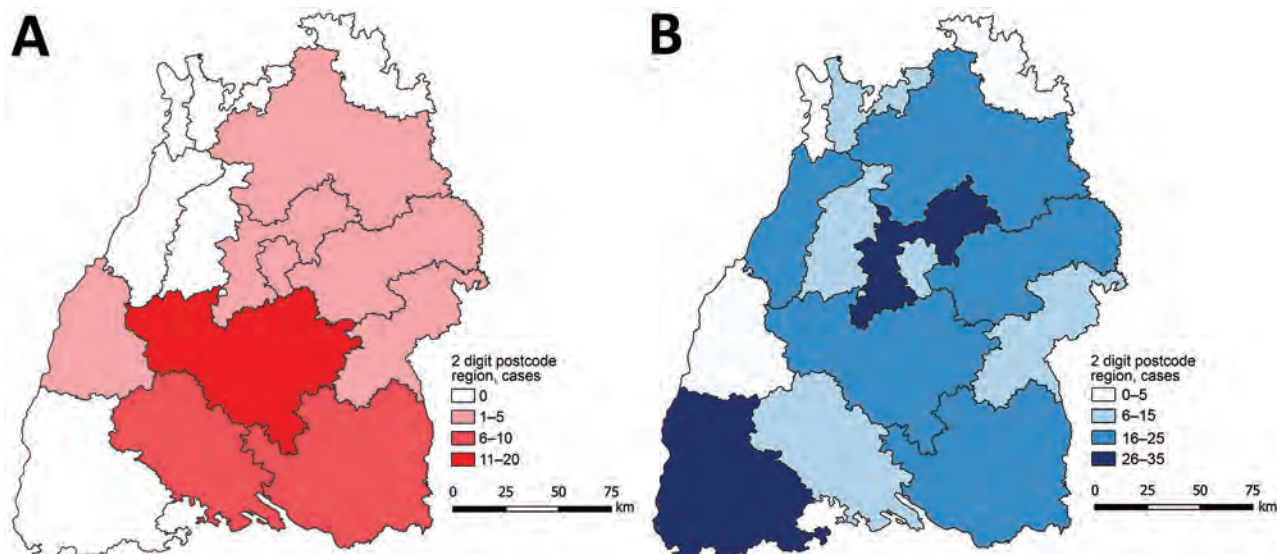


**Figure 3.** Choropleth map showing the distribution and frequency of 43 patients with alveolar echinococcosis (A) and 214 controls (B) who participated in case-control study of dog ownership and human risk for alveolar echinococcosis, by 2-digit postal code region, Baden-Württemberg, Germany, January 2019–February 2020.

frequencies. For variables that may influence the occurrence of alveolar echinococcosis, we used a multivariable logistic regression model to determine adjusted odds ratios (aORs), 95% CIs, and *p* values. Confounding variables determined a priori were included in the adjusted logistic regression model. We used Pearson  $\chi^2$  and Fisher exact tests to identify possible relationships and differences in frequency distributions between dichotomous variables. The significance level was set at  $\alpha = 0.05$ . Dot-density maps and choropleth maps of cases and controls and their distributions were created by using the QGIS geographic information system version 3.16.0 (<https://www.qgis.org>).

#### Ethics Statement

The study was approved by the local ethics committees of the University of Ulm (approval no. 125/20) and conducted according to the Declaration of Helsinki. Written informed consent was obtained from all case-patients and controls.

#### Results

The study included 43 persons with cases that fit the World Health Organization case definition of confirmed or probable (case-patients) and 214 controls from Baden-Württemberg. The mean age of the case-patients was  $50.09 \pm 17.62$  years and of controls was  $44.23 \pm 15.23$  years ( $p = 0.0347$ ). The proportion of women was significantly lower among case-patients (26/43 [60.47%]) than controls (177/214 [82.71%]) ( $\chi^2 = 10.6757$ ;  $p = 0.0011$ ).

A total of 41/43 (95.35%) case-patients and 182/214 (85.05%) controls reported that they had lived in Baden-Württemberg for >20 years ( $p = 0.0839$  by Fisher exact test) (Table 1). The main country of origin is Germany for dogs owned by case-patients 21/24 (87.50%) and 89/128 (69.53%) for dogs owned by controls ( $p = 0.08417$  by Fisher exact test). No information was available for the origin of the dogs for 19/43 (44.19%) of the case-patients and 86/214 (40.19%) of the controls.

#### Dog Ownership

The duration of dog ownership and regular contact with dogs was >20 years for 27/43 (62.79%) of the case-patients and 116/214 (54.21%) of the controls. The duration of dog ownership and regular contact with dogs was 11–20 years for 10/43 (23.26%) of the case-patients and for 48/214 (22.43%) of the controls. Thus, duration of dog ownership and regular contact with dogs did not differ significantly between the groups ( $\chi^2 = 1.2533$ ;  $p = 0.2629$ ).

The number of dogs owned also did not differ significantly between the groups ( $\chi^2 = 3.6938$ ;  $p = 0.0546$ ) but was remarkably discrepant between the groups (Table 1). In the case group, the proportion of dog owners with 1 dog was 32/43 (74.42%), and in the control group it was 122/214 (57.01%). The survey further revealed that 6/43 (13.95%) of the case-patients and 56/214 (26.17%) of the controls owned 2 dogs. The percentage of dog owners with >3 dogs was 3/43 (6.98%) for case-patients and 14/214 (6.54%) for controls (Table 1).

### Risk Behavior and Habits of Dog Owners

The aOR for alveolar echinococcosis increased by ≈7-fold for owners whose dogs roamed unattended in fields compared with owners whose dogs roamed unattended in yards (aOR 7.081, 95% CI 1.523–32.931;  $p = 0.0126$ ) (Table 2). For dog owners whose dogs rarely rolled in other animals' feces, odds of acquiring alveolar echinococcosis were lower (aOR 0.205, 95% CI 0.078–0.538;  $p = 0.0013$ ). Furthermore, the analysis revealed a nearly 13-fold increase in OR for alveolar echinococcosis among dog owners who fed their dogs organic waste daily (aOR 12.840, 95% CI 1.127–146.278;  $p = 0.0398$ ) (Table 2). ORs were potentially increased but not statistically significant for dog owners from rural communities (aOR 4.175, 95% CI 0.711–24.534,  $p = 0.9559$ ) and those whose dogs ate carrion or rodents (aOR 2.125, 95% CI 0.542–8.340,  $p = 0.2798$ ). Odds increased 7-fold for those who owned a herding dog (aOR 6.831, 95% CI 1.028–45.371), and having a dog with an undercoat seemed to be significantly protective (aOR 0.319, 95% CI 0.102–0.997) (Table 2).

### Dog Cleaning and Prevention Behavior

Multivariable logistic regression adjusted for age and sex revealed an almost 4-fold increased odds ratio for dog owners who took their dog to a veterinary facility only for illness compared with dog owners who sought veterinary care >1 time/year (aOR 3.657, 95% CI 1.480–9.039;  $p = 0.0050$ ). For dog owners who

never received information from a veterinarian about their own risk for *E. multilocularis* infection and possible prevention, the analysis further revealed a 10-fold increase in odds for alveolar echinococcosis (aOR 10.006, 95% CI 4.282–23.383;  $p < 0.0001$ ) (Table 2).

In contrast, for dog owners who never had their dog's feces tested for worm eggs, the odds for alveolar echinococcosis were not significantly increased (aOR 2.262, 95% CI 0.598–8.562;  $p = 0.2292$ ) (Table 2). Odds were increased by 7-fold for dog owners who never cleaned their dog's coat compared with dog owners who cleaned their dog's coat daily (aOR 7.567, 95% CI 0.655–87.406;  $p = 0.1050$ ), but the difference was not statistically significant. Furthermore, odds were not significantly increased between case-patient and control groups with regard to dog deworming ( $p > 0.05$ ).

### Discussion

Our case-control study of the potential contributions of factors of dog ownership to the risk for human alveolar echinococcosis in Baden-Württemberg was based on the findings of previous case-control studies and systematic reviews that described dog ownership as an evident risk factor for human alveolar echinococcosis (10–15). We found a significantly increased risk for alveolar echinococcosis among dog owners whose dogs roamed unattended in fields. Other factors that may increase risk are ownership of dogs in rural communities, dogs that roll in the feces of other animals, and dogs that eat carrion or prey.

**Table 1.** Characteristics of 257 dog owners with alveolar echinococcosis and healthy controls in case-control study of dog ownership and human risk for alveolar echinococcosis, Baden-Württemberg, Germany, January 2019–February 2020\*

| Characteristic                        | Case-patients, n = 43 | Controls, n = 214   | p value           |
|---------------------------------------|-----------------------|---------------------|-------------------|
| Sex, no. (%)                          |                       |                     | <b>0.0011</b>     |
| F                                     | 26 (60.47%)           | 177 (82.71%)        |                   |
| M                                     | 17 (39.53%)           | 37 (17.29%)         |                   |
| Age, y, no. (%)                       |                       |                     | <b>&lt;0.0001</b> |
| 18–30                                 | 8 (18.60%)            | 56 (26.17%)         |                   |
| 31–50                                 | 13 (30.23%)           | 71 (33.18%)         |                   |
| 51–70                                 | 15 (34.88%)           | 80 (37.38%)         |                   |
| >70                                   | 7 (16.28%)            | 7 (3.27%)           |                   |
| Age, y                                |                       |                     | <b>0.0347</b>     |
| Mean ± SD                             | 50.09 ± 17.62         | 44.23 ± 15.23       |                   |
| Median (range)                        | 51.00 (18.00–79.00)   | 44.00 (19.00–88.00) |                   |
| Time lived in Baden-Württemberg, y    |                       |                     | 0.0839            |
| 5–20                                  | 2 (4.65%)             | 32 (14.95%)         |                   |
| >20                                   | 41 (95.35%)           | 182 (85.05%)        |                   |
| Dogs owned, no. (%)                   |                       |                     | 0.0546            |
| 1                                     | 32 (74.42)            | 122 (57.01)         |                   |
| 2                                     | 6 (13.95)             | 56 (26.17)          |                   |
| 3                                     | 2 (4.65)              | 22 (10.28)          |                   |
| >3                                    | 3 (6.98)              | 14 (6.54)           |                   |
| Regular contact with dogs, y, no. (%) |                       |                     | 0.2629            |
| 0–5                                   | 4 (9.30)              | 16 (7.48)           |                   |
| 6–10                                  | 2 (4.65)              | 34 (15.89)          |                   |
| 11–20                                 | 10 (23.26)            | 48 (22.43)          |                   |
| >20                                   | 27 (62.79)            | 116 (54.21)         |                   |

\*Boldface indicates significance ( $p < 0.05$ ).

## RESEARCH

**Table 2.** Multivariable logistic regression analysis with estimations of odds of acquiring alveolar echinococcosis, Baden-Württemberg, Germany, January 2019–February 2020\*

| Variable                                   | Alveolar echinococcosis  |                   |
|--|--------------------------|-------------------|
|  | aOR (95% CI)             | p value†          |
| Community type, no. residents              |                          |                   |
| Large city, >100,000                       | Referent                 |                   |
| Middle city, 20,000–100,000                | 0.127 (0.009–1.789)      | 0.1263            |
| Small city, 5,000–20,000                   | 1.054 (0.161–6.917)      | 0.9559            |
| Rural community, <5,000                    | 4.175 (0.711–24.534)     | 0.9559            |
| Unattended                                 |                          |                   |
| Garden                                     | Referent                 |                   |
| Field                                      | 7.081 (1.523–32.931)     | <b>0.0126</b>     |
| Forest                                     | 1.221 (0.362–4.120)      | 0.7473            |
| Dog eats carrion or prey                   |                          |                   |
| Frequently                                 | 2.125 (0.542–8.340)      | 0.2798            |
| Rarely                                     | 0.514 (0.233–1.135)      | 0.0998            |
| Never                                      | Referent                 |                   |
| Dog rolls in feces from other animals      |                          |                   |
| Frequently                                 | 2.570 (0.962–6.865)      | 0.0598            |
| Rarely                                     | 0.205 (0.078–0.538)      | <b>0.0013</b>     |
| Never                                      | Referent                 |                   |
| Dog hunts mice or prey                     |                          |                   |
| Frequently                                 | 0.664 (0.242–1.821)      | 0.4260            |
| Rarely                                     | 0.766 (0.334–1.756)      | 0.5292            |
| Never                                      | Referent                 |                   |
| Dog eats organic waste from other animals  |                          |                   |
| Daily                                      | 12.840 (1.127–146.278)   | <b>0.0398</b>     |
| Weekly                                     | <0.001 (<0.001–>999.999) | 0.9843            |
| Monthly                                    | <0.001 (<0.001–>999.999) | 0.9908            |
| Never/ sporadic                            | Referent                 |                   |
| Frequency of fur cleaning                  |                          |                   |
| Daily                                      | Referent                 |                   |
| Weekly                                     | 0.472 (0.163–1.368)      | 0.1665            |
| Monthly                                    | 0.400 (0.075–2.140)      | 0.2840            |
| When soiled                                | 0.543 (0.216–1.366)      | 0.1945            |
| Never                                      | 7.567 (0.655–87.406)     | 0.1050            |
| Veterinary visits                          |                          |                   |
| Only in case of illness                    | 3.657 (1.480–9.039)      | <b>0.0050</b>     |
| 1 visit/y                                  | 2.003 (0.767–5.233)      | 0.1560            |
| >1 visit/y                                 | Referent                 |                   |
| Deworming frequency                        |                          |                   |
| 1 time/mo                                  | Referent                 |                   |
| 3–4 times/y                                | 0.183 (0.031–1.061)      | 0.0582            |
| 1 time/y                                   | 0.799 (0.125–5.091)      | 0.8124            |
| If infection is suspected                  | 0.190 (0.022–1.599)      | 0.1264            |
| Never                                      | 0.734 (0.064–8.437)      | 0.8040            |
| Feces tested for worm eggs                 |                          |                   |
| Regularly                                  | Referent                 |                   |
| If infection is suspected                  | 0.225 (0.045–1.118)      | 0.0681            |
| Never                                      | 2.262 (0.598–8.562)      | 0.2292            |
| Owner received education from veterinarian |                          |                   |
| Yes  | Referent                 |                   |
| No   | 10.006 (4.282–23.383)    | <b>&lt;0.0001</b> |
| Purpose of dog ownership                   |                          |                   |
| Hunting                                    | 0.332 (0.083–1.329)      | 0.1192            |
| Herding                                    | 6.831 (1.028–45.371)     | <b>0.0467</b>     |
| Sporting                                   | 0.668 (0.077–5.808)      | 0.7148            |
| Guard/watch dog                            | 2.776 (0.819–9.412)      | 0.1011            |
| Breeding                                   | <0.001 (<0.001–>999.999) | 0.1011            |
| Pet  | Referent                 |                   |
| Other                                      | 2.132 (0.149–30.566)     | 0.5773            |
| Coat length of the dog                     |                          |                   |
| Short, 1–2 cm                              | Referent                 |                   |
| Medium, 2–7 cm                             | 0.902 (0.371–2.192)      | 0.8205            |
| Long, >7 cm                                | 0.709 (0.205–2.446)      | 0.5860            |
| Undercoat                                  | 0.319 (0.102–0.997)      | <b>0.0493</b>     |

\*Model adjusted for age and sex. Boldface indicates significance (p<0.05).

Kern et al. demonstrated increased risk for owners of dogs that poach, owners of dogs that run unattended outdoors, and persons who live close to a field (10). Those results and ours are consistent with the fact that in the rural areas of the study region, there is a potential reservoir of the parasite in wildlife populations, particularly foxes (definitive hosts) and their natural prey (i.e., small mammals) (18). The overall risk may be elevated by increased environmental contamination with *E. multilocularis* eggs, including increased prevalence of dog feces in the environment.

Studies suggest that the prevalence of *E. multilocularis* parasites in dogs as the final host can vary greatly, depending on the study region, and may play a substantial role in transmitting the pathogen (19–25). In rural areas, such as southern Germany, dogs that roam unattended in fields and prey on rodents have an increased chance of ingesting infected prey and thus enabling completion of the parasite's life and development cycle. If dogs then excrete worm eggs, it is plausible that their owners' risk of contracting alveolar echinococcosis is increased. However, the general risk for persons living in rural, echinococcosis-endemic areas is also likely to be increased because of the higher level of environmental contamination with *E. multilocularis* eggs.

We found also a significantly increased risk for alveolar echinococcosis for dog owners who took their dog to a veterinarian only if it was ill, who had never been informed by a veterinarian about their own risk for infection with the fox tapeworm *E. multilocularis*, and who dewormed their dog(s) infrequently. These results seem plausible because studies have shown that dogs in rural areas where risk for infection is higher receive less veterinary care (8,22) and that dogs in rural areas, specifically unattended dogs, are more likely to be infected (21). Studies of dog feces from different countries show *E. multilocularis* infestation rates of 1.5%–20%, depending on the study setting (19–25). PCR analysis of 21,588 dog feces samples collected during 2004–2005 in Germany indicated an overall *E. multilocularis* prevalence of 0.24% (43/17,894); prevalence was higher in southern Germany (0.35%, 31/8,941) than in northern Germany (0.13%, 12/8,953) (26). The authors estimated that the chance of a dog becoming infected with the parasite within 10 years was 8.7%. Knapp et al. found that the high occurrence of dog feces in the cities studied, despite a lower prevalence of *E. multilocularis* infection, posed a clear risk for humans (27). Accordingly, dogs kept for private reasons were less likely to be carriers of the parasite (<1.5%) than were herding or hunting dogs that had free range and hunted rodents

(3%–8%). Towes et al. also found higher proportions of infected animals among hunting and herding dogs that were allowed to roam freely (21), as did we in our study.

Strube et al. argued that, depending on the active ingredient and anthelmintic, 62.4% (312/500) of dogs should be dewormed 12 times per year, according to European Scientific Counsel Companion Animal Parasites (28). Those guidelines also said that another 30.8% (154/500) of the dogs studied should be dewormed according to category C, 4.8% (24/500) 4 times/year and 2.0% (10/500) 1 or 2 times/year. The study showed poor deworming practices, with an average of only 2.07 dewormings/year. Dog fur contaminated with *E. multilocularis* eggs may be another source of transmission to humans (29). That possibility contrasts with our finding that a dog having an undercoat is protective. Given the denseness of this coat structure, the possibility of transmission can be assumed. The study by Nagy et al. shows that contamination via the coat is possible, which in turn means that inadequate coat care may be associated with increased risk for disease, as our study suggests (29). Thus, lack of education and knowledge about the potential risk for infection with *E. multilocularis* parasites and poor canine hygiene/grooming may be associated with higher odds of possible human infection.

We do not have a plausible explanation for the increased risk for dog owners who feed dogs organic waste on a daily basis. Possibly this feeding behavior is confounded by the behavior of dogs with a certain purpose (e.g., hunting, herding, and guarding [watch dogs]).

Limitations of our study are the heterogeneous distribution of case-patients and controls, as well as possible recall bias. Because patients with alveolar echinococcosis and the risk factor of dog ownership in Baden-Württemberg are in a highly selected, heterogeneously distributed group, this potential confounding factor may be overcome only by conducting an international study, perhaps in a multicentered format. Because of the small number of cases and often heterogeneous group sizes, values may scatter substantially, and CIs can vary widely.

Our study shows that certain factors of dog ownership are associated with increased odds of human alveolar echinococcosis and provides an overview of other potential risk factors. Considering the rapidly increasing number of dog owners in Germany, the results emphasize the role of veterinary facilities and others in informing dog owners about preventing or reducing their risk for infection with *E. multilocularis* parasites.

The study was supported by the German Research Foundation funded projects “Establishment of a national database for alveolar echinococcosis” (reference no. KA 4356/3-1) and “Implementation of interfaces for the standardization of national database systems for alveolar echinococcosis and its transformation processes” (reference no. KR 5204/1-2). It was further supported by the Ministry of Rural Areas and Consumer Protection Baden-Württemberg “Fuchsbandwurm-Erkrankung: eine Baden-Württembergische Erkrankung” (reference no. AZ: 14-(33)-8402.43/419E), and by the Bavarian State Government in the context of the funding of the “National Echinococcosis Database Germany” (reference no. AZ: K1-2490-PF-2020-FBW).

### About the Author

Dr. Schmidberger is a research scientist at the Department of Internal Medicine I at Ulm University Hospital and an expert in public health, specializing in infectious disease epidemiology.

### References

- Kratzer W, Schmidberger J, Hillenbrand A, Henne-Bruns D, Gräter T, Barth TFE, et al. Alveoläre echinokokkose: eine herausforderung für diagnostik, therapie und klinisches management. *Epid Bull.* 2019;41:423-30.
- Brunetti E, Kern P, Vuitton DA; Writing Panel for the WHO-IWGE. Expert consensus for the diagnosis and treatment of cystic and alveolar echinococcosis in humans. *Acta Trop.* 2010;114:1-16. <https://doi.org/10.1016/j.actatropica.2009.11.001>
- Oksanen A, Siles-Lucas M, Karamon J, Possenti A, Conraths FJ, Romig T, et al. The geographical distribution and prevalence of *Echinococcus multilocularis* in animals in the European Union and adjacent countries: a systematic review and meta-analysis. *Parasit Vectors.* 2016;9:519. <https://doi.org/10.1186/s13071-016-1746-4>
- Conraths FJ, Deplazes P. *Echinococcus multilocularis*: Epidemiology, surveillance and state-of-the-art diagnostics from a veterinary public health perspective. *Vet Parasitol.* 2015;213:149-61. <https://doi.org/10.1016/j.vetpar.2015.07.027>
- Baumann S, Shi R, Liu W, Bao H, Schmidberger J, Kratzer W, et al.; Interdisciplinary Echinococcosis Working Group Ulm. Worldwide literature on epidemiology of human alveolar echinococcosis: a systematic review of research published in the twenty-first century. *Infection.* 2019;47:703-27. <https://doi.org/10.1007/s15010-019-01325-2>
- Schmidberger J, Kratzer W, Stark K, Grüner B; Echinococcosis Working Group. Alveolar echinococcosis in Germany, 1992-2016. An update based on the newly established national AE database. *Infection.* 2018;46:197-206. <https://doi.org/10.1007/s15010-017-1094-0>
- Conraths FJ, Maksimov P. Epidemiology of *Echinococcus multilocularis* infections: a review of the present knowledge and of the situation in Germany. *Berl Munch Tierarztl Wochenschr.* 2020;OA-133. <https://doi.org/10.2376/0005-9366-2020-5>
- Deplazes P, van Knapen F, Schweiger A, Overgaauw PA. Role of pet dogs and cats in the transmission of helminthic zoonoses in Europe, with a focus on echinococcosis and toxocarosis. *Vet Parasitol.* 2011;182:41-53. <https://doi.org/10.1016/j.vetpar.2011.07.014>
- Kapel CM, Torgerson PR, Thompson RC, Deplazes P. Reproductive potential of *Echinococcus multilocularis* in experimentally infected foxes, dogs, raccoon dogs and cats. *Int J Parasitol.* 2006;36:79-86. <https://doi.org/10.1016/j.ijpara.2005.08.012>
- Kern P, Ammon A, Kron M, Sinn G, Sander S, Petersen LR, et al. Risk factors for alveolar echinococcosis in humans. *Emerg Infect Dis.* 2004;10:2088-93.
- Piarroux M, Piarroux R, Knapp J, Bardonnnet K, Dumortier J, Watelet J, et al.; FrancEchino Surveillance Network. Populations at risk for alveolar echinococcosis, France. *Emerg Infect Dis.* 2013;19:721-8. <https://doi.org/10.3201/eid1905.120867>
- Kreidl P, Allerberger F, Judmaier G, Auer H, Aspöck H, Hall AJ. Domestic pets as risk factors for alveolar hydatid disease in Austria. *Am J Epidemiol.* 1998;147:978-81. <https://doi.org/10.1093/oxfordjournals.aje.a009388>
- Stehr-Green JK, Stehr-Green PA, Schantz PM, Wilson JF, Lanier A. Risk factors for infection with *Echinococcus multilocularis* in Alaska. *Am J Trop Med Hyg.* 1988;38:380-5. <https://doi.org/10.4269/ajtmh.1988.38.380>
- Conraths FJ, Probst C, Possenti A, Boufana B, Saulle R, La Torre G, et al. Potential risk factors associated with human alveolar echinococcosis: systematic review and meta-analysis. *PLoS Negl Trop Dis.* 2017;11:e0005801. <https://doi.org/10.1371/journal.pntd.0005801>
- Torgerson PR, Robertson LJ, Enemark HL, Foehr J, van der Giessen JWB, Kapel CMO, et al. Source attribution of human echinococcosis: a systematic review and meta-analysis. *PLoS Negl Trop Dis.* 2020;14:e0008382. <https://doi.org/10.1371/journal.pntd.0008382>
- Zentralverband Zoologischer Fachbetrieb, Industrieverband Heimtierbedarf. Der Deutsche heimtiermarkt 2016 [cited 2019 Aug 29] [https://www.zzf.de/fileadmin/files/ZZF/Marktdaten/ZZF\\_IVH\\_Der\\_Deutsche\\_Heimtiermarkt\\_2016\\_A4.pdf](https://www.zzf.de/fileadmin/files/ZZF/Marktdaten/ZZF_IVH_Der_Deutsche_Heimtiermarkt_2016_A4.pdf)
- Zentralverband Zoologischer Fachbetrieb, Industrieverband Heimtierbedarf. Der Deutsche heimtiermarkt 2017 [cited 2019 Aug 29]. [https://www.zzf.de/fileadmin/files/ZZF/Marktdaten/IVH\\_ZZF\\_Der\\_Deutsche\\_Heimtiermarkt\\_Anzahl\\_Heimtiere\\_2017.pdf](https://www.zzf.de/fileadmin/files/ZZF/Marktdaten/IVH_ZZF_Der_Deutsche_Heimtiermarkt_Anzahl_Heimtiere_2017.pdf)
- Schelling U, Frank W, Will R, Romig T, Lucius R. Chemotherapy with praziquantel has the potential to reduce the prevalence of *Echinococcus multilocularis* in wild foxes (*Vulpes vulpes*). *Ann Trop Med Parasitol.* 1997;91:179-86. <https://doi.org/10.1080/00034983.1997.11813128>
- Pouille ML, Bastien M, Richard Y, Josse-Dupuis É, Aubert D, Villena I, et al. Detection of *Echinococcus multilocularis* and other foodborne parasites in fox, cat and dog faeces collected in kitchen gardens in a highly endemic area for alveolar echinococcosis. *Parasite.* 2017;24:29. <https://doi.org/10.1051/parasite/2017031>
- Karamon J, Sroka J, Dąbrowska J, Bilska-Zajac E, Zdybel J, Kochanowski M, et al. First report of *Echinococcus multilocularis* in cats in Poland: a monitoring study in cats and dogs from a rural area and animal shelter in a highly endemic region. *Parasit Vectors.* 2019;12:313. <https://doi.org/10.1186/s13071-019-3573-x>
- Toews E, Musiani M, Checkley S, Visscher D, Massolo A. A global assessment of *Echinococcus multilocularis* infections in domestic dogs: proposing a framework to overcome past methodological heterogeneity. *Int J Parasitol.* 2021;51:379-92. <https://doi.org/10.1016/j.ijpara.2020.10.008>

22. Hegglin D, Deplazes P. Control of *Echinococcus multilocularis*: strategies, feasibility and cost-benefit analyses. *Int J Parasitol*. 2013;43:327–37. <https://doi.org/10.1016/j.ijpara.2012.11.013>
23. Liu CN, Xu YY, Cadavid-Restrepo AM, Lou ZZ, Yan HB, Li L, et al. Estimating the prevalence of *Echinococcus* in domestic dogs in highly endemic for echinococcosis. *Infect Dis Poverty*. 2018;7:77. <https://doi.org/10.1186/s40249-018-0458-8>
24. Hao L, Yang A, Yuan D, Guo L, Hou W, Mo Q, et al. Detection of *Echinococcus multilocularis* in domestic dogs of Shiqu County in the summer herding. *Parasitol Res*. 2018;117:1965–8. <https://doi.org/10.1007/s00436-018-5862-2>
25. Ziadinov I, Mathis A, Trachsel D, Rysmukhambetova A, Abdyjaparov TA, Kuttubaev OT, et al. Canine echinococcosis in Kyrgyzstan: using prevalence data adjusted for measurement error to develop transmission dynamics models. *Int J Parasitol*. 2008;38:1179–90. <https://doi.org/10.1016/j.ijpara.2008.01.009>
26. Dyachenko V, Pantchev N, Gawlowska S, Vrhovec MG, Bauer C. *Echinococcus multilocularis* infections in domestic dogs and cats from Germany and other European countries. *Vet Parasitol*. 2008;157:244–53. <https://doi.org/10.1016/j.vetpar.2008.07.030>
27. Knapp J, Giraudoux P, Combes B, Umhang G, Boué F, Said-Ali Z, et al. Rural and urban distribution of wild and domestic carnivore stools in the context of *Echinococcus multilocularis* environmental exposure. *Int J Parasitol*. 2018;48:937–46. <https://doi.org/10.1016/j.ijpara.2018.05.007>
28. Strube C, Neubert A, Springer A, von Samson-Himmelstjerna G. Survey of German pet owners quantifying endoparasitic infection risk and implications for deworming recommendations. *Parasit Vectors*. 2019;12:203. <https://doi.org/10.1186/s13071-019-3410-2>
29. Nagy A, Ziadinov I, Schweiger A, Schnyder M, Deplazes P. Hair coat contamination with zoonotic helminth eggs of farm and pet dogs and foxes [in German]. *Berl Munch Tierarztl Wochenschr*. 2011;124:503–11.

Address for correspondence: Julian Schmidberger, Department of Internal Medicine I, University Hospital Ulm, Albert-Einstein-Allee 23, 89081 Ulm, Germany; email: [julian.schmidberger@uniklinik-ulm.de](mailto:julian.schmidberger@uniklinik-ulm.de)

## The Public Health Image Library



The Public Health Image Library (PHIL), Centers for Disease Control and Prevention, contains thousands of public health-related images, including high-resolution (print quality) photographs, illustrations, and videos.

PHIL collections illustrate current events and articles, supply visual content for health promotion brochures, document the effects of disease, and enhance instructional media.

PHIL images, accessible to PC and Macintosh users, are in the public domain and available without charge.

Visit PHIL at:  
<http://phil.cdc.gov/phil>

# Characterization of Emerging Serotype 19A Pneumococcal Strains in Invasive Disease and Carriage, Belgium

Stefanie Desmet, Heidi Theeten, Lies Laenen, Lize Cuyppers, Piet Maes, Wouter Bossuyt, Liesbet Van Heirstraeten, Willy E. Peetermans, Katrien Lagrou

After switching from 13-valent to 10-valent pneumococcal conjugate vaccine (PCV10) (2015–2016) for children in Belgium, we observed rapid reemergence of serotype 19A invasive pneumococcal disease (IPD). Whole-genome sequencing of 166 serotype 19A IPD isolates from children ( $n = 54$ ) and older adults ( $n = 56$ ) and carriage isolates from healthy children ( $n = 56$ ) collected after the vaccine switch (2017–2018) showed 24 sequence types (STs). ST416 (global pneumococcal sequence cluster [GPSC] 4) and ST994 (GPSC146) accounted for 75.9% of IPD strains from children and 65.7% of IPD (children and older adults) and carriage isolates in the PCV10 period (2017–2018). These STs differed from predominant 19A IPD STs after introduction of PCV7 (2011) in Belgium (ST193 [GPSC11] and ST276 [GPSC10]), which indicates that prediction of emerging strains cannot be based solely on historical emerging strains. Despite their susceptible antimicrobial drug profiles, these clones spread in carriage and IPD during PCV10 use.

**P**neumococcal serotype 19A is one of the 100 known serotypes of *Streptococcus pneumoniae* (1). The high potential of serotype 19A to cause invasive pneumococcal disease (IPD), its high rates of antimicrobial drug resistance, the variable inclusion of this serotype in conjugate vaccines, and its high genetic plasticity makes it one of the most studied pneumococcal

serotypes (2–4). Serotype 19A became more prevalent after 7-valent pneumococcal conjugate vaccine (PCV7) was introduced into childhood vaccination programs. As a consequence of the decrease of PCV7 serotype IPD, serotypes not included in PCV7, such as serotype 19A, became a more critical issue because of process called serotype replacement. In the United States, capsular switching and antimicrobial drug resistance played a major role in the increase of serotype 19A after introduction of PCV7 (2,3).

In Belgium, introduction of the 13-valent vaccine, which includes serotype 19A, resulted in a 10-fold decrease of serotype 19A incidence in the youngest children (5). As in Belgium, in most countries that use PCV13, a decrease in serotype 19A IPD in children was observed, resulting in a low residual serotype 19A IPD incidence during PCV13 use (6,7). By an indirect effect, use of PCV13 in children also resulted in a decrease in the incidence of serotype 19A IPD in older adults in Belgium and other countries (7,8). However, serotype 19A has remained one of the major serotypes, accounting for 5.6% of IPD cases in older adults during 2015 (9). In addition, in other countries (e.g., England and Wales), serotype 19A did not completely disappear after PCV13 introduction, and the number of serotype 19A IPD cases remained on a plateau (10).

For >20 years, a stable national laboratory-based surveillance of IPD has been in place in Belgium (5). Since 2016, a national nasopharyngeal carriage study investigating pneumococcal carriage in children attending day care centers was also conducted in parallel with IPD surveillance (11). These 2 parallel surveillances make it possible to study in detail changes over time in the pneumococcal population (4,5,11). After

Author affiliations: University Hospitals Leuven, Leuven, Belgium (S. Desmet, L. Laenen, L. Cuyppers, W. Bossuyt, W.E. Peetermans, K. Lagrou); Katholieke Universiteit Leuven, Leuven (S. Desmet, P. Maes, W. Bossuyt, W.E. Peetermans, K. Lagrou); University of Antwerp, Antwerp, Belgium (H. Theeten, L. Van Heirstraeten); Katholieke Universiteit Leuven–University Hospitals Leuven, Leuven (W. Bossuyt)

DOI: <https://doi.org/10.3201/eid2808.212440>

a decrease in pediatric IPD incidence after the switch from PCV7 to PCV13 in Belgium, a major increase in IPD incidence in the youngest children was again observed during 2017–2018, two years after the switch from PCV13 to PCV10 (2015–2016) (5). This increase was attributed mainly to the major increase in serotype 19A IPD (from 2.2 cases/100,000 children <2 years old in the PCV13 period to 12.5 cases/100,000 children <2 years old in PCV10 period) (5). In older adults, an increase in the proportion of serotype 19A IPD was detected from 5.6% during 2015 to 13.2% during 2019 (9). In parallel, an increase in the proportion of serotype 19A in nasopharyngeal carriage of young children in Belgium was observed from 0.4% during 2016 to 6.4% during 2017–2018 (11).

To elucidate the rapid increase in serotype 19A IPD and carriage, we performed phenotypic and molecular characterization of the serotype 19A strains isolated during 2017–2018. We investigated whether the same serotype 19A strains were detected in children and adults who had IPD, and if they correspond to the ones carried by the youngest children during 2017–2018. Moreover, we aimed to compare these serotype 19A strains from Belgium with serotype 19A IPD strains that were detected after introduction of PCV7 in Belgium and other countries to investigate whether there was a clonal expansion of previous dominant clones and whether capsular switching or antimicrobial drug resistance played a role in reemergence of serotype 19A.

## Materials and Methods

### Bacterial Strains

We included in the study all serotype 19A *S. pneumoniae* isolates sent to the Belgian Reference Centre for Invasive *S. pneumoniae* and collected from a normally sterile site (e.g., blood culture, cerebrospinal fluid, pleural fluid, or synovial fluid) during 2010, during 2012–2018 from children  $\leq 2$  years of age (IPD children), and during 2018 from older adults (65–85 years of age) (IPD older adults). Data collection was part of the national passive surveillance network that showed a mean representativeness for IPD in Belgium of 90.5% (2007–2018) (5).

We collected serotype 19A pneumococcal strains carried by young healthy children 6–30 months of age during a national nasopharyngeal carriage study (carriage children). This study has been described in detail (12). Healthy children were recruited in randomly selected daycare centers in 3 regions of Belgium (Flanders, Wallonia, and Brus-

sels). We obtained a nasopharyngeal flocculated swab specimen from 1,855 children during the winter of years 2 (2016–2017) and years 3 (2017–2018). For this study, we included only serotype 19A strains collected during 2017 and 2018. We defined 2010 as the PCV7 year, January 2012–December 2014 as the PCV13 period, and January 2017–December 2018 as the PCV10 period.

### Phenotypic Characterization

We performed serotyping of pneumococcal strains by detection of the Quellung reaction using serotype-specific antisera (SSI Diagnostica, <https://ssidiagnostica.com>). We conducted antimicrobial susceptibility testing by using disk diffusion for penicillin (oxacillin), erythromycin, tetracycline, trimethoprim/sulfamethoxazole, and levofloxacin. If the oxacillin zone diameter was <20 mm, we determined the MIC by using Etest (bioMérieux, <https://www.biomerieux.com>) for penicillin and cefotaxime. We interpreted results by using the European Committee on Antimicrobial Susceptibility Testing (<https://www.eucast.org>) 2019 guidelines. We interpreted a penicillin MIC >0.064 mg/L and a cefotaxime MIC >0.5 mg/L as indicating resistance.

### Genotypic Characterization

We extracted DNA by using the DSP DNA Mini Kit on the QIASymphony SP/AP Instrument (QIAGEN, <https://www.qiagen.com>) and the protocol for gram-negative bacteria. We prepared libraries by using the Nextera XT DNA Library Prep Kit (Illumina, <https://www.illumina.com>) and the Echo 525 Liquid Handler Instrument (Beckman-Coulter, <https://www.beckmancoulter.com>), followed by solid-phase reversible immobilization bead purification (Hamilton, <https://www.hamiltoncompany.com>).

We used a genomic DNA concentration of 0.2 ng/ $\mu$ L dissolved in 500 nL of nuclease-free water. We prepared a Nextera library according to the manufacturer's (Illumina) protocol with a tagment DNA buffer to amplicon tagment mixture ratio of 2:1 and tagmentation time of 15 min at 55°C. We performed amplification of the library by using 12 PCR cycles of 95°C for 10 s, 55°C for 30 s, and 72°C for 30 s.

We purified beads by using Hamilton NGS Star and AMPure XP beads (Beckman-Coulter) at a ratio of 30%. We verified library quality by using Bioanalyzer (Agilent, <https://www.agilent.com>) and a quantitative PCR (Kapa Biosystems, <https://kapabiosystems.com>). We performed sequencing by using the MiSeq System with MiSeq version 3 PE300 reagents and HiSeq2500 with version 2 reagents (Illumina). We

submitted read data for all *S. pneumoniae* serotype 19 isolates to the National Center for Biotechnology Information Short Read Archive (BioProject accession no. PRJNA780376).

We analyzed demultiplexed sequence reads by using 2 pipelines. First, we used an in-house cloud-based pipeline based on Kraken 2, the Centers for Disease Control and Prevention StrepLab pipeline, and SeroBA (13,14). We used Kraken 2 and information about identification of the strain to check whether there was contamination with other bacterial species (15). Combining of the Centers for Disease Control and Prevention StrepLab pipeline and SeroBA resulted in an output of serotype, multilocus sequence typing (MLST) results, presence of pilus genes, presence of antimicrobial drug resistance genes, assignment of penicillin-binding protein (PBP) profile, and prediction of antimicrobial drug susceptibility of the strain.

Second, we used the INNUca pipeline (<https://innuca-nf.readthedocs.io>) for performing quality control and de novo assembly of the genome. We performed quality control of reads by using FastQC version 0.11.5 (<https://guix.gnu.org>), and cleaned and trimmed reads by using Trimmomatic version 0.36 ([https://kbase.us/applist/apps/kb\\_trimmomatic/run\\_trimmomatic/release](https://kbase.us/applist/apps/kb_trimmomatic/run_trimmomatic/release)).

We assembled the genome by using SPAdes version 3.11.0 (<https://cab.spbu.ru>) and subsequently polished the genome by using Pilon version 1.18 (<https://github.com/broadinstitute/pilon>). We used the assembled genome for assignment of global pneumococcal sequence clustering (GPSC) by using Pathogenwatch (Wellcome Sanger Institute, <https://pathogen.watch>) (16). We used PopPUNK 2.4 (<https://poppunk.readthedocs.io>) and a newer GPSC reference database (n = 42,000) for strains that had a novel GPSC assignment by Pathogenwatch (accessed on January 11, 2021).

### Data Analysis

We compared phenotypic and genotypic characteristics of serotype 19A strains causing IPD in older adults and carried (isolated during 2017–2018) by healthy young children with serotype 19A IPD strains isolated from children during the PCV7 period (2010), the PCV13 period (2012–2014), and the PCV10 period (2017–2018). We compiled descriptive statistics for these comparisons.

### Results

A total of 255 serotype 19A strains were included in this study, of which 166 strains were isolated in the

PCV10 period (2017–2018): 54 IPD strains from children, 56 IPD strains from older adults, and 56 carriage strains from children. A total of 89 strains that were isolated in children <2 years old in the PCV7 (2010) (n = 67) and PCV13 period (2012–2014) (n = 23) were included to analyze the evolution over time of the serotype 19A strains in children <2 years of age.

### Antimicrobial Drug Susceptibility and Pilus Genes of Serotype 19A Strains Isolated during 2017–2018

Resistance rates for serotype 19A strains were 9.0% for penicillin, 23.5% for erythromycin, 0.0% for levofloxacin, and 22.3% for tetracycline. Higher resistance rates for penicillin were detected in IPD strains (13.0% for children and 11.1% for older adults) compared with carriage strains (5.4%). For erythromycin and tetracycline, higher resistance rates were observed in IPD strains from children (29.6% and 27.8%) compared with IPD strains from older adults (17.9% and 17.9%) and carriage strains (23.2% and 21.4%) (Table 1). The pilus 1 gene was found in 47.6% of the serotype 19A strains in the PCV10 period, with a similar proportion in the different groups (range 46.3%–48.2% pilus-1-positive strains in each group). Both pilus 1 and pilus 2 genes were detected in only 3 strains causing IPD in young children, 2 strains causing IPD in older adults, and 4 strains carried by young children in the PCV10 period. A total of 77 (46.4%) of the 166 serotype 19A strains had no pilus genes.

### MLST Types of Serotype 19A Isolated during 2017–2018

We detected 24 MLST types. ST416 (47.6%, 79/166), ST994 (18.1%, 30/166), ST2081 (5.4%, 9/166), ST320 (3.0%, 5/166), and ST419 (3.0%, 5/166) were the predominant types (Table 2, <https://wwwnc.cdc.gov/EID/article/28/810/21-2440-T2.htm>). We detected 11 STs only once: ST63, ST1756, ST2013, ST2669, ST2927, ST3012, SST9387, ST13097, ST13701, ST16628, and ST16627. ST16628 and ST16627 were assigned as new pneumococcal STs. Of the predominant STs, we detected ST416, ST994, and ST320 in all 3 groups, and these STs accounted for >60% of the strains in each group: 43/54 (79.6%) for IPD young children, 36/56 (64.3%) for IPD older adults, and 35/56 (62.5%) for carriage strains. We detected ST416 in all groups, and it was the most predominant ST, accounting for 45%–48% of the strains in each group. ST2081, ST419 and ST1848 accounted for 26.8% (15/56) of carriage strains but were not detected as the cause of IPD in young children and only rarely (3.6%, 2/56) in older adults who had IPD. We detected 5 STs in children who had IPD, but we did not detect those STs in carriage. We detected ST994

**Table 1.** Characteristics and antimicrobial drug susceptibility for serotype 19A strains of pneumococci isolated during the period after the PCV13 to PCV10 switch, Belgium\*

| Characteristic               | IPD, young children | IPD, older persons | Carriage, young children | Total     |
|------------------------------|---------------------|--------------------|--------------------------|-----------|
| No. strains                  | 54                  | 56                 | 56                       | 166       |
| Year of isolation            | 2017–2018           | 2018               | 2017–2018                | 2017–2018 |
| Age                          |                     |                    |                          |           |
| 0–11 mo                      | 41                  | 0                  | 8                        | 49        |
| 13–23 mo                     | 13                  | 0                  | 32                       | 45        |
| 2–3 y                        | 0                   | 0                  | 15                       | 15        |
| 3–4 y                        | 0                   | 0                  | 1                        | 1         |
| 65–85 y                      | 0                   | 56                 | 0                        | 56        |
| Sex, M/F                     | 32/22               | 27/29              | 28/28                    | 87        |
| Source of isolation          |                     |                    |                          |           |
| Blood                        | 48                  | 56                 | 0                        | 104       |
| CSF                          | 5                   | 0                  | 0                        | 5         |
| Pleural fluid                | 1                   | 0                  | 0                        | 1         |
| Nasopharyngeal swab specimen | 0                   | 0                  | 56                       | 56        |
| Penicillin resistant         | 7 (13.0)            | 5 (11.1)           | 3 (5.4)                  | 15 (9.0)  |
| Levofloxacin resistant       | 0 (0)               | 0 (0)              | 0 (0)                    | 0 (0)     |
| Erythromycin resistant       | 16 (29.6)           | 10 (17.9)          | 13 (23.2)                | 39 (23.5) |
| Tetracycline resistant       | 15 (27.8)           | 10 (17.9)          | 12 (21.4)                | 37 (22.3) |
| Pilus 1                      | 25 (46.3)           | 27 (48.2)          | 27 (48.2)                | 79 (47.6) |
| Pilus 1 and pilus 2          | 3 (5.6)             | 2 (3.6)            | 4 (7.1)                  | 9 (5.4)   |

\*Values are no. or no. (%). CSF, cerebrospinal fluid; IPD, invasive pneumococcal disease; PCV, pneumococcal conjugate vaccine.

at a higher proportion in IPD (15/54; 27.8%) than in carriage (6/56, 10.7%) in children.

Comparing the strains causing IPD in children and older adults in the PCV10 period indicated the same predominant STs (ST416 and ST994). Two STs, ST199 and ST276, accounted for 14.3% (8/56) of 19A strains in older adults; we did not detect those STs in the IPD cases in young children. Conversely, 4 STs we detected in young children who had IPD were not found in older adults.

Serotype 19A strains from the PCV10 period grouped into 9 GPSCs. Strains that had the same ST always grouped together into 1 GPSC. A total of 6 GPSCs consisted of different STs. A total of 63.3% (105/166) of the strains grouped in GPSC4, and 18.1% (30/166) grouped in GPSC146. The other GPSC accounted for <5% of the strains.

#### Genomic Characterization of Predominant MLST Types during 2017–2018

ST416 strains are mainly pilus 1 gene positive (76/79), and all are penicillin susceptible, based on the 0-0-0 PBP profile in 74 of the 79 strains. A total of 20.2% (16/79) had the *erm(B)* gene, and all those strains were erythromycin resistant. In 20.2% of ST416 strains, we detected the *tet(M)* gene, conferring phenotypically tetracycline resistance in these strains. ST416 is part of clonal complex 199 and is a double-locus variant of the worldwide distributed penicillin nonsusceptible ST199. According to the pubMLST database (<https://pubmlst.org>), ST416 has been associated with serotype 19A and to a lesser extent with serotype 19F (only 3 strains in the

database as of May 14, 2021). ST416 strains belonged to GPSC4, which is the GPSC with the highest number of serotype 19A strains in the GPSC database (Pathogenwatch, <https://www.pneumogen.net>; 25,731 pneumococcal genomes as of May 14, 2021). The ST994 strains from Belgium clustered in GPSC146, which is a small GPSC with only 23 public genomes assigned, all ST994 strains.

Of the other predominant 19A strains, ST994 and ST2081 did not have pilus genes and had no erythromycin or tetracycline resistance genes detected; they were phenotypically susceptible to all tested antimicrobial drugs. ST994 has been identified in only 77 isolates, all serotype 19A except 1 serotype 19C isolate, which indicates that it is even less frequently described than ST416 (179 isolates) in the pubMLST database. It is unlikely that this ST results from a serotype switch.

Conversely, ST320 strains carried the 13-11-16 PBP profile associated with penicillin resistance. We also detected *erm(B)*, *mef(A)*, and *tet(M)* genes in all ST320 strains, which correlated with the phenotypical resistance to erythromycin and tetracycline.

#### Comparing Pre-PCV10 to PCV10 Serotype 19A Clones

Comparing serotype 19A strains causing IPD in children in the PCV7 period (2010) and PCV13 period (2012–2014) to those from the PCV10 period (2017–2018) indicated a change in predominant STs and GPSCs over time (Table 3; Figure). The predominant clones in the PCV10 period, ST416 (GPSC4) and ST994 (GPSC146), which accounted for 75.9% (41/54) of serotype 19A IPD strains

during 2017–2018, were also detected in the PCV7 and PCV13 period but at much lower proportions: 11.9% (8/67) for the PCV period and 30.4% (7/23) for the PCV13 period. Of the clones that were predominant during the PCV7 period, ST193 (GPSC11) and ST276 (GPSC10) (together 40/67; 59.7%), only 1 ST193 (GPSC11) isolate was detected as the cause of IPD in the youngest children during the PCV10 period. ST416, ST994, ST193 and ST276 clustered in 4 different GPSC, indicating they were not closely related to each other.

## Discussion

After the PCV13 to PCV10 switch in Belgium, a rapid emergence of serotype 19A occurred in IPD and nasopharyngeal carriage in the youngest children. Emergence in both groups was associated with the increase in a variety of mainly penicillin-susceptible serotype 19A clones. Two serotype 19A clones, ST416 (GPSC4) and ST994 (GPSC146), accounted for most 19A isolates. Those clones were not only predominant in the youngest children but were also the predominant clones causing IPD in adults after vaccine switch. These emerging clones

differed from the serotype 19A clones (ST193 and ST276) that were mainly responsible for the increase in serotype 19A IPD in children after PCV7 introduction in Belgium and other countries in Europe (17–20).

The 2 predominant STs are greatly involved in carriage in the youngest children, as well as in invasive disease in the youngest children and older adults, which might indicate that these strains have an advantage to spread compared with other STs of serotype 19A. Although ST416 and ST994 were already on the increase before the vaccine switch in Belgium, they were not the predominant serotype 19A STs in childhood IPD at that time. Instead, ST193 and ST276 still accounted for most of the serotype 19A strains causing IPD in the youngest children during the PCV7 and PCV13 periods. The number of ST193 and ST276 serotype 19A IPD strains in young children did not increase after the vaccine switch. We observed that after introduction of PCV7 and PCV10, an increase in serotype 19A was detected, but the effect on the microepidemiology of serotype 19A was different because of emergence of different clones.

**Table 3.** GPSC and ST assignment for serotype 19A invasive pneumococci isolated during PCV7 period (2010), PCV13 period (2012–2014), and PCV10 period (2017–2018), from children <2 years of age, Belgium\*

| GPSC    | Sequence type | No. isolated         |                            |                            | Total |
|---------|---------------|----------------------|----------------------------|----------------------------|-------|
|         |               | PCV7 period,<br>2010 | PCV13 period,<br>2012–2014 | PCV10 period,<br>2017–2018 |       |
| GPSC4   | Total         | 7                    | 4                          | 28                         | 39    |
|         | ST199         | 2                    | 0                          | 0                          | 2     |
|         | ST416         | 2                    | 4                          | 26                         | 32    |
|         | ST876         | 1                    | 0                          | 0                          | 1     |
|         | ST3012        | 2                    | 0                          | 0                          | 2     |
|         | ST3017        | 0                    | 0                          | 1                          | 1     |
| GPSC11  | ST15414       | 0                    | 0                          | 1                          | 1     |
|         | Total         | 31                   | 5                          | 1                          | 37    |
|         | ST193         | 26                   | 5                          | 1                          | 32    |
|         | ST1228        | 1                    | 0                          | 0                          | 1     |
|         | ST2927        | 2                    | 0                          | 0                          | 2     |
|         | ST16995       | 1                    | 0                          | 0                          | 1     |
| GPSC10  | ST16996       | 1                    | 0                          | 0                          | 1     |
|         | Total         | 20                   | 6                          | 3                          | 29    |
|         | ST276         | 14                   | 6                          | 0                          | 20    |
|         | ST2013        | 4                    | 0                          | 1                          | 5     |
|         | ST15077       | 0                    | 0                          | 2                          | 2     |
| GPSC146 | ST16994       | 2                    | 0                          | 0                          | 2     |
|         | ST994         | 6                    | 3                          | 15                         | 24    |
| GPSC1   | Total         | 1                    | 1                          | 3                          | 5     |
|         | ST320         | 1                    | 1                          | 2                          | 4     |
|         | ST9387        | 0                    | 0                          | 1                          | 1     |
| GPSC9   | ST63          | 1                    | 1                          | 1                          | 3     |
| GPSC18  | Total         | 0                    | 2                          | 0                          | 3     |
|         | ST4831        | 0                    | 1                          | 0                          | 1     |
|         | ST99          | 0                    | 0                          | 0                          | 1     |
|         | ST1848        | 0                    | 1                          | 0                          | 1     |
| GPSC109 | ST13096       | 0                    | 0                          | 2                          | 2     |
| Unknown | Total         | 1                    | 1                          | 1                          | 1     |
| Total   | Total         | 67                   | 23                         | 54                         | 143   |

\*GPSC, global pneumococcal sequence cluster; PCV, pneumococcal conjugate vaccine; ST, sequence type.

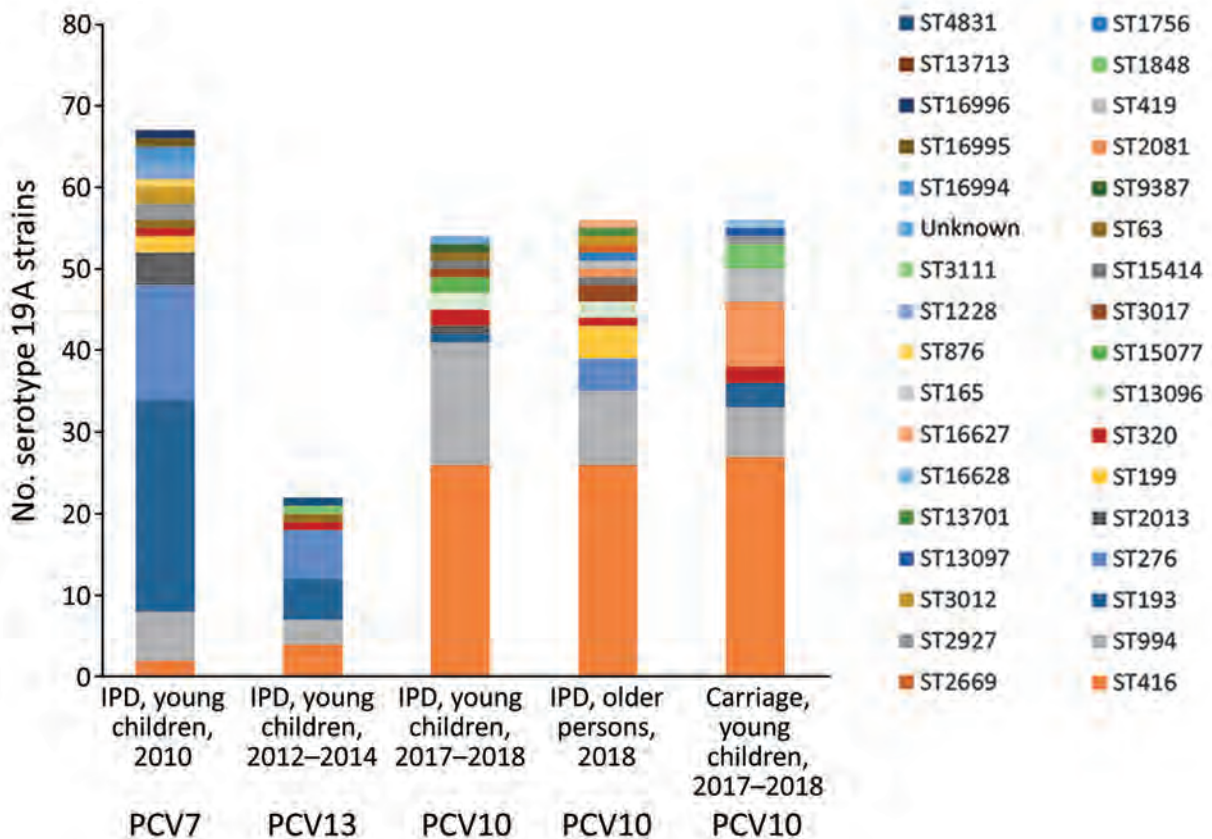


**Figure.** Number and ST distribution of pneumococcal serotype 19A strains isolated from invasive disease and carriage, Belgium. Shown are IPD cases in young children during 2010, 2012–2014, and 2017–2018; serotype 19A strains isolated from IPD cases in older persons during 2018; and serotype 19A strains carried by children during 2017–2018. Different colors indicate different STs. IPD, invasive pneumococcal disease; PCV, pneumococcal conjugate vaccine; ST, sequence type.

Although serotype 19A is well known for its high level of antimicrobial drug resistance, emergence of serotype 19A after introduction of PCV10 in Belgium is driven mainly by drug-susceptible pneumococci. Although the penicillin resistance rate is somewhat higher in serotype 19A IPD strains (13.0% in adults and 11.1% in young children) compared with carriage strains (5.4%), those resistance rates are much lower than the resistance rates for serotype 19A IPD strains isolated from children before the PCV13 period (e.g., 38.6% in 2011; data from the Belgian Reference Centre for Invasive *S. pneumoniae*).

An influencing factor could be different antimicrobial drug pressure during the PCV7 period in comparison with the PCV10 period. In the PCV10 period (2015–2018; 23.4 defined daily doses [DDD]/1,000 inhabitants/day) a slightly lower consumption of systemic antimicrobial drugs in community and hospital settings was detected than during the PCV7 period (2007–2010; 23.9 DDDs/1,000 inhabitants/day) (21). In addition,

during 2007–2015, macrolide consumption gradually increased (2.7 to 3.7 DDDs/1,000 inhabitants/day), and nonpenicillin  $\beta$ -lactam (code J01D in the World Health Organization ATC classification system, [https://www.whocc.no/atc\\_ddd\\_index](https://www.whocc.no/atc_ddd_index); 2.73 to 1.8 DDDs/1,000 inhabitants/day) consumption gradually decreased (21). However, because ST416 and ST994 strains are mainly macrolide susceptible, it is unlikely that the modest increase in macrolide antimicrobial drug pressure is the driver of the spread of these specific clones.

Looking into more detail for ST416 and ST994 is useful to clarify why these STs expanded in comparison with other serotype 19A STs. In contrast to the ancestral ST199, ST416 strains were all penicillin susceptible in this study. Some diversity was observed regarding macrolide and tetracycline resistance within the emerging ST416 strains in Belgium, but the resistant strains were seen in equal proportions in the 3 studied groups (IPD children, IPD adults, and carriage children). ST416 has been detected in countries in

Europe at relatively low frequencies. In Germany, France, Spain, and Finland, it has been detected after PCV introduction, but it was only responsible for <10% of serotype 19A strains (17–20). Also in Belgium, ST416 has sporadically been detected before the PCV13 to PCV10 vaccine switch. An exception is Italy, where ST416 accounted for >60% of serotype 19A IPD strains and was the driver of the increase of serotype 19A IPD after introduction of PCV7 (17). These data for Italy underscores the potential of ST416 to rapidly increase.

Before 2015, ST994 was sporadically detected in Belgium and in other countries in Europe (e.g., Germany, Spain, and the Netherlands). ST994 was also the predominant 19A clone in children <5 years old after PCV10 introduction in Finland.

A detailed comparison of 19A strains from Belgium with 19A strains from countries using PCV13 and PCV10 is needed to investigate a correlation between presence of ST994 and use of PCV10. Publicly available databases do not contain genome sequences with relevant metadata for ST994 and ST416 serotype 19A strains to investigate whether the serotype 19A from Belgium is distinct from the serotype 19A strains from other countries in Europe using PCV13 or PCV10. To study this possibility in detail, collaboration between national reference centers is needed.

Pilus genes are major virulence factors promoting adhesion, invasion, and spreading of the pneumococcus in the human host. Almost all ST416 strains carry the pilus 1 gene, which might be a competitive advantage for this clone. In general, <40% of all invasive pneumococci carry pilus genes, and the presence of pilus genes has been associated with serotype 19A. Presence of pili is frequently associated with antimicrobial drug resistance in pneumococcal strains. In contrast, in this study, pilus genes were detected in penicillin-susceptible strains. The emerging ST416 accounts for most of these pilus 1-positive strains. ST416 and ST994 could also carry other virulence factors, which could explain their competitive advantage compared with other STs.

Only some serotype 19A clones are detected in carriage but not in IPD and vice versa. Children act as a reservoir for the pneumococci that cause invasive disease in older adults, but the dynamics between pneumococcal carriage in young children and IPD in the same age group and older age groups are not yet fully understood (22–24). In this study, the same predominant clones of serotype 19A are responsible for the emergence of serotype 19A, indicating an association between strains that are carried by young children and strains that cause invasive disease in

children and adults. Other invasive serotypes (e.g., serotype 1, 8, and 12F) are not frequently carried in the youngest children, which suggests that also other factors are essential for the spread of pneumococci that cause invasive disease.

Based on the increase of total IPD and serotype 19A IPD in the youngest children in Belgium, PCV10 was again replaced by PCV13 in September 2019 (25,26). Data from Belgium for emerging serotype 19A clones in adults and children are useful for other countries that switched from PCV13 to PCV10 or that plan to make changes on the dose schedule and type of vaccine. Close monitoring of IPD epidemiology by surveillance is needed to rapidly detect emerging clones. Investigation of the microepidemiology of serotype 19A after this switch back from PCV10 to PCV13 will be useful for further investigation of correlations between the use of the different PCVs and the circulation of specific serotype 19A clones. However, confounding variables caused by the coronavirus disease pandemic and its related containment measures during 2020 and 2021, which resulted in a perturbation of the IPD epidemiology in Belgium and other countries, will make this analysis more complicated (27,28).

S.D. received an investigator-initiated research grant from Pfizer for this study; K.L. received consultancy fees from SMB Laboratoires, Merck, and Gilead, travel support from Pfizer, speaker fees from FUJIFILM WAKO, Pfizer, and Gilead, and a service fee from Thermo Fisher Scientific; and W.E.P. received consultancy fees from Merck and Pfizer and travel support from GlaxoSmithKline.

## About the Author

Dr. Desmet is a clinical microbiologist at the University Hospitals, Leuven, Belgium, and head of the Belgian Reference Center for invasive pneumococcal disease. Her primary research interests are clinical microbiology and epidemiology of *S. pneumoniae*.

## References

1. Ganaie F, Saad JS, McGee L, van Tonder AJ, Bentley SD, Lo SW, et al. A new pneumococcal capsule type, 10D, is the 100th serotype and has a large *cps* fragment from an oral *Streptococcus*. MBio. 2020;11:e00937-20. <https://doi.org/10.1128/mBio.00937-20>
2. Beall BW, Gertz RE, Hulkower RL, Whitney CG, Moore MR, Brueggemann AB. Shifting genetic structure of invasive serotype 19A pneumococci in the United States. J Infect Dis. 2011;203:1360–8. <https://doi.org/10.1093/infdis/jir052>
3. Moore MR, Gertz RE Jr, Woodbury RL, Barkocy-Gallagher GA, Schaffner W, Lexau C, et al. Population snapshot of emergent *Streptococcus pneumoniae* serotype 19A in the United States, 2005. J Infect Dis. 2008;197:1016–27. <https://doi.org/10.1086/528996>

4. Desmet S, Wouters I, Heirstraeten LV, Beutels P, Van Damme P, Malhotra-Kumar S, et al. In-depth analysis of pneumococcal serotypes in Belgian children (2015–2018): diversity, invasive disease potential, and antimicrobial susceptibility in carriage and disease. *Vaccine*. 2021;39:372–9. <https://doi.org/10.1016/j.vaccine.2020.11.044>
5. Desmet S, Lagrou K, Wyndham-Thomas C, Braeys T, Verhaegen J, Maes P, et al. Dynamic changes in paediatric invasive pneumococcal disease after sequential switches of conjugate vaccine in Belgium: a national retrospective observational study. *Lancet Infect Dis*. 2021;21:127–36. [https://doi.org/10.1016/S1473-3099\(20\)30173-0](https://doi.org/10.1016/S1473-3099(20)30173-0)
6. Savulescu C, Krizova P, Lepoutre A, Mereckiene J, Vestheim DF, Ciruela P, et al.; SpIDnet group. Effect of high-valency pneumococcal conjugate vaccines on invasive pneumococcal disease in children in SpIDnet countries: an observational multicentre study. *Lancet Respir Med*. 2017;5:648–56. [https://doi.org/10.1016/S2213-2600\(17\)30110-8](https://doi.org/10.1016/S2213-2600(17)30110-8)
7. Moore MR, Link-Gelles R, Schaffner W, Lynfield R, Lexau C, Bennett NM, et al. Effect of use of 13-valent pneumococcal conjugate vaccine in children on invasive pneumococcal disease in children and adults in the USA: analysis of multisite, population-based surveillance. *Lancet Infect Dis*. 2015;15:301–9. [https://doi.org/10.1016/S1473-3099\(14\)71081-3](https://doi.org/10.1016/S1473-3099(14)71081-3)
8. Hanquet G, Krizova P, Valentiner-Branth P, Ladhani SN, Nuorti JP, Lepoutre A, et al.; SpIDnet/I-MOVE+ Pneumo Group. Effect of childhood pneumococcal conjugate vaccination on invasive disease in older adults of 10 European countries: implications for adult vaccination. *Thorax*. 2019;74:473–82. <https://doi.org/10.1136/thoraxjnl-2018-211767>
9. Desmet SP, Verhaegen J, Flamaing J, Lagrou K. Increase in PCV13-only serotype invasive pneumococcal disease in children and older persons during PCV10 period (2015–2019) in Belgium. Presented at: International Symposium on Pneumococci and Pneumococcal Diseases (ISPPD). Toronto, Ontario, Canada; June 19–23, 2022.
10. Ladhani SN, Collins S, Djennad A, Sheppard CL, Borrow R, Fry NK, et al. Rapid increase in non-vaccine serotypes causing invasive pneumococcal disease in England and Wales, 2000–17: a prospective national observational cohort study. *Lancet Infect Dis*. 2018;18:441–51. [https://doi.org/10.1016/S1473-3099\(18\)30052-5](https://doi.org/10.1016/S1473-3099(18)30052-5)
11. Wouters I, Desmet S, Van Heirstraeten L, Herzog SA, Beutels P, Verhaegen J, et al.; NPcarriage Study Group. How nasopharyngeal pneumococcal carriage evolved during and after a PCV13-to-PCV10 vaccination programme switch in Belgium, 2016 to 2018. *Euro Surveill*. 2020;25:1900303. <https://doi.org/10.2807/1560-7917.ES.2020.25.5.1900303>
12. Wouters I, Van Heirstraeten L, Desmet S, Blaizot S, Verhaegen J, Goossens H, et al.; NPcarriage Study Group. Nasopharyngeal s. pneumoniae carriage and density in Belgian infants after 9 years of pneumococcal conjugate vaccine programme. *Vaccine*. 2018;36:15–22. <https://doi.org/10.1016/j.vaccine.2017.11.052>
13. Epping L, van Tonder AJ, Gladstone RA, The Global Pneumococcal Sequencing Consortium, Bentley SD, Page AJ, et al. SeroBA: rapid high-throughput serotyping of *Streptococcus pneumoniae* from whole genome sequence data. *Microb Genom*. 2018;4:e000186.
14. Metcalf BJ, Gertz RE Jr, Gladstone RA, Walker H, Sherwood LK, Jackson D, et al.; Active Bacterial Core surveillance team. Strain features and distributions in pneumococci from children with invasive disease before and after 13-valent conjugate vaccine implementation in the USA. *Clin Microbiol Infect*. 2016;22:60.e9–29. <https://doi.org/10.1016/j.cmi.2015.08.027>
15. Wood DE, Lu J, Langmead B. Improved metagenomic analysis with Kraken 2. *Genome Biol*. 2019;20:257. <https://doi.org/10.1186/s13059-019-1891-0>
16. Gladstone RA, Lo SW, Lees JA, Croucher NJ, van Tonder AJ, Corander J, et al.; Global Pneumococcal Sequencing Consortium. International genomic definition of pneumococcal lineages, to contextualise disease, antibiotic resistance and vaccine impact. *EBioMedicine*. 2019;43:338–46. <https://doi.org/10.1016/j.ebiom.2019.04.021>
17. Del Grosso M, Camilli R, D'Ambrosio F, Petrucci G, Melchiorre S, Moschioni M, et al. Increase of pneumococcal serotype 19A in Italy is due to expansion of the piliated clone ST416/CC199. *J Med Microbiol*. 2013;62:1220–5. <https://doi.org/10.1099/jmm.0.061242-0>
18. van der Linden M, Reinert RR, Kern WV, Imöhl M. Epidemiology of serotype 19A isolates from invasive pneumococcal disease in German children. *BMC Infect Dis*. 2013;13:70. <https://doi.org/10.1186/1471-2334-13-70>
19. Marimón JM, Alonso M, Rolo D, Ardanuy C, Liñares J, Pérez-Trallero E. Molecular characterization of *Streptococcus pneumoniae* invasive serotype 19A isolates from adults in two Spanish regions (1994–2009). *Eur J Clin Microbiol Infect Dis*. 2012;31:1009–13. <https://doi.org/10.1007/s10096-011-1399-3>
20. Mahjoub-Messai F, Doit C, Koeck JL, Billard T, Evrard B, Bidet P, et al. Population snapshot of *Streptococcus pneumoniae* serotype 19A isolates before and after introduction of seven-valent pneumococcal vaccination for French children. *J Clin Microbiol*. 2009;47:837–40. <https://doi.org/10.1128/JCM.01547-08>
21. European Centre for Disease Prevention and Control. Antimicrobial consumption database (ESAC-Net), 2021 [cited 2021 Jan 7]. <https://www.ecdc.europa.eu/en/antimicrobial-consumption/surveillance-and-disease-data/database>
22. Wyllie AL, Rümke LW, Arp K, Bosch AA, Bruin JP, Rots NY, et al. Molecular surveillance on *Streptococcus pneumoniae* carriage in non-elderly adults; little evidence for pneumococcal circulation independent from the reservoir in children. *Sci Rep*. 2016;6:34888. <https://doi.org/10.1038/srep34888>
23. Simell B, Auranen K, Käyhty H, Goldblatt D, Dagan R, O'Brien KL; Pneumococcal Carriage Group. The fundamental link between pneumococcal carriage and disease. *Expert Rev Vaccines*. 2012;11:841–55. <https://doi.org/10.1586/erv.12.53>
24. Wyllie AL, Warren JL, Regev-Yochay G, Givon-Lavi N, Dagan R, Weinberger DM. Serotype patterns of pneumococcal disease in adults are correlated with carriage patterns in older children. *Clin Infect Dis*. 2021;72:e768–75. <https://doi.org/10.1093/cid/ciaa1480>
25. Health Belgium. Vaccination against pneumococci: children and adolescents (HGR 9519) [in Dutch]. 2018 [cited 2022 Apr 4]. [https://www.health.belgium.be/sites/default/files/uploads/fields/fpshealth\\_theme\\_file/hgr\\_9519\\_advies\\_vaccinatie\\_pneumokokken\\_kinderen\\_.pdf](https://www.health.belgium.be/sites/default/files/uploads/fields/fpshealth_theme_file/hgr_9519_advies_vaccinatie_pneumokokken_kinderen_.pdf)
26. Care and Health. Duration of government contracts for vaccines and vaccination policy in Flanders. [in Dutch] [cited 2022 Apr 12]. <https://www.zorg-en-gezondheid.be/duur-en-looptijd-van-de-overheidsopdrachten-voor-vaccins-en-het-vaccinatiebeleid-in-vlaanderen>
27. Brueggemann AB, Jansen van Rensburg MJ, Shaw D, McCarthy ND, Jolley KA, Maiden MCJ, et al. Changes in the incidence of invasive disease due to *Streptococcus pneumoniae*,

*Haemophilus influenzae*, and *Neisseria meningitidis* during the COVID-19 pandemic in 26 countries and territories in the Invasive Respiratory Infection Surveillance Initiative: a prospective analysis of surveillance data. *Lancet Digit Health*. 2021;3:e360–70. [https://doi.org/10.1016/S2589-7500\(21\)00077-7](https://doi.org/10.1016/S2589-7500(21)00077-7)

28. Amin-Chowdhury Z, Aiano F, Mensah A, Sheppard CL, Litt D, Fry NK, et al. Impact of the coronavirus disease 2019 (COVID-19) pandemic on invasive pneumococcal disease and risk of pneumococcal coinfection with severe acute

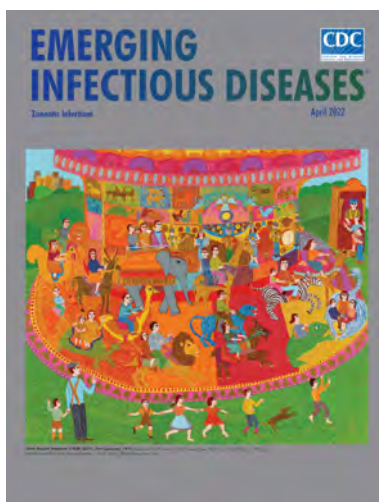
respiratory syndrome coronavirus 2 (SARS-CoV-2): Prospective National Cohort Study, England. *Clin Infect Dis*. 2021;72:e65–75. <https://doi.org/10.1093/cid/ciaa1728>

Address for correspondence: Stefanie Desmet, Microbiology, Immunology, and Transplantation, Katholieke Universiteit Leuven, Herestraat 49, 3000 Leuven, Belgium; email: stefanie.desmet@uzleuven.be

April 2022

## Zoonotic Infections

- Citywide Integrated *Aedes aegypti* Mosquito Surveillance as Early Warning System for Arbovirus Transmission, Brazil
- *Shewanella* spp. Bloodstream Infections in Queensland, Australia
- Increasing Antimicrobial Resistance in World Health Organization Eastern Mediterranean Region, 2017–2019
- Phylogenetic Analysis of Spread of Hepatitis C Virus Identified during HIV Outbreak Investigation, Unnao, India
- SARS-CoV-2 IgG Seroprevalence among Blood Donors as a Monitor of the COVID-19 Epidemic, Brazil
- Diminishing Immune Responses against Variants of Concern in Dialysis Patients 4 Months after SARS-CoV-2 mRNA Vaccination
- Genomic Epidemiology of Early SARS-CoV-2 Transmission Dynamics, Gujarat, India
- Reassessing Reported Deaths and Estimated Infection Attack Rate during the First 6 Months of the COVID-19 Epidemic, Delhi, India
- Mapping the Risk for West Nile Virus Transmission, Africa
- Increased Attack Rates and Decreased Incubation Periods in Raccoons with Chronic Wasting Disease Passaged through Meadow Voles



- Fatal Human Alphaherpesvirus 1 Infection in Free-Ranging Black-Tufted Marmosets in Anthropized Environments, Brazil, 2012–2019
- Molecular Surveillance for Imported Antimicrobial Resistant *Plasmodium falciparum*, Ontario, Canada
- Decrease in Tuberculosis Cases during COVID-19 Pandemic as Reflected by Outpatient Pharmacy Data, United States, 2020
- Unique Clinical, Immune, and Genetic Signature in Patients with Borrelial Meningoradiculoneuritis
- Durability of Antibody Response and Frequency of SARS-CoV-2 Infection 6 Months after COVID-19 Vaccination in Healthcare Workers
- SARS-CoV-2 Outbreak among Malayan Tigers and Humans, Tennessee, USA, 2020
- Zika Virus after the Public Health Emergency of International Concern Period, Brazil
- Vehicle Windshield Wiper Fluid as Potential Source of Sporadic Legionnaires' Disease in Commercial Truck Drivers
- *Bordetella hinzii* Pneumonia in Patient with SARS-CoV-2 Infection
- Coccidioidomycosis Cases at a Regional Referral Center, West Texas, USA, 2013–2019
- In Vitro Confirmation of Artemisinin Resistance in *Plasmodium falciparum* from Patient Isolates, Southern Rwanda, 2019
- *Rigidoporus corticola* Colonization and Invasive Fungal Disease in Immunocompromised Patients, United States
- Zoonotic Pathogens in Wildlife Traded in Markets for Human Consumption, Laos
- Infectious Toscana Virus in Seminal Fluid of Young Man Returning from Elba Island, Italy
- Multisystem Inflammatory Syndrome in Adult after First Dose of mRNA Vaccine

**EMERGING  
INFECTIOUS DISEASES**

To revisit the April 2022 issue, go to:

<https://wwwnc.cdc.gov/eid/articles/issue/28/4/table-of-contents>

# Invasive Pneumococcal Disease and Long-Term Mortality Rates in Adults, Alberta, Canada

Kristen A. Versluys, Dean T. Eurich, Thomas J. Marrie, Gregory J. Tyrrell

The relationship between increased short-term mortality rates after invasive pneumococcal disease (IPD) has been frequently studied. However, the relationship between IPD and long-term mortality rates is unknown. IPD patients in Alberta, Canada, had clinical data collected that were linked to administrative databases. We used Cox proportional hazards modeling, and the primary outcome was time to all-cause deaths. First IPD events were identified in 4,522 patients, who had a median follow-up of 3.2 years (interquartile range 0.8–9.1 years). Overall all-cause mortality rates were consistently higher among cases than controls at 30 days (adjusted hazard ratio [aHR] 3.75, 95% CI 3.29–4.28), 30–90 days (aHR 1.56, 95% CI 1.27–1.93), and >90 days (aHR 1.43, 95% CI 1.33–1.54). IPD increases risk for short, intermediate, and long-term mortality rates regardless of age, sex, or concurrent conditions. These findings can help clinicians focus on postdischarge patient plans to limit long-term effects after acute IPD infection.

Despite introduction and recommendation of the capsular polysaccharide pneumococcal vaccine in Canada during 1989 to persons  $\geq 65$  years of age, *Streptococcus pneumoniae* is still a cause of major illness and death in Canada and worldwide (1–3). The most serious manifestation of infection is invasive pneumococcal disease (IPD), which is characterized by bacteria invading normally sterile body sites, such as blood, lungs, or cerebrospinal fluid. In Canada, the incidence of IPD is around 8.8–9.9 cases/100,000 persons (4,5) and consistently highest in persons >60 years of age (27.1 cases/100,000 men and 20.2 cases/100,000 women) (6).

Short-term 30-day mortality rates after IPD have been frequently studied (estimated case-fatality rate within 30 days ranging from 13% to 21%) (7,8).

Increasing age and concurrent conditions are associated with increased case-fatality rates (7,8). However, studies on long-term mortality rates after IPD have been largely deficient, despite IPD being a reportable disease in Canada since 2000 (9).

Two studies conducted in Norway and the Netherlands investigated 1-year and 5-year mortality rates after IPD compared with those for age- and sex-matched controls in the general population (7,10). In persons who survived initial hospitalization or survived 30 days after acute infection, IPD mortality rates were higher for cases than for controls (1-year mortality rate 10%–30% for cases vs. 1%–3% for controls; 5-year mortality rate 35%–42% for cases vs. 7%–15% for controls) (7,10). However, the study noted that, in the Netherlands, most deaths occurred within the first 30 days (case-mortality rate 17%) (7). Thus, it remains unclear whether IPD increases long-term mortality rates. Moreover, these were highly selected samples because both studies used data from only 1 hospital in a large urban center, which are unlikely to be representative of the broader IPD population (7,10).

Widespread pneumococcal vaccination has seen major success (11). However, with an aging population at risk for IPD, and pneumococcal serotypes changing to evade current vaccinations, IPD remains a disease of public health concern (12). We have shown a change in serotypes and associated potential increases in severity of disease among IPD patients in Alberta, Canada (13). To determine how IPD is affecting mortality rates, we investigated short, intermediate, and long-term mortality outcomes for persons who had IPD compared with age- and sex-matched controls in Alberta over a 20-year period.

Author affiliations: University of Alberta, Edmonton, Alberta, Canada (K.A. Versluys, D.T. Eurich, G.T. Tyrrell); Dalhousie University, Halifax, Nova Scotia, Canada (T.J. Marrie); Provincial Laboratory for Public Health, Edmonton (G.T. Tyrrell)

DOI: <https://doi.org/10.3201/eid2808.212469>

## Methods

### IPD Cases

Community cases of IPD were defined by laboratory-confirmed isolation of *S. pneumoniae* from a sterile site,

including blood, cerebrospinal fluid (CSF), and pleural fluid (14). In Alberta, all IPD cases are reported to Alberta Health; thus, case ascertainment is accurate and complete. Data were collected on all adult IPD patients ( $\geq 18$  years of age) in Alberta during 1999–2019. The population of Alberta was estimated at 2.9 million at the start of follow-up and 4.3 million by the end of follow-up (15). Data for case-patients were collected by using standardized case reports. These data included demographic information, concurrent conditions, pharmacy data, laboratory results, diagnostic imaging, and vitals for the entirety of their hospital stay. Concurrent conditions for IPD patients have been described (16). This study was approved by the University of Alberta Health Ethics Research Board (Pro00071271) and Alberta Health Services.

### Matched Controls

We age- and sex-matched case-patients with up to 2 population controls who did not have a history of IPD. Because case-patients were hospitalized, where possible, hospital controls were preferred because both groups probably had poorer underlying health than nonhospitalized controls. Hospitalized controls were defined as being alive at the time of the index case, the same age ( $\pm 1$  year) and sex, and hospitalized within a  $\pm 3$ -month time frame as the case IPD diagnosis date. If  $> 2$  controls were identified, we randomly selected 2 controls from the pool of eligible controls for that case-patient. If no suitable hospitalized controls were available, we selected nonhospitalized age- and sex-matched controls from the Alberta general population registry. Unlike case-patients, who had extensive data collected as part of their hospital stays, controls had no specific data collected, other than administrative data.

### Linkage to Administrative Data

Using lifetime personal healthcare numbers (PHNs), we linked patients to the provincial administrative health databases. This linkage included Alberta Vital statistics to determine mortality rate (the provincial registry system that captures all migration within the province). We obtained all hospitalizations, ambulatory visits, and physician claims from the Discharge Abstract Database, the National Ambulatory Care Reporting System, the Ambulatory Care Classification System, and Physician Claim data. We used the standardized International Classification of Diseases, 9th and 10th Revisions (ICD-9 and ICD-10), for diagnostic coding preceding IPD date, hospitalization date for controls, or pseudodiagnosis date for nonhospitalized controls, for up to 5 years, to identify concurrent conditions.

### Outcome Measures

The primary outcome was time to all-cause mortality after IPD diagnosis date or pseudodiagnosis date for controls. We assessed short-term ( $< 30$  days after IPD), intermediate-term (30–90 days), and long-term ( $> 90$  days) mortality rates to determine the relationship between infection and survival. Mortality rates within 30 days are expected to be directly associated with acute IPD infection, as noted (7,8); intermediate and long-term mortality rates might not explicitly be from acute infection but rather a result of downstream, yet unknown, sequelae.

### Statistical Analysis

To describe the relationship between IPD patients and mortality rates, we performed logistic regression and survival analysis. Time zero was defined as date of IPD diagnosis, or pseudo-date for matched controls. Patients were followed up until death, censoring (person left the province) or March 31, 2019, if the person was alive at the end of the follow-up period. The maximum follow-up time possible was 20 years. If death or censoring preceded the start of the intermediate or long-term follow-up (for 30–90-day and  $> 90$ -day analyses), we subsequently excluded those persons so as to observe the effects of IPD on these outcomes among persons who survived to these time periods. Completing the segmented analysis enabled a clearer picture of long-term mortality rates to be understood, after removing the shorter mortality rates from the estimates. Finally, an analysis was completed to look at overall survival over the entire potential 20 years of follow-up (i.e., 30-day, 30–90-day, and  $> 90$ -day time periods were not assessed). If multiple IPD episodes occurred, only the first event was used.

We used Kaplan-Meier survival curves and log-rank tests to describe mortality rates over time, which we stratified by age and sex. We divided age categories into  $< 45$ , 45–60, 60–75, and  $> 75$  years. To characterize the population, we identified all relevant diagnostic codes (ICD-9 and ICD-10 classifications) in the administrative databases, including hospitalization, ambulatory, and physicians claims before each person's respective diagnosis date. We also calculated the Elixhauser comorbidity index (17), which incorporates 31 comorbidities, each comorbidity category is dichotomous: it is either present or absent based on administrative coding. Thus, a person could have a range of no comorbidities (0) or upwards of all comorbidities identified (18). We also included 3 additional cardiovascular risk factors (hyperlipidemia, previous stroke, and previous ischemic heart disease), because cardiovascular disease is associated with increased

risk for IPD. Scores were categorized into 2 groups, 0–1 comorbidities or  $\geq 2$  comorbidities, which is often used a marker of multimorbidity in health services research (19).

We used Cox proportional hazard modeling to compare case-patients and controls. We performed adjusted analyses by using models that had case-patient/control status, age categories, and Elixhauser comorbidity categories, but we used no specific model building strategy. We forced the Elixhauser comorbidity score into the model to ensure that differences in outcomes were not driven by differences in comorbidity. We also included age in our models to control for any residual confounding. We performed stratified analysis by using age, comorbidity category, and sex. In addition, to determine whether mortality rate trends have changed over time, we stratified IPD cases occurring  $>10$  years ago, 5–10 years ago, and  $<5$  years ago and measured this trend by using a linear trend test. Finally, we tested interactions between case status with age, sex, and comorbidity score. We tested a Cox proportional hazards assumption by using log-log plots and Schoenfeld residuals. A  $p$  value  $<0.05$  was considered significant in modeling. All analyses were performed by using Stata software version 15 (StataCorp LLC, <https://www.stata.com>).

In a sensitivity analysis, we excluded all IPD cases (and their controls) if no hospitalized controls were identified for the IPD case. In addition, we also excluded all IPD case-patients who had  $>1$  IPD event to ensure these events were not influencing our mortality rate estimates.

## Results

### Patient Characteristics

Our study comprised 4,522 IPD case-patients, and 4,315 (95%) were matched with 8,837 controls; there were 2 controls/case-patient (Figure 1). Overall, 4,357 (96.4%) IPD case-patients had  $\geq 1$  hospitalized control; for some IPD case-patients ( $n = 165$ , 3.6%), nonhospitalized controls were required. The mean ( $\pm$ SD) age of case-patients was 55.8 ( $\pm 17.7$ ) years, and 56.7% of case-patients were male; this distribution remained consistent over time (Table 1; Appendix Table 1, <https://wwwnc.cdc.gov/EID/article/28/8/21-2469-App1.pdf>).

Data on site of infection were available for patients only during 1999–2014. Of those patients, 67% had *S. pneumoniae* identified in  $>1$  sterile body site. There were 2,008 (44.4%) cases of invasive pneumonia, of which 1,961 (97.7%) also had a positive blood culture; the remaining 2.3% had *S. pneumoniae*

isolated from another sterile body site (pleural fluid, pericardial fluid, and peritoneal fluid). There were 116 (2.6%) cases of meningitis, 2,315 (51.2%) cases of bacteremia/sepsis, and 646 (14.3%) cases from an unspecified/other sterile source (not mutually exclusive) (Table 1).

### All-Cause Mortality Rate within 30 Days

Within 30 days of the IPD diagnosis date (or pseudo-date for controls), there were 614 deaths among IPD cases (1,915 deaths/1,000 person-years), compared with 348 deaths in the control group (510 deaths/1,000 person-years) (Figure 2, panel A). After adjustment, IPD cases were strongly associated with increased risk for 30-day mortality rate (adjusted odds ratio [aOR] 4.08, 95% CI 3.54–4.69; adjusted hazard ratio [aHR] 3.75, 95% CI 3.29–4.28) compared with controls (Table 2; Appendix Table 2).

We observed a major increase in risk for mortality rate in IPD case-patients in every age category for both male and female patients, as well as level of Elixhauser comorbidity category (Table 3). No interactions with age categories or Elixhauser scores were noted.

When stratified by year of IPD occurrence, we found that mortality rate differences decreased over time. These decreases were for case-patients  $>10$  years ago (1999–2009) (aHR 4.66, 95% CI 3.75–5.78), for case-patients 5–10 years ago (2009–2014) (aHR 4.07, 95% CI 3.09–5.35), and for case-patients within the past 5 years (2014–2019) (aHR 2.88, 95% CI 2.33–3.56;  $p < 0.001$  for trend).

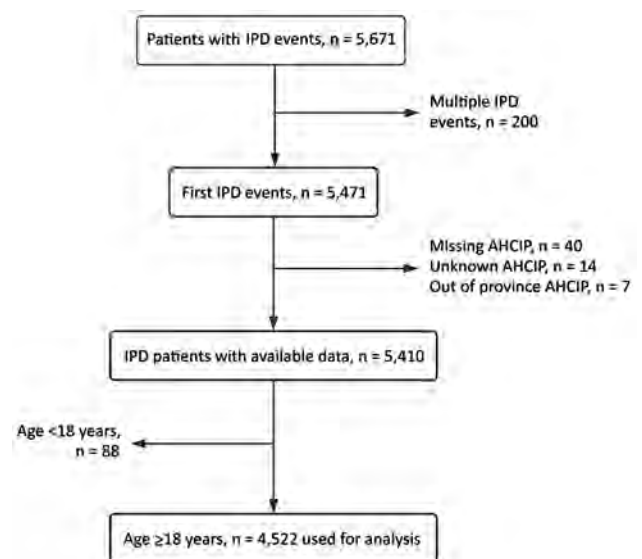


**Figure 1.** Flowchart diagram of case inclusion for study of IPD long-term mortality rates in adults, Alberta, Canada. AHCIP, Alberta Health Care Insurance Plan; IPD, invasive pneumococcal disease.

**Table 1.** Characteristics for case-patients and controls for invasive pneumococcal disease long-term mortality rates in adults, Alberta, Canada\*

| Characteristic                        | Case-patients | Controls      |
|---------------------------------------|---------------|---------------|
| Total                                 | 4,522 (100.0) | 8,837 (100.0) |
| Sex                                   |               |               |
| M                                     | 2,565 (56.7)  | 4,994 (56.5)  |
| F                                     | 1,957 (43.3)  | 3,843 (43.5)  |
| Age, y                                |               |               |
| <45                                   | 1,324 (29.3)  | 2,579 (29.2)  |
| 45–60                                 | 1,388 (30.7)  | 2,735 (30.9)  |
| 60–75                                 | 1,054 (23.3)  | 2,060 (23.3)  |
| >75                                   | 756 (16.7)    | 1,463 (16.6)  |
| Mean age, y (+SD)                     | 55.8 (17.7)   | 55.8 (17.7)   |
| Type of IPD                           |               |               |
| Pneumonia                             | 2,008 (44.4)  |               |
| Positive blood culture                | 1,961 (97.7)  |               |
| Positive pleural fluid                | 16 (0.8)      |               |
| Positive pericardial fluid            | 3 (0.1)       |               |
| Positive peritoneal fluid             | 2 (0.1)       |               |
| Unknown                               | 26 (1.3)      |               |
| Meningitis                            | 116 (2.6)     |               |
| Bacteremia/sepsis                     | 2,315 (51.2)  |               |
| Unspecified type                      | 646 (14.3)    |               |
| Unknown                               | 1,496 (33.0)  |               |
| Median comorbidity score (IQR)        | 5 (2–9)       | 5 (2–8)       |
| Comorbidities                         |               |               |
| Asplenia                              | 25 (0.6)      | 22 (0.5)      |
| Solid organ transplant                | 113 (2.5)     | 187 (4.2)     |
| HIV infection                         | 136 (3.0)     | 41 (0.9)      |
| Other immunosuppression conditions†   | 1,456 (32.2)  | 2,252 (50.0)  |
| Malignancies                          | 1,052 (23.3)  | 1,889 (41.9)  |
| Chronic obstructive pulmonary disease | 1,193 (26.4)  | 1,469 (32.6)  |
| Other respiratory diseases‡           | 771 (17.1)    | 1,139 (25.3)  |
| Asthma                                | 1,045 (23.1)  | 1,506 (33.4)  |
| Chronic renal disease                 | 502 (11.1)    | 881 (19.6)    |
| Hypertension                          | 1,790 (39.6)  | 2,744 (60.9)  |
| Ischemic heart disease                | 990 (21.9)    | 1,925 (42.7)  |
| Arrhythmias                           | 1,662 (36.8)  | 2,785 (61.8)  |
| Valvular heart disease                | 244 (5.4)     | 512 (11.4)    |
| Congestive heart failure              | 645 (14.3)    | 1,207 (26.8)  |
| Chronic liver disease                 | 806 (17.8)    | 863 (19.2)    |
| Diabetes                              | 1,057 (23.4)  | 1,768 (39.2)  |
| Smoking                               | 907 (20.1)    | 1,136 (25.2)  |
| Harmful alcohol use§                  | 1,968 (43.5)  | 2,503 (55.6)  |

\*Values are no. (%) except as indicated.

†Neutropenia, leukopenia, leukocyte disease, functional and genetic leukocyte cell abnormalities, myelofibrosis, disorders of immune mechanism.

‡Acute bronchitis, pneumoconiosis, pneumonitis, pulmonary embolism, and other pulmonary circulation disorders.

§Alcohol related disorders, toxic effects of alcohol, alcoholic polyneuropathy, alcoholic cardiomyopathy, alcoholic gastritis, alcoholic fatty liver disease, alcoholic cirrhosis, alcoholic liver disease, alcohol abuse counseling and surveillance.

### All-Cause Mortality Rates at 30–90 Days

After removing IPD cases (and controls) who died or were censored within 30 days, we found that 3,888 case-patients (86.0%) and 8,459 (95.7%) controls remained. Compared with age- and sex-matched controls, for which 220 deaths (107 deaths/1,000 patient-years) occurred, case-patients had 149 total deaths (158 deaths/1,000 patient-years) during 30–90 days after the diagnosis date (Figure 2, panel B). Both unadjusted and adjusted models demonstrated an increased risk for death for persons who had IPD (unadjusted HR [uHR] 1.49, 95% CI 1.21–1.83; unadjusted OR [uOR] 1.49, 95% CI 1.21–1.84; aHR 1.56, 95% CI 1.27–1.93;

aOR 1.58, 95% CI 1.28–1.96) (Table 2; Appendix Table 2).

When we stratified patients by age group, we observed an increased risk for death only among those >75 years of age. We observed a major increased risk for death for male and female patients, as well as by level of Elixhauser comorbidity category (Table 3). However, few events occurred in patients who had only 0–1 comorbidities (n = 31, 1.2%). No major interactions with age or comorbidities were noted.

Case-patients entering the study >10 years ago had higher observed mortality rates during 30–90 days after diagnosis date than did controls (aHR

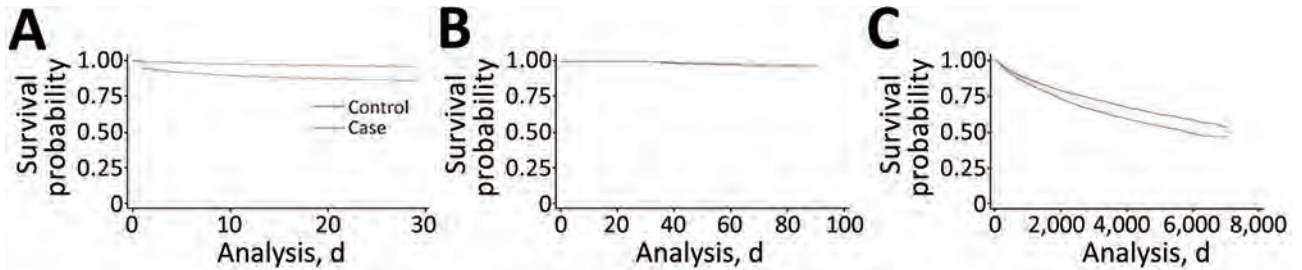


**Figure 2.** Invasive pneumococcal disease long-term mortality rates in adults, Alberta, Canada. Overall Kaplan-Meier survival estimates comparing case-patients with population controls. A) <30-day survival estimates; B) 30–90-day survival estimates. C) >90-day survival estimates.

2.12, 95% CI 1.55–2.92). Case-patients identified during 5–10 years ago had an aHR of 1.40 (95% CI 0.84–2.33), and those identified <5 years ago had an aHR 1.19 (95% CI 0.85–1.66;  $p < 0.001$  for trend).

**All-Cause Mortality Rate after 90 Days**

After removing IPD case-patients (and controls) who had an event within 90 days, we followed those who survived (and were not removed before 90 days) through March 31, 2019. At the end of this follow-up period, 1,174 case-patients (49 deaths/1,000 PYs) and 2,086 controls (37 deaths/1,000 PYs) died (Figure 2, panel C). Again, there was a major difference observed in mortality rates between case-patients and controls (uHR 1.32, 95% CI 1.23–1.42; uOR 1.35, 95% CI 1.24–1.47; aHR 1.43, 95% CI 1.33–1.54; aOR 1.49, 95% CI 1.36–1.64) (Table 2; Appendix Table 2).

Both groups that had 0–1 and  $\geq 2$  comorbidities showed higher mortality rates, as did every age group with the exception of patients >75 years of age. Again, female and male case-patients had similar increased risks when compared with controls. No interactions were noted. Cases identified >10 years ago had an aHR of 1.50 (95% CI 1.37–1.64), cases from 5–10 years ago had an aHR of 1.41

(95% CI 1.20–1.67), and cases from <5 years ago had an aHR of 1.26 (95% CI 1.06–1.51) ( $p < 0.001$  for trend).

**All-Cause Overall Mortality Rates**

When observing the entire follow-up period of 20 years, we found that the median follow-up period was 3.9 (interquartile range 1.3–10.2) years. Overall, 1,937 case-patients died (81 deaths/1,000 PYs) compared with 2,654 controls (47 deaths/1,000 PYs) (Figure 2). By age, event rates in cases were as follows: <45 years, 1,324 case-patients (29.3%), 88 deaths (14.3%); 45–60 years, 1,388 case-patients (30.7%), 170 deaths (27.7%); 60–75 years, 1,054 case-patients (23.3%), 173 deaths (28.2%); and >75 years, 756 case-patients (16.7%), 183 deaths (29.8%). Unadjusted and adjusted models provided similar results: uHR 1.66 (95% CI 1.56–1.76), uOR 1.75 (95% CI 1.62–1.88), aHR 1.77 (95% CI 1.67–1.88), and aOR 1.97 (95% CI 1.81–2.14) (Table 2; Appendix Table 2).

Models stratified by age, sex, and comorbidity category showed that case-patients had increased mortality rates when compared with controls ( $p < 0.01$ ) (Table 3). Interaction models were tested, and none were noted. log-minus-log plots and Schoenfeld residuals were generated, and no violations were noted.

**Table 2.** Death outcomes of invasive pneumococcal disease (IPD) patients compared with age- and sex-matched controls, Alberta, Canada\*

| Time, days | Controls                    |                      | Case-patients               |                      | log-rank test            |                          | HR (95% CI), p value |                          |                          |
|------------|-----------------------------|----------------------|-----------------------------|----------------------|--------------------------|--------------------------|----------------------|--------------------------|--------------------------|
|            | No. positive/no. tested (%) | No. events/1,000 PYs | No. positive/no. tested (%) | No. events/1,000 PYs | OR (95% CI), p value     |                          | Unadjusted           |                          |                          |
|            |                             |                      |                             |                      | Unadjusted               | Adjusted                 | Unadjusted           | Adjusted                 |                          |
| <30        | 348/8,837 (3.9)             | 510                  | 614/4,522 (13.6)            | 1,915                | 3.83 (3.34–4.39), <0.001 | 4.08 (3.54–4.69), <0.001 | 431.40, <0.001       | 3.65 (3.20–4.17), <0.001 | 3.75 (3.29–4.28), <0.001 |
| 30–90      | 220/8,459 (2.6)             | 107                  | 149/3,888 (3.8)             | 158                  | 1.49 (1.21–1.84), <0.001 | 1.58 (1.28–1.96), <0.001 | 14.09, <0.001        | 1.49 (1.21–1.83), <0.001 | 1.56 (1.27–1.93), <0.001 |
| >90        | 2,086/8,236 (25.3)          | 37                   | 1,174/3,733 (31.4)          | 49                   | 1.35 (1.24–1.47), <0.001 | 1.49 (1.36–1.64), <0.001 | 57.44, <0.001        | 1.32 (1.23–1.42), <0.001 | 1.43 (1.33–1.54), <0.001 |
| Overall    | 2,654/8,837 (30.0)          | 47                   | 1,937/4,522 (42.8)          | 81                   | 1.75 (1.62–1.88), <0.001 | 1.97 (1.81–2.14), <0.001 | 291.34, <0.001       | 1.66 (1.56–1.76), <0.001 | 1.77 (1.67–1.88), <0.001 |

\*HR, hazard ratio; OR, odds ratio, PY, person-year.

**Table 3.** Stratified hazard ratios for case-patients versus controls for invasive pneumococcal disease long-term mortality rates in adults, Alberta, Canada

| Characteristic       | Hazard ratio (95% CI), p value |                            |                          | Overall                  |
|----------------------|--------------------------------|----------------------------|--------------------------|--------------------------|
|                      | <30 d                          | 30–90 d                    | >90 d                    |                          |
| Age <45 y            | 8.88 (5.46–14.42), <0.001      | 1.75 (0.88–3.47), 0.110    | 2.41 (1.97–2.95), <0.001 | 2.97 (2.49–3.53), <0.001 |
| Age 45–60 y          | 4.66 (3.56–6.09), <0.001       | 1.44 (0.94–2.21), 0.098    | 1.64 (1.43–1.89), <0.001 | 2.02 (1.80–2.27), <0.001 |
| Age 60–75 y          | 3.85 (3.00–4.95), <0.001       | 1.36 (0.92–2.00), 0.127    | 1.36 (1.19–1.55), <0.001 | 1.69 (1.51–1.89), <0.001 |
| Age >75 y            | 2.54 (2.05–3.15), <0.001       | 1.79 (1.28–2.50), 0.001    | 1.10 (0.97–1.26), 0.137  | 1.41 (1.27–1.56), <0.001 |
| Male                 | 3.57 (3.00–4.25), <0.001       | 1.48 (1.12–1.94), 0.005    | 1.40 (1.27–1.54), <0.001 | 1.71 (1.58–1.85), <0.001 |
| Female               | 4.02 (3.29–4.91), <0.001       | 1.71 (1.24–2.35), 0.001    | 1.50 (1.34–1.66), <0.001 | 1.86 (1.71–2.04), <0.001 |
| Elixhauser score 0–1 | 6.41 (4.01–10.24), <0.001      | 16.73 (5.09–55.06), <0.001 | 1.72 (1.47–2.02), <0.001 | 2.16 (1.87–2.49), <0.001 |
| Elixhauser score ≥2  | 3.55 (3.10–4.08), <0.001       | 1.32 (1.06–1.65), 0.015    | 1.36 (1.26–1.48), <0.001 | 1.70 (1.59–1.81), <0.001 |

Case-patients identified >10 years ago (aHR 1.80, 95% CI 1.66–1.94), 5–10 years ago (aHR 1.85, 95% CI 1.62–2.11), and in the past 5 years (aHR 1.67, 95% CI 1.48–1.89) had similar estimates over time (p<0.01). However when compared with controls, we found that case-patients still had higher mortality rates (Figure 3; Appendix Table 3).

**Sensitivity Analysis**

In a sensitivity analysis, after excluding all IPD case-patients (and their controls) if no hospitalized controls were identified for the case-patient (n = 164, 3.6%), we found that our results were unchanged (<30 days aHR 3.71, 95% CI 3.24–4.24; 30–90 days aHR 1.43, 95% CI 1.16–1.78; >90 days aHR 1.37, 95% CI 1.27–1.47; overall mortality rate aHR 1.70, 95% CI 1.61–1.81). In addition, after we excluded IPD case-patients (and their matched controls) who had >1 IPD event (n = 142, 3.1%), we observed similar results (<30 days aHR

3.92, 95% CI 3.43–4.48; 30–90 days aHR 1.59, 95% CI 1.29–1.97; >90 days aHR 1.39, 95% CI 1.29–1.49; overall mortality rate aHR 1.75, 95% CI 1.65–1.86).

**Discussion**

This study showed that an episode of IPD increases the risk for death not only in the short term, which is expected, but is also a prognostic marker in the intermediate- and long-term periods. The observed aHR for 30-day mortality rate was the highest estimate because acute infection is believed to be directly associated with death. As time after infection increases, risk for death is believed to be influenced by lasting sequalee after acute infection, which this study showed remains substantial (20). Although the absolute difference in events per PY between cases and controls was nearly 4-fold higher in the initial 30-day period, the absolute event rate remained almost 50% higher throughout the

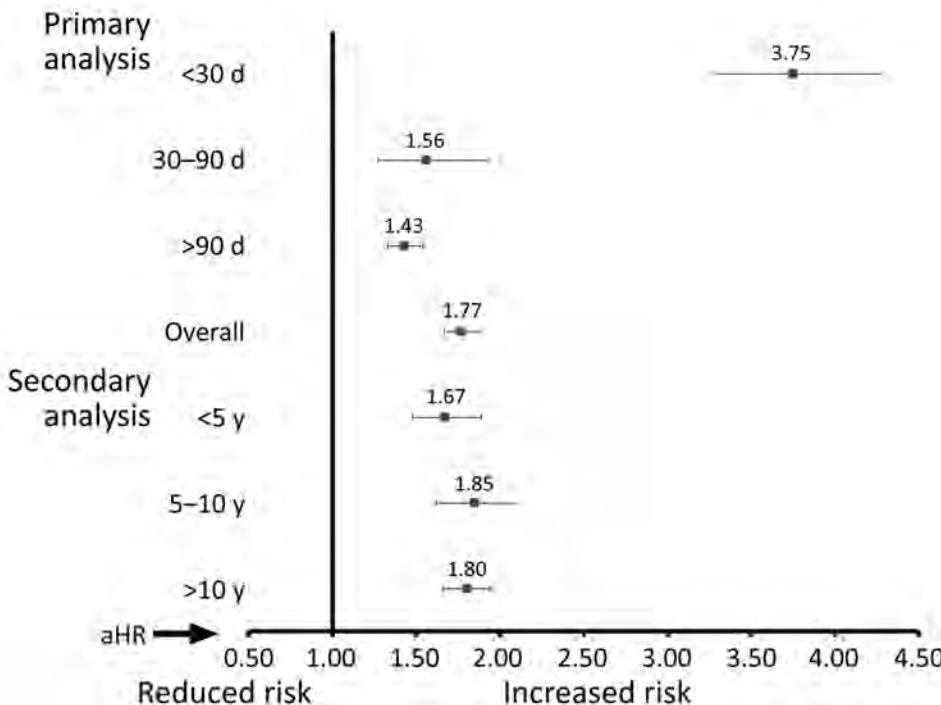


**Figure 3.** Invasive pneumococcal disease (IPD) long-term mortality rates in adults, Alberta, Canada. aHRs describing illness risk comparing IPD cases versus controls after adjusting for age and Elixhauser comorbidity scores. Primary analysis: short (<30 days), intermediate (30–90 days), and long-term (>90 days) and overall (entire time period) follow-up. Secondary analysis: IPD cases and matched controls identified <5 years ago, 5–10 years ago, and >10 years ago. Error bars indicate 95% CIs. aHR, adjusted hazard ratio.

entire follow-up period, irrespective of age or comorbidity level.

Our results were similar to those of previous studies (30-day mortality rate of 14% vs. 13%–21% published, >90-day mortality rate of 31% compared with 10%–42% previously published) (7,8,10,21). In terms of specific risk groups, like others, we observed a higher absolute rate difference in case-patients who had multimorbidities compared with those without multimorbidities irrespective of time frame (7,8,22). However, the relative HRs compared with those for controls were highest in persons who did not have a comorbidity. A similar trend was seen with increasing age. Although persons <45 years of age had the lowest absolute rate difference in terms of events per PY, the relative increase in deaths compared with that of controls was the highest among persons <45 years of age, and the relative difference decreased with increasing age. Although published reports frequently describe male sex as being a risk factor for increased death from IPD (7,8), our findings differ. We observed few differences in sex with respect to short- or long-term deaths. The reason for the discrepancy is unknown, but several previous studies were completed in specific populations and locations, whereas our analysis was a large population-based approach, which might partially or fully explain the reported differences. In addition, unknown confounding in previous studies or ours might also explain the differences.

Because our study spanned a wide period, it is useful to recognize advancements in medicine and preventive care for IPD. There have been decreases of aHRs over time, and the gap has decreased particularly in the past 5 years. Although the exact mechanisms of why this decrease is occurring is unknown, some possible explanations are increased use of vaccinations, herd immunity protection, and advances in use of antimicrobial drugs and supportive care (1). In Canada, vaccine recommendations have been consistent with the 23-valent pneumococcal polysaccharide vaccine recommended for immunocompetent adults  $\geq 65$  years of age (the recommended target population) and immunocompromised adults 18–65 years of age. Estimated vaccine uptake in adults >65 years of age during 2014 was  $\approx 37\%$  (in Canada) (3) and increased to  $\approx 53\%$  during 2020–2021 (in Alberta) (23). One possible reason for the increase might be related to policy changes that enabled pharmacists in Alberta to provide routine 23-valent pneumococcal polysaccharide vaccine to eligible adults. In addition, changing serotype distribution and

pathogenicity might have influenced differences in mortality rates observed between different periods.

Our study evaluated outcomes for up to 20 years in a cohort of IPD patients, covered a large sample size of persons who were identified from rural and urban areas, and had case ascertainment that is complete as a result of the provincial surveillance system and reportable requirements of IPD, but several limitations to our study should be recognized. First, because of the nature of the data, we were unable to account for some clinical differences (e.g., clinical markers such as blood pressure) that might have existed between patients who had IPD and controls. However, we adjusted for a well-known and validated Elixhauser comorbidity index, and controls were matched on site of care. Although it is not possible to adjust for every variable, our control matching on sex and age and adjustments for comorbidities provide a good understanding of IPD mortality rates. Second, the source of infection was not investigated for this study. It is hypothesized that persons who have nosocomial infections have worse outcomes than persons who have community-acquired infections (8), and our sample was IPD based on community-acquired infections. Third, the statistical power was low in some stratum analyses in which there were fewer deaths, in particular persons who had limited comorbidities. Thus, CIs were wide and should be interpreted with caution. Moreover, all-cause death was used as the outcome as opposed to a more cause-specific death (i.e., infectious-related death), and cause of death data were not fully available for the cohort, particularly in the early years. Fourth, history of comorbidities was based on the well-validated Elixhauser comorbidity index by using a 5-year history before diagnosis. Thus, comorbidities that might have occurred before this period for which the patient never received any subsequent care or follow-up for the condition could potentially be misclassified. Moreover, it is possible that residual confounding might exist at the level of the individual person (e.g., adherence to treatments, severity of illness) or at the population level (e.g., access to clinical care), which we could not account for in our analyses. Thus, if potential differences exist in this regard between case-patients and controls, the estimates of mortality rates could be potentially confounded. Fifth, enrollment was limited to a single province in Canada, which might limit generalizability of our findings. However, Alberta has a population of >4 million persons, so we do not see this limitation as a major concern.

In conclusion, IPD confers increased short, intermediate, and long-term mortality rates, irrespective of age or comorbidity. In particular, short-term

mortality rate outcomes are most noticeable compared with those for controls. However, persons who survive past 30 days are still at increased risk for death. In aging populations at risk, combined with increasing pneumococcal serotype switching and antimicrobial drug resistance (12,13), IPD remains a major disease. Thus, focused efforts on prevention of IPD and how best to prevent downstream sequelae are required. We believe that our findings might help front-line clinicians in recognizing the high-risk nature of IPD patients, even after the acute event has been managed, and might assist in long-term postdischarge care plans and preventive strategies to mitigate the risk for longer-term adverse events in these patients.

This study was supported by a grant-in-aid from Pfizer, Canada.

This study is based on data approved by The Alberta Strategy for Patient Orientated Research (ABSPOR) (<https://absporu.ca>) Support Unit, Alberta Health, and Alberta Health Services. Interpretations and conclusions contained herein are those of the researchers and do not necessarily represent the views of the Government of Alberta, Alberta Health Services, or ABSPOR. Neither the Government of Alberta, Alberta Health Services, or ABSPOR expresses any opinion in relation to this study. The administrative data that support the findings of this study are from ABSPOR. We had full permission to use these data; however, restrictions apply to the public availability of these data, which are under data access agreements for this study.

### About the Author

Ms. Versluys is a research scientist at the School of Public Health, University of Alberta, Edmonton, Alberta, Canada. Her primary research interests are invasive pneumococcal disease, other vaccine preventable diseases, medical laboratory science, and clinical epidemiology.

### References

- Feldman C, Anderson R. Recent advances in the epidemiology and prevention of *Streptococcus pneumoniae* infections. *F1000Research*. 2020;9:F1000 Faculty Rev-338.
- Mook-Kanamori BB, Geldhoff M, van der Poll T, van de Beek D. Pathogenesis and pathophysiology of pneumococcal meningitis. *Clin Microbiol Rev*. 2011;24:557-91. <https://doi.org/10.1128/CMR.00008-11>
- Public Health Agency of Canada. National Advisory Committee on Immunization. Advisory Committee Statement: update on the use of pneumococcal vaccines in adults 65 years and older – a public health perspective, 2018 [cited 2022 Apr 10]. <https://www.canada.ca/en/public-health/services/publications/healthy-living/update-on-the-use-of-pneumococcal-vaccines-in-adult.html>
- Desai S, Policarpio ME, Wong K, Gubbay J, Fediurek J, Deeks S. The epidemiology of invasive pneumococcal disease in older adults from 2007 to 2014 in Ontario, Canada: a population-based study. *CMAJ Open*. 2016;4:E545-50. <https://doi.org/10.9778/cmajo.20160035>
- Public Health Agency of Canada. Vaccine preventable disease: surveillance report to December 31, 2017 [cited 2021 Jun 1]. <https://www.canada.ca/en/public-health/services/publications/vaccines-immunization/vaccine-preventable-disease-surveillance-report-december-31-2017.html>
- Public Health Agency of Canada. Reported cases by age group in Canada, grouped by sex: notifiable diseases on-line. Pneumococcal disease, invasive, 2021 [cited 2021 Jun 5]. <https://diseases.canada.ca/notifiable/charts?c=abs>
- Wagenvoort GH, Sanders EA, de Melker HE, van der Ende A, Vlamincx BJ, Knol MJ. Long-term mortality after IPD and bacteremic versus non-bacteremic pneumococcal pneumonia. *Vaccine*. 2017;35:1749-57. <https://doi.org/10.1016/j.vaccine.2017.02.037>
- Christensen JS, Jensen TG, Kolmos HJ, Pedersen C, Lassen A. Bacteremia with *Streptococcus pneumoniae*: sepsis and other risk factors for 30-day mortality – a hospital-based cohort study. *Eur J Clin Microbiol Infect Dis*. 2012;31:2719-25. <https://doi.org/10.1007/s10096-012-1619-5>
- Government of Canada. Invasive pneumococcal disease, 2019 [cited 2021 Jun 5]. <https://www.canada.ca/en/public-health/services/immunization/vaccine-preventable-diseases/invasive-pneumococcal-disease/health-professionals.html>
- Floeystad HK, Holm A, Sandvik L, Vestrheim DF, Brandsaeter B, Berild D. Increased long-term mortality after survival of invasive pneumococcal disease: a population-based study. *Infect Dis (Lond)*. 2017;49:365-72. <https://doi.org/10.1080/23744235.2016.1271997>
- Wijayasri S, Hillier K, Lim GH, Harris TM, Wilson SE, Deeks SL. The shifting epidemiology and serotype distribution of invasive pneumococcal disease in Ontario, Canada, 2007-2017. *PLoS One*. 2019;14:e0226353. <https://doi.org/10.1371/journal.pone.0226353>
- Golden AR, Adam HJ, Karlowsky JA, Baxter M, Nichol KA, Martin I, et al.; Canadian Antimicrobial Resistance Alliance (CARA). Molecular characterization of predominant *Streptococcus pneumoniae* serotypes causing invasive infections in Canada: the SAVE study, 2011-15. *J Antimicrob Chemother*. 2018;73(suppl\_7):vii20-31. <https://doi.org/10.1093/jac/dky157>
- Marrie TJ, Tyrrell GJ, Majumdar SR, Eurich DT. Invasive pneumococcal disease in northern Alberta, not a red queen but a dark horse. *Vaccine*. 2018;36:2985-90. <https://doi.org/10.1016/j.vaccine.2018.04.032>
- Ministry of Health, Government of Alberta. Alberta Public Health Disease Management Guidelines: pneumococcal disease, invasive (IPD), 2019 [cited 2021 Jun 7]. <https://open.alberta.ca/dataset/67a2161b-d849-4fd4-8c02-9a1be7c65809/resource/f9750e6df-ed5d-48b5-93b4-bd70a9b41b00/download/health-phdmng-pneumococcal-disease-invasive-2021-09.pdf>
- Alberta Government. Alberta population estimates, data tables: quarterly Alberta total population estimates: 1951-2021. March 2021 [cited 2021 Jun 7]. <https://open.alberta.ca/dataset/alberta-population-estimates-data-tables#summary>
- Marrie TJ, Tyrrell GJ, Majumdar SR, Eurich DT. Invasive pneumococcal disease: still lots to learn and a need for standardized data collection instruments. *Can Respir J*. 2017;2017:2397429. <https://doi.org/10.1155/2017/2397429>

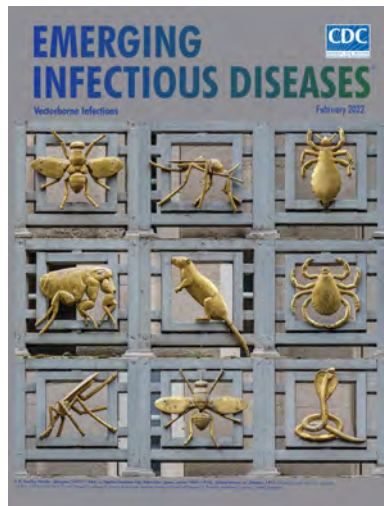
17. Li B, Evans D, Faris P, Dean S, Quan H. Risk adjustment performance of Charlson and Elixhauser comorbidities in ICD-9 and ICD-10 administrative databases. *BMC Health Serv Res.* 2008;8:12. <https://doi.org/10.1186/1472-6963-8-12>
18. Quan H, Sundararajan V, Halfon P, Fong A, Burnand B, Luthi JC, et al. Coding algorithms for defining comorbidities in ICD-9-CM and ICD-10 administrative data. *Med Care.* 2005;43:1130-9. <https://doi.org/10.1097/01.mlr.0000182534.19832.83>
19. Johnston MC, Crilly M, Black C, Prescott GJ, Mercer SW. Defining and measuring multimorbidity: a systematic review of systematic reviews. *Eur J Public Health.* 2019;29:182-9. <https://doi.org/10.1093/eurpub/cky098>
20. Hughes GJ, Wright LB, Chapman KE, Wilson D, Gorton R. Serotype-specific differences in short- and longer-term mortality following invasive pneumococcal disease. *Epidemiol Infect.* 2016;144:2654-69. <https://doi.org/10.1017/S0950268816000856>
21. Sandvall B, Rueda AM, Musher DM. Long-term survival following pneumococcal pneumonia. *Clin Infect Dis.* 2013;56:1145-6. <https://doi.org/10.1093/cid/cis1207>
22. Torres A, Blasi F, Dartois N, Akova M. Which individuals are at increased risk of pneumococcal disease and why? Impact of COPD, asthma, smoking, diabetes, and/or chronic heart disease on community-acquired pneumonia and invasive pneumococcal disease. *Thorax.* 2015;70:984-9. <https://doi.org/10.1136/thoraxjnl-2015-206780>
23. CanAge, Canada's National Seniors' Advocacy Organization. Adult vaccination in Canada: cross-country report Card 2021, 2021 [cited 2022 Apr 10]. <https://www.canage.ca/wp-content/uploads/2021/03/VaccineReportCard-2021-02-23-FINAL-1.pdf>

Address for correspondence: Dean Eurich, University of Alberta School of Public Health, 2-040 Li Ka Shing Centre for Health Research Innovation, Edmonton, AB T6G 2E1, Canada; email: [deurich@ualberta.ca](mailto:deurich@ualberta.ca)

February 2022

# Vectorborne Infections

- Novel Clinical Monitoring Approaches for Reemergence of Diphtheria Myocarditis, Vietnam
- Clinical and Laboratory Characteristics and Outcome of Illness Caused by Tick-Borne Encephalitis Virus without Central Nervous System Involvement
- Role of *Anopheles* Mosquitoes in Cache Valley Virus Lineage Displacement, New York, USA
- Burden of Tick-Borne Encephalitis, Sweden
- Invasive *Burkholderia cepacia* Complex Infections among Persons Who Inject Drugs, Hong Kong, China, 2016–2019
- Comparative Effectiveness of Coronavirus Vaccine in Preventing Breakthrough Infections among Vaccinated Persons Infected with Delta and Alpha Variants
- Effectiveness of mRNA BNT162b2 Vaccine 6 Months after Vaccination among Patients in Large Health Maintenance Organization, Israel
- Comparison of Complications after Coronavirus Disease and Seasonal Influenza, South Korea
- Epidemiology of Hospitalized Patients with Babesiosis, United States, 2010–2016
- Rapid Spread of Severe Fever with Thrombocytopenia Syndrome Virus by Parthenogenetic Asian Longhorned Ticks



- Wild Boars as Reservoir of Highly Virulent Clone of Hybrid Shiga Toxigenic and Enterotoxigenic *Escherichia coli* Responsible for Edema Disease, France
- Public Acceptance of and Willingness to Pay for Mosquito Control, Texas, USA
- Widespread Detection of Multiple Strains of Crimean-Congo Hemorrhagic Fever Virus in Ticks, Spain
- SARS-CoV-2 Cross-Reactivity in Prepandemic Serum from Rural Malaria-Infected Persons, Cambodia

- West Nile Virus Transmission by Solid Organ Transplantation and Considerations for Organ Donor Screening Practices, United States
- Viral Interference between Respiratory Viruses
- Serial Interval and Transmission Dynamics during SARS-CoV-2 Delta Variant Predominance, South Korea
- Postvaccination Multisystem Inflammatory Syndrome in Adult with No Evidence of Prior SARS-CoV-2 Infection
- Postmortem Surveillance for Ebola Virus Using OraQuick Ebola Rapid Diagnostic Tests, Eastern Democratic Republic of the Congo, 2019–2020
- SARS-CoV-2 Seroprevalence before Delta Variant Surge, Chattogram, Bangladesh, March–June 2021
- SARS-CoV-2 B.1.619 and B.1.620 Lineages, South Korea, 2021
- *Neisseria gonorrhoeae* FC428 Subclone, Vietnam, 2019–2020
- Zoonotic Infection with Oz Virus, a Novel Thogotovirus
- Tonate Virus and Fetal Abnormalities, French Guiana, 2019
- *Babesia crassa*-Like Human Infection Indicating Need for Adapted PCR Diagnosis of Babesiosis, France

**EMERGING  
INFECTIOUS DISEASES**

To revisit the February 2022 issue, go to:  
<https://wwwnc.cdc.gov/eid/articles/issue/28/2/table-of-contents>

# COVID-19 Symptoms and Deaths among Healthcare Workers, United States

Shao Lin,<sup>1</sup> Xinlei Deng,<sup>2</sup> Ian Ryan,<sup>2</sup> Kai Zhang,<sup>3</sup> Wangjian Zhang,<sup>3</sup>  
Ese Oghaghare,<sup>3</sup> DeeDee Bennett Gayle,<sup>3</sup> Benjamin Shaw<sup>3</sup>

We evaluated whether demographics and COVID-19 symptoms predicted COVID-19 deaths among healthcare workers (HCWs) in the United States by comparing COVID-19 deaths in HCWs with 3 control groups (HCW nondeaths, non-HCW deaths, and non-HCW nondeaths) using a case-control design. We obtained patient-level data of 33 variables reported during January 1, 2020–October 12, 2021, in all US states. We used logistic regression analysis while controlling for confounders. We found that persons who were  $\geq 50$  years of age, male, Black, or Asian experienced significantly more deaths than matched controls. In addition, HCWs who died had higher risks for the most severe clinical indicators. We also found that the most indicative symptoms were preexisting medical conditions, shortness of breath, fever, cough, and gastrointestinal symptoms. In summary, minority, male, and older HCWs had greater risk for COVID-19 death. Severe clinical indicators and specific symptoms may predict COVID-19–related deaths among HCWs.

COVID-19 is one of the longest-lasting and largest global pandemics in history (1), but its typical symptoms and relevant clinical predictors are still unknown. By March 2022, >79 million Americans had contracted COVID-19, and >963,000 had died (2,3). Multiple studies have found that older adults (4,5) and persons with chronic medical conditions, such as diabetes, hypertension, and renal

failure, were particularly susceptible to contracting COVID-19 (6,7).

Healthcare workers (HCWs) are another highly susceptible subpopulation (8–10) because of their time spent caring for COVID-19 patients (11). Of importance, 40% of HCWs identify as a racial minority; of those, 16% are Black, 13% Hispanic, and 7% Asian/other (12–14). Kirby reported that doctors from racial and ethnic minority communities were twice as likely to deal with patients without access to personal protective equipment (PPE) than White colleagues (15). Available data suggest that Black persons are more likely to hold jobs considered essential (e.g., HCW, medical assistant, food preparation, home care aide) than their White counterparts. In addition, ethnic minorities work disproportionately in the top 9 occupations exposed to COVID-19 and, therefore, are at high risk for infection (16). However, they are less likely to publicly express their workplace safety concerns for fear of job loss (17).

The initial surge in COVID-19 cases led to a profound increase in HCWs' exposure to the virus. However, the extent to which increased exposure in HCWs led to increased risk for death—and which demographic characteristics, severity indicators, and symptoms best predict this risk—remains unclear. Most previous research has used non-HCWs as controls, leading to biases due to differences in occupation, education, and treatment accessibility. In addition, a nationwide study evaluating COVID-19 symptoms and deaths among HCWs is lacking, especially one that accounts for the second and third COVID-19 surges.

To fill these knowledge gaps, we used COVID-19 surveillance data from the Centers for Disease Control

Author affiliations: University of Albany School of Public Health, Rensselaer, New York, USA (S. Lin, X. Deng, I. Ryan, K. Zhang, E. Oghaghare, B. Shaw); Sun Yat-Sen University School of Public Health, Guangzhou, China (W. Zhang); University at Albany College of Emergency Preparedness, Homeland Security and Cybersecurity, Albany, New York, USA (D. Bennett Gayle); University of Illinois Chicago School of Public Health, Chicago, Illinois, USA (B. Shaw)

DOI: <https://doi.org/10.3201/eid2808.212200>

<sup>1</sup>This author was the principal investigator and first author.

<sup>2</sup>These senior authors contributed equally to this article.

<sup>3</sup>These authors contributed equally to this article.

and Prevention (CDC) to compare the differences in demographic characteristics and symptoms between HCWs who died and those who did not (HCW deaths and nondeaths) and compared to the general population (non-HCW deaths and nondeaths). We also examined the temporal trends of COVID-19 infection and deaths in HCWs versus the general population.

## Methods

### Study Design and Controls

Our study population included all COVID-19 infection cases reported by the CDC. We used a case-control design to compare demographics and symptoms between HCW deaths and HCW nondeaths (control 1). HCW nondeaths were the primary control group, representing the source population and controlling for important confounders, including occupation, education, medical knowledge, and access to medical care. To compare our findings with previous research, we added 2 other reference groups from the US general population: non-HCW deaths (control 2), which is commonly used by other studies, and non-HCW nondeaths (control 3).

### Data Acquisition

We obtained data on laboratory-confirmed COVID-19 cases, probable cases, and deaths across the United States from the Restricted Access Dataset operated by the CDC. In January 2020, COVID-19 data collection commenced, and COVID-19 was added to the nationally notifiable condition list; on April 5, 2020, COVID-19 was classified as immediately notifiable, urgent (within 24 hours) (interim-20-ID-01). All states and territories were encouraged to enact laws in their jurisdictions to submit case notifications to CDC. CDC also requested that public health departments report all COVID-19 cases using standardized case report forms and case definitions for laboratory-confirmed or probable cases. This surveillance system includes patient-level data reported by all US territories and states. This study covers the timeframe January 1, 2020–October 12, 2021.

We obtained demographic and medical information for each record in this dataset, including COVID-19 case status (confirmed or probable case), date of first positive specimen collection, and demographics (sex, age group, race, ethnicity, and county and state of residence) (Table 1). We also obtained information on presence of severe COVID-19 clinical indicators and of less severe symptoms (Table 2). CDC suppressed data cells reporting <5 records and uncommon combinations of

demographic characteristics (recoded to NA) to prevent releasing personally identifiable data.

### Outcomes and Predictors

The health outcomes in this study were COVID-19-related deaths. Among HCW deaths and control groups 1, 2, and 3, a total of 97.8% were confirmed COVID-19 cases, and 2.2% were probable cases. We calculated fatality as the number of COVID-19 deaths divided by all COVID-19 cases in the United States. We used 20 predictors in the analysis, including demographic variables, severe COVID-19 clinical indicators, and less severe reported symptoms.

### Statistical Analysis and Confounders

We first compared all 20 predictor variables between HCW deaths and the 3 control groups using  $\chi^2$  tests. We then developed logistic regression models by regressing fatality against each symptom predictor while controlling for potential confounders, including sex, age group, race, ethnicity, and periods of different SARS-CoV-2 variants and COVID-19 vaccines. We selected these confounders because they were associated with SARS-CoV-2 infection and various symptoms based on the literature and our data. We defined viral variant periods when specific SARS-CoV-2 variants were dominant in the United States (18): the original variants were dominant until March 20, 2021; the Alpha variant during March 21–May 30, 2021; the Delta variant during May 31–December 10, 2021; and Omicron since December 11, 2021. However, Omicron was not included because its dominance fell outside our study period (January 1, 2020–October 12, 2021). In addition, the first vaccine was given in America on December 14, 2020 (19). To account for these confounders, we included 3 dummy variables representing the periods of different SARS-CoV-2 variants and when vaccinations started in the United States and controlled these variables in each symptom model. Finally, we examined and compared the temporal trends of confirmed cases and deaths among HCWs and the general population. To reduce the instance of false-positive findings due to multiple testing, we conducted sensitivity analyses using the Bonferroni test method (Tables 1–3). We accomplished all data cleaning, analysis, and results using R version 3.6.1 (<https://www.r-project.org>).

## Results

Among 6,271,313 laboratory-confirmed COVID-19 cases reported during January 1, 2020–October 12, 2021, by CDC, 7.02% (440,044) were in HCWs. The fatality rate among HCWs was 0.33% versus 24.64%

RESEARCH

for non-HCWs. The percentages we report represent the proportion of each specific variable (numerator) among HCW deaths or 1 of the 3 control groups (denominator) (Table 1). A total of 1,469 HCW deaths were reported among 440,044 cases. The proportion of male HCWs was significantly higher in HCW deaths (39.21%) compared with HCW nondeaths (control 1: 18.64%), although it was still lower than for non-HCWs (55.03% for deaths [control 2] and 48.93% for nondeaths [control 3]). The percentage of persons in the 50–59-year age group among HCW death cases was 28.05% and in the 60–69-year group, 37.51%;

these rates were higher than those from all 3 control groups (8.08%–17.24% in the 50–59-year age group and 8.36%–17.24% in the 60–69-year group). The percentage of Hispanic persons in the HCW deaths category (19.71%) was not significantly different from other reference groups except for control 3 (30.89%). Furthermore, the percentages of Black (27.17%) and Asian (21.47%) persons in the HCW deaths category were greater than those in all 3 control groups (Black, 13.39%–15.66%; Asian 4.37%–7.58%).

Of note, we found that COVID-19 deaths among HCWs increased from March to June. June and then

**Table 1.** Comparison of sociodemographics among HCWs who died from COVID-19 versus 3 control groups, United States, January 1, 2020–October 12, 2021\*

| Variable                                   | HCW deaths, no. (%) | Control 1: HCW nondeaths |          | Control 2: non-HCW deaths |          | Control 3: non-HCW nondeaths |          |
|--|---------------------|--------------------------|----------|---------------------------|----------|------------------------------|----------|
|  |                     | No. (%)                  | p value† | No. (%)                   | p value‡ | No. (%)                      | p value§ |
| Sex  |                     |                          |          |                           |          |                              |          |
| F  | 893 (60.79)         | 356,553 (81.36)          | <0.001   | 50,104 (44.97)            | <0.001   | 2,240,363 (51.07)            | <0.001   |
| M  | 576 (39.21)         | 81,700 (18.64)           |          | 61,306 (55.03)            |          | 2,146,333 (48.93)            |          |
| Age group, y                               |                     |                          |          |                           |          |                              |          |
| 10–19                                      | 1 (0.07)            | 10,866 (2.48)            | <0.001   | 104 (0.09)                | <0.001   | 610,578 (13.89)              | <0.001   |
| 20–29                                      | 27 (1.84)           | 109,220 (24.90)          |          | 536 (0.48)                |          | 794,483 (18.08)              |          |
| 30–39                                      | 86 (5.85)           | 111,437 (25.41)          |          | 1,471 (1.32)              |          | 698,099 (15.89)              |          |
| 40–49                                      | 160 (10.89)         | 90,003 (20.52)           |          | 3,613 (3.24)              |          | 633,574 (14.42)              |          |
| 50–59                                      | 412 (28.05)         | 75,625 (17.24)           |          | 9,013 (8.08)              |          | 593,951 (13.52)              |          |
| 60–69                                      | 551 (37.51)         | 36,657 (8.36)            |          | 18,621 (16.69)            |          | 423,500 (9.64)               |          |
| 70–79                                      | 176 (11.98)         | 3,382 (0.77)             |          | 28,157 (25.23)            |          | 224,251 (5.10)               |          |
| 80+  | 56 (3.81)           | 294 (0.07)               |          | 50,026 (44.83)            |          | 123,222 (2.80)               |          |
| Ethnicity                                  |                     |                          |          |                           |          |                              |          |
| Non-Hispanic                               | 1,104 (80.29)       | 299,362 (80.63)          | 0.774    | 79,520 (76.84)            | <0.001   | 2,588,535 (69.11)            | <0.001   |
| Hispanic                                   | 271 (19.71)         | 71,899 (19.37)           |          | 23,973 (23.16)            |          | 1,157,127 (30.89)            |          |
| Race                                       |                     |                          |          |                           |          |                              |          |
| White                                      | 530 (48.01)         | 208,585 (69.68)          | <0.001   | 59,586 (74.93)            | <0.001   | 1,878,386 (72.57)            | <0.001   |
| Black                                      | 300 (27.17)         | 46,883 (15.66)           |          | 10,644 (13.39)            |          | 350,133 (13.53)              |          |
| Asian                                      | 237 (21.47)         | 19,156 (6.40)            |          | 6,031 (7.58)              |          | 113,042 (4.37)               |          |
| American Indian/<br>Alaska Native          | 0                   | 497 (0.17)               |          | 292 (0.37)                |          | 13,813 (0.53)                |          |
| Native Hawaiian/<br>other Pacific Islander | 3 (0.27)            | 988 (0.33)               |          | 327 (0.41)                |          | 11,837 (0.46)                |          |
| Multiple/other                             | 34 (3.08)           | 23,253 (7.77)            |          | 2,640 (3.32)              |          | 221,324 (8.55)               |          |
| Month                                      |                     |                          |          |                           |          |                              |          |
| January                                    | 89 (7.00)           | 47,353 (11.52)           | <0.001   | 11,209 (12.81)            | <0.001   | 512,018 (12.61)              | <0.001   |
| February                                   | 30 (2.36)           | 15,997 (3.89)            |          | 3,455 (3.95)              |          | 217,736 (5.36)               |          |
| March                                      | 51 (4.01)           | 17,412 (4.24)            |          | 3,500 (4.00)              |          | 198,717 (4.90)               |          |
| April                                      | 95 (7.47)           | 35,111 (8.55)            |          | 7,079 (8.09)              |          | 268,465 (6.61)               |          |
| May  | 86 (6.77)           | 27,006 (6.57)            |          | 5,938 (6.79)              |          | 223,827 (5.51)               |          |
| June                                       | 347 (27.30)         | 43,318 (10.54)           |          | 10,658 (12.18)            |          | 318,614 (7.85)               |          |
| July                                       | 87 (6.85)           | 30,810 (7.50)            |          | 6,860 (7.84)              |          | 331,432 (8.16)               |          |
| August                                     | 107 (8.42)          | 34,256 (8.34)            |          | 7,088 (8.10)              |          | 405,229 (9.98)               |          |
| September                                  | 82 (6.45)           | 29,824 (7.26)            |          | 5,726 (6.54)              |          | 348,613 (8.59)               |          |
| October                                    | 49 (3.86)           | 23,615 (5.75)            |          | 4,492 (5.13)              |          | 238,337 (5.87)               |          |
| November                                   | 109 (8.58)          | 51,872 (12.62)           |          | 9,349 (10.68)             |          | 480,294 (11.83)              |          |
| December                                   | 139 (10.94)         | 54,316 (13.22)           |          | 12,149 (13.88)            |          | 516,249 (12.72)              |          |
| Season                                     |                     |                          |          |                           |          |                              |          |
| Spring                                     | 232 (18.25)         | 79,529 (19.36)           | <0.001   | 16,517 (18.88)            | <0.001   | 691,009 (17.02)              | <0.001   |
| Summer                                     | 541 (42.56)         | 108,384 (26.38)          |          | 24,606 (28.12)            |          | 1,055,275 (25.99)            |          |
| Fall                                       | 240 (18.88)         | 105,311 (25.63)          |          | 19,567 (22.36)            |          | 1,067,244 (26.29)            |          |
| Winter                                     | 258 (20.30)         | 117,666 (28.64)          |          | 26,813 (30.64)            |          | 1,246,003 (30.69)            |          |

\*A total of 440,044 healthcare workers were reported to have COVID-19, including 1,469 in the HCW deaths group and 438,575 in HCW nondeaths group. HCW, healthcare worker.

†Comparison of HCW deaths vs. HCW nondeaths (control 1).

‡Comparison of HCW deaths vs. non-HCW deaths (control 2).

§Comparison of HCW deaths vs. non-HCW nondeaths (control 3).

**Table 2.** Multivariable analyses for severe clinical indicators and reported symptoms among HCWs who died of COVID-19 compared with HCW nondeaths, United States, January 1, 2020–October 12, 2021\*

| Variables                          | HCW deaths, no. (%) | Control 1: HCW nondeaths |                        |
|------------------------------------|---------------------|--------------------------|------------------------|
|                                    |                     | No. (%)                  | OR (95% CI)†           |
| Total numbers                      | 1,469               | 438,575                  |                        |
| Hospitalized                       | 1,152 (83.84)       | 18,018 (5.20)            | 56.22 (47.40–66.70)    |
| Admitted to ICU                    | 663 (77.00)         | 1,530 (1.51)             | 102.51 (83.53–125.82)  |
| Had pneumonia                      | 281 (64.75)         | 4,363 (3.13)             | 30.97 (24.53–39.10)    |
| Abnormal radiograph                | 207 (69.93)         | 2,647 (3.73)             | 28.75 (21.51–38.41)    |
| Acute respiratory disease symptoms | 138 (46.62)         | 1,120 (0.83)             | 61.96 (46.60–82.38)    |
| MV intubation                      | 296 (58.04)         | 306 (0.29)               | 230.94 (178.10–299.45) |
| Fever                              | 305 (66.02)         | 57,293 (36.50)           | 3.11 (2.50–3.86)       |
| Subjective fever                   | 169 (52.98)         | 57,236 (37.68)           | 1.75 (1.37–2.23)       |
| Chills                             | 217 (48.98)         | 73,019 (42.77)           | 1.10 (0.90–1.35)       |
| Myalgia                            | 245 (53.38)         | 106,971 (59.10)          | 0.88 (0.72–1.08)       |
| Running nose                       | 69 (30.67)          | 63,003 (51.99)           | 0.51 (0.37–0.71)       |
| Sore throat                        | 106 (25.00)         | 72,053 (41.11)           | 0.65 (0.51–0.83)       |
| Cough                              | 440 (78.15)         | 124,345 (66.30)          | 1.65 (1.33–2.06)       |
| Dyspnea, shortness of breath       | 399 (70.74)         | 51,547 (30.04)           | 6.06 (4.95–7.41)       |
| Nausea/vomiting                    | 127 (27.73)         | 39,179 (23.04)           | 1.49 (1.19–1.87)       |
| Headache                           | 195 (43.82)         | 121,960 (66.47)          | 0.50 (0.41–0.62)       |
| Abdominal pain                     | 47 (12.95)          | 17,180 (12.49)           | 1.03 (0.73–1.45)       |
| Diarrhea                           | 171 (37.58)         | 48,559 (28.68)           | 1.47 (1.20–1.82)       |
| Underlying medical conditions      | 627 (88.31)         | 93,519 (43.94)           | 6.44 (4.95–8.39)       |

\*The ORs in this table controlled for sex, age group, race, ethnicity, dominant periods of SARS-CoV-2 variants, and vaccination starting time. HCW, healthcare worker; ICU, intensive care unit; MV, mechanical ventilation; OR, odds ratio.

†Comparison of HCW deaths vs. HCW nondeaths (control 1).

July–August contained the most HCW COVID-19 deaths compared with all controls: 27.30% versus 7.86%–12.18% in June and 42.56% versus 25.99%–28.12% in summer.

We conducted multivariate analysis for HCW deaths compared with 3 reference groups (Tables 2, 3). We calculated odds ratios (ORs) by severity indicators and COVID-19 related symptoms after adjusting for sex, age group, race/ethnicity, dominant periods of SARS-CoV-2 variants, and vaccination start time. All 6 severity indicators for COVID-19 were consistently higher in HCW death cases than in the 3 control groups (OR 1.24–230.94). The highest ORs occurred for mechanical ventilation, followed by intensive care unit admission, acute respiratory disease symptoms, hospitalization, pneumonia, and abnormal chest radiograph. In addition, compared with control 1, HCWs deaths showed significantly increased ORs for multiple symptoms, including specific preexisting medical conditions (OR 6.44, 95% CI 4.95–8.39), followed by shortness of breath, fever, subjective fever, cough, nausea/vomiting, and diarrhea (ORs 1.47–6.06;  $p < 0.05$ ). Chills, myalgia, and abdominal pain in HCW deaths group were not significantly different from those in the control groups. However, sore throat, running nose, and headache were significantly lower in the HCW deaths group than in the control 1 and control 2 groups. Those results remained significant and of similar magnitudes (<5% changes) after Bonferroni test adjustment (Tables 1–3). However, 4 severity indicators among HCWs (hospitalization,

pneumonia, abnormal chest radiograph, and acute respiratory disease symptoms) became statistically nonsignificant compared with control 2 after the Bonferroni correction.

We compared the temporal patterns of COVID-19 infections and deaths among HCWs with those in the general population (Figure). Three surges of COVID-19 infections and deaths occurred in the United States around April 2020, July 2020, and November 2020–January 2021. Although infections peaked during November 2020–January in the general population, the highest death numbers occurred in the first surge (April 2020). Of note, the temporal trend of COVID-19 infections among HCWs was similar to that among the US general population. However, the COVID-19 deaths among HCWs declined after April 2020 and remained flat, whereas 2 subsequent death surges occurred among the general population.

### Discussion

We found that HCWs who died of COVID-19 in the United States were disproportionately older ( $\geq 50$  years of age), male, and Black or Asian. Consistent with our findings, previous research found that older age groups are more vulnerable to COVID-19 infection and death, likely because of their lower immunity against viral infections and multiple preexisting medical conditions, both known to exacerbate COVID-19–related deaths (5,20,21). Of interest, we found that the highest risk for death among HCWs

occurs in a relatively younger group (50–59 years of age) than the general population of hospitalized patients ( $\geq 65$  years of age). A possible explanation is that HCWs are generally a younger working population compared with retirees in the general population who suffer a higher COVID-19 burden. Unfortunately, there was no available literature in this area to confirm our findings.

Although this study found that female deaths were higher among HCWs than non-HCWs, female deaths were significantly lower than for HCW-controls, implying no significant increase in deaths among female HCWs after controlling for occupation. This finding could be attributable to the confounding factor of HCWs composition; that is, women are more likely to work in healthcare occupations (22). Therefore, using non-HCWs as a control group may lead to biases due to occupational confounders. On the other hand, worldwide, men were more likely to be infected by COVID-19 and have severe symptoms than were women, which is consistent with our findings of a 2-fold increase in death risk for male HCWs compared with male HCW nondeaths. Furthermore, several studies suggest that sex differences in the susceptibility to COVID-19 may be because of differences in immune response (23,24). These studies found higher plasma levels of innate immune cytokines, such as interleukin 8 and 18, among male patients but more robust T-cell activation among female patients infected by COVID-19.

Our findings regarding the increased risk for COVID-19 death among ethnic minority populations (Black and Asian) agree with several studies on the general population. For instance, Rogers et al. (12) and Kirby (15) reported an increased risk for COVID-19 deaths among non-Hispanic Black and Hispanic minority populations (13,15). In addition, two thirds of HCWs in the United Kingdom who died of COVID-19 identified as an ethnic minority (25). Another study found that COVID-19 infection and death were strongly linked with overcrowded neighborhoods, higher body mass index, and low incomes, all categories that are overrepresented in Hispanic and Black communities (26). However, we did not detect an increased risk for COVID-19 deaths among Hispanic HCWs, which could be caused by the small sample size ( $n = 271$ ) or missing ethnicity information.

Our study also reported a significantly higher risk for COVID-19 deaths (3- to 5-fold) among Asian HCWs than in all 3 control groups. Sze et al. (27) reviewed 50 studies, including 18,728,893 COVID patients from the United States and the United Kingdom, and found that Black and Asian persons were at an increased risk for COVID-19 infection compared with White persons. Pooled adjusted OR for Black persons was 2.02 (95% CI 1.67–2.44), and for Asian persons, 1.50 (95% CI 1.24–1.83) (27). Nevertheless, few studies have reported that Asian persons are also at higher risk. Coronary heart disease, a high-risk comorbidity of COVID-19 death, is

**Table 3.** Multivariable analyses for severe clinical indicators and reported symptoms among HCWs who died of COVID-19 compared with non-HCW deaths and non-HCW nondeaths, United States, January 1, 2020–October 12, 2021\*

| Variables                          | HCW deaths,   | Control 2: non-HCW deaths |                  | Control 3: non-HCW nondeaths |                        |
|------------------------------------|---------------|---------------------------|------------------|------------------------------|------------------------|
|                                    | no. (%)       | No. (%)                   | OR (95% CI)†     | No. (%)                      | OR (95% CI)‡           |
| Total numbers                      | 1,469         | 1,436,898                 |                  | 4,394,371                    |                        |
| Hospitalized                       | 1,152 (83.84) | 81,094 (79.22)            | 1.24 (1.04–1.46) | 239,761 (6.21)               | 46.16 (38.88–54.79)    |
| Admitted ICU                       | 663 (77.00)   | 33,066 (64.85)            | 1.57 (1.30–1.90) | 25,754 (2.61)                | 76.80 (63.22–93.30)    |
| Had pneumonia                      | 281 (64.75)   | 13,722 (56.88)            | 1.32 (1.05–1.65) | 53,506 (3.80)                | 26.55 (21.09–33.44)    |
| Abnormal radiograph                | 207 (69.93)   | 9,997 (62.37)             | 1.19 (0.89–1.58) | 34,944 (5.38)                | 21.89 (16.41–29.19)    |
| Acute respiratory disease symptoms | 138 (46.62)   | 7,994 (35.33)             | 1.46 (1.12–1.90) | 11,452 (0.84)                | 62.43 (47.63–81.83)    |
| MV intubation                      | 296 (58.04)   | 8,729 (34.77)             | 1.85 (1.50–2.28) | 4,123 (0.44)                 | 156.19 (125.65–194.16) |
| Fever                              | 305 (66.02)   | 15,800 (54.89)            | 1.39 (1.12–1.74) | 532,385 (36.13)              | 3.38 (2.72–4.19)       |
| Subjective fever                   | 169 (52.98)   | 8,205 (36.34)             | 1.82 (1.42–2.34) | 548,940 (36.23)              | 1.99 (1.56–2.54)       |
| Chills                             | 217 (48.98)   | 7,963 (30.64)             | 1.84 (1.48–2.28) | 643,555 (38.88)              | 1.28 (1.04–1.57)       |
| Myalgia                            | 245 (53.38)   | 10,051 (36.51)            | 1.88 (1.52–2.32) | 913,780 (51.95)              | 1.08 (0.88–1.32)       |
| Running nose                       | 69 (30.67)    | 3,244 (20.37)             | 1.75 (1.26–2.42) | 495,995 (47.70)              | 0.58 (0.42–0.79)       |
| Sore throat                        | 106 (25.00)   | 4,225 (16.22)             | 1.59 (1.23–2.06) | 641,523 (37.43)              | 0.71 (0.56–0.91)       |
| Cough                              | 440 (78.15)   | 23,085 (66.81)            | 1.63 (1.31–2.04) | 1,159,870 (62.77)            | 1.70 (1.37–2.11)       |
| Dyspnea, shortness of breath       | 399 (70.74)   | 23,545 (66.50)            | 1.11 (0.91–1.37) | 405,746 (24.21)              | 5.95 (4.88–7.26)       |
| Nausea/vomiting                    | 127 (27.73)   | 5,304 (18.73)             | 1.42 (1.13–1.80) | 297,213 (18.27)              | 1.60 (1.28–2.01)       |
| Headache                           | 195 (43.82)   | 6,821 (25.71)             | 1.87 (1.49–2.33) | 1,068,424 (59.68)            | 0.59 (0.48–0.72)       |
| Abdominal pain                     | 47 (12.95)    | 2,079 (9.93)              | 1.07 (0.75–1.52) | 136,869 (11.24)              | 1.05 (0.74–1.47)       |
| Diarrhea                           | 171 (37.58)   | 7,219 (25.56)             | 1.62 (1.31–2.01) | 430,488 (25.88)              | 1.45 (1.18–1.78)       |
| Underlying medical conditions      | 627 (88.31)   | 42,515 (93.01)            | 0.65 (0.49–0.85) | 790,854 (42.64)              | 6.29 (4.82–8.21)       |

\*The ORs in this table controlled for sex, age group, race, ethnicity, dominant periods of SARS-CoV-2 variants, and vaccination starting time. HCW, healthcare worker; ICU, intensive care unit; MV, mechanical ventilation; OR, odds ratio.

†Comparison of HCW deaths vs. non-HCW deaths (control 2).

‡Comparison of HCW deaths vs. non-HCW nondeaths (control 3).

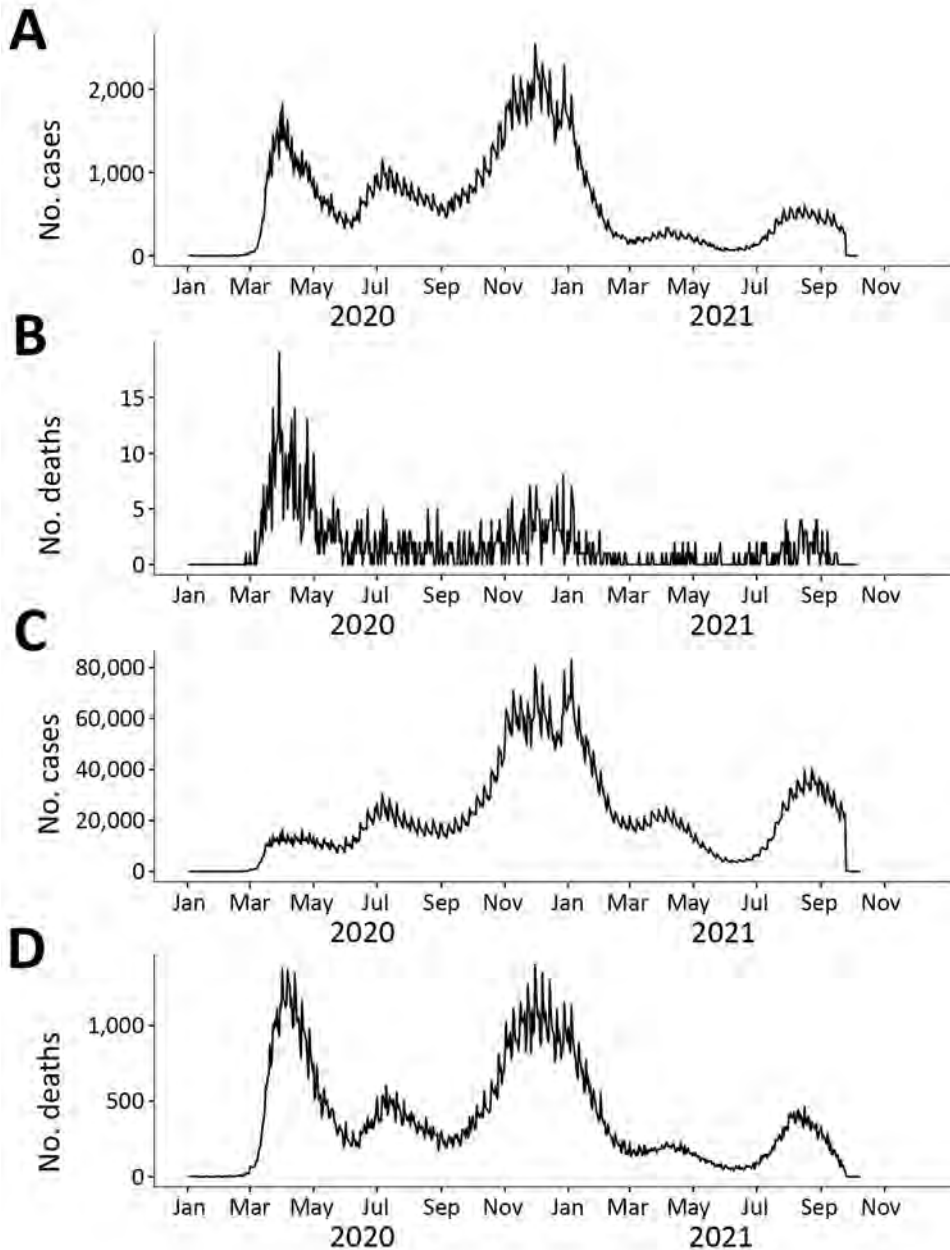


**Figure.** Comparison of COVID-19 cases and deaths among HCWs and in the non-HCW population, United States, January 2020–October 2021. A) Confirmed cases in HCW. B) HCW deaths. C) Confirmed cases in the non-HCW population. D) Confirmed deaths in non-HCW population. HCW, healthcare worker.

more common among Black persons, Asian persons, and persons of other ethnic minorities (28). Overcrowded households may be another risk factor associated with the spread of COVID-19 among Asian persons (29). Our results contradicted the belief we noted among Asian populations that they are at a lower risk of contracting COVID-19 because of genetic protection. Therefore, these findings are of critical public health importance in terms of communicating accurate COVID-19 information to particularly at-risk populations.

We found that almost one third of the HCW death cases in the United States occurred in June,

and >40% occurred in the summer months (June–August) of 2020. The initial surge in COVID-19 cases led to a profound increase in HCWs’ exposure to the virus. This surge is likely the result of inadequate intensive care units and hospital beds, insufficient PPE supply, inadequate training and experience among HCWs, and heavy workloads due to a large and rapid influx of patients. Another study reported that HCWs with inadequate access to PPE had increased SARS-CoV-2 infection compared with those with adequate PPE access (30).

We found that the fatality rate in the US general population (2.48%) was more than 7-fold

higher than that among HCWs (0.33%). This finding is consistent with that of Sahu et al. (9), who also found that the mortality rate among HCWs was 7 times lower than that among all cases (10). However, almost all severe indicators and symptoms were higher among HCW deaths than in the 3 control groups in this study, which may be because of HCWs' proximity to and longer duration of exposure to COVID-19 patients. Alternatively, HCWs may have better access to healthcare and treatment, which prevented deaths in this population. Unfortunately, there is a paucity of literature regarding the severity indicators for COVID-19 to compare with our study.

We found that underlying conditions were the most important predictor of COVID-19 deaths among HCWs, followed by shortness of breath, fever, cough, nausea/vomiting, and diarrhea. Multiple studies found that chronic conditions were the most critical COVID-19 severity and death indicators in different countries (6,7). Other studies have shown that shortness of breath is another important symptom of COVID infection (31,32). Our findings that fever >100.4°F, even subjective fever (felt feverish), was consistently more common for HCW deaths than for the 3 control groups, indicating that fever may be an early indicator of disease severity. Another finding is that HCW death cases reported significantly higher gastrointestinal symptoms (diarrhea, nausea, vomiting, abdominal pain) than all 3 control groups. Consistent with our findings, Wiersinga et al. (31) reported that initial COVID-19 symptoms might include shortness of breath, fever, cough, nausea/vomiting, or diarrhea. The general public expects respiratory symptoms but may be unaware of gastrointestinal symptoms related to COVID-19. Therefore, this study may provide valuable insight for public education and severity prediction.

We also found that cough is among the top 3 reported symptoms of COVID-19 infections and deaths in HCWs and the general population (62.77%–78.15%). However, although headache (59.68%–66.47%) and myalgia (51.95%–59.10%) were the other 2 top symptoms among COVID-19 infection cases, preexisting conditions (88.31%–93.01%) and shortness of breath (66.5%–70%) were the commonly reported symptoms for COVID-19 deaths. In addition, we found that runny nose, sore throat, and headache symptoms were notably lower in HCW deaths than in nondeath controls, implying that these symptoms may not be essential predictors of COVID-19 death. Unfortunately, we found no relevant literature with which to compare our results.

Temporal patterns of infection and death in our study showed that, whereas COVID-19 deaths in the general US population experienced 3 distinct peaks, deaths among HCWs only peaked during the first surge. Deaths among HCWs went down after April 2020 and remained low. This finding is consistent with CDC reports and other studies that show a large initial surge and subsequent decline. The similar peaks in both HCWs and non-HCWs illustrate how quickly the COVID-19 pandemic spread from the general population to HCWs who took care of the deadliest cases (2,22,33). The flatter COVID-19 death trend after the first surge among HCWs could be attributed to their early and high immunization rate, improved PPE, access to healthcare facilities, and early detection and treatment for HCWs compared with the general population.

A strength of our study is that we used multiple reference groups to minimize different biases. We further validated our findings using HCW controls with similar exposure opportunities and socioeconomic backgrounds. In addition, using 2 general-population reference groups helped us examine how demographics and symptoms differed between HCWs and the general population. We also used dynamic, nationwide CDC surveillance data. These objective data reduce reporting bias, which is typically a major concern in studies relying on media reports or questionnaires. Finally, we controlled for several known risk factors for COVID-19, including demographics, different dominant SARS-CoV-2 variants, and the start of vaccinations.

Our findings illustrate how timely CDC surveillance data, reported every 2 weeks, can be used to monitor the temporal trend of infections and deaths among different populations. In addition, unique findings, such as HCW deaths increasing in younger age groups and in Asian persons, could be used in targeted interventions. Furthermore, clinical agencies could use the severe clinical indicators and symptoms we identified to predict deaths and plan hospital beds.

A limitation of our study is that, because the COVID-19 case surveillance system is passive, our data may underestimate the number of cases, although reporting cases to the CDC is federally mandated. In addition, the availability of diagnostic testing, resources, and the priorities of health officials may influence the completeness of reporting. To address this issue, we included total cases (both laboratory confirmed and probable cases); most COVID-19 deaths (>99%) were laboratory confirmed. Although the case report form captures severity indicators, these data may be inaccurate or underreported because some outcomes

were unknown at the time of reporting. We repeated the analyses multiple times using different lengths of the cohort after the initial analysis by adding updated data, and the results are robust. Missing values, especially demographic information for death cases in the general population, are also important limitations, suggesting that control 2 would not be a good control group. Furthermore, we examined race and ethnicity variables separately and could not combine these 2 variables because of a lack of personal identifiers and the arbitrary coding in the data; only 1 variable (race or ethnicity) was coded. We used race/ethnicity as a surrogate for sociodemographic status; however, household income and deprivation indices, which correlate with COVID infection, were not available. Although multiple testing may cause false positives, our results are robust after Bonferroni correction, a conservative test used to protect from type I error.

Another challenge we faced was determining whether a reported death was caused by COVID-19 or other diseases. We believe that COVID-19 was the primary cause of death for the cases we used because the death-related question from the CDC questionnaire is specific to COVID-19 (i.e., “Did the patient die as a result of this illness [COVID-19]?”). In addition, similar to other infectious diseases under mandatory reporting, all COVID-19 cases and causes of death were confirmed and validated by hospitals or health departments. Finally, we could not separate unique infections from reinfections because no personal identifier is available. However, this problem may not have a substantial effect for several reasons. We aimed to examine fatality (deaths per infection) rather than infection. Although death was almost certainly reported only once, infections could be reported multiple times because of reinfection. Therefore, we may have underestimated fatalities because reinfections increased the denominator. This underestimation bias is likely similar between the HCW deaths and HCW controls because of identical occupations and similar sociodemographic status, which would be nondifferential and toward the null. When comparing HCW deaths to non-HCW controls, the denominator, including reinfection numbers, is likely larger among HCWs than the general population because of HCWs’ frequency and duration of exposure to patients. Therefore, the fatality ratio of these 2 groups may have been underestimated. Finally, the effect of such bias may be minimal because most COVID-19 reinfections occurred when the Omicron variant was dominant (86.9%) after December 31, 2021 (34), which occurred after our study period (January 1, 2020–October 12, 2021). For instance, the COVID-19 reinfection

rate in New York through December 31, 2021, was 0.56%, but as of January 1, 2022, it was 3.74% (34).

In conclusion we found that HCWs who were  $\geq 50$  years of age, male, Black, or Asian experienced higher deaths from COVID-19. In addition, HCW COVID-19 patients experienced fewer deaths but significantly higher risks for the most severe indicators than the 3 reference groups. We also found that underlying conditions, shortness of breath, fever, cough, nausea/vomiting, and diarrhea were the most relevant indicators for COVID-19–related deaths among HCWs. Conversely, runny nose, sore throat, and headache may not be critical indicators for COVID-19 death in this population.

### About the Author

Dr. Lin is a professor in the Department of Environmental Health Sciences and the associate director of global health research at the School of Public Health, University at Albany. She has 30 years of research experience directing large environmental health studies assessing the health impacts of manmade and natural disasters, and various environmental exposures like climate change, extreme weather, and ambient/indoor air pollution. She has also led a series of school environment-health projects.

### References

1. Mallapaty S. The coronavirus is most deadly if you are older and male—new data reveal the risks. *Nature*. 2020;585:16–7. <https://doi.org/10.1038/d41586-020-02483-2>
2. Burrer SL, de Perio MA, Hughes MM, Kuhar DT, Luckhaupt SE, McDaniel CJ, et al.; CDC COVID-19 Response Team. Characteristics of health care personnel with COVID-19—United States, February 12–April 9, 2020. *MMWR Morb Mortal Wkly Rep*. 2020;69:477–81. <https://doi.org/10.15585/mmwr.mm6915e6>
3. Johns Hopkins Coronavirus Resource Center. COVID-19 dashboard. 2021 [cited 2021 Oct 21]. <https://coronavirus.jhu.edu/map.html>
4. Palaiodimos L, Kokkinidis DG, Li W, Karamanis D, Ognibene J, Arora S, et al. Severe obesity, increasing age and male sex are independently associated with worse in-hospital outcomes, and higher in-hospital mortality, in a cohort of patients with COVID-19 in the Bronx, New York. *Metabolism*. 2020;108:154262. <https://doi.org/10.1016/j.metabol.2020.154262>
5. Pence BD. Severe COVID-19 and aging: are monocytes the key? *Geroscience*. 2020;42:1051–61. <https://doi.org/10.1007/s11357-020-00213-0>
6. Chen Y, Klein SL, Garibaldi BT, Li H, Wu C, Osevala NM, et al. Aging in COVID-19: vulnerability, immunity and intervention. *Ageing Res Rev*. 2021;65:101205. <https://doi.org/10.1016/j.arr.2020.101205>
7. Shahid Z, Kalayanamitra R, McClafferty B, Kepko D, Ramgobin D, Patel R, et al. COVID-19 and older adults: what we know. *J Am Geriatr Soc*. 2020;68:926–9. <https://doi.org/10.1111/jgs.16472>

8. Dy LF, Rabajante JFAA. COVID-19 infection risk model for frontline health care workers. *Netw Model Anal Health Inform Bioinform*. 2020;9:57. <https://doi.org/10.1007/s13721-020-00258-3>
9. Sahu AK, Amrithanand VT, Mathew R, Aggarwal P, Nayer J, Bhoi S. COVID-19 in health care workers – a systematic review and meta-analysis. *Am J Emerg Med*. 2020;38:1727–31. <https://doi.org/10.1016/j.ajem.2020.05.113>
10. Shields A, Faustini SE, Perez-Toledo M, Jossi S, Aldera E, Allen JD, et al. SARS-CoV-2 seroprevalence and asymptomatic viral carriage in healthcare workers: a cross-sectional study. *Thorax*. 2020;75:1089–94. <https://doi.org/10.1136/thoraxjnl-2020-215414>
11. Xiang B, Li P, Yang X, Zhong S, Manyande A, Feng M. The impact of novel coronavirus SARS-CoV-2 among healthcare workers in hospitals: An aerial overview. *Am J Infect Control*. 2020;48:915–7. <https://doi.org/10.1016/j.ajic.2020.05.020>
12. Rogers TN, Rogers CR, VanSant-Webb E, Gu LY, Yan B, Qeadan F. Racial disparities in COVID-19 mortality among essential workers in the United States. *World Med Health Policy*. 2020;12:311–27. <https://doi.org/10.1002/wmh3.358>
13. Salsberg E, Richwine C, Westergaard S, Portela Martinez M, Oyeyemi T, Vichare A, et al. Estimation and comparison of current and future racial/ethnic representation in the US health care workforce. *JAMA Netw Open*. 2021;4:e213789. <https://doi.org/10.1001/jamanetworkopen.2021.3789>
14. Artiga S, Rae M, Pham O, Hamel L, Muñana C. COVID-19 risks and impacts among health care workers by race/ethnicity. 2020 Nov 11 [cited 2022 Jun 15]. <https://www.kff.org/racial-equity-and-health-policy/issue-brief/covid-19-risks-impacts-health-care-workers-race-ethnicity/>
15. Kirby T. Evidence mounts on the disproportionate effect of COVID-19 on ethnic minorities. *Lancet Respir Med*. 2020; 8:547–8. [https://doi.org/10.1016/S2213-2600\(20\)30228-9](https://doi.org/10.1016/S2213-2600(20)30228-9)
16. Shah ASV, Wood R, Gribben C, Caldwell D, Bishop J, Weir A, et al. Risk of hospital admission with coronavirus disease 2019 in healthcare workers and their households: nationwide linkage cohort study. *BMJ*. 2020;371:m3582. <https://doi.org/10.1136/bmj.m3582>
17. Zhou F, Yu T, Du R, Fan G, Liu Y, Xiang J, et al. Clinical course and risk factors for mortality of adult in patients with COVID-19 in Wuhan, China: a retrospective cohort study. *Lancet*. 2020;395:1054–62 [Erratum in: *Lancet*. 2020 Mar 28;395:1038]. [https://doi.org/10.1016/S0140-6736\(20\)30566-3](https://doi.org/10.1016/S0140-6736(20)30566-3)
18. CoVariants. Overview of variants in countries. 2022 [cited 2022 Mar 9]. <https://covariants.org/per-country>
19. US Centers for Disease Control and Prevention. New COVID-19 viral testing tool – CDC. 2021 [cited 2022 Jun 21]. <https://www.cdc.gov/coronavirus/2019-ncov/testing/viral-testing-tool.html>
20. Asfahan S, Deokar K, Dutt N, Niwas R, Jain P, Agarwal M. Extrapolation of mortality in COVID-19: exploring the role of age, sex, comorbidities and healthcare related occupation. *Monaldi Arch Chest Dis*. 2020;90:313–7. <https://doi.org/10.4081/monaldi.2020.1325>
21. Kim R, Nachman S, Fernandes R, Meyers K, Taylor M, LeBlanc D, et al. Comparison of COVID-19 infections among healthcare workers and non-healthcare workers. *PLoS One*. 2020;15:e0241956. <https://doi.org/10.1371/journal.pone.0241956>
22. Díez-Manglano J, Solís-Marquín MN, Álvarez García A, Alcalá-Rivera N, Maderuelo Riesco I, Gericó Aseguinolaza M, et al.; SEMI-COVID-19 Network. Healthcare workers hospitalized due to COVID-19 have no higher risk of death than general population. Data from the Spanish SEMI-COVID-19 Registry. *PLoS One*. 2021;16:e0247422. <https://doi.org/10.1371/journal.pone.0247422>
23. Klein SL, Flanagan KL. Sex differences in immune responses. *Nat Rev Immunol*. 2016;16:626–38. <https://doi.org/10.1038/nri.2016.90>
24. Takahashi T, Ellingson MK, Wong P, Israelow B, Lucas C, Klein J, et al.; Yale IMPACT Research Team. Sex differences in immune responses that underlie COVID-19 disease outcomes. *Nature*. 2020;588:315–20. <https://doi.org/10.1038/s41586-020-2700-3>
25. Rimmer A. COVID-19: Two thirds of healthcare workers who have died were from ethnic minorities. *BMJ*. 2020;369:m1621. <https://doi.org/10.1136/bmj.m1621>
26. Arasteh K. Prevalence of comorbidities and risks associated with COVID-19 among Black and Hispanic populations in New York City: an examination of the 2018 New York City Community Health Survey. *J Racial Ethn Health Disparities*. 2021;8:863–9. <https://doi.org/10.1007/s40615-020-00844-1>
27. Sze S, Pan D, Nevill CR, Gray LJ, Martin CA, Nazareth J, et al. Ethnicity and clinical outcomes in COVID-19: a systematic review and meta-analysis. *EClinicalMedicine*. 2020;29–30:100630. <https://doi.org/10.1016/j.eclinm.2020.100630>
28. Raisi-Estabragh Z, McCracken C, Bethell MS, Cooper J, Cooper C, Caulfield MJ, et al. Greater risk of severe COVID-19 in Black, Asian and minority ethnic populations is not explained by cardiometabolic, socioeconomic or behavioural factors, or by 25(OH)-vitamin D status: study of 1,326 cases from the UK Biobank. *J Public Health (Oxf)*. 2020;42:451–60. <https://doi.org/10.1093/pubmed/fdaa095>
29. Abuelgasim E, Saw LJ, Shirke M, Zeinah M, Harky A. COVID-19: Unique public health issues facing Black, Asian and minority ethnic communities. *Curr Probl Cardiol*. 2020;45:100621. <https://doi.org/10.1016/j.cpcardiol.2020.100621>
30. Nguyen LH, Drew DA, Graham MS, Joshi AD, Guo CG, Ma W, et al.; Coronavirus Pandemic Epidemiology Consortium. Risk of COVID-19 among front-line health-care workers and the general community: a prospective cohort study. *Lancet Public Health*. 2020;5:e475–83. [https://doi.org/10.1016/S2468-2667\(20\)30164-X](https://doi.org/10.1016/S2468-2667(20)30164-X)
31. Wiersinga WJ, Rhodes A, Cheng AC, Peacock SJ, Prescott HC. Pathophysiology, transmission, diagnosis, and treatment of coronavirus disease 2019 (COVID-19): a review. *JAMA*. 2020;324:782–93. <https://doi.org/10.1001/jama.2020.12839>
32. Li L-Q, Huang T, Wang Y-Q, Wang Z-P, Liang Y, Huang T-B, et al. COVID-19 patients' clinical characteristics, discharge rate, and fatality rate of meta-analysis. *J Med Virol*. 2020;92:577–83. <https://doi.org/10.1002/jmv.25757>
33. McNicholas JE, Kosnik R, Blanc PD, Taylor BR, Guntur S. Temporal trends in COVID-19 incidence in two healthcare worker cohorts. *J Occup Environ Med*. 2021;63:528–31. <https://doi.org/10.1097/JOM.0000000000002208>
34. New York State Department of Health. COVID-19 reinfection data. 2022 [cited 2022 Jun 15]. <https://coronavirus.health.ny.gov/COVID-19-reinfection-data>

Address for correspondence: Shao Lin, Department of Environmental Health Sciences, School of Public Health, University at Albany, State University of New York, 1 University Pl, Rm 212d, Rensselaer, NY 12144, USA; email: [slin@albany.edu](mailto:slin@albany.edu)

---

# Factors Associated with Delayed or Missed Second-Dose mRNA COVID-19 Vaccination among Persons $\geq 12$ Years of Age, United States

Lu Meng, Neil Chandra Murthy, Bhavini Patel Murthy, Elizabeth Zell, Ryan Saelee, Megan Irving, Hannah E. Fast, Patricia Castro Roman, Adam Schiller, Lauren Shaw, Carla L. Black, Lynn Gibbs-Scharf, LaTrece Harris, Terence Chorba

To identify demographic factors associated with delaying or not receiving a second dose of the 2-dose primary mRNA COVID-19 vaccine series, we matched 323 million single Pfizer-BioNTech (<https://www.pfizer.com>) and Moderna (<https://www.modernatx.com>) COVID-19 vaccine administration records from 2021 and determined whether second doses were delayed or missed. We used 2 sets of logistic regression models to examine associated factors. Overall, 87.3% of recipients received a timely second dose ( $\leq 42$  days between first and second dose), 3.4% received a delayed second dose ( $>42$  days between first and second dose), and 9.4% missed the second dose. Persons more likely to have delayed or missed the second dose belonged to several racial/ethnic minority groups, were 18–39 years of age, lived in more socially vulnerable areas, and lived in regions other than the northeastern United States. Logistic regression models identified specific subgroups for providing outreach and encouragement to receive subsequent doses on time.

**I**n December 2020, the US Food and Drug Administration (FDA) issued Emergency Use Authorizations (EUAs) for the Pfizer BioNTech (<https://www.pfizer.com>) and Moderna (<https://www.modernatx.com>) 2-dose primary mRNA COVID-19 vaccine series

(1,2). The Centers for Disease Control and Prevention (CDC) Advisory Committee on Immunization Practices, part of the National Center for Immunization and Respiratory Diseases, prioritized certain populations to be offered the COVID-19 vaccination first, including healthcare personnel, long-term care facility residents, persons  $\geq 65$  years of age, persons 16–64 years of age with high-risk medical conditions, and essential workers (3). Starting in March 2021, Pfizer-BioNTech and Moderna COVID-19 vaccines have been available at pharmacies and from other medical practice providers for anyone  $\geq 16$  years of age. In the 1-year period of this analysis, the recommended intervals between the 2 primary doses were 21 days for the Pfizer-BioNTech vaccine and 28 days for the Moderna vaccine (4). On May 10, 2021, FDA expanded the EUA for the Pfizer COVID-19 vaccine to include persons 12–15 years of age (5). During August–November 2021, FDA approved a series of EUAs: 1 for an additional primary dose for immunocompromised persons and 1 for a booster dose for persons  $\geq 18$  years of age (6).

In the summer of 2021, one of every 10 US persons received the first dose of an mRNA COVID-19 vaccine,  $\approx 15$  million still had not received the second dose, and many more had received the second dose outside the recommended intervals between doses (7). Persons who start the primary series are presumably amenable to initial vaccination but may then either delay completing or may fail to complete the series. Delayed or missed recommended COVID-19 vaccine doses can hamper national efforts to reduce COVID-19–associated illness, hospitalization, and death (8–10). More information about this population is valuable for addressing second-dose vaccination

---

Author affiliations: Centers for Disease Control and Prevention Atlanta, Georgia, USA (L. Meng, N.C. Murthy, B.P. Murthy, E. Zell, R. Saelee, M. Irving, H.E. Fast, P. Castro Roman, A. Schiller, L. Shaw, C.L. Black, L. Gibbs-Scharf, L. Harris, T. Chorba); General Dynamics Information Technology Inc., Falls Church, Virginia, USA (L. Meng); Stat-Epi Associates, Inc., Ponte Vedra Beach, Florida, USA (E. Zell); Deloitte Consulting LLP, New York, New York, USA (M. Irving); Booz Allen Hamilton, Inc., McLean, Virginia, USA (A. Schiller)

DOI: <https://doi.org/10.3201/eid2808.220557>

barriers and devising interventions to increase primary series completion.

To support nationwide COVID-19 immunization efforts, we performed an analysis to identify demographic factors associated with receiving 1 dose of the 2-dose primary mRNA vaccine series but delaying the second dose or not completing the series. The study was reviewed by CDC and conducted consistent with applicable federal law and CDC policy.

## Methods

We analyzed COVID-19 mRNA vaccine administration data among persons  $\geq 12$  years of age in the United States during December 14, 2020–December 31, 2021. US COVID-19 vaccine administration data are reported from jurisdictions, pharmacies, and federal entities to CDC via immunization information systems, the CDC Vaccine Administration Management System, or direct data submission (11). De-identified vaccination records from Idaho were reported for persons  $\geq 18$  years of age; all other states, excluding Texas, and the District of Columbia reported vaccination records for persons  $\geq 12$  years of age. For this analysis, so that all persons who had received a first dose had sufficient time to receive a second dose within a conventionally permissible time frame, we included in our analysis all persons  $\geq 12$  years of age who received a first dose of an mRNA vaccine on or before September 30, 2021, which would allow  $\geq 3$  months (October 1, 2021–December 31, 2021) after a first dose to have received a second dose. We matched de-identified first- and second-dose records according to a unique recipient number (not associated with recipients' personally identified information) assigned by the reporting entity and an 8-12-digit reporting source code. For each recipient, we calculated the number of days between the first and second doses. To enable scheduling considerations and other unintended or systematic delays, we defined receipt of a timely second dose as a second dose administered  $\leq 42$  days after the first dose. We defined a delayed second dose as a second dose administered  $>42$  days after the first dose. Although data on the efficacy of second mRNA COVID-19 vaccine doses administered beyond this window are limited, we chose a cutoff of 42 days because that has been the limit of days between doses conventionally considered permissible when a delay is unavoidable (4). We defined a missed second dose as receipt of the first dose but not having a matching second dose on record. We excluded from analysis persons whose records indicated that the second dose was administered earlier than the vaccine brand-specific recommended dosing interval, with a

4-day grace period, which for this study we defined as 17 days (Pfizer-BioNTech) and 24 days (Moderna). We included recipients of both mRNA vaccine brands (e.g., first dose Pfizer-BioNTech and second dose Moderna vaccine). We determined second-dose timing according to brand of the first-dose vaccine.

On the basis of the inclusion criteria and definitions, we attempted to match 323 million mRNA COVID-19 vaccine administration records reported to CDC as doses having been administered during December 14, 2020–December 31, 2021, including 170,865,184 first-dose records issued by September 30, 2021, and 153,791,171 second-dose records issued by December 31, 2021. We excluded 15,017,733 (8.8%) records for which county of residence was missing. We built logistic regression models to examine sociodemographic factors associated with a delayed second dose (model 1) or a missed second dose (model 2) (Figure 1).

## Dependent Variables

In model 1, recipients whose second dose was delayed were classified as 1 and recipients who received a timely second dose were classified as 0. Recipients who did not receive a second dose were excluded from this model.

In model 2, recipients who did not receive a second dose were classified as 1 and recipients who received a timely second dose were classified as 0. Recipients who received a delayed second dose were excluded from this model.

## Independent Variables

We included in the model the fundamental demographic information reported to CDC in the vaccine administration records, including recipient's age, sex, race/ethnicity, and postal code. In addition, we derived the CDC/Agency for Toxic Substances and Disease Registry Social Vulnerability Index (SVI) scores and the CDC Urban-Rural Classification scores from vaccination records according to the recipient's county of residence (12,13). We generated urban-rural classification and SVI score tertiles of county of residence (low, medium, high) for each record. Higher SVI scores indicated counties that were more socially vulnerable. Independent variables for the 2 logistic regression models included first-dose vaccine type (Pfizer-BioNTech, Moderna), age group (12–17, 18–39, 40–64,  $\geq 65$  years), sex (male, female), race/ethnicity (Hispanic, non-Hispanic Asian/Other Pacific Islander, non-Hispanic Black, non-Hispanic White, non-Hispanic American Indian/Alaska Native, other/unknown), US region of residence (South,

| Second dose timing  | Pfizer                    | Moderna | Records from initial query | %     |
|---------------------|---------------------------|---------|----------------------------|-------|
| Timely second dose  | ≤42 days after first dose |         | 148,021,753                | 86.63 |
| Delayed second dose | >42 days after first dose |         | 5,769,418                  | 3.38  |
| Missed second dose  | No record of second dose  |         | 17,074,013                 | 9.99  |
| Total               |                           |         | 170,865,184                | —     |

Logistic regression model 1: Factors associated with a delayed second dose

| Second dose timing  | Records included in model | %     |
|---------------------|---------------------------|-------|
| Timely second dose  | 135,979,226               | 96.30 |
| Delayed second dose | 5,224,993                 | 3.70  |
| Missed second dose  | 14,643,232                | —     |

Defined as 0

Defined as 1

Logistic regression model 2: Factors associated with a missing second dose

| Second dose timing  | Records included in model | %     |
|---------------------|---------------------------|-------|
| Timely second dose  | 135,979,226               | 90.28 |
| Delayed second dose | 5,224,993                 | —     |
| Missed second dose  | 14,643,232                | 9.72  |

**Figure 1.** Logistic regression models built to examine sociodemographic factors associated with missed or delayed second doses in primary series of mRNA COVID vaccination among persons ≥12 years of age, United States. The table at the top includes all records from initial query that met the inclusion criteria. The lower 2 sub-tables provide the number of records included in each of the 2 multivariable logistic regression models. Pfizer-BioNTech, <https://www.pfizer.com>; Moderna, <https://www.modernatx.com>.

Midwest, Mountain, Pacific, Northeast, Noncontiguous [Figure 2]), SVI tertile of county of residence (low, medium, high), and urbanicity (metro, nonmetro). In our results, racial/ethnic groups are reported as Hispanic, Asian, Black, White, American Indian/Alaska Native, and other/unknown.

We based odds ratio (OR) and 95% CI calculations on regression estimates and performed descriptive analyses for all input variables. We included in this study factors for which OR was >1.150 or <0.850. All analyses were conducted in the cloud-based data platform Microsoft Azure DataBricks (<https://azure.microsoft.com/en-us/services/databricks>).

**Results**

In total, we attempted to match 155,847,451 records of first-dose mRNA vaccine receipt containing recipient’s county of residence (91.2% of the total 170,865,184 first-dose records) to records of second-dose mRNA vaccine receipt. We merged those records with SVI and urbanicity variables and included them in the descriptive analyses and multivariable

logistic regression models. Of the 155,847,451 first-dose mRNA vaccination records, matching indicated that 135,979,226 (87.3%) persons received a timely second dose and that 5,224,993 (3.4%) received a delayed second dose; 14,643,232 (9.4%) first-dose records lacked a matched second-dose record and the first-dose recipients were considered to have missed the second dose (Table 1). Of all first-dose recipients, 41.9% were White, 11.3% were Hispanic, 7.2% were Black, 4.4% were Asian, 0.7% were American Indian/Alaska Native, and 34.5% were of other/unknown race/ethnicity. Of all recipients, 46.2% were male, and mean (±SD) age was 48.0 (±20.3) years.

Model 1 of the 2 logistic regression models (Table 2) shows the results of the logistic regression model examining factors associated with a delayed second dose, conditional on receiving a second dose. Model 1 analyzed a total of 141,204,219 matched first- and second-dose pairs; of those, 135,979,226 (96.3%) first-dose recipients received a timely second dose and 5,224,993 (3.7%) received a delayed second dose. Compared with initial Pfizer-BioNTech vaccine recipients, initial

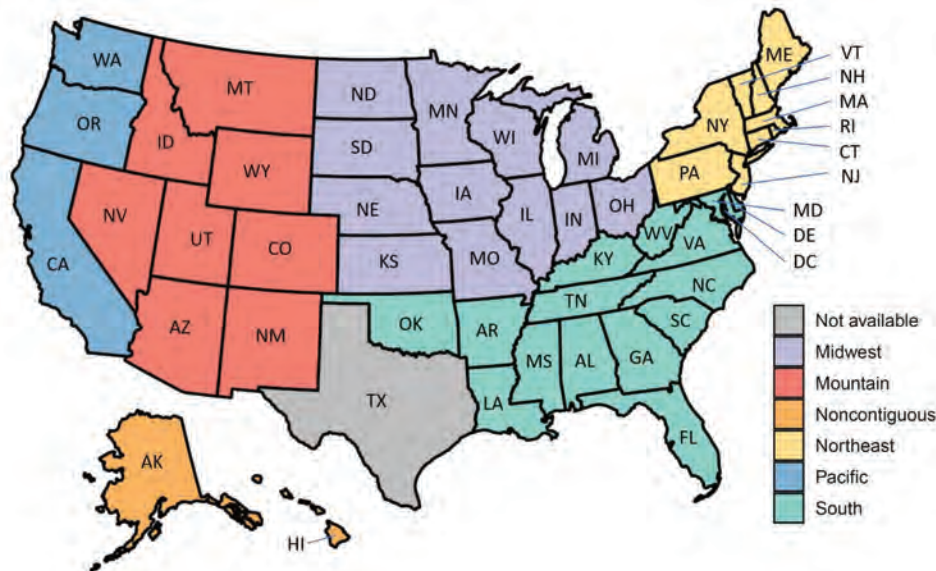


**Figure 2.** States in each region used in study of factors associated with delayed or missed second-dose mRNA COVID-19 vaccination among persons  $\geq 12$  years of age, United States.

Moderna vaccine recipients were more likely to have received a delayed second dose (OR 1.267, 95% CI 1.265–1.270). Recipients 18–39 years of age were more likely to have received a delayed second dose compared with recipients 12–17 years of age (OR 0.763, 95% CI 0.759–0.766). Compared with recipients who resided in low SVI tertile counties, those in high SVI tertile counties were more likely to have received a delayed second dose (OR 1.198, 95% CI 1.196–1.201). Compared with White recipients, delayed receipt of a second dose was more likely among American Indian/Alaska Native (OR 1.508, 95% CI 1.494–1.522), Black (OR 1.310, 95% CI 1.305–1.314), and Hispanic (OR 1.172, 95% CI 1.168–1.175) persons. Compared with recipients who resided in counties in the Northeast, delayed receipt of a second dose was more likely among persons who resided in counties in the South (OR 1.425, 95% CI 1.421–1.429), Pacific (OR 1.507, 95% CI 1.503–1.512), Noncontiguous (OR 1.886, 95% CI 1.863–1.909), and Mountain (OR 1.648, 95% CI 1.641–1.655) regions.

Model 2 of the 2 logistic regression models (Table 2) shows the result of the model examining factors associated with a missed second dose. Model 2 analyzed a total of 150,622,458 first-dose records; of these, 135,979,226 (90.3%) first-doses recipients received a timely second dose and 14,643,232 (9.7%) missed the second dose. First-dose recipients 18–39 years of age were more likely to have missed the second dose compared with those 40–64 (OR 0.740, 95% CI 0.739–0.741) and  $\geq 65$  (OR 0.743, 95% CI 0.742–0.744) years of age. Compared with first-dose recipients who resided in counties in the low SVI tertile, the second dose was more likely to have been missed by persons in medium

(OR 1.297, 95% CI 1.295–1.299) and high SVI tertile counties (OR 1.168, 95% CI 1.166–1.170). Compared with White first-dose recipients, the second dose was more likely to have been missed by American Indian/Alaska Native (OR 2.760, 95% CI 2.746–2.774), Black (OR 1.377, 95% CI 1.373–1.380), Hispanic (OR 1.751, 95% CI 1.748–1.754) recipients, and those of other or unknown race (OR 1.487, 95% CI 1.485–1.489). Compared with first-dose recipients who resided in counties in the Northeast, the second dose was more likely to have been missed by persons who resided in counties in the Pacific (OR 1.566, 95% CI 1.563–1.568), Noncontiguous (OR 3.038, 95% CI 3.020–3.056), and South (OR 1.319, 95% CI 1.317–1.322) regions.

## Discussion

By building models based on millions of US vaccination records to analyze sociodemographic factors associated with delayed or missed second doses in a 2-dose primary mRNA COVID-19 vaccine series, we identified population subgroups that might benefit from targeted interventions aimed at encouraging timely receipt of a second dose and at increasing access and demand for a booster dose. Findings from this study (Table 1) align with previous US reports that nearly 1 in 10 persons who began a 2-dose COVID-19 mRNA vaccination series had not received a second dose (7).

Compared with first-dose recipients 18–39 years of age, recipients 40–64 and  $\geq 65$  years of age were less likely to have missed a second dose. Persons in older age groups had more time to complete their primary series, given the prioritization when COVID-19 vaccine first became available. Older adults also are at

higher risk for severe COVID-19 illness and may have been more motivated to become fully vaccinated (14,15). Compared with persons 18–39 years of age, persons 12–17 years of age were less likely to have received a delayed second dose. On May 10, 2021, EUA was granted for COVID-19 vaccine use in persons 12–15 years of age, and peak adolescent vaccination rates were observed during summer 2021, immediately before the start of the 2021–22 school year (16,17). Lower rates of delayed second-dose vaccine receipt by those 12–17 years of age may have partially resulted from parent and child desire to return to in-person learning and from vaccination encouragement by or mandates from schools (18–20).

In our analyses, receipt of the second vaccine dose was more likely to have been delayed by initial Moderna vaccine recipients than by initial Pfizer-BioNTech recipients. In the context of our analysis, given the shorter recommendation period for the second dose of Pfizer-BioNTech vaccine, the definition of delayed

second dose (>42 days) gave Pfizer recipients a window of 7 more days (beyond the vaccine-specific recommended dosing interval) than Moderna recipients to complete a second dose, which might contribute to the result. Previous studies suggested that Moderna recipients were more likely to have experienced side effects (especially after the second dose) than were Pfizer-BioNTech recipients (21,22). Fear of side effects may also have contributed to the higher percentage of delayed second doses among Moderna recipients (23).

When compared with first-dose recipients who were White, members of several racial/ethnic minority groups were more likely to have delayed or missed the second dose, including Hispanic, Black, and American Indian/Alaska Native; this finding is consistent with reports from other studies that uptake of COVID-19 vaccination and other vaccinations was lower among members of these minority groups (24–26). Many factors may contribute to this disparity. Poverty rates are higher among Black (19.5%) and

**Table 1.** Timing of second dose of a 2-dose primary mRNA COVID-19 vaccine series, by sociodemographic factors, United States, December 14, 2020–December 31, 2021\*

| Variable                        | Second dose timing, no. (%) |                  |                   | Total, no. (%) |
|---------------------------------|-----------------------------|------------------|-------------------|----------------|
|                                 | Timely†                     | Delayed‡         | Missed§           |                |
| Total                           | 135,979,226 (87.25)         | 5,224,993 (3.35) | 14,643,23 (9.40)  | 155,847,451    |
| Vaccine type, dose 1            |                             |                  |                   |                |
| Moderna                         | 53,478,853 (87.04)          | 2,384,368 (3.88) | 5,577,569 (9.08)  | 61,440,790     |
| Pfizer-BioNTech                 | 82,500,373 (87.39)          | 2,840,625 (3.01) | 9,065,663 (9.60)  | 94,406,661     |
| Age group, y                    |                             |                  |                   |                |
| 12–17                           | 9,762,549 (86.60)           | 280,348 (2.49)   | 1,230,395 (10.91) | 11,273,292     |
| 18–39                           | 39,414,160 (85.13)          | 1,621,400 (3.50) | 5,264,452 (11.37) | 46,300,012     |
| 40–64                           | 52,589,787 (88.27)          | 1,934,658 (3.25) | 5,053,236 (8.48)  | 59,577,681     |
| ≥65                             | 34,212,730 (88.41)          | 1,388,587 (3.59) | 3,095,149 (8.00)  | 38,696,466     |
| Sex                             |                             |                  |                   |                |
| M                               | 62,548,887 (86.85)          | 2,393,426 (3.32) | 7,076,540 (9.83)  | 72,018,853     |
| F                               | 73,430,339 (87.60)          | 2,831,567 (3.38) | 7,566,692 (9.03)  | 83,828,598     |
| Urbanicity                      |                             |                  |                   |                |
| Metro                           | 120,443,535 (87.14)         | 4,633,895 (3.35) | 13,145,421 (9.51) | 138,222,851    |
| Nonmetro                        | 15,535,691 (88.15)          | 591,098 (3.35)   | 1,497,811 (8.50)  | 17,624,600     |
| Social Vulnerability Index (12) |                             |                  |                   |                |
| High                            | 41,938,563 (85.92)          | 1,873,526 (3.84) | 5,003,810 (10.25) | 48,815,899     |
| Medium                          | 54,681,094 (86.36)          | 2,090,878 (3.30) | 6,544,599 (10.34) | 63,316,571     |
| Low                             | 39,359,569 (90.04)          | 1,260,589 (2.88) | 3,094,823 (7.08)  | 43,714,981     |
| Race/ethnicity                  |                             |                  |                   |                |
| Hispanic                        | 14,678,149 (83.38)          | 622,364 (3.54)   | 2,302,543 (13.08) | 17,603,056     |
| Black                           | 9,711,675 (86.24)           | 446,893 (3.97)   | 1,102,700 (9.79)  | 11,261,268     |
| American Indian/Alaska Native   | 860,111 (75.91)             | 54,520 (4.81)    | 218,355 (19.27)   | 1,132,986      |
| Asian/OPI                       | 6,047,962 (88.09)           | 210,615 (3.07)   | 607,609 (8.85)    | 6,866,186      |
| White                           | 58,829,793 (90.17)          | 1,972,730 (3.02) | 4,445,116 (6.81)  | 65,247,639     |
| Other/unknown                   | 45,851,536 (85.33)          | 1,917,871 (3.57) | 5,966,909 (11.10) | 53,736,316     |
| Region                          |                             |                  |                   |                |
| South                           | 41,188,846 (86.15)          | 1,775,680 (3.71) | 4,844,461 (10.13) | 47,808,987     |
| Midwest                         | 28,738,970 (91.57)          | 811,360 (2.59)   | 1,832,846 (5.84)  | 31,383,176     |
| Mountain                        | 11,446,355 (86.39)          | 574,949 (4.34)   | 1,227,706 (9.27)  | 13,249,010     |
| Pacific                         | 27,077,135 (83.19)          | 1,254,754 (3.86) | 4,216,649 (12.95) | 32,548,538     |
| Noncontiguous                   | 517,084 (74.17)             | 28,439 (4.08)    | 151,668 (21.75)   | 697,191        |
| Northeast                       | 27,010,836 (89.56)          | 779,811 (2.59)   | 2,369,902 (7.86)  | 30,160,549     |

\*Pfizer-BioNTech, <https://www.pfizer.com>; Moderna, <https://www.modernatx.com>. OPI, other Pacific Islander.

†Second dose administered ≤42 d after first dose.

‡Second dose administered >42 d after second dose.

§Received the first dose but no matching second dose on record.

RESEARCH

**Table 2.** Logistic regression models examining sociodemographic factors associated with delayed or missed second dose of a 2-dose primary mRNA COVID-19 vaccine series, United States, December 14, 2020–December 31, 2021\*

| Variable                        | Model 1                                |                      | Model 2                               |                      |
|---------------------------------|--|----------------------|---------------------------------------|----------------------|
|                                 | Delayed second dose, † n = 141,204,219 |                      | Missed second dose, ‡ n = 155,847,451 |                      |
|                                 | Coefficient estimate                   | OR (95% CI)          | Coefficient estimate                  | OR (95% CI)          |
| Vaccine type, dose 1            |  |                      |                                       |                      |
| Moderna                         | 0.237                                  | 1.267 (1.265–1.270)§ | -0.012                                | 0.988 (0.987–0.989)  |
| Pfizer-BioNTech                 | Referent                               |                      | Referent                              |                      |
| Age group, y                    |  |                      |                                       |                      |
| 12–17                           | -0.271                                 | 0.763 (0.759–0.766)§ | -0.064                                | 0.938 (0.936–0.940)  |
| 40–64                           | -0.112                                 | 0.894 (0.892–0.896)  | -0.301                                | 0.740 (0.739–0.741)§ |
| ≥65                             | -0.008                                 | 0.992 (0.990–0.995)  | -0.298                                | 0.743 (0.741–0.744)§ |
| 18–39                           | Referent                               |                      | Referent                              |                      |
| Sex                             |  |                      |                                       |                      |
| F                               | 0.006                                  | 1.006 (1.004–1.008)  | -0.082                                | 0.922 (0.921–0.923)  |
| M                               | Referent                               |                      | Referent                              |                      |
| Urbanicity                      |  |                      |                                       |                      |
| Metro                           | 0.048                                  | 1.049 (1.046–1.052)  | -0.038                                | 0.963 (0.961–0.965)  |
| Nonmetro                        | Referent                               |                      | Referent                              |                      |
| Social Vulnerability Index (12) |  |                      |                                       |                      |
| High                            | 0.181                                  | 1.198 (1.196–1.201)§ | 0.155                                 | 1.168 (1.166–1.170)§ |
| Medium                          | 0.092                                  | 1.096 (1.094–1.099)  | 0.260                                 | 1.297 (1.295–1.299)§ |
| Low                             | Referent                               |                      | Referent                              |                      |
| Race/ethnicity                  |  |                      |                                       |                      |
| Hispanic                        | 0.159                                  | 1.172 (1.168–1.175)§ | 0.560                                 | 1.751 (1.748–1.754)§ |
| Black                           | 0.270                                  | 1.310 (1.305–1.314)§ | 0.320                                 | 1.377 (1.373–1.380)§ |
| American Indian/Alaska Native   | 0.411                                  | 1.508 (1.494–1.522)§ | 1.015                                 | 2.760 (2.746–2.774)§ |
| Asian/OPI                       | 0.010                                  | 1.010 (1.005–1.015)  | 0.128                                 | 1.137 (1.134–1.140)  |
| Other/unknown                   | 0.117                                  | 1.124 (1.122–1.127)  | 0.397                                 | 1.487 (1.485–1.489)§ |
| White                           | Referent                               |                      | Referent                              |                      |
| Region                          |  |                      |                                       |                      |
| South                           | 0.354                                  | 1.425 (1.421–1.429)§ | 0.277                                 | 1.319 (1.317–1.322)§ |
| Midwest                         | -0.007                                 | 0.993 (0.990–0.996)  | -0.246                                | 0.782 (0.780–0.783)§ |
| Mountain                        | 0.499                                  | 1.648 (1.641–1.655)§ | 0.070                                 | 1.072 (1.069–1.075)  |
| Pacific                         | 0.410                                  | 1.507 (1.503–1.512)§ | 0.448                                 | 1.566 (1.563–1.568)§ |
| Noncontiguous                   | 0.634                                  | 1.886 (1.863–1.909)§ | 1.111                                 | 3.038 (3.020–3.056)§ |
| Northeast                       | Referent                               |                      | Referent                              |                      |

\*Pfizer-BioNTech, <https://www.pfizer.com>; Moderna, <https://www.modernatx.com>. OPI, Other Pacific Islander; OR, odds ratio.

†Second dose administered >42 d after first dose. This model examines factors associated with a delayed second dose, conditional on receiving a second dose.

‡Received the first dose but no matching second dose on record.

§Factors with OR >1.150 or <0.850.

Hispanic (17.0%) than among White (8.2%) persons (27). Lower-income persons may be concerned about taking time off work to get vaccinated and to recuperate should they experience side effects (28,29). In addition, this racial/ethnic disparity may in part reflect vaccine access barriers for getting a timely second dose among Black and Hispanic persons (30). In comparison, Asian first-dose recipients were more likely to receive a timely second dose, which may reflect lower vaccine hesitancy observed among this group (24). These observations all highlight the value of knowing which barriers prevent timely second-dose completion for racial/ethnic minority recipients.

Delayed or missed second doses were less likely among those who reside in low SVI tertile counties than among those who reside in high SVI tertile counties. SVI comprises 4 themes (socioeconomic status, household composition and disability, minority status and language, and housing and transportation) con-

structed by using 15 social and environmental variables from the US Census (13). Lower SVI scores indicate that an area is less socially vulnerable. Previous research found that COVID-19 vaccine coverage was lower in rural counties than in urban counties (31). Residents of communities within more socially vulnerable areas may have more barriers to accessing vaccination providers, including limited transportation options, higher disability, and reduced ability to seek out or engage with vaccine providers (32,33). Technologic disparities and reduced health literacy resulting from language and education barriers could contribute to the finding that those able to receive a first dose missed or delayed receipt of their second dose, especially if challenges involved accessing information regarding vaccine availability or scheduling a second dose within the appropriate time interval (34).

Recipients who resided in counties in the Northeast region were more likely than recipients in other

regions to receive a timely second dose and less likely to miss their second dose. The Northeast region has reported the highest vaccination coverage since vaccine availability, which may in part reflect the fact that this region has the highest per capita income and the lowest percentage of uninsured persons, both of which have been correlated with vaccination coverage (35). The population in the Northeast region is also older and has more college graduates, which are 2 population characteristics associated with lower vaccine hesitancy and higher COVID-19 vaccination coverage (36,37). In addition, compared with other US regions, Northeast jurisdictions promoted vaccinations at different administrative levels (e.g., local or state), including vaccine mandates and proof-of-vaccination requirements for indoor dining, indoor entertainment venues, and large gatherings (38,39). Such policies and cultural norms may also have contributed to populations receiving their second vaccine dose on time.

First among the limitations of our study, a small percentage of records submitted to CDC lacked recipients' county of residence information (8.8%), which in some states contributed to the loss of sample size for generation of SVI and urbanicity measures. Race/ethnicity data were missing on 30% of records, which may affect the accuracy of findings related to race/ethnicity. Race/ethnicity information is not a customary unit of data gathered when arranging vaccination appointments, unlike age (date of birth) or sex. Missing race/ethnicity data result in part from data-reporting limitations in some counties and states and from incomplete data collection/reporting at the beginning of vaccine rollout. Second, in our analysis, identifying second-dose recipients depended on the link between vaccination records in jurisdiction-specific immunization information systems. Persons who received a second dose in a different jurisdiction from that of their first dose or for whom we were unable to match first and second primary series doses could not be represented accurately in these results. Third, persons who received the first dose in the fall of 2021 (e.g., September) had fewer months in which to receive their second dose and be matched than did those who received their first dose early in 2021 (because of our cutoff of December 31, 2021). Thus, we would not have captured any delayed second doses for those who received their second dose in 2022 (i.e., after the cutoff); this population would have been defined as having missed the second dose and was included in the model examining risk factors associated with having missed the second dose. Fourth, characteristics other than the sociodemographic factors that we analyzed could have been associated with series completion.

Because vaccine effectiveness against infection and hospitalization has been found to be higher with an extended (6–8-week) interval than with a standard (3–4-week) interval (40), CDC provided guidance in March 2022 that an 8-week interval might be optimal for some persons, especially for men and boys 12–39 years of age (41). Future studies of delayed second-dose completion of the mRNA primary series should consider that newer recommended intervals between first and second doses may be longer than the intervals that we considered here.

Our study highlights demographic factors associated with delayed or missed second doses in the 2-dose primary series of mRNA COVID-19 vaccine in the United States and identifies population subgroups that may benefit from outreach and encouragement to receive subsequent doses on time. Second doses were more likely to be delayed or missed for members of several racial/ethnic minority groups, persons <40 years of age, persons living in more socially vulnerable or nonmetro areas, and persons living in regions other than the Northeast. Interventions and efforts addressing social and health inequalities and promoting vaccine-related policies can potentially increase access and demand for COVID-19 vaccine and improve subsequent dose completion.

### Acknowledgments

We thank the COVID-19 Vaccine Task Force, the US Department of Defense, immunization program managers, immunization information system managers, and other staff members of the immunization programs in the 64 jurisdictions and 5 federal entities who provided these data.

### About the Author

Dr. Meng, with CDC's National Center for Immunization and Respiratory Diseases, has served as data science advisor/manager for the CDC COVID-19 response for the past 2 years, including on the Vaccine Task Force, the Health Systems & Worker Safety Task Force, and the Data, Analytics & Visualization Task Force. Her primary research interest is the use of big data and modeling to understand factors associated with vaccine uptake and coverage and vaccination intent.

### References

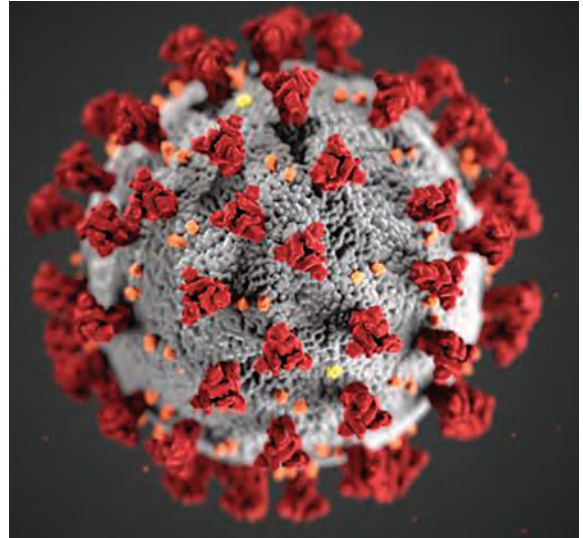
1. Oliver SE, Gargano JW, Marin M, Wallace M, Curran KG, Chamberland M, et al. The Advisory Committee on Immunization Practices' interim recommendation for use of Pfizer-BioNTech COVID-19 vaccine – United States, December 2020. *MMWR Morb Mortal Wkly Rep.* 2020;69:1922–4. <https://doi.org/10.15585/mmwr.mm6950e2>

2. Oliver SE, Gargano JW, Marin M, Wallace M, Curran KG, Chamberland M, et al. The Advisory Committee on Immunization Practices' interim recommendation for use of Moderna COVID-19 vaccine – United States, December 2020. *MMWR Morb Mortal Wkly Rep.* 2021;69:1653–6. <https://doi.org/10.15585/mmwr.mm695152e1>
3. Dooling K, Marin M, Wallace M, McClung N, Chamberland M, Lee GM, et al. The Advisory Committee on Immunization Practices' updated interim recommendation for allocation of COVID-19 vaccine—United States, December 2020. *MMWR Morb Mortal Wkly Rep.* 2021;69:1657–60. <https://doi.org/10.15585/mmwr.mm695152e2>
4. Kriss JL, Reynolds LE, Wang A, Stokley S, Cole MM, Harris LQ, et al.; CDC COVID-19 Vaccine Task Force. COVID-19 vaccine second-dose completion and interval between first and second doses among vaccinated persons – United States, December 14, 2020–February 14, 2021. *MMWR Morb Mortal Wkly Rep.* 2021;70:389–95. <https://doi.org/10.15585/mmwr.mm7011e2>
5. Wallace M, Woodworth KR, Gargano JW, Scobie HM, Blain AE, Moulia D, et al. The Advisory Committee on Immunization Practices' interim recommendation for use of Pfizer-BioNTech COVID-19 vaccine in adolescents aged 12–15 years—United States, May 2021. *MMWR Morb Mortal Wkly Rep.* 2021;70:749–52. <https://doi.org/10.15585/mmwr.mm7020e1>
6. Fast HE, Zell E, Murthy BP, Murthy N, Meng L, Scharf LG, et al. Booster and additional primary dose COVID-19 vaccinations among adults aged ≥65 years – United States, August 13, 2021–November 19, 2021. *MMWR Morb Mortal Wkly Rep.* 2021;70:1735–9. <https://doi.org/10.15585/mmwr.mm7050e2>
7. Anders C. 15 million people in the U.S. have missed their second dose of the coronavirus vaccine, CDC says [cited 2022 Jan 30]. <https://www.washingtonpost.com/health/2021/07/02/missed-second-dose-covid19-vaccine>
8. Bradley T, Grundberg E, Selvarangan R, LeMaster C, Fraley E, Banerjee D, et al. Antibody responses after a single dose of SARS-CoV-2 mRNA vaccine. *N Engl J Med.* 2021;384:1959–61. <https://doi.org/10.1056/NEJMc2102051>
9. Bar-On YM, Goldberg Y, Mandel M, Bodenheimer O, Freedman L, Kalkstein N, et al. Protection of BNT162b2 vaccine booster against Covid-19 in Israel. *N Engl J Med.* 2021;385:1393–400. <https://doi.org/10.1056/NEJMoa2114255>
10. Doria-Rose N, Suthar MS, Makowski M, O'Connell S, McDermott AB, Flach B, et al. mRNA-1273 Study Group. Antibody persistence through 6 months after the second dose of mRNA-1273 vaccine for Covid-19. *N Engl J Med.* 2021;384:2259–61. <https://doi.org/10.1056/NEJMc2103916>
11. Centers for Disease Control and Prevention. Vaccine Administration Management System (VAMS) program information [cited 2022 Jan 30]. <https://www.cdc.gov/vaccines/covid-19/reporting/vams/program-information.html>
12. Agency for Toxic Substances and Disease Registry. CDC/ATSDR Social Vulnerability Index [cited 2022 Jan 30]. <https://www.atsdr.cdc.gov/placeandhealth/svi/index.html>
13. Centers for Disease Control and Prevention. NCHS urban-rural classification scheme for counties [cited 2022 Jan 30]. [https://www.cdc.gov/nchs/data\\_access/urban\\_rural.htm#2013\\_urban-rural\\_classification\\_scheme\\_for\\_counties](https://www.cdc.gov/nchs/data_access/urban_rural.htm#2013_urban-rural_classification_scheme_for_counties)
14. Berek MA, Aziz MA, Islam MS. Impact of age, sex, comorbidities and clinical symptoms on the severity of COVID-19 cases: a meta-analysis with 55 studies and 10014 cases. *Heliyon.* 2020;6:e05684. <https://doi.org/10.1016/j.heliyon.2020.e05684>
15. Centers for Disease Control and Prevention. COVID-19 risks and vaccine information for older adults [cited 2021 Aug 4]. <https://www.cdc.gov/aging/covid19/covid19-older-adults.html>
16. Kates J, Michaud J, Tolbert J, Artiga S, Orgera K; Kaiser Family Foundation. KFF COVID-19 Vaccine Monitor: winter 2021 update on parents' views of vaccines for kids [cited 2022 Jan 30]. <https://www.kff.org/coronavirus-covid-19/polling/kff-covid-19-vaccine-monitor-winter-2021-update-on-parents-views-of-vaccines>
17. Murthy BP, Zell E, Saelee R, Murthy N, Meng L, Meador S, et al. COVID-19 vaccination coverage among adolescents aged 12–17 years – United States, December 14, 2020–July 31, 2021. *MMWR Morb Mortal Wkly Rep.* 2021;70:1206–13. <https://doi.org/10.15585/mmwr.mm7035e1>
18. Camera L. Survey shows parents clamoring for in-person learning despite spike in COVID-19 cases [cited 2022 Mar 4]. <https://www.usnews.com/news/education-news/articles/2021-08-18/survey-shows-parents-clamoring-for-in-person-learning-despite-spike-in-covid-19-cases>
19. Goldstein D. Los Angeles mandates vaccines for students 12 and older [cited 2022 Mar 4]. <https://www.nytimes.com/2021/09/09/us/la-vaccine-mandate-students-schools.html>
20. Camera L. School vaccine mandates: here they come [cited 2022 Mar 4]. <https://www.usnews.com/news/national-news/articles/2021-08-31/school-vaccine-mandates-here-they-come>
21. Meo SA, Bukhari IA, Akram J, Meo AS, Klonoff DC. COVID-19 vaccines: comparison of biological, pharmacological characteristics and adverse effects of Pfizer/BioNTech and Moderna vaccines. *Eur Rev Med Pharmacol Sci.* 2021;25:1663–9. <https://doi.org/10.26355/eurrev.202102.24877>
22. Chapin-Bardales J, Gee J, Myers T. Reactogenicity following receipt of mRNA-based COVID-19 vaccines. *JAMA.* 2021;325:2201–2. <https://doi.org/10.1001/jama.2021.5374>
23. Ismail L. Doctors say some are opting out of second vaccine dose in fear of side effects [cited 2022 Mar 4]. <https://www.newschannel5.com/news/doctors-say-some-are-opting-out-of-second-vaccine-dose-in-fear-of-side-effects>
24. Momplaisir FM, Kuter BJ, Ghadimi F, Browne S, Nkwihoreze H, Feemster KA, et al. Racial/ethnic differences in COVID-19 vaccine hesitancy among health care workers in 2 large academic hospitals. *JAMA Netw Open.* 2021;4:e2121931. <https://doi.org/10.1001/jamanetworkopen.2021.21931>
25. Lu PJ, O'Halloran A, Williams WW, Lindley MC, Farrall S, Bridges CB. Racial and ethnic disparities in vaccination coverage among adult populations in the U.S. *Am J Prev Med.* 2015;49(Suppl 4):S412–25. <https://doi.org/10.1016/j.amepre.2015.03.005>
26. Nguyen KH, Anneser E, Toppo A, Allen JD, Scott Parott J, Corlin L. Disparities in national and state estimates of COVID-19 vaccination receipt and intent to vaccinate by race/ethnicity, income, and age group among adults ≥ 18 years, United States. *Vaccine.* 2022;40:107–13. <https://doi.org/10.1016/j.vaccine.2021.11.040>
27. Shrider EA, Kollar M, Chen F, Semega J. Income and poverty in the United States: 2020 [cited 2022 Mar 4]. <https://www.census.gov/library/publications/2021/demo/p60-273.html>
28. Goldman N, Pebley AR, Lee K, Andrasfay T, Pratt B. Racial and ethnic differentials in COVID-19-related job exposures by occupational standing in the US. *PLoS One.* 2021;16:e0256085. <https://doi.org/10.1371/journal.pone.0256085>

29. Hamel L, Lopes L, Sparks G, Kirzinger A, Kearney A, Strokes M, et al.; Kaiser Family Foundation. KFF COVID-19 vaccine monitor: October 2021 [cited 2022 Jan 30]. <https://www.kff.org/coronavirus-covid-19/poll-finding/kff-covid-19-vaccine-monitor-october-2021>
30. Rusoja EA, Thomas BA. The COVID-19 pandemic, Black mistrust, and a path forward. *EclinicalMedicine*. 2021; 35:100868. <https://doi.org/10.1016/j.eclinm.2021.100868>
31. Saelee R, Zell E, Murthy BP, Castro-Roman P, Fast H, Meng L, et al. Disparities in COVID-19 vaccination coverage between urban and rural counties – United States, December 14, 2020–January 31, 2022. *MMWR Morb Mortal Wkly Rep*. 2022;71:335–40. <https://doi.org/10.15585/mmwr.mm7109a2>
32. Ryerson AB, Rice CE, Hung MC, Patel SA, Weeks JD, Kriss JL, et al. Disparities in COVID-19 vaccination status, intent, and perceived access for noninstitutionalized adults, by disability status – National Immunization Survey Adult COVID module, United States, May 30–June 26, 2021. *MMWR Morb Mortal Wkly Rep*. 2021;70:1365–71. <https://doi.org/10.15585/mmwr.mm7039a2>
33. Haggerty J, Levesque JF, Harris M, Scott C, Dahrouge S, Lewis V, et al. Does healthcare inequity reflect variations in peoples' abilities to access healthcare? Results from a multi-jurisdictional interventional study in two high-income countries. *Int J Equity Health*. 2020;19:167. <https://doi.org/10.1186/s12939-020-01281-6>
34. Press VG, Huisingh-Scheetz M, Arora VM. Inequities in technology contribute to disparities in COVID-19 vaccine distribution. *JAMA Health Forum*. 2021;2:e210264. <https://doi.org/10.1001/jamahealthforum.2021.0264>
35. Mollalo A, Tatar M. Spatial modeling of COVID-19 vaccine hesitancy in the United States. *Int J Environ Res Public Health*. 2021;18:9488. <https://doi.org/10.3390/ijerph18189488>
36. Levenson E. These are the states with the highest and lowest vaccination rates [cited 2021 May 10]. <https://www.cnn.com/2021/05/10/us/us-vaccination-rates-states>
37. Willis DE, Andersen JA, Bryant-Moore K, Selig JP, Long CR, Felix HC, et al. COVID-19 vaccine hesitancy: race/ethnicity, trust, and fear. *Clin Transl Sci*. 2021;14:2200–7. <https://doi.org/10.1111/cts.13077>
38. Kaiser Family Foundation. State COVID-19 data and policy actions [cited 2022 Jan 30]. <https://www.kff.org/report-section/state-covid-19-data-and-policy-actions-policy-actions>
39. Levenson E. New York City now enforcing Covid-19 vaccine requirement for most indoor activities [cited 2022 Mar 4]. <https://www.cnn.com/2021/09/13/us/new-york-vaccine-passport/index.html>
40. Amirthalingam G, Bernal JL, Andrews NJ, Whitaker H, Gower C, Stowe J, et al. Serological responses and vaccine effectiveness for extended COVID-19 vaccine schedules in England. *Nat Commun*. 2021;12:7217. <https://doi.org/10.1038/s41467-021-27410-5>
41. Wallace M, Moulia D, Blain AE, Ricketts EK, Minhaj FS, Link-Gelles R, et al.; Centers for Disease Control and Prevention. The Advisory Committee on Immunization Practices' recommendation for use of Moderna COVID-19 vaccine in adults aged ≥18 years and considerations for extended intervals for administration of primary series doses of mRNA COVID-19 vaccines – United States, February 2022. *MMWR Morb Mortal Wkly Rep*. 2022;71:416–21. <https://doi.org/10.15585/mmwr.mm7111a4>

Address for correspondence: Terence Chorba, Centers for Disease Control and Prevention, 1600 Clifton Rd NE, Mailstop US 12-4, Atlanta, GA 30329-4027, USA; email: [tlc2@cdc.gov](mailto:tlc2@cdc.gov)

## EID Podcast Isolation Cocoon, May 2020—After Zhuangzi's Butterfly Dream



For many people, the prolonged period of social distancing during the coronavirus disease pandemic felt frightening, uncanny, or surreal.

For Ron Louie, the sensation was reminiscent of a moth taking refuge in its cocoon, slumbering in isolation as he waited for better days ahead.

In this EID podcast, Dr. Ron Louie, a clinical professor in Pediatrics Hematology-Oncology at the University of Washington in Seattle, reads and discusses his poem about the early days of the pandemic.

Visit our website to listen:  
<https://go.usa.gov/x6W9A>

**EMERGING  
INFECTIOUS DISEASES®**

# COVID-19 Vaccination Intent and Belief that Vaccination Will End the Pandemic

Marion de Vries, Liesbeth Claassen, Mattijs Lambooi, Ka Yin Leung, Kees Boersma, Aura Timen

High vaccination coverage is considered to be key in dealing with the coronavirus disease (COVID-19) pandemic. However, vaccine hesitancy can limit uptake. We examined the specific coronavirus beliefs that persons have regarding COVID-19 and COVID-19 vaccines and to what extent these beliefs explain COVID-19 vaccination intentions. We conducted a survey among 4,033 residents of the Netherlands that examined COVID-19 vaccination intentions and various beliefs. Random forest regression analysis explained 76% of the variance in vaccination intentions. The strongest determinant in the model was the belief the COVID-19 crisis will only end if many persons get vaccinated. Other strong determinants were beliefs about safety of vaccines, specifically in relation to vaccine development and approval process; (social) benefits of vaccination; social norms regarding vaccination behavior; and effectiveness of vaccines. We propose to address these specific beliefs in communications about COVID-19 vaccinations to stimulate vaccine uptake.

The COVID-19 pandemic has profoundly affected global health and well-being. Since 2020, countries worldwide have experienced high rates of illness and death caused by COVID-19, and many societies have dealt with often stringent outbreak control measures. The successful development of effective vaccines has provided a much-wanted major step toward controlling the pandemic. However, for the vaccines to be successful during outbreak control, a high and equally distributed vaccine uptake is essential. Next to possible barriers of limited COVID-19 vaccine availability and accessibility, vaccine hesitancy can also form a considerable barrier to reaching a high vaccine uptake.

The public acceptance of vaccines has been a global concern for decades. Before the COVID-19

crisis, in 2019, the World Health Organization declared vaccine hesitancy as one of the top 10 global public health threats (1). Vaccine hesitancy has been defined as a broad range of vaccine-related attitudes and behavior, from having some doubts and delaying vaccinations up to complete refusal of vaccines (2). Various studies have provided insights into beliefs underlying vaccination hesitancy and vaccination intentions for childhood vaccinations (3–5); influenza vaccinations (5,6), including pandemic influenza A(H1N1) vaccination (5–7); and COVID-19 vaccinations (8–12). Personal beliefs that are known to have a major role in vaccination decision-making are beliefs about the need for, safety of, and effectiveness of vaccines.

Many studies that examine determinants of vaccination hesitancy, intentions, or behavior (e.g., studies applying the health belief model [9–13]) explore beliefs in relatively general terms. For example, surveys may simply ask respondents whether they have concerns about the safety of vaccines. It is useful to have more detailed knowledge of these beliefs for 3 reasons. First, in-depth insights into beliefs can provide more concrete input toward developing well-adapted communication (14). For example, concerns about safety of vaccines might be related to beliefs about the vaccine production process, long-term side-effects, and composition of vaccines. Such specific beliefs should be addressed in communications. Second, COVID-19 vaccination intentions are likely to be associated with specific beliefs that differ from those found in research during other vaccination campaigns. This reaction might be the case for beliefs about the rapid vaccine development process, the new technologies used (mRNA), and the personal freedom associated with vaccination (through vaccination entry passes). Third, there might be major differences in (the influence of certain) beliefs underlying vaccination decisions between countries or communities (15) (e.g., due to differences in experiences with the COVID-19 pandemic, information streams, and vaccination campaign history).

Author affiliations: National Institute for Public Health and the Environment, Bilthoven, the Netherlands (M. de Vries, L. Claassen, M. Lambooi, K.Y. Leung, A. Timen); Vrije Universiteit, Amsterdam, the Netherlands (K. Boersma, A. Timen)

DOI: <https://doi.org/10.3201/eid2808.212556>

Consistent with earlier research on vaccination decisions (16), we adopted a mental models perspective in studying beliefs underlying COVID-19 vaccination intentions among persons in the Netherlands (14). This perspective entails a detailed study of interrelated beliefs of a subject, in this case COVID-19 and the COVID-19 vaccinations. These beliefs form a mental model underlying decisions of persons regarding COVID-19 vaccination. By gaining in-depth insights into these various beliefs, we can identify knowledge gaps and misbeliefs that need to be addressed in communications. In addition, by studying which beliefs are useful determinants of vaccination intentions, we aimed to identify beliefs that should be addressed and prioritized in communications to optimize vaccine acceptability and uptake.

## Methods

### Study Population and Procedure

We conducted an online survey during March 12–22, 2021. At that time, 1.5 million of the 17.5 million residents of the Netherlands were partly or fully vaccinated against COVID-19 (data from March 14, 2021) (17). We sent the survey (in Dutch) to 6,810 persons in the Netherlands ( $\geq 18$  years of age) by using an online survey panel (ISO/IEC 27001:2013; I&O Research, <https://www.ioresearch.nl>). Members from this survey panel were recruited by using random samples of name and address data. The sample invited for participation to this survey was selected to be representative of the general population of the Netherlands ( $\geq 18$  years of age) on the basis of demographic characteristics.

Panel members provided informed consent for participation to the survey panel. Survey completion took  $\approx 10$ –15 minutes. The Clinical Expertise Centre at the National Institute for Public Health and the Environment reviewed the study protocol and determined that the study was exempt from needing further approval from an ethics research committee (study no. LCI-485).

### Development of Survey Measurements

We measured vaccination intention as follows. All respondents who indicated to have received an invitation for a COVID-19 vaccination but who had not yet been vaccinated were asked, “Do you want to get vaccinated against the corona virus?” Respondents who indicated not yet to be invited for a COVID-19 vaccination were asked, “If you are invited for a COVID-19 vaccination, do you then want to get vaccinated?” Both questions could be answered on a 5-point Likert scale: 1. Certainly not; 2. Probably not; 3. Don’t know; 4. Probably yes; 5. Certainly yes. The answers to both

questions were taken together in 1 variable that was called COVID-19 vaccination intention.

To identify the beliefs about COVID-19 and the COVID-19 vaccines that should be assessed in this study, we studied literature on sociopsychological determinants of vaccination intentions to identify main elements in mental models of persons underlying COVID-19 vaccination intentions (2,4,18,19). In addition, we used recent qualitative studies (survey open answer categories and in-depth interviews) on COVID-19 vaccination acceptability among members of the public in the Netherlands (20,21) to identify specific beliefs within the familiar mental model themes and to identify beliefs that might not have been identified in studies on other vaccination campaigns.

We studied beliefs about COVID-19 and COVID-19 vaccines by using this question: “We would like to know what you think about the corona virus/vaccination against the corona virus. For each statement, indicate to what extent it aligns with what you think. I think ....” The question was followed by 25 statements that were scored on a 5-point Likert scale (1 = certainly not to 5 = certainly yes) (Table 1, <https://wwwnc.cdc.gov/EID/article/28/8/21-2556-T1.htm>). The 25 beliefs can be categorized into 7 elements of mental models of persons, namely beliefs about risk for COVID-19 regarding oneself, risk for COVID-19 regarding one’s loved ones, safety of vaccination, effectiveness of vaccination, (social) benefits of vaccination, alternatives to vaccination, social norms regarding vaccination behavior, and accessibility of vaccination.

### Analyses

We analyzed responses of (at that time) unvaccinated respondents. Descriptive analyses were performed for vaccination intention and the 25 beliefs about COVID-19 and the vaccines. In addition, we calculated Pearson correlations (2-tailed) between vaccination intention and all 25 beliefs and between all beliefs separately.

We subsequently performed a regression analysis by using Random forest (RF) (22) in R (23) to assess the extent to which beliefs explain variance in vaccination intentions, and to identify which specific beliefs are good determinants of vaccination intentions (Appendix, <https://wwwnc.cdc.gov/EID/article/28/8/21-2556-App1.pdf>). RF is a machine learning method for regression and classification based on an ensemble of decision trees. This method makes no assumptions about data distribution and is well suited to address 3 complicating features of the study responses for analyses: a dependent variable (COVID-19 vaccination intention) that is not normally distributed, many

(partly intercorrelated) independent variables (beliefs), and potentially nonlinear relationships between independent variables and the dependent variable. The RF method has been successfully applied in explaining vaccination intentions (16) and screening intentions (24). We controlled the RF regression analysis for age, sex, education level, region of residence, migration background, health status, previous coronavirus infection, being invited for a COVID-19 vaccination, perceived allergy for vaccinations, employment in health-care, and religious motivations (Appendix) by adding these as independent variables to the RF model.

We considered 4 types of output from the RF regression analyses. The first output was the variable importance ranking (VIR), which ranks independent and control variables in terms of how much these contribute to explaining the dependent variable. The second output was the partial dependence (also known as marginal means) that indicates the direction and strength of the relationship between the independent and dependent variable. The third output was the cumulative variance explained, which is the variance explained after adding an independent variable to the model in the sequence of the VIR. The fourth output was the total variance explained.

## Results

### Study Population

The survey response rate was 59% ( $n = 4,033$ ). The survey population was reasonably comparable to the general population in the Netherlands ( $\geq 18$  years of age) for demographic characteristics (Table 2).

### COVID-19 Vaccination Intention

Most (2,266/3,628, 62.5%) unvaccinated respondents indicated that they would certainly want to get vaccinated against COVID-19, 645 (17.8%) would probably want to get vaccinated, 257 (7.1%) did not know (yet), 213 (5.9%) would probably not want to get vaccinated, and 247 (6.8%) indicated certainly not. The mean ( $\pm$ SD) response of vaccination intention was 4.2 ( $\pm 1.2$ ).

### Beliefs about COVID-19 and COVID-19 Vaccines

Descriptive statistics and Pearson correlations (2-tailed) with vaccination intention showed that all 25 beliefs were significantly ( $p < 0.001$ ) correlated with vaccination intention (Table 1). Correlations between different beliefs about COVID-19 and COVID-19 vaccinations (Figure 1) showed moderate-to-strong correlations between different risk perception beliefs of COVID-19 (for self and loved ones), and, at the

same time, mostly weak correlations between these COVID-19 beliefs and the several beliefs about COVID-19 vaccinations. In addition, we observed many strong correlations between the various beliefs about COVID-19 vaccinations, especially in relation to beliefs about the safety of vaccination.

Personal risk perceptions of respondents for COVID-19 were moderate, with values of 2.9 ( $\pm 1.0$ ) for the belief about high likelihood of infection and 3.0 ( $\pm 1.3$ ) for the belief about possibility of severe illness. For loved ones, these COVID-19 risk perceptions were scored relatively higher: 3.5 ( $\pm 1.1$ ) for high likelihood of infection and 3.9 ( $\pm 1.1$ ) for possibility of severe illness. Respondents valued the likelihood to infect others if infected themselves with a value of 3.3 ( $\pm 1.2$ ).

Safety of vaccinations was generally trusted by respondents (Table 3), but some notable variations in responses were observed. For example, 27.7% of respondents indicated not believing that the side effects of vaccinated were well researched (mean 3.3, SD  $\pm 1.3$ ), and 28.3% of respondents believed that the vaccines were developed too quickly (mean 2.7, SD  $\pm 1.3$ ). With regard to the effectiveness of vaccinations, respondents believed that vaccines would protect them well against COVID-19 (mean 3.8, SD  $\pm 1.1$ ). Respondents seemed somewhat unsure about whether vaccines only protect for a short while (mean 3.1, SD  $\pm 1.0$ ) and whether one can still infect others after vaccination (mean 3.0, SD  $\pm 1.1$ ). At the time of data collection, scientific knowledge about those last 2 vaccine aspects was also limited.

In terms of (social) benefits of vaccinations, vaccinations were commonly seen as the only way out of the COVID-19 crisis (mean 4.1, SD  $\pm 1.2$ ) and as a means to return to a life without COVID-19 restrictions sooner (mean 3.8, SD  $\pm 1.3$ ). With regard to alternatives to vaccination, respondents generally did not believe that there were (sufficient) drugs that could cure COVID-19 (mean 1.9, SD  $\pm 1.0$ ), and few respondents believed that they were immune to COVID-19 (mean 2.0, SD  $\pm 1.1$ ). Some support was found for the belief that one's good health would protect against COVID-19 (mean 2.8, SD  $\pm 1.2$ ).

We found that perceived social norms were generally in favor of vaccination. Beliefs that friends and family expected that the respondent would get vaccinated (mean 4.0, SD  $\pm 1.2$ ), and the beliefs that most of the respondent's family and friends (mean 4.2, SD  $\pm 1.0$ ), as well as most residents in the Netherlands (mean 4.0, SD  $\pm 0.8$ ), would get vaccinated were largely supported. Accessibility of vaccination did not seem a large obstacle because the belief that getting vaccinated would take a lot of time or effort

was not strongly supported among the respondents (mean 2.0, SD  $\pm$ 1.2).

**Variance in COVID-19 Vaccination Intention**

The random forest model explained 76% of the variance in COVID-19 vaccination intentions. This analysis was performed using data for 3,614 of the 3,628 unvaccinated respondents (14 respondents were excluded from the analysis because of missing values). We provide the VIR with the 10 best explaining beliefs (Figure 2). We also provide the cumulative variances explained and partial dependence of the 10 best explaining beliefs (Table 3). Of these 10 best explaining beliefs, 5 beliefs concern safety of vaccinations, 2 beliefs are about social benefits of vaccination, 2 beliefs concern social norms regarding vaccination behavior, and 1 belief is about effectiveness of vaccination.

There was no clear selection of the 25 beliefs that explained variance in vaccination intention considerably more strongly than all other beliefs. Instead we observe a gradual progression in explanatory value of various beliefs (VIR with all determinants; Appendix). Because there are many intercorrelations between the beliefs (Figure 1), and many of the beliefs are associated with vaccination intentions, the partial dependence ranges were also small (Table 3). Our findings confirm that vaccination decisions are made on the basis of a complex web of interrelated beliefs (mental models), rather than on a few independent perceptions. Although a small number of these beliefs can (statistically) explain a large part of the variance in vaccination intentions, one needs to keep in mind that in reality beliefs never stand on their own. This said, the belief “the corona crisis will only end if many people get vaccinated” seems, distinctively, the strongest determinant in the model. By adding only this variable to the model, we can explain 54% of the variance in vaccination intentions.

We conducted sensitivity analyses in which we repeated the main RF analyses for 3 age groups (18–34 years, 35–64 years, and  $\geq$ 65 years). We repeated the main analysis with a binary dependent variable, explaining differences between those with low vaccination intentions (original values 1 and 2) and those who were unsure (value 3). Results were consistent with those of the main analyses and did not affect our conclusions.

**Discussion**

Our findings provide detailed insights into COVID-19 vaccination intentions and the underlying beliefs about COVID-19 and the COVID-19 vaccines among residents in the Netherlands during 2021. No

**Table 2.** Variables for study population testing major role for the belief that COVID-19 vaccination will end the pandemic, the Netherlands\*

| Variable                               | Answer categories    | No. (%)     |
|--|----------------------|-------------|
| Sex                                    | M                    | 1,991 (49)  |
|  | F                    | 2,042 (51)  |
| Age, y                                 | 18–29                | 560 (14)    |
|  | 30–39                | 503 (12)    |
|  | 40–49                | 574 (14)    |
|  | 50–59                | 765 (19)    |
|  | 60–69                | 805 (20)    |
|  | 70–79                | 613 (15)    |
|  | $\geq$ 80            | 213 (5)     |
| Level of education                     | Low                  | 824 (20)    |
|  | Moderate             | 1,535 (38)  |
|  | High                 | 1,674 (42)  |
| Region of residence in the Netherlands | West                 | 1,736 (43)  |
|  | North                | 470 (12)    |
|  | East                 | 866 (22)    |
|  | South                | 961 (24)    |
| Migration background                   | None                 | 3,267 (81)  |
|  | Western              | 444 (11)    |
|  | Other                | 306 (8)     |
|  | Unknown              | 16 (0)      |
| Invited for a COVID-19 vaccination     | Invited              | 642 (16)    |
|  | Not (yet) invited    | 3,391 (84)  |
| Vaccinated against COVID-19            | Vaccinated           | 405 (10)    |
|  | Not (yet) vaccinated | 3,628 (90)  |
| Total                                  | NA                   | 4,033 (100) |

\*COVID-19, coronavirus disease; NA, not applicable.

major knowledge gaps or misbeliefs were observed, but we did observe some considerable concerns with regard to the vaccine development and approval process. The beliefs assessed in our study explained a large part of the variance in COVID-19 vaccination intentions. Beliefs about the safety of vaccines, (social) benefits of vaccination, social norms regarding vaccination behavior and the effectiveness of vaccines were, relative to other beliefs, strong determinants of vaccination intention for persons. The strongest determinant in the model was the belief “the corona crisis will only end if many people get vaccinated.”

Our study results showed strong beliefs, and the explanatory value of these beliefs, about (social) benefits after being vaccinated or reaching a high vaccination coverage. The belief that the COVID-19 crisis will only end if many persons get vaccinated could (statistically) explain more than half of the variance in COVID-19 vaccination intentions. It is striking that this belief seemed to be, at least somewhat, a better determinant of vaccination intentions than beliefs about personal protection against the vaccine-preventable disease or beliefs about safety of vaccines, which have often been identified as the most essential psychosocial determinants of vaccination intentions (5,17,18). The wish for relaxation of COVID-19 control measures and for the ending of the enduring crisis seem to have been stronger among many than the wish for personal protection against disease (although these wishes are not

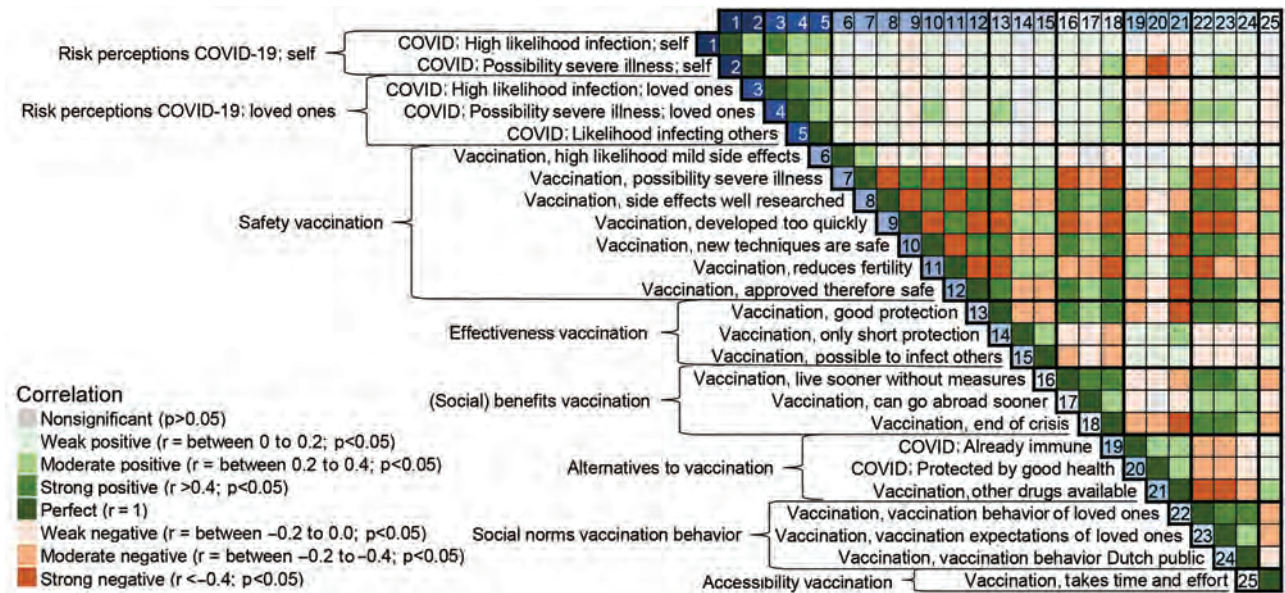


**Figure 1.** COVID-19 vaccination intent and belief that COVID-19 vaccination will end the pandemic among persons in the Netherlands. Pearson correlation matrix (2-tailed) heat map with all beliefs about COVID-19 and COVID-19 vaccinations was visualized per mental models element (risk perceptions COVID-19: self, risk perceptions COVID-19: loved ones, safety vaccination, effectiveness vaccination, (social) benefits vaccination, alternatives to vaccination, social norms vaccination behavior, accessibility vaccination). For a more detailed correlation matrix, see Appendix. (<https://wwwnc.cdc.gov/EID/article/28/8/21-2556-App1.pdf>).

mutually exclusive). This finding might be explained by the considerable effect of COVID-19 measures on lives of persons (25) and the observed moderate COVID-19 risk perceptions. Our results also suggest that persons who did not believe that high vaccination coverage is the only solution to end the COVID-19 crisis were not less likely to vaccinate.

We might expect that over time fewer persons will have the belief of vaccination being the only solution to end the crisis, because during the winter of 2021, when lockdown measures were again necessary, despite relatively high vaccination coverage (26). A decrease in this belief might lead to a decrease in vaccination acceptability. In communications, we are faced with a

dilemma. In the short run, providing clear future perspectives regarding personal and societal benefits after reaching a high vaccination coverage, might considerably help in motivating persons to get vaccinated. At the same time, transparency about uncertainties regarding these perspectives are necessary from an ethical point of view, but also to prevent disappointments in the future resulting from too optimistic expectations. Transparency is also crucial in remaining trust and support for control measures (27,28).

Consistent with previous research, we found that various beliefs about the safety of the vaccines were major determinants of COVID-19 vaccination intentions (12,29). Five of the 10 major explanatory beliefs

**Table 3.** Cumulative variance explained and partial dependence of 10 strongest determinants of COVID-19 vaccination intention in random forest model for residents of the Netherlands

| Ten strongest determinants in random forest model | Cumulative variance explained, % | Partial dependence, lowest–highest value* | Direction of relationship with vaccination intention |
|---|----------------------------------|---|--|
| Vaccination, end of crisis                        | 54                               | 3.9–4.3                                   | Positive   |
| Vaccination, expectations of loved ones           | 62                               | 4.0–4.4                                   | Positive   |
| Vaccination, developed too quickly                | 70                               | 4.5–4.2                                   | Negative   |
| Vaccination, side effects well researched         | 72                               | 4.1–4.3                                   | Positive   |
| Vaccination, approved therefore safe              | 72                               | 3.9–4.2                                   | Positive   |
| Vaccination, good protection                      | 73                               | 4.2–4.5                                   | Positive   |
| Vaccination, new techniques are safe              | 73                               | 4.2–4.4                                   | Positive   |
| Vaccination, live sooner without measures         | 74                               | 4.2–4.3                                   | Positive   |
| Vaccination, behavior of loved ones               | 74                               | 4.0–4.3                                   | Positive   |
| Vaccination, possibility severe illness           | 74                               | 4.4–4.3                                   | Negative   |

\*Interpretation of the partial dependence figures, first row (end of crisis) as an example: When all other determinants are kept constant, the lowest value for this belief (1, certainly not) matches a mean vaccination intention of 3.9 and the highest value of this belief (5, certainly yes) matches a mean vaccination intention of 4.3. Because many of the beliefs correlate strongly, and the partial dependence figures are controlled for all other determinants in the model, the partial dependence ranges are small. Partial dependence figures corresponding to all of the 10 best determinants values (1–5) are shown in the Appendix (<https://wwwnc.cdc.gov/EID/article/28/8/21-2556-App1.pdf>).

were related to safety. Four of these 5 beliefs were about vaccine development and approval processes. Rapid development of vaccines and the approval process, and the use of new techniques (e.g., mRNA vaccines) have probably increased public concerns about vaccine safety. Concerns about rapid development of vaccines were also observed in previous research on COVID-19 vaccination perceptions (8) and pandemic influenza A(H1N1) virus vaccination perceptions (30). Authorities must provide persons with timely and transparent information about development, approval, and safety monitoring of COVID-19 vaccines to fulfil their information needs. If such information is not, or is scarcely, provided by authorities, persons are likely to search for this information elsewhere on the internet, with the considerable risk that this would lead them to vaccine skeptical sources (31,32).

We showed that beliefs about descriptive and subjective social norms, specifically with regard to vaccination expectations and behavior of friends and family, were also major determinants of COVID-19 vaccination intentions. The role of social norms in vaccination behavior was also suggested in previous research with regard to COVID-19 vaccinations (8,33), influenza vaccinations (34,35), and human papillomavirus vaccinations (36,37). These findings suggest the

potential for interventions focused on endorsing social norms with regard to vaccination (e.g., providing narratives in communication materials for peers who vaccinated). In addition, this finding might indicate that persons are, at least partly, segregated in like-minded groups on the basis of COVID-19 vaccination intentions, which could increase the risk for local outbreaks.

Beliefs about the health risks posed by COVID-19 were not found among the major determinants of vaccination intentions. A similar result was seen in a study on meningococcal vaccination intentions that had a similar study approach (16). An explanation for this result can lie in the distribution of responses in vaccination intentions. Because most of our respondents intended to vaccinate against COVID-19, the explanatory analysis shows mainly how persons who are not (so) willing to vaccinate differ from those who do want to vaccinate, because that is where the variance in responses can be found. Perceptions of the health risk posed by COVID-19 are likely major reasons for persons to vaccinate but might not be among the most essential reasons for those who do not intend to vaccinate.

The first limitation of our study is that, although the study population is at large fairly comparable with the population in the Netherlands in terms of main demographic characteristics, it is not a perfect

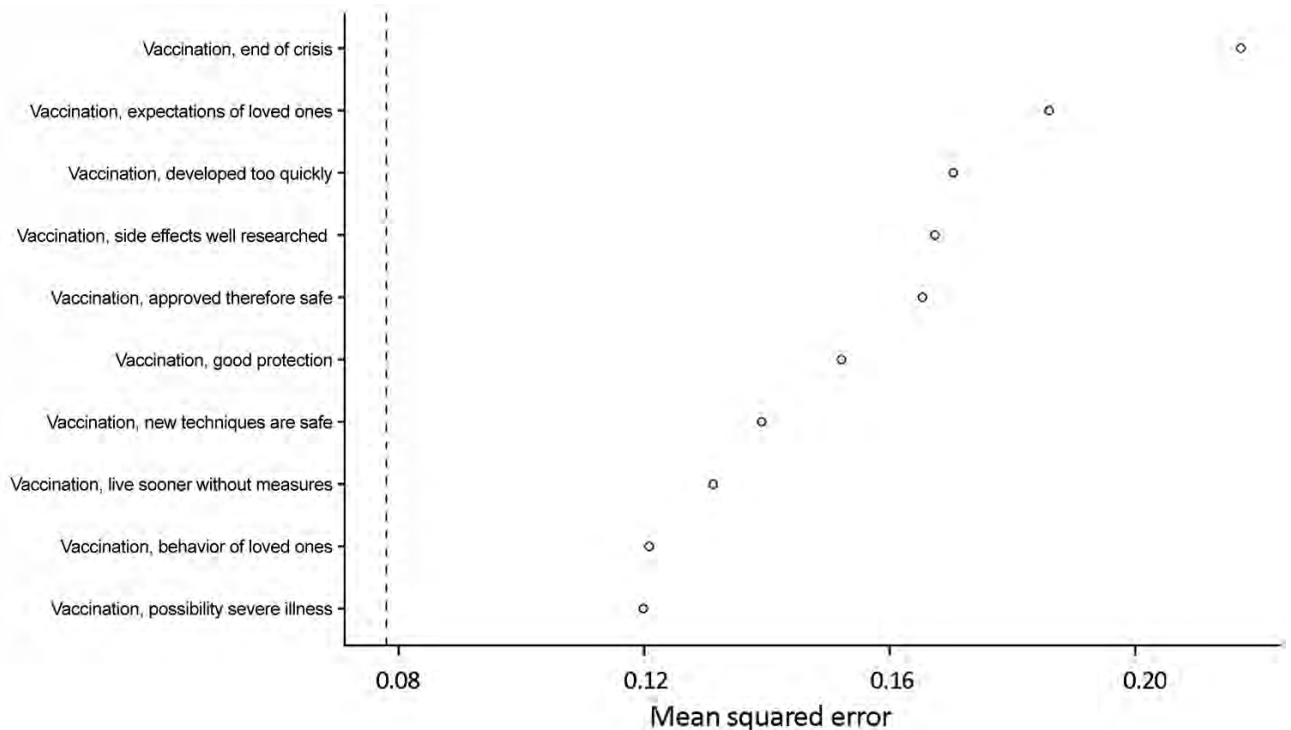


**Figure 2.** COVID-19 vaccination intent and belief that COVID-19 vaccination will end the pandemic among persons in the Netherlands. Variable ranking random forest model shows the 10 strongest determinants. n = 3,614, explained variance 0.76, mean squared error 0.078 (dashed vertical line).

representation. Presumably, there is an overlap between those persons who are difficult to reach for vaccination with those persons who are difficult to reach for research purposes. Second, our study was cross-sectional and conducted in a period that had rapid developments in information about COVID-19 vaccinations. For example, just before the start of our data collection, Denmark announced suspending use of vaccine from AstraZeneca (<https://www.astrazeneca.com>) after reports of possible severe adverse events; during the second half of our data collection, the Netherlands also temporarily suspended these vaccinations (38). Such developments might have affected the outcomes of our study (e.g., through a potential decrease in people's trust in vaccine safety). Also, subsequent events might lead to slightly different results if the study was repeated. It would be highly valuable to repeat research like ours throughout prolonged crises and in multiple settings to monitor changes and differences. Third, our study focused on beliefs about COVID-19 and COVID-19 vaccinations to provide concrete input for communication. Our study did not address other possible major determinants of vaccination intentions, such as trust in institutions or health literacy. Fourth, we did not include beliefs about conspiracy theories in this study, which in hindsight could have added interesting insights. Such beliefs were not included because these were not pronounced in the literature nor in the qualitative data at the time we developed our survey.

Results of this study provide several essential key points for future research, policy, and communication. First, COVID-19 vaccination decisions are not made purely by considering the pros and cons for one's own health. Other (social) benefits of COVID-19 vaccination, related to the relaxation of COVID-19 control measures, are likely to play a major role in vaccination decisions of persons. Providing clear perspectives with regard to these benefits might increase vaccination uptake. At the same time, it is highly essential to address the uncertainties with regard to those social benefits and to prevent future disappointments and decreases in trust and support. Second, social norms regarding peers have been shown to be an essential factor in COVID-19 vaccination intentions, which suggests the potential for norms to induce interventions to increase vaccination uptake. Future research should focus on the characterization and identification of like-minded social networks who are hesitant to vaccinate against COVID-19 to provide well-tailored interventions. Finally, it is highly essential to provide transparent and accessible information about vaccine development and approval process and

the probability of potential adverse events caused by vaccination to address concerns about safety of COVID-19 vaccines.

### Acknowledgments

We thank Kim van Zoonen, Christiaan Oostdijk, Renske Eilers, Anne-Romy Peelen, Floor Kroese, Koen van der Swaluw, Nora Hamdiui, Rob Ruiters, Vincent Buskens, Pepijn van Empelen, Danielle Timmermans, Mirjam Fransen, Ellen Uiters, and Marion Bouwer for contributing to survey development and colleagues from the panel organization I&O Research, specifically Jolijn Polet and Annemarijn Smit, for contributing to data collection.

This study was supported by the National Institute for Public Health and the Environment in the Netherlands and the European Union Horizon2020 project HERoS.

### About the Author

Dr. de Vries is a senior research scientist at the National Institute for Public Health and the Environment, Bilthoven, the Netherlands. Her primary research interests are social dynamics during disease outbreaks, risk and crisis communication, and vaccination behavior.

### References

1. World Health Organization. Ten threats to global health in 2019 [cited 2022 Jun 15]. <https://www.who.int/news-room/spotlight/ten-threats-to-global-health-in-2019>
2. Dubé É, Ward JK, Verger P, MacDonald NE. Vaccine hesitancy, acceptance, and anti-vaccination: trends and future prospects for public health. *Annu Rev Public Health*. 2021;42:175–91. <https://doi.org/10.1146/annurev-publhealth-090419-102240>
3. Gidengil C, Chen C, Parker AM, Nowak S, Matthews L. Beliefs around childhood vaccines in the United States: a systematic review. *Vaccine*. 2019;37:6793–802. <https://doi.org/10.1016/j.vaccine.2019.08.068>
4. Downs JS, de Bruin WB, Fischhoff B. Parents' vaccination comprehension and decisions. *Vaccine*. 2008;26:1595–607. <https://doi.org/10.1016/j.vaccine.2008.01.011>
5. Karafillakis E, Larson HJ; ADVANCE consortium. The benefit of the doubt or doubts over benefits? A systematic literature review of perceived risks of vaccines in European populations. *Vaccine*. 2017;35:4840–50. <https://doi.org/10.1016/j.vaccine.2017.07.061>
6. Schmid P, Rauber D, Betsch C, Lidolt G, Denker ML. Barriers of influenza vaccination intention and behavior – a systematic review of influenza vaccine hesitancy, 2005–2016. *PLoS One*. 2017;12:e0170550. <https://doi.org/10.1371/journal.pone.0170550>
7. Prematunge C, Corace K, McCarthy A, Nair RC, Pugsley R, Garber G. Factors influencing pandemic influenza vaccination of healthcare workers: a systematic review. *Vaccine*. 2012;30:4733–43. <https://doi.org/10.1016/j.vaccine.2012.05.018>
8. Latkin CA, Dayton L, Yi G, Konstantopoulos A, Boodram B. Trust in a COVID-19 vaccine in the US: a social-ecological perspective. *Soc Sci Med*. 1982;2021:113684.

9. Wong MC, Wong EL, Huang J, Cheung AW, Law K, Chong MK, et al. Acceptance of the COVID-19 vaccine based on the health belief model: a population-based survey in Hong Kong. *Vaccine*. 2021;39:1148–56. <https://doi.org/10.1016/j.vaccine.2020.12.083>
10. Thaker J. The persistence of vaccine hesitancy: COVID-19 vaccination intention in New Zealand. *J Health Commun*. 2021;26:104–11. <https://doi.org/10.1080/10810730.2021.1899346>
11. Salmon DA, Dudley MZ, Brewer J, Kan L, Gerber JE, Budigan H, et al. COVID-19 vaccination attitudes, values and intentions among United States adults prior to emergency use authorization. *Vaccine*. 2021;39:2698–711. <https://doi.org/10.1016/j.vaccine.2021.03.034>
12. Karlsson LC, Soveri A, Lewandowsky S, Karlsson L, Karlsson H, Nolvi S, et al. Fearing the disease or the vaccine: the case of COVID-19. *Pers Individ Dif*. 2021;172:110590. <https://doi.org/10.1016/j.paid.2020.110590>
13. Zampetakis LA, Melas C. The health belief model predicts vaccination intentions against COVID-19: a survey experiment approach. *Appl Psychol Health Well-Being*. 2021;13:469–84. <https://doi.org/10.1111/aphw.12262>
14. Morgan MG. Risk communication: a mental models approach. New York: Cambridge University Press; 2002.
15. Lazarus JV, Ratzan SC, Palayew A, Gostin LO, Larson HJ, Rabin K, et al. A global survey of potential acceptance of a COVID-19 vaccine. *Nat Med*. 2021;27:225–8. <https://doi.org/10.1038/s41591-020-1124-9>
16. de Vries M, Claassen L, Te Wierik MJ, Coban F, Wong A, Timmermans DR, et al. Meningococcal W135 disease vaccination intent, the Netherlands, 2018–2019. *Emerg Infect Dis*. 2020;26:1420–9. <https://doi.org/10.3201/eid2607.191812>
17. Government of the Netherlands. Coronavirus dashboard: COVID-19 vaccinations, 2021 [cited 2021 Aug 11]. <https://coronadashboard.rijksoverheid.nl/landelijk/vaccinaties>
18. Betsch C, Böhm R, Chapman GB. Using behavioral insights to increase vaccination policy effectiveness. *Policy Insights Behav Brain Sci*. 2015;2:61–73. <https://doi.org/10.1177/2372732215600716>
19. Larson HJ, Cooper LZ, Eskola J, Katz SL, Ratzan S. Addressing the vaccine confidence gap. *Lancet*. 2011;378:526–35. [https://doi.org/10.1016/S0140-6736\(11\)60678-8](https://doi.org/10.1016/S0140-6736(11)60678-8)
20. National Institute for Public Health and the Environment (RIVM). Corona behavioral unit in-depth interviews, round 9, 2021 [in Dutch] [cited 2021 Aug 11]. <https://www.rivm.nl/documenten/corona-gedragsunit-verdiepende-interviews-ronde-9>
21. National Institute for Public Health and the Environment (RIVM). Participation in COVID-19 vaccination: update June 5, 2021 [in Dutch] [cited 2021 Aug 11]. <https://www.rivm.nl/documenten/deelname-aan-covid-19-vaccinatie-stand-van-zaken>
22. Breiman L. Random forests. *Mach Learn*. 2001;45:5–32. <https://doi.org/10.1023/A:1010933404324>
23. Liaw A, Wiener M. Classification and regression by randomForest. *R News*. 2002;2:18–22.
24. Hamdiui N, Stein ML, Timen A, Timmermans D, Wong A, van den Muijsenbergh ME, et al. Hepatitis B in Moroccan-Dutch: a quantitative study into determinants of screening participation. *BMC Med*. 2018;16:47. <https://doi.org/10.1186/s12916-018-1034-6>
25. Serafini G, Parmigiani B, Amerio A, Aguglia A, Sher L, Amore M. The psychological impact of COVID-19 on the mental health in the general population. *QJM*. 2020;113:531–7. <https://doi.org/10.1093/qjmed/hcaa201>
26. National Institute for Public Health and the Environment (RIVM). Nearly 85% of people aged 18 and over have had at least one vaccination, 2021 [cited: 2021 Aug 11]. <https://www.rivm.nl/en/news/nearly-85-of-people-aged-18-and-over-have-had-at-least-one-vaccination>
27. Seeger MW. Best practices in crisis communication: an expert panel process. *J Appl Commun Res*. 2006;34:232–44. <https://doi.org/10.1080/00909880600769944>
28. Covello VT. Best practices in public health risk and crisis communication. *J Health Commun*. 2003;8(Suppl 1):5–8, discussion 148–51. <https://doi.org/10.1080/713851971>
29. Sanders JG, Spruijt P, van Dijk M, Elberse J, Lambooi MS, Kroese FM, et al. Understanding a national increase in COVID-19 vaccination intention, the Netherlands, November 2020–xMarch 2021. *Euro Surveill*. 2021;26:2100792. <https://doi.org/10.2807/1560-7917.ES.2021.26.36.2100792>
30. Seale H, Heywood AE, McLaws ML, Ward KF, Lowbridge CP, Van D, et al. Why do I need it? I am not at risk! Public perceptions towards the pandemic (H1N1) 2009 vaccine. *BMC Infect Dis*. 2010;10:99. <https://doi.org/10.1186/1471-2334-10-99>
31. Davies P, Chapman S, Leask J. Antivaccination activists on the world wide web. *Arch Dis Child*. 2002;87:22–5. <https://doi.org/10.1136/adc.87.1.22>
32. Betsch C, Renkewitz F, Betsch T, Ulshöfer C. The influence of vaccine-critical websites on perceiving vaccination risks. *J Health Psychol*. 2010;15:446–55. <https://doi.org/10.1177/1359105309353647>
33. Graupensperger S, Abdallah DA, Lee CM. Social norms and vaccine uptake: college students' COVID vaccination intentions, attitudes, and estimated peer norms and comparisons with influenza vaccine. *Vaccine*. 2021;39:2060–7. <https://doi.org/10.1016/j.vaccine.2021.03.018>
34. Bruine de Bruin W, Parker AM, Galesic M, Vardavas R. Reports of social circles' and own vaccination behavior: a national longitudinal survey. *Health Psychol*. 2019;38:975–83. <https://doi.org/10.1037/hea0000771>
35. Quinn SC, Hilyard KM, Jamison AM, An J, Hancock GR, Musa D, et al. The influence of social norms on flu vaccination among African American and White adults. *Health Educ Res*. 2017;32:473–86. <https://doi.org/10.1093/her/cyx070>
36. de Visser R, Waites L, Parikh C, Lawrie A. The importance of social norms for uptake of catch-up human papillomavirus vaccination in young women. *Sex Health*. 2011;8:330–7. <https://doi.org/10.1071/SH10155>
37. Stout ME, Christy SM, Winger JG, Vadapampall ST, Mosher CE. Self-efficacy and HPV vaccine attitudes mediate the relationship between social norms and intentions to receive the HPV vaccine among college students. *J Community Health*. 2020;45:1187–95. <https://doi.org/10.1007/s10900-020-00837-5>
38. Government of the Netherlands. As a precaution, temporarily no vaccinations with AstraZeneca, 2021 [in Dutch] [cited 2021 Dec 12]. <https://www.rijksoverheid.nl/actueel/nieuws/2021/03/14/uit-voorzorg-tijdelijk-geen-vaccinaties-met-astrazeneca>

---

Address for correspondence: Marion de Vries, National Institute of Public Health and the Environment, Centre for Infectious Disease Control, Antonie van Leeuwenhoeklaan 9, Bilthoven, Utrecht 3721 MA, the Netherlands; email: marion.de.vries@rivm.nl

# Association of Environmental Factors with Seasonal Intensity of *Erysipelothrix rhusiopathiae* Seropositivity among Arctic Caribou

O. Alejandro Aleuy, Michele Anholt, Karin Orsel, Fabien Mavrot, Catherine A. Gagnon, Kimberlee Beckmen, Steeve D. Côté, Christine Cuyler, Andrew Dobson, Brett Elkin, Lisa-Marie Leclerc, Joëlle Taillon, Susan Kutz

Several caribou (*Rangifer tarandus*) populations have been declining concurrently with increases in infectious diseases in the Arctic. *Erysipelothrix rhusiopathiae*, a zoonotic bacterium, was first described in 2015 as a notable cause of illness and death among several Arctic wildlife species. We investigated epidemiologic and environmental factors associated with the seroprevalence of *E. rhusiopathiae* in the Arctic and found that seropositivity was highest during warmer months, peaking in September, and was highest among adult males. Summer seroprevalence increases tracked with the oestrid index from the previous year, icing and snowing events, and precipitation from the same year but decreased with growing degree days in the same year. Seroprevalence of *E. rhusiopathiae* varied more during the later years of the study. Our findings provide key insights into the influence of environmental factors on disease prevalence that can be instrumental for anticipating and mitigating diseases associated with climate change among Arctic wildlife and human populations.

Author affiliations: University of Notre Dame, Notre Dame, Indiana, USA (O.A. Aleuy); University of Calgary, Calgary, Alberta, Canada (O.A. Aleuy, K. Orsel, F. Mavrot, S. Kutz); One Health at UCalgary, Calgary (M. Anholt); Canada Research Chair on Northern Biodiversity, Université du Québec à Rimouski Centre of Northern Studies and Quebec Center for Biodiversity Science, Rimouski, Quebec, Canada (C.A. Gagnon); Alaska Department of Fish and Game, Fairbanks, Alaska, USA (K. Beckmen); Laval University, Quebec City, Quebec, Canada (S.D. Côté); Greenland Institute of Natural Resources, Nuuk, Greenland (C. Cuyler); Princeton University, Princeton, New Jersey, USA (A. Dobson); Government of the Northwest Territories, Yellowknife, Northwest Territories, Canada (B. Elkin); Government of Nunavut, Kugluktuk, Nunavut, Canada (L.-M. Leclerc); Government of Quebec, Quebec City (J. Taillon)

DOI: <https://doi.org/10.3201/eid2808.212144>

A 2021 report of the Intergovernmental Panel on Climate Change (1) reinforced that anthropogenic influences on climate systems are causing increases in temperature and extremes of weather and climate events at rates unprecedented in at least the last 2,000 years. In the Arctic, climate warming will continue at rates  $\approx 2$  times higher than those in the rest of the world, profoundly affecting biotic and abiotic systems (1,2). For example, development and death rates among pathogens and vectors and host factors such as immune response and aggregation are very sensitive to environmental conditions and extremes in climate (3). As a consequence, as climate change progresses and weather events become less predictable, changes in the dynamics of wildlife disease are likely to increase (e.g., changes in prevalence), directly affecting conservation biology, human health, and food safety and security in Arctic ecosystems.

*Erysipelothrix rhusiopathiae*, a gram-positive zoonotic bacterium, was first detected infecting muskoxen (*Ovibos moschatus*) in the western Canadian Arctic (4). During 2010–2014, a single genotype of this bacterium was associated with unusual and widespread mortality events and population declines among muskoxen in this region (4,5). During the same period, multiple genotypes of *E. rhusiopathiae* were isolated from muskoxen in Alaska, USA, and moose (*Alces americanus*) and woodland caribou (*R. tarandus caribou*) from British Columbia and Alberta, Canada, during periods of unusually high mortality for all 3 species (6,7). Recently, *E. rhusiopathiae* was identified as the cause of a disease syndrome in Pribilof Arctic foxes (*Vulpes lagopus pribilofensis*) in Alaska (8), and concerns have emerged regarding possible public health issues in Arctic communities (9). Clinical disease manifests

similarly in animals and humans, including skin lesions, fever, endocarditis, and septicemia (10). Among domestic animals, illness from *E. rhusiopathiae* occurs under stressful circumstances, and while illness is acute, the bacteria sheds in large amounts through nasal secretions, saliva, and feces; animals with chronic infections are long-term sources of contamination (11). This pattern is particularly relevant because *E. rhusiopathiae* can persist for prolonged periods in the environment, including in soil and water, which are notable sources of indirect transmission (12). In wild systems, *E. rhusiopathiae* has been associated with individual cases, clusters, and large-scale illness events (4,8,13,14).

*Rangifer tarandus* caribou (called reindeer outside North America) are core to the structure and function of Arctic ecosystems and have profound regulatory effects on vegetation growth and diversity, as well as population dynamics among top predators (15). In addition, these animals are fundamental to the culture, economy, and socioeconomic wellbeing of circumpolar indigenous peoples (16). Several *Rangifer* populations have declined, some by 99%, in the past 15 years, with little to no evidence of recovery (17). Some of these declines have coincided with the emergence of pathogens and changes in the distribution, epidemiology, and effects of endemic diseases (18–20). Wildlife managers, indigenous wildlife comanagement organizations, scientists, and public health officials in the Arctic face the substantial challenge of understanding and managing the effects of emerging infectious diseases on caribou health, conservation, and food security. Determining interactions between seasonal and large-scale weather and climatic events and the dynamics of relevant pathogens is a first step towards anticipating, preparing for, and adapting to perturbations in disease ecology linked to climate changes in the Arctic (21).

The effects of *E. rhusiopathiae* on caribou survival and food security and on human health, along with its distribution throughout the Arctic, make it an ideal model for understanding how pathogens will be influenced by changes in environmental conditions in the future. We investigated the epidemiology of *E. rhusiopathiae* in migratory tundra caribou to quantify and report the association of environmental conditions with *E. rhusiopathiae* seropositivity in caribou. Elucidating the epidemiology of *E. rhusiopathiae* and the environmental factors influencing its seropositivity in caribou is instrumental for developing predictive frameworks to anticipate and mitigate disease risks influenced by climate change.

## Methods

### Sample Collection

We obtained frozen serum and blood on filter paper samples collected from 21 migratory tundra caribou herds during 1980–2019. Samples were collected opportunistically during capture-and-collar programs across Canada, Alaska, and Greenland. We collected information for the sampled animals on the herd name, sex, age class (immature [ $<24$  mo of age] or adult [ $\geq 24$  mo of age]), pregnancy status, body condition status (lean, good, or very good) visually assessed at sampling as described elsewhere (22), and collection dates.

### Seroprevalence Analysis and Cutoff Determination

To determine the seroprevalence of *E. rhusiopathiae*, we used a modified ELISA (5). Results were expressed as percentage positivity based on a benchmark positive control; we assumed a bimodal Gaussian distribution of percentage positivity values and determined the optimal cutoffs using maximum-likelihood estimation. We calculated 95% CIs around estimated point values using bootstrapping. We classified any sample with a percentage positivity above the CI as seropositive and below the CI as seronegative. We considered serum and filter paper samples as 2 different sets and determined separate cutoffs (5).

### Herd-Specific Weather Conditions

We obtained weather data from the CircumArctic Rangifer Monitoring and Assessment (CARMA) network's caribou range climate database (<https://carma.caff.is>) (23). This dataset includes 26 variables describing daily environmental conditions in each of the seasonal territorial ranges of 22 caribou (reindeer) herds across North America, Greenland, and Eurasia; these data enabled us to calculate monthly mean residuals specific to the seasonal range used by each herd during the study period (1980–2015). As dates for caribou seasonal ranges, we used September 1–November 30 for fall range, December 1–March 31 for winter range, April 1–May 31 for spring range, June 1–30 for calving range, and July 1–August 31 for summer range. We conducted a literature review to determine weather and climatic events affecting the performance of caribou herds (Appendix 1 Table, <https://wwwnc.cdc.gov/EID/article/28/8/21-2144-App1.pdf>).

### Data Analysis

We used the entire dataset to calculate descriptive seroprevalence and binomial proportion 95% CIs for each caribou herd for sex, age class, and body condition class.

We investigated associations among these variables and seroprevalence using a generalized linear mixed model (GLMM) with binomial distribution using herd and year of sample collection as nested random effects to address the uneven distribution of samples.

The Western Arctic, Central Arctic, and Teshekpuk Lake herds in Alaska and the Alaska–Canada transboundary Porcupine herd provided relatively rich data with samples taken across most months and over several decades; thus, we focused analyses on data from these herds. We investigated monthly distribution of *E. rhusiopathiae* seroprevalence using a GLMM with binomial distribution. We included month, age class, and sex as independent variables in the models. To account for the nonlinearity of seasonal trends, we included different polynomial degrees of the variable month in the model. We fitted models with different combinations of these independent variables and then compared models using the Akaike information criterion (AIC) (24).

We investigated the association between seropositivity of *E. rhusiopathiae* and weather and environmental factors using GLMM with binomial distribution. The dependent variable was seropositivity of *E. rhusiopathiae* in individual caribou during June, July, August, and September, the months with highest seroprevalence. Month of sampling was included as a random effect in the model. We obtained the independent variables from the CARMA database using temporal and spatial scales specific to each herd including effective growing degree days above 5°C (GDD5) (used to estimate growth and development of plants and insects), daily total surface precipitation, and oestrid index (as a proxy for insect harassment) from the calving range and current and previous year's summer ranges. We included those variables in the model as the residuals of their mean values for the period under study. In addition, we pooled variables pertaining to snowing and icing events from the fall, winter, and spring ranges. We performed a sepa-

rate analysis to transform correlated variables into uncorrelated principal components for snowing and icing events (25). We decided the number of principal components to be used as final variables on the basis of a sharp decline in consecutive eigenvalues and eigenvalues >1.0 (26), which identified 2 principal components describing snowing events, PCsnow1 and PCsnow2, and 2 describing icing events, PCice1 and PCice2 (Table 1; Appendix 2 Table 1, <https://wwwnc.cdc.gov/EID/article/28/8/21-2144-App2.pdf>). We compared models that included different combinations of fixed effects, which were not highly correlated ( $r < 0.7$ ), and interactions based on AIC and analysis of variance (ANOVA).

To investigate trends and variability of *E. rhusiopathiae* seroprevalence during the study period, we calculated the monthly residuals of mean seroprevalence; we used data from the 4 herds in Alaska and only from months with >8 samples. After dividing the 30-year study period into 10 groups of 3 years each, we combined 3-year totals for each month to increase monthly sample sizes. We obtained monthly residuals by calculating the absolute monthly seroprevalence over the entire study period and then subtracting it from monthly prevalence in each of these 10 periods. We quantified seroprevalence of *E. rhusiopathiae* as the proportion of seropositive samples within each period.

## Results

We analyzed 3,170 caribou samples, then randomly selected and removed duplicate samples from 125 animals sampled in  $\geq 1$  period, leaving 3,045 test results for the analysis. Three Alaska herds (Western Arctic, Central Arctic, and Teshekpuk Lake) and the transboundary (Alaska–Canada) Porcupine herd provided 68.4% of the samples. Seropositivity was found in 18/19 herds included in the study. In the herd with no positives (Boothia Peninsula, Nunavut, Canada), only 4 samples were analyzed. Overall, 31.4% (95% CI 29.6%–33.1%) of the samples analyzed were seropositive (Figure 1; Appendix 2 Table 2).

**Table 1.** Components used as climate indices to characterize snowing and icing events during the fall, winter, and spring seasonal ranges in the caribou territorial ranges of 4 Western Arctic herds during 1985–2014\*

| Event          | Variable name | Description of component  |
|----------------|---------------|---|
| Snowing events | PCsnow1       | High snow depth and snow density in the fall, winter, and spring seasonal ranges and large proportion of surface area of total geographic range covered by snow in the fall |
|                | PCsnow2       | Low snow melt rate in spring and fall seasonal ranges, high snow depth and large proportion of surface area of total geographic range covered by snow in the spring.        |
| Icing events   | PCice1        | High number of days with freeze/thaw events and rain on snow in fall, winter, and spring seasonal ranges.   |
|                | PCice2        | High number of days with freeze/thaw events and rain during snow events in the fall seasonal range, but low in the winter and spring.                                       |

\*Three herds were in Alaska (Western Arctic, Central Arctic, and Teshekpuk Lake) and 1 Alaska–Canada transboundary (Porcupine). Seasonal ranges: fall, September 1–November 30; winter, December 1–March 31; spring, April 1–May 31; calving, June 1–30; and summer, July 1–August 31. PC, principal component.

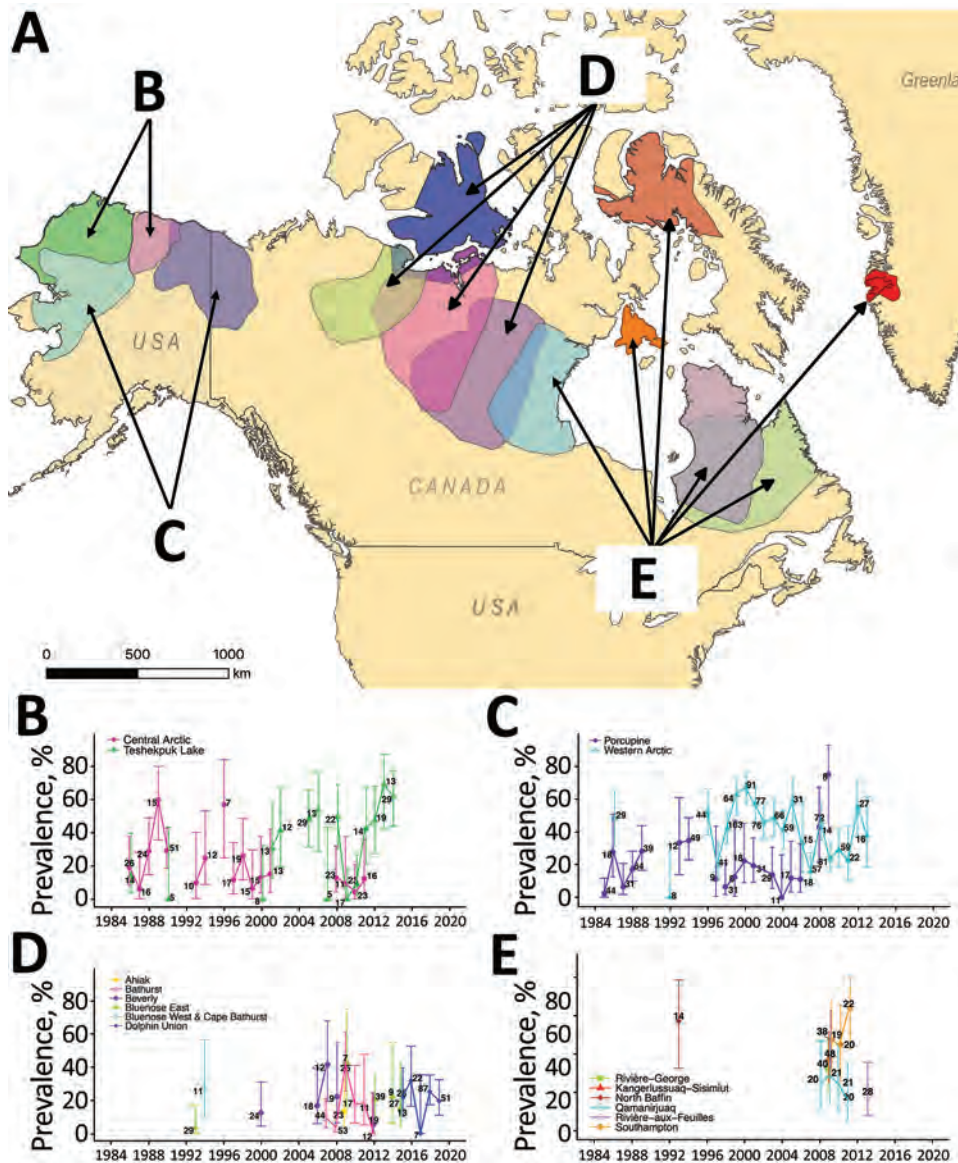


**Figure 1.** Yearly seroprevalence of *Erysipelothrix rhusiopathiae* in caribou herds with territorial ranges in B) Alaska, USA; C) Alaska and Yukon, Canada; D) north central Canada; and E) northeastern Canada, Baffin Island, Canada, and Greenland during 1980–2019. Line colors in graphs B–E correspond to colors of territorial ranges on map of sampled herds. Numbers indicate the sample size for each year; error bars indicate 95% CIs.

**Effects of Individual Traits**

In the best model for investigating the association of age class and sex with *E. rhusiopathiae* seroprevalence, male caribou had a significantly higher seroprevalence than female caribou (odds ratio [OR] 1.4, 95% CI 1.1–1.8). This same model indicated that, for the age class variable, adult caribou had higher *E. rhusiopathiae* seroprevalence, but the effect was small (OR 0.7, 95% CI 0.5–1.0) (Appendix 2 Table 3). We observed no overall association between caribou body condition class and seroprevalence (n = 249) (Appendix 2 Table 4), although in winter we observed a trend in which seroprevalence in animals in poor body condition was 2 times that of animals in good body condition ( $\chi^2_{(1,70)} = 1.8$ ;

p = 0.2) (Appendix 2 Table 3). Pregnancy was not associated with seroprevalence.

**Seasonal Distribution of Seroprevalence**

In the 4 herds from western North America (Western Arctic, Central Arctic, Teshekpuk Lake, and Porcupine), we observed a clear seasonal pattern of higher seroprevalence during warmer months (June–September). Seasonal seroprevalence varied widely, showing a significant increase from 9.8% (binomial confidence interval [BCI] 6.2%–15.2%) in April to 32.7% (BCI 27.4%–38.5%) in June (GLMM, June vs. April: b = 1.42, SE 0.28, z = 5.1; p<0.01), reaching a peak of 45.9% seroprevalence (BCI 42.1%–49.75%) in September and significantly decreasing to 20.6% (BCI 12.7%–31.6%)

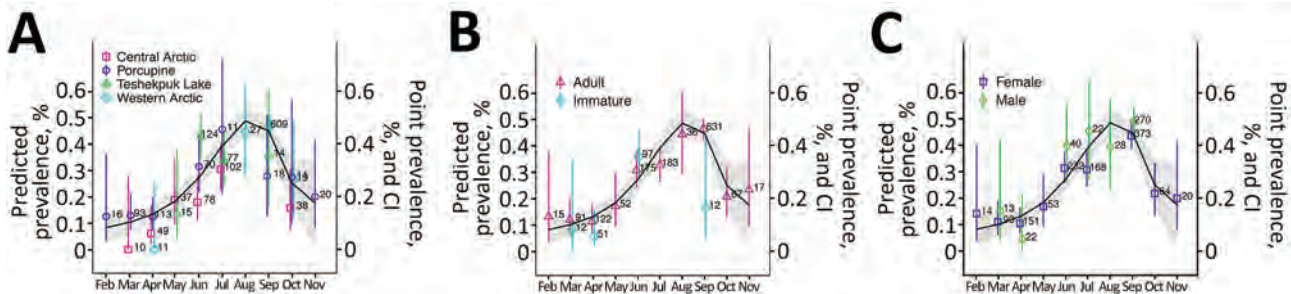


**Figure 2.** Monthly seroprevalence and predicted prevalence of *Erysipelothrix rhusiopathiae* in caribou from western North America during 1980–2019. A) By herd; B) by age; C) by sex. The predicted prevalence was determined using generalized linear models with binomial distribution using month of collection as an independent variable. We included only months with >8 samples. Error bars indicate 95% CIs.

in October (GLMM, October vs. September:  $b = -1.14$ , SE 0.24,  $z = -4.6$ ;  $p < 0.01$ ) (Figure 2, panel A; Appendix 2 Table 5). The odds for *E. rhusiopathiae* seropositivity in September were >6 times higher than in February (OR 6.5, 95% CI 1.8–40.9), March (OR 6.3, 95% CI 3.7–11.2), or April (OR 6.7, 95% CI 4.2–11.4). Including sex or age class did not improve model fit (Figure 2, panels B, C; Appendix 2 Table 6).

### Climatic and Environmental Factors Influencing Seropositivity

Seropositivity of *E. rhusiopathiae* was associated with weather and environmental conditions during different seasonal ranges (Table 2; Figure 3). Including month of sample collection as a random effect significantly improved model fit ( $\Delta$ AIC 11.3, ANOVA;  $p < 0.001$ ) (Appendix 2 Table 7). An increase in GDD5 during calving season was negatively associated with seropositivity of *E. rhusiopathiae* (OR 0.9, 95% CI 0.8–1.0). Icing events occurring during the entire length of the cold season (i.e., in fall, winter, and spring), significantly increased the chances of seropositivity for *E. rhusiopathiae* the following summer (PCice1 OR 1.13, 95% CI 1.0–1.3). More important, icing events occurring only during the fall range were enough to cause a similar increase in seropositivity the following

summer (PCice2 OR 1.3, 95% CI 1.1–1.5). Summer conditions, including the surface precipitation from the same year and oestrid harassment from the previous summer, increased seropositivity of *E. rhusiopathiae* (surface precipitation OR 1.2, 95% CI 1.1–1.4; oestrid index OR 1.3, 95% CI 1.2–1.5) (Table 2; Figure 3).

### Long-Term Trends in Seroprevalence

The variability of *E. rhusiopathiae* seroprevalence residuals in western North America trended upward during 1985–2014. In the first part of this period, the residuals were mostly negative with positive values that were close to 0. Conversely, during the second half of the period, the range between positive and negative residuals gradually increased, leading to more variability in seroprevalence. The 4 highest residuals occurred during the second half of the study period (Figure 4).

### Discussion

Drawing on a large repository of samples, we demonstrated that *E. rhusiopathiae* is widely distributed among North American tundra caribou herds with seroprevalence varying over space and time. We detected a seasonal pattern of higher seroprevalence during summer months; the amplitude of this seasonal pattern was associated with various environmental variables that are known stressors for caribou. Finally, the variability in seroprevalence of *E. rhusiopathiae* appeared to increase during the later years of the study period. Although the data we used for analyses originated from a complex array of sampling protocols, resulting in an unbalanced dataset, the sheer volume of samples across space and time enabled insights into factors that might influence seropositivity. Our study provides key insights into the influence of environmental factors on seroprevalence, which is instrumental for anticipating and mitigating

**Table 2.** Estimates of final model to investigate association between seroprevalence of *Erysipelothrix rhusiopathiae* in caribou and herd-specific environmental conditions\*

| Environmental condition       | Estimate (SE) | p value      |
|-------------------------------|---------------|--------------|
| Summer surface precipitation  | 0.19 (0.061)  | 0.002        |
| Previous summer oestrid index | 0.27 (0.058)  | <0.001       |
| Calving GDD5                  | -0.15 (0.068) | 0.027        |
| PCsnow2†                      | 0.18 (0.066)  | <b>0.006</b> |
| PCice1†                       | 0.12 (0.059)  | <b>0.034</b> |
| PCice2†                       | 0.25 (0.066)  | <0.001       |

\*All results were significant ( $p < 0.05$ ). GDD5, effective growing degree days above 5°C (used to estimate growth and development of plants and insects); PC, principal component.

†Described in Table 1.



and other disease issues, might be the trigger for the increased circulation of *E. rhusiopathiae* in the summer.

The amplitude of the seasonal increase in seropositivity of *E. rhusiopathiae* in a given year was influenced by weather and environmental factors in the previous year that are known to cause substantial distress in caribou: oestrid harassment and icing and snowing events (Figure 3; Appendix Table 1). Insect harassment, particularly from oestrid flies, warbles (*Hypoderma tarandi*) and nose bots (*Cephenemyia trompe*), because of the increased time spent avoiding insect harassment negatively affects food intake among caribou (30–33). During the summer, warble flies lay eggs on the hair of caribou, which then hatch into larvae that penetrate the skin. Larvae migrate to the subcutaneous region on the animal's back where they remain as third instars until the following summer when they depart their host through breathing holes in the caribou's skin, then pupate in the environment (34). The migration and growth of larvae in the caribou are energetically costly. At the same time, the parasitic larvae release enzymes, serine proteases, that down-regulate host immune function, negatively influencing immune response to other pathogens (35), such as *E. rhusiopathiae*. Finally, the lesions in the skin left by emergent larvae may provide *Erysipelothrix* entry points, mostly because of flying insects that can act as fomites (36). Similarly, icing and snowing events can also negatively affect caribou performance, including body condition and pregnancy rates, and cause mass die-offs and declines in herd populations (37–41). Conversely, conditions supporting good vegetation growth, which we estimated using GDD5 as a proxy, decreased the likelihood of elevated *E. rhusiopathiae* seropositivity in the same year potentially by positively influencing intrinsic caribou health factors, such as body mass and thus, likely pathogen resistance (40,42).

Different theoretical and disease-specific approaches have demonstrated that climate variability and extreme weather events likely affect disease dynamics in hard-to-predict ways (43). Our study results indicating an increasing trend in the variability of *E. rhusiopathiae* seroprevalence are consistent with this dynamic and might result from the increasing variability of the Arctic climate during the study period. Environmental drivers can alter disease transmission and manifestations through direct influences on the development, persistence and mortality of pathogens, as well as by influencing the physiologic and behavioral responses of both hosts and vectors. An increase in seroprevalence in the Arctic might suggest a negative impact on caribou populations as this bacterium has been implicated in

several caribou deaths in western Canada and on Arctic islands (6,7). Further understanding how weather and climate variability interacts with hosts, pathogens, and vectors to influence the epidemiology and ecology of *E. rhusiopathiae* would offer essential insights into how this host-pathogen relationship works, when measures to mitigate infections should be applied, and how disease risk for humans and wildlife will respond to anthropogenic climate change.

Determining how *E. rhusiopathiae* is maintained at high latitudes between summer peak seasons, fall, winter, and spring, is critical to understanding the seasonal dynamics of *E. rhusiopathiae*; animal reservoirs play roles in other wild systems (10). Close to a hundred species of birds and mammals are susceptible to *E. rhusiopathiae*, including a variety of high-latitude species (5,6,8). Wild rodents are a well-known host for the bacterium (10). Because *E. rhusiopathiae* can survive in the environment for long periods (10), reservoir species such as rodents that overwinter in the subnivean environment, where temperatures are milder, more stable, and perhaps more conducive for pathogen survival, might play an important role in its persistence in the extreme Arctic environment. Lemmings (e.g., *Dicrostonyx* spp., *Lemmus trimucronatus*) and voles (e.g., *Clethrionomys rutilus*, *Microtus oeconomus*) in the Arctic, display strong subnivean activity with seasonal increases in population density during winter months and profound interannual variation in population size (44). Another hypothesis to explain the overwinter persistence of pathogens involves migratory wild water birds, which are notable carriers of poultry pathogens like Newcastle and avian influenza viruses (45,46), meaning *E. rhusiopathiae* is not the lone exception (47).

We have documented the seasonality, ecology, and historical trends of *E. rhusiopathiae*, an emerging pathogen in the Arctic. Our work highlights the role of environmental factors on the seroprevalence of this zoonotic pathogen, which is infecting a key Arctic ungulate in one of the regions most affected by anthropogenic climate change. Changes in the dynamics of pathogens from the Arctic have already been documented and are expected to increasingly affect human health, food security, and wildlife conservation (48–50). Environmental conditions can affect the physiology and behaviors of caribou and have both proximate and remote consequential influences on the transmission of infectious disease pathogens such as *E. rhusiopathiae*. This information is instrumental for developing predictive frameworks to anticipate and mitigate climate change-related disease risks. For example, intensifying passive and active caribou surveillance efforts, and strengthening public health campaigns to educate persons who

might be exposed (e.g., from hunted animals) on safe practices to avoid *Erysipelothrix* infections, especially in years preceded by summer seasons with a high oestrid index. Enacting efforts to mitigate the effects of emerging climate change-related disease threats offer direct benefits for developing adaptations to public health, food security, and conservation efforts.

### Acknowledgments

The authors are grateful to the many biologists and technicians who collected, processed, and archived the serum samples and data used in this study, especially Alaska herd researchers Jim Dau, Lincoln Parrett, Elizabeth Lenart, Geoff Carroll, and Randy Zarnke, Angie Schneider, and James Wang from the University of Calgary for their technical support in the laboratory.

Research was performed in collaboration with CircumArctic Rangifer Monitoring and Assessment (CARMA) and supported through funding from Morris Animal Foundation, Natural Sciences and Engineering Research Council of Canada Discovery, and International Polar Year grants (S.K.), University of Calgary Eyes High PhD scholarship, Caribou Ungava, and the territorial and state government employers of coauthors. We would like to thank the territorial and state governments as well as communities, hunters, trappers and, hunter and trapper committees that collaborated with samples collection.

### References

1. Intergovernmental Panel on Climate Change. Climate change 2021: the physical science basis. Contribution of working group I to the sixth assessment report of the intergovernmental panel on climate change. Masson-Delmotte V Zhai, Pirani A, Connors SL, Péan C, Berger S, Caud N, et al., editors. Cambridge: Cambridge University Press; 2021 [cited 2021 Sep 10]. <https://www.ipcc.ch/report/ar6/wg1>
2. Intergovernmental Panel on Climate Change. Climate change 2014: synthesis report. Contribution of working groups I, II and III to the fifth assessment report of the intergovernmental panel on climate change. Pachauri RK, Meyer L, editors. Geneva: The Panel; 2014 [cited 2021 Mar 25]. <https://www.ipcc.ch/report/ar5/syr>
3. Aleuy OA, Kutz S. Adaptations, life-history traits and ecological mechanisms of parasites to survive extremes and environmental unpredictability in the face of climate change. *Int J Parasitol Parasites Wildl.* 2020;12:308–17. <https://doi.org/10.1016/j.ijppaw.2020.07.006>
4. Kutz S, Bollinger T, Branigan M, Checkley S, Davison T, Dumond M, et al. *Erysipelothrix rhusiopathiae* associated with recent widespread muskox mortalities in the Canadian Arctic. *Can Vet J.* 2015;56:560–3.
5. Mavrot F, Orsel K, Hutchins W, Adams LG, Beckmen K, Blake JE, et al. Novel insights into serodiagnosis and epidemiology of *Erysipelothrix rhusiopathiae*, a newly recognized pathogen in muskoxen (*Ovibos moschatus*). *PLoS One.* 2020;15:e0231724. <https://doi.org/10.1371/journal.pone.0231724>
6. Bondo KJ, Macbeth B, Schwantje H, Orsel K, Culling D, Culling B, et al. Health survey of boreal caribou (*Rangifer tarandus caribou*) in northeastern British Columbia, Canada. *J Wildl Dis.* 2019;55:544–62. <https://doi.org/10.7589/2018-01-018>
7. Forde TL, Orsel K, Zadoks RN, Biek R, Adams LG, Checkley SL, et al. Bacterial genomics reveal the complex epidemiology of an emerging pathogen in Arctic and boreal ungulates. *Front Microbiol.* 2016;7:1759. <https://doi.org/10.3389/fmicb.2016.01759>
8. Spraker TR, White PA. Shaggy lame fox syndrome in Pribilof Island Arctic foxes (*Alopex lagopus pribilofensis*), Alaska. *Vet Pathol.* 2017;54:258–68. <https://doi.org/10.1177/0300985816660745>
9. Groeschel M, Forde T, Turvey S, Joffe AM, Hui C, Naidu P, et al. An unusual case of *Erysipelothrix rhusiopathiae* prosthetic joint infection from the Canadian Arctic: whole genome sequencing unable to identify a zoonotic source. *BMC Infect Dis.* 2019;19:282. <https://doi.org/10.1186/s12879-019-3913-7>
10. Wang Q, Chang BJ, Riley TV. *Erysipelothrix rhusiopathiae*. *Vet Microbiol.* 2010;140:405–17. <https://doi.org/10.1016/j.vetmic.2009.08.012>
11. Wang Q, Riley TV. *Erysipelothrix rhusiopathiae*. In: Tang Y-W, Sussman M, Liu D, Poxton I, Schwartzman J, editors. *Molecular medical microbiology*. Vol. 2. Cambridge, MA, USA: Academic Press; 2015.
12. Opriessnig T, Shen HG, Bender JS, Boehm JR, Halbur PG. *Erysipelothrix rhusiopathiae* isolates recovered from fish, a harbour seal (*Phoca vitulina*) and the marine environment are capable of inducing characteristic cutaneous lesions in pigs. *J Comp Pathol.* 2013;148:365–72. <https://doi.org/10.1016/j.jcpa.2012.08.004>
13. Campbell GD, Addison EM, Barker IK, Rosendal S. *Erysipelothrix rhusiopathiae*, serotype 17, septicemia in moose (*Alces alces*) from Algonquin Park, Ontario. *J Wildl Dis.* 1994;30:436–8. <https://doi.org/10.7589/0090-3558-30.3.436>
14. Fiorito CD, Bentancor A, Lombardo D, Bertellotti M. *Erysipelothrix rhusiopathiae* isolated from gull-inflicted wounds in southern right whale calves. *Dis Aquat Organ.* 2016;121:67–73. <https://doi.org/10.3354/dao03041>
15. Festa-Bianchet M, Ray JC, Boutin S, Côté SD, Gunn A. Conservation of caribou (*Rangifer tarandus*) in Canada: an uncertain future. *Can J Zool.* 2011;89:419–34. <https://doi.org/10.1139/z11-025>
16. Kenny T-A, Fillion M, Simpkin S, Wesche SD, Chan HM. Caribou (*Rangifer tarandus*) and Inuit nutrition security in Canada. *EcoHealth.* 2018;15:590–607. <https://doi.org/10.1007/s10393-018-1348-z>
17. Fauchald P, Park T, Tømmervik H, Myneni R, Hausner VH. Arctic greening from warming promotes declines in caribou populations. *Sci Adv.* 2017;3:e1601365. <https://doi.org/10.1126/sciadv.1601365>
18. Taillon J, Brodeur V, Rivard S. Biological status report of migratory caribou, Leaf River herd. Gouvernement du Québec, Ministère des forêts, de la faune et des parcs. 2016 [cited 2021 Feb 20]. <https://mffp.gouv.qc.ca/documents/wildlife/biological-status-caribou-leaf-river.pdf>
19. Ducrocq J, Beauchamp G, Kutz S, Simard M, Taillon J, Côté SD, et al. Variables associated with *Besnoitia tarandi* prevalence and cyst density in barren-ground caribou (*Rangifer tarandus*) populations. *J Wildl Dis.* 2013;49:29–38. <https://doi.org/10.7589/2012-05-125>
20. Kafle P, Peller P, Massolo A, Hoberg E, Leclerc L-M, Tomaselli M, et al. Range expansion of muskox lungworms track rapid Arctic warming: implications for geographic colonization under climate forcing. *Sci Rep.* 2020;10:17323. <https://doi.org/10.1038/s41598-020-74358-5>

21. Hudson PJ, Cattadori IM, Boag B, Dobson AP. Climate disruption and parasite-host dynamics: patterns and processes associated with warming and the frequency of extreme climatic events. *J Helminthol*. 2006;80:175–82. <https://doi.org/10.1079/JOH2006357>
22. Gunn A, Nixon W. Rangifer health body condition manual. CircumArctic Rangifer Monitoring and Assessment Network (CARMA); 2008 [cited 2021 Feb 20]. [https://www.caff.is/images/\\_Organized/CARMA/Resources/Field\\_Protocols/RangiferHealthBodyConditionManualforweb42d.pdf](https://www.caff.is/images/_Organized/CARMA/Resources/Field_Protocols/RangiferHealthBodyConditionManualforweb42d.pdf)
23. Russell DE, Whitfield PH, Cai J, Gunn A, White RG, Poole K. CARMA's MERRA-based caribou range climate database. *Rangifer*. 2013;33:145–51.
24. Burnham KP, Anderson DR, Huyvaert KP. AIC model selection and multimodel inference in behavioral ecology: some background, observations, and comparisons. *Behav Ecol Sociobiol*. 2011;65:23–35 [Erratum in *Behav Ecol Sociobiol*. 2011;65:415]. <https://doi.org/10.1007/s00265-010-1029-6>
25. Graham MH. Confronting multicollinearity in ecological multiple regression. *Ecology*. 2003;84:2809–15. <https://doi.org/10.1890/02-3114>
26. Jolliffe IT, Cadima J. Principal component analysis: a review and recent developments. *Philos Trans A Math Phys Eng Sci*. 2016;374:20150202. <https://doi.org/10.1098/rsta.2015.0202>
27. Giménez-Lirola LG, Xiao CT, Halbur PG, Opriessnig T. Development of a novel fluorescent microbead-based immunoassay and comparison with three enzyme-linked immunoassays for detection of anti-*Erysipelothrix* spp. IgG antibodies in pigs with known and unknown exposure. *J Microbiol Methods*. 2012;91:73–9. <https://doi.org/10.1016/j.mimet.2012.07.014>
28. Gurarie E, Hebblewhite M, Joly K, Kelly AP, Adamczewski J, Davidson SC, et al. Tactical departures and strategic arrivals: divergent effects of climate and weather on caribou spring migrations. *Ecosphere*. 2019;10:e02971. <https://doi.org/10.1002/ecs2.2971>
29. Hing S, Narayan EJ, Andrew Thompson RC, Godfrey SS. The relationship between physiological stress and wildlife disease: consequences for health and conservation. *Wildl Res*. 2016;43:51–60. <https://doi.org/10.1071/WR15183>
30. Mörschel FM, Klein DR. Effects of weather and parasitic insects on behavior and group dynamics of caribou of the Delta Herd, Alaska. *Can J Zool*. 1997;75:1659–70. <https://doi.org/10.1139/z97-793>
31. Witter LA, Johnson CJ, Croft B, Gunn A, Gillingham MP. Behavioural trade-offs in response to external stimuli: time allocation of an Arctic ungulate during varying intensities of harassment by parasitic flies. *J Anim Ecol*. 2012;81:284–95. <https://doi.org/10.1111/j.1365-2656.2011.01905.x>
32. Thomas DD, Kiliaan HPL. Warble infestations in some Canadian caribou and their significance. *Rangifer*. 1990;10:409–17. <https://doi.org/10.7557/2.10.3.889>
33. Cuyler C, White RR, Lewis K, Soulliere C, Gunn A, Russell DE, et al. Are warbles and bots related to reproductive status in West Greenland caribou? *Rangifer*. 2012;32:243–57. <https://doi.org/10.7557/2.32.2.2273>
34. Smythe RH. *Veterinary parasitology*. Indianapolis, Indiana, USA: Alpha Editions; 2019.
35. Otranto D. The immunology of myiasis: parasite survival and host defense strategies. *Trends Parasitol*. 2001;17:176–82. [https://doi.org/10.1016/S1471-4922\(00\)01943-7](https://doi.org/10.1016/S1471-4922(00)01943-7)
36. Timofeeva AA, Shcherbina RD, Evseeva TI, Olsuf'ev NG, Meshcheriakova IS. Erysipeloid on the islands of the Sea of Okhotsk. I. The sources and vectors of the causative agent of erysipeloid [in Russian]. *Zh Mikrobiol Epidemiol Immunobiol*. 1975;0:119–26.
37. Le Corre M, Dussault C, Côté SD. Weather conditions and variation in timing of spring and fall migrations of migratory caribou. *J Mammal*. 2016;98:260–71. <https://doi.org/10.1093/jmammal/gyw177>
38. Joly K, Klein DR, Verbyla DL, Rupp TS, Chapin FS III. Linkages between large-scale climate patterns and the dynamics of Arctic caribou populations. *Ecography*. 2011;34:345–52. <https://doi.org/10.1111/j.1600-0587.2010.06377.x>
39. Ferguson SH, Mahoney SP. The relationship between weather and caribou productivity for the La-Poile caribou herd, Newfoundland. *Rangifer*. 1991;11:151–6. <https://doi.org/10.7557/2.11.4.1005>
40. Gagnon CA, Hamel S, Russell DE, Powell T, Andre J, Svoboda MY, et al. Merging indigenous and scientific knowledge links climate with the growth of a large migratory caribou population. *J Appl Ecol*. 2020;57:1644–55. <https://doi.org/10.1111/1365-2664.13558>
41. Gunn A, Dragon J. Peary caribou and muskox abundance and distribution on the western Queen Elizabeth Islands, Northwest Territories and Nunavut, June–July 1997. Yellowknife, Northwest Territories, Canada: Department of Resources, Wildlife and Economic Development, Government of the Northwest Territories; 2002.
42. Couturier S, Côté SD, Otto RD, Weladji RB, Huot J. Variation in calf body mass in migratory caribou: the role of habitat, climate and movements. *J Mammal*. 2009;90:442–52. <https://doi.org/10.1644/07-MAMM-A-279.1>
43. Cohen JM, Sauer EL, Santiago O, Spencer S, Rohr JR. Divergent impacts of warming weather on wildlife disease risk across climates. *Science*. 2020;370:eabb1702. <https://doi.org/10.1126/science.abb1702>
44. Fauteux D, Gauthier G, Berteaux D. Seasonal demography of a cyclic lemming population in the Canadian Arctic. *J Anim Ecol*. 2015;84:1412–22. <https://doi.org/10.1111/1365-2656.12385>
45. Pedersen JC, Senne DA, Woolcock PR, Kinde H, King DJ, Wise MG, et al. Phylogenetic relationships among virulent Newcastle disease virus isolates from the 2002–2003 outbreak in California and other recent outbreaks in North America. *J Clin Microbiol*. 2004;42:2329–34. <https://doi.org/10.1128/JCM.42.5.2329-2334.2004>
46. Soares PBM, Demétrio C, Sanfilippo L, Kawanoto AHN, Brentano L, Durigon EL. Standardization of a duplex RT-PCR for the detection of influenza A and Newcastle disease viruses in migratory birds. *J Virol Methods*. 2005;123:125–30. <https://doi.org/10.1016/j.jviromet.2004.09.011>
47. Wolcott MJ. Erysipeloid. In: Thomas BJ, Hunter DB, Atkinson CT, editors. *Infectious diseases of wild birds*. Ames, IA, USA: Blackwell Publishing; 2007. p. 332–40. <https://doi.org/10.1002/9780470344668.ch17>
48. Kutz SJ, Jenkins EJ, Veitch AM, Ducrocq J, Polley L, Elkin B, et al. The Arctic as a model for anticipating, preventing, and mitigating climate change impacts on host-parasite interactions. *Vet Parasitol*. 2009;163:217–28. <https://doi.org/10.1016/j.vetpar.2009.06.008>
49. Van Hemert C, Pearce JM, Handel CM. Wildlife health in a rapidly changing North: focus on avian disease. *Front Ecol Environ*. 2014;12:548–56. <https://doi.org/10.1890/130291>
50. Parkinson AJ, Butler JC. Potential impacts of climate change on infectious diseases in the Arctic. *Int J Circumpolar Health*. 2005;64:478–86. <https://doi.org/10.3402/ijch.v64i5.18029>

---

Address for correspondence: Alejandro Aleuy, Department of Ecosystem and Public Health, University of Calgary, 2500 University Dr NW, Calgary, AB T2N 1N4, Canada; email: oaleuy@ucalgary.ca

# Culling of Urban Norway Rats and Carriage of *Bartonella* spp. Bacteria, Vancouver, British Columbia, Canada

Kaylee A. Byers,<sup>1</sup> Michael J. Lee,<sup>1</sup> Janet E. Hill, Champika Fernando, Laura Speerin, Christina M. Donovan, David M. Patrick, Chelsea G. Himsworth

We investigated the effects of culling on *Bartonella* spp. bacteria carriage among urban rats in Canada. We found that the odds of *Bartonella* spp. carriage increased across city blocks except those in which culling occurred. Removing rats may have prevented an increase in *Bartonella* spp. prevalence, potentially lowering human health risks.

Urban Norway rats (*Rattus norvegicus*) carry *Bartonella* spp., which are bacteria transmitted among rats and to humans through vectors including fleas (1). Infection in humans can result in fever, fatigue, myalgia, and endocarditis (2). In Vancouver, British Columbia, Canada, a serosurvey of residents of an underresourced neighborhood found that 3% of participants had been exposed to *B. tribocorum* (3), a species found in rats in this neighborhood (4), suggesting that rats may be an exposure source for humans in this area.

Although aimed at decreasing disease risks, culling methods (i.e., lethal removal) may increase zoonotic pathogen prevalence by altering normal behaviors that modify pathogen transmission (5,6). We sought to determine whether culling rats altered *Bartonella* spp. prevalence in rats and their fleas in

the Downtown Eastside neighborhood of Vancouver. The University of British Columbia's Animal Care Committee (A14-0265) approved study procedures.

## The Study

We trapped rats in 12 study sites (5 intervention, 7 control), each comprising 3 contiguous city blocks (36 total blocks) (Figure, panel A) during June 2016–January 2017 (Appendix, <https://wwwnc.cdc.gov/EID/article/28/8/21-1164-App1.pdf>). We placed 10 live traps (Tomahawk Live Traps, <https://www.livetraps.com>) in the alley of each block. We conducted the experiment in 3 trapping phases: before, during, and after the intervention (Figure, panel B). Before and after the intervention, we captured rats, gave each a numbered ear tag, and released it to its capture site. In the center block of intervention sites culling occurred during the second trapping phase. In flanking blocks (those adjacent to the intervention block) and control blocks, no culling occurred (Figure, panel A).

We collected blood from all rats via jugular puncture under isoflurane anesthesia. We collected fleas by brushing the coat.

We identified fleas to species (7), and pooled  $\leq 5$  fleas per rat. We extracted DNA from rat blood and fleas using the DNEasy Blood and Tissue Kit (QIAGEN, <https://www.qiagen.com>). We tested DNA extracts for *Bartonella* spp. by real-time PCR. For rat blood, we used primers to detect a 380-bp segment of the citrate synthase gene (*gltA*) (8). For fleas, we used a probe-based real-time PCR assay to detect a 302-bp fragment of the *ssrA* gene (9). We conducted our analysis as described in Himsworth et al. (10).

We used generalized linear mixed models to assess the relationship between the intervention and *Barton-*

Author affiliations: The University of British Columbia School of Population and Public Health, Vancouver, British Columbia, Canada (K.A. Byers, M.J. Lee, C.M. Donovan, D.M. Patrick); The University of British Columbia, Vancouver (K.A. Byers, C.G. Himsworth); Canadian Wildlife Health Cooperative, Abbotsford, British Columbia, Canada (K.A. Byers, M.J. Lee, C.G. Himsworth); University of Saskatchewan, Saskatoon, Saskatchewan, Canada (J.E. Hill, C. Fernando, L. Speerin); British Columbia Centre for Disease Control, Vancouver (D.M. Patrick); British Columbia Ministry of Agriculture, Abbotsford (C.G. Himsworth)

DOI: <https://doi.org/10.3201/eid2808.211164>

<sup>1</sup>These first authors contributed equally to this article.

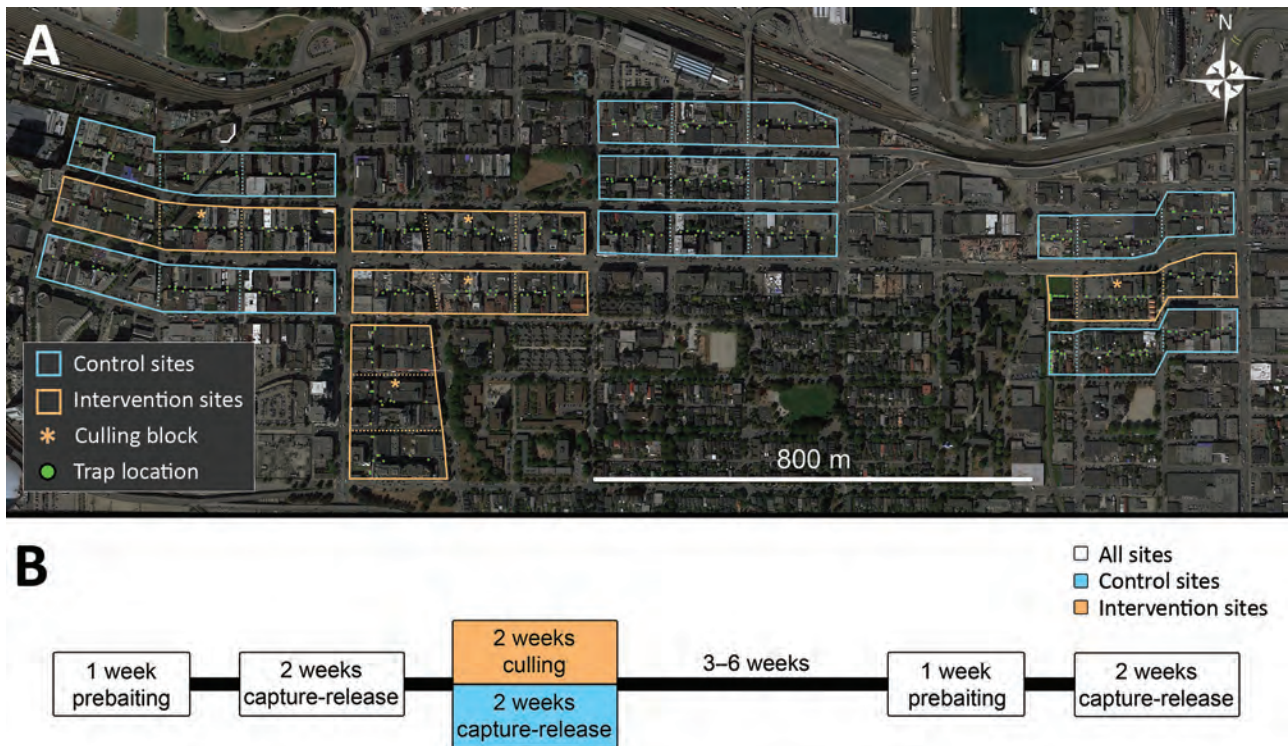


**Figure.** Trapping locations for Norway rats (*Rattus norvegicus*) caught in Vancouver, British Columbia, Canada. A) Trapping sites consisting of 3 contiguous city blocks. Each site was designated as a control or intervention site. Control sites did not involve culling (lethal animal removal); intervention sites included culling in the central block. B) Depiction of the study timeline. We first baited traps without capture to acclimatize rats to traps, then trapped and tagged rats with numbered ear tags and released the rats to their site of capture. After an intervention that involved culling rats in intervention sites, we resampled 3–6 weeks later to determine whether *Bartonella* spp. carriage differed between trapping periods before and after the intervention.

*ella* spp. carriage. We controlled for spatial clustering by city block as a random effect. We assessed positive or negative carriage by rats (model A) and fleas (model B) and the number of fleas per rat (model C). We analyzed carriage models A and B by logistic regression and model C by negative binomial regression. For all models, the intervention variable consisted of 4 categories indicating when rats or fleas were caught: before the intervention in all blocks; after the intervention in control blocks; after the intervention in flanking blocks; and after the intervention in intervention blocks.

We used a hypothesis-testing model building approach to estimate the effect of the intervention while accounting for covariates (Table). We retained covariates if they confounded the relationship between the intervention and the outcome (i.e., if they changed the effect of any level of the intervention by  $\geq 10\%$  or if their association with the outcome and intervention had  $p \leq 0.25$ ). We also kept independent predictors of the outcome if they significantly improved the model, as indicated by a likelihood ratio test result of  $p \leq 0.05$ ; that test compared 2 nested models, each with the intervention variable and all confounders present, but

with and without the potential predictor variable.

We trapped 512 Norway rats; 206 (40.2%) of them had fleas. The median number of fleas per rat was 0 (range 0–58; mean 1.18). All fleas were *Nosopsyllus fasciatus*. We obtained blood from 454 rats; 90 (20%) tested positive for *Bartonella* spp. We tested 201 flea pools; 86 (42.8%) tested positive for *Bartonella* spp. (Table). In the final model A, which contained the variables season, presence of *Bartonella* spp.–positive fleas, and wound presence as covariates, the odds of *Bartonella* spp. carriage were significantly higher among rats caught after the intervention in control blocks (odds ratio [OR] 2.68; 95% CI 1.22–6.67) and flanking blocks (OR 7.26; 95% CI 1.56–38.17), but not in the intervention blocks (OR 2.03; 95% CI 0.22–15.41), when compared with the odds of carriage before the intervention in all block types (Table). We saw no association between the intervention and the number of fleas per rat or *Bartonella* spp. carriage by fleas.

## Conclusions

The prevalence of *Bartonella* spp. bacteria among rats in this neighborhood has been shown to increase in

the fall (4). Our study suggests that culling rats may have prevented this increase within the blocks where culling occurred.

Removing rats may change how individual rats interact within colonies, which alters pathogen transmission. *Bartonella* spp. transmission via fleas (1) requires close contact among individual rats. Rats burrow communally, establishing a network of chambers with some shared nests (11). Those

nests promote close contact among rats and act as a source of fleas that spend time in the nest (12). Decreased rat population density may lessen nest sharing and behaviors such as social grooming, thereby reducing opportunities for fleas to transmit *Bartonella* spp. among individual rats. A reduction in *Bartonella* spp. prevalence may decrease exposure risk for humans, but the relationship between rodents, vectors, pathogens, and humans is

**Table.** Mixed effects logistic regression models of the effect of intervention on *Bartonella* spp. carriage by Norway rats (*Rattus norvegicus*), Vancouver, British Columbia, Canada\*

| Variable  | <i>Bartonella</i> prevalence, no. positive/no. tested (%) | Bivariable models      |                  |              | Final model†         |                  |
|---|---|------------------------|------------------|--------------|----------------------|------------------|
|   |   | Unadjusted OR (95% CI) | p value in model | LRT p value‡ | Adjusted OR (95% CI) | p value in model |
| <b>Intervention</b>                                       |   |                        |                  |              |                      |                  |
| Rats caught before the intervention in all blocks         | 58/267 (22)   | Referent               | Referent         | Referent     | Referent             | Referent         |
| Rats caught after the intervention in control blocks      | 24/109 (22)   | 1.26 (0.67–2.39)       | 0.47             | <0.01        | 2.68 (1.22–6.67)     | 0.02             |
| Rats caught after the intervention in flanking blocks     | 6/37 (16)   | 0.56 (0.18–1.46)       | 0.26             | NA           | 7.26 (1.56–38.17)    | 0.01             |
| Rats caught after the intervention in intervention blocks | 2/41 (5)  | 0.12 (0.02–0.46)       | <0.01            | NA           | 2.03 (0.22–15.41)    | 0.50             |
| <b>Sex</b>  |   |                        |                  |              |                      |                  |
| F   | 38/221 (17)   | Referent               | Referent         | Referent     | NA                   | NA               |
| M   | 52/233 (22)   | 1.32 (0.82–2.14)       | 0.26             | 0.26         | NA                   | NA               |
| <b>Sexual maturity</b>                                    |   |                        |                  |              |                      |                  |
| Juvenile  | 34/177 (19)   | Referent               | Referent         | Referent     | NA                   | NA               |
| Mature  | 56/277 (20)   | 0.98 (0.60–1.63)       | 0.95             | 0.95         | NA                   | NA               |
| <b>Wound presence</b>                                     |   |                        |                  |              |                      |                  |
| Absent  | 59/339 (17)   | Referent               | Referent         | Referent     | Referent             | Referent         |
| Present   | 31/115 (27)   | 1.67 (0.97–2.81)       | 0.06             | 0.06         | 1.49 (0.83–2.63)     | 0.17             |
| <b>Weight§</b>  |   |                        |                  |              |                      |                  |
|   | NA  | 1.04 (0.81–1.32)       | 0.75             | 0.75         | NA                   | NA               |
| <b>Presence of fleas on rats</b>                          |   |                        |                  |              |                      |                  |
| Absent  | 46/261 (18)   | Referent               | Referent         | Referent     | NA                   | NA               |
| Present   | 44/193 (23)   | 1.39 (0.86–2.25)       | 0.18             | 0.18         | NA                   | NA               |
| <b>No. fleas on rat</b>                                   |   |                        |                  |              |                      |                  |
|   | NA  | 1.02 (0.95–1.09)       | 0.50             | 0.52         | NA                   | NA               |
| <b>Flea index#</b>  |   |                        |                  |              |                      |                  |
|   | NA  | 1.13 (0.90–1.43)       | 0.31             | 0.32         | NA                   | NA               |
| <b>Presence of positive fleas per rat</b>                 |   |                        |                  |              |                      |                  |
| Absent  | 67/376 (18)   | Referent               | Referent         | Referent     | Referent             | Referent         |
| Present   | 23/78 (30)  | 1.83 (1.00–3.25)       | 0.04             | 0.05         | 1.94 (1.00–3.69)     | 0.05             |
| <b>Season</b>   |   |                        |                  |              |                      |                  |
| Summer, June–August                                       | 16/124 (13)   | Referent               | Referent         | Referent     | Referent             | Referent         |
| Fall, September–November                                  | 65/208 (31)   | 3.16 (1.59–6.73)       | <0.01            | <0.01        | 2.90 (1.32–6.31)     | <0.01            |
| Winter, December–March                                    | 9/122 (7)   | 0.50 (0.18–1.30)       | 0.15             | NA           | 0.16 (0.03–0.68)     | 0.02             |

\*OR refers to the odds of *Bartonella* spp. carriage among rats in each group relative to the reference group for that variable. Variables were included in the final model if they confounded the relationship between the intervention and the outcome (changed the effect of any level of the intervention by  $\geq 10\%$  and/or were associated with the outcome and intervention;  $p \leq 0.25$ ) or if they were independent predictors that improved the model as indicated by a significant ( $p \leq 0.05$  likelihood ratio test with all confounders and intervention present). LRT, likelihood ratio test; NA, not applicable; OR, odds ratio.

†Final multivariable model: *Bartonella* status ~ intervention + wound presence + presence of positive fleas per rat + season + (city.block).

‡Likelihood ratio test comparing the generalized linear mixed model with and without the indicated variable;  $p \leq 0.05$  indicates that the variable significantly improved the model with all confounders and as such was a significant predictor and was retained in the final model.

§Scaled and centered around its mean.

#Average number of fleas per rat per city block.

complex (13). For example, although a previous study revealed that residents in this neighborhood had been exposed to *Bartonella* spp. (3), it is unclear whether this exposure was associated with rats and to what extent humans encounter fleas. Furthermore, for other fleaborne pathogens such as *Yersinia pestis* (agent of the plague), culling rats may increase disease transmission to humans as fleas seek new hosts (14). Understanding how rat abundance and rat removal impacts intraspecies and interspecies dynamics and pathogen prevalence is necessary to anticipate management impacts on pathogen transmission.

Whereas our intervention involved removing rats and their fleas, we did not observe a change in the number of fleas on rats. The steady number suggests that culling did not reduce flea abundance, perhaps because *N. fasciatus* fleas also reside in the burrows, such that the number of fleas per rat does not reflect the total number of fleas in a city block (12). It is possible that our intervention removed a negligible proportion of the flea population. In addition, we did not observe a change in the odds of *Bartonella* spp. carriage among fleas. A past study in this neighborhood showed that *Bartonella* spp. carriage among rats was not related to flea presence or abundance; therefore, the role of *N. fasciatus* fleas in the ecology of *Bartonella* spp. in this ecosystem remains enigmatic (15).

Our findings counter a study of *Leptospira interrogans* using the same experimental design, in which culling was associated with an increased odds of infection among rats (5). This difference is likely attributable to differences in transmission; *L. interrogans* is spread via urine (13) and *Bartonella* spp. via fleas (1). Culling may alter a variety of social interactions (e.g., fighting, nest-sharing, grooming) which affect the spread of these pathogens differently. Together, these studies illustrate the complexity of managing rat-associated zoonoses; the intervention may have opposite effects on different pathogens. Indeed, past literature has shown that culling wildlife to control zoonoses can have unpredictable consequences (6) and that ecosystem-based approaches that manage the human-wildlife interface may be more effective.

### Acknowledgments

We thank the Vancouver Area Network of Drug Users for their assistance in enacting this study. We also thank Charles Krebs, Bobby Corrigan, and Michael Whitlock for their suggestions regarding the design of this study. Finally, we thank Geoffrey Knaub, Sophia Kontou, and Emilia Mackowiak for their assistance in the field.

This study was funded in part by the Public Scholars Initiative at the University of British Columbia (K.A.B.), a Natural Sciences and Engineering Research Council of Canada Discovery Grant (D.M.P.), and the Public Health Agency of Canada (J.E.H.).

### About the Author

Dr. Byers is the deputy director of the British Columbia Node of the Canadian Wildlife Health Cooperative and a university research associate at Simon Fraser University. At time this research was conducted, she was a PhD student at the University of British Columbia. Her research focus is using systems approaches to derive actionable solutions to One Health issues affecting wildlife, people, and the environment.

### References

- Gutiérrez R, Krasnov B, Morick D, Gottlieb Y, Khokhlova IS, Harrus S. *Bartonella* infection in rodents and their flea ectoparasites: an overview. *Vector Borne Zoonotic Dis.* 2015;15:27–39. <https://doi.org/10.1089/vbz.2014.1606>
- Kosoy M, Bai Y, Sheff K, Morway C, Baggett H, Maloney SA, et al. Identification of *Bartonella* infections in febrile human patients from Thailand and their potential animal reservoirs. *Am J Trop Med Hyg.* 2010;82:1140–5. <https://doi.org/10.4269/ajtmh.2010.09-0778>
- McVea DA, Himsforth CG, Patrick DM, Lindsay LR, Kosoy M, Kerr T. Exposure to rats and rat-associated *Leptospira* and *Bartonella* species among people who use drugs in an impoverished, inner-city neighborhood of Vancouver, Canada. *Vector Borne Zoonotic Dis.* 2018;18:82–8. <https://doi.org/10.1089/vbz.2017.2179>
- Himsforth CG, Bai Y, Kosoy MY, Wood H, DiBernardo A, Lindsay R, et al. An investigation of *Bartonella* spp., *Rickettsia typhi*, and Seoul hantavirus in rats (*Rattus* spp.) from an inner-city neighborhood of Vancouver, Canada: is pathogen presence a reflection of global and local rat population structure? *Vector Borne Zoonotic Dis.* 2015;15:21–6. <https://doi.org/10.1089/vbz.2014.1657>
- Lee MJ, Byers KA, Donovan CM, Bidulka JJ, Stephen C, Patrick DM, et al. Effects of culling on *Leptospira interrogans* carriage by rats. *Emerg Infect Dis.* 2018;24:356–60. <https://doi.org/10.3201/eid2402.171371>
- Donnelly CA, Woodroffe R, Cox DR, Bourne FJ, Cheeseman CL, Clifton-Hadley RS, et al. Positive and negative effects of widespread badger culling on tuberculosis in cattle. *Nature.* 2006;439:843–6. <https://doi.org/10.1038/nature04454>
- Holland GP. The fleas of Canada, Alaska, and Greenland (Siphonaptera). *Memoirs of the Entomological Society of Canada.* 1985;117(S130):3–632. <https://doi.org/10.4039/entm117130fv>
- Hornok S, Beck R, Farkas R, Grima A, Orranto D, Kontschán J, et al. High mitochondrial sequence divergence in synanthropic flea species (Insecta: Siphonaptera) from Europe and the Mediterranean. *Parasit Vectors.* 2018;11:221. <https://doi.org/10.1186/s13071-018-2798-4>
- Diaz MH, Bai Y, Malania L, Winchell JM, Kosoy MY. Development of a novel genus-specific real-time PCR assay for detection and differentiation of *Bartonella* species and genotypes. *J Clin Microbiol.* 2012;50:1645–9. <https://doi.org/10.1128/JCM.06621-11>

10. Himsforth CG, Byers KA, Fernando C, Speerin L, Lee MJ, Hill JE. When the sum of the parts tells you more than the whole: The advantage of using metagenomics to characterize *Bartonella* spp. infections in Norway rats (*Rattus norvegicus*) and their fleas. *Front Vet Sci*. 2020;7:584724. <https://doi.org/10.3389/fvets.2020.584724>
11. Calhoun JB. The ecology and sociology of the Norway rat. Bethesda, MD: US Department of Health, Education, and Welfare, Public Health Service; 1963.
12. Bitam I, Dittmar K, Parola P, Whiting MF, Raoult D. Fleas and flea-borne diseases. *Int J Infect Dis*. 2010;14:e667–76. <https://doi.org/10.1016/j.ijid.2009.11.011>
13. Meerburg BG, Singleton GR, Kijlstra A. Rodent-borne diseases and their risks for public health. *Crit Rev Microbiol*. 2009;35:221–70. <https://doi.org/10.1080/10408410902989837>
14. Keeling MJ, Gilligan CA. Metapopulation dynamics of bubonic plague. *Nature*. 2000;407:903–6. <https://doi.org/10.1038/35038073>
15. Himsforth CG, Byers KA, Whelan T, Bai Y, Kosoy MY. Flea presence and abundance are not predictors of *Bartonella tribocorum* carriage in Norway rats (*Rattus norvegicus*) from an underserved neighborhood of Vancouver, Canada. *Vector-Borne and Zoonotic Diseases*. 2021;21:121–24. <https://doi.org/10.1089/vbz.2020.2665>

Address for correspondence: Kaylee Byers, School of Population and Public Health, University of British Columbia, 2206 East Mall, Vancouver, BC V6T 1Z3, Canada; email: [kaylee\\_byers@sfu.ca](mailto:kaylee_byers@sfu.ca)

## etymologia

### *Dermatophilus congolensis* [dur"mə-tof'ī-ləs con-gō-len'sis]

Rüdiger D. Ollhoff, Fabio C. Pogliani, Fábio P. Sellera

**D***ermatophilus congolensis* From the Greek *derma* (skin) + *philos* (loving), *Dermatophilus congolensis* is a Gram-positive, aerobic actinomycete, and facultatively anaerobic bacteria. *D. congolensis* infects the epidermis and produces exudative dermatitis termed dermatophilosis that was previously known as rain rot, rain scald, streptotrichosis, and mycotic dermatitis.



**Figure 1.** Photomicrograph of *Dermatophilus congolensis*, showing a Giemsa-stained, gram-positive bacteria. Source: Dr. Jerrold Kaplan, Centers for Disease Control, 1965.

In 1915, René Van Saceghem, a Belgian military veterinarian stationed at a veterinary laboratory in the former Belgian Congo (thus, the species name *congolensis*), reported *D. congolensis* from exudative dermatitis in cattle. Local breeders and veterinarians had observed the disease since 1910, but the causal agent was not identified.

Dermatophilosis affects animals, mainly cattle, and more rarely humans. Outbreaks of *D. congolensis* infection have severe economic implications in the livestock and leather industries.



**Figure 2.** René Van Saceghem (1884–1965). Source: Mortelmans J. Veterinary medicine in Belgian Congo and Ruanda-Urundi from 1885 to 1962 [in French]. *Vlaams Diergeneeskundig Tijdschrift*. 2003;72:83–95. Courtesy of the Institute of Tropical Medicine (Antwerp). <https://vdt.ugent.be/?q=nl/content/72-2-83-95>

#### Sources

1. Amor A, Enríquez A, Corcuera MT, Toro C, Herrero D, Baquero M. Is infection by *Dermatophilus congolensis* underdiagnosed? *J Clin Microbiol*. 2011;49:449–51. <https://doi.org/10.1128/JCM.01117-10>
2. Branford I, Johnson S, Chapwanya A, Zayas S, Boyen F, Mielcarska MB, et al. Comprehensive molecular dissection of *Dermatophilus congolensis* genome and first observation of *tet(z)* tetracycline resistance. *Int J Mol Sci*. 2021;22:7128. <https://doi.org/10.3390/ijms22137128>
3. Dorland's illustrated medical dictionary. 32nd ed. Philadelphia: Elsevier Saunders; 2012.
4. Van Saceghem R. Contagious skin disease (contagious impetigo) [in French]. *Bull Soc Pathol Exot*. 1915;8:354–9.

Author affiliations: Pontifícia Universidade Católica do Paraná, Curitiba, Brazil (R.D. Ollhoff); Universidade de São Paulo, São Paulo, Brazil (F.P. Sellera, F.C. Pogliani); Universidade Metropolitana de Santos, Santos, Brazil (F.P. Sellera)

DOI: <https://doi.org/10.3201/eid2808.212573>

Address for correspondence: Address for correspondence: Rüdiger D. Ollhoff, Programa de Pós-Graduação em Ciência Animal, Pontifícia Universidade Católica do Paraná, Rua Imaculada Conceição, 1155 Prado Velho, Curitiba 80215 901, Paraná, Brazil; email: [daniel.ollhoff@puccpr.br](mailto:daniel.ollhoff@puccpr.br)

# Zoonotic Threat of G4 Genotype Eurasian Avian-Like Swine Influenza A(H1N1) Viruses, China, 2020

Min Gu,<sup>1</sup> Kaibiao Chen,<sup>1</sup> Zhichuang Ge, Jun Jiao, Tianyu Cai, Suhan Liu, Xiaoquan Wang, Xinan Jiao, Daxin Peng, Xiufan Liu

We investigated genetic and biologic characteristics of 2 Eurasian avian-like H1N1 swine influenza viruses from pigs in China that belong to the predominant G4 genotype. One swine isolate exhibited strikingly great homology to contemporaneous human Eurasian avian-like H1N1 isolates, preferential binding to the human-type receptor, and vigorous replication in mice without adaptation.

Pigs have long been considered a crucial genetic mixing vessel for influenza A viruses (IAVs) of different hosts (1) because of the dual expression of human (SA $\alpha$ -2,6Gal) and avian (SA $\alpha$ -2,3Gal) viral receptors on their respiratory epithelium. Swine IAVs such as H1N1 and H3N2 subtypes sporadically infect humans and are prone to cause bidirectional interspecies transmission at the swine-human interface (2-5). So far, Eurasian avian-like (EA) H1N1 has dominated prevalence in pig herds in China and caused >10 human infections (6-9). In particular, the dominant genotype 4 (G4) EA H1N1 containing 2009 pandemic influenza A(H1N1) polymerase basic (PB) 1 and 2, polymerase acid (PA), nucleoprotein (NP), and matrix (M) genes, plus the triple-reassortant (TR) nonstructural (NS) gene, is thought to be a candidate virus of potential pandemic (10,11). Indeed, a case of human infection with G4 EA H1N1 was reported in Yunan Province, China, in 2021 (8). It is imperative to conduct surveillance on swine IAVs and evaluate their risk to public health.

## The Study

During monthly surveillance of swine IAVs in China during October-December 2020, we collected a total

of 376 nasal swab samples from apparently healthy pigs in a slaughterhouse accommodating swine from neighboring regions (Jiangsu, Shandong, and Anhui Provinces in eastern China). We detected H1 subtype swine influenza virus in 9 of those by real-time reverse transcription quantitative PCR; 2 were confirmed as hemagglutinin (HA) positive after inoculating into MDCK cells (12). We further evaluated these 2 swine IAV isolates, A/swine/Jiangsu/HD11/2020 (H1N1) [HD11] and A/swine/Anhui/HD21/2020 (H1N1) [HD21], for their genetic and biologic characteristics.

The genome sequences of HD11 and HD21 deposited in the GenBank database (accession no. OL744678-93) shared 95.4%-99.0% nucleotide identities across the coding regions of 8 genes. We performed searches of those sequences on BLAST (<https://blast.ncbi.nlm.nih.gov/Blast.cgi>) and the GISAID database (<http://platform.gisaid.org>) to present a more comprehensive scene of the homologous reference influenza viruses. As shown by the closest BLAST hits (Table 1), HD11 and HD21 were not only highly related to swine origin IAVs collected during 2012-2018 but also remarkably similar to contemporaneous human H1N1 isolates from 2020 and 2021.

We constructed a phylogenetic gene tree analysis with H1N1 reference strains to confirm the intimate genetic relationship between these 2 swine IAVs and human viruses (Appendix Figure 1, <https://wwwnc.cdc.gov/EID/article/28/8/21-2530-App1.pdf>). In each tree, HD11 consistently clustered with 3 human H1N1 viruses, A/Tianjin/00030/2020(H1N1), A/Shandong/00204/2021(H1N1), and A/Sichuan/01208/2021(H1N1). As for HD21, the virus aggregated closely with the HD11-involved subbranch in PB2, HA, NP, NA, and M gene trees but gathered more intimately with another 3 human H1N1 viruses containing A/Hubei-Wujiagang/1324/2020(H1N1),

Author affiliations: Yangzhou University, Yangzhou, China (M. Gu, K. Chen, Z. Ge, J. Jiao, T. Cai, S. Liu, X. Wang, X. Jiao, D. Deng, X. Liu); Jiangsu Co-innovation Center for Prevention and Control of Important Animal Infectious Diseases and Zoonoses, Yangzhou (M. Gu, X. Wang, X. Jiao, D. Peng, X. Liu)

DOI: <https://doi.org/10.3201/eid2808.212530>

<sup>1</sup>These authors contributed equally to this article.

**Table 1.** Comparison of 2 G4 Eurasian avian-like H1N1 swine isolates from pigs in China with similar influenza viruses retrieved from the GISAID and GenBank databases\*

| Gene and isolate | Most homologous sequence in GISAID |              |        |                                     | Most homologous sequence in GenBank |       |  |  |
|------------------|------------------------------------|--------------|--------|-------------------------------------|-------------------------------------|-------|--|--|
|                  | Virus strain                       | % Similarity |        | Virus strain                        | % Similarity                        |       |  |  |
|                  |                                    | nt           | aa     |                                     | nt                                  | aa    |  |  |
| <b>PB2</b>       |                                    |              |        |                                     |                                     |       |  |  |
| HD11             | A/Sichuan/01208/2021(H1N1)         | 99.25        | 99.47  | A/swine/Liaoning/PJ89/2014(H1N1)    | 97.72                               | 98.69 |  |  |
| HD21             | A/Sichuan/01208/2021(H1N1)         | 97.11        | 98.03  | A/swine/Liaoning/PJ89/2014(H1N1)    | 97.54                               | 98.29 |  |  |
| <b>PB1</b>       |                                    |              |        |                                     |                                     |       |  |  |
| HD11             | A/Shandong/00204/2021(H1N1)        | 99.60        | 100.00 | A/swine/Liaoning/CY102/2014(H1N1)   | 97.98                               | 98.42 |  |  |
| HD21             | A/Hubei-Wujiagang/1324/2020(H1N1)  | 97.58        | 98.68  | A/swine/Liaoning/CY102/2014(H1N1)   | 97.71                               | 98.68 |  |  |
| <b>PA</b>        |                                    |              |        |                                     |                                     |       |  |  |
| HD11             | A/Tianjin/00030/2020(H1N1)         | 99.67        | 99.86  | A/swine/Liaoning/PJ43/2014(H1N1)    | 97.44                               | 99.30 |  |  |
| HD21             | A/swine/China/Qingdao/2018(H1N1)   | 97.49        | 99.02  | A/swine/China/Qingdao/2018(H1N1)    | 97.49                               | 99.02 |  |  |
| <b>HA</b>        |                                    |              |        |                                     |                                     |       |  |  |
| HD11             | A/Tianjin/00030/2020(H1N1)         | 99.47        | 99.47  | A/swine/Liaoning/CY102/2014(H1N1)   | 97.47                               | 97.18 |  |  |
| HD21             | A/Tianjin/00030/2020(H1N1)         | 98.71        | 98.59  | A/swine/Liaoning/CY102/2014(H1N1)   | 97.30                               | 97.35 |  |  |
| <b>NP</b>        |                                    |              |        |                                     |                                     |       |  |  |
| HD11             | A/Tianjin/00030/2020(H1N1)         | 99.73        | 100.00 | A/swine/Guangxi/NS1402/2012(H3N2)   | 97.80                               | 98.20 |  |  |
| HD21             | A/Tianjin/00030/2020(H1N1)         | 98.00        | 98.60  | A/swine/Guangdong/NS2883/2012(H3N2) | 97.80                               | 99.00 |  |  |
| <b>NA</b>        |                                    |              |        |                                     |                                     |       |  |  |
| HD11             | A/Shandong/00204/2021(H1N1)        | 99.57        | 99.36  | A/swine/Ningjin/03/2014(H1N1)       | 97.02                               | 95.96 |  |  |
| HD21             | A/Sichuan/01208/2021(H1N1)         | 97.02        | 97.45  | A/swine/Liaoning/PJ43/2014(H1N1)    | 96.67                               | 95.74 |  |  |
| <b>M</b>         |                                    |              |        |                                     |                                     |       |  |  |
| HD11             | A/Tianjin/00030/2020(H1N1)         | 99.69        | 99.70  | A/swine/Shandong/LY142/2017(H1N1)   | 98.78                               | 98.78 |  |  |
|                  | A/Sichuan/01208/2021(H1N1)         |              |        |                                     |                                     |       |  |  |
| HD21             | A/Tianjin/00030/2020(H1N1)         | 98.47        | 98.48  | A/swine/Shandong/LY142/2017(H1N1)   | 98.57                               | 99.39 |  |  |
|                  | A/Sichuan/01208/2021(H1N1)         | 98.47        | 98.48  |                                     |                                     |       |  |  |
| <b>NS</b>        |                                    |              |        |                                     |                                     |       |  |  |
| HD11             | A/Shandong/00204/2021(H1N1)        | 100.00       | 100.00 | A/swine/Guangxi/1874/2012(H3N2)     | 97.97                               | 96.43 |  |  |
|                  | A/Sichuan/01208/2021(H1N1)         | 100.00       | 100.00 |                                     |                                     |       |  |  |
| HD21             | A/Hubei-Wujiagang/1324/2020(H1N1)  | 97.49        | 95.00  | A/swine/China/Qingdao/2018(H1N1)    | 97.14                               | 95.00 |  |  |

\*HD11 is the isolate A/swine/Jiangsu/HD11/2020(H1N1); HD21 is the isolate A/swine/Anhui/HD21/2020(H1N1). GISAID, <https://www.gisaid.org>. HA, hemagglutinin; M, matrix; NA, neuraminidase; NP, nucleoprotein; NS, nonstructural protein; PA, polymerase acid; PB, polymerase basic.

A/Gansu-Xifeng/1143/2021(H1N1) and A/Gansu-Xifeng/1194/2021(H1N1) in PB1, PA, and NS gene trees. Taken together, HD11 and HD21 were both closest to contemporaneous human H1N1 strains, and they uniformly possessed the EA H1N1-like HA and NA genes, pandemic influenza-like RNP (PB2, PB1, PA, and NP) and M genes, and TR-like NS gene that made the G4 type gene constellation. We

observed that 2 additional swine reference viruses of A/swine/Shandong/LY142/2017(H1N1) and A/swine/China/Qingdao/2018(H1N1) assembled tightly with the HD11/HD21 cluster, further supporting the possibility of IAV interspecies transmission from swine to human.

The 2 G4 genotype EA H1N1 swine isolates both propagated well in specific-pathogen-free chicken

**Table 2.** Virus replication of 2 G4 Eurasian avian-like H1N1 swine isolates from pigs in China in vitro and in vivo\*

| Virus strain | log <sub>10</sub> EID <sub>50</sub> /0.1 TCID <sub>50</sub> /0.1 mL |        | Virus growth in MDCK cells, mean titer ±SD, log <sub>10</sub> TCID <sub>50</sub> /0.1 mL † |        |        |        |         |        | Virus replication in infected mice, mean titer ±SD, log <sub>10</sub> copies/μL ‡ |        |        |        |        |  |
|--------------|---|--------|--|--------|--------|--------|---------|--------|---|--------|--------|--------|--------|--|
|              | 0.1 mL  | 0.1 mL | 12 hpi   |        | 24 hpi |        | 36 hpi  |        | 3 dpi   |        | 5 dpi  |        |        |  |
|              |   |        | 12 hpi   | 24 hpi | 36 hpi | 48 hpi | 60 hpi  | Lung   | Turb  | Brain  | Lung   | Turb   | Brain  |  |
| HD11         | 9.5   | 7.5    | 3.872§   | 5.041  | 7.000¶ | 5.556# | 5.667** | 5.679# | 4.295**   | 2.495  | 3.828  | 2.385  | 2.703  |  |
|              |   |        | ±0.645   | ±0.219 | ±0.441 | ±0.096 | ±0.000  | ±0.355 | ±0.181  | ±0.318 | ±1.484 | ±0.219 | ±0.661 |  |
| HD21         | 9.375   | 5.769  | 3.055  | 4.389  | 4.556  | 4.556  | 4.444   | 3.894  | 2.008   | 1.667  | 4.550  | 2.334  | 2.692  |  |
|              |   |        | ±0.481   | ±0.096 | ±0.096 | ±0.096 | ±0.096  | ±0.195 | ±0.988  | ±0.537 | ±0.53  | ±0.221 | ±0.132 |  |

\*We conducted 2-way analysis of variance in Prism software version 8 (GraphPad, <https://www.graphpad.com>) for virus titer comparison between HD11 and HD21 groups in each time point in cells or each tissue of the same sampling day in mice. dpi, days postinfection; EID<sub>50</sub>, 50% egg infectious dose; HD11, A/swine/Jiangsu/HD11/2020(H1N1); HD21, A/swine/Anhui/HD21/2020(H1N1); hpi, hours postinfection; TCID<sub>50</sub>, 50% tissue culture infectious dose (determined in MDCK cells); turb, turbinate.

†MDCK monolayers were infected with HD11 and HD21 at a multiplicity of infection (MOI) of 0.1. The virus titers of cell supernatants collected at different time points of 12, 24, 36, 48, and 60 h postinfection were determined via the TCID<sub>50</sub> assay in MDCK cells.

‡Three 6-week-old BALB/c mice per group challenged with 10<sup>6.0</sup> EID<sub>50</sub> virus in 50 μL volume were euthanized to collect tissue samples including the lung, turbinate, and brain for virus titration on 3 and 5 d postinoculation. The viral load expressed with virus copies in tissue homogenates was measured through the real-time quantitative reverse transcription PCR method as described (12).

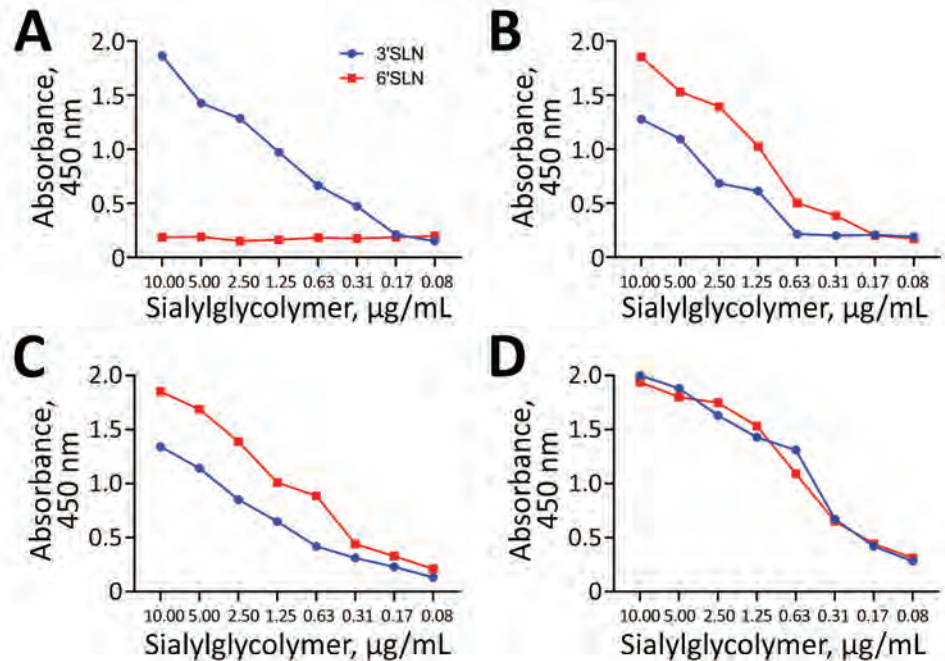
§p<0.05.

¶p<0.0001.

#p<0.01.

\*\*p<0.001.

**Figure 1.** Receptor-binding property of 2 G4 Eurasian avian-like influenza A(H1N1) swine isolates from pigs in China. A) The control virus A/mallard/Huadong/S/2005(H5N1) (HDS05) showed an absolute preference for avian-type SA $\alpha$ -2,3Gal. B) The control virus A/Jiangsu/202/2010(H3N2) (JS202) displayed double affinities to both human-type SA $\alpha$ -2,6Gal and avian-type SA $\alpha$ -2,3Gal, but with an overt bias toward SA $\alpha$ -2,6Gal. C) The tested virus A/swine/Jiangsu/HD11/2020(H1N1) (HD11) resembled the human-origin JS202 to possess an obviously advantageous avidity for SA $\alpha$ -2,6Gal over SA $\alpha$ -2,3Gal. D) The tested virus A/swine/Anhui/HD21/2020(H1N1) (HD21) exhibited comparable binding capacity to SA $\alpha$ -2,6Gal and SA $\alpha$ -2,3Gal without apparent preference. The solid-phase direct binding ELISA assay with the synthetic sialyl glycopolymers containing either 3'SLN-PAA and 6'SLN-PAA was applied to estimate the virus binding to avian-type SA $\alpha$ -2,3Gal and human-type SA $\alpha$ -2,6Gal, respectively. The data shown are representative of 3 independent binding experiments. SLN, sialyl-N-acetylglucosamine.



embryos with virus titers per 0.1mL  $>9 \log_{10}$  50% egg infectious dose (EID<sub>50</sub>) (Table 2). However, HD11 replicated much better than HD21 in MDCK cells through the titration of the 50% culture infectious dose (TCID<sub>50</sub>) value and virus growth at 12-hours intervals across 12–60 hours postinfection (hpi). At  $\geq 24$  hpi, HD11 had generated more than  $5 \log_{10}$  TCID<sub>50</sub> and reached a peak of  $7 \log_{10}$  TCID<sub>50</sub> at 36 hpi, where-

as the titer of HD21 virus remained at the relatively lower level  $<5 \log_{10}$  TCID<sub>50</sub> until the endpoint.

Subsequently, we conducted a solid-phase direct binding ELISA assay with the synthetic glycopolymer-based receptor mimics Neu5Aca2-3Galb1-4GlcNAcb(3-SLN)-PAA-biotin and Neu5Aca2-3Galb1-4GlcNAcb(6-SLN)-PAA-biotin (GlycoTech, <https://www.glycotech.com>) to evaluate

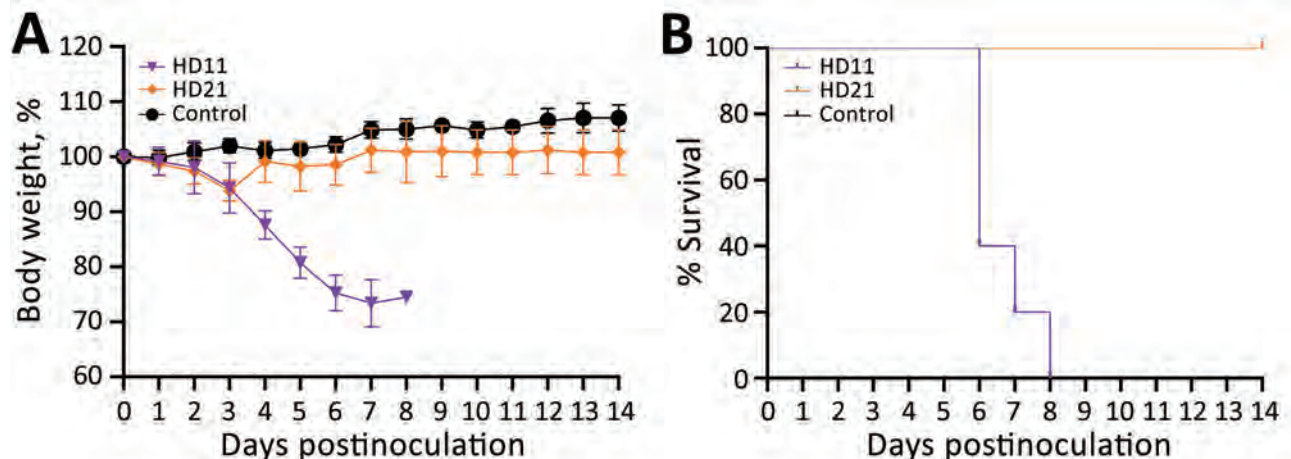


**Figure 2.** Pathogenicity of 2 G4 Eurasian avian-like influenza A(H1N1) swine isolates from pigs in China in BALB/c mice. A) Body weight change of infected mice. B) Survival curve of infected mice. Two groups of five 6-week-old BALB/c mice were inoculated intranasally with A/swine/Jiangsu/HD11/2020(H1N1) (HD11) or A/swine/Anhui/HD21/2020(H1N1) (HD21) at a dose of  $10^6$  50% egg infectious dose/50  $\mu$ L. Another 5 mice mock-infected with phosphate-buffered saline were served as control. Body weight change and survival rate were recorded daily until 14 days postinoculation, and mice that lost  $\geq 25\%$  of the initial body weight were humanely euthanized.

the viral receptor-binding preference as previously described (13). We used 1 avian H5N1 virus and 1 human seasonal H3N2 virus as controls; the avian virus displayed a complete 3-sialyl-N-acetylglucosamine (SLN) affinity, whereas the human virus possessed a dual binding property to both 3-SLN and the more advantageous 6-SLN (Figure 1). Unlike HD21, which was endowed with comparable avidity between 3-SLN and 6-SLN, HD11 resembled the binding feature of the human-origin H3N2 virus that preferentially binds the human-type SA $\alpha$ -2,6Gal (Figure 1).

We then investigated the pathogenicity of HD11 and HD21 in mice. We infected 6-week-old BALB/c mice in groups of 5 intranasally with  $10^{6.0}$  EID<sub>50</sub> virus dose or mock-inoculated them with phosphate-buffered saline (PBS). We monitored body weight changes and clinical symptoms of the mice daily for 14 days. We humanely euthanized an additional 3 challenged mice per group and analyzed them for virus load in tissues at 3 and 5 days postinfection (dpi). Mice in the control group displayed a steady increase in body weight, the HD21 group experienced a slightly transient weight loss on 3 dpi, and all mice survived during the entire experiment (Figure 2). In contrast, HD11 resulted in a steady decrease in body weights starting at 1 dpi, and all died within 8 days. In addition, we observed that both HD11 and HD21 replicated efficiently in the lungs without prior adaptation and readily disseminated into nasal turbinates and the brain (Table 2). Of note, the virus load in respiratory tissues of HD11-infected mice was significantly higher ( $p < 0.01$  in lungs and  $p < 0.001$  in turbinates) than that of HD21-infected mice on 3 dpi. On 5 dpi, we observed no significant difference in virus titers in the 3 tissues of the mice infected with these 2 isolates. Moreover, HD11 infections increased the mRNA levels of inflammatory cytokines, including interleukin 6 and 10, interferon  $\beta$  and  $\gamma$ , MX1, and C-X-C motif chemokine ligand 10/11 on 3 dpi, 5 dpi, or both, more dramatically than HD21 virus. Both HD21 and HD11 infections increased tumor necrosis factor  $\alpha$  expression at relatively low levels (Appendix Figure 2).

## Conclusions

Homology alignment and phylogenetic tree construction analysis suggest that HD11 and HD21, two G4 EA H1N1 swine IAVs isolated in 2020 in China, are strongly related to recent human-origin EA H1N1 viruses. In particular, HD11 had higher affinity for human-type 6-SLN at the level that is equivalent to the human seasonal H3N2 virus. Moreover, HD11 replicated much faster in vitro in MDCK cells and in vivo

in the lung than did HD21 and was highly pathogenic to BALB/c mice, as evidenced by its lethality, higher viral loads in pulmonary tissues, and higher levels of inflammatory cytokines in the lung. We propose that the HD11-like G4 swine isolates whose genomic sequences share great homology with that of contemporary human EA H1N1 viruses may lead to interspecies transmission. Therefore, the public health threat from the zoonotic G4 EA H1N1 viruses should not be underestimated.

## Acknowledgments

We thank Xiulong Xu for revising and editing the manuscript.

This work was supported by the National Key Research and Development Program of China (no. 2021YFD1800202), the National Natural Science Foundation of China (no. 32072892), the Jiangsu Provincial Postdoctoral Science Foundation (no. 1501075C), the Priority Academic Program Development of Jiangsu Higher Education Institutions, the Jiangsu Qinglan Project, and the High-end talent support program of Yangzhou University.

## About the Author

Dr. Gu is a faculty member at College of Veterinary Medicine, Yangzhou University. Her research primarily focuses on the epidemiology of zoonotic influenza viruses and the mechanisms of virus evolution.

## References

1. Crisci E, Mussá T, Fraile L, Montoya M. Review: influenza virus in pigs. *Mol Immunol*. 2013;55:200–11. <https://doi.org/10.1016/j.molimm.2013.02.008>
2. Nelson MI, Vincent AL. Reverse zoonosis of influenza to swine: new perspectives on the human-animal interface. *Trends Microbiol*. 2015;23:142–53. <https://doi.org/10.1016/j.tim.2014.12.002>
3. Chastagner A, Enouf V, Peroz D, Hervé S, Lucas P, Quéguiner S, et al. Bidirectional human–swine transmission of seasonal influenza A(H1N1)pdm09 virus in pig herd, France, 2018. *Emerg Infect Dis*. 2019;25:1940–3. <https://doi.org/10.3201/eid2510.190068>
4. Deng YM, Wong FYK, Spirason N, Kaye M, Beazley R, Grau MLL, et al. Locally acquired human infection with swine-origin influenza A(H3N2) variant virus, Australia, 2018. *Emerg Infect Dis*. 2020;26:143–7. <https://doi.org/10.3201/eid2601.191144>
5. Anderson TK, Chang J, Arendsee ZW, Venkatesh D, Souza CK, Kimble JB, et al. Swine influenza A viruses and the tangled relationship with humans. *Cold Spring Harb Perspect Med*. 2021;11:a038737. <https://doi.org/10.1101/cshperspect.a038737>
6. Feng Z, Zhu W, Yang L, Liu J, Zhou L, Wang D, et al. Epidemiology and genotypic diversity of Eurasian avian-like H1N1 swine influenza viruses in China. *Virol Sin*. 2021;36:43–51. <https://doi.org/10.1007/s12250-020-00257-8>
7. Li X, Guo L, Liu C, Cheng Y, Kong M, Yang L, et al. Human infection with a novel reassortant Eurasian-avian lineage

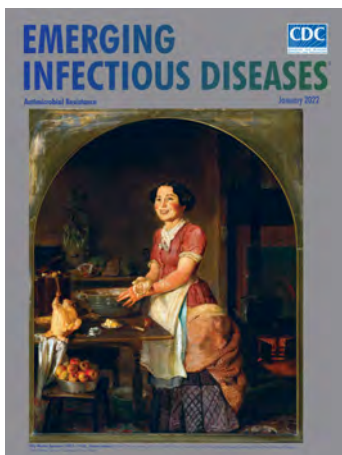
- swine H1N1 virus in northern China. *Emerg Microbes Infect.* 2019;8:1535–45. <https://doi.org/10.1080/22221751.2019.1679611>
8. Li Z, Zhao X, Huang W, Yang L, Cheng Y, Tan M, et al. Etiological characteristics of the first human infection with the G4 genotype Eurasian avian-like H1N1 swine influenza virus in Yunnan province, China [in Chinese]. *Chinese Journal of Virology.* 2022;38:290–7.
  9. World Health Organization. Influenza at the human-animal interface summary and assessment, 1 October 2021. 2021 [cited 2021 Dec 14]. <https://www.who.int/publications/m/item/influenza-at-the-human-animal-interface-summary-and-assessment-1-october-2021>
  10. Yang H, Chen Y, Qiao C, He X, Zhou H, Sun Y, et al. Prevalence, genetics, and transmissibility in ferrets of Eurasian avian-like H1N1 swine influenza viruses. *Proc Natl Acad Sci U S A.* 2016;113:392–7. <https://doi.org/10.1073/pnas.1522643113>
  11. Sun H, Xiao Y, Liu J, Wang D, Li F, Wang C, et al. Prevalent Eurasian avian-like H1N1 swine influenza virus with 2009 pandemic viral genes facilitating human infection. *Proc Natl Acad Sci U S A.* 2020;117:17204–10. <https://doi.org/10.1073/pnas.1921186117>
  12. Chen K, Kong M, Liu J, Jiao J, Zeng Z, Shi L, et al. Rapid differential detection of subtype H1 and H3 swine influenza viruses using a TaqMan-MGB-based duplex one-step real-time RT-PCR assay. *Arch Virol.* 2021;166:2217–24. <https://doi.org/10.1007/s00705-021-05127-6>
  13. Yamada S, Suzuki Y, Suzuki T, Le MQ, Nidom CA, Sakai-Tagawa Y, et al. Haemagglutinin mutations responsible for the binding of H5N1 influenza A viruses to human-type receptors. *Nature.* 2006;444:378–82. <https://doi.org/10.1038/nature05264>

Address for correspondence: Xiufan Liu, Animal Infectious Diseases Laboratory, College of Veterinary Medicine, Yangzhou University, 48 East Wenhui Road, Yangzhou, Jiangsu 225009, China; email: xfliu@yzu.edu.cn

January 2022

## Antimicrobial Resistance

- Outbreak of Mucormycosis in Coronavirus Disease Patients, Pune, India
- Severe Acute Respiratory Syndrome Coronavirus 2 and Respiratory Virus Sentinel Surveillance, California, USA, May 10, 2020–June 12, 2021
- Using the Acute Flaccid Paralysis Surveillance System to Identify Cases of Acute Flaccid Myelitis, Australia, 2000–2018
- Fungal Infections Caused by *Kazachstania* spp., Strasbourg, France, 2007–2020
- Multistate Outbreak of SARS-CoV-2 Infections, Including Vaccine Breakthrough Infections, Associated with Large Public Gatherings, United States
- Potential Association of Legionnaires' Disease with Hot Spring Water, Hot Springs National Park and Hot Springs, Arkansas, USA, 2018–2019
- Mask Effectiveness for Preventing Secondary Cases of COVID-19, Johnson County, Iowa, USA



- Transmission Dynamics of Large Coronavirus Disease Outbreak in Homeless Shelter, Chicago, Illinois, USA, 2020
- Risk Factors for SARS-CoV-2 Infection Among US Healthcare Personnel, May–December 2020
- Systematic Genomic and Clinical Analysis of Severe Acute Respiratory Syndrome Coronavirus 2 Reinfections and Recurrences Involving the Same Strain
- High-Level Quinolone-Resistant *Haemophilus haemolyticus* in Pediatric Patient with No History of Quinolone Exposure
- New Sequence Types and Antimicrobial Drug-Resistant Strains of *Streptococcus suis* in Diseased Pigs, Italy, 2017–2019
- Invasive Multidrug-Resistant *emm93.0 Streptococcus pyogenes* Strain Harboring a Novel Genomic Island, Israel, 2017–2019
- Coronavirus Disease Spread during Summer Vacation, Israel, 2020
- Extensively Drug-Resistant Carbapenemase-Producing *Pseudomonas aeruginosa* and Medical Tourism from the United States to Mexico, 2018–2019
- Effects of Nonpharmaceutical COVID-19 Interventions on Pediatric Hospitalizations for Other Respiratory Virus Infections, Hong Kong
- Global Genome Diversity and Recombination in *Mycoplasma pneumoniae*

**EMERGING  
INFECTIOUS DISEASES**

To revisit the January 2022 issue, go to:  
<https://wwwnc.cdc.gov/eid/articles/issue/28/1/table-of-contents>

# Increased Incidence of Invasive Pneumococcal Disease among Children after COVID-19 Pandemic, England

Marta Bertran, Zahin Amin-Chowdhury, Carmen L. Sheppard, Seyi Eletu, Dania V. Zamarreño, Mary E. Ramsay, David Litt, Norman K. Fry, Shamez N. Ladhani

During July–December 2021, after COVID-19 restrictions were removed in England, invasive pneumococcal disease incidence in children <15 years of age was higher (1.96/100,000 children) than during the same period in 2020 (0.7/100,000 children) and in prepandemic years 2017–2019 (1.43/100,000 children). Childhood vaccine coverage should be maintained to protect the population.

The COVID-19 pandemic and its associated lockdowns, social isolation, and other interventions led to large declines in respiratory infections, including invasive pneumococcal disease (IPD) (1,2). In England, IPD cases declined by 30% after the first lockdown in March 2020 and remained low during the subsequent winter until February 2021, when cases increased by 8% above the 3-year prepandemic mean incidence for February (3). As the country ended its third national lockdown in March 2021, after emergence of SARS-CoV-2 Alpha variant, IPD cases started to gradually increase. By June 2021, case numbers remained 25% lower than prepandemic levels, but we observed a proportionately higher increase in cases among children <15 years of age (3). We describe IPD trends during July–December 2021, after England removed all COVID-19 control measures on July 19, 2021.

## The Study

We compared IPD cases during July–December 2021 to July–December 2020 and July–December in 3

prepandemic years (2017–2019) by using national enhanced surveillance data for England (2). In brief, National Health Service (NHS) hospitals electronically report notifiable infections and routinely submit invasive pneumococcal isolates for serotyping to the UK Health Security Agency (UKHSA). For confirmed cases, the UKHSA sends general practitioners a questionnaire regarding risk factors, clinical characteristics, vaccination history, and patient outcomes. To calculate incidence, we used mid-year Office of National Statistics population estimates as denominators, using 2020 data for 2021 because 2021 data were not yet available.

During July–December 2021, a total of 1,632 IPD cases were reported to UKHSA, compared with a mean of 2,403 during July–December of 3 prepandemic years, 2017–2019 (Figure 1, panels A, B). Among children <15 years of age, the number of IPD and incidence (cases per 100,000 children) declined by 50% ( $n = 71$ ) during July–December 2020 but gradually increased in February 2021 and remained above the 3-year prepandemic mean of 145 cases (incidence 1.43, 95% CI 1.21–1.68) during July–December 2021 ( $n = 200$ ; 1.96, 95% CI, 1.70–2.25) (Figure 1, panel B). Case rates rose earlier in younger age groups (Figure 1, panel C) among whom incidence was highest during this period: 10.63 (95% CI 8.19–13.58) among <1-year-olds; 3.22 (95% CI 2.57–3.98) among 1–4-year-olds; 1.02 (95% CI 0.71–1.41) among 5–9-year-olds; and 0.44 (95% CI 0.24–0.72) among 10–14-year-olds. Cases also increased ( $n = 1,432$ ) among persons  $\geq 15$  years age during February–December 2021 (Figure 1, panel A), but the incidence during July–December 2021 remained lower (2.60, 95% CI 2.47–2.74) than the prepandemic mean during July–December in 2017–2019 (4.14, 95% CI 3.97–4.32).

Author affiliations: UK Health Security Agency, London, UK (M. Bertran, Z. Amin-Chowdhury, C.L. Sheppard, S. Eletu, D.V. Zamarreño, M.E. Ramsay, D. Litt, N.K. Fry, S.N. Ladhani); St George's University of London, London (S.N. Ladhani)

DOI: <https://doi.org/10.3201/eid2808.220304>

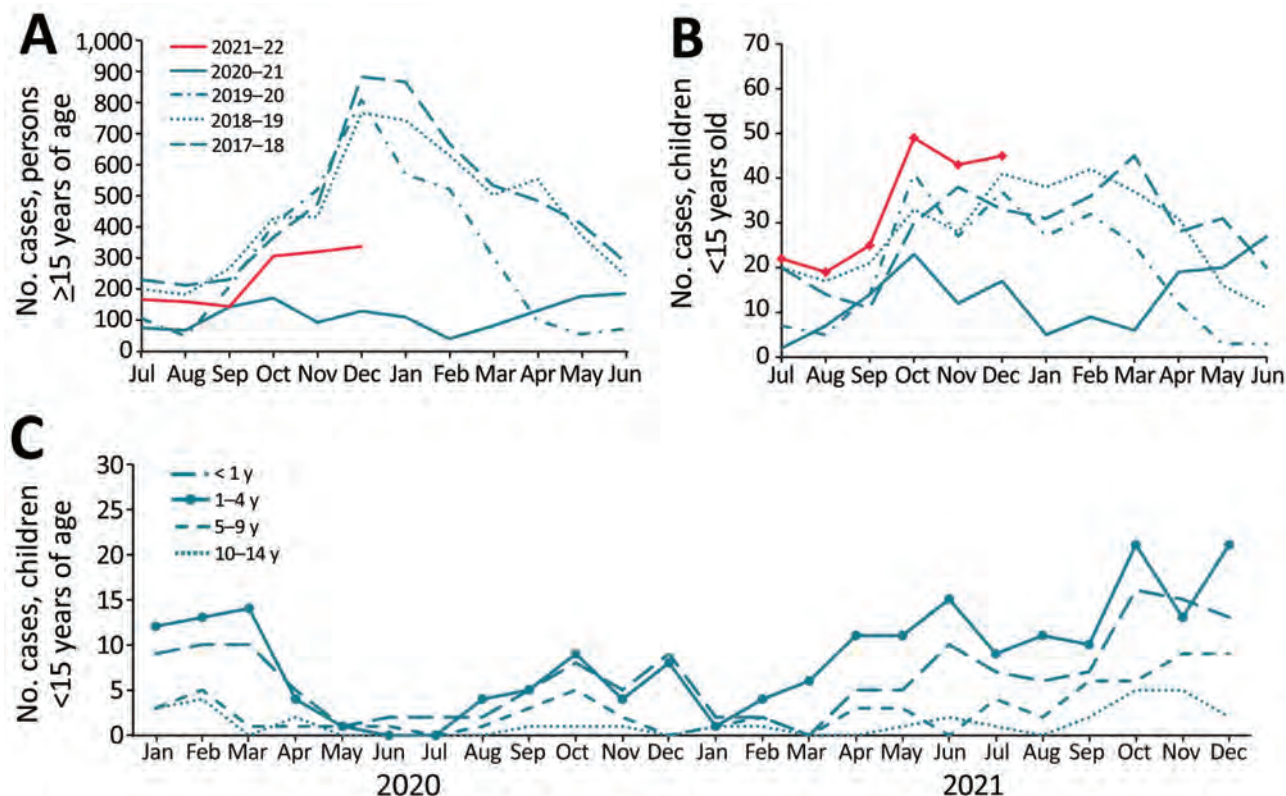


**Figure 1.** Number of IPD cases among persons before and after COVID-19 pandemic, England. A) Number of IPD cases among persons  $\geq 15$  years of age during July–June by epidemiologic year 2017–18 to 2021–22. B) Number of IPD cases among children  $< 15$  years of age during July–June by epidemiologic year 2017–18 to 2021–22. C) Number of IPD cases in children  $\leq 15$  years of age, by month and age group, January 2020–December 2021. IPD, invasive pneumococcal disease.

Age distribution of childhood IPD cases resembled the prepandemic period ( $p = 0.08$ ): 32% of cases were among  $< 1$ -year-olds, 42.5% among 1–4-year-olds, 18% among 5–9-year-olds, and 7.5% among 10–14-year-olds. Of 172 (86%) pneumococcal isolates serotyped, we noted no difference in serotype distribution between years nor within age groups. Nonvaccine types (43%) and serotypes in the 23-valent pneumococcal polysaccharide vaccine (PPV23; 37%) but not in the 13-valent pneumococcal conjugate vaccine (PCV13) predominated compared with PCV7 (5%) and additional PCV13 (16%) serotypes (Figure 2, panel A).

The most frequent serotypes among childhood cases remained similar in 2021 to those in prepandemic years (Figure 2, panel A). Of the PCV13 cases, serotypes 3, 19A, and 19F continued to predominate (91% [32/35] compared with 97% [62/64] during the prepandemic period;  $p = 0.3$ ). Of the additional PPV23 serotypes, the greatest decrease was in serotype 12F, which caused 20% (37/187) of PPV23 cases in the prepandemic period but was not detected during July–December 2021 (Figure 2, panel B). In addition,

of the PPV23 serotypes, the proportion of cases attributed to serotype 11A increased from 2% (95% CI 1%–6%;  $n = 4$ ) prepandemic to 13% (95% CI 7%–24%;  $n = 8$ ) in 2021. We noted no substantial changes among nonvaccine serotypes.

More IPD cases in 2021 involved bacteremia (50/125; 40%, 95% CI, 32%–49%) compared with the prepandemic period (105/422; 25%, 95% CI 21%–29%) ( $p = 0.003$ ). The proportion of cases with meningitis (22%), pneumonia (31%), and other clinical manifestations (7%) were not substantially different. The prepandemic and postpandemic 30-day case-fatality rates also were similar (5% vs. 4%;  $p = 0.6$ ).

## Conclusions

After lifting COVID-19 social restrictions, England experienced an increase in childhood IPD cases that exceeded prepandemic levels. England's pandemic social restrictions led to large declines in many infectious diseases, including IPD (1,2). However, a study from Israel reported that pneumococcal carriage in young children declined only slightly during the pandemic (4). Reduced social contact and exposure

to respiratory pathogens have led to concerns of immunity debt and risk for higher infection rates as restrictions are lifted globally (5). Immunity debt is typified in the emergence of respiratory viruses outside their typical season, as observed with respiratory syncytial virus (6). Of note, respiratory virus infections that usually peak in winter (e.g., influenza, rhinovirus) remained low during winter 2021–22 (6).

Other countries experienced increasing IPD cases after easing national restrictions (7,8). Germany reported higher IPD rates in children <5 years of age during June–July 2021 than during the prepandemic period (8), consistent with our data (Figure 1, panel C). An initial increase among the highest carriage age group that then extends to other age groups was reported with the resurgence of *Haemophilus influenzae* serotype b after mass vaccination in England (9), in which the first increases were among 1–3-year-olds. More recently, meningococcal group B disease was highest among university-age students (S. Clark et al., unpub. data, <https://doi.org/10.2139/ssrn.3998164>), who are the main nasopharyngeal carriers of *Neisseria meningitidis*. Our observed IPD case increase among children is counter to modeling studies that predicted IPD incidence would continue to decline after COVID-19 restrictions were lifted, even accounting for decreased vaccine coverage (10). However, these decreases might be because the model did not consider the higher proportion of susceptible children who were not exposed to pneumococci during lockdown (10).

Adult IPD cases in England remained lower during 2021 than prepandemic levels. This finding likely is because older adults, who are most at risk for IPD

and IPD-related deaths, have continued to socially isolate because of ongoing SARS-CoV-2 infections and emergence of more transmissible variants.

In the United Kingdom, the PCV13 vaccination schedule for infants born after January 1, 2020, was changed from a 2+1 schedule (8 weeks, 16 weeks, and 1 year) that had been in place since 2010 to a reduced 1+1 schedule (12 weeks and 1 year). This change was made on the basis that most protection is through indirect herd or population protection offered by preventing carriage among toddlers, thus interrupting transmission to others (11). However, the program relies on maintaining high vaccine coverage in infants to provide adequate population protection. In England, PCV13 coverage data for the 12-month dose were not available for 2020–21 during our study, but uptake of other childhood vaccines was lower after the pandemic started and improved during August–December 2021 (12). Because of the COVID-19 pandemic restrictions, evaluation of the effect of the 1+1 schedule is not yet possible.

In our cohort, serotype distribution of childhood IPD cases did not change, consistent with the childhood carriage study in Israel and reports from Germany (4,8). Switzerland reported an increase in serotype 23B (7), but we did not see a major increase in this serotype, although it remains among the most prevalent serotypes responsible for IPD in England.

In conclusion, although total IPD cases remained lower in 2021 than the 3 pre-COVID-19 pandemic years, increases in childhood cases exceeding prepandemic levels could portend increases across all age groups. Maintaining high childhood PCV13 uptake will be critical for ongoing population protection.

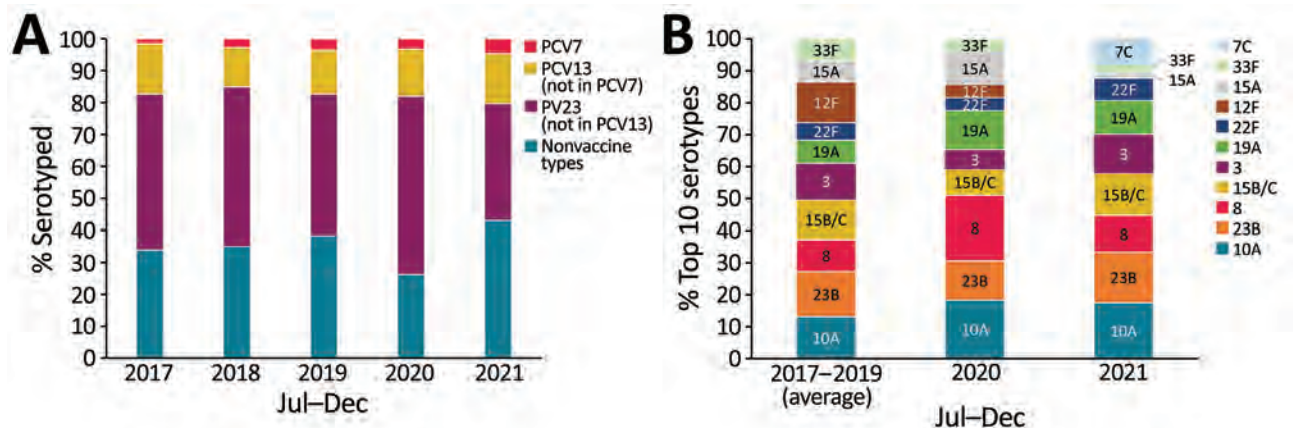


**Figure 2.** Serotype distribution of pneumococcal isolates from IPD among children <15 years of age, England. A) Percentage of IPD cases by serotype group and year during July–December 2017–2021. PCV7 includes serotypes in the 7-valent PCV; PCV13 includes serotypes in the 13-valent PCV, excluding PCV7 serotypes; PPV23 includes serotypes in the 23-valent pneumococcal polysaccharide vaccine, excluding PCV13 serotypes. B) Top 10 serotypes isolated during July–December 2017–2021. Note these values represent percentages of the top 10 isolated serotypes in each timeframe; the average number of cases of these serotypes compared with all IPD cases was 97/129 for 2017–2019, 49/61 for 2020, and 114/172 for 2021. IPD, invasive pneumococcal disease; PCV, pneumococcal conjugate vaccine.

This article was preprinted at [https://papers.ssrn.com/sol3/papers.cfm?abstract\\_id=4026121](https://papers.ssrn.com/sol3/papers.cfm?abstract_id=4026121).

### Acknowledgments

We thank staff in the Immunisation and Vaccine Preventable Diseases Division and Respiratory and Vaccine Preventable Bacterial Reference Unit who provided surveillance data for invasive pneumococcal disease, and Rashmi Malkani and Natalie Mensah for follow-up of confirmed cases and data administration. We also thank the staff at hospital laboratories across England for referring pneumococcal isolates for serotyping at the reference laboratory and general practitioners of patients with invasive pneumococcal disease for completing the surveillance questionnaires.

This work was supported by the UK Health Security Agency.

The Immunisation and Vaccine Preventable Diseases Division provided vaccine manufacturers with postmarketing surveillance reports on pneumococcal and meningococcal infection, which the companies are required to submit to the UK Licensing authority in compliance with their risk management strategy. A cost recovery charge is made for these reports. S.N.L. performs contract research on behalf of St. George's University of London and UK Health Security Agency for pharmaceutical companies but receives no personal remuneration. C.L.S., S.E., D.L., and N.K.F. report payment to their institution for investigator-led research in pneumococcal pneumonia or carriage, or both, in humans by GlaxoSmithKline and Pfizer.

### About the Author

Ms. Bertran is an epidemiologist at the UK Health Security Agency, London. She currently conducts national surveillance for invasive pneumococcal disease, *Haemophilus Influenzae*, and rotavirus. Her research interests include epidemiology of vaccine-preventable diseases and evaluation of vaccination programs.

### References

- Kadambari S, Goldacre R, Morris E, Goldacre MJ, Pollard AJ. Indirect effects of the COVID-19 pandemic on childhood infection in England: population based observational study. *BMJ*. 2022;376:e067519. <https://doi.org/10.1136/bmj-2021-067519>
- Amin-Chowdhury Z, Aiano F, Mensah A, Sheppard CL, Litt D, Fry NK, et al. Impact of the coronavirus disease 2019 (COVID-19) pandemic on invasive pneumococcal disease and risk of pneumococcal coinfection with severe acute respiratory syndrome coronavirus 2 (SARS-CoV-2): prospective national cohort study, England. *Clin Infect Dis*. 2021;72:e65–75. <https://doi.org/10.1093/cid/ciaa1728>
- Amin-Chowdhury Z, Bertran M, Sheppard CL, Eletu S, Litt D, Fry NK, et al. Does the rise in seasonal respiratory viruses foreshadow the return of invasive pneumococcal disease this winter? *Lancet Respir Med*. 2022;10:e1–2. [https://doi.org/10.1016/S2213-2600\(21\)00538-5](https://doi.org/10.1016/S2213-2600(21)00538-5)
- Danino D, Ben-Shimol S, Van Der Beek BA, Givon-Lavi N, Avni YS, Greenberg D, et al. Decline in pneumococcal disease in young children during the COVID-19 pandemic in Israel associated with suppression of seasonal respiratory viruses, despite persistent pneumococcal carriage: a prospective cohort study. *Clin Infect Dis*. 2021 Dec 14 [Epub ahead of print]. <https://doi.org/10.1093/cid/ciab1014>
- Cohen R, Ashman M, Taha M-K, Varon E, Angoulvant F, Levy C, et al. Pediatric Infectious Disease Group (GPIP) position paper on the immune debt of the COVID-19 pandemic in childhood, how can we fill the immunity gap? *Infect Dis Now*. 2021;51:418–23. <https://doi.org/10.1016/j.idnow.2021.05.004>
- UK Health Security Agency. Weekly national influenza and COVID-19 surveillance report: week 2 report (up to week 1 data) 13 January 2022. London: The Agency; 2022.
- Casanova C, Küffer M, Leib SL, Hilty M. Re-emergence of invasive pneumococcal disease (IPD) and increase of serotype 23B after easing of COVID-19 measures, Switzerland, 2021. *Emerg Microbes Infect*. 2021;10:2202–4. <https://doi.org/10.1080/22221751.2021.2000892>
- Perniciaro S, van der Linden M, Weinberger DM. Re-emergence of invasive pneumococcal disease in Germany during the spring and summer of 2021. *Clin Infect Dis*. 2022 Feb 7 [Epub ahead of print]. <https://doi.org/10.1093/cid/ciac100>
- Ladhani S, Slack MP, Heys M, White J, Ramsay ME. Fall in *Haemophilus influenzae* serotype b (Hib) disease following implementation of a booster campaign. *Arch Dis Child*. 2008;93:665–9. <https://doi.org/10.1136/adc.2007.126888>
- Choi YH, Miller E. Impact of COVID-19 social distancing measures on future incidence of invasive pneumococcal disease in England and Wales: a mathematical modelling study. *BMJ Open*. 2021;11:e045380. <https://doi.org/10.1136/bmjopen-2020-045380>
- Ladhani SN, Andrews N, Ramsay ME. Summary of evidence to reduce the two-dose infant priming schedule to a single dose of the 13-valent pneumococcal conjugate vaccine in the National Immunisation Programme in the UK. *Lancet Infect Dis*. 2021;21:e93–102. [https://doi.org/10.1016/S1473-3099\(20\)30492-8](https://doi.org/10.1016/S1473-3099(20)30492-8)
- UK Health Security Agency. Impact of COVID-19 on routine childhood immunisations: early vaccine coverage data to August 2021 in England. Health Protection Report volume 15. London: The Agency; 2021.

---

Address for correspondence: Shamez Ladhani, Immunisation and Vaccine Preventable Diseases, UK Health Security Agency, 61 Colindale Ave, London NW9 5EQ, UK; email: [shamez.ladhani@ukhsa.gov.uk](mailto:shamez.ladhani@ukhsa.gov.uk)

# Novel Chronic Anaplasmosis in Splenectomized Patient, Amazon Rainforest

Olivier Duron, Rachid Koual, Lise Musset, Marie Buisse, Yann Lambert, Benoît Jaulhac, Denis Blanchet, Kinan Drak Alsibai, Yassamine Lazrek, Loïc Epelboin, Pierre Deshuillers, Céline Michaud, Maylis Douine

We report a case of unusual human anaplasmosis in the Amazon rainforest of French Guiana. Molecular typing demonstrated that the pathogen is a novel *Anaplasma* species, distinct to all known species, and more genetically related to recently described *Anaplasma* spp. causing infections in rainforest wild fauna of Brazil.

Anaplasmoses are emerging tickborne zoonoses caused by intracellular bacteria of the *Anaplasma* genus. In total, 8 *Anaplasma* species and several candidate species have been described, including at least 5 species infecting humans (1,2). Of particular concern, the agent of human granulocytic anaplasmosis, *A. phagocytophilum*, has a specific tropism to polymorphonuclear neutrophils (1,3). Another species, provisionally named *A. capra*, recently described from asymptomatic goats, is now recognized as an agent of human intraerythrocytic anaplasmosis in China (4). The 3 other species detected in humans are major veterinary agents sporadically identified in few patients worldwide: *A. ovis* and *A. bovis* in erythrocytes and *A. platys* in platelets (1,5). Human anaplasmosis are consistently associated with persons who live in rural areas in habitats favorable to ticks or who work closely with domestic animals (1,6). However, recent surveys

report the presence of novel *Anaplasma* species of undetermined zoonotic potential in wild fauna (1,2).

## The Study

We assessed the presence of *Anaplasma* in blood samples of clandestine gold miners working in the Amazon rainforest of French Guiana. This 83,000 km<sup>2</sup> territory, located between Suriname and Brazil, is one of the regions of highest biodiversity in the world, with >280 species of wild mammals (7). The human population of French Guiana (≈284,000 inhabitants) is concentrated principally in a handful of towns spread along the coastline and the 2 main rivers (8). The interior is largely uninhabited and covered by dense rainforest, where illegal gold mining camps are located (9,10).

We examined 363 archived DNA extracts obtained from human blood samples. We primarily collected these samples in 2019 as part of Malakit, a malaria survey in remote mining camps in French Guiana (11). To characterize the whole bacterial diversity, we typed DNA blood samples by using a high-throughput bacterial 16S rDNA (*rrs*) sequencing approach (bacterial barcoding) (12). Bacteria were characterized as operational taxonomic units (OTUs) and amplicon sequence variants (ASVs) and taxonomically assigned by using the Silva database (<https://www.arb-silva.de>).

Examination of OTUs and ASVs revealed the presence of *Anaplasma* sequences in 1 DNA sample. No OTU or ASV assigned to the *Anaplasma* genus or to the Anaplasmataceae family was detected in the 362 other samples. We further conducted 2 independent *Anaplasma*-specific PCRs targeting a region of the 16S rDNA gene (544 bp) and the 23S–5S (ITS2) intergenic region (423 bp) using techniques described by Calchi et al. (13) and obtained amplicons of correct sizes for the positive sample. The Sanger sequencing of amplicons obtained with each pair of primers

Author affiliations: Centre National de la Recherche Scientifique, Montpellier, France (O. Duron, R. Koual); MIVEGEC, Montpellier (O. Duron, R. Koual, M. Buisse); Institut Pasteur de la Guyane, Cayenne, French Guiana (L. Musset, Y. Lazrek); University of Montpellier, Montpellier (M. Buisse); Centre Hospitalier Andree Rosemon, Cayenne (Y. Lambert, L. Epelboin, M. Douine); University of Strasbourg, ITI InnoVec, and Hôpitaux Universitaires de Strasbourg, Strasbourg, France (B. Jaulhac); Centre Hospitalier de Cayenne, Cayenne (D. Blanchet, K. Drak Alsibai, L. Epelboin, C. Michaud); Ecole Nationale Vétérinaire d'Alfort, Maisons-Alfort, France (P. Deshuillers)

DOI: <https://doi.org/10.3201/eid2808.212425>

confirmed the presence of *Anaplasma*. These sequences have been deposited to GenBank (accession nos. ON513878, ON521229).

We used BLAST (<http://www.ncbi.nlm.nih.gov/blast/Blast.cgi>) to compare the 16S rDNA and ITS2 nt sequences with *Anaplasma* sequences available in GenBank. None of the nucleotide sequences observed in this study are 100% identical to known *Anaplasma* sequences. The 16S rRNA sequence showed highest identities with *Anaplasma* found in wild fauna of Brazil, including an *Anaplasma* sp. detected in *Amblyomma coelebs* ticks collected on South American coatis, *Nasua nasua* (99.8%; GenBank accession no. MT019560); another *Anaplasma* sp. of black rats, *Rattus rattus* (99.8%; GenBank accession no. KY391803); and *Candidatus Anaplasma amazonensis* (13) of brown-throated sloths (*Bradypus variegatus*) and two-toed sloths (*Choloepus didactylus*) (99.1%; GenBank accession no. MT199827). All other *Anaplasma* species showed identities <99%. The ITS2 sequences showed highest nucleotide identity with *Candidatus A. amazonensis* of sloths (96.8%; GenBank accession no. MT267354) and lower identities with other *Anaplasma* species or

strains (<92%). On account of these distinct genetic traits, we propose the designation *Candidatus Anaplasma sparouinense* for this novel bacterium. The specific name refers to the Sparouine River, where the infected patient lived.

We conducted phylogenetic analyses on the basis of these 16S rDNA and ITS2 nucleotide sequences by using the maximum-likelihood method. We obtained trees of similar topologies with a robust clustering of *Candidatus A. sparouinense* with some *Anaplasma* associated with Brazilian wild fauna: *Candidatus A. sparouinense* is phylogenetically related to *Anaplasma* sp. infections detected in ticks of coatis, black rats, and, to a lesser extent, to *Candidatus A. amazonensis* of sloths (Figure 1). Altogether, they delineate a clade of neotropical *Anaplasma* divergent to all other *Anaplasma* species (Figure 1).

The DNA sample positive for *Candidatus A. sparouinense* was from a 58-year-old man who had a history of posttraumatic splenectomy and malaria attacks caused by *Plasmodium vivax*. This patient originated from Maranhão, Brazil, but had been working exclusively in the rainforest of French Guiana for the

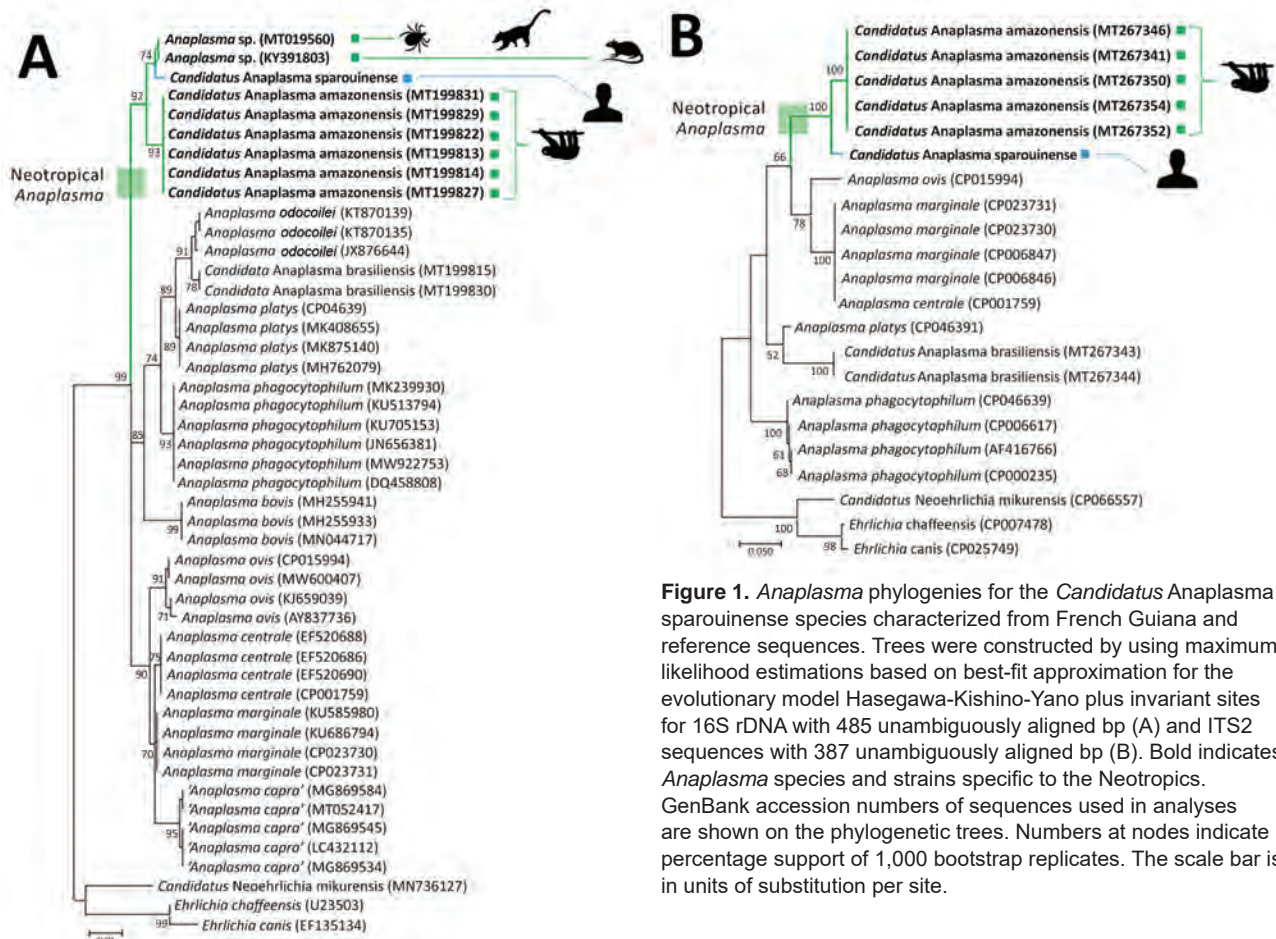


**Figure 1.** *Anaplasma* phylogenies for the *Candidatus Anaplasma sparouinense* species characterized from French Guiana and reference sequences. Trees were constructed by using maximum-likelihood estimations based on best-fit approximation for the evolutionary model Hasegawa-Kishino-Yano plus invariant sites for 16S rDNA with 485 unambiguously aligned bp (A) and ITS2 sequences with 387 unambiguously aligned bp (B). Bold indicates *Anaplasma* species and strains specific to the Neotropics. GenBank accession numbers of sequences used in analyses are shown on the phylogenetic trees. Numbers at nodes indicate percentage support of 1,000 bootstrap replicates. The scale bar is in units of substitution per site.

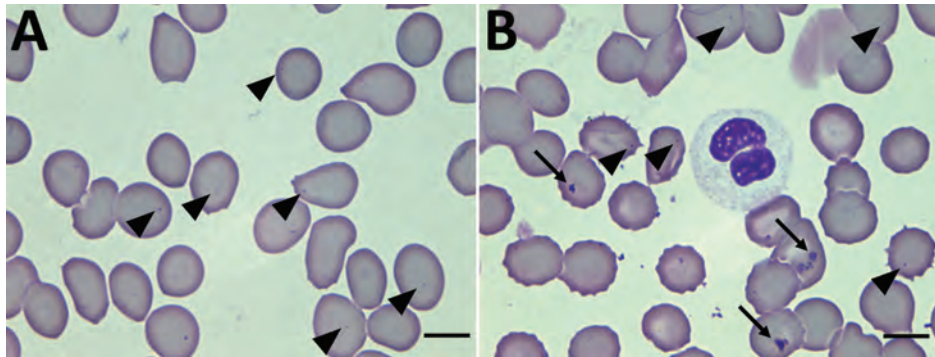


**Figure 2.** Thin films of a blood sample collected in October 2019 from a patient in French Guiana. Inclusions of *Candidatus Anaplasma sparouinense* are located at the periphery of the red blood cells as small round dots of 0.3–0.4  $\mu\text{m}$  (arrowheads). Other red blood cells contain Howell-Jolly bodies of various shapes and sizes  $>1 \mu\text{m}$  (arrows). Some Howell-Jolly bodies are found in the background of the smears. Wright-Giemsa stain; original magnification  $\times 100$ .

past 3 years. The Sparouine anaplasmosis was retrospectively diagnosed in September 2021 on the basis of PCR survey of previous blood samples (October 2019 and May 2021) and blood smears (October 2019).

We primarily detected the presence of *Candidatus A. sparouinense* in a blood sample collected in October 2019. At that time, the patient was asymptomatic, including no fever and blood pressure at reference levels; tests were negative for agents of diseases usually tested for in French Guiana (serologic assays for yellow fever, Q fever, hepatitis B and C, HIV, and syphilis and molecular tests for malaria and leptospirosis). He displayed anemia, a hemoglobin level of 10.5 g/dL. The reexamination of Giemsa-stained thin blood film taken for malaria diagnosis at that time revealed the presence of intraerythrocytic bodies, which could be *Candidatus A. sparouinense*. No infection was detected in granulocytes and platelets, but around one third of erythrocytes harbored 1 or 2 small, round, dark purple inclusions located at their periphery, which could be *Anaplasma* (Figure 2). We also detected the presence of Howell-Jolly bodies in erythrocytes (Figure 2, panel B), which could be a consequence of splenectomy.

Eighteen months later (May 2021), the patient was admitted to the Cayenne Hospital Center with fever, myalgia, headache, epistaxis, and severe anemia (hemoglobin 6.6g/dL). A broad microbiologic investigation ruled out COVID-19, dengue, chikungunya virus, Zika virus, influenza, malaria, HIV, hepatitis B and C, and leptospirosis. The only positive test was a subnormal level of *Coxiella burnetii* IgM and IgG (phase II IgG 64, IgM 96; phase I negative), which led to the introduction of antibiotic treatment (doxycycline 100 mg 2 $\times$ /d for 21 d and ceftriaxone 1 g/d for 5 d). The anemia was considered autoimmune hemolytic because of a positive Coombs test and was thus treated with prednisolone with decreasing doses from 60 mg/day to 10 mg/day for 3 months. The patient recovered within 3 weeks; symptoms resolved, and his hemoglobin level improved to 9.4 g/dL at discharge. Our

a posteriori *Anaplasma* PCR survey of May 2021 blood samples (before and at day 7 of antibiotic treatment) again revealed the presence of *Candidatus A. sparouinense*. No further blood sample was preserved; thus, the disappearance of the *Anaplasma* infection at the end of antibiotic treatment could not be confirmed.

### Conclusions

We characterized *Candidatus A. sparouinense* as a novel human intraerythrocytic pathogen. The infection arose over at least 18 months in a patient living in the rainforest of French Guiana who was potentially more susceptible because of a previous splenectomy. The phylogenetic proximity of *Candidatus A. sparouinense* to other *Anaplasma* associated with Amazon ticks and wild mammals highlights that a genetic cluster of *Anaplasma* is circulating in French Guiana and Brazil. These neotropical *Anaplasma* species might represent a source of novel infections to humans. Better documentation of the diversity and transmission cycles of *Anaplasma* in the Amazon rainforest is needed, as recently highlighted for other novel tickborne pathogens described in French Guiana (14,15).

### Acknowledgments

We thank the medical staffs of health centers in French Guiana, especially the staff of Grand Santi and the field team that collected the data (Louise Hureau-Mutricy, Audrey Godin, Mylène Cebe, and Alan Ribeiro).

The research was supported by funding from Investissements d'Avenir grants managed by the Agence Nationale de la Recherche (ANR, France, Laboratoire d'Excellence CEBA, ref. ANR-10-LABX-25-01).

### About the Author

Dr. Duron is an evolutionary ecologist in the MIVEGEC Research Unit, French National Centre for Scientific Research, France. His research interest includes the molecular study of tickborne microbes and their epidemiologic relevance.

## References

1. Rar V, Tkachev S, Tikunova N. Genetic diversity of *Anaplasma* bacteria: twenty years later. *Infect Genet Evol.* 2021;91:104833. <https://doi.org/10.1016/j.meegid.2021.104833>
2. Battilani M, De Arcangeli S, Balboni A, Dondi F. Genetic diversity and molecular epidemiology of *Anaplasma*. *Infect Genet Evol.* 2017;49:195–211. <https://doi.org/10.1016/j.meegid.2017.01.021>
3. Bakken JS, Dumler JS. Human granulocytic anaplasmosis. *Infect Dis Clin North Am.* 2015;29:341–55. <https://doi.org/10.1016/j.idc.2015.02.007>
4. Beyer AR, Carlyon JA. Of goats and men: rethinking anaplasmoses as zoonotic infections. *Lancet Infect Dis.* 2015; 15:619–20. [https://doi.org/10.1016/S1473-3099\(15\)70097-6](https://doi.org/10.1016/S1473-3099(15)70097-6)
5. Lu M, Li F, Liao Y, Shen J-J, Xu J-M, Chen Y-Z, et al. Epidemiology and diversity of Rickettsiales bacteria in humans and animals in Jiangsu and Jiangxi provinces, China. *Sci Rep.* 2019;9:13176. <https://doi.org/10.1038/s41598-019-49059-3>
6. Atif FA. Alpha proteobacteria of genus *Anaplasma* (Rickettsiales: Anaplasmataceae): epidemiology and characteristics of *Anaplasma* species related to veterinary and public health importance. *Parasitology.* 2016;143:659–85. <https://doi.org/10.1017/S0031182016000238>
7. Hollowell T, Reynolds RP. Checklist of the terrestrial vertebrates of the Guiana Shield. *Natl Mus Nat Hist MRC.* 2013;106.
8. Institut National de la Statistique et des Études Économiques (INSEE). Bilan démographique de Guyane 2018. Une croissance démographique toujours soutenue. Report no. 121. 2020 [cited 2021 Oct 7]. <https://www.insee.fr/fr/statistiques/4285434>
9. Douine M, Musset L, Corlin F, Pelleau S, Pasquier J, Mutricy L, et al. Prevalence of *Plasmodium* spp. in illegal gold miners in French Guiana in 2015: a hidden but critical malaria reservoir. *Malar J.* 2016;15:315. <https://doi.org/10.1186/s12936-016-1367-6>
10. Douine M, Mosnier E, Le Hingrat Q, Charpentier C, Corlin F, Hureau L, et al. Illegal gold miners in French Guiana: a neglected population with poor health [Erratum in: *BMC Public Health.* 2017;17:736]. *BMC Public Health.* 2017;18:23. <https://doi.org/10.1186/s12889-017-4557-4>
11. Douine M, Lambert Y, Galindo MS, Mutricy L, Sanna A, Peterka C, et al. Self-diagnosis and self-treatment of malaria in hard-to-reach and mobile populations of the Amazon: results of Malakit, an international multicentric intervention research project. *Lancet Reg Health Am.* 2021;4:100047.
12. Binetruy F, Buysse M, Lejarre Q, Barosi R, Villa M, Rahola N, et al. Microbial community structure reveals instability of nutritional symbiosis during the evolutionary radiation of Amblyomma ticks. *Mol Ecol.* 2020;29:1016–29. <https://doi.org/10.1111/mec.15373>
13. Calchi AC, Vultão JG, Alves MH, Yogui DR, Desbiez ALJ, De Santi M, et al. Ehrlichia spp. and Anaplasma spp. in Xenarthra mammals from Brazil, with evidence of novel 'Candidatus Anaplasma spp.'. *Sci Rep.* 2020;10:12615. <https://doi.org/10.1038/s41598-020-69263-w>
14. Binetruy F, Garnier S, Boulanger N, Talagrand-Reboul É, Loire E, Faivre B, et al. A novel *Borrelia* species, intermediate between Lyme disease and relapsing fever groups, in neotropical passerine-associated ticks. *Sci Rep.* 2020;10:10596. <https://doi.org/10.1038/s41598-020-66828-7>
15. Binetruy F, Buysse M, Barosi R, Duron O. Novel *Rickettsia* genotypes in ticks in French Guiana, South America. *Sci Rep.* 2020;10:2537. <https://doi.org/10.1038/s41598-020-59488-0>

---

Address for correspondence: Olivier Duron, Centre National de la Recherche Scientifique (CNRS), Laboratoire MiVEGEC, 911 Avenue Agropolis, 34394 Montpellier, France; email: [olivier.duron@cnrs.fr](mailto:olivier.duron@cnrs.fr)

# Anthelmintic Baiting of Foxes against *Echinococcus multilocularis* in Small Public Area, Japan

Kohji Uraguchi,<sup>1</sup> Takao Irie,<sup>1,2</sup> Hirokazu Kouguchi,<sup>1</sup> Azusa Inamori,<sup>1</sup> Mariko Sashika,<sup>1</sup> Michito Shimozuru,<sup>1</sup> Toshio Tsubota,<sup>1</sup> Kinpei Yagi<sup>1,3</sup>

We distributed anthelmintic baits on a university campus in Japan inhabited by foxes infected with *Echinococcus multilocularis* to design an effective baiting protocol for small public areas. High-density baiting can reduce the risk for human exposure to the parasite to near zero. However, monthly baiting is recommended to maintain this effect.

**A**lveolar echinococcosis is a potentially fatal disease caused by the larvae of the *Echinococcus multilocularis* tapeworm, which is widely distributed in the Northern Hemisphere (1). This parasite primarily depends on red foxes as definitive hosts, along with small mammals (mainly *Myodes rufocanus* gray-backed voles) as intermediate hosts in Japan (2). Human infection occurs by accidental ingestion of the parasite eggs excreted through the feces of definitive hosts.

Field trials aimed at reducing the rate of *E. multilocularis* infection in foxes through the distribution of praziquantel-containing baits have been conducted in Europe and Japan (3–7). These studies showed that anthelmintic baiting over a large area effectively reduces the infection rate in foxes; however, in most cases, eradicating the parasite from the area is difficult. Urban fox populations have increased in many countries in recent decades. In Hokkaido, Japan, foxes invade and breed on smaller spatial scales, such as university campuses and zoos in urban areas (8). Several deaths in zoo animals infected with echinococcosis have also been reported (9). Reducing the risk for infection among workers, students or visitors, and zoo animals has become an important issue for

facility managers. Anthelmintic baiting may be an efficient measure against echinococcosis in such areas with many users on a small spatial scale. However, the effect of baiting on such small public areas has not been widely examined (10).

We conducted this study to provide a basic dataset for designing an effective baiting protocol for small public areas. We investigated the effect of high-density baiting on contamination by *E. multilocularis* eggs on a university campus in Japan.

## The Study

The study was conducted on the Hokkaido University campus (an area of 1.8 km<sup>2</sup>) in an urban area of Sapporo, Japan (Figure 1, panel A). We evenly distributed anthelmintic baits manually by using 100-m grids on a map (Figure 1, panel B). We structured bait distribution into 2 phases. In phase 1 (August 2014–early July 2016), we distributed 100 baits/km<sup>2</sup> monthly across the campus during the summer and fall of 2014 and 2015. In phase 2 (late July 2016–December 2018), we distributed baits monthly throughout the year. We excluded the building area (Figure 1, panel B) from baiting in this phase because the bait consumption and frequency of foxes in the camera survey in this area were relatively low compared with the farm area in phase 1. We reduced the baiting area to ≈70% of the campus (an area of 1.3 km<sup>2</sup>), and the density of baits on the campus decreased to ≈70/km<sup>2</sup>. These baiting densities in this study are higher than those used in previous studies. We prepared anthelmintic baits for this study by mixing praziquantel with fishmeal and 2 types of edible fats, which we formed into pellets containing 50 mg praziquantel each (11).

Author affiliations: Hokkaido Institute of Public Health, Sapporo, Japan (K. Uraguchi, T. Irie, H. Kouguchi, K. Yagi); Hokkaido University, Sapporo (A. Inamori, M. Sashika, M. Shimozuru, T. Tsubota)

DOI: <https://doi.org/10.3201/eid2808.212016>

<sup>1</sup>These authors contributed equally to this article.

<sup>2</sup>Current affiliation: University of Miyazaki, Miyazaki, Japan.

<sup>3</sup>Current affiliation: Hokkaido University, Sapporo, Japan.

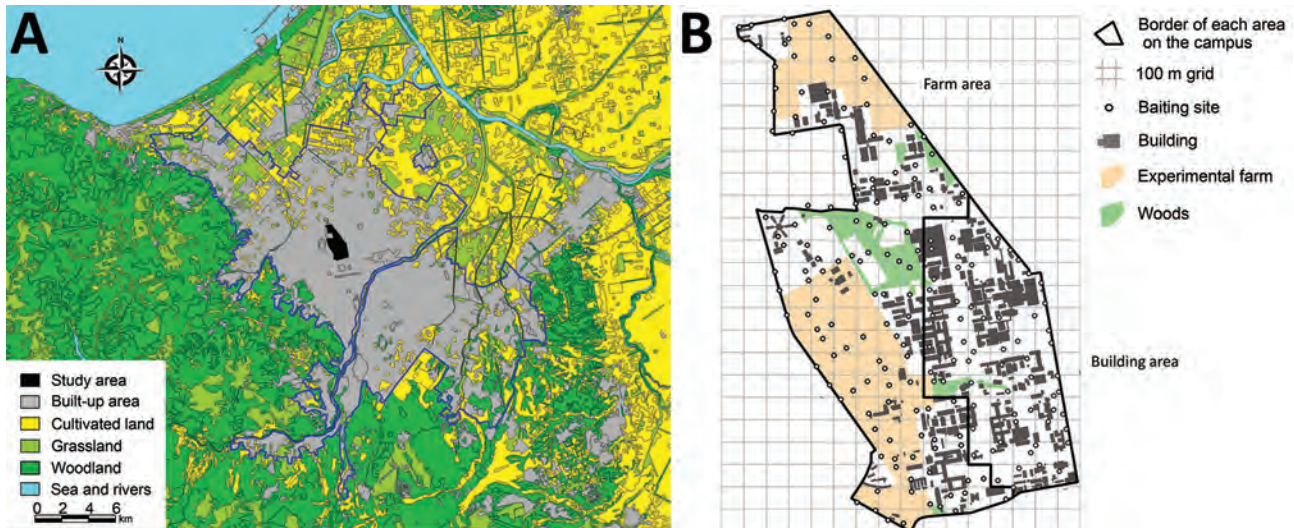


**Figure 1.** Study area for anthelmintic baiting experiment to control *Echinococcus multilocularis* tapeworms in Sapporo, Japan. A) Land use map around the study area, the Hokkaido University campus. The bold blue line shows the border of the urban area of Sapporo. B) Baiting sites and locations of buildings, farm areas, and wooded areas on the Hokkaido University campus.

To determine the effect of baiting, we detected *E. multilocularis* eggs in fox feces, we collected fox fecal samples on campus mainly during the snowless season (Figure 2). We examined parasite eggs in all fecal samples by using a sugar flotation method with 1 g of feces (12), and then we molecularly analyzed the species of detected taeniid egg by using PCR/sequencing of the cytochrome *c* oxidase subunit 1 and nuclear U1 spliceosomal RNA genes (13). We also examined fecal samples collected in phase 2 for copro-DNA derived from the body of an adult *E. multilocularis* worm by using 3 g of feces (14). We recorded the number of fox fecal samples collected on the campus and presence or absence of *E. multilocularis* eggs or DNA in the samples (Figure 2). Before the first bait campaign, 53.4% (31/58) of the collected feces contained eggs. In phase 1, we collected 144 fecal samples, 2.1% (3/144) of which were egg-positive. We identified all detected eggs as *E. multilocularis* by analyzing the cytochrome *c* oxidase subunit 1 and nuclear U1 spliceosomal RNA gene sequences. We found no egg-positive feces during the baiting period (Figure 2). In phase 2, none of the 282 fecal samples collected during September 2016–October 2018 contained eggs (Table). However, we detected *E. multilocularis*-specific DNA by using the copro-DNA test on 5 fecal samples collected in phase 2 (Figure 2).

We investigated the prevalence of *E. multilocularis* larvae in intermediate hosts on the campus. We set 150–250 traps (H.B. Sherman Traps Inc., <https://www.shermantraps.com>) for 3 consecutive days in the spring, summer, and fall seasons of 2014–2018, except for the spring of 2014 (Figure 2). We dissected all cap-

tured mammals and examined them macroscopically for lesions in the liver and other organs. We investigated lesions for *E. multilocularis* metacestode tissues by examining morphologic features. We determined the age of *M. rufocanus* voles, the most important intermediate host in Hokkaido (2), by examining the shape and root ratio of the molars (15). In total, we captured 649 small mammals of 6 species on the campus (Appendix Table, <https://wwwnc.cdc.gov/EID/article/28/8/21-2016-App1.pdf>). Seven of the 508 *M. rufocanus* voles were infected with *E. multilocularis*. The age of all *M. rufocanus* voles ranged from 20 days to 16 months. Of these, 6.8% were older than 12 months. The ages ( $\pm$  SD of the z score) of the 7 infected voles were  $51 \pm 20$  days and  $5 \pm 1.0$  (2 individual voles),  $6 \pm 1.5$ ,  $12 \pm 3.0$ ,  $13 \pm 3.8$ , and  $14 \pm 3.8$  months. Judging from their ages, we determined that the lifespan of all infected voles included the nonbaiting period (Figure 2). None of the 286 voles born in phase 2 were infected. These results show that if egg-positive fox feces are present during the nonbaiting period, voles can be infected with *E. multilocularis* worms and remain a source for infection of foxes for a year or more.

## Conclusions

Although the egg-positive rate of fecal samples is not equivalent to the infection rate in foxes, this rate directly represents the risk for exposure to the parasite eggs when university staff and students come into contact with the feces on campus. The goal of baiting on the campus is not to reduce the infection rate in foxes, but to reduce the egg-positive rate to near

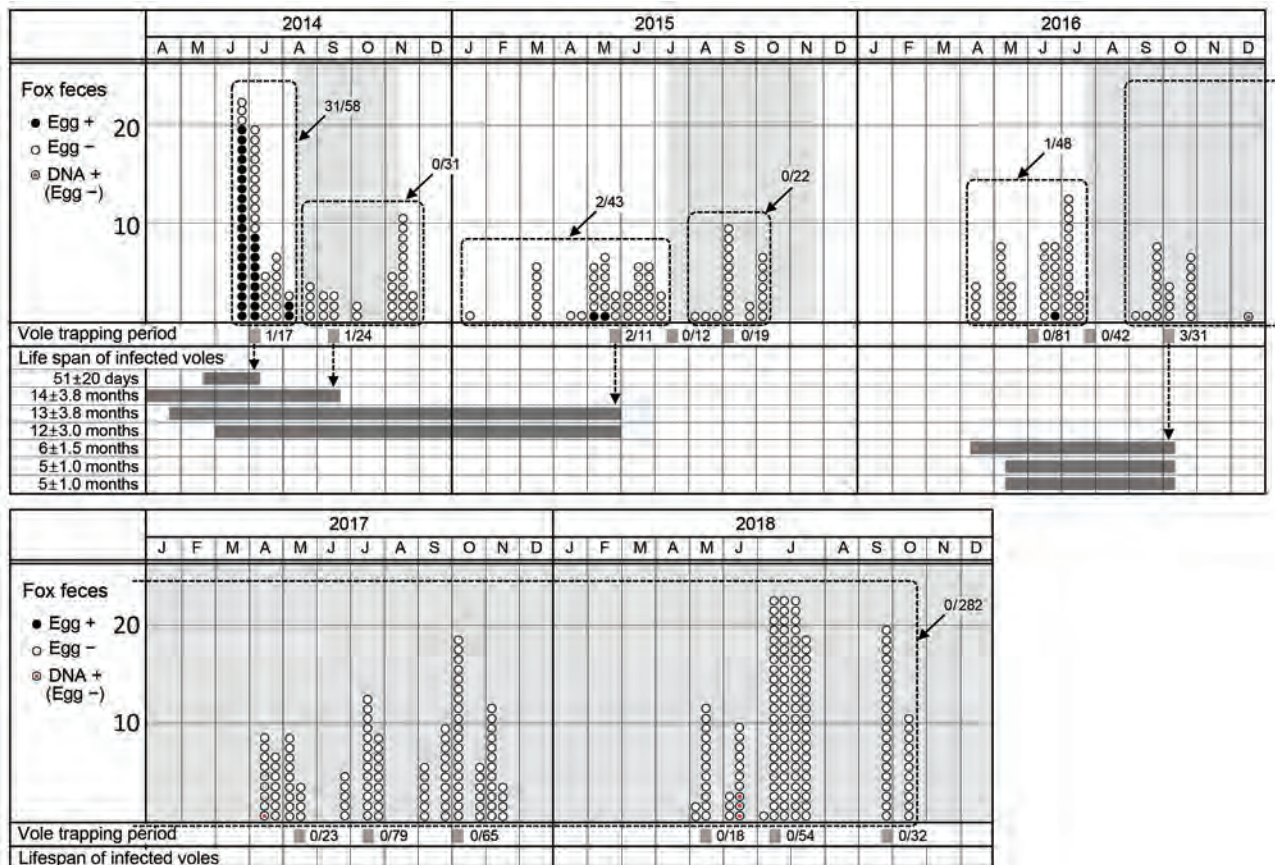


**Figure 2.** *Echinococcus multilocularis* tapeworm prevalence in foxes and voles at Hokkaido University campus, Sapporo, Japan, June 2014–October 2018. In the fox feces section, circles in each month show the fecal samples collected at the beginning, middle, and end of the month (88 fecal samples were collected in the middle of July 2018). Black circles indicate fecal samples that were *E. multilocularis* egg-positive. White circles indicate fecal samples that were *E. multilocularis* egg-negative. Circled red dots show fecal samples that were egg-negative and positive for *E. multilocularis*-specific copro-DNA. Fractions indicate the egg-positive rate of fecal samples collected during each period enclosed by a dashed line. Light gray shaded areas indicate the baiting periods. In the vole trapping period section, gray strips show the vole trapping periods. Fractions indicate the infection rate of *E. multilocularis* in *Myodes rufocanus* voles in each trapping period. In the lifespan of infected voles section, dark gray bars show the life span of 7 infected *M. rufocanus* voles, estimated from the age on the day of trapping ( $\pm$  SD of the z score). +, positive; –, negative.

zero to prevent human infection with *E. multilocularis* tapeworms within the campus.

In this study, high-density, monthly baiting nearly eradicated the parasite eggs in a campus for >2 years. The effectiveness of high-density baiting has also been demonstrated in Europe, although the evaluation methods were different (3,10). In contrast, when the baiting was suspended, egg-positive feces

were found again in 6–7 months, possibly because of the long lifespan of the intermediate host. Even after monthly baiting for 22 months, longer than the generation time of voles, DNA-positive feces were found in June 2018, possibly because of migrating foxes. These results suggest that preventing reinfection of foxes is difficult, even in a small area. However, even if reinfection occurs, monthly baiting will probably

**Table.** *Echinococcus multilocularis* egg-positive rate of fox fecal samples collected on Hokkaido University campus, Sapporo, Japan, June 2014–October 2018

| Baiting phase | Fecal sample collection period | Implementation of baiting | Total no. fecal samples | No. egg-positive fecal samples | Egg-positive rate of fecal samples, % |
|---------------|--------------------------------|---------------------------|-------------------------|--------------------------------|---------------------------------------|
| Pre-survey    | 2014 Jun–Aug                   | Before baiting            | 58                      | 31                             | 53.4                                  |
| Phase 1       | 2014 Aug–Nov                   | Baiting                   | 31                      | 0                              | 0.0                                   |
|               | 2015 Jan–Jul                   | Nonbaiting                | 43                      | 2                              | 4.7                                   |
|               | 2015 Aug–Oct                   | Baiting                   | 22                      | 0                              | 0.0                                   |
|               | 2016 Apr–Jul                   | Nonbaiting                | 48                      | 1                              | 2.1                                   |
| Phase 2       | 2016 Sep–2018 Oct              | Baiting                   | 282                     | 0                              | 0.0                                   |

eliminate the parasites before the foxes excrete the parasite eggs, because the monthly interval is approximately the same as the prepatent period for *E. multilocularis* tapeworms. Eradicating *E. multilocularis* tapeworms from an area is difficult, but eradicating the parasite eggs may be possible.

These findings are subject to limitations because results may not be completely generalizable. Further studies are needed to identify individual feces using genetic analysis to achieve a more detailed understanding of the mechanism of small area baiting. In summary, high-density, monthly baiting is effective for preventing human infection with *E. multilocularis* tapeworms within small public areas.

### Acknowledgments

We thank Takashi Saitoh for his valuable comments on the manuscript. We also thank the experimental farm staff of Hokkaido University for providing important information about foxes on campus.

This research was supported by JSPS KAKENHI (grant no. JP20K06402).

### About the Author

Mr. Uruguchi studied forestry and zoology at Hokkaido University, Japan, and is currently a senior researcher of Hokkaido Institute of Public Health. His main research interests are animal ecology, medical zoology, and urban ecology.

### References

- World Health Organization/World Health Organization for Animal Health. Geographic distribution and prevalence. In: Eckert J, Gemmell MA, Meslin FX, Pawłowski ZS, editors. WHO/OIE manual on echinococcosis in humans and animals: a public health problem of global concern. Paris: World Health Organization/World Health Organization for Animal Health; 2001. p. 101–43 [cited 2022 May 1]. <https://apps.who.int/iris/handle/10665/42427>
- Ito A, Romig T, Takahashi K. Perspective on control options for *Echinococcus multilocularis* with particular reference to Japan. *Parasitology*. 2003;127(Suppl):S159–72. <https://doi.org/10.1017/S0031182003003718>
- König A, Romig T, Holzhofer E. Effective long-term control of *Echinococcus multilocularis* in a mixed rural-urban area in southern Germany. *PLoS One* 2019;14:e0214993.
- Tackmann K, Löschner U, Mix H, Staubach C, Thulke HH, Ziller M, et al. A field study to control *Echinococcus multilocularis*-infections of the red fox (*Vulpes vulpes*) in an endemic focus. *Epidemiol Infect*. 2001;127:577–87. <https://doi.org/10.1017/S0950268801006112>
- Romig T, Bilger B, Dinkel A, Merli M, Thoma D, Will R, et al. Impact of praziquantel baiting on intestinal helminths of foxes in southwestern Germany. *Helminthologia*. 2007;44:137–44. <https://doi.org/10.2478/s11687-007-0021-9>
- Tsukada H, Hamazaki K, Ganzorig S, Iwaki T, Konno K, Lagapa JT, et al. Potential remedy against *Echinococcus multilocularis* in wild red foxes using baits with anthelmintic distributed around fox breeding dens in Hokkaido, Japan. *Parasitology*. 2002;125:119–29. <https://doi.org/10.1017/S0031182002001968>
- Takahashi K, Uruguchi K, Hatakeyama H, Giraudoux P, Romig T. Efficacy of anthelmintic baiting of foxes against *Echinococcus multilocularis* in northern Japan. *Vet Parasitol*. 2013;198:122–6. <https://doi.org/10.1016/j.vetpar.2013.08.006>
- Uruguchi K. Red fox. In: Masuda R, editor. *Carnivores in Japan: mammals at the top of the ecosystem* [in Japanese]. Tokyo: University of Tokyo Press; 2018. p. 67–88.
- Yamano K, Kouguchi H, Uruguchi K, Mukai T, Shibata C, Yamamoto H, et al. First detection of *Echinococcus multilocularis* infection in two species of nonhuman primates raised in a zoo: a fatal case in *Cercopithecus diana* and a strongly suspected case of spontaneous recovery in *Macaca nigra*. *Parasitol Int*. 2014;63:621–6. <https://doi.org/10.1016/j.parint.2014.04.006>
- Hegglin D, Deplazes P. Control strategy for *Echinococcus multilocularis*. *Emerg Infect Dis*. 2008;14:1626–8. <https://doi.org/10.3201/eid1410.080522>
- Takahashi K, Uruguchi K, Abe S, Hirakawa H. Making acceptable bait by red foxes [in Japanese]. Report of the Hokkaido Institute of Public Health. 2010;60:81–2.
- Ito S. Modified Wisconsin sugar centrifugal-flotation technique for nematode eggs in bovine feces [in Japanese.]. *Nippon Juishikai Zasshi*. 1980;33:424–9. <https://doi.org/10.12935/jvma1951.33.424>
- Irie T, Mukai T, Yagi K. *Echinococcus multilocularis* surveillance using copro-DNA and egg examination of shelter dogs from an endemic area in Hokkaido, Japan. *Vector Borne Zoonotic Dis*. 2018;18:390–2. <https://doi.org/10.1089/vbz.2017.2245>
- Irie T, Ito T, Kouguchi H, Yamano K, Uruguchi K, Yagi K, et al. Diagnosis of canine *Echinococcus multilocularis* infections by copro-DNA tests: comparison of DNA extraction techniques and evaluation of diagnostic deworming. *Parasitol Res*. 2017;116:2139–44. <https://doi.org/10.1007/s00436-017-5514-y>
- Abe H. Age determination of *Clethrionomys rufocanus bedfordiae* (THOMAS) [in Japanese.]. *Jap J Ecol*. 1976;26:221–7.

Address for correspondence: Kohji Uruguchi, Department of Infectious Diseases, Hokkaido Institute of Public Health, N19 W12, Sapporo 060-0819, Japan; email: [ura@iph.pref.hokkaido.jp](mailto:ura@iph.pref.hokkaido.jp)

# *Spiroplasma ixodetis* Infections in Immunocompetent and Immunosuppressed Patients after Tick Exposure, Sweden

Johannes Eimer,<sup>1,2</sup> Louise Fernström,<sup>2</sup> Louise Rohlén, Anna Grankvist, Kristoffer Loo, Erik Nyman, Anna J. Henningson, Mats Haglund, Viktor Hultqvist, Johanna Sjöwall, Christine Wennerås,<sup>3</sup> Thomas Schön<sup>3</sup>

We report 2 cases of *Spiroplasma ixodetis* infection in an immunocompetent patient and an immunocompromised patient who had frequent tick exposure. Fever, thrombocytopenia, and increased liver aminotransferase levels raised the suspicion of anaplasmosis, but 16S rRNA PCR and Sanger sequencing yielded a diagnosis of spiroplasmosis. Both patients recovered after doxycycline treatment.

Acute febrile illness after tick bites may be caused by various agents (e.g., *Borrelia* spp., tick-borne encephalitis virus, *Babesia* spp., *Rickettsia* spp., *Neorhlichia mikurensis*, *Anaplasma phagocytophilum*). *Spiroplasma ixodetis* was initially described as a cause of neonatal cataract and uveitis (1,2). Systemic infections caused by other *Spiroplasma* spp. have been reported in 3 immunocompromised patients (3–5).

*Spiroplasma* spp. are intracellular organisms that belong to the class Mollicutes, which include *Mycoplasma* spp. These bacteria have a single-layer cell membrane, cannot be visualized by Gram staining, require special substrates for growth, and can be diagnosed by genetic methods (6). Plants, insects, and ticks are known reservoirs (7). *S. ixodetis* was initially reported in *Ixodes pacificus* ticks from Oregon, USA

(8), and has since been detected in many arthropod species, including *Ixodes ricinus* ticks in several countries in Europe, but not yet in Sweden (9,10). We report *S. ixodetis* infections in an immunocompetent patient and an immunocompromised patient after tick exposure in Sweden.

## The Study

Oral and written informed consent were obtained from the 2 patients. Case-patient 1 was an 81-year-old previously healthy woman who sought care at the emergency department of Kalmar County Hospital (Kalmar, Sweden) in July 2021 because of a 3-day history of fever (temperature up to 39°C) and mild headache. She reported frequent tick exposure in southeastern Sweden but no history of opportunistic infections or immunosuppressive diseases or treatments that would have compromised immune defenses. She was admitted because of clinical suspicion of anaplasmosis.

Blood tests showed thrombocytopenia and increased levels of C-reactive protein (CRP) and alanine aminotransferase (ALT) (Table). Real-time PCR specific for *A. phagocytophilum* (11) and *N. mikurensis* (12) on EDTA-anticoagulated whole blood showed negative results. However, 3 days after admission, 16S rRNA PCR and Sanger sequencing analysis (Appendix, <https://wwwnc.cdc.gov/EID/article/28/8/21-2524-App1.pdf>) identified *S. ixodetis* that had 99.72% sequence homology with a reference strain of *S. ixodetis* (GenBank accession no. MN166761) (Figure 1). The *S. ixodetis* sequence has been deposited in GenBank (accession no. OL636349).

Author affiliations: Visby County Hospital, Visby, Sweden (J. Eimer, E. Nyman); Linköping University, Linköping, Sweden (L. Fernström, L. Rohlén, K. Loo, A.J. Henningson, M. Haglund, V. Hultqvist, J. Sjöwall, T. Schön); Kalmar County Hospital, Kalmar, Sweden (L. Fernström, L. Rohlén, K. Loo, M. Haglund, V. Hultqvist, T. Schön); Sahlgrenska University Hospital, Gothenburg, Sweden (A. Grankvist, C. Wennerås); Jönköping County Hospital, Jönköping, Sweden (A.J. Henningson); Linköping University Hospital, Linköping, Sweden (J. Sjöwall, T. Schön); University of Gothenburg, Gothenburg (C. Wennerås)

DOI: <https://doi.org/10.3201/eid2808.212524>

<sup>1</sup>Current affiliation: Sorbonne University, Paris, France.

<sup>2</sup>These authors contributed equally to this article.

<sup>3</sup>These senior authors contributed equally to this article.

**Table.** Results of analysis for *Spiroplasma ixodetis* infections in immunocompetent and immunosuppressed patients after tick exposure, Sweden\*

| Analysis                               | Reference value | Case-patient 1, immunocompetent† |       |        |      | Case-patient 2, immunosuppressed‡ |        |        |      |
|--|-----------------|----------------------------------|-------|--------|------|-----------------------------------|--------|--------|------|
|  |                 | D0                               | D1    | D2     | D16  | D0                                | D2     | D4     | D25  |
| Clinical chemistry                     |                 |                                  |       |        |      |                                   |        |        |      |
| Blood                                  |                 |                                  |       |        |      |                                   |        |        |      |
| Hemoglobin, g/L                        | 134–170         | 143                              | 162   | NT     | 145  | 114                               | 118    | 110    | 108  |
| Leukocytes, × 10 <sup>9</sup> cells/L  | 3.5–8.8         | 4.2                              | 3.0   | NT     | 6.4  | 6.1                               | 6.4    | 8.8    | 6.4  |
| Lymphocytes, × 10 <sup>9</sup> cells/L | 1.1–3.5         | NT                               | NT    | NT     | 1.9  | 0.3                               | NT     | 0.6    | NT   |
| Neutrophils, × 10 <sup>9</sup> cells/L | 1.6–5.9         | NT                               | NT    | NT     | 3.7  | 4.9                               | NT     | 7.7    | NT   |
| Platelet count, × 10 <sup>9</sup> /L   | 140–350         | 150                              | 118   | NT     | 287  | 47                                | 43     | 41     | 159  |
| Plasma                                 |                 |                                  |       |        |      |                                   |        |        |      |
| ALT, µkat/L                            | <1.1            | 1.6                              | 2.1   | NT     | 0.85 | 3.82                              | 8.18   | 13.34  | 0.48 |
| Creatinine, µmol/L                     | 45–90           | 66                               | 73    | NT     | 72   | 75                                | 90     | 149    | 71   |
| CRP, mg/L                              | <5              | 59                               | 59    | 38     | <1   | 197                               | 158    | 164    | <3   |
| Vital signs                            |                 |                                  |       |        |      |                                   |        |        |      |
| O <sub>2</sub> saturation, %           | 95–100          | 95                               | 95    | 97     |      | 95                                | 97     | 97     | NT   |
| Respiratory rate, breathes/min         | 12–16           | 20                               | 18    | 20     |      | 20                                | 24     | 20     | NT   |
| Blood pressure, mm Hg                  | 90/60–120/80    | 108/50                           | 94/69 | 114/56 |      | 117/72                            | 119/66 | 120/74 | NT   |
| Heart rate, beats/min                  | 60–100          | 66                               | 90    | 79     |      | 73                                | 74     | 94     | NT   |
| Temperature, °C                        | 37              | 38.6                             | 37.4  | 36.2   |      | 37.1                              | 39.9   | 36.4   | NT   |
| Immunology/microbiology                |                 |                                  |       |        |      |                                   |        |        |      |
| Serum                                  |                 |                                  |       |        |      |                                   |        |        |      |
| IgG1, g/L                              | 4.0–10          | NT                               | NT    | NT     | 7.0  | NT                                | NT     | NT     | NT   |
| IgG2, g/L                              | 1.7–7.9         | NT                               | NT    | NT     | 3.4  | NT                                | NT     | NT     | NT   |
| IgG3, g/L                              | 0.1–0.85        | NT                               | NT    | NT     | 0.48 | NT                                | NT     | NT     | NT   |
| IgG4, g/L                              | 0.03–2          | NT                               | NT    | NT     | 0.15 | NT                                | NT     | NT     | NT   |
| IgA, g/L                               | 0.9–4.5         | NT                               | NT    | NT     | 3.7  | NT                                | 2.4    | NT     | NT   |
| IgG, g/L                               | 6.7–15          | NT                               | NT    | NT     | 12   | NT                                | 10.6   | NT     | NT   |
| IgM, g/L                               | 0.3–2.1         | NT                               | NT    | NT     | 2.7  | NT                                | 0.80   | NT     | NT   |
| Blood culture                          | NR              | –                                | NT    | NT     | NT   | –                                 | NT     | NT     | NT   |
| Urine culture                          | NR              | –                                | NT    | NT     | NT   | –                                 | NT     | NT     | NT   |
| COVID-19 PCR/rapid test                | NR              | –                                | NT    | NT     | NT   | –                                 | NT     | NT     | NT   |

\*Day 0 indicates day of admission. ALT, alanine aminotransferase; COVID-19, coronavirus disease; CRP, C-reactive protein; D, day; NT, not tested; NR, not relevant; –, negative.

†Case-patient 1 had negative PCR results for *Anaplasma* spp. and *Neorickettsia* spp. at admission to the emergency department.

‡Case-patient 2 had negative PCR results in serum for *Anaplasma* spp. and *Neorickettsia* spp. at admission, as well as negative IgG results for *Anaplasma* spp. Results were positive in serum for IgG against *Borrelia burgdorferi* and tick borne encephalitis virus, which were compatible with past infection.

Molecular testing (DNA) for Epstein-Barr virus, cytomegalovirus, adenovirus, and parvovirus B19 showed negative results. Test results were negative for antinuclear antibodies and antineutrophil cytoplasmic antibodies, and urine sediment test result was unremarkable.

A slight increase in IgG convalescent-phase titer against *A. phagocytophilum* was observed (from 1:160 to 1:320 during a 4-week interval; reference titer <1:160). However, the result was disregarded because of the negative *A. phagocytophilum* PCR result at admission.

The fever decreased promptly when oral doxycycline treatment (100 mg 2×/d) was initiated. The patient was discharged, and treatment was continued for a total of 10 days. Upon follow-up, the patient had recovered and had no remaining laboratory result abnormalities (Table). Total serum immunoglobulins, including IgG subclasses, were within reference ranges, and a follow-up blood sample was negative by 16S rRNA PCR.

Case-patient 2 was a 76-year-old man who had insulin-dependent type 2 diabetes and Crohn's disease who had been given infliximab maintenance therapy. He was on a prednisolone taper after an exacerbation of his inflammatory bowel disease. The patient sought care at the emergency department of Visby

County Hospital (Visby, Sweden) in October 2021 for a 2-week history of spiking fevers and fatigue. He reported multiple tick bites throughout summer and had been given penicillin V for erythema migrans. No other focal signs or symptoms were reported.

At admission, blood tests showed pancytopenia with predominant thrombocytopenia and increased CRP and ALT levels (Table). Empirical treatment with intravenous cefotaxime was started. Aminotransferase levels quadrupled during the next 4 days, and acute kidney injury developed (Figure 2). Results of routine examinations, such as blood cultures, serologic tests, and molecular tests, were inconclusive (Table).

Given the progressive clinical picture, cefotaxime was replaced on day 5 by doxycycline (100 mg 2×/d), which resulted in return of liver and kidney functions to reference values within 1 week and improved clinical condition (Figure 2). The patient was discharged after 11 days; doxycycline treatment was continued for 21 days. A serum sample (1 mL) from day 4 was ana-

lyzed for *N. mikurensis* and *A. phagocytophilum* by PCR and unbiased bacterial 16S rRNA sequencing. Analysis identified *S. ixodetis* in serum that had 99.86% sequence homology with a reference strain of *S. ixodetis*. The patient sequence has been deposited in GenBank (accession no. OL636350) (Figure 1). The patient remained well 6 weeks after symptom onset and had no residual abnormal laboratory results.

## Conclusions

We report 2 cases of systemic *S. ixodetis* infection that were presumably acquired by tick bites in southeastern Sweden. This organism has not been reported in *Ix. ricinus* ticks from Sweden, but *A. phagocytophilum*, *N. mikurensis*, *Rickettsia* spp., and *Babesia* spp. are endemic tickborne microorganisms that may cause febrile illness. However, thrombocytopenia and increased levels of liver enzymes rarely occur in neoehrlichiosis (13). *A. phagocytophilum* infections can cause thrombocytopenia and increased levels of liver enzymes, but are an uncommon cause of fever in Scandinavia, and *Babesia* spp. affects primarily severely immunocompromised persons (14).

A case of human *Spiroplasma* infection was reported in Germany during 2002 and involved a 4-month-old premature child who had unilateral cataract and uveitis (1). Three case reports have described systemic infections caused by *Spiroplasma* spp. The first case involved a 73-year-old woman from Spain who had selective IgM deficiency, rheumatoid arthritis, fever, myalgia, headache, and bilateral conjunctivitis; she was receiving tumor necrosis- $\alpha$  and interleukin-6 inhibitors (4). *S. turonicum* was identified by 16S rRNA PCR performed on blood cultures. Her fever was unresponsive to cefuroxime but resolved after she received doxycycline and levofloxacin for 2 months.

The second case involved a 70-year-old woman from Switzerland who had diffuse abdominal pain and fatigue. She was a lung transplant recipient and was afebrile. Laboratory analysis showed, consistent with our cases, thrombocytopenia and increased liver enzyme levels. Liver biopsy and blood samples analyzed by 16S rRNA PCR identified *Spiroplasma* sp. that had 98.2% homology with *S. ixodetis*, referred to as *Spiroplasma* sp. Zurich (5). The patient received doxycycline and azithromycin for 2 months and slowly recovered.

The third case involved a 40-year-old man who had X-linked agammaglobulinemia and febrile polyarthritis. Blood and synovial fluid cultures grew small bacterial colonies unidentifiable by routine methods, but 16S rRNA PCR identified *S. apis* (3).

He recovered after a 12-week course of levofloxacin and doxycycline.

In reports on systemic *S. ixodetis* infection, doxycycline was prescribed in combination with either levofloxacin or azithromycin (2). In our study, the patients showed improvement after doxycycline monotherapy and were cured without relapse, supporting the notion that doxycycline is effective against *S. ixodetis* infections. The previously described systemic infections were caused by other

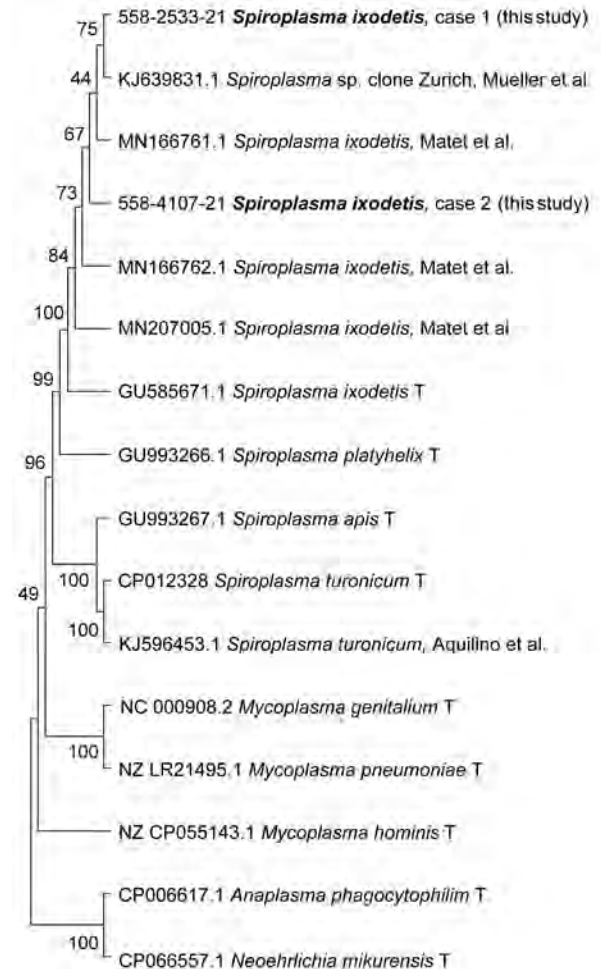


**Figure 1.** *Spiroplasma ixodetis* infections in immunocompetent and immunosuppressed patients after tick exposure, Sweden. Neighbor-joining tree based on partial 16S rRNA sequences of clinical isolates of *Spiroplasma* spp., other members of the family Mollicutes (*Mycoplasma* spp.), and tickborne bacterial pathogens of the family Anaplasmataceae (*Anaplasma phagocytophilum* and *Neoehrlichia mikurensis*). Type strains are indicated by T, and clinical samples from this study are indicated in bold. Percentage values of replicate trees in which the associated taxa clustered together in the bootstrap test (1,000 replicates) are shown next to the branches. Evolutionary distances were computed by using the Kimura 2-parameter method and are in the units of number of base substitutions per site. Evolutionary analyses were conducted by using MEGA11 (<https://www.megasoftware.net>).

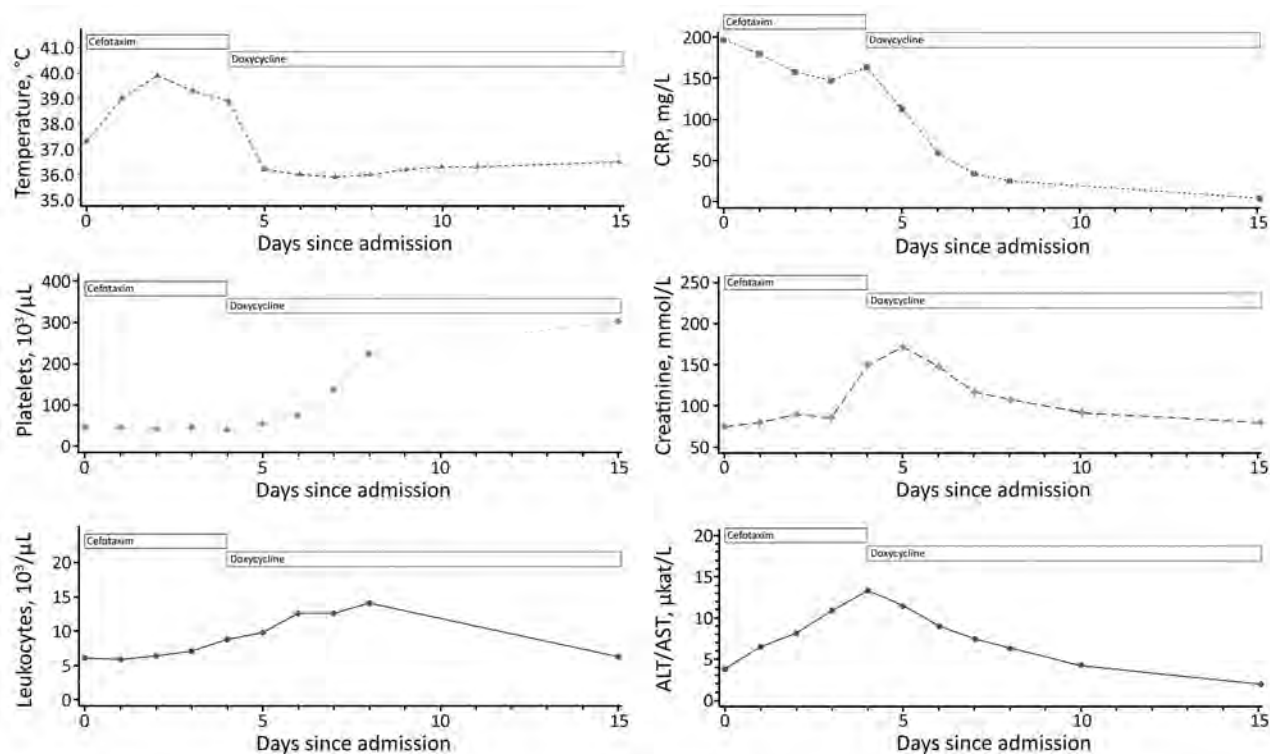


**Figure 2.** Clinical course of *Spiroplasma ixodetis* infection in an immunocompromised 76-year-old man (case-patient 2) after tick exposure, Sweden. ALT, alanine aminotransferase; CRP, C-reactive protein.

species of *Spiroplasma* (*S. turonicum*, *S. apis*, and *Spiroplasma* sp. Zurich). The route of transmission was unclear except for the *S. apis* case, for which a hornet sting was the plausible route of transmission. In contrast, the *S. ixodetis* patients we describe were most likely infected via tick bites acquired in the coastal areas of southeastern Sweden, including the islands of Öland and Gotland.

Our study suggests an association between tick exposure and human *S. ixodetis* infection. Previous case reports of human *Spiroplasma* infection have been associated with an immunocompromised state, either in the form of immature eyes of newborns or conditions requiring immunosuppressive treatment. We report a systemic *Spiroplasma* infection in an apparently immunocompetent person. However, immunosenescence of the aged immune system might have compromised innate or acquired immune defenses (15).

In conclusion, we report 2 case-patients who had *S. ixodetis* infection and acute febrile illness after tick exposure. Treatment with doxycycline was successful. This finding shows the clinical utility of unbiased 16S rRNA analysis for correct diagnosis and treatment, as well as its potential for identifying novel pathogens in the febrile host. We are developing a

*Spiroplasma*-specific PCR that might increase sensitivity of detection. *S. ixodetis* is an emerging pathogen that should be considered in patients with febrile illness after tick exposure.

This study was supported by the Swedish Research Council grants 2016-02043 (to T.S.) and 2020-01287 (to C.W.), core funding from Linköping University (to T.S.), and the Swedish state under the agreement between the Swedish government and the county councils, the ALF agreement (ALFGBG-827291).

C.W. and T.S. conceptualized and supervised the study and provided resources; C.W., A.G., and A.H. analyzed laboratory data; T.S., K.L., J.E., and E.N. analyzed case reports; L.R., L.F., K.L., J.E., T.S., and C.W. wrote the original draft of the paper; and J.S., A.H., M.H., T.S., C.W., A.G., and V.H. wrote and edited the paper.

### About the Author

At the time of the study, Dr. Eimer was an infectious disease and respiratory consultant at Gotland County Hospital, Visby, Sweden. He is currently a scientist at the Centre of Immunology and Microbial Infections, Sorbonne University, Paris, France. His primary research interest is treatment for multidrug-resistant tuberculosis.

## References

- Lorenz B, Schroeder J, Reischl U. First evidence of an endogenous *Spiroplasma* sp. infection in humans manifesting as unilateral cataract associated with anterior uveitis in a premature baby. *Graefes Arch Clin Exp Ophthalmol*. 2002;240:348–53. <https://doi.org/10.1007/s00417-002-0453-3>
- Matet A, Le Flèche-Matéos A, Doz F, Dureau P, Cassoux N. Ocular *Spiroplasma ixodetis* in newborns, France. *Emerg Infect Dis*. 2020;26:340–4. <https://doi.org/10.3201/eid2602.191097>
- Etienne N, Bret L, Le Brun C, Lecuyer H, Moraly J, Lanternier F, et al. Disseminated *Spiroplasma apis* infection in patient with agammaglobulinemia, France. *Emerg Infect Dis*. 2018;24:2382–6. <https://doi.org/10.3201/eid2412.180567>
- Aquilino A, Masiá M, López P, Galiana AJ, Tovar J, Andrés M, et al. First human systemic infection caused by *Spiroplasma*. *J Clin Microbiol*. 2015;53:719–21. <https://doi.org/10.1128/JCM.02841-14>
- Mueller NJ, Tini GM, Weber A, Gaspert A, Husmann L, Bloemberg G, et al. Hepatitis from *Spiroplasma* sp. in an immunocompromised patient. *Am J Transplant*. 2015;15:2511–6. <https://doi.org/10.1111/ajt.13254>
- Harne S, Gayathri P, Béven L. Exploring *Spiroplasma* biology: opportunities and challenges. *Front Microbiol*. 2020;11:589279. <https://doi.org/10.3389/fmicb.2020.589279>
- Cisak E, Wójcik-Fatla A, Zajac V, Sawczyn A, Sroka J, Dutkiewicz J. *Spiroplasma*: an emerging arthropod-borne pathogen? *Ann Agric Environ Med*. 2015;22:589–93. <https://doi.org/10.5604/12321966.1185758>
- Tully JG, Rose DL, Yunker CE, Carle P, Bové JM, Williamson DL, et al. *Spiroplasma ixodetis* sp. nov., a new species from *Ixodes pacificus* ticks collected in Oregon. *Int J Syst Bacteriol*. 1995;45:23–8. <https://doi.org/10.1099/00207713-45-1-23>
- Binetruy F, Bailly X, Chevillon C, Martin OY, Bernasconi MV, Duron O. Phylogenetics of the *Spiroplasma ixodetis* endosymbiont reveals past transfers between ticks and other arthropods. *Ticks Tick Borne Dis*. 2019;10:575–84. <https://doi.org/10.1016/j.ttbdis.2019.02.001>
- Olsthoorn F, Sprong H, Fonville M, Rocchi M, Medlock J, Gilbert L, et al. Occurrence of tick-borne pathogens in questing *Ixodes ricinus* ticks from Wester Ross, northwest Scotland. *Parasit Vectors*. 2021;14:430. <https://doi.org/10.1186/s13071-021-04946-5>
- Wass L, Grankvist A, Mattsson M, Gustafsson H, Krogfelt K, Olsen B, et al. Serological reactivity to *Anaplasma phagocytophilum* in neohrlichiosis patients. *Eur J Clin Microbiol Infect Dis*. 2018;37:1673–8. <https://doi.org/10.1007/s10096-018-3298-3>
- Grankvist A, Sandelin LL, Andersson J, Fryland L, Wilhelmsson P, Lindgren P-E, et al. Infections with *Candidatus Neohrlichia mikurensis* and cytokine responses in 2 persons bitten by ticks, Sweden. *Emerg Infect Dis*. 2015;21:1462–5. <https://doi.org/10.3201/eid2108.150060>
- Sjöwall J, Kling K, Ochoa-Figueroa M, Zachrisson H, Wennerås C. *Neohrlichia mikurensis* causing thrombosis and relapsing fever in a lymphoma patient receiving rituximab. *Microorganisms*. 2021;9:2138. <https://doi.org/10.3390/microorganisms9102138>
- Madison-Antenucci S, Kramer LD, Gebhardt LL, Kauffman E. Emerging tick-borne diseases. *Clin Microbiol Rev*. 2020;33:e00083–18. <https://doi.org/10.1128/CMR.00083-18>
- Rodrigues LP, Teixeira VR, Alencar-Silva T, Simonassi-Paiva B, Pereira RW, Pogue R, et al. Hallmarks of aging and immunosenescence: connecting the dots. *Cytokine Growth Factor Rev*. 2021;59:9–21. <https://doi.org/10.1016/j.cytogfr.2021.01.006>

---

Address for correspondence: Thomas Schön, Department of Infectious Diseases, Kalmar County Hospital (Linköping University), SE-391 85 Kalmar, Sweden. Email: thomas.schon@liu.se

# Toxigenic *Corynebacterium diphtheriae* Infection in Cat, Texas, USA

Ronald Tyler Jr.,<sup>1</sup> Layda Rincon,<sup>1</sup> Michael R. Weigand, Lingzi Xiaoli, Anna M. Acosta, Daniel Kurien, Hong Ju, Sonia Lingsweiler, Emilie Yvonne Prot

We report a toxigenic strain of *Corynebacterium diphtheriae* isolated from an oozing dermal wound in a pet cat in Texas, USA. We also describe the epidemiologic public health efforts conducted to identify potential sources of infection and mitigate its spread and the molecular and genetic studies performed to identify the bacterium.

Diphtheria, caused by toxigenic strains of the bacterium *Corynebacterium diphtheriae*, can result in life-threatening respiratory disease or cutaneous infections. Toxigenicity is contingent on successful bacterial expression of diphtheria toxin, encoded by a toxin gene (*tox*). Toxigenic *C. diphtheriae* is considered nearly exclusively a human pathogen, and humans are believed to be the reservoir. Because of high population coverage with diphtheria toxoid-containing vaccines, few diphtheria cases are reported in the United States. The most recently reported toxigenic infections were cutaneous and associated with international travel (1–4).

A 2016 article reviewing available literature on *C. diphtheriae* isolated from animals identified 12 cases globally, 4 in dogs, 4 in cats, 2 in horses, 1 in a cow, and 1 in a fox. These infections were toxigenic only in 2 dogs and the 2 horses; 1 of the horses was identified in the United States (5,6). In contrast, toxigenic *Corynebacterium ulcerans* is a zoonotic organism that causes diphtheria-like illness in humans clinically

indistinguishable from illness caused by toxigenic *C. diphtheriae*; it is more common than the diphtheria pathogen among household pets and their owners (7).

To date, toxigenic diphtheria has not been detected in cats; however, nontoxigenic strains have been identified, including 2 from the ears of cats in the United States and 1 from the nose of a cat in Belgium (8,9). Although these 3 strains contained the *tox* gene, they were not toxin producing. Of note, the strains identified in the United States have recently been reclassified as a novel species, *C. rouxii*, because of biochemical and genetic differences with *C. diphtheriae* (10).

Recommended public health response to toxigenic diphtheria infections in humans in the United States involves isolating and treating the index case-patient, identifying contacts, and vaccinating the patient and contacts with diphtheria toxoid-containing vaccine if it has been  $\geq 5$  years since the last dose (11). After treatment is completed, the index case-patient should be tested to confirm eradication of toxigenic *C. diphtheriae* and contacts monitored for development of diphtheria illness for 7–10 days after their most recent exposure; nasal and throat swab specimens should be collected to test for carriage, and prophylactic antibiotics should be administered. No formal recommendations exist for toxigenic diphtheria in animals because of its rarity, but health departments may pursue interventions similar to those to prevent transmission in humans.

In October 2020, a veterinary clinic in southern Texas, USA, evaluated a male domestic shorthair cat 10 years of age for an oozing wound with multiple abscess pockets in its left flank. The clinic reported culturing *Mycobacterium farcinogenes* from a similar lesion on the cat in May 2018. A swab of the new wound was submitted for culturing to the Texas A&M Veterinary

Author affiliations: Texas Department of State Health Services, Harlingen, Texas, USA (R. Tyler Jr., E.Y. Prot); Cameron County Public Health Department, San Benito, Texas, USA (L. Rincon); Centers for Disease Control and Prevention, Atlanta, Georgia, USA (M.R. Weigand, A.M. Acosta, H. Ju); IHRC, Inc., Atlanta (L. Xiaoli); ASRT, Inc., Atlanta (D. Kurien); Texas A&M College of Veterinary Medicine, College Station, Texas, USA (S. Lingsweiler)

DOI: <https://doi.org/10.3201/eid2808.220018>

<sup>1</sup>These authors contributed equally to this article.

Medical Diagnostic Laboratory (College Station, TX, USA). The cat was empirically started on marbofloxacin, but after the owner reported worsening of the wound 2 days later, the attending veterinarian added amoxicillin/clavulanic acid to the regimen. The laboratory isolated 2 bacteria, *C. diphtheriae* and *M. farcinogenes*, and sent the *C. diphtheriae* isolate to the Centers for Disease Control and Prevention (CDC; Atlanta, GA, USA) for confirmation and toxigenicity testing. An investigation was conducted to identify possible exposures to toxicogenic *C. diphtheriae*, identify potential human and animal carriers, and provide prevention measures. We report details of the investigation and subsequent molecular and genetic studies.

### The Study

The owner of the index cat lived in a house with her husband and reported having no regular visitors the month before the cat developed the flank abscess. The owner reported they had 5 indoor-only cats, including the index cat, and 4 dogs that spent time both indoors and outdoors. The cat's owner had received tetanus toxoid, reduced diphtheria toxoid, and acellular pertussis (Tdap) vaccine 3 years earlier; her husband provided no vaccine history. Cameron County Public Health (San Benito, TX, USA) collected an oropharyngeal swab specimen from the owner in November 2020 and submitted it to the Texas Department of State Health Services laboratory (Harlingen, TX, USA) for testing; the sample was negative for *C. diphtheriae*. Her husband did not submit a specimen. Both refused antibiotic prophylaxis, and the husband refused diphtheria toxoid-containing vaccine.

The owners allowed oropharyngeal swab specimens to be collected from the 4 contact cats but refused to have their dogs tested. The cat samples were submitted to CDC but were negative for *C. diphtheriae* by isolation or PCR detection. One posttreatment swab specimen collected from the wound of the index cat in November was negative for *C. diphtheriae*. In December, the owner reported the wound appeared to be healing.

Ten veterinary staff were identified as having potential exposures to the *C. diphtheriae* wound; 9 worked with the abscess wearing gloves and masks but no eye protection, and 1 was bitten while handling the cat. The Cameron County Public Health clinic collected oropharyngeal swab specimens from 9/10 exposed staff, and all tested negative for *C. diphtheriae* at the Texas Department of State Health Services laboratory. Six of 10 exposed staff received prophylactic antibiotics; 5/10 reported receiving no diphtheria toxoid vaccine within 5 years and so

received vaccine boosters, and the remaining 5 reported having received diphtheria toxoid vaccine within 5 years. Human and animal contacts were assessed for clinical signs and symptoms, including skin lesions, consistent with diphtheria, but no signs or symptoms were observed.

CDC conducted microbiologic and molecular characterization of the *C. diphtheriae* isolate (named PC1297), as described elsewhere (12,13). The isolate was confirmed as *C. diphtheriae* biotype gravis, and PCR confirmed presence of the tox gene. Modified Elek testing showed the isolate produced diphtheria toxin (14). The isolate was further characterized by whole-genome shotgun sequencing on an Illumina Miseq (<https://www.illumina.com>) (Appendix, <https://wwwnc.cdc.gov/EID/article/28/8/22-0018-App1.pdf>). Genome sequence-based multilocus sequence typing identified the isolate as ST705, unique among the 754 publicly available *C. diphtheriae* isolate sequences, and genome assembly confirmed presence of tox-encoding corynephage (Appendix) (15). Phylogenetic reconstruction of 273 *C. diphtheriae* isolate sequences, representing 270 unique sequence types and including 8 isolates from domestic animals. The results indicated that PC1297 was not related to isolates from previous cases reported in cats, including those now classified as *C. rouxii* (Appendix), nor was it closely related to any available human sequences; the nearest neighboring sequence in the phylogenetic tree, ERR3932636, sequence type 669, was 6,948 single-nucleotide polymorphisms distant.

### Conclusion

We report public health response to a rare case of cutaneous toxicogenic diphtheria in a pet cat. Not all animal and human contacts could be tested, but *C. diphtheriae* was not detected among those tested; no source for the infection was identified. Comparative genomic analyses suggested that the identified strain differed from publicly available sequences of *C. diphtheriae*, including those from domestic pets, and the strain was not related to the neighboring *C. rouxii* sp. nov. Because of the limited availability of *C. diphtheriae* sequences from animals, there was insufficient data to determine whether the source of infection was from human or animal contact. Whereas our findings do not confirm whether animals might serve as reservoirs for diphtheria, they highlight the need for further study regarding transmission and environmental health. This case also reiterates the criticality of promptly discovering and identifying *C. diphtheriae* infections in companion animals for preventing spread of the disease to susceptible animals and humans.

## Acknowledgments

We thank the Cameron County Public Health Department for leading the investigations and our CDC partners for their guidance and laboratory analysis of the samples collected.

## About the Author

Dr. Tyler Jr. is a regional zoonosis veterinarian with the Texas Department of State Health Services. He is a veterinary pathologist with an interest in infectious diseases, diagnostic pathology, and veterinary public health. Ms. Rincon is an epidemiologist with the Cameron County Public Health Department. She is interested in infectious diseases and public health prevention.

## References

- Hill HA, Yankey D, Elam-Evans LD, Singleton JA, Sterrett N. Vaccination coverage by age 24 months among children born in 2017 and 2018—National Immunization Survey-Child, United States, 2018–2020. *MMWR Morb Mortal Wkly Rep.* 2021;70:1435–40. <https://doi.org/10.15585/mmwr.mm7041a1>
- Pingali C, Yankey D, Elam-Evans LD, Markowitz LE, Williams CL, Fredua B, et al. National, regional, state, and selected local area vaccination coverage among adolescents aged 13–17 years—United States, 2020. *MMWR Morb Mortal Wkly Rep.* 2021;70:1183–90. <https://doi.org/10.15585/mmwr.mm7035a1>
- Otshudiema JO, Acosta AM, Cassidy PK, Hadler SC, Hariri S, Tiwari TSP. Respiratory illness caused by *Corynebacterium diphtheriae* and *C. ulcerans*, and use of diphtheria antitoxin in the United States, 1996–2018. *Clin Infect Dis.* 2021;73:e2799–806. <https://doi.org/10.1093/cid/ciaa1218>
- Griffith J, Bozio CH, Poel AJ, Fitzpatrick K, DeBolt CA, Cassidy P, et al. Imported toxin-producing cutaneous diphtheria—Minnesota, Washington, and New Mexico, 2015–2018. *MMWR Morb Mortal Wkly Rep.* 2019;68:281–4. <https://doi.org/10.15585/mmwr.mm6812a2>
- Sing A, Konrad R, Meinel DM, Mauder N, Schwabe I, Sting R. *Corynebacterium diphtheriae* in a free-roaming red fox: case report and historical review on diphtheria in animals. *Infection.* 2016;44:441–5. <https://doi.org/10.1007/s15010-015-0846-y>
- Henricson B, Segarra M, Garvin J, Burns J, Jenkins S, Kim C, et al. Toxigenic *Corynebacterium diphtheriae* associated with an equine wound infection. *J Vet Diagn Invest.* 2000;12:253–7. <https://doi.org/10.1177/104063870001200309>
- Monaco M, Sacchi AR, Scotti M, Mancini F, Riccio C, Errico G, et al. Respiratory diphtheria due to *Corynebacterium ulcerans* transmitted by a companion dog, Italy 2014. *Infection.* 2017;45:903–5. [Erratum in *Infection.* 2017;45:931.] <https://doi.org/10.1007/s15010-017-1040-1>
- Hall AJ, Cassidy PK, Bernard KA, Bolt F, Steigerwalt AG, Bixler D, et al. Novel *Corynebacterium diphtheriae* in domestic cats. *Emerg Infect Dis.* 2010;16:688–91. <https://doi.org/10.3201/eid1604.091107>
- Detemmerman L, Rousseaux D, Efstratiou A, Schirvel C, Emmerechts K, Wybo I, et al. Toxigenic *Corynebacterium ulcerans* in human and non-toxigenic *Corynebacterium diphtheriae* in cat. *New Microbes New Infect.* 2013;1:18–9. <https://doi.org/10.1002/2052-2975.9>
- Badell E, Hennart M, Rodrigues C, Passet V, Dazas M, Panunzi L, et al. *Corynebacterium rouxii* sp. nov., a novel member of the diphtheriae species complex. *Res Microbiol.* 2020;171:122–7. <https://doi.org/10.1016/j.resmic.2020.02.003>
- Faulkner AE, Bozio CH, Acosta AM, Tiwari TSP. Chapter 1: Diphtheria. In: Roush SM, Baldy LM, Kirkconnell Hall MA, editors. *Manual for the surveillance of vaccine-preventable diseases.* Atlanta: Centers for Disease Control and Prevention; 2020.
- Efstratiou A, Maple PAC; World Health Organization Regional Office for Europe. *Manual for the laboratory diagnosis of diphtheria.* Copenhagen: The Office; 1994.
- Williams MM, Waller JL, Aneke JS, Weigand MR, Diaz MH, Bowden KE, et al. Detection and characterization of diphtheria toxin gene-bearing *Corynebacterium* species through a new real-time PCR assay. *J Clin Microbiol.* 2020;58:e00639–20. PubMed <https://doi.org/10.1128/JCM.00639-20>
- Engler KH, Glushkevich T, Mazurova IK, George RC, Efstratiou A. A modified Elek test for detection of toxigenic corynebacteria in the diagnostic laboratory. *J Clin Microbiol.* 1997;35:495–8. <https://doi.org/10.1128/jcm.35.2.495-498.1997>
- Jolley KA, Bray JE, Maiden MC. Open-access bacterial population genomics: BIGSdb software, the PubMLST.org website and their applications. *Wellcome Open Res.* 2018;3:124. PubMed <https://doi.org/10.12688/wellcomeopenres.14826.1>

---

Address for correspondence: Ronald Tyler Jr., Texas Department of State Health Services, Public Health Region 11, 601 W Sesame Dr, Harlingen, TX 78550, USA; email: [Ronald.Tyler@dshs.texas.gov](mailto:Ronald.Tyler@dshs.texas.gov)

# Child Melioidosis Deaths Caused by *Burkholderia pseudomallei*–Contaminated Borehole Water, Vietnam, 2019

Quyen T.L. Tran, Phuc H. Phan, Linh N.H. Bui, Ha T.V. Bui, Ngoc T.B. Hoang, Dien M. Tran, Trung T. Trinh

Within 8 months, 3 children from 1 family in northern Vietnam died from melioidosis. *Burkholderia pseudomallei* of the same sequence type, 541, was isolated from clinical samples, borehole water, and garden and rice field soil. Boreholes should be properly constructed and maintained to avoid *B. pseudomallei* contamination.

The gram-negative soil-dwelling saprophytic bacterium *Burkholderia pseudomallei* causes melioidosis, a fatal disease highly endemic to Southeast Asia and northern Australia (1). Humans can be infected with *B. pseudomallei* via inoculation, inhalation, and ingestion. Rice farmers are at high risk for infection because of their frequent exposure to soil and water, but newborns, children, and older persons also are at risk (2,3). We report 3 melioidosis deaths among children in northern Vietnam.

## The Study

In November 2019, the Preventive Health Center of Soc Son district in Vietnam reported the deaths of 3 children from 1 family. The first child, a 7-year-old girl, had a high fever and abdominal pain on April 6, 2019. Two days later, she was admitted to a local hospital; after 1 day, she was transferred to St. Paul Hospital in Hanoi, where septic shock was diagnosed. She died on April 9, shortly after admission, before any diagnostic tests were performed.

On October 27, 2019, the second child, a 5-year-old boy, had a high fever and abdominal pain around the umbilicus. He was admitted to Vietnam National Children's Hospital in Hanoi on October 28 with diagnosed septic shock. Abdominal and chest radiographs

and abdominal ultrasound results were unremarkable. His blood culture grew *B. pseudomallei*, and he died on October 31.

The third child, a 13-month-old boy, had a high fever and poor appetite on November 10, 2019. According to his grandparents, he had black stool, like his sister and brother. He was admitted to Vietnam National Children's Hospital; chest radiography results were unremarkable, but *B. pseudomallei* was cultured from his blood sample. He died on November 16.

We retrieved laboratory findings from all hospitals to which these children were admitted. Results showed leukopenia, neutropenia, thrombocytopenia, and high procalcitonin and C-reactive protein in all children's blood. Liver dysfunction was diagnosed in all 3 children, but kidney dysfunction was recognized only in the 2 older children. We detected no identifiable risk factors (Table 1).

To trace the source of infection, on November 17, 2019, we visited the family home in the midland region of northern Vietnam (Figure 1). During our active surveillance for melioidosis cases admitted to provincial and tertiary hospitals surrounding Hanoi (4), no previous cases had been reported from this area.

We interviewed the parents and grandparents using epidemiologic questions about all the children's daily activities inside and outside the house. The family used water supplied from 3 boreholes: 1 for bathing (borehole A), 1 for livestock (borehole B), and 1 for human consumption (borehole C). During our first environmental investigation, we collected samples of front garden soil (n = 7), borehole water (n = 9), and boiled drinking water (n = 1). We performed qualitative culture for *B. pseudomallei*, and all 3 water samples collected from borehole A tested positive (Appendix, <https://wwwnc.cdc.gov/EID/article/28/8/22-0113-App1.pdf>).

Author affiliations: Vietnam National University, Hanoi, Vietnam (Q.T.L. Tran, L.N.H. Bui, H.T.V. Bui, T.T. Trinh); Vietnam National Children's Hospital, Hanoi (P.H. Phan, N.T.B. Hoang, D.M. Tran)

DOI: <https://doi.org/10.3201/eid2808.220113>

**Table 1.** Demographic and clinical characteristics and corresponding isolates from 3 children who died of melioidosis caused by *Burkholderia pseudomallei*-contaminated borehole water, Vietnam, 2019\*

| Characteristics                        | Case 1  | Case 2  | Case 3  |       |       |       |       |       |
|--|---|---|---|-------|-------|-------|-------|-------|
| Age, y/sex                             | 7/F   | 5/M   | 1/M   |       |       |       |       |       |
| Date                                   |   |   |   |       |       |       |       |       |
| Symptom onset                          | Apr 6   | Oct 27  | Nov 10  |       |       |       |       |       |
| Hospital admission                     | Apr 9   | Oct 28  | Nov 11  |       |       |       |       |       |
| Death                                  | Apr 9   | Oct 31  | Nov 16  |       |       |       |       |       |
| Signs and symptoms                     | High fever, abdominal pain, vomiting, diarrhea with mucous, tachycardia, and cyanosis | High fever, abdominal pain, vomiting, tachypnea, and tachycardia  | High fever, poor appetite, mild pitting edema in the feet and hands, tachypnea, and tachycardia |       |       |       |       |       |
| Underlying disease                     | Not detectable  | Not detectable  | Not detectable  |       |       |       |       |       |
| Microbiology                           |   |   |   |       |       |       |       |       |
| Blood culture                          | ND  | <i>B. pseudomallei</i> -positive  | <i>B. pseudomallei</i> -positive  |       |       |       |       |       |
| Sequence type                          | ND  | 541   | 541   |       |       |       |       |       |
| Other sample cultures                  | ND  | ND  | ND  |       |       |       |       |       |
| Antimicrobial drug treatment           | Cefoperazone in the first day; then efoperazone and amikacin on subsequent days       | Ceftriaxone, tobramycin, and metronidazole in the first day; then meropenem and levofloxacin on subsequent days | Ceftazidime in the first 2 days; meropenem in the last 3 days                                   |       |       |       |       |       |
| Imaging at admission                   |   |   |   |       |       |       |       |       |
| Chest radiograph                       | NA  | No abnormalities noted  | No abnormalities noted  |       |       |       |       |       |
| Abdominal radiograph                   | NA  | No abnormalities noted  | NA  |       |       |       |       |       |
| Abdominal ultrasound                   | NA  | No abnormalities noted  | NA  |       |       |       |       |       |
| Laboratory findings                    | Day 1   | Day 2   | Day 1   | Day 2 | Day 1 | Day 3 | Day 4 | Day 5 |
| WBC, × 10 <sup>9</sup> cells/L         | 0.6   | 0.7   | 25.2  | 0.35  | 10.8  | 7.5   | 1.35  | 1.06  |
| Neutrophils, × 10 <sup>9</sup> cells/L | NA  | 0.12  | 22.8  | 0.05  | 8.4   | 4.0   | 0.76  | 0.38  |
| Lymphocytes, × 10 <sup>9</sup> cells/L | NA  | 0.48  | 1.07  | 0.29  | 1.52  | 3.07  | 0.50  | 0.55  |
| Platelets, × 10 <sup>9</sup> cells/L   | 47  | 36  | 272   | 29    | 264   | 172   | 67    | 32    |
| Urea, mmol/L                           | 8.9   | 9.9   | NA  | 9.8   | 2.2   | 1.4   | 3.7   | 4.1   |
| Creatinine, μmol/L                     | 91  | 123   | NA  | 124   | 45    | 33    | 55    | 71    |
| AST, U/L                               | 571   | 713   | NA  | 602   | 23    | 59    | 185   | 269   |
| ALT, U/L                               | 226   | 258   | NA  | 166   | 10    | 40    | 94    | 73    |
| CRP, mg/L                              | 124   | NA  | 26  | 148   | 57    | NA    | 209   | 158   |
| PCT, ng/mL                             | NA  | >100  | NA  | >100  | 9     | 43    | NA    | NA    |

\*Data were collected from the St. Paul Hospital and Vietnam National Children's Hospital, except for the laboratory findings for case 1, which were retrieved from the child's local hospital. ALT, alanine aminotransferase; AST, aspartate aminotransferase; CRP, C-reactive protein; NA, not available; ND, not done; PCT, procalcitonin; WBC, white blood cell count.

We revisited the home on November 23, 2019, and asked the family about the history of borehole A. In brief, the borehole was drilled in 2010. In 2015, the family reconstructed the back garden and added a new soil layer, resulting in the bore cap being ≈80 cm below the soil surface (Figure 2, panel A). At the end of 2018, the foot valve in the suction pipe of the dynamic electric pump was damaged, and the bore cap was not sealed after the damage was repaired (Figure 2, panel B). We suspected rainwater and surface soil particles contaminated with *B. pseudomallei* drained into the groundwater via the opened borehole. To test this hypothesis, we conducted a second round of environmental sampling, focusing on borehole A and the nearby surface soil. We collected 26 borehole water and 46 garden soil samples. Within a 1-km radius of the home, we also collected 39 water samples from other boreholes, 30 surface water samples from 10 ponds, and 40 soil samples from 8 rice fields (Figure 1; Appendix).

We found 26 (100%) water samples collected from borehole A and 27 (58.7%) garden soil samples from 8 (80%) sampling points near the borehole were *B. pseudomallei*-positive by qualitative culture. These findings supported our hypothesis that *B. pseudomallei* from surface soil might have contaminated the groundwater through the unsealed bore cap during the rainy season, which starts in April and coincided with the first child's illness and death. Another 5 (12.5%) soil samples from 2 (25%) rice fields also tested *B. pseudomallei*-positive. Quantitative culture showed that the median *B. pseudomallei* count was 406 CFU/g (range 12–746 CFU/g) in soil (Appendix). Of 26 water samples collected from borehole A, 2 (7.7%) grew *B. pseudomallei* on the initial agar plates and had a median *B. pseudomallei* count of 2 CFU/mL (Table 2).

We selected 20 *B. pseudomallei* isolates for multi-locus sequence typing (MLST) (5): 7 from borehole A, 6 from back garden soil, 5 from rice field soil,

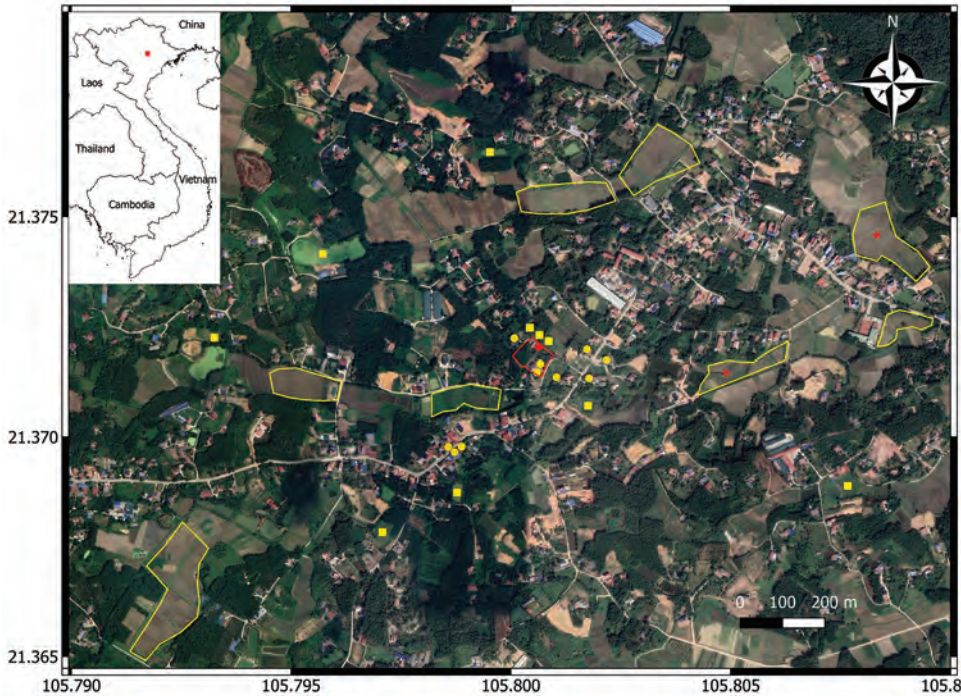


**Figure 1.** Environmental sampling sites in an investigation of 3 child deaths from melioidosis caused by *Burkholderia pseudomallei*–contaminated borehole water, Vietnam, 2019. The satellite map was created using QGIS software version 3.22.1 (<https://www.qgis.org>). Red outline indicates the family property where the children lived; red circle is borehole A from which *B. pseudomallei* was isolated. Yellow outlines are rice fields from which soil samples were collected; red stars indicate rice fields that tested positive for *B. pseudomallei*. Yellow circles indicate neighbors’ boreholes and yellow squares indicate neighbors’ ponds from which water samples were collected. Inset map shows Vietnam; red square indicates sampling area.

and 2 from blood samples from cases 2 and 3. MLST showed an identical sequence type (ST), 541, among all samples (Table 2).

**Conclusions**

*B. pseudomallei* is ubiquitously distributed in soil and surface water throughout the tropics, including in Asia, the Pacific Islands, sub-Saharan Africa, and Latin America, where boreholes are the most common water supply in the rural areas (1,6,7). In addition to other waterborne infections (7), untreated water supplies have been implicated in previous human *B. pseudomallei* infections (8–10). *B. pseudomallei* also was isolated from the compacted earth floor under

the bathing tub of a woman who died from septicemic melioidosis in Brazil (11).

Studies in Australia and Thailand detected diverse STs among *B. pseudomallei* isolates from an unchlorinated bore water site and a single soil sample (12,13), but our analysis revealed a single ST in the borehole, nearby garden, and surrounding rice fields. Because all 3 infections occurred in children, we believe *B. pseudomallei* transmission likely occurred through ingestion of contaminated water during bathing, especially considering that the 13-month-old boy was not in contact with garden or rice field soil. Ingestion also could explain the gastrointestinal symptoms the children exhibited.



**Figure 2.** Borehole involved in 3 child melioidosis deaths caused by *Burkholderia pseudomallei*–contaminated borehole water, Vietnam, 2019. A) View of area around borehole. The bore cap is ≈80 cm below the soil surface inside the masonry area. Red arrow indicates cracks in the masonry construction that might enable rainwater and soil particles to drain into the borehole area. B) View from above the borehole. Red arrow indicates the unsealed, opened gap around the borehole, which likely enabled rainwater and soil particles to drain into the groundwater during the rainy season.

**Table 2.** Culture results and genotype data from environmental samples in a study of 3 child melioidosis deaths caused by *Burkholderia pseudomallei*-contaminated borehole water, Vietnam, 2019\*

| Sample type, date                | No. samples | No. sampling points† | Qualitative culture      |                                   | Median quantitative count, CFU (range) | No. isolates selected for MLST‡ | ST  |
|----------------------------------|-------------|----------------------|--------------------------|-----------------------------------|--|---------------------------------|-----|
|                                  |             |                      | No. (%) positive samples | No. (%) positive sampling points† |  |                                 |     |
| Sampling 1, 2019 Nov 17          |             |                      |                          |                                   |  |                                 |     |
| Front garden soil                | 7           | 7                    | 0                        | 0                                 | NP                                     | NA                              |     |
| Water from borehole A            | 3           | 1                    | 3 (100)                  | 1 (100)                           | 2§                                     | 3                               | 541 |
| Water from borehole B            | 3           | 1                    | 0                        | 0                                 | NP                                     | NA                              | NA  |
| Water from borehole C            | 3           | 1                    | 0                        | 0                                 | NP                                     | NA                              | NA  |
| Boiled drinking water            | 1           | 1                    | 0                        | 0                                 | NP                                     | NA                              | NA  |
| Sampling 2, 2019 Nov 23          |             |                      |                          |                                   |  |                                 |     |
| Back garden soil near borehole A | 46          | 10                   | 27 (58.7)                | 8 (80)                            | 406 (12–746)§                          | 6                               | 541 |
| Rice field soil                  | 40          | 8                    | 5 (12.5)                 | 2 (25)                            | ND                                     | 5                               | 541 |
| Water from borehole A            | 26          | 1                    | 26 (100)                 | 1 (100)                           | ND                                     | 4                               | 541 |
| Water from borehole B            | 3           | 1                    | 0                        | 0                                 | NP                                     | NA                              | NA  |
| Water from borehole C            | 3           | 1                    | 0                        | 0                                 | NP                                     | NA                              | NA  |
| Water from neighbors' borehole   | 33          | 11                   | 0                        | 0                                 | NP                                     | NA                              | NA  |
| Water from ponds                 | 30          | 10                   | 0                        | 0                                 | NP                                     | NA                              | NA  |

\*CFU, colony forming unit; MLST, multilocus sequence typing; NA, not applicable; ND, not detected; NP, not performed; ST, sequence type.

†Sampling points refer to garden, borehole, field, and pond sites.

‡We selected 20 *B. pseudomallei* isolates for sampling; 2 patient isolates are not shown here.

§*B. pseudomallei* colonies were countable only in 2 borehole water samples and 5 garden soil samples (Appendix, <https://wwwnc.cdc.gov/EID/article/28/8/22-0113-App1.pdf>). In water samples CFU/mL; in soil samples CFU/g.

*B. pseudomallei* ST541 has been reported from human melioidosis cases in northern Vietnam (3) and has only been described from southeast Asia thus far. During previous surveillance (4), we found other ST541 isolates in clinical and environmental samples from north and north-central Vietnam. An ST541 isolate available in a public MLST database (<https://pubmlst.org/organisms/burkholderia-pseudomallei>; accessed 2021 Dec 8) was from a human case in Hainan, China, which is close to the area of Vietnam where these 3 melioidosis deaths occurred. From our clinical data retrieval (3,4), 5 of 8 patients infected with *B. pseudomallei* ST541 died, which could mean ST541 is more virulent than other STs, but further data are needed.

From the epidemiologic investigation and field study at the family home, we became aware of the construction and maintenance of the borehole, which had an unsealed cap and an open borehole below the soil surface. The unsealed borehole probably enabled *B. pseudomallei* from surface soil to contaminate groundwater during rainfall. Other studies have reported higher rates of gastrointestinal pathogens in water from boreholes with unsealed annuli (14,15). Therefore, persons using boreholes in countries where melioidosis is endemic should ensure proper construction and maintenance to avoid contamination with *B. pseudomallei* and other pathogens from surface soil.

### Acknowledgments

We express our deepest condolences to the family members and sincerely thank them for providing information during the investigation.

This work was supported by Vietnam National University, Hanoi, Vietnam (grant no. QG.21.57). Q.T.L.T. received a PhD scholarship from the Vingroup Innovation Foundation (award no. 2020.TS.33).

### About the Author

Mrs. Tran is a PhD candidate at the Laboratory for Microbial Pathogens, VNU–Institute of Microbiology and Biotechnology, Vietnam National University, Hanoi, Vietnam. Her research interests include melioidosis diagnosis and detection of *B. pseudomallei* from environmental samples.

### References

- Limmathurotsakul D, Golding N, Dance DA, Messina JP, Pigott DM, Moyes CL, et al. Predicted global distribution of *Burkholderia pseudomallei* and burden of melioidosis. *Nat Microbiol*. 2016;1:15008. PubMed <https://doi.org/10.1038/nmicrobiol.2015.8>
- Limmathurotsakul D, Kanoksil M, Wuthiekanun V, Kitphati R, deStavola B, Day NP, et al. Activities of daily living associated with acquisition of melioidosis in northeast Thailand: a matched case-control study. *PLoS Negl Trop Dis*. 2013;7:e2072. <https://doi.org/10.1371/journal.pntd.0002072>
- Phuong DM, Trung TT, Breitbach K, Tuan NQ, Nübel U, Flunker G, et al. Clinical and microbiological features of melioidosis in northern Vietnam. *Trans R Soc Trop Med Hyg*. 2008;102(Suppl 1):S30–6. [https://doi.org/10.1016/S0035-9203\(08\)70009-9](https://doi.org/10.1016/S0035-9203(08)70009-9)
- Trinh TT, Nguyen LDN, Nguyen TV, Tran CX, Le AV, Nguyen HV, et al. Melioidosis in Vietnam: recently improved recognition but still an uncertain disease burden after almost a century of reporting. *Trop Med Infect Dis*. 2018;3:39. <https://doi.org/10.3390/tropicalmed3020039>
- Godoy D, Randle G, Simpson AJ, Aanensen DM, Pitt TL, Kinoshita R, et al. Multilocus sequence typing and evolutionary relationships among the causative agents of

melioidosis and glanders, *Burkholderia pseudomallei* and *Burkholderia mallei*. J Clin Microbiol. 2003;41:2068–79. <https://doi.org/10.1128/JCM.41.5.2068-2079.2003>

6. Foster I, Priadi C, Kotra KK, Odagiri M, Rand EC, Willetts J. Self-supplied drinking water in low- and middle-income countries in the Asia-Pacific. npj Clean Water. 2021;4:37. <https://doi.org/10.1038/s41545-021-00121-6>
7. Odiyo JO, Mathoni MM, Makungo R. Health risks and potential sources of contamination of groundwater used by public schools in Vhuronga 1, Limpopo Province, South Africa. Int J Environ Res Public Health. 2020;17:6912. <https://doi.org/10.3390/ijerph17186912>
8. Limmathurotsakul D, Wongsuvan G, Aanensen D, Ngamwilai S, Saiprom N, Rongkard P, et al. Melioidosis caused by *Burkholderia pseudomallei* in drinking water, Thailand, 2012. Emerg Infect Dis. 2014;20:265–8. <https://doi.org/10.3201/eid2002.121891>
9. Inglis TJ, Garrow SC, Henderson M, Clair A, Sampson J, O'Reilly L, et al. *Burkholderia pseudomallei* traced to water treatment plant in Australia. Emerg Infect Dis. 2000;6:56–9.
10. Currie BJ, Mayo M, Anstey NM, Donohoe P, Haase A, Kemp DJ. A cluster of melioidosis cases from an endemic region is clonal and is linked to the water supply using molecular typing of *Burkholderia pseudomallei* isolates. Am J Trop Med Hyg. 2001;65:177–9. <https://doi.org/10.4269/ajtmh.2001.65.177>
11. Rolim DB, Vilar DC, Sousa AQ, Miralles IS, Almeida de Oliveira DC, Harnett G, et al. Melioidosis, northeastern Brazil. Emerg Infect Dis. 2005;11:1458–60. <https://doi.org/10.3201/eid1109.050493>
12. Mayo M, Kaesti M, Harrington G, Cheng AC, Ward L, Karp D, et al. *Burkholderia pseudomallei* in unchlorinated domestic bore water, tropical northern Australia. Emerg Infect Dis. 2011;17:1283–5. <https://doi.org/10.3201/eid1707.100614>
13. Wuthiekanun V, Limmathurotsakul D, Chantratita N, Feil EJ, Day NP, Peacock SJ. *Burkholderia pseudomallei* is genetically diverse in agricultural land in northeast Thailand. PLoS Negl Trop Dis. 2009;3:e496. <https://doi.org/10.1371/journal.pntd.0000496>
14. Knappett PS, McKay LD, Layton A, Williams DE, Alam MJ, Mailloux BJ, et al. Unsealed tubewells lead to increased fecal contamination of drinking water. J WaterHealth. 2012;10:565–78. <https://doi.org/10.2166/wh.2012.102>
15. MacDonald AM, Calow RC. Developing groundwater for secure rural water supplies in Africa. Desalination. 2009;248:546–56. <https://doi.org/10.1016/j.desal.2008.05.100>

Address for correspondence: Trung T. Trinh, Laboratory for Microbial Pathogens, VNU–Institute of Microbiology and Biotechnology, Vietnam National University, 144 Xuan Thuy, Cau Giay, Hanoi, Vietnam; email: [ttrung@vnu.edu.vn](mailto:ttrung@vnu.edu.vn)

## Emerging Infectious Diseases Spotlight Topics

**etymologia**

Antimicrobial resistance • Ebola • Etymologia  
 Food safety • HIV-AIDS • Influenza • Rabies  
 Lyme disease • Malaria • MERS • Pneumonia  
 Tuberculosis • Ticks • Zika • Coronavirus

<https://wwwnc.cdc.gov/eid/page/spotlight-topics>

EID's spotlight topics highlight the latest articles and information on emerging infectious disease topics in our global community.

# Association of Phylogenomic Relatedness among *Neisseria gonorrhoeae* Strains with Antimicrobial Resistance, Austria, 2016–2020

Justine Schaeffer, Kathrin Lippert, Sonja Pleininger, Anna Stöger, Petra Hasenberger, Silke Stadlbauer, Florian Heger, Angelika Eigentler, Alexandra Geusau, Alexander Indra, Franz Allerberger, Werner Ruppitsch

We investigated genomic determinants of antimicrobial resistance in 1,318 *Neisseria gonorrhoeae* strains isolated in Austria during 2016–2020. Sequence type (ST) 9363 and ST11422 isolates had high rates of azithromycin resistance, and ST7363 isolates correlated with cephalosporin resistance. These results underline the benefit of genomic surveillance for antimicrobial resistance monitoring.

Gonorrhea, a sexually transmissible infection (STI) caused by *Neisseria gonorrhoeae*, is the second most common bacterial STI (1). Most gonorrhea cases are mild, but serious complications can occur. Gonorrhea is treated with antibiotics, and the recommended treatment is dual extended-spectrum cephalosporin (ESC)/azithromycin therapy or ceftriaxone monotherapy (2).

One of the main characteristics of *N. gonorrhoeae* is the plasticity of its genome, favoring the acquisition and dispersion of antimicrobial resistance (AMR). AMR is an increasing issue for gonorrhea treatment, and untreatable gonorrhea represents an imminent global health threat (3).

Whole-genome sequencing (WGS) provides high-resolution data that can support AMR surveillance.

We combined phenotypic AMR testing with WGS to investigate 1,318 *N. gonorrhoeae* strains isolated in Austria during 2016–2020 and identify genetic risk factors associated with AMR.

## The Study

This study encompassed 1,318 *N. gonorrhoeae* isolates collected in Austria during 2016–2020; isolates were available at the National Reference Centre for Gonococci. We tested all isolates for phenotypic resistance to azithromycin, cefixime, ceftriaxone, ciprofloxacin, tetracycline, and benzylpenicillin, as well as production of  $\beta$ -lactamase (i.e., cefinase positive) (Appendix, <https://wwwnc.cdc.gov/EID/article/28/8/22-0071-App1.pdf>). We followed European Committee on Antimicrobial Susceptibility Testing guidelines (4) to determine MIC thresholds used in this study.

We performed genomic DNA isolation, WGS, assembly, and contig filtering as described previously (5) (Appendix). We deposited raw reads in the National Center for Biotechnology Information Sequence Read Archive (project no. PRJNA771206). We obtained sequence types (STs) from WGS data by using the PubMLST schemes (6,7). We generated a local *N. gonorrhoeae* core-genome multilocus sequence typing (cgMLST) scheme with SeqSphere+ target definer tool version 6.0.0 (Ridom, <https://www.ridom.de>) (7) (Appendix). We investigated AMR genes by using allele libraries based on PathogenWatch in TOML format version 0.0.14 (8).

We performed time series analysis, linear regression, univariate analysis, multivariate analysis (logistic regression), and data visualization by using R version 4.0.4 (Appendix). We defined statistical significance as  $p < 0.05$ . We computed neighbor-joining

Author affiliations: European Centre for Disease Prevention and Control, Stockholm, Sweden (J. Schaeffer); Austrian Agency for Health and Food Safety, Vienna, Austria (J. Schaeffer, K. Lippert, S. Pleininger, A. Stöger, P. Hasenberger, S. Stadlbauer, F. Heger, A. Indra, F. Allerberger, W. Ruppitsch); MB-LAB Clinical Microbiology Laboratory, Innsbruck, Austria (A. Eigentler); Medical University of Vienna, Vienna (A. Geusau); Paracelsus Medical University of Salzburg, Salzburg, Austria (A. Indra); University of Natural Resources and Life Sciences, Vienna (W. Ruppitsch)

DOI: <https://doi.org/10.3201/eid2808.220071>

trees in SeqSphere+ by using the number of cgMLST allelic differences and exported the trees into R.

We classified isolates according to AMR (Figure 1, panel A; Table) and determined MIC distributions (Figure 1, panel B). We observed high levels of resistance to ciprofloxacin (60%) and tetracycline (46%) (Figure 1, panel A), which increased 5% per year for ciprofloxacin ( $p < 0.0001$ ) and 6% per year for tetracycline ( $p < 0.0001$ ). The percentage of penicillin-resistant isolates was 16% and decreased over the study period (2% per year;  $p < 0.0001$ ) (Figure 1, panel C); 14% of isolates were cefinase-positive, which increased by 2.7% per year ( $p < 0.0001$ ).

We detected azithromycin resistance in 9% of the isolates, which increased by 5% per year ( $p < 0.0001$ ) (Figure 1). Two isolates from 2020 exhibited high levels

of azithromycin resistance ( $MIC \geq 256 \mu\text{g/mL}$ ) but no other AMR. Resistance to ESC was rare; only 3% of isolates were resistant to cefixime, none were resistant to ceftriaxone, and 2.5% had reduced susceptibility to ceftriaxone ( $MIC > 0.032 \mu\text{g/mL}$ ). Cefixime resistance decreased by 0.9% per year ( $p < 0.0001$ ). Among cefixime-resistant isolates, 23/35 were resistant to ciprofloxacin and penicillin, qualifying as multidrug resistant.

The isolates belonged to 119 different STs in multilocus sequence typing, including 23 newly defined (STs 15803–15825). The most prevalent STs were ST7363 (170 isolates), ST9363 (151 isolates), and ST8156 (113 isolates), which comprised 33% of the isolates. We identified 215 NG-MAST types for 873/1,318 isolates; the most prevalent STs were 12302 (73 isolates), 5441 (59 isolates), and 387 (50 isolates).

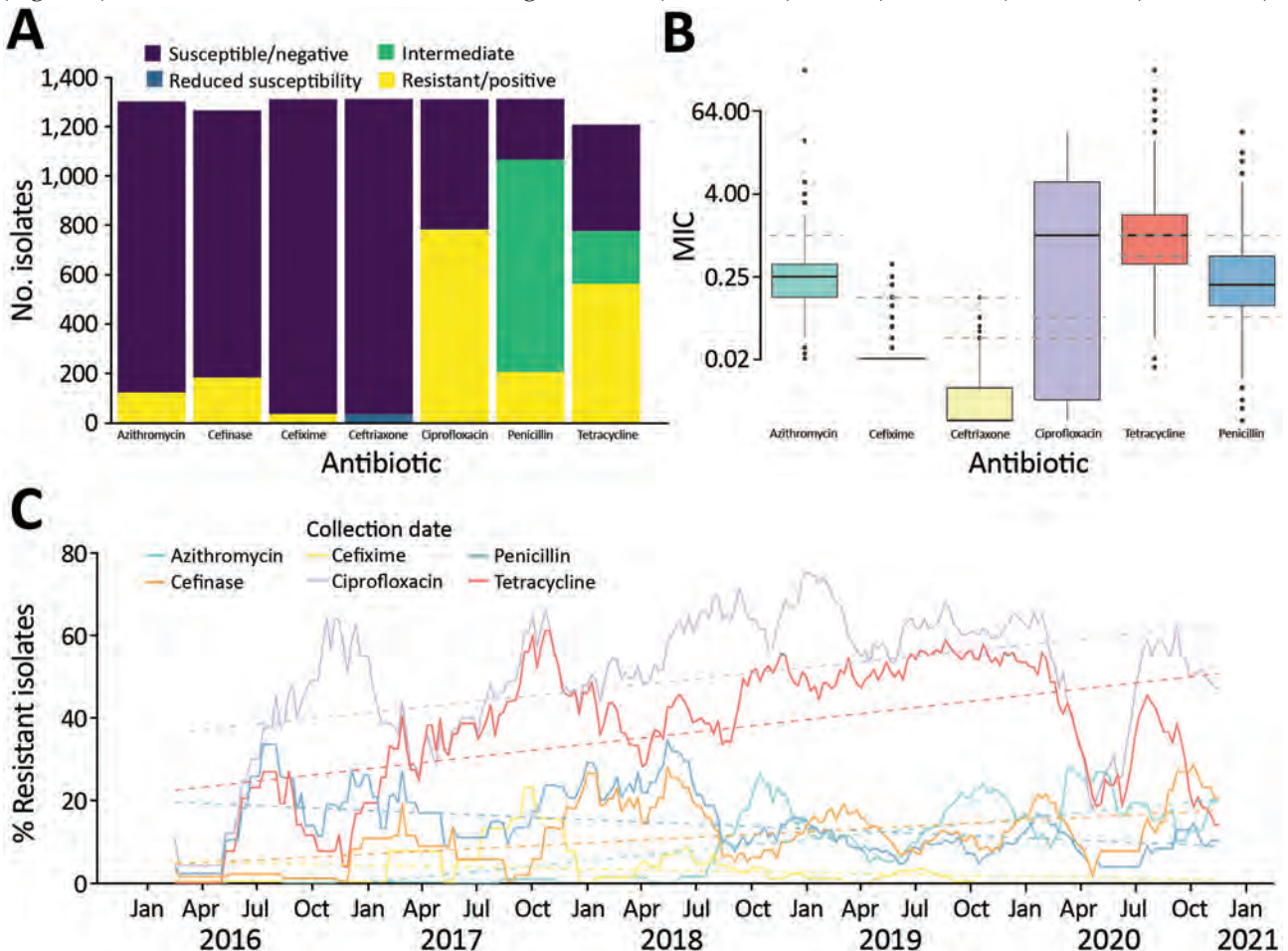


**Figure 1.** Antimicrobial resistance in 1,318 *Neisseria gonorrhoeae* isolates, Austria, 2016–2020. A) Number of isolates classified as susceptible, intermediate, or resistant. For ceftriaxone, isolates with reduced susceptibility are indicated in blue. For cefinase,  $\beta$ -lactamase producing isolates are indicated as positive (yellow). B) Boxplots of MIC obtained by Etest. Dashed lines indicate the thresholds used to classify the isolates as susceptible, intermediate, or resistant for ciprofloxacin, tetracycline, and penicillin, as susceptible or resistant for azithromycin, cefixime, and as susceptible, reduced susceptibility, or resistant for ceftriaxone. Horizontal lines within boxes indicate median, box tops and bottoms indicate quartiles 1 and 3, and dots indicate potential outliers. C) Evolution of the frequency of resistant isolates over time. Plain lines indicate the 13-week moving average of the percentage of isolates classified as resistant. Trends over time (obtained by linear regression) are represented by the dashed lines.

**Table.** Antimicrobial resistance classification and mean MIC of 1,318 *Neisseria gonorrhoeae* isolates, Austria, 2016–2020

| Antibiotic    | Antimicrobial resistance         | No. isolates | Total no. isolates*    | Frequency, % |
|---------------|----------------------------------|--------------|------------------------|--------------|
| Azithromycin  | Susceptible ( $\leq 1$ )         | 1,180        | 1,302                  | 90.6         |
|               | Resistant ( $>1$ )               | 122          | 1,302                  | 9.4          |
|               | MIC, $\mu\text{g/mL}$            |              | 0.8432 (0.2937–1.3927) |              |
| Cefixime      | Susceptible ( $\leq 0.125$ )     | 1,276        | 1,311                  | 97.3         |
|               | Resistant ( $>0.125$ )           | 35           | 1,311                  | 2.7          |
|               | MIC, $\mu\text{g/mL}$            |              | 0.0289 (0.0266–0.0311) |              |
| Ceftriaxone   | Susceptible ( $\leq 0.032$ )     | 1,279        | 1,312                  | 97.5         |
|               | Reduced Sensitivity ( $>0.032$ ) | 33           | 1,312                  | 2.5          |
|               | Resistant ( $>0.125$ )           | 0            | 1,312                  |              |
|               | MIC, $\mu\text{g/mL}$            |              | 0.007 (0.0064–0.0076)  |              |
| Ciprofloxacin | Susceptible ( $\leq 0.032$ )     | 528          | 1,311                  | 40.3         |
|               | Intermediate                     | 1            | 1,311                  | 0.1          |
|               | Resistant ( $>0.064$ )           | 782          | 1,311                  | 59.6         |
|               | MIC, $\mu\text{g/mL}$            |              | 6.4455 (5.8446–7.0463) |              |
| Tetracycline  | Susceptible ( $\leq 0.5$ )       | 431          | 1,208                  | 35.7         |
|               | Intermediate                     | 215          | 1,208                  | 17.8         |
|               | Resistant ( $>1$ )               | 562          | 1,208                  | 46.5         |
|               | MIC, $\mu\text{g/mL}$            |              | 7.0349 (5.9602–8.1096) |              |
| Penicillin    | Susceptible ( $\leq 0.064$ )     | 246          | 1,312                  | 18.8         |
|               | Intermediate                     | 861          | 1,312                  | 65.6         |
|               | Resistant ( $>1$ )               | 205          | 1,312                  | 15.6         |
|               | MIC, $\mu\text{g/mL}$            |              | 2.2397 (1.8598–2.6196) |              |
| Cefinase      | Negative                         | 1,083        | 1,266                  | 85.5         |
|               | Positive                         | 183          | 1,266                  | 14.5         |
| All           |                                  |              | 1,318                  | 100          |

\*Total number of isolates for which variable data were available.

cgMLST showed a branch including isolates with no or little AMR (Figure 2). We found no clear correlation with the cgMLST classification for penicillin, cefinase, tetracycline, and ciprofloxacin resistance. All cefixime-resistant isolates belonged to a single branch of ST7363 isolates, which also contained 24/32 isolates with reduced susceptibility to ceftriaxone. This branch had above average rates of ciprofloxacin, tetracycline, and penicillin resistance. A branch containing ST9363 and ST11422 isolates had a high rate of azithromycin resistance.

We searched isolate sequences for genes and point mutations associated with AMR (Appendix Table 3). For ciprofloxacin resistance, *gyrA* D95 substitutions were the main risk factor (adjusted odds ratio [aOR] 7.56 [95% CI 2.33–33.1]) and explained >99% of ciprofloxacin resistance. Tetracycline resistance was strongly associated with *tetM* carriage (aOR 157 [95% CI 48–965]), which we found in 33% of tetracycline-resistant isolates. For  $\beta$ -lactams, the main risk factor was *bla*<sub>TEM</sub> carriage (aOR 67.9 [95% CI 35.2–139] for penicillin and aOR 234 [95% CI 93.3–683] for cefinase). Mutations in *penA* were also associated with cefinase positivity (aOR 35.6 [95% CI 14–97.4]).

We found mutations in the *macAB* promoter or mosaic *mtr* genes in 138/149 azithromycin-resistant isolates (93%). All cefixime-resistant isolates carried *penA* G545S substitution. The major risk factor for reduced susceptibility to ceftriaxone was *penA* A501T/V (aOR 73.9 [95% CI 6.9–3,170]).

## Conclusions

This study combined phenotypic AMR and genomic data to analyze *N. gonorrhoeae* strains isolated in Austria during 2016–2020. We used a convenience sample (National Reference Centre for Gonococci collection) and results should be interpreted in light of this limitation. The percentage of *N. gonorrhoeae* strains resistant to azithromycin, ciprofloxacin, and tetracycline, or producing  $\beta$ -lactamase was increasing during the study period. The rate of azithromycin resistance rate was >13% during 2019–2020, which was high considering that an azithromycin/cefixime combination is a standard treatment for gonorrhea (2). We found no ceftriaxone-resistant isolates, and cefixime resistance rate was low.

We performed isolate typing by using multilocus sequence typing, *N. gonorrhoeae* multiantigen sequence typing (NG-MAST), and cgMLST. Only 37 isolates belonged to ST1901, which was predominant in isolates from Austria in a European study in 2013, highlighting the fast diversification of *N. gonorrhoeae* (9). The most common NG-MAST type was 12302; all isolates belonged to ST9363 and 71% were resistant to azithromycin. NG-MAST type 12302 and ST9363 have been associated with azithromycin resistance in other studies (10,11). cgMLST classification highlighted 3 branches with specific AMR patterns: 1 with low rates of AMR, 1 including azithromycin-resistant isolates, and 1 including ESC-resistant isolates. Previous studies comparing AMR and phylogenomic distributions in



We used our WGS data to search for genetic determinants of AMR (8,14). Ciprofloxacin resistance matched well with *gyrA* mutations (9,12). Tetracycline resistance correlated with *tetM*, and penicillin resistance correlated *bla<sub>TEM</sub>*. Mutations in *penA* and *mtrR* were associated with ESC resistance. Neither substitution C1192U in *16S rDNA* nor *rpsE* V25 mutations, associated with spectinomycin resistance, were found, suggesting a low prevalence of spectinomycin resistance.

Our study provides an overview of the *N. gonorrhoeae* strains circulating in Austria and their evolution over the past 5 years, both at the phenotypic and genomic level. It also underlines the benefits of genomic surveillance of *N. gonorrhoeae*, which can support epidemiologic investigations and provide information on specific genes and alleles thought to confer AMR (14).

### Acknowledgments

We thank the staff of the Gonococci National Reference Centre and other partner institutions for the collection, isolation, and characterization of the study isolates. We thank Loredana Ingrassio for her feedback throughout the project and on the manuscript.

All co-authors in this manuscript declare that no funding was received from any funding agency in the public, commercial, or not-for-profit sectors. J.S. was supported by a grant from the European Public Health Microbiology Training Programme, European Centre for Disease Prevention and Control (grant agreement no. 1 ECD.7550, implementing ECDC/GRANT/2017/003).

### About the Author

Dr. Schaeffer is a public health microbiologist at the Austrian Agency for Health and Food Safety, Vienna, Austria. Her research interests include emerging pathogens, severe human diseases, and genomic analysis.

### References

- Rowley J, Vander Hoorn S, Korenromp E, Low N, Unemo M, Abu-Raddad LJ, et al. Chlamydia, gonorrhoea, trichomoniasis and syphilis: global prevalence and incidence estimates, 2016. *Bull World Health Organ*. 2019;97:548–562P. <https://doi.org/10.2471/BLT.18.228486>
- World Health Organization. WHO guidelines for the treatment of *Neisseria gonorrhoeae*. Report no. 978–92–4–154969–1. 2016 [cited 2022 Jan 8]. <https://apps.who.int/iris/bitstream/handle/10665/246114/9789241549691-eng.pdf>
- World Health Organization. Global priority list of antibiotic-resistant bacteria to guide research, discovery, and development of new antibiotics. 2017 [cited 2022 Jan 8]. <https://www.who.int/news/item/27-02-2017-who-publishes-list-of-bacteria-for-which-new-antibiotics-are-urgently-needed>
- European Committee on Antimicrobial Susceptibility Testing. Breakpoint tables for interpretation of MICs and zone diameters, version 11.0. 2021 [cited 2022 Jan 8]. [https://www.eucast.org/fileadmin/src/media/PDFs/EUCAST\\_files/Breakpoint\\_tables/v\\_10.0\\_Breakpoint\\_Tables.pdf](https://www.eucast.org/fileadmin/src/media/PDFs/EUCAST_files/Breakpoint_tables/v_10.0_Breakpoint_Tables.pdf)
- Hirk S, Lepuschitz S, Cabal Rosel A, Huhulescu S, Blaschitz M, Stöger A, et al. Draft genome sequences of interpatient and intrapatient epidemiologically linked *Neisseria gonorrhoeae* isolates. *Genome Announc*. 2018; 6:e00319–18. <https://doi.org/10.1128/genomeA.00319-18>
- Maiden MC, Bygraves JA, Feil E, Morelli G, Russell JE, Urwin R, et al. Multilocus sequence typing: a portable approach to the identification of clones within populations of pathogenic microorganisms. *Proc Natl Acad Sci U S A*. 1998;95:3140–5. <https://doi.org/10.1073/pnas.95.6.3140>
- Martin IM, Ison CA, Aanensen DM, Fenton KA, Spratt BG. Rapid sequence-based identification of gonococcal transmission clusters in a large metropolitan area. *J Infect Dis*. 2004;189:1497–505. <https://doi.org/10.1086/383047>
- Sánchez-Busó L, Yeats CA, Taylor B, Goater RJ, Underwood A, Abudahab K, et al. A community-driven resource for genomic epidemiology and antimicrobial resistance prediction of *Neisseria gonorrhoeae* at Pathogenwatch. *Genome Med*. 2021;13:61. <https://doi.org/10.1186/s13073-021-00858-2>
- Harris SR, Cole MJ, Spiteri G, Sánchez-Busó L, Golparian D, Jacobsson S, et al.; Euro-GASP study group. Public health surveillance of multidrug-resistant clones of *Neisseria gonorrhoeae* in Europe: a genomic survey. *Lancet Infect Dis*. 2018;18:758–68. [https://doi.org/10.1016/S1473-3099\(18\)30225-1](https://doi.org/10.1016/S1473-3099(18)30225-1)
- Sawatzky P, Demczuk W, Lefebvre B, Allen V, Diggie M, Hoang L, et al. Increasing azithromycin resistance in *Neisseria gonorrhoeae* due to NG-MAST 12302 clonal spread in Canada, 2015 to 2018. *Antimicrob Agents Chemother*. 2022;66:e0168821. <https://doi.org/10.1128/aac.01688-21>
- Williamson DA, Chow EPF, Gorrie CL, Seemann T, Ingle DJ, Higgins N, et al. Bridging of *Neisseria gonorrhoeae* lineages across sexual networks in the HIV pre-exposure prophylaxis era. *Nat Commun*. 2019;10:3988. <https://doi.org/10.1038/s41467-019-12053-4>
- Lee RS, Seemann T, Heffernan H, Kwong JC, Gonçalves da Silva A, Carter GP, et al. Genomic epidemiology and antimicrobial resistance of *Neisseria gonorrhoeae* in New Zealand. *J Antimicrob Chemother*. 2018;73:353–64. <https://doi.org/10.1093/jac/dkx405>
- Harrison OB, Cehovin A, Skett J, Jolley KA, Massari P, Genco CA, et al. *Neisseria gonorrhoeae* population genomics: use of the gonococcal core genome to improve surveillance of antimicrobial resistance. *J Infect Dis*. 2020;222:1816–25. <https://doi.org/10.1093/infdis/jiaa002>
- Demczuk W, Martin I, Sawatzky P, Allen V, Lefebvre B, Hoang L, et al. Equations to predict antimicrobial MICs in *Neisseria gonorrhoeae* using molecular antimicrobial resistance determinants. *Antimicrob Agents Chemother*. 2020;64:e02005–19. <https://doi.org/10.1128/AAC.02005-19>

Address for correspondence: Justine Schaeffer, Österreichische Agentur für Gesundheit und Ernährungssicherheit, Währinger Straße 25A, 1096 Vienna, Austria; email: justine.schaeffer@ages.at; Werner Ruppitsch, Österreichische Agentur für Gesundheit und Ernährungssicherheit, Währinger Straße 25A, 1096 Vienna, Austria; email: werner.ruppitsch@ages.at

---

# Serial Intervals for SARS-CoV-2 Omicron and Delta Variants, Belgium, November 19–December 31, 2021

Cécile Kremer,<sup>1</sup> Toon Braeye,<sup>1</sup> Kristiaan Proesmans, Emmanuel André, Andrea Torneri, Niel Hens

We investigated the serial interval for SARS-CoV-2 Omicron BA.1 and Delta variants and observed a shorter serial interval for Omicron, suggesting faster transmission. Results indicate a relationship between empirical serial interval and vaccination status for both variants. Further assessment of the causes and extent of Omicron dominance over Delta is warranted.

The World Health Organization designated the SARS-CoV-2 Omicron BA.1 variant (B.1.1.529) as a variant of concern (VOC) on November 26, 2021 (1). Omicron shows a fast epidemic growth and has taken over as the dominant VOC from the previously dominant Delta variant (B.1.617.2) worldwide. In Belgium, the Omicron variant was the dominant circulating strain during December 27, 2021–January 9, 2022, identified in 88.5% of sequenced samples (2). The Omicron variant is more efficient at evading immunity, acquired from previous infection or vaccination (3,4), compared with the Delta variant. Another epidemiologic characteristic that may contribute to the rapid spread of Omicron is increased transmissibility, possibly attributable to an increase in the reproduction number or a shortened serial interval (i.e., the time difference between symptom onset in an infector and infectee) (5). In this study, we estimate the means and SDs of the serial interval for the Omicron and Delta variants and assess whether these variants are associated with different observed serial intervals. To gain more insights on the possible effects of vaccination, we also compare the observed serial intervals for different combinations of vaccination status in transmission pairs.

## The Study

Belgium has a contact tracing system in place, where COVID-19 confirmed case-patients are asked about their contacts from 2 days before symptom onset until 10 days after. We used genotype sequencing to detect variants. If a variant was found in a transmission chain, all case-patients belonging to that chain were assumed to be infected by that variant. We collected transmission pairs that could be linked either to Omicron or Delta infections in which the infector reported first symptoms during November 19–December 31, 2021. During this period, Omicron started to spread in Belgium and took over dominance from the Delta variant (6). The same nonpharmaceutical interventions were in place throughout this period; the stringency index (indicating the strictness of measures on a scale from 0 to 100) was 48. We assumed that the first confirmed case in a reconstructed transmission pair (i.e., the index case-patient) was the infector and the contact was the infectee. We excluded transmission pairs for which symptom onset was not available for either case, as well as pairs for which the observed serial interval was <−5 days or >15 days to ensure biologically plausible serial intervals (7,8). We assigned vaccination status to both cases in a transmission pair as unvaccinated (including partially vaccinated), vaccinated (i.e., completed vaccination cycle), and vaccinated plus booster (Appendix, <https://wwwnc.cdc.gov/EID/article/28/6/22-0220-App1.pdf>).

Of the 2,495 included transmission pairs, 86.61% were linked to transmission of the Omicron variant (Appendix Figure 1). We report the means and SDs of the observed serial intervals; the median was 3 days for all stratifications. All reported p values are based on a Mann-Whitney U test. We further stratified transmission pairs by household and vaccination status (Appendix Tables 1, 2).

---

Author affiliations: Hasselt University, Hasselt, Belgium (C. Kremer, A. Torneri, N. Hens); Sciensano, Brussels, Belgium (T. Braeye, K. Proesmans); Katholieke Universiteit Leuven, Leuven, Belgium (E. André); University Hospitals Leuven, Leuven (E. André); University of Antwerp, Antwerp, Belgium (N. Hens)

DOI: <https://doi.org/10.3201/eid2808.220220>

<sup>1</sup>These first authors contributed equally to this article.

The empirical serial interval distribution for Omicron had a mean of 2.75 days (SD 2.53 days), compared with 3.00 days (SD 2.48 days) for Delta ( $p = 0.019$ ) (Figures 1, panels A, B). We estimated parameters of the normal distribution fit to both empirical serial interval distributions (Table; Figure 1, panel C). The empirical serial interval distribution for Omicron also was shorter than that for Delta within households (Table; Appendix Figure 2).

No difference in mean empirical serial intervals was found for pairs where both case-patients were unvaccinated or only partially vaccinated (2.69 vs. 2.54 days;  $p = 0.931$ ) (Figure 2, panels A, B). For transmission pairs in which both case-patients were vaccinated (without booster), the mean empirical serial interval for Omicron was significantly shorter than that for Delta (2.63 vs. 3.38 days;  $p = 0.004$ ) (Figure 2, panels C, D). The mean empirical serial interval for Omicron was longer for pairs that received a booster vaccine than for pairs that were vaccinated with only 2 doses (3.34 vs. 2.63 days;  $p = 0.065$ ) (Figure 2, panels C–E). The mean empirical serial interval was significantly longer for the Delta variant in transmission pairs in which both

case-patients completed the vaccination cycle, compared with those where both case-patients were unvaccinated or only partially vaccinated (3.38 versus 2.54 days;  $p = 0.045$ ) (Figure 2, panels B–D).

### Conclusions

Our estimates of the empirical serial interval for Omicron are in line with those previously reported. Lee et al. (9) reported a mean serial interval of 2.8 days, and Kim et al. (10) estimated the mean serial interval to be 2.22 days (SD 1.62 days). Backer et al. (7) reported a mean serial interval of 3.5 and 3 days in 2 consecutive weeks for Omicron within-household pairs; in line with our findings, they found the interval to be shorter than that for Delta pairs. Shorter serial intervals suggest a possibly shorter generation time for the Omicron variant compared with Delta, pointing to faster transmission, which could explain the rapid growth that is observed for the Omicron variant. However, control measures and asymptomatic transmission may lead to different serial and generation interval distributions (11). Future studies estimating the generation interval for both variants are needed to shed more light on this matter.

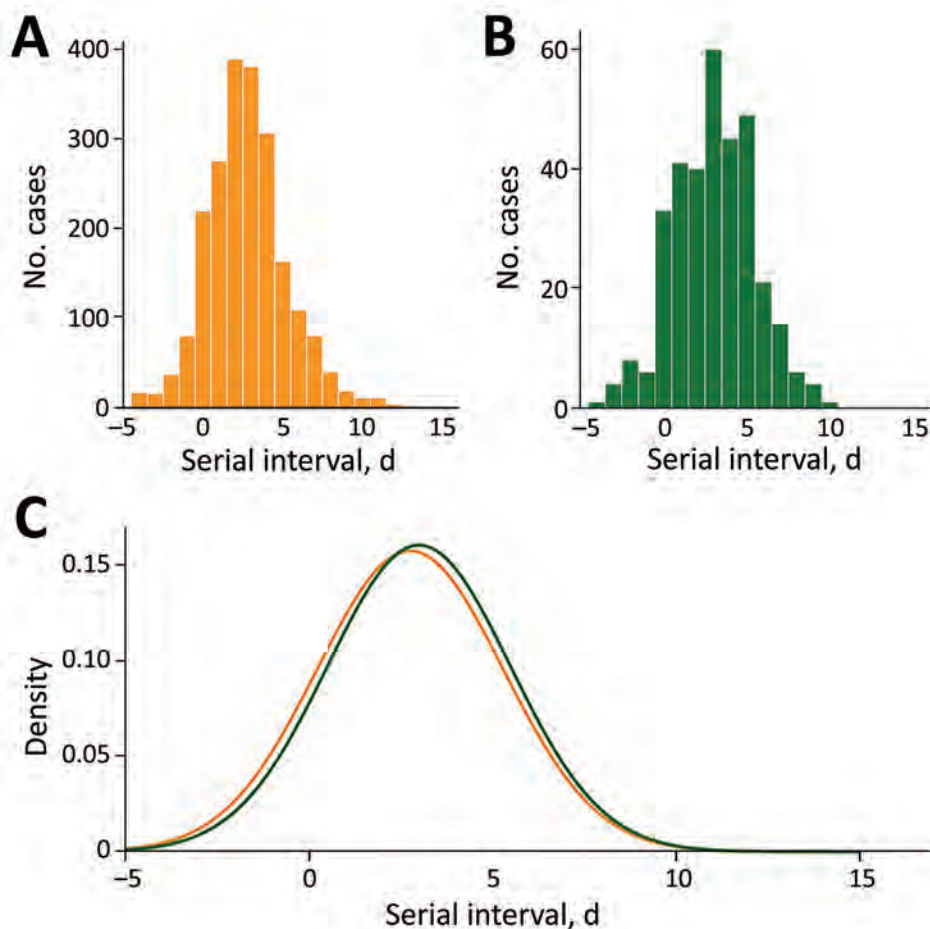


**Figure 1.** Empirical (A–B) and fitted normal (C) distributions of the serial intervals for SARS-CoV-2 Omicron and Delta variants, Belgium, for cases with onset date of infector during November 19–December 31, 2021.

**Table.** Estimated parameters of a normal distribution for the serial interval of SARS-CoV-2 Omicron and Delta variants, by different stratifications, Belgium, November 19–December 31, 2021\*

| Variant | Stratification            | No. transmission pairs | Posterior median (95% CrI) | SD (95% CrI)     |
|---------|---------------------------|------------------------|----------------------------|------------------|
| Omicron | None                      | 2,161                  | 2.75 (2.65–2.86)           | 2.54 (2.46–2.61) |
| Delta   | None                      | 334                    | 3.00 (2.73–3.26)           | 2.49 (2.31–2.69) |
| Omicron | Within-household          | 1,412                  | 2.80 (2.67–2.93)           | 2.60 (2.50–2.70) |
| Delta   | Within-household          | 278                    | 3.04 (2.75–3.33)           | 2.43 (2.24–2.65) |
| Omicron | Between-household         | 672                    | 2.72 (2.53–2.90)           | 2.44 (2.31–2.57) |
| Delta   | Between-household         | 50                     | 2.78 (2.00–3.56)           | 2.78 (2.30–3.45) |
| Omicron | Both unvaccinated         | 346                    | 2.69 (2.40–2.98)           | 2.75 (2.55–2.96) |
| Delta   | Both unvaccinated         | 61                     | 2.54 (1.96–3.12)           | 2.29 (1.93–2.78) |
| Omicron | Both vaccinated           | 774                    | 2.63 (2.46–2.81)           | 2.45 (2.33–2.58) |
| Delta   | Both vaccinated           | 97                     | 3.38 (2.89–3.88)           | 2.47 (2.16–2.86) |
| Omicron | Both vaccinated + booster | 47                     | 3.34 (2.58–4.10)           | 2.59 (2.13–3.24) |
| Delta   | Both vaccinated + booster | 0                      | NA                         | NA               |

\*No Delta transmission pairs in which both case-patients had received a booster vaccine were reported. CrI, credible interval; NA, not available

The first limitation of our study is that self-reported symptom onset dates and contacts may be subject to recall bias. Likewise, the level of reporting contacts may differ for each person. We have used all reported transmission pairs, although some of them may have been wrongly assigned. We further assume that directionality of transmission was from index to contact, which may not be correct for each pair. However, because the same assumption was made for both variants, the comparison of serial intervals still holds, although serial interval lengths should be interpreted with caution. In addition, contacts were required to quarantine, which limited possible exposure from sources other than the reported index case-patient. We also do not explicitly account for right truncation (12); this choice is assumed not to affect our estimates because symptomatic infectees probably were not missed, given that we used the data available on January 17, 2022, but limited the serial interval to no more than 15 days. However, because contacts are reconstructed until 2 days before

symptom onset of the index case-patient, possible left truncation might lead to exclusion of some transmission pairs. Selection bias attributable to targeted genotype sequencing of suspected Omicron cases (such as previously infected cases or travelers) might also have occurred, whereas genotype sequencing resulting in confirmed Delta cases might have been performed on samples from a hospital setting because severe disease was an indication for sequencing during the study period. This analysis does not correct for age or for previous infection; reinfections might be overrepresented among the Omicron cases.

Our results suggest that the empirical mean serial interval increases when both case-patients have a higher level of vaccine-induced immunity. However, possibly because of limited sample size, we did not observe this pattern for all possible combinations of vaccination status (Appendix Figure 3); more data are needed to properly assess the relationship between vaccination and serial interval. The empirical

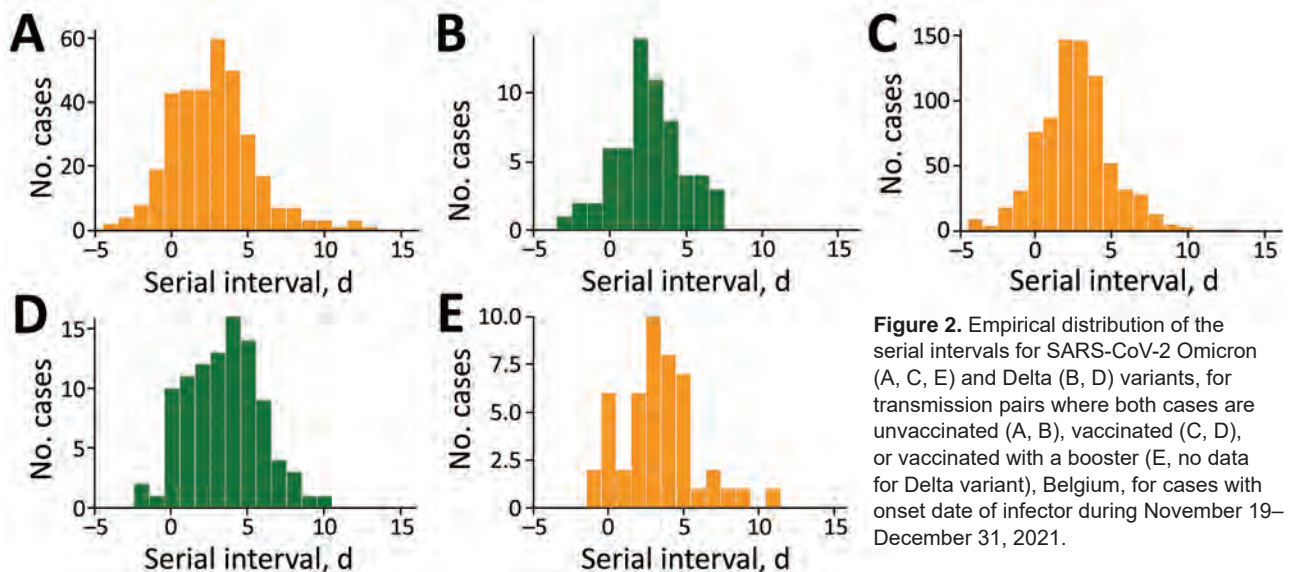


**Figure 2.** Empirical distribution of the serial intervals for SARS-CoV-2 Omicron (A, C, E) and Delta (B, D) variants, for transmission pairs where both cases are unvaccinated (A, B), vaccinated (C, D), or vaccinated with a booster (E, no data for Delta variant), Belgium, for cases with onset date of infector during November 19–December 31, 2021.

mean serial interval for unvaccinated and vaccinated (without booster) transmission pairs was similar for the Omicron variant. If vaccine-induced immunity and serial interval are positively correlated, this result might be explained by lower vaccine efficacy against Omicron for persons who have not yet received a booster vaccine. As the vaccination campaign progresses and more persons receive a booster vaccine, the reasons for and extent of Omicron's dominance over Delta might need to be reassessed.

### Acknowledgments

We thank Nicola Low for the insightful comments on an earlier draft of this manuscript. Data are provided by Sciensano, the Belgian institute for health. Transmission pair data (without vaccination status for identifiability reasons) and R code for the analysis are available at [https://github.com/cecilekremer/serial\\_interval](https://github.com/cecilekremer/serial_interval).

N.H. and A.T. acknowledge funding from the European Union's Horizon 2020 Research and Innovation Programme's EpiPose project (grant agreement no. 101003688). N.H. acknowledges funding from the Antwerp Study Centre for Infectious Diseases and the chair in evidence-based vaccinology at the Methusalem Centre of Excellence Consortium VAX-IDEA. This project was supported by the VERDI project (grant no. 101045989), funded by the European Union. Views and opinions expressed are those of the authors only and do not necessarily reflect those of the European Union or the Health and Digital Executive Agency. Neither the European Union nor the granting authority can be held responsible for them.

The data analyses conducted in this work are among the legal tasks of Sciensano (artikel 4.4 Wet tot oprichting van Sciensano; article 4.4 Law establishment Sciensano). Article 4.4 explicitly states that Sciensano is authorized to collect, validate, analyze, report and archive data of a personal nature concerning public health. Sciensano is further authorized to make these processed data available with approval of the qualified sectoral committees. Such approval for these data was obtained from the Information Security Committee Social Security and Health.

Study conceptualization: N.H., A.T., C.K., T.B.; literature research: C.K., A.T., N.H.; data collection: T.B., K.P.; data analysis code: C.K.; data analysis: C.K., A.T., N.H.; results interpretation: A.T., C.K., N.H., E.A., T.B., K.P.; manuscript writing: C.K., A.T., N.H.; manuscript review: T.B., K.P., E.A., N.H., A.T., C.K.; coordination: N.H.

### About the Author

Ms. Kremer is a PhD student in infectious disease modelling at Hasselt University, Hasselt, Belgium. Her research interests include infectious disease epidemiology

with a focus on public health policy. Dr. Braeys is a senior epidemiologist at Belgium's public health institute, Sciensano. He has been working mostly on vaccine-preventable infectious diseases.

### References

1. World Health Organization. Tracking SARS-CoV-2 variants. 2021 [cited 2022 Jan 27]. <https://www.who.int/en/activities/tracking-SARS-CoV-2-variants>
2. Sciensano. COVID-19 weekly report. 2022 [cited 2022 Jan 27]. [https://covid-19.sciensano.be/sites/default/files/Covid19/COVID-19\\_Weekly\\_report\\_NL.pdf](https://covid-19.sciensano.be/sites/default/files/Covid19/COVID-19_Weekly_report_NL.pdf)
3. Cele S, Jackson L, Khoury DS, Khan K, Moyo-Gwete T, Tegally H, et al. SARS-CoV-2 Omicron has extensive but incomplete escape of Pfizer BNT162b2 elicited neutralization and requires ACE2 for infection. *Nature*. 2022;602:654–6. <https://doi.org/10.1038/s41586-021-04387-1>
4. Pulliam JRC, van Schalkwyk C, Govender N, von Gottberg A, Cohen C, Groome MJ, et al. Increased risk of SARS-CoV-2 reinfection associated with emergence of Omicron in South Africa. *Science*. 2022;376:eabn4947. <https://doi.org/10.1126/science.abn4947>
5. Svensson A. A note on generation times in epidemic models. *Math Biosci*. 2007;208:300–11. <https://doi.org/10.1016/j.mbs.2006.10.010>
6. Cuypers L, Maes P, Dellicour S, Van Weyenbergh J, Keyaerts E, Baele G, et al. Genomic surveillance of SARS-CoV-2 in Belgium. 2021 [cited 2022 Jan 27]. [https://assets.uzleuven.be/files/2021-12/genomic\\_surveillance\\_update\\_211130.pdf](https://assets.uzleuven.be/files/2021-12/genomic_surveillance_update_211130.pdf)
7. Backer JA, Eggink D, Andeweg SP, Veldhuijzen IK, van Maarseveen N, Vermaas K, et al. Shorter serial intervals in SARS-CoV-2 cases with Omicron variant compared to Delta variant in the Netherlands, 13–19 December 2021. *Euro Surveill*. 2022;27:2200042. <https://doi.org/10.2807/1560-7917.ES.2022.27.6.2200042>
8. He X, Lau EHY, Wu P, Deng X, Wang J, Hao X, et al. Temporal dynamics in viral shedding and transmissibility of COVID-19. *Nat Med*. 2020;26:672–5. <https://doi.org/10.1038/s41591-020-0869-5>
9. Lee JJ, Choe YJ, Jeong H, Kim M, Kim S, Yoo H, et al. Importation and transmission of SARS-CoV-2 B.1.1.529 (Omicron) variant of concern in Korea, November 2021. *J Korean Med Sci*. 2021;36:e346. <https://doi.org/10.3346/jkms.2021.36.e346>
10. Kim D, Ali ST, Kim S, Jo J, Lim J-S, Lee S, et al. estimation of serial interval and reproduction number to quantify the transmissibility of SARS-CoV-2 Omicron variant in South Korea. *Viruses*. 2022;14:533. <https://doi.org/10.3390/v14030533>
11. Torneri A, Libin P, Scalia Tomba G, Faes C, Wood JG, Hens N. On realized serial and generation intervals given control measures: The COVID-19 pandemic case. *PLOS Comput Biol*. 2021;17:e1008892. <https://doi.org/10.1371/journal.pcbi.1008892>
12. Linton NM, Kobayashi T, Yang Y, Hayashi K, Akhmetzhanov AR, Jung SM, et al. Incubation period and other epidemiological characteristics of 2019 novel coronavirus infections with right truncation: a statistical analysis of publicly available case data. *J Clin Med*. 2020;9:538. <https://doi.org/10.3390/jcm9020538>

Address for correspondence: Cécile Kremer, Hasselt University, Agoralaan gebouw D, 3590 Diepenbeek, Belgium; email [cecile.kremer@uhasselt.be](mailto:cecile.kremer@uhasselt.be)

# Novel Reassortant Avian Influenza A(H5N6) Virus, China, 2021

Junhong Chen,<sup>1</sup> Lingyu Xu,<sup>1</sup> Tengfei Liu,<sup>1</sup> Shumin Xie,<sup>1</sup> Ke Li, Xiao Li, Mengmeng Zhang, Yifan Wu, Xinkai Wang, Jinfeng Wang, Keyi Shi, Beibei Niu, Ming Liao, Weixin Jia

Although reports of human infection with influenza A(H5N6) increased in 2021, reports of similar H5N6 virus infection in poultry are few. We detected 10 avian influenza A(H5N6) clade 2.3.4.4b viruses in poultry from 4 provinces in China. The viruses showed strong immune-escape capacity and complex genetic reassortment, suggesting further transmission risk.

Severe human infection with influenza A(H5N6) virus was identified in China in 2014. During 2014–2020, a total of 26 cases of human infection were laboratory confirmed (1,2). Sporadic cases did not attract widespread attention until 2021 (3,4). During February–October 2021, China reported 24 laboratory-confirmed cases of human infection with H5N6 virus and 5 deaths (Figure 1, panel A); the number of human infections within only 8 months was close to the total for the previous 7 years.

The policy of compulsory poultry immunizations in China was adopted to prevent and control infection with highly pathogenic avian influenza (HPAI) subtype H5Nx (5). Although vaccination can reduce the likelihood of severe clinical disease and reduce shedding of virus in poultry, it cannot prevent sporadic infections with H5N6 virus in waterfowl. Because it is difficult to achieve a qualified 100% rate of H5N6 virus antibodies in waterfowl (6), these birds have become a weak link in prevention and control

of the virus. In the context of selection pressure for vaccines and the absence of immunity in waterfowl, antigenic drift causes the H5N6 virus to continuously evolve (7), making currently available H5N6 vaccines ineffective.

On November 27, 2020, an outbreak of influenza A(H5N8) virus infections among wild swans was reported in China, resulting in the death of 2 swans (8,9). Since then, H5N8 clade 2.3.4.4b virus has spread throughout China, resulting in co-endemicity of H5N6 clade 2.3.4.4h/b and H5N8 clade 2.3.4.4b viruses. This 2020 outbreak was not the first outbreak of H5N8 virus in China; the earliest introduction of the virus into China was reported in Liaoning on September 12, 2014 (10,11). Because of China's immunization policies for poultry, H5N8 virus was quickly eliminated, only to reemerge in 2020.

The reappearance and spread of H5N8 virus is a serious threat to the poultry industry. The ecologic environment of the virus has been altered, given the increasing number of influenza A(H5N6) cases in humans. The current prevalence and mode of virus reassortment is of great concern. We discovered a novel H5N6 virus that has spread throughout the poultry industry, and similar viruses caused a sharp rise in human infections.

## The Study

In June 2021, we isolated an H5N6 virus from a sick duck on a live poultry farm in Chengdu, Sichuan, China. In July 2021, we isolated another H5N6 virus from a dead chicken in the backyard of a human patient with confirmed infection in Chongqing. In August 2021, we detected an H5N6 virus on a chicken farm in Maoming City and another on a goose farm in Huizhou City (both cities in Guangdong, China). In September 2021, we detected an H5N6 virus on a chicken farm in Qinzhou, Guangxi. Last, in October 2021, we detected 5 H5N6 viruses at live poultry

Author affiliations: South China Agricultural University College of Veterinary Medicine, Guangzhou, China (J. Chen, L. Xu, T. Liu, S. Xie, X. Li, M. Zhang, Y. Wu, X. Wang, J. Wang, K. Shi, B. Niu, M. Liao, W. Jia); Experimental Animal Center, South China Agricultural University, Guangzhou (S. Xie); Yunnan Animal Science and Veterinary Institute, Kunming, Yunnan, China (K. Li); Key Laboratory of Zoonoses and Key Laboratory of Animal Vaccine Development, Ministry of Agriculture, Guangzhou, China (M. Liao, W. Jia); Key Laboratory of Zoonoses Prevention and Control of Guangdong Province, Guangzhou (W. Jia)

DOI: <https://doi.org/10.3201/eid2808.212241>

<sup>1</sup>These authors contributed equally to this article.

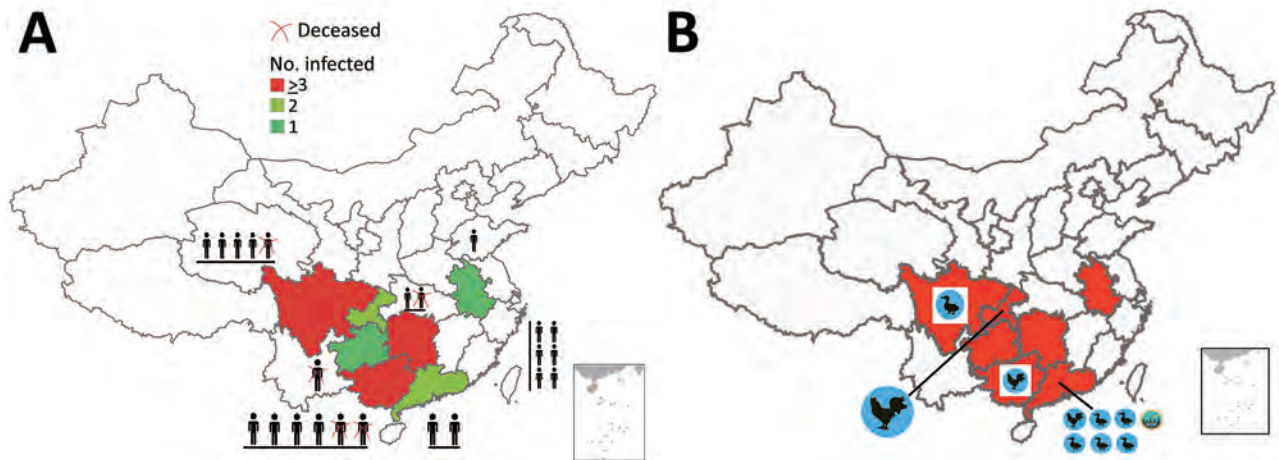


**Figure 1.** Distribution of confirmed cases of avian influenza A(H5N6) virus in humans, China, 2021. A) Provinces of the outbreaks and number of infected persons. A red X indicates a deceased person, and colors represent the number of infected persons. B) Region of novel H5N6 virus isolation from birds (chickens, ducks) and the environment (green icon). The red areas on the map indicate the provinces where human cases occurred in 2021. Insets indicate islands of China, additional sites of poultry breeding and human habitation.

markets in Dongguan City of Guangdong Province (3 from ducks, 1 from a goose, and 1 from the environment) (Figure 1, panel B).

To examine the genetic relationships of the viruses, we sequenced the genomes of the 10 H5N6

viruses and constructed maximum-likelihood phylogenetic trees divided into H5N6 epidemic clades (12), according to the protocol established by the World Health Organization (Figure 2, panel A). The H5N6 virus fell within 8 hemagglutinin (HA)

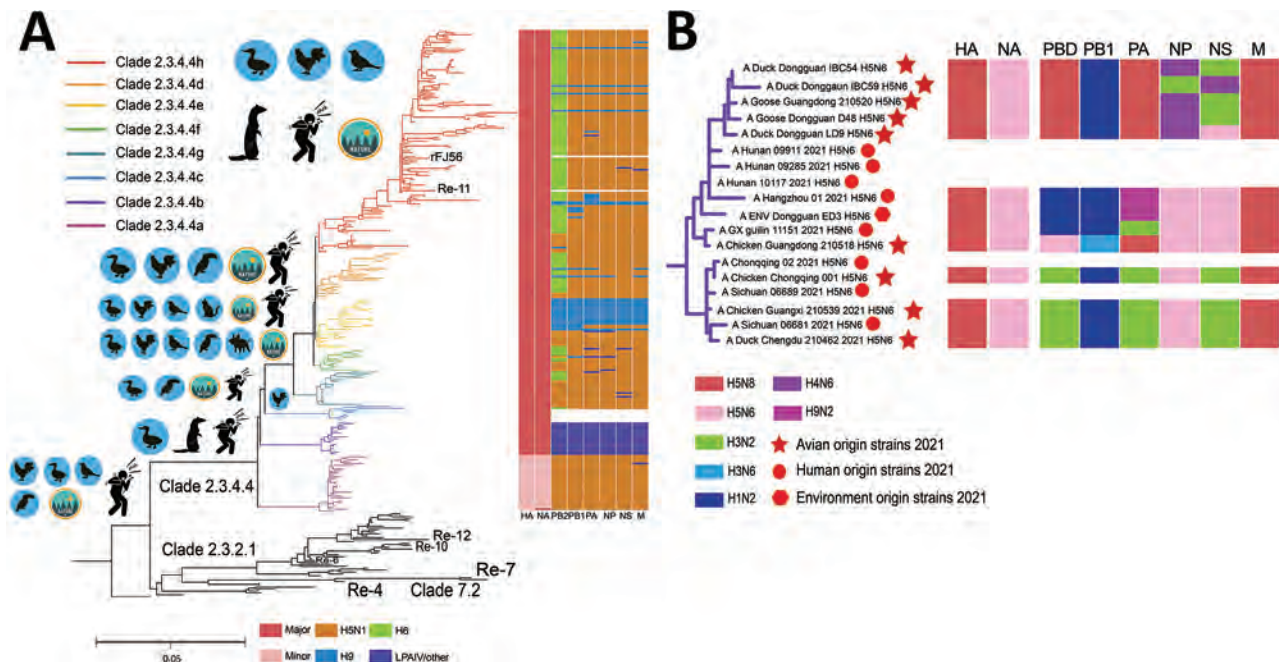


**Figure 2.** Visual depictions of avian influenza A(H5N6) viruses from China, 2021, and reference viruses. A) Maximum-likelihood phylogenetic tree showing comparisons with 332 H5 reference sequences downloaded from the GISAID database (<http://www.gisaid.org>). The Guizhou strain (A/Guizhou/1/2012) was set as the tree root, and all influenza A(H5N1) strains were set as the outgroup. RE-X/rFJ56 represents vaccine strains. To the left of each clade are images showing the corresponding primary hosts. On the right side is the dynamic reassortment profile of each avian (H5N6) virus in the phylogenetic tree; colors represent gene segments. Colored boxes below the graph correspond to possible potential donor viruses. B) Novel avian and environmental origin H5N6 strains. Red circles represent human strains (Appendix Tables 13–17, <https://wwwnc.cdc.gov/EID/article/28/8/21-2241-App1.pdf>). HA, hemagglutinin; LPAIV, low-pathogenicity avian influenza virus; NA, neuraminidase; NS, nonstructural; M, matrix. PA, polymerase acidic; PB, polymerase basic.

clades (2.3.4.4a to 2.3.4.4h). The similarity between the HA genes of all 10 viruses was 99.1%–100%, and all belonged to clade 2.3.4.4b. The HA genes of all the strains had the typical HPAI virus amino acid sequence RRKR↓GLF at the cleavage site (Appendix Table 1, <https://wwwnc.cdc.gov/EID/article/28/8/21-2241-App1.pdf>). All viruses contain the S137A and T192I mutations in the HA gene, which enable it to bind to the human  $\alpha$ -2, 6-linked sialic acid receptor, thereby increasing human susceptibility to the virus (8,13). Mammalian adaptive mutations, such as T33K, L89V, and G309D (14), were detected in the polymerase basic (PB) 2 gene of all strains, which increases the virulence of H5 viruses in mice (Table 1). Those variants are uncommon in previously circulating H5N6 (clade 2.3.4.4h) viruses.

Because there was an epidemiologic correlation between the avian virus strains from Chongqing and the human infections in Chongqing, we used Chongqing avian strains as a representative virus for the control analysis with human-origin virus sequences (Table 2). We deemed this approach to be the appropriate way to reveal links between the human-origin and avian-origin viruses. We found many similarities between the PB2, polymerase acidic, and nonstructural genes of the Chongqing avian-origin strain and those in influenza A(H3N2) virus, which suggests that the novel virus reassorted with H3N2 virus. The PB1 gene is derived from influenza A(H1N2) virus. The HA gene of the Chongqing H5N6 virus was 99.2% similar to that of the H5N8 virus and the matrix genes were 99.9% similar to those of the H5N8 virus, which leads us to believe that both genes

originated from the H5N8 virus. The neuraminidase gene was derived from the H5N6 virus, however, and we speculate that the novel H5N6 virus is a reassortment of the H5N8 and H5N6 viruses. The HA and matrix genes of all viruses were derived from H5N8, which suggests that the novel H5N6 virus may use the gene backbone of the H5N8 virus. Other low-pathogenicity avian influenza viruses have been found to be involved in reassortment, which makes the internal genes of all strains appear complex but inconsistent (Appendix Tables 2–11). Notably, >1 pattern of reassortment seems to be present. Some human-derived strains have internal genes that are close to known H5N6 HPAI virus genes, and others are less closely related (Figure 2, panel B).

Bayesian analysis indicated that the viruses in the Pearl River Delta region (Guangdong), the upper reaches of the Yangtze River (Sichuan/Chongqing), and the middle and lower reaches of the Yangtze River (Hunan/Hangzhou) formed 3 subclades according to geographic characteristics (Appendix Figure 1). Compared with the study of Gu et al. (15), we found that the domestic novel H5N6 virus initially formed 3 subclades and an additional 7 types of genomes (Figure 2, panel B). Current vaccine strains lack protection (hemagglutination inhibition test) against novel H5N6 circulating virus strains (Appendix Table 12). This result differs from that reported by Gu et al. (15), which may result from isolation of the virus from different regions. Our study suggests that the virus poses a high risk for further transmission, which can be reduced or avoided by updating the vaccine strains. In January 2022, the Chinese government introduced

**Table 1.** Mutation sites for novel influenza A(H5N6) avian influenza viruses detected from humans and birds, China, 2021\*

| Strain                                | HA gene     | Function  | PB2 gene        | Function                                 | Host        |
|---------------------------------------|-------------|---|-----------------|--|-------------|
| A/Chongqing/00013/2021/H5N6           | S137A/T192I | Increased $\alpha$ -2,6 sialic acid receptor affinity | T33K/L89V/G309D | Enhanced virulence of H5 viruses in mice | Human       |
| A/Sichuan/06681/2021/H5N6             |             |   |                 |  | Human       |
| A/Sichuan/06689/2021/H5N6             |             |   |                 |  | Human       |
| A/Hunan/09285/2021/H5N6               |             |   |                 |  | Human       |
| A/Hunan/09911/2021/H5N6               |             |   |                 |  | Human       |
| A/Chongqing/02/2021/H5N6              |             |   |                 |  | Human       |
| A/chicken/Chongqing/001/2021/H5N6V†   |             |   |                 |  | Avian       |
| A/goose/Guangdong/210520/2021/H5N6V†  |             |   |                 |  | Avian       |
| A/chicken/Guangdong/210518/2021/H5N6† |             |   |                 |  | Avian       |
| A/duck/Chengdu/210462/2021/H5N6†      |             |   |                 |  | Avian       |
| A/goose/Dongguan/D48/2021/H5N6†       |             |   |                 |  | Avian       |
| A/duck/Dongguan/LD9/2021/H5N6†        |             |   |                 |  | Avian       |
| A/ENV/Dongguan/ED3/2021/H5N6†         |             |   |                 |  | Environment |
| A/duck/Dongguan/IBC54/2021/H5N6†      |             |   |                 |  | Avian       |
| A/duck/Dongguan/IBC59/2021/H5N6†      |             |   |                 |  | Avian       |
| A/chicken/Guangxi/210539/2021/H5N6†   |             |   |                 |  | Avian       |
| A/whooper swan/Xinjiang/13/2020/H5N6‡ | 137S/192T   | None  |                 |  | Avian       |
| A/chicken/Suzhou/j6/2019/H5N6‡        | 137S/192T   | None  |                 |  | Avian       |
| A/China/Original/2018/H5N6‡           | 137S/192T   | None  |                 |  | Human       |

\*HA, hemagglutinin; PB2, polymerase basic 2.

†Avian and environmental strains isolated in study of novel reassortant avian influenza A(H5N6) virus, China, in 2021. The remaining reference strains were downloaded from GISAID (<http://www.gisaid.org>). All strains isolated from humans in 2021 were novel A(H5N6) viruses.

‡Reference strain (clade 2.3.4.4h) that did not have HA gene mutation before 2021.

**Table 2.** Genomic similarity of influenza virus isolate A/chicken/Chongqing/001/2021/H5N6 from a bird in China, 2021, to previously detected influenza viruses from birds in China\*

| Gene | Name                                     | Subtype | Similarity, % | Host    | Year |
|------|--|---------|---------------|---------|------|
| PB2  | A/chicken/Guangxi/165C7/2014(H3N2)       | H3N2    | 96.90         | Chicken | 2014 |
| PB1  | A/duck/Guangxi/293D21/2017(H1N2)         | H1N2    | 97.90         | Duck    | 2017 |
| PA   | A/duck/China/322D22/2018(H3N2)           | H3N2    | 96.51         | Duck    | 2018 |
| NP   | A/Muscovy duck/China/H5N6/2020(H5N6)     | H5N6    | 95.20         | Duck    | 2020 |
| NS   | A/chicken/Ganzhou/GZ43/2016(H3N2)        | H3N2    | 97.90         | Chicken | 2016 |
| M    | A/Cygnus columbianus/Hubei/56/2020(H5N8) | H5N8    | 99.90         | Cygnus  | 2020 |
| HA   | A/Cygnus columbianus/Hubei/53/2020(H5N8) | H5N8    | 99.20         | Cygnus  | 2020 |
| NA   | A/Muscovy duck/China/H5N6/2020(H5N6)     | H5N6    | 99.28         | Duck    | 2020 |

\*The virus isolate came from a dead chicken in the backyard of a patient with confirmed infection in Chongqing, China. The host, subtype, and similarity of reference sequences were obtained from the National Center for Biotechnology Information (<https://www.ncbi.nlm.nih.gov>). HA, hemagglutinin; NA, neuraminidase; NS, nonstructural; M, matrix. PA, polymerase acidic; PB, polymerase basic.

new vaccine strains H5-Re14 and rHN5801 to prevent an epidemic of poultry infection with H5N6 virus.

Because reported cases in humans were concentrated in southern China within a short time and most of these cases happened during the noninfluenza season, we suspect that transmissibility or viral load of the novel H5N6 viruses has increased. Furthermore, the virus that was isolated from environmental swab specimens (sewage ditch swab in a live poultry market) in Dongguan indicates that the virus is already present in the surrounding environment, which could increase the likelihood that the virus will infect humans.

## Conclusions

At the peak of human cases, we isolated a total of 10 novel reassortment H5N6 virus strains from local poultry and the environment that were highly similar to the H5N6 (human-origin) virus reported during the same period. The human and avian viruses belong to clade 2.3.4.4b. The initial epidemic strains clustered into 3 geographically characterized subclades, and each avian strain had the same mammalian susceptibility mutation. The apparent antigenic differences between the virus and vaccine antiserum suggest further transmission risk.

## Acknowledgments

We acknowledge all contributors who submitted the sequence data on which this research is based to the GISAID EpiFlu Database. All submitters of data may be contacted directly through GISAID (<http://www.gisaid.org>). Human case reports and data were obtained from <http://www.flu.org.cn/scn/news>.

This work was supported by the Science and Technology Program of Guangdong Province (2021B1212030015), China Agriculture Research System of MOF and MARA (CARS-41), China National Animal Disease Surveillance and Epidemiological Survey Program(2021-2025) (No.202111), Yunnan Liaoming expert workstation, Basic research project of Yunnan Animal Science and Veterinary Institute (2019RW011).

## About the Author

Dr. Chen is a postgraduate student at South China Agricultural University in Guangzhou, China. His research interests are the epidemiology and pathogenesis of emerging and re-emerging infectious diseases.

## References

- Bi F, Jiang L, Huang L, Wei J, Pan X, Ju Y, et al. Genetic characterization of two human cases infected with the avian influenza A (H5N6) viruses—Guangxi Zhuang Autonomous Region, China, 2021. *China CDC Wkly.* 2021;3:923–8. <https://doi.org/10.46234/ccdcw2021.199>
- Xiao C, Xu J, Lan Y, Huang Z, Zhou L, Guo Y, et al. Five independent cases of human infection with avian influenza H5N6—Sichuan Province, China, 2021. *China CDC Wkly.* 2021;3:751–6. <https://doi.org/10.46234/ccdcw2021.187>
- Zhu W, Li X, Dong J, Bo H, Liu J, Yang J, et al. Epidemiologic, clinical, and genetic characteristics of human infections with influenza A(H5N6) viruses, China. *Emerg Infect Dis.* 2022;28.
- Jiang W, Dong C, Liu S, Peng C, Yin X, Liang S, et al. Emerging novel reassortant influenza A(H5N6) viruses in poultry and humans, China, 2021. *Emerg Infect Dis.* 2022;28:1064–6. <https://doi.org/10.3201/eid2805.212163>
- Bai R, Sikkema RS, Li CR, Munnink BBO, Wu J, Zou L, et al. Antigenic variation of avian influenza A(H5N6) viruses, Guangdong Province, China, 2014–2018. *Emerg Infect Dis.* 2019;25:1932–45. <https://doi.org/10.3201/2510.190274>
- Qin J, Zhang Y, Shen X, Gong L, Xue C, Cao Y. Biological characteristics and immunological properties in Muscovy ducks of H5N6 virus-like particles composed of HA-TM/HA-TM<sub>H3</sub> and M1. *Avian Pathol.* 2019;48:35–44. <https://doi.org/10.1080/03079457.2018.1546375>
- Chen J, Li X, Xu L, Xie S, Jia W. Health threats from increased antigenicity changes in H5N6-dominant subtypes, 2020 China. *J Infect.* 2021;83:e9–11. <https://doi.org/10.1016/j.jinf.2021.06.013>
- Li J, Zhang C, Cao J, Yang Y, Dong H, Cui Y, et al. Re-emergence of H5N8 highly pathogenic avian influenza virus in wild birds, China. *Emerg Microbes Infect.* 2021;10:1819–23. <https://doi.org/10.1080/22221751.2021.1968317>
- He G, Ming L, Li X, Song Y, Tang L, Ma M, et al. Genetically divergent highly pathogenic avian influenza A(H5N8) viruses in wild birds, eastern China. *Emerg Infect Dis.* 2021;27:2940–3. <https://doi.org/10.3201/eid2711.204893>
- Zhou LC, Liu J, Pei EL, Xue WJ, Lyu JM, Cai YT, et al. Novel avian influenza A(H5N8) viruses in migratory birds, China,

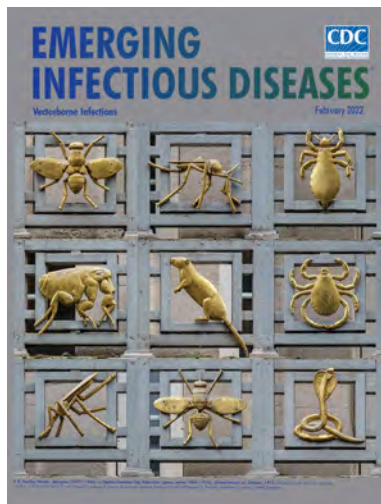
- 2013–2014. *Emerg Infect Dis.* 2016;22:1121–3. <https://doi.org/10.3201/eid2206.151754>
11. Poen MJ, Venkatesh D, Bestebroer TM, Vuong O, Scheuer RD, Oude Munnink BB, et al. Co-circulation of genetically distinct highly pathogenic avian influenza A clade 2.3.4.4 (H5N6) viruses in wild waterfowl and poultry in Europe and East Asia, 2017–18. *Virus Evol.* 2019;5:vez004. <https://doi.org/10.1093/ve/vez004>
  12. Zhang D, Gao F, Jakovlić I, Zou H, Zhang J, Li WX, et al. PhyloSuite: an integrated and scalable desktop platform for streamlined molecular sequence data management and evolutionary phylogenetics studies. *Mol Ecol Resour.* 2020;20:348–55. <https://doi.org/10.1111/1755-0998.13096>
  13. Huang J, Wu S, Wu W, Liang Y, Zhuang H, Ye Z, et al. The biological characteristics of novel H5N6 highly pathogenic avian influenza virus and its pathogenesis in ducks. *Front Microbiol.* 2021;12:628545. <https://doi.org/10.3389/fmicb.2021.628545>
  14. Wu Y, Lin J, Yang S, Xie Y, Wang M, Chen X, et al. The molecular characteristics of avian influenza viruses (H9N2) derived from air samples in live poultry markets. *Infect Genet Evol.* 2018;60:191–6.
  15. Gu W, Shi J, Cui P, Yan C, Zhang Y, Wang C, et al. Novel H5N6 reassortants bearing the clade 2.3.4.4b HA gene of H5N8 virus have been detected in poultry and caused multiple human infections in China. *Emerg Microbes Infect.* 2022;11:1174–85. <https://doi.org/10.1080/22221751.2022.2063076>

Address for correspondence Weixin Jia and Ming Liao, College of Veterinary Medicine, South China Agricultural University, 483 Wushan Rd, Tianhe, Guangzhou, Guangdong 510642, China; email: [jjaweixin@scau.edu.cn](mailto:jjaweixin@scau.edu.cn) and [mliao@scau.edu.cn](mailto:mliao@scau.edu.cn)

February 2022

## Vectorborne Infections

- Viral Interference between Respiratory Viruses
- Novel Clinical Monitoring Approaches for Reemergence of Diphtheria Myocarditis, Vietnam
- Clinical and Laboratory Characteristics and Outcome of Illness Caused by Tick-Borne Encephalitis Virus without Central Nervous System Involvement
- Role of *Anopheles* Mosquitoes in Cache Valley Virus Lineage Displacement, New York, USA
- Burden of Tick-Borne Encephalitis, Sweden
- Invasive *Burkholderia cepacia* Complex Infections among Persons Who Inject Drugs, Hong Kong, China, 2016–2019
- Comparative Effectiveness of Coronavirus Vaccine in Preventing Breakthrough Infections among Vaccinated Persons Infected with Delta and Alpha Variants
- Effectiveness of mRNA BNT162b2 Vaccine 6 Months after Vaccination among Patients in Large Health Maintenance Organization, Israel
- Comparison of Complications after Coronavirus Disease and Seasonal Influenza, South Korea
- Wild Boars as Reservoir of Highly Virulent Clone of Hybrid Shiga Toxigenic and Enterotoxigenic *Escherichia coli* Responsible for Edema Disease, France



- Widespread Detection of Multiple Strains of Crimean–Congo Hemorrhagic Fever Virus in Ticks, Spain
- Rapid Spread of Severe Fever with Thrombocytopenia Syndrome Virus by Parthenogenetic Asian Longhorned Ticks
- Public Acceptance of and Willingness to Pay for Mosquito Control, Texas, USA
- West Nile Virus Transmission by Solid Organ Transplantation and Considerations for Organ Donor Screening Practices, United States

- Serial Interval and Transmission Dynamics during SARS-CoV-2 Delta Variant Predominance, South Korea
- Postvaccination Multisystem Inflammatory Syndrome in Adult with No Evidence of Prior SARS-CoV-2 Infection
- Postmortem Surveillance for Ebola Virus Using OraQuick Ebola Rapid Diagnostic Tests, Eastern Democratic Republic of the Congo, 2019–2020
- SARS-CoV-2 Seroprevalence before Delta Variant Surge, Chattogram, Bangladesh, March–June 2021
- SARS-CoV-2 B.1.619 and B.1.620 Lineages, South Korea, 2021
- *Neisseria gonorrhoeae* FC428 Subclone, Vietnam, 2019–2020
- Zoonotic Infection with Oz Virus, a Novel Thogotovirus
- SARS-CoV-2 Cross-Reactivity in Prepandemic Serum from Rural Malaria-Infected Persons, Cambodia
- Tonate Virus and Fetal Abnormalities, French Guiana, 2019
- *Babesia crassa*-Like Human Infection Indicating Need for Adapted PCR Diagnosis of Babesiosis, France
- Clinical Features and Neurodevelopmental Outcomes for Infants with Perinatal Vertical Transmission of Zika Virus, Colombia

**EMERGING  
INFECTIOUS DISEASES**

To revisit the February 2022 issue, go to:  
<https://wwwnc.cdc.gov/eid/articles/issue/28/2/table-of-contents>

# Effectiveness of Naturally Acquired and Vaccine-Induced Immune Responses to SARS-CoV-2 Mu Variant

Edmilson F. de Oliveira-Filho,<sup>1</sup> Bladimiro Rincon-Orozco,<sup>1</sup> Natalia Jones-Cifuentes, Brigitte Peña-López, Barbara Mühlemann, Christian Drosten, Andres Moreira-Soto, Jan Felix Drexler

SARS-CoV-2 Mu variant emerged in Colombia in 2021 and spread globally. In 49 serum samples from vaccinees and COVID-19 survivors in Colombia, neutralization was significantly lower ( $p < 0.0001$ ) for Mu than a parental strain and variants of concern. Only the Omicron variant of concern demonstrated higher immune evasion.

Diverse SARS-CoV-2 variants have arisen during the pandemic. As of May 4, 2022, there had been 2 recognized variants of concern (VOC), Delta and Omicron, in addition to earlier emerging VOCs Alpha, Beta, and Gamma and strains previously categorized as variants of interest (VOI). Many VOIs have been understudied in terms of pathogenesis, transmissibility, and potential for immune escape. Delta and Omicron illustrate how variants emerging in tropical settings can spread globally.

Mu was first reported as a VOI in early January 2021 in northern Colombia. While outcompeting other locally circulating variants, Mu spread to additional countries, such as Ecuador, United States, Mexico, and Spain; as of early 2022, it was still circulating at low levels in Colombia (1). Mu caused 70% of all COVID-19 cases in Colombia during May–July 2021 (Figure 1), a period which also accounted for the highest number of deaths in Colombia during the pandemic, suggesting substantial

pathogenicity of Mu (1). Mu was later outcompeted by Delta and Omicron, and the number of Mu-related cases gradually decreased through the end of 2021 (Figure 1).

Recent studies relying on data from spike-based pseudovirus testing suggested substantially lower neutralization of Mu compared with the parental B.1 virus in antiserum samples from persons in Japan and China who had received either the BNT162b2 (Pfizer-BioNTech, <https://www.pfizer.com>) or Sinovac (<http://www.sinovac.com>) vaccines or recovered from COVID-19 (2,3). Because of inherent limitations in pseudovirus-based systems for reproducing response variations based on natural infection (4), regional differences of immune responses (5), and different vaccines used in Colombia, we comparatively characterized the neutralization of Mu and VOCs using fully infectious viruses and serum samples from persons in Colombia. The study was approved by the Ethics Committee of the Universidad Industrial de Santander (protocol 4110) and by the Ethics Committee of the Charité-Universitätsmedizin Berlin (protocol EA2/031/22). All participants provided written informed consent.

## The Study

By March 2022, ≈68% of the population of Colombia had been vaccinated, predominantly with spike-based mRNA (BNT162b2), vectored (AZD1222; AstraZeneca, <https://www.astrazeneca.com>), and chemically inactivated whole virus-based vaccines (CoronaVac) (Appendix Figure 1, <https://wwwnc.cdc.gov/EID/article/28/8/22-0584-App1.pdf>). To investigate the potency of natural and vaccine-derived immunity, we tested and compared the

Author affiliations: Charité-Universitätsmedizin Berlin, corporate member of Freie Universität Berlin and Humboldt-Universität zu Berlin, Institute of Virology, Berlin, Germany (E.F. de Oliveira-Filho, B. Mühlemann, C. Drosten, A. Moreira-Soto, J.F. Drexler); Universidad Industrial de Santander School of Medicine, Bucaramanga, Colombia (B. Rincon-Orozco, N. Jones-Cifuentes, B. Peña-López); German Centre for Infection Research, Berlin (B. Mühlemann, C. Drosten, J.F. Drexler)

DOI: <https://doi.org/10.3201/eid2808.220584>

<sup>1</sup>These first authors contributed equally to this article.

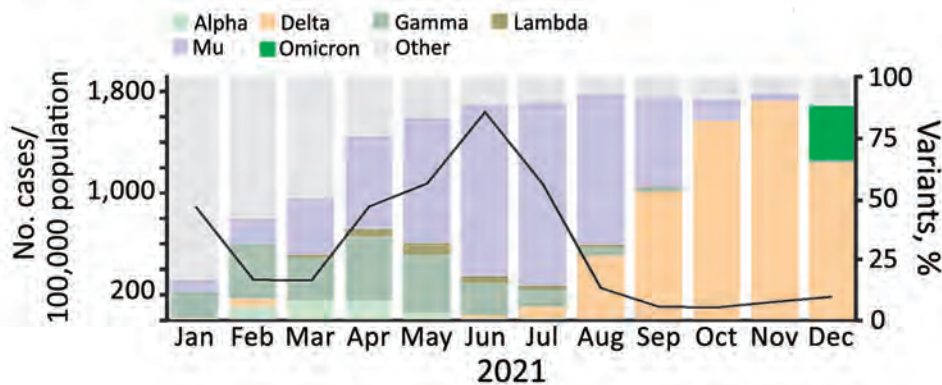


**Figure 1.** Incidence of SARS-CoV-2 and circulation of variants, by month, Colombia, 2021. Data on variant circulation was obtained from GISAID (<https://www.gisaid.org>) and data on the number of cases in Colombia from the Our World in Data database (<https://www.ourworldindata.org>).

neutralization activity in 49 serum samples from vaccinated and naturally infected persons in Colombia. Among vaccinated persons, we tested serum from 32 persons sampled in October 2021. Of those, 10 vaccinated with BioNTech-Pfizer were tested a median 99.5 d (range 65–170) after completing vaccination, 7 vaccinated with AstraZeneca were tested a median 146.0 d (range 129–173) after completing vaccination, and 15 vaccinated with Sinovac were tested a median 46.0 d (range 28–131) after completing vaccination. We tested serum samples from 17 persons who tested positive for SARS-CoV-2 antibodies (MAGLUMI 2019-nCoV IgG; Snibe Diagnostic, <https://www.snibe.com>) (Table 1; Appendix Table 1) during a seroprevalence study conducted in November 2020. To control whether persons vaccinated with spike-based vaccines were not previously infected, serum samples were tested against the SARS-CoV-2 IgG nucleocapsid protein by ELISA (SARS-CoV-2 NCP kit; Euroimmun, <https://www.euroimmun.com>) (Table 2). We used 50% plaque reduction neutralization tests to obtain neutralizing titers against an early isolate and the Alpha, Beta, Delta, Gamma, Omicron BA.1, and Mu variants (Appendix).

Neutralizing antibody titers against Mu were significantly lower than those against the parental isolate ( $p < 0.0001$  by Wilcoxon matched-pairs signed-rank test) in all serum samples tested in this study, irrespective of whether immune responses were elicited by vaccination or by natural infection. Vaccine-derived antibodies neutralized Mu on average 8.1-fold ( $p < 0.0001$  by Wilcoxon test) less than the parental strain resembling the vaccine backbones (Figure 2, panels A–C; Appendix Figure 2). We found a similar 8.0-fold reduced neutralization of Mu ( $p < 0.0001$  by Wilcoxon test) for the group of naturally infected persons (Figure 2, panel D). Despite the relatively lower neutralization potency observed in serum samples from persons immunized with the inactivated full

virus-based vaccine Sinovac, observed differences in the ability to neutralize Mu compared with the parental strain among the 3 vaccine groups were not statistically significant (range 7.7–11.4-fold;  $p = 0.8298$  by Kruskal-Wallis test) (Figure 2).

Compared with other variants, neutralizing antibody titers from serum samples of both naturally infected persons and vaccinees were lower against Mu than against all VOCs except for Omicron (Figure 2, panels A and B). Therefore, our results provide strong evidence for immune evasion of the Mu VOI on the basis of results from robust neutralization testing using full viral isolates. Neutralization of Mu by vaccine-induced antibodies was significantly lower than for Beta ( $p = 0.0083$  by Wilcoxon test), for which immune evasion properties led to the suspension of AstraZeneca usage in South Africa (6), and Gamma, which resulted in breakthrough infections in Latin America (7). Immune evasion of Mu is consistent with shared mutations in spike protein residues associated with immune evasion in Beta and Gamma, such as E484K (8). In addition, the mutation leading to the amino acid exchange R346K in Mu is known to be involved in the evasion of monoclonal antibody-mediated neutralization (9), and genomic exchanges occurring at 3 adjacent sites (Y144T, Y145S, and insertion of the amino acid asparagine [N] between spike residues 145 and 146) have been associated with the immune escape properties of Mu (10,11).

**Table 1.** Median age and days after the second dose of vaccinated persons, by vaccine type, at time of sampling among persons in Colombia\*

| Vaccine groups  | Days after second dose (range) | Age, y (range) |
|-----------------|--------------------------------|----------------|
| AstraZeneca     | 146 (129–173)                  | 66.0 (61–72)   |
| Pfizer-BioNTech | 99.5 (65–170)                  | 44.6 (27–65)   |
| Sinovac         | 46.0 (23–131)                  | 44.5 (23–92)   |

\*AstraZeneca (AZD1222), <https://www.astrazeneca.com>; Pfizer-BioNTech (BNT162b2), <https://www.pfizer.com>; Sinovac (CoronaVac), <http://www.sinovac.com>.

Antigenic cartography was recently employed to map the antigenic relationship between the SARS-CoV-2 Omicron and Delta VOCs and other previously circulating VOCs and VOIs (S.H. Wilks et al., unpub. data, <https://www.biorxiv.org/content/10.1101/2022.01.28.477987v1>). Among the serum samples from Colombia vaccinees, there was a high antigenic

distance between Mu and most variants from other serum samples, which clustered together with the parental strain and Alpha (Appendix Figure 3). Of note, antibody responses in naturally infected persons supported past infection with strains bearing similarities to early SARS-CoV-2 isolates and the Gamma variant (Figure 2, panel D). Antibody reactivity in naturally

**Table 2.** ELISA results and endpoint titers for vaccinee and naturally infected individual serum samples from persons in Colombia\*

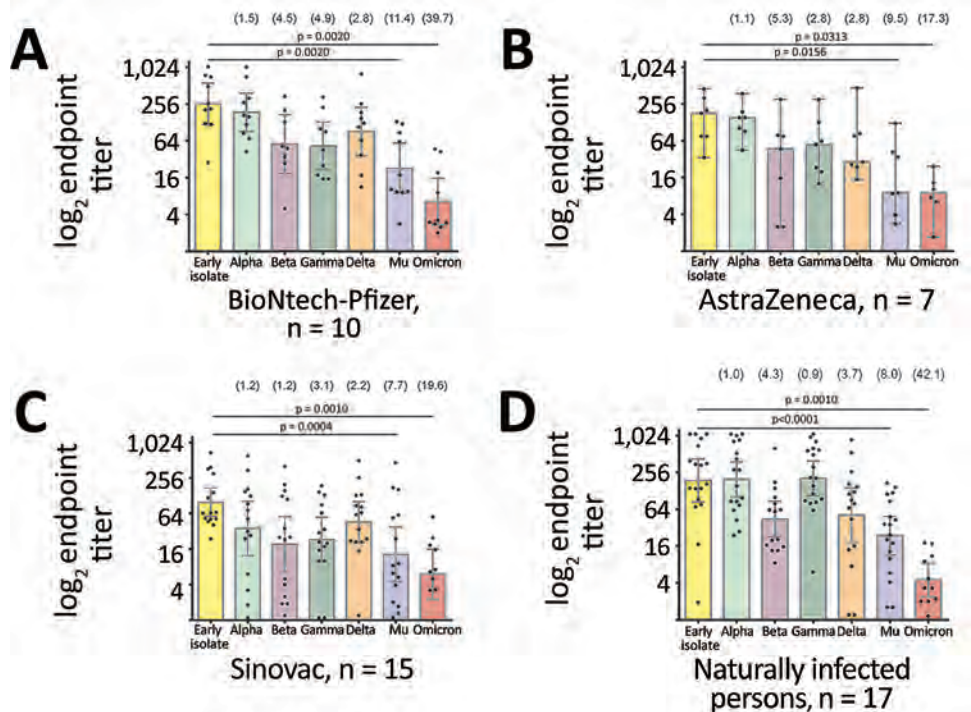
| Group              | Patient ID | Nucleocapsid |       | Neutralizing titer by PRNT <sub>50</sub> |       |       |       |       |         |
|--------------------|------------|--------------|-------|--|-------|-------|-------|-------|---------|
|                    |            | IgG ELISA†   | WT    | Mu                                       | Alpha | Beta  | Gamma | Delta | Omicron |
| AstraZeneca        | AZ2        | 0.15         | 204   | 41                                       | 154   | 79    | 64    | 77    | 13      |
|                    | AZ3        | 0.07         | 453   | 123                                      | 381   | 305   | 306   | 470   | 25      |
|                    | AZ4        | 0.11         | 75    | 3  | 91    | 16    | 20    | 24    | 6       |
|                    | AZ5        | 0.12         | 76    | 9  | 104   | 3     | 13    | 29    | 2       |
|                    | AZ6        | 0.13         | 34    | 4  | 45    | 3     | 23    | 15    | 0       |
|                    | AZ9        | 0.08         | 179   | 35                                       | 189   | 75    | 128   | 84    | 10      |
|                    | AZ10       | 0.07         | 319   | 9  | 153   | 47    | 55    | 26    | 8       |
| Pfizer-BioNTech    | PF1        | 0.14         | 119   | 9  | 85    | 1     | 18    | 38    | 3       |
|                    | PF2        | 0.04         | 28    | 3  | 43    | 35    | 15    | 17    | 3       |
|                    | PF3        | 0.15         | 262   | 62                                       | 158   | 130   | 101   | 149   | 19      |
|                    | PF4        | 0.06         | 754   | 121                                      | 715   | 204   | 226   | 187   | 43      |
|                    | PF5        | 0.05         | 501   | 87                                       | 320   | 48    | 91    | 259   | 9       |
|                    | PF6        | 0.07         | 123   | 10                                       | 119   | 52    | 15    | 11    | 3       |
|                    | PF7        | 0.19         | 214   | 9  | 70    | 5     | 0     | 125   | 3       |
|                    | PF8        | 0.05         | 207   | 18                                       | 167   | 28    | 25    | 66    | 3       |
|                    | PF9        | 0.09         | 715   | 10                                       | 273   | 0     | 46    | 108   | 2       |
|                    | PF10       | 0.62         | 1043  | 132                                      | 1036  | 343   | 333   | 799   | 47      |
| Sinovac            | SVN1       | 2.96         | 51    | 54                                       | 72    | 36    | 66    | 83    | 0       |
|                    | SVN2       | 1.68         | 47    | 9  | 24    | 23    | 21    | 22    | 0       |
|                    | SVN3       | 0.46         | 41    | 6  | 1     | 1     | 18    | 1     | 0       |
|                    | SVN4       | 2.43         | 118   | 61                                       | 151   | 111   | 89    | 87    | 25      |
|                    | SVN7       | 0.97         | 363   | 162                                      | 347   | 407   | 188   | 259   | 56      |
|                    | SVN8       | 0.81         | 303   | 5  | 93    | 26    | 30    | 61    | 5       |
|                    | SVN9       | 0.69         | 53    | 0  | 32    | 3     | 15    | 35    | 0       |
|                    | SVN10      | 1.61         | 65    | 4  | 27    | 0     | 10    | 66    | 1       |
|                    | SVN12      | 0.29         | 52    | 8  | 52    | 1     | 20    | 21    | 0       |
|                    | SVN13      | 0.39         | 387   | 24                                       | 126   | 126   | 35    | 130   | 7       |
|                    | SVN15      | 2.81         | 145   | 175                                      | 168   | 197   | 147   | 133   | 19      |
|                    | SVN16      | 0.40         | 67    | 2  | 6     | 25    | 10    | 21    | 3       |
|                    | SVN17      | 0.07         | 24    | 1  | 1     | 5     | 0     | 15    | 3       |
| SVN18              | 0.37       | 65           | 0     | 3  | 4     | 0     | 24    | 7     |         |
| SVN20              | 1.88       | 686          | 464   | 612                                      | 155   | 131   | 503   | 16    |         |
| Naturally infected | EA210      | ND           | 696   | 146                                      | 825   | 595   | 167   | 177   | 2       |
|                    | EA234      | ND           | 142   | 4  | 86    | 83    | 67    | 9     | 0       |
|                    | EA238      | ND           | 1,080 | 48                                       | 1080  | 314   | 541   | 79    | 5       |
|                    | EA245      | ND           | 70    | 2  | 61    | 154   | 44    | 0     | 0       |
|                    | EA332      | ND           | 93    | 10                                       | 43    | 94    | 1     | 20    | 0       |
|                    | EA334      | ND           | 140   | 6  | 74    | 115   | 7     | 16    | 3       |
|                    | EA340      | ND           | 77    | 2  | 24    | 61    | 0     | 14    | 2       |
|                    | EA352      | ND           | 1,080 | 113                                      | 1,080 | 578   | 870   | 59    | 3       |
|                    | EA354      | ND           | 336   | 119                                      | 423   | 972   | 90    | 628   | 0       |
|                    | EA380      | ND           | 918   | 43                                       | 281   | 630   | 151   | 63    | 17      |
|                    | EA396      | ND           | 139   | 24                                       | 98    | 88    | 14    | 21    | 0       |
|                    | EA413      | ND           | 1,080 | 18                                       | 864   | 1,080 | 260   | 17    | 11      |
|                    | EA422      | ND           | 2     | 20                                       | 28    | 6     | 123   | 100   | 0       |
|                    | EA439      | ND           | 398   | 171                                      | 283   | 812   | 79    | 62    | 9       |
|                    | EA485      | ND           | 357   | 87                                       | 531   | 206   | 114   | 14    | 0       |
|                    | EA501      | ND           | 17    | 13                                       | 86    | 80    | 1     | 0     | 2       |
|                    | EA520      | ND           | 166   | 36                                       | 154   | 211   | 16    | 141   | 1       |

\*AstraZeneca (AZD1222), <https://www.astrazeneca.com>; Pfizer-BioNTech (BNT162b2), <https://www.pfizer.com>; Sinovac (CoronaVac), <http://www.sinovac.com>. ND, not determined; PRNT<sub>50</sub>, 50% plaque reduction neutralization test; WT, wild-type.

†Cut-off  $\geq 0.8$  was considered positive.

**Figure 2.** Comparative neutralization of the Mu SARS-CoV-2 variant in Colombia.

A–C) Neutralization of SARS-CoV-2 variants from serum samples from persons fully immunized with BNT162b2 (Pfizer-BioNTech, <https://www.pfizer.com>) (A), AZD1222 (AstraZeneca, <https://www.astrazeneca.com>) (B), or CoronaVac (Sinovac, <http://www.sinovac.com>) (C). D) Neutralization of SARS-CoV-2 variants by serum samples from naturally infected persons who tested positive for SARS-CoV-2 antibodies during a seroprevalence study in November 2020. For all panels, each point represents the reciprocal plaque reduction neutralization test endpoint titer of 1 tested serum sample for different SARS-CoV-2 variants; colored bars indicate geometric mean titers, and error bars represent 95% CIs. Values in parentheses above bars represent reduction compared to the parental strain. Statistical significance was determined by the Wilcoxon matched signed-rank test; p values are indicated. For clarity of presentation, only significant values between the early isolate and the Mu variant are shown.



infected persons was thus in concordance with the circulation of SARS-CoV-2 variants in South America during the time of sampling in late 2020 (12), supporting the robustness of our data.

Our study was limited by different time points for sampling of vaccinees and the lack of information on natural infections altering immune responses in vaccinees. However, lack of detectable N-protein antibody responses and the absence of clinical records suggestive of COVID-19 infection in vaccinees immunized with spike-based vaccines supports the robustness of our data despite the vaccinees' unclear infection histories.

## Conclusions

Our data highlight the importance of continuous monitoring for the emergence of new SARS-CoV-2 variants and strains and the timely identification of those variants with potential to evade naturally elicited and vaccine-derived immune responses, using local sampling specimens in the context of regional epidemiologic conditions. Moreover, our data confirmed the potential of Mu to partially evade immune responses, which may affect the efficacy of vaccination programs in southern America and other areas (7,13). Further studies are warranted to evaluate the

pathogenicity of and cell-mediated immunity against Mu and the ability of immune responses associated with Mu to neutralize other SARS-CoV-2 variants. However, because vaccination boosters still provide some degree of protection against severe disease from Omicron (3,14), which shows more immunity evasion than Mu, vaccination will likely still provide protection against severe disease from Mu.

## Acknowledgments

We thank Victor Carvalho Urbieto, Ana María Arboleda, Karina Freyle, and Arne Kühne for their technical support. The Gamma and the Omicron SARS-CoV-2 isolates were obtained from the European Virus Archive) and provided by Dr. Chantal Reusken from the National Institute for Public Health and the Environment.

This work was supported by the Deutsche Gesellschaft für Internationale Zusammenarbeit GmbH (project nos. 88114108 and 81263203), Universidad Industrial de Santander, and MinCiencias-SGR (project no. BPIN 2020000100126).

## About the Author

Dr. Oliveira-Filho is a virologist at the Institute of Virology, Charité Universitätsmedizin Berlin. His research interests include the epidemiology and evolution of emerging viruses.

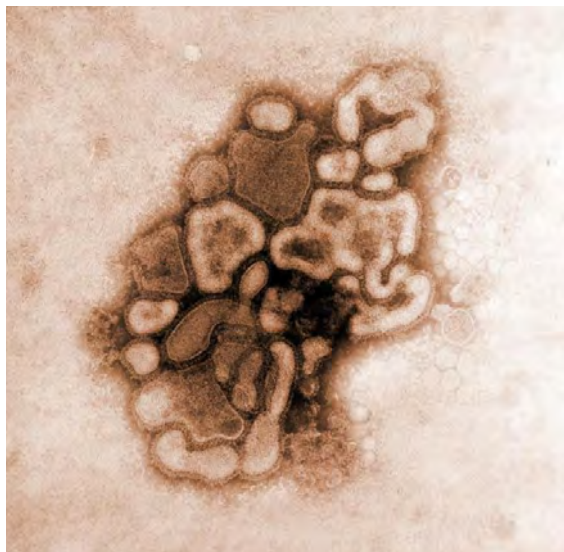
## References

- Laiton-Donato K, Franco-Muñoz C, Álvarez-Díaz DA, Ruiz-Moreno HA, Usme-Ciro JA, Prada DA, et al. Characterization of the emerging B.1.621 variant of interest of SARS-CoV-2. *Infect Genet Evol.* 2021;95:105038. <https://doi.org/10.1016/j.meegid.2021.105038>
- Uriu K, Kimura I, Shirakawa K, Takaori-Kondo A, Nakada TA, Kaneda A, et al.; Genotype to Phenotype Japan (G2P-Japan) Consortium. Neutralization of the SARS-CoV-2 Mu variant by convalescent and vaccine serum. *N Engl J Med.* 2021;385:2397–9. <https://doi.org/10.1056/NEJMc2114706>
- Wang Y, Ma Y, Xu Y, Liu J, Li X, Chen Y, et al. Resistance of SARS-CoV-2 Omicron variant to convalescent and CoronaVac vaccine plasma. *Emerg Microbes Infect.* 2022; 11:424–7. <https://doi.org/10.1080/22221751.2022.2027219>
- Chen M, Zhang XE. Construction and applications of SARS-CoV-2 pseudoviruses: a mini review. *Int J Biol Sci.* 2021;17:1574–80. <https://doi.org/10.7150/ijbs.59184>
- Kollmann TR. Variation between populations in the innate immune response to vaccine adjuvants. *Front Immunol.* 2013;4:81. <https://doi.org/10.3389/fimmu.2013.00081>
- Madhi SA, Izu A, Pollard AJ. ChAdOx1 nCoV-19 vaccine efficacy against the B.1.351 variant. [Reply]. *N Engl J Med.* 2021;385:571–2. <https://doi.org/10.1056/NEJMc2110093>
- Vignier N, Bérout V, Bonnave N, Peugny S, Ballet M, Jacoud E, et al. Breakthrough infections of SARS-CoV-2 Gamma variant in fully vaccinated gold miners, French Guiana, 2021. *Emerg Infect Dis.* 2021;27:2673–6. <https://doi.org/10.3201/eid2710.211427>
- Cai Y, Zhang J, Xiao T, Lavine CL, Rawson S, Peng H, et al. Structural basis for enhanced infectivity and immune evasion of SARS-CoV-2 variants. *Science.* 2021;373:642–8. <https://doi.org/10.1126/science.abi9745>
- McCallum M, Czudnochowski N, Rosen LE, Zepeda SK, Bowen JE, Walls AC, et al. Structural basis of SARS-CoV-2 Omicron immune evasion and receptor engagement. *Science.* 2022;375:864–8. <https://doi.org/10.1126/1659science.abn8652>
- Hossain MJ, Rabaan AA, Mutair AA, Alhumaid S, Emran TB, Saikumar G, et al. Strategies to tackle SARS-CoV-2 Mu, a newly classified variant of interest likely to resist currently available COVID-19 vaccines. *Hum Vaccin Immunother.* 2022;18:2027197. <https://doi.org/10.1080/21645515.2022.2027197>
- Uriu K, Cardenas P, Munoz E, Barragan V, Kosugi Y, Shirakawa K, et al. Characterization of the immune resistance of SARS-CoV-2 Mu variant and the robust immunity induced by Mu infection. *J Infect Dis.* 2022;jiac053.
- Gutierrez B, Marquez S, Prado-Vivar B, Becerra-Wong M, Guadalupe JJ, Candido DDS, et al. Genomic epidemiology of SARS-CoV-2 transmission lineages in Ecuador. *Virus Evol.* 2021;7:veab051. 13. Collie S, Champion J, Moultrie H, Bekker LG, Gray G. Effectiveness of BNT162b2 vaccine against Omicron variant in South Africa. *N Engl J Med.* 2022;386:494–6. <https://doi.org/10.1056/NEJMc2119270>
- Khoury DS, Cromer D, Reynaldi A, Schlub TE, Wheatley AK, Juno JA, et al. Neutralizing antibody levels are highly predictive of immune protection from symptomatic SARS-CoV-2 infection. *Nat Med.* 2021;27:1205–11. <https://doi.org/10.1038/s41591-021-01377-8>

Address for correspondence: Jan Felix Drexler, Institute of Virology, Charitéplatz 1, 10117 Berlin, Germany; email: felix.drexler@charite.de

## EID Podcast

# Farmer Infected with Avian-Like Swine Influenza



Viruses are constantly mutating, and with those mutations can come shifts in their abilities to infect different hosts. Sometimes these mutations allow a virus to “jump” from one species to another, such as an avian influenza virus adapting to pigs.

Zoonotic transmission can have catastrophic effects on global and environmental health. Researchers document and study these events, prepare for them, and if possible, minimize the risk for zoonotic transmission in the first place.

In this EID podcast, Dr. Kristien Van Reeth, a professor of virology at Ghent University in Belgium, tells the events of how an avian-like influenza virus infected a pig farmer in the Netherlands.

Visit our website to listen:  
<https://go.usa.gov/xHgBx>

**EMERGING  
INFECTIOUS DISEASES®**

## Lymphocytic Choriomeningitis Virus Infection, Australia

Leon Caly, Ashleigh F. Porter, Joanna Chua, James P. Collet, Julian D. Druce, Michael G. Catton, Sebastian Duchene

Author affiliations: Monash University, Clayton, Victoria, Australia (L. Caly); The Peter Doherty Institute of Infection and Immunity, Melbourne, Victoria, Australia (L. Caly, A.F. Porter, J. Chua, J.D. Druce, M.G. Catton, S. Duchene); University of Sydney, Sydney, New South Wales, Australia (J.P. Collet); Dubbo Hospital, Dubbo, New South Wales, Australia (J.P. Collet)

DOI: <http://doi.org/10.3201/eid2808.220119>

During a mouse plague in early 2021, a farmer from New South Wales, Australia, sought treatment for aseptic meningitis and was subsequently diagnosed with locally acquired lymphocytic choriomeningitis virus infection. Whole-genome sequencing identified a divergent and geographically distinct lymphocytic choriomeningitis virus strain compared with other published sequences.

A member of the Arenaviridae family, lymphocytic choriomeningitis virus (LCMV) is an enveloped virus comprised of a bisegmented (large [L] and small [S]), negative-stranded RNA genome encoding 2 polypeptides per segment. First discovered in the 1930s during a study of epidemic encephalitis in St. Louis, Missouri, USA (1), LCMV is presumed now to be localized to all continents (excluding Antarctica) based on the distribution of its primary host, the common house mouse (*Mus musculus*). In early 2021, a mouse plague started in western New South Wales, Australia, and spread to the adjoining jurisdictions of Queensland, Victoria, and South Australia, causing considerable losses to the Australia agricultural and grain industry. We report a case of acute LCMV infection in a male farmer from New South Wales.

Although LCMV is considered a truly global virus, acute LCMV infection is rarely diagnosed, possibly because most infected, immunocompetent patients have mild, self-limiting symptoms, such as headache, fever, and myalgia, or are completely asymptomatic and thus never seek treatment. In rare instances, patients have onset of aseptic meningitis or meningoencephalitis but usually recover with no sequelae (2). Furthermore, LCMV is not routinely considered as part of a differential diagnosis (outside of a mouse plague), and testing

is not widely available. Fatal infections are rare but have been associated with organ transplantation (3). LCMV infection in pregnant women has been associated with pregnancy loss and permanent congenital neurologic malformations and chorio retinitis (4). Sampling and subsequent genomic sequencing occur only sporadically, usually during a marked spillover event from the reservoir rodent host to humans (5).

In early 2021, a 51-year-old male farmer in New South Wales, Australia, sought treatment for headache, neck stiffness, photophobia, and a lower abdominal rash. The patient described a month-long history of arthralgia affecting his low back, left hip, and knee. Serologic and PCR tests were negative for *Neisseria meningitidis*, *Streptococcus pneumoniae*, herpes simplex viruses, enterovirus, parechovirus, cytomegalovirus, and varicella zoster virus. Given the patient's high zoonotic exposure as a cattle and horse farmer and his recent contact with mice, their carcasses, and droppings (all occurring during a concurrent regional mouse plague), we conducted PCR testing for LCMV on a sample of cerebrospinal fluid, which returned a positive result (6). With supportive care, the patient's symptoms resolved, and he was discharged and remains well.

After the patient's diagnosis, we sought to determine the evolutionary origin of this specimen in a global context. From 50  $\mu$ L of the patient's cerebrospinal fluid, we obtained an almost complete genome sequence for both the L and S viral genome segments by using a nontargeted, sequence-independent, single-primer amplification strategy prior to Illumina library preparation (<https://www.illumina.com>) (7). We estimated a highest clade credibility phylogenetic tree from both S and L (GenBank accession nos. OK356607 and OK356608) gene segments of the LCMV genome (Figure). Our Australia sample was highly divergent ( $\approx$ 75% nucleotide identity) compared with other S and L gene sequences within GenBank. Bayesian molecular dating of the sequence estimated a divergence from the most common recent ancestor in the mid-16th century, with a mean value of 488 years before present (95% highest posterior density 477.9–531.2) for the S segment and a mean value of 443 years (95% highest posterior density 416.2–470.0) for the L segment. Determining the closest relative to our strain is difficult because of a low representation and diversity of complete LCMV genomes worldwide; there is a high bias toward sequences from the United States and China and a gross underrepresentation of strains from Europe.

LCMV may have been introduced to Australia with the arrival of feral rodents brought by the Dutch and Spanish (17th century) or the French and British (18th century) (8). It makes sense, then, that the ancestor of our gene sequences might have

been brought to Australia during early European exploration and colonization. This hypothesis can be tested only by monitoring occurrences and gathering more samples of LCMV in rodent populations in both Europe and Australia.

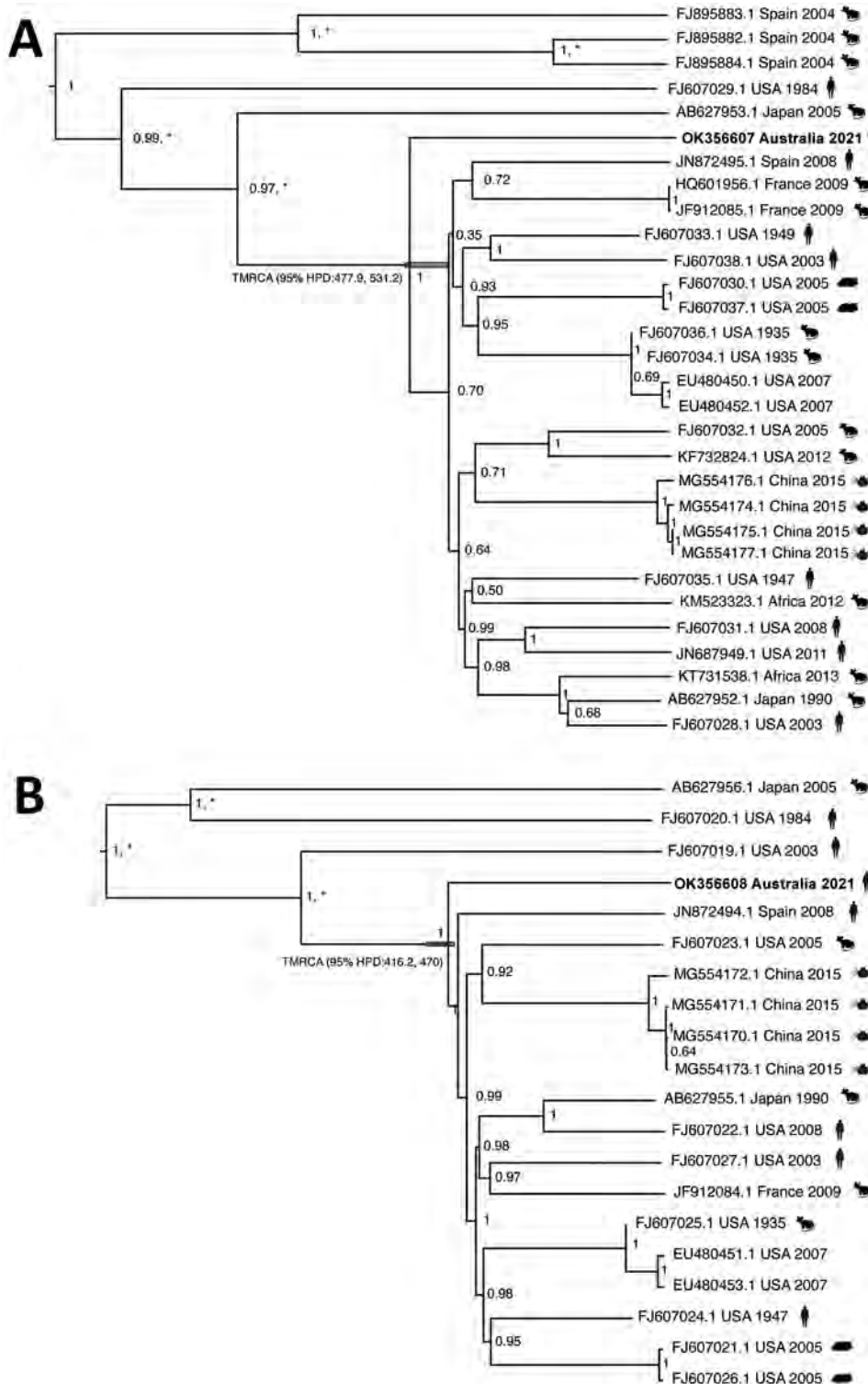


**Figure.** Phylogenetic relationships of a strain of lymphocytic choriomeningitis virus from a man in Australia and the broader lymphocytic choriomeningitis virus phylogeny. Tips are labeled with GenBank sequence accession number, country of origin, year of collection, and host (mice, hamsters, humans, ticks). Trees were generated by using BEAST 1.10.4 (9) to estimate the time to the most recent common ancestor between the novel virus sequence and its closest phylogenetic relative. We used the Hasegawa-Kishino-Yano plus gamma substitution model with a strict clock and an exponential growth coalescent tree prior. Because the dataset exhibits high sequence divergence, we calibrated the molecular clock by using previous independent estimates of the substitution rate, with a fixed clock rate for the long segment of  $3.7 \times 10^{-4}$  substitutions/site/year and  $3.3 \times 10^{-4}$  substitutions/site/year for the short segment (10). Highest clade credibility tree of the short segment (GenBank accession no. OK356607) sequences (n = 29) (A) and highest clade credibility tree of the long segment (GenBank accession no. OK356608) sequences (n = 19) (B). Node labels denote the posterior support, and an asterisk represents a bootstrap percentage of >70% support for a specific clade, using 1,000 ultra-fast bootstrap replicates in a maximum-likelihood tree approach using IQ-TREE2 (11). The 95% highest posterior density for the divergence time before present of the Australia sample is annotated in the respective node.

## About the Author

Dr. Caly is a senior medical scientist at the Peter Doherty Institute of Infection and Immunity in Melbourne, Australia. He is currently working toward validating whole-genome sequencing methodologies targeting viral pathogens for implementation into a public health diagnostic service.

## References

1. Armstrong C, Lillie RD. Experimental lymphocytic choriomeningitis of monkeys and mice produced by a virus encountered in studies of the 1933 St. Louis encephalitis epidemic. *Public Health Reports* (1896–1970). 1934;49: 1019–27.
2. Lewis JM, Utz JP. Orchitis, parotitis and meningoencephalitis due to lymphocytic-choriomeningitis virus. *N Engl J Med*. 1961;265:776–80. <https://doi.org/10.1056/NEJM196110192651604>
3. Palacios G, Druce J, Du L, Tran T, Birch C, Briese T, et al. A new arenavirus in a cluster of fatal transplant-associated diseases. *N Engl J Med*. 2008;358:991–8. <https://doi.org/10.1056/NEJMoa073785>
4. Bonthius DJ, Wright R, Tseng B, Barton L, Marco E, Karacay B, et al. Congenital lymphocytic choriomeningitis virus infection: spectrum of disease. *Ann Neurol*. 2007;62:347–55. <https://doi.org/10.1002/ana.21161>
5. Gregg MB. Recent outbreaks of lymphocytic choriomeningitis in the United States of America. *Bull World Health Organ*. 1975;52:549–53.
6. Holdsworth RL, Downie E, Georgiades MJ, Bradbury R, Druce J, Collett J. Lymphocytic choriomeningitis virus in western New South Wales. *Med J Aust*. 2022;216:71–2. <https://doi.org/10.5694/mja2.51383>
7. Kafetzopoulou LE, Efthymiadis K, Lewandowski K, Crook A, Carter D, Osborne J, et al. Assessment of metagenomic Nanopore and Illumina sequencing for recovering whole genome sequences of chikungunya and dengue viruses directly from clinical samples. *Euro Surveill*. 2018;23:23. <https://doi.org/10.2807/1560-7917.ES.2018.23.50.1800228>
8. Gabriel SI, Stevens ML, Mathias Mda L, Searle JB. Of mice and ‘convicts’: origin of the Australian house mouse, *Mus musculus*. *PLoS One*. 2011;6:e28622. doi:10.1371/journal.pone.0028622
9. Suchard MA, Lemey P, Baele G, Ayres DL, Drummond AJ, Rambaut A. Bayesian phylogenetic and phylodynamic data integration using BEAST 1.10. *Virus Evol*. 2018;4:vey016. <https://doi.org/10.1093/ve/vey016>
10. Albariño CG, Palacios G, Khristova ML, Erickson BR, Carroll SA, Comer JA, et al. High diversity and ancient common ancestry of lymphocytic choriomeningitis virus. *Emerg Infect Dis*. 2010;16:1093–100. <https://doi.org/10.3201/eid1607.091902>
11. Minh BQ, Schmidt HA, Chernomor O, Schrempf D, Woodhams MD, von Haeseler A, et al. IQ-TREE 2: new models and efficient methods for phylogenetic inference in the genomic era. *Mol Biol Evol*. 2020;37:1530–4. <https://doi.org/10.1093/molbev/msaa015>

Address for correspondence: Leon Caly, Victorian Infectious Diseases Reference Laboratory, Peter Doherty Institute for Infection and Immunity, 792 Elizabeth St, Melbourne, VIC 3000, Australia; email: leon.caly@mh.org.au

## Public Health Risk of Foodborne Pathogens in Edible African Land Snails, Cameroon

Mary Nkongho Tanyitiku, Graeme Nicholas, Igor C. Njombissie Petcheu, Jon J. Sullivan, Stephen L.W. On

Author affiliations: Lincoln University, Christchurch, New Zealand (M.N. Tanyitiku, G. Nicholas, I.C. Njombissie Petcheu, J.J. Sullivan, S.L.W. On); Global Mapping and Environmental Monitoring, Yaounde, Cameroon (I.C. Njombissie Petcheu).

DOI: <https://doi.org/10.3201/eid2808.220722>

In tropical countries, land snails are an important food source; however, foodborne disease risks are poorly quantified. We detected *Campylobacter* spp., *Yersinia* spp., *Listeria* spp., *Salmonella* spp., or Shiga-toxicogenic *Escherichia coli* in 57%–86% of snails in Cameroon. Snail meat is a likely vector for enteric diseases in sub-Saharan Africa countries.

African land snails (*Achatina achatina*, *Achatina fulica*, *Archachatina marginata*) are a source of food for many persons in sub-Saharan Africa (1–5). Snail meat contains 37%–51% protein, which is higher than the protein content in poultry (18.3%), fish (18.0%), cattle (17.5%), sheep (16.4%), and swine (14.5%) (1,2,5).

In rural settings, commercial snail farming is uncommon. Rural dwellers may spend up to 20 hours a week in search of edible snails in environments that include marshes, decaying vegetation, domestic wastes, roadsides, footpaths, and bushes (2,4–6). Those local practices of collecting, handling, and consuming snails could expose handlers and consumers to foodborne pathogens.

Although several studies (2,3,6) have highlighted the close association of edible snails with pathogenic microorganisms, their potential contribution to the burden of foodborne diseases in Africa has been overlooked. In Cameroon, no data on foodborne pathogens in snail meat are available, and their role in causing enteric diseases in the local population is unknown. Our study assessed the prevalence of potential foodborne pathogens in African land snails consumed in Buea, Cameroon.

We collected live snails from 3 locations (in persons’ homes, on arable land, and in local markets) during June–October 2019. We sampled within persons’ homes from 9 PM to 5 AM on rainy nights and on arable land during the day. In Buea, live snails are

**Table.** Frequency of pathogens detected by PCR in African land snails, Buea, Cameroon, June–October 2019\*

| Pathogen     | STEC | <i>Campylobacter</i> spp. | <i>Salmonella</i> spp. | <i>Listeria</i> spp. | <i>Yersinia</i> spp. |
|--------------|------|---------------------------|------------------------|----------------------|----------------------|
| Frequency, % | 57   | 75                        | 69                     | 86                   | 71                   |

\*STEC, Shiga toxin–producing *Escherichia coli*.

found actively moving around at night, and during the day, they usually are present underneath decaying vegetation in farmlands (7). We purchased samples from local markets weekly from snail vendors. Our choice of these sampling locations emerged from participants' responses to questions such as, "Where do you get the snails you eat or sell at the market?"; "How do you get the snails you eat or sell?"; "How do you know snails are present there?"; and "If you are to teach your daughter on how to get snails, what will you teach her?" (7)

We collected live snails weekly from the 3 locations and stored them at room temperature in a laboratory in 2-L sterile Sistema containers (Sistema Plastics, <https://www.sistemaplastics.com>). We aseptically collected the feces of 6–12 edible snails/sample within 12–18 hours, pooled them, and placed them in 15-mL sterile tubes manufactured by Eppendorf (<https://corporate.eppendorf.com>). We then stored the samples at –80°C before DNA extraction. We then stored DNA extracts at 4°C before air freighting them to Lincoln University (Christchurch, New Zealand), for PCR analysis. We examined for the presence of Shiga toxin–producing *Escherichia coli*, *Campylobacter* spp., *Salmonella* spp., *Listeria* spp.,

and *Yersinia* spp. by using a high-fidelity DNA polymerase (repliQa Hifi toughmix; Quantabio, <https://www.quantabio.com>) (Appendix, <https://wwwnc.cdc.gov/EID/article/28/8/22-0722-App1.pdf>). We validated PCR methods in-house by using authenticated reference strains as positive and negative controls and then detecting them by electrophoresis. We recorded the presence of an amplicon of the appropriate size for each PCR in each sample as a positive result. For Shiga toxin–producing *Escherichia coli*, a positive result required the detection of both *stx1* and *stx2* genes. These criteria determined the occurrences of each pathogen in the samples (Table; Figure).

We detected  $\geq 1$  pathogen in every sample examined; most samples contained multiple pathogens. We also calculated the prevalence of each pathogen within the 3 sampling locations (Figure). The overall pathogen prevalence among the samples examined was high, ranging from 57% to 86%.

Although detailed information regarding the consumption of snail meat is not available in Cameroon, live snails are sold in almost every local market in the country (8). As for other sub-Saharan countries, an increase in the demand for snail meat has

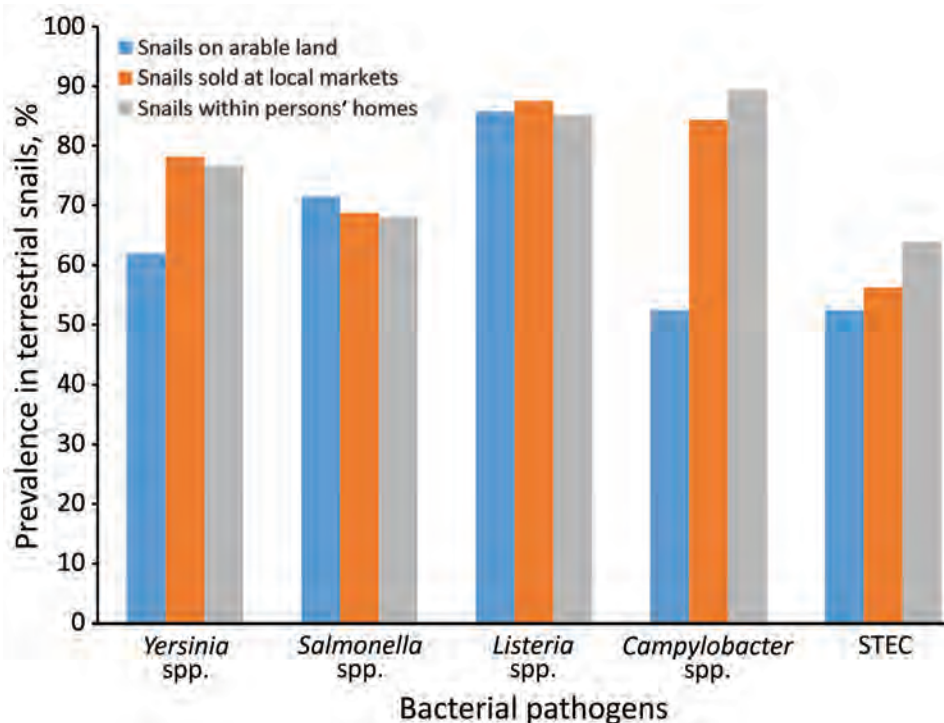


**Figure.** Prevalence of foodborne pathogens in land snails sampled in 3 selected locations, Buea, Cameroon, June–October 2019. STEC, Shiga toxin–producing *Escherichia coli*.

prompted the random collection of edible snails from locations that could be considered unhygienic (2,3,6). Our results identify the public health risks in the handling and consumption of raw or undercooked edible snails collected from natural habitats in Cameroon. Similar pathogenic microorganisms have been isolated in edible snails consumed in Nigeria (2) and Ghana (3,6).

Moreover, the pathogens isolated in this study are associated with many foodborne outbreaks in developed countries such as the United States (9). Higher prevalences of *Campylobacter* spp. (75.37%) and *Listeria* spp. (86.10%) may reflect the common practice of free-range poultry farming in Buea and the direct contact of snails with the soil and decaying vegetation (3,6). Although previous studies highlighted that the local residents believed their practices of snail washing with aluminum sulfate or salt and lime in addition to boiling and then stewing could kill all microorganisms (3,7), Akpomie et al. (2) described substantial bacterial loads in snail meat after boiling, frying, smoking, and oven drying in Nigeria. Thus, our results strongly suggest that foodborne outbreaks from edible snail consumption may be occurring, but are unidentified, in Cameroon, and probably other sub-Saharan Africa countries. The situation clearly indicates a pressing need for interventions to improve public health, for which best results may be obtained in conjunction with a deeper understanding of community attitudes and practices (7,10).

The New Zealand Aid Programme provided financial support during sample collection and analysis. M.N.T is the grateful recipient of a New Zealand Aid Scholarship.

### About the Author

Ms. Tanyitiku is currently finishing her doctoral studies at Lincoln University, New Zealand. In combination with her experiences in food process engineering, her research interests are in the food safety of locally produced foods.

### References

1. Adeyeye SAO, Bolaji OT, Abegunde TA, Adesina TO. Processing and utilization of snail meat in alleviating protein malnutrition in Africa: a review. *Nutr Food Sci*. 2020;50:1085-97. <https://doi.org/10.1108/NFS-08-2019-0261>
2. Akpomie OO, Akponah E, Onoharigho I, Isiakpere OP, Adewuyi IS. Microbiological analysis and nutritional constituents of *Achatina achatina* subjected to various cooking methods. *Nigerian Journal of Microbiology*. 2019;33:4415-22.
3. Barimah MNYS. Microbiological quality of edible land snails from selected markets in Ghana: MPHIL Thesis; Department of Microbiology, University of Ghana Medical School, Ghana; 2013 [cited 2020 Jun 17]. <http://ugspace.ug.edu.gh/handle/123456789/23446>
4. Mohammed S, Ahmed A, Adjei D. Opportunities for increasing peasant farmers income through snail production in Ghana *Sch J Agric*. 2014;1:195-200.
5. Ndah NR, Celestine FCL, Chia EL, Enow EA, Yengo T, Ngwa AD. Assessment of snail farming from selected villages in the Mount Cameroon Range, South West Region of Cameroon. *Asian Research Journal of Agriculture*. 2017;6:1-11. <https://doi.org/10.9734/ARJA/2017/35113>
6. Nyoagbe LA, Appiah V, Josephine N, Daniel L, Isaac A. Evaluation of African giant snails (*Achatina* and *Archachatina*) obtained from markets (wild) and breeding farms. *Afr J Food Sci*. 2016;10:94-104. <https://doi.org/10.5897/AJFS2015.1320>
7. Tanyitiku MN, Nicholas G, Sullivan JJ, Njombissie Petcheu IC, On SLW. Snail meat consumption in Buea, Cameroon: the methodological challenges in exploring its public health risks. *Int J Qual Methods*. 2022;21:1-12. <https://doi.org/10.1177/16094069221078132>
8. Meffowoet CP, Kouam KM, Kana JR, Tchakounte FM. Infestation rate of African giant snails (*Achatina fulica* and *Archachatina marginata*) by parasites during the rainy season in three localities of Cameroon. *Journal of Veterinary Medicine and Research*. 2020;7:1-8.
9. Centers for Disease Control and Prevention. Reports of selected *E. coli* outbreak investigations, 2021 [cited 2022 Mar 12]. <https://www.cdc.gov/ecoli/outbreaks.html>
10. Kaldjob MC, Enangue NA, Siri BN, Etchu K. Socio-economic perception of snail meat consumption in Fako Division, South-West Region Cameroon. *Int J Livest Prod*. 2019;10:143-50. <https://doi.org/10.5897/IJLP2018.0543>

Address for correspondence: Stephen L.W. On, Department of Wine, Food and Molecular Biosciences, Faculty of Agriculture and Life Sciences, PO Box 85084, Lincoln University, RFH Bldg, Rm 081, Lincoln 7647, New Zealand; email: [stephen.on@lincoln.ac.nz](mailto:stephen.on@lincoln.ac.nz)

## *Bacillus subtilis* variant *natto* Bacteremia of Gastrointestinal Origin, Japan

Ippei Tanaka, Satoshi Kutsuna, Misako Ohkusu, Tomoyuki Kato, Mari Miyashita, Ataru Moriya, Kiyofumi Ohkusu

Author affiliations: Japanese Red Cross Musashino Hospital, Tokyo, Japan (I. Tanaka, T. Kato, M. Miyashita); Osaka University, Osaka, Japan (S. Kutsuna); Chiba University, Chiba, Japan (M. Ohkusu); National Center for Global Health and Medicine, Tokyo (A. Moriya); Tokyo Medical University, Tokyo (K. Ohkusu)

DOI: <https://doi.org/10.3201/eid2808.211567>

We report a case of bacteremia caused by *Bacillus subtilis* variant *natto* after a gastrointestinal perforation in a patient in Japan. Genotypic and phenotypic studies of biotin identified *B. subtilis* var. *natto*. This case and 3 others in Japan may have been caused by consuming natto (fermented soybeans).

*Bacillus subtilis* is a gram-positive, rod-shaped, spore-forming bacterium temporarily present in the human gastrointestinal tract (1). The presence of *B. subtilis* in clinical specimens indicates contamination, but rare cases of bacteremia have been reported in Japan (2). Previous reports have attributed bacteremia in Japan to gastrointestinal origin but of

unknown cause. We identified a case of *B. subtilis* variant *natto* bacteremia in a patient in Japan.

In May 2021, a 56-year-old woman was referred to the Japanese Red Cross Musashino Hospital (Musashino-shi, Tokyo, Japan) for a 2-day history of abdominal pain after having taken barium for gastric radiographic examination. The patient had a history of hypertension and ate natto (fermented soybeans) almost every day. At admission, the patient exhibited spontaneous abdominal pain, muscular defense, and rebound tenderness. Laboratory findings showed a decreased leukocyte count (1,800 cells/ $\mu$ L, reference range 3,300–8,600 cells/ $\mu$ L) and mildly increased C-reactive protein concentration (0.75 mg/dL, reference range 0–0.14 mg/dL). Contrast-enhanced computed tomography revealed contrast accumulation in the colon and free air around the sigmoid rectum. Lower gastrointestinal perforation and generalized peritonitis were suspected, and 2 sets of blood cultures were obtained. Emergency proctosigmoidectomy (Hartmann surgery) was performed on the same day, and perforation of the sigmoid colon was confirmed.

Intravenous antimicrobial treatment was initiated. Initial treatment was piperacillin/tazobactam (18 g/d). On day 5, because both blood culture sets were positive for gram-positive rod bacteria, teicoplanin (800 mg/d) was added. On day 11, only *B. subtilis* was isolated from the culture by matrix-assisted laser desorption/ionization-time of flight mass spectrometry, and the antimicrobial drugs

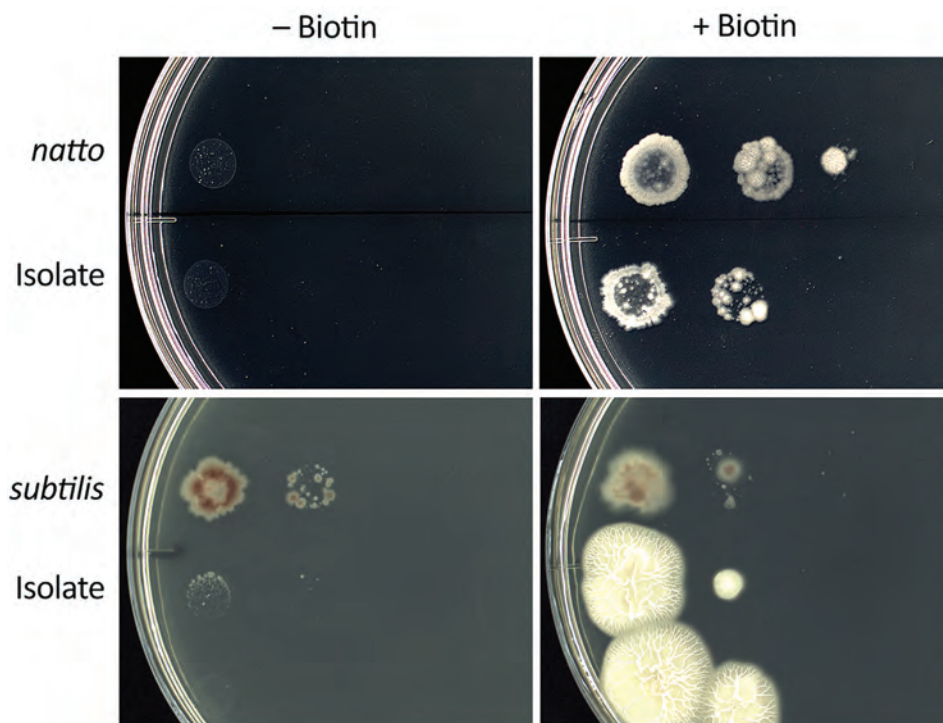


**Figure.** *Bacillus subtilis* cultures on E9 minimal medium agar plates with and without biotin. From left to right in each column, 0.5 McFarland standard was diluted  $\times 1$ ,  $\times 10$ , and  $\times 10^2$ , and 10  $\mu$ L was incubated at 35°C for 72 hours under aerobic conditions. The isolate showed a biotin requirement. Isolate, *Bacillus subtilis* variant *natto* from patient in Japan with bacteremia of gastrointestinal origin; *natto*, *B. subtilis* var. *natto* standard strain; *subtilis*, *B. subtilis* subspecies *subtilis* standard strain.

were changed to ampicillin/sulbactam (12 g/d) as indicated by antimicrobial susceptibility testing by broth microdilution (Appendix Table, <https://wwwnc.cdc.gov/EID/article/28/8/21-1567-App1.pdf>). *B. subtilis* was also detected along with multiple other bacteria by culture of ascites fluid collected intraoperatively. After 39 days of antimicrobial therapy, the patient was discharged.

We investigated whether the blood culture isolate was *B. subtilis* var. *natto*. DNA analysis showed that in the *bioF* region, the isolate was 100% homologous to the *B. subtilis* var. *natto* standard strain. Compared with the *B. subtilis* subspecies *subtilis* standard strain, the isolate had  $\approx 50$  fewer bases and the *bioW* region of the isolate had a single-nucleotide mutation that resulted in a termination codon for amino acid synthesis (Appendix Figures 1–4). The isolate and *B. subtilis* var. *natto* standard strain grew abundantly on a biotin-supplemented medium but did not thrive on a nonsupplemented medium (Figure).

Our biotin gene and biotin requirement testing confirmed that the isolate in this case was *B. subtilis* var. *natto*. Previous genotypic and phenotypic studies on biotin were helpful in identifying this variant. Kubo et al. reported that natto-fermented *B. subtilis* requires biotin and that nonfermented *B. subtilis* does not (3). *bioF* and *bioW* are biotin biosynthetic operons in *B. subtilis* (4). Compared with the *B. subtilis* subsp. *subtilis* standard strain, the 2 biotin genes of the isolate in this study and the *B. subtilis* var. *natto* standard strain were partially defective. According to the biotin requirement test, the isolate required biotin.

We conclude that this case of bacteremia caused by *B. subtilis* var. *natto* resulted from a gastrointestinal perforation. In Japan, the most common causative organism of community-acquired bloodstream infections is gram-negative *Escherichia coli* (25.4%); gram-positive bacilli rarely induce bacteremia (2.7%) (5). *B. subtilis* bacteremia typically originates from the gastrointestinal tract (2); Tamura et al. have reported 3 cases of *B. subtilis* bacteremia arising from the gastrointestinal tract (6). In patients with gastrointestinal bacteremia, the causative organism differs according to the food consumed (7). Oggioni et al. reported a case of *B. subtilis* bacteremia caused by probiotics (8). However, the patient that we report was not taking any probiotics but frequently ate natto. Most of the previously reported cases of *B. subtilis* bacteremia in Japan (2,6) were possibly related to natto consumption, although dietary history was not mentioned in their reports.

This case of bacteremia caused by *B. subtilis* var. *natto* resulted from gastrointestinal tract perforation.

Genotypic and phenotypic studies on biotin effectively identified *B. subtilis* var. *natto*. In Japan, natto consumption is common, and *B. subtilis* bacteremia of gastrointestinal origin is most likely associated with *B. subtilis* var. *natto*.

### Acknowledgments

We thank the clinical staff at the Japanese Red Cross Musashino Hospital for their dedicated clinical practice and patient care.

### About the Author

Mr. Tanaka is a pharmacist at the Japanese Red Cross Musashino Hospital in Musashino-shi, Tokyo, Japan. His main research interest is microbiology.

### References

- García-Arribas ML, de la Rosa MC, Mosso MA. Characterization of the strains of *Bacillus* isolated from orally administered solid drugs [in French]. *Pharm Acta Helv*. 1986;61:303–7.
- Hashimoto T, Hayakawa K, Mezaki K, Kutsuna S, Takeshita N, Yamamoto K, et al. Bacteremia due to *Bacillus subtilis*: a case report and clinical evaluation of 10 cases [in Japanese]. *Kansenshogaku Zasshi*. 2017;91:151–4. <https://doi.org/10.11150/kansenshogakuzasshi.91.151>
- Kubo Y, Rooney AP, Tsukakoshi Y, Nakagawa R, Hasegawa H, Kimura K. Phylogenetic analysis of *Bacillus subtilis* strains applicable to natto (fermented soybean) production. *Appl Environ Microbiol*. 2011;77:6463–9. <https://doi.org/10.1128/AEM.00448-11>
- Sasaki M, Kawamura F, Kurusu Y. Genetic analysis of an incomplete *bio* operon in a biotin auxotrophic strain of *Bacillus subtilis* natto OK2. *Biosci Biotechnol Biochem*. 2004;68:739–42. <https://doi.org/10.1271/bbb.68.739>
- Takeshita N, Kawamura I, Kurai H, Araoka H, Yoneyama A, Fujita T, et al. Unique characteristics of community-onset healthcare-associated bloodstream infections: a multi-centre prospective surveillance study of bloodstream infections in Japan. *J Hosp Infect*. 2017;96:29–34. <https://doi.org/10.1016/j.jhin.2017.02.022>
- Tamura T, Yoshida J, Kikushi T. *Bacillus subtilis* bacteremia originated from gastrointestinal perforation: report of 3 cases [in Japanese]. *Journal of the Japan Society for Surgical Infection*. 2020;5:456.
- Hosoya S, Kutsuna S, Shiojiri D, Tamura S, Isaka E, Wakimoto Y, et al. *Leuconostoc lactis* and *Staphylococcus nepalensis* bacteremia, Japan. *Emerg Infect Dis*. 2020;26:2283–5. <https://doi.org/10.3201/eid2609.191123>
- Oggioni MR, Pozzi G, Valensin PE, Galieni P, Bigazzi C. Recurrent septicemia in an immunocompromised patient due to probiotic strains of *Bacillus subtilis*. *J Clin Microbiol*. 1998;36:325–6. <https://doi.org/10.1128/JCM.36.1.325-326.1998>

Address for correspondence: Satoshi Kutsuna, Department of Infection Control, Graduate School of Medicine Faculty of Medicine, Osaka University, 2-2 Yamadaoka, Suita, Osaka 565-0871, Japan; email: kutsuna@hp-infect.med.osaka-u.ac.jp

## Invasive *Streptococcus oralis* Expressing Serotype 3 Pneumococcal Capsule, Japan

Bin Chang, Masatomo Morita, Akiyoshi Nariai, Kei Kasahara, Akira Kakutani, Michinaga Ogawa, Makoto Ohnishi, Kazunori Oishi

Author affiliations: National Institute of Infectious Diseases, Tokyo, Japan (B. Chang, M. Morita, M. Ogawa, M. Ohnishi); Matsue Red Cross Hospital, Shimane, Japan. (A. Nariai); Nara Medical University, Nara, Japan (K. Kasahara); Nara City Hospital, Nara (A. Kakutani); Toyama Institute of Health, Toyama, Japan (K. Oishi)

DOI: <https://doi.org/10.3201/eid2808.212176>

We report 2 adult cases of invasive disease in Japan caused by *Streptococcus oralis* that expressed the serotype 3 pneumococcal capsule and formed mucoid colonies. Whole-genome sequencing revealed that the identical serotype 3 pneumococcal capsule locus and *hyl* fragment were recombined into the genomes of 2 distinct *S. oralis* strains.

*Streptococcus oralis* is a viridans streptococcus that is divided into 3 subspecies *S. oralis* subsp. *oralis*, *dentisani*, and *tigurinus* (1). Differentiation between these subspecies and other  $\alpha$ -hemolytic streptococci, including *S. pneumoniae*, remains difficult because they share similar biochemical properties. *S. oralis* inhabits the oral cavity and can cause severe infections in persons with immunodeficiency (2). Antimicrobial drug resistance and capsule expression studies have demonstrated that gene transfer can occur from oral *Streptococcus* spp. to *S. pneumoniae* (3–5). Most oral *Streptococcus* spp. have a pneumococcus-like capsule locus and produce capsular polysaccharides (6).

We report 2 cases of invasive streptococcal disease in older adults in Japan (Table). Case 1 occurred in a 69-year-old man with gastric cancer; case 2 occurred in a 78-year-old man with bacteremic meningitis who had no underlying disease. Both patients were successfully treated with antimicrobial agents. The bacterial isolates (ASP0312-Sp from case 1 and SP2752 from case 2) contained  $\alpha$ -hemolytic bacteria that formed characteristic mucoid colonies on blood agar (Table). Quellung reactions were strongly positive for pool R or pneumococcal serotype 3 antisera (Statens Serum Institut, <https://en.ssi.dk>), suggesting that the isolates were *S. pneumoniae* serotype 3. However, both isolates were optochin-resistant and bile-insoluble. Moreover, multilocus sequence

typing (MLST) showed that the sequences of all 7 alleles of ASP0312-Sp and 5 alleles of SP2752 differed from those registered in the MLST database (<https://pubmlst.org>) (Table). For SP2752, the allele numbers were 341 for *gdh* and 406 for *spi*. Furthermore, we observed nucleotide differences between ASP0312-Sp and SP2752 in *aroE* (31 different bp), *gdh* (34 bp), *gki* (25 bp), *recP* (25 bp), *spi* (14 bp), *xpt* (47 bp), and *ddl* (15 bp), which indicated that the strains were distinct. These results suggested that the 2 strains were non-pneumococcal *Streptococcus* spp.

For species identification, we performed phylogenetic analyses of whole-genome sequences (Appendix, <https://wwwnc.cdc.gov/EID/article/28/8/21-2176-App1.pdf>). Homologous core gene clustering showed that ASP0312-Sp and SP2752 belonged to the *S. oralis* clade (Figure); they were distant from one another, which was consistent with the MLST results.

To investigate recombination events, we compared the sequences surrounding the capsule loci of ASP0312-Sp and SP2752 with those of *S. oralis* subsp. *tigurinus* osk\_001 and *S. pneumoniae* serotype 3 OXC141 (Appendix Figure). For ASP0312-Sp, the sequence corresponding to the downstream region of *nsik* up to the 5' terminus of the gene encoding the cell wall binding repeat protein in osk\_001 was replaced by a fragment of  $\approx 30$  kb from pneumococcus. For SP2752, the sequence encoding an ATPase up to the 5' terminus of the gene encoding the cell wall binding repeat protein in osk\_001 was replaced by a fragment of  $\approx 16$  kb from pneumococcus. The capsule sequences of ASP0312-Sp and SP2752 were 100% identical to the corresponding sequences located from 303730 to 312820 bp in HU-OH (GenBank accession no. AP018937.1), a serotype 3 pneumococcal strain that was isolated in Japan (7).

We performed homology searches of 36 known pneumococcal virulence genes because multifragment recombination has been demonstrated during the capsular transformation process in pneumococcal populations (8). In ASP0312-Sp and SP2752, the *hyl* gene, which encodes hyaluronate lyase (9), was located distantly from the capsule locus and shared 96% identity with that of *S. pneumoniae*. We did not detect homologs of the other 35 genes for either isolate.

A recent study reported that acapsular pneumococcus became virulent after transformation with the capsule gene from SK95, which is an oral *S. mitis* strain (5). This previous study demonstrated a cross-species transformation from a commensal streptococcal species to pneumococcus (5). Our results complement this report, although the direction of transformation in our study was reversed. Our analyses of 2 human

**Table.** Characteristics of invasive *Streptococcus oralis* expressing serotype 3 pneumococcal capsule from 2 adult patients, Japan\*

| Case | Onset date   | Isolate ID | Source     | Positive Quellung reaction | No. different bases |            |            |             |            |            |            |
|------|--------------|------------|------------|----------------------------|---------------------|------------|------------|-------------|------------|------------|------------|
|      |              |            |            |                            | <i>aroE</i>         | <i>gdh</i> | <i>gki</i> | <i>recP</i> | <i>spi</i> | <i>xpt</i> | <i>ddl</i> |
| 1    | January 2015 | ASP0312-Sp | Blood      | Pool R, serotype 3         | 61                  | 30         | 44         | 32          | 4          | 41         | 37         |
| 2    | April 2014   | SP2752     | Blood, CSF | Pool R, serotype 3         | 54                  | -†         | 40         | 33          | -†         | 47         | 36         |

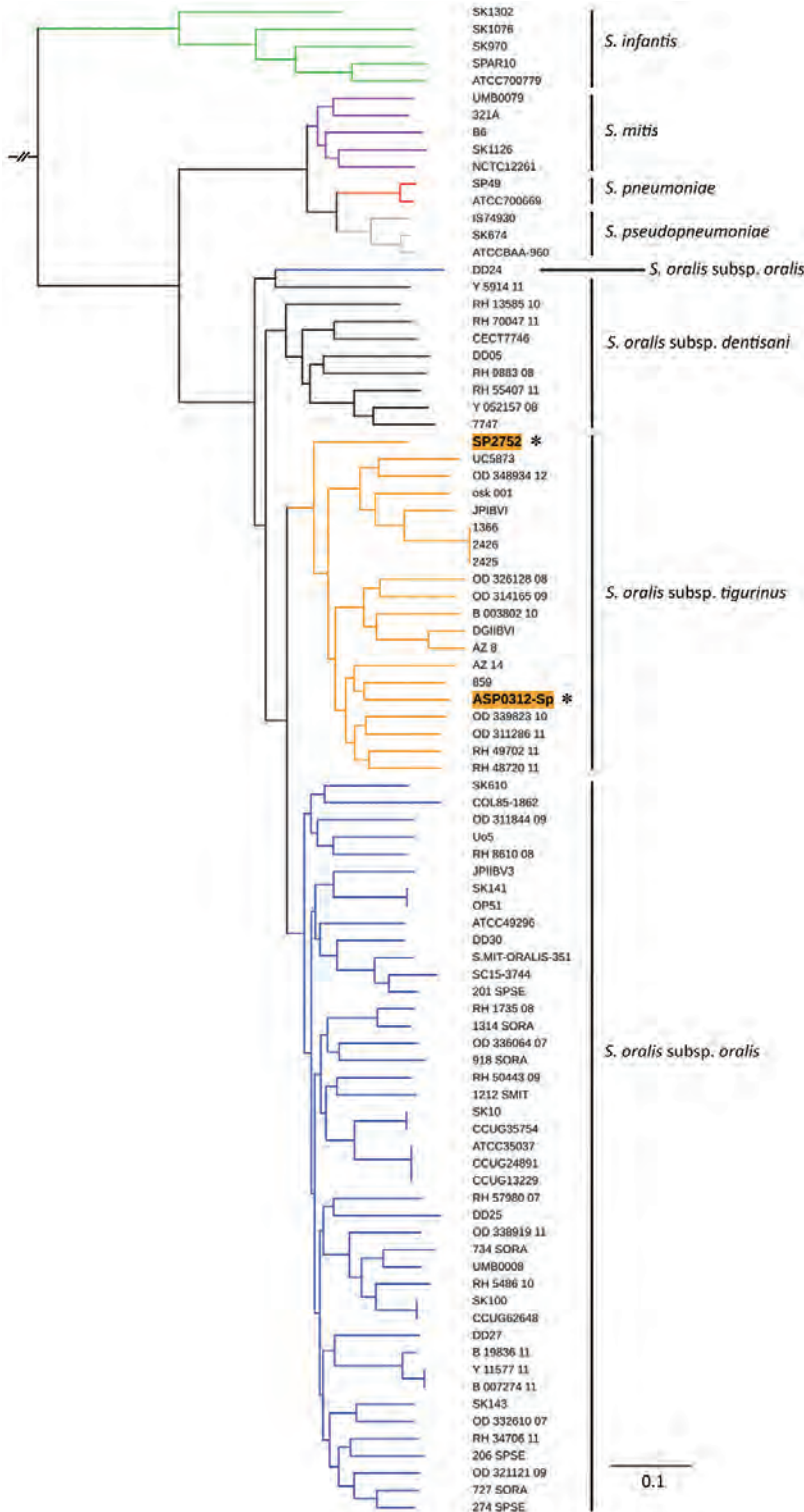


**Figure.** Phylogenetic analysis of invasive *Streptococcus oralis* expressing serotype 3 pneumococcal capsule from 2 adult patients, Japan. Asterisks and orange shading indicate genomes from isolates ASP0312-Sp and SP2752 identified in this study. Homologous core gene clusters of 71 strains from 3 *Streptococcus oralis* subsp., 2 *S. pneumoniae*, 5 *S. mitis*, 5 *S. infantis*, and 3 *S. pseudopneumoniae* were downloaded from the National Center for Biotechnology Information database (<https://www.ncbi.nlm.nih.gov>) and compared with the ASP0312-Sp and SP2752 genomes. Branch lengths represent the genetic distance. Scale bar indicates nucleotide substitutions per site.

patients with invasive disease caused by *S. oralis* provided evidence of cross-species gene transfer from pneumococcus to a commensal streptococcal species. Acquisition of capsule and *hyl* genes might have increased pathogenicity (9,10) and contributed to progression of invasive disease in these 2 cases.

In conclusion, because of discrepancies between phenotypic and biochemical analyses, we used MLST and whole-genome sequencing to identify streptococcal species in these 2 patients. Our study indicates a potential pitfall for identifying and serotyping pneumococci that can occur if the bacteria are not isolated. Thus, when  $\alpha$ -hemolytic streptococci are isolated from a sterile site, clinicians should request molecular analyses to identify the causative species, regardless of the mucoid phenotype.

### Acknowledgments

We thank Moon H. Nahm for his valuable comments.

This work was supported by grants from the Japan Agency for Medical Research and Development (AMED; no. JP20fk0108139) and Ministry of Health, Labour and Welfare (no. JPMH19HA1005).

### About the Author

Dr. Chang is a microbiologist at the National Institute of Infectious Diseases, Tokyo, Japan. Her research interests focus on the microbiology of *Streptococcus pneumoniae*.

### References

- Jensen A, Scholz CFP, Kilian M. Re-evaluation of the taxonomy of the Mitis group of the genus *Streptococcus* based on whole genome phylogenetic analyses, and proposed reclassification of *Streptococcus dentisani* as *Streptococcus oralis* subsp. *dentisani* comb. nov., *Streptococcus tigurinus* as *Streptococcus oralis* subsp. *tigurinus* comb. nov., and *Streptococcus oligofermentans* as a later synonym of *Streptococcus cristatus*. *Int J Syst Evol Microbiol*. 2016;66:4803–20. <https://doi.org/10.1099/ijsem.0.001433>
- Nakamura Y, Uemura T, Kawata Y, Hirose B, Yamauchi R, Shimohama S. *Streptococcus oralis* meningitis with gingival bleeding in a patient: a case report and review of the literature. *Intern Med*. 2021;60:789–93. <https://doi.org/10.2169/internalmedicine.5628-20>
- Bryskier A. Viridans group streptococci: a reservoir of resistant bacteria in oral cavities. *Clin Microbiol Infect*. 2002;8:65–9. <https://doi.org/10.1046/j.1198-743x.2001.00398.x>
- Ganaie F, Saad JS, McGee L, van Tonder AJ, Bentley SD, Lo SW, et al. A new pneumococcal capsule type, 10D, is the 100th serotype and has a large *cps* fragment from an oral *Streptococcus*. *mBio*. 2020;11:e00937–20. <https://doi.org/10.1128/mBio.00937-20>
- Nahm MH, Brissac T, Kilian M, Vlach J, Orihuela CJ, Saad JS, et al. Pneumococci can become virulent by acquiring a new capsule from oral streptococci. *J Infect Dis*. 2020;222:372–80. <https://doi.org/10.1093/infdis/jjz456>
- Skov Sørensen UB, Yao K, Yang Y, Tettelin H, Kilian M. Capsular polysaccharide expression in commensal *Streptococcus pneumoniae* species: genetic and antigenic similarities to *Streptococcus pneumoniae*. *mBio*. 2016;7:e01844–16. <https://doi.org/10.1128/mBio.01844-16>
- Nagaoka K, Konno S, Murase K, Kikuchi T, Morinaga Y, Yanagihara K, et al. Complete genome sequences of *Streptococcus pneumoniae* strains HU-OH (serotype 3, sequence type 183 [ST183]), NU83127 (serotype 4, ST246), and ATCC 49619 (serotype 19F, ST1203). *Microbiol Resour Announc*. 2019;8:e01504–18. <https://doi.org/10.1128/MRA.01504-18>
- Golubchik T, Brueggemann AB, Street T, Gertz RE Jr, Spencer CCA, Ho T, et al. Pneumococcal genome sequencing tracks a vaccine escape variant formed through a multi-fragment recombination event. *Nat Genet*. 2012;44:352–5. <https://doi.org/10.1038/ng.1072>
- Suits MDL, Pluvinaige B, Law A, Liu Y, Palma AS, Chai W, et al. Conformational analysis of the *Streptococcus pneumoniae* hyaluronate lyase and characterization of its hyaluronan-specific carbohydrate-binding module. *J Biol Chem*. 2014;289:27264–77. <https://doi.org/10.1074/jbc.M114.578435>
- Kadioglu A, Weiser JN, Paton JC, Andrew PW. The role of *Streptococcus pneumoniae* virulence factors in host respiratory colonization and disease. *Nat Rev Microbiol*. 2008;6:288–301. <https://doi.org/10.1038/nrmicro1871>

Address for correspondence: Bin Chang, Department of Bacteriology I, National Institute of Infectious Diseases, 1-23-1, Toyama, Shinjuku-ku, Tokyo 162-8640, Japan; email: b-chang@niid.go.jp

## Hepatitis E Virus Outbreak among Tigray War Refugees from Ethiopia, Sudan

Ayman Ahmed, Yousif Ali, Emmanuel Edwar Siddig, Jehan Hamed, Nouh S. Mohamed, Amna Khairy, Jakob Zinsstag

Author affiliations: University of Khartoum, Khartoum, Sudan (A. Ahmed, E.E. Siddig, J. Hamed); Sirius Training and Research Centre, Khartoum (A. Ahmed, N.S. Mohamed); Swiss Tropical and Public Health Institute, Allschwil, Switzerland (A. Ahmed, J. Zinsstag); University of Basel, Basel, Switzerland (A. Ahmed, J. Zinsstag); Sudan Federal Ministry of Health, Khartoum (Y. Ali, A. Khairy); Erasmus MC University Medical Center, Rotterdam, the Netherlands (E.E. Siddig)

DOI: <https://doi.org/10.3201/eid2808.220397>

We report hepatitis E virus (HEV) outbreaks among refugees from Ethiopia in Sudan during June 2021–February 2022. We identified 1,589 cases of acute jaundice syndrome and used PCR to confirm HEV infection in 64% of cases. Implementing vaccination, water, sanitation, and hygiene programs might reduce HEV outbreak risk.

**H**epatitis E is a hygiene- and sanitation-related disease caused by hepatitis E virus (HEV), a member of the Hepeviridae viral family (1,2). HEV has 4 genotypes: genotypes 1 and 2, predominantly found in humans, and genotypes 3 and 4, found in both humans and animals (1,2). Main zoonotic virus reservoirs include domestic pigs, wild boars, rodents, and sika deer (2). Risk factors for transmission differ depending on the genotype. However, genotype 1 is associated with maternal mortality, waterborne transmission, and outbreaks in Africa (3,4). In low- and middle-income countries, HEV is mainly transmitted through contaminated drinking water (2). The clinical manifestation of HEV infection is largely genotype-dependent (2–4).

HEV is a common cause of acute hepatitis and jaundice worldwide. The World Health Organization estimates that 20 million HEV infections (16.5% symptomatic) and 44,000 HEV-related fatalities occur annually (2). The public health threat of HEV infection is exceptionally high in Africa, and biennial outbreaks result in  $\approx$ 35,300 cases of infection and 650 fatalities (3). Pregnant women in Africa are at higher risk for HEV infection than other persons and have an HEV-related mortality rate 10 times higher than the general population (4). Outbreaks of HEV infections in Africa are associated with camps for refugees and internally displaced persons (4). Limited knowledge of the disease is a major challenge for prevention and control of HEV infection in Africa (4).

Gedaref State is in the southeastern region of Sudan, along the borders of Ethiopia and Eritrea (Appendix Figure, <https://wwwnc.cdc.gov/EID/article/28/8/22-0397-App1.pdf>). In early 2022, the area was hosting >60,000 refugees who fled from the Tigray War in Ethiopia. After arriving at the reception camp in Hamdayet, Sudan, the refugees were assigned to 1 of 3 long-term humanitarian camps: Tunaydbah, Um Rakuba, or Village 8 (5). During recent years, the region has had severe weather events, including heavy rains and flooding, that increased risks for infectious disease outbreaks (5,6).

On June 2, 2021, cases of acute jaundice syndrome appeared among the refugees in the Um Rakuba camp and were reported from the other humanitarian camps 2 weeks later. Patients were 3 months–64 years of age, and most (50.1%) were 16–30 years of age; 81 (5.2%) patients were <5 years of age, and 95 (6.1%) were >50 years of age. The male to female ratio was 1.9:1. Of 1,589 patients, 100% had jaundice; 83% had yellowish urine; and 78% had anorexia, nausea, and fatigue. Other symptoms included fever (61%), abdominal pain (56%), and headache and vomiting (44%). Among 22 initial acute jaundice syndrome cases, samples from 14 (64%) patients tested positive for HEV at the National Public Health Laboratory in Khartoum, Sudan, by using real-time PCR kits (Altona Diagnostics, <https://www.altona-diagnostics.com>). The outbreak appeared to peak in July 2021 during which 395 cases were reported (Figure). By February 21, 2022,  $\approx$ 1,589 cases that included 21 pregnant women and 1 fatality (nonpregnant woman) were identified by using the Rapid Anti-HEV-IgM Test (InTec Products, <https://www.intecasi.com>) (Figure). Most (75%) cases were reported from the Um Rakuba camp (Appendix).

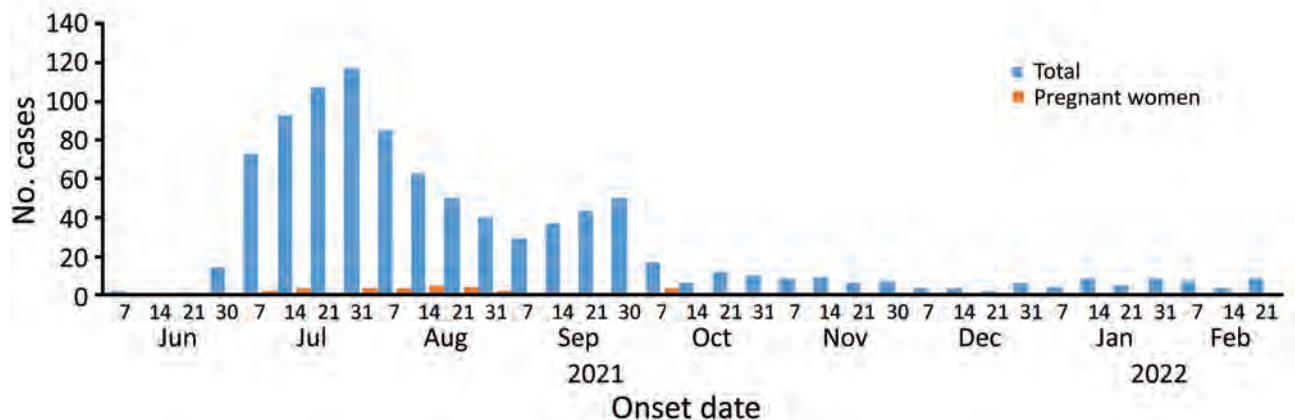


**Figure.** Number of cases of HEV infections per week among Tigray War refugees from Ethiopia in Sudan, June 2, 2021–February 21, 2022. HEV infections occurred in 3 humanitarian camps for refugees in Gedaref State, Sudan. The HEV outbreak peaked in July 2021 during which 395 cases were reported. HEV, hepatitis E virus.

The HEV outbreak in Sudan was associated with heavy rainstorms that flooded the humanitarian settlements and destroyed >1,231 latrines and >1,500 family shelters (5). A similar HEV outbreak occurred among refugees from South Sudan hosted in humanitarian camps in western Ethiopia, where >1,000 cases and a 2% mortality rate were reported (7). However, we report a relatively low mortality rate of <0.1% (1/1,589). Among pregnant women attending antenatal clinics in Tigray, Ethiopia, in 2018, lower hygiene and rural residency were associated with a high (43.4%) HEV seroprevalence, suggesting that a large outbreak could have been prevented by improving hygienic conditions (4).

HEV vaccination is recommended for preventing and controlling HEV outbreaks in humanitarian settings, particularly for pregnant women (1,3). However, the success of vaccination is dependent on the HEV genotype. Because of limited resources, we were unable to genotype the HEV that was circulating in the camps.

Recent outbreaks of Rift Valley fever in northern Sudan and dengue fever in western Sudan have occurred (8–10). These outbreaks highlight the association between massive population displacements because of war or armed conflict and the emergence of infectious diseases (5,6,8–10). Most (50%) HEV outbreaks in sub-Saharan Africa have occurred among refugees and displaced persons living in humanitarian crisis settings (3,4). Open defecation and flooding, both of which occur in the camps, are additional risk factors for HEV emergence and can lead to contamination of nearby open sources of drinking water and food (5).

In summary, we report an outbreak of HEV infection among refugees from Ethiopia hosted in humanitarian camps in Gedaref State, Sudan. Implementing HEV vaccination, water, sanitation, and hygiene programs to improve the living conditions and drinking water among refugees and displaced persons in these camps might reduce the risk for HEV outbreaks. In addition, genotyping circulating HEV could clarify virus transmission routes and inform control measures.

### Acknowledgments

We thank all our colleagues at the National Public Health Laboratory, Federal Ministry of Health, and Ministry of Health of Gedaref State, Sudan, and nongovernment organizations for their support and help in data collection, diagnosis, and case management.

### About the Author

Mr. Ahmed is an epidemiologist with the University of Khartoum, Khartoum, Sudan, and a PhD candidate at the Swiss Tropical and Public Health Institute University of Basel, Switzerland. His research interests include the use of One Health strategies for surveillance, prevention, and control of viral zoonotic diseases.

### References

1. Pavio N, Meng XJ, Renou C. Zoonotic hepatitis E: animal reservoirs and emerging risks. *Vet Res.* 2010;41:46. <https://doi.org/10.1051/vetres/2010018>
2. Wang B, Meng XJ. Hepatitis E virus: host tropism and zoonotic infection. *Curr Opin Microbiol.* 2021;59:8–15. <https://doi.org/10.1016/j.mib.2020.07.004>
3. Kim JH, Nelson KE, Panzner U, Kasture Y, Labrique AB, Wierzbica TF. A systematic review of the epidemiology of hepatitis E virus in Africa. *BMC Infect Dis.* 2014;14:308. <https://doi.org/10.1186/1471-2334-14-308>
4. Bagulo H, Majekodunmi AO, Welburn SC. Hepatitis E in sub-Saharan Africa – a significant emerging disease. *One Health.* 2020;11:100186. <https://doi.org/10.1016/j.onehlt.2020.100186>
5. Ahmed A, Mohamed NS, Siddiq EE, Algaily T, Sulaiman S, Ali Y. The impacts of climate change on displaced populations: a call for action. *J Clim Chang Health.* 2021;3:100057. <https://doi.org/10.1016/j.joclim.2021.100057>
6. Ahmed A, Mahmoud I, Eldigail M, Elhassan RM, Weaver SC. The emergence of Rift Valley fever in Gedaref State urges the need for a cross-border One Health strategy and enforcement of the International Health Regulations. *Pathogens.* 2021;10:885. <https://doi.org/10.3390/pathogens10070885>
7. Browne LB, Menkir Z, Kahi V, Maina G, Asnakew S, Tubman M, et al.; Centers for Disease Control and Prevention (CDC). Notes from the field: hepatitis E outbreak among refugees from South Sudan – Gambella, Ethiopia, April 2014–January 2015. *MMWR Morb Mortal Wkly Rep.* 2015;64:537.
8. Ahmed A, Eldigail M, Elduma A, Breima T, Dietrich I, Ali Y, et al. First report of epidemic dengue fever and malaria co-infections among internally displaced persons in humanitarian camps of North Darfur, Sudan. *Int J Infect Dis.* 2021;108:513–6. <https://doi.org/10.1016/j.ijid.2021.05.052>
9. Ahmed A, Ali Y, Elduma A, Eldigail MH, Mhmoud RA, Mohamed NS, et al. Unique outbreak of Rift Valley fever in Sudan, 2019. *Emerg Infect Dis.* 2020;26:3030–3. <https://doi.org/10.3201/eid2612.201599>
10. Ahmed A, Ali Y, Elmagboul B, Mohamed O, Elduma A, Bashab H, et al. Dengue fever in the Darfur area, western Sudan. *Emerg Infect Dis.* 2019;25:2126. <https://doi.org/10.3201/eid2511.181766>

Address for correspondence: Ayman Ahmed, Human and Animal Health Unit, Department of Epidemiology and Public Health, Swiss Tropical and Public Health Institute, Kreuzstrasse 2, 4123 Allschwil, Switzerland; email: ayman.ame.ahmed@gmail.com

## Emergence of Dengue Virus Serotype 2 Cosmopolitan Genotype, Brazil

Marta Giovanetti,<sup>1</sup> Luiz Augusto Pereira, Gilberto A. Santiago, Vagner Fonseca, Maria Paqueta García Mendoza, Carla de Oliveira, Laise de Moraes, Joilson Xavier, Stephane Tosta, Hegger Fristch, Emerson de Castro Barbosa, Evandra Strazza Rodrigues, Dana Figueroa-Romero, Carlos Padilla-Rojas, Omar Cáceres-Rey, Ana Flávia Mendonça, Fernanda de Bruycker Nogueira, Rivaldo Venancio da Cunha, Ana Maria Bispo de Filippis, Carla Freitas, Cassio Roberto Leonel Peterka, Carlos Frederico Campelo de Albuquerque, Leticia Franco, Jairo Andrés Méndez Rico, Jorge L. Muñoz-Jordán,<sup>1</sup> Vinícius Lemes da Silva,<sup>1</sup> Luiz Carlos Junior Alcantara<sup>1</sup>

Author affiliations: Fundação Oswaldo Cruz, Rio de Janeiro, Brazil (M. Giovanetti, C. de Oliveira, F. de Bruycker Nogueira, R.V. da Cunha, A.M.B. de Filippis, L.C.J. Alcantara); Università Campus Bio-Medico di Roma, Rome, Italy (M. Giovanetti); Universidade Federal de Minas Gerais, Belo Horizonte, Brazil (M. Giovanetti, J. Xavier, S. Tosta, H. Fristch, L.C.J. Alcantara); Laboratório Central de Saúde Pública Dr. Giovanni Cysneiros, Goiânia, Brazil (L.A. Pereira, A.F. Mendonça, V.L. da Silva); Centers for Disease Control and Prevention, San Juan, Puerto Rico, USA (G.A. Santiago, J.L. Muñoz-Jordán); Organização Pan-Americana da Saúde/Organização Mundial da Saúde, Brasília, Brazil (V. Fonseca, C.F.C. de Albuquerque); Instituto Nacional de Salud, Lima, Peru (M.P. García Mendoza, D. Figueroa Romero, C. Padilla-Rojas, O. Cáceres-Rey); Fundação Oswaldo Cruz and Universidade Federal da Bahia, Salvador, Brazil (L. de Moraes); Fundação Ezequiel Dias, Belo Horizonte (E. de Castro Barbosa); University of São Paulo, Ribeirão Preto, Brazil (E.S. Rodrigues); Ministério da Saúde, Brasília (C. Freitas, C.R.L. Peterka); Pan American Health Organization–World Health Organization, Washington, DC, USA (L. Franco, J.A.M. Rico)

DOI: <https://doi.org/10.3201/eid2808.220550>

We used nanopore sequencing and phylogenetic analyses to identify a cosmopolitan genotype of dengue virus serotype 2 that was isolated from a 56-year-old male patient from the state of Goiás in Brazil. The emergence of a cosmopolitan genotype in Brazil will require risk assessment and surveillance to reduce epidemic potential.

**D**engue virus (DENV) is a single-stranded, positive-sense RNA virus that has a genome consisting of ≈11 kb. DENV belongs to the Flaviviridae

family (genus *Flavivirus*) and is transmitted by *Aedes aegypti* and *Ae. albopictus* mosquitoes (1). DENV has caused a substantial global economic and public health burden and numerous mild to severe epidemics in the Americas, particularly during recent decades (1). DENV can be divided into 4 antigenically distinct serotypes (DENV-1–4), which have an interserotype nucleotide variability of ≈30% (2). Each serotype is further subdivided into phylogenetically distinct genotypes often named according to their geographic origin, even though some DENV serotypes have spread to other regions (2). According to epidemiologic reports, recent dengue epidemics in Brazil and South America were mainly driven by the circulation of DENV-1 and DENV-2 serotypes (3,4). DENV-2 contributed substantially to dengue-related mortality in the region.

DENV-2 includes 5 distinct nonsylvatic genotypes. Circulation of the Asian I and II genotypes (also known as DENV-2 genotype IV) is mostly circumscribed to Asia. The Asian–American genotype, also known as the Southeast Asian–American or genotype III, replaced the American genotype (DENV-2 genotype I) in the 1980s (5). The cosmopolitan genotype (DENV-2 genotype II) is the most widespread and genetically heterogeneous genotype (6). This genotype is circulating in Asia, the Middle East, the Pacific Islands, and Africa and contributes substantially to the global dengue burden (6). The global dispersal of this genotype might have driven extensive intragenotypic diversity, potentially favoring widespread expansion (6).

Cosmopolitan lineages continue to expand geographically, and recent introductions have been reported in Asia and Africa (7,8). In South America, the cosmopolitan genotype was detected in Peru in 2019 and spread mainly in Madre de Dios Province, where 4,893 total dengue cases were reported during that year (9). However, much is still unknown about its genomic diversity, evolution, and transmission dynamics in the region. Because each genotype might result in different clinical outcomes or enhanced virus dispersal, surveillance of circulating strains is pivotal for public health preparedness (5).

We report a case of DENV-2 cosmopolitan genotype in Goiás state, a well-connected region located in midwestern Brazil. We combined mobile genomic sequencing and phylogenetic data to provide preliminary insight regarding the transmission dynamics of this genotype in Brazil.

The patient was a health worker at the Control Center and Zoonosis in Aparecida de Goiânia,

<sup>1</sup>These authors contributed equally to this article.

located in Goiás, who had no travel history. The patient had symptoms (fever, myalgia, nausea, retro-orbital pain, back pain, headache) compatible with an arbovirus infection on November 26, 2021. A serum sample was collected and sent to the Central Public Health Laboratory of Goiás for molecular screening. Viral RNA was extracted by using the QIAmp Viral RNA Mini Kit (QIAGEN, <https://www.qiagen.com>) and tested by quantitative reverse transcription PCR for arboviruses, including Zika, chikungunya, and yellow fever viruses and DENV-1–4. Molecular testing confirmed DENV-2 infection. We performed genome sequencing by using nanopore technology to rapidly identify the DENV genotype as part of an active arboviral

real-time monitoring effort in collaboration with public health laboratories in Brazil (Appendix, <https://wwwnc.cdc.gov/EID/article/28/8/22-0550-App1.pdf>).

We performed phylogenetic analysis by using the DENV Typing Tool (Genome Detective, <http://genomedetective.com>), which consistently placed the strain from Brazil in a clade within the cosmopolitan lineage and showed maximum statistical bootstrap support (100%) (Appendix Figure 1). Time-resolved maximum-likelihood trees demonstrated that the isolate obtained in this study clustered with 2 recently described DENV-2 strains isolated in Peru in 2019 (bootstrap support, 96%) (Figure; Appendix Figure 2), suggesting a possible

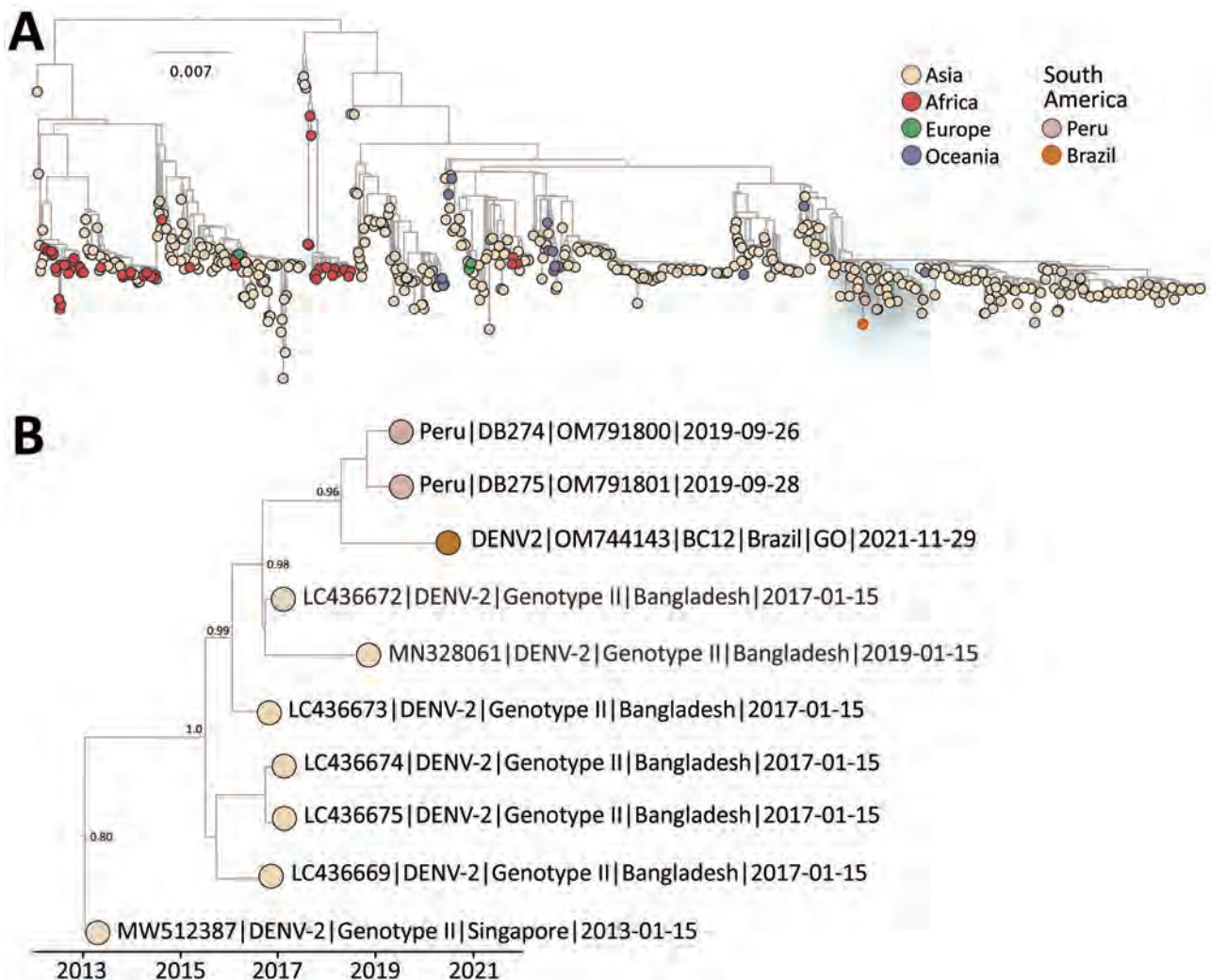


**Figure.** Maximum-likelihood phylogenetic analysis for DENV-2 cosmopolitan genotype, Brazil. A) Midpoint rooted tree shows the evolutionary relationships of the complete genome sequence from the DENV-2 cosmopolitan genotype identified from a patient in Goiás state, Brazil (orange circle), and 1,089 publicly available sequences from GenBank. Scale bar indicates nucleotide substitutions per site. Colors represent different sampling locations. Blue highlighting shows area enlarged in panel B. B) Time-resolved maximum-likelihood tree showing the blue highlighted area from the larger tree in panel A. Colors indicate geographic location of sampling. Support for branching structure is shown by bootstrap values at key nodes. DENV-2, dengue virus serotype 2.

cross-border transmission. This cluster in South America diverged from strains observed in Bangladesh that were collected during 2017–2019 (bootstrap support 100%), suggesting a complex transmission scenario mediated by transcontinental travel (Figure; Appendix Figure 3).

In summary, although genetic data alone cannot determine transmission directionality, phylogenetic analyses indicated that the DENV-2 cosmopolitan genotype sequence recovered from Goiás clustered with strains isolated in Peru, which deviated from a robust clade of sequences isolated in Bangladesh during 2017–2019 (Appendix Table). Brazil will need to improve DENV screening and sequencing to determine whether the virus is endemic or represents a recent introduction from elsewhere, such as Peru and Asia. The emergence of a DENV-2 cosmopolitan genotype in Brazil will require active outbreak risk assessment to reduce epidemic potential. Considering the potential for spread in this region, we advocate for a shift to active surveillance to ensure adequate control of any potential outbreak of this genotype across South America.

This work was supported in part by a National Institutes of Health grant (no. U01 AI151698) for the United World Antiviral Research Network; the Brazilian National Council for Scientific and Technological Development (grant no. 421598/2018-2); and Brazilian Ministry of Health (grant no. SCON2021-00180).

M.G. and L.C.J.A. are supported by Fundação de Amparo a Pesquisa do Estado do Rio de Janeiro. M.G. is funded by Programma Operativo Nazionale Ricerca e Innovazione 2014–2020. Dengue virus serotype 2 sequences from Peru were obtained from the Pan American Health Organization project Vigilancia Genómica del Dengue en las Américas.

Author contributions: M.G. and L.C.J.A. were responsible for the study concept and design; M.G., L.A.P., G.A.S., V.F., M.P.G.M., C.O., L.M., J.X., S.T., H.F., E.C.B., E.S.R., D.F.R., C.P.R., O.C.R., A.N.M., and F.B.N. performed the investigations; M.G., V.F., L.M., and G.B. analyzed the data; L.A.P., A.F.M., M.P.G.M., A.M.B.F., R.V.C., V.L.S., C.F.C.A., C.R.L.P., C.F., J.A.M.M.R., J.L.M.J., M.G., and L.C.J.A. were responsible for data curation; all authors have read and agreed to the published version of the manuscript.

## About the Author

Dr. Giovanetti is a visiting researcher at the Flavivirus Reference Laboratory of the Oswaldo Cruz Foundation in Rio de Janeiro, Brazil. Her primary research interest focuses on the patterns of gene flow in pathogen populations as determinants of viral outbreaks and translating this information into public policy recommendations.

## References

1. Brathwaite Dick O, San Martín JL, Montoya RH, del Diego J, Zambrano B, Dayan GH. The history of dengue outbreaks in the Americas. *Am J Trop Med Hyg.* 2012;87:584–93. <https://doi.org/10.4269/ajtmh.2012.11-0770>
2. Cuypers L, Libin PJK, Simmonds P, Nowé A, Muñoz-Jordán J, Alcántara LCJ, et al. Time to harmonize dengue nomenclature and classification. *Viruses.* 2018;10:569. <https://doi.org/10.3390/v10100569>
3. Adelino TÊR, Giovanetti M, Fonseca V, Xavier J, de Abreu ÁS, do Nascimento VA, et al. Field and classroom initiatives for portable sequence-based monitoring of dengue virus in Brazil. *Nat Commun.* 2021;12:2296. <https://doi.org/10.1038/s41467-021-22607-0>
4. Forshey BM, Reiner RC, Olkowski S, Morrison AC, Espinoza A, Long KC, et al. Incomplete protection against dengue virus type 2 re-infection in Peru. *PLoS Negl Trop Dis.* 2016;10:e0004398. <https://doi.org/10.1371/journal.pntd.0004398>
5. Rico-Hesse R, Harrison LM, Salas RA, Tovar D, Nisalak A, Ramos C, et al. Origins of dengue type 2 viruses associated with increased pathogenicity in the Americas. *Virology.* 1997;230:244–51. <https://doi.org/10.1006/viro.1997.8504>
6. Yenamandra SP, Koo C, Chiang S, Lim HSJ, Yeo ZY, Ng LC, et al. Evolution, heterogeneity and global dispersal of cosmopolitan genotype of dengue virus type 2. *Sci Rep.* 2021;11:13496. <https://doi.org/10.1038/s41598-021-92783-y>
7. Ayolabi CI, Olusola BA, Ibemgbo SA, Okonkwo GO. Detection of dengue viruses among febrile patients in Lagos, Nigeria and phylogenetics of circulating dengue serotypes in Africa. *Infect Genet Evol.* 2019;75:103947. <https://doi.org/10.1016/j.meegid.2019.103947>
8. Suzuki K, Phadungsombath J, Nakayama EE, Saito A, Egawa A, Sato T, et al. Genotype replacement of dengue virus type 3 and clade replacement of dengue virus type 2 genotype Cosmopolitan in Dhaka, Bangladesh in 2017. *Infect Genet Evol.* 2019;75:103977. <https://doi.org/10.1016/j.meegid.2019.103977>
9. Paquita García M, Padilla C, Figueroa D, Manrique C, Cabezas C. Emergence of the cosmopolitan genotype of dengue virus serotype 2 (DENV2) in Madre de Dios, Peru, 2019 [in Spanish]. *Rev Peru Med Exp Salud Publica.* 2022;39:126–8. <http://dx.doi.org/10.17843/rpmesp.2022.391.10861>

Address for correspondence: Luiz Carlos Júnior Alcántara, Instituto Oswaldo Cruz/IOC/FIOCRUZ, Rio de Janeiro 21040-360, Brazil; email: [luiz.alcantara@ioc.fiocruz.br](mailto:luiz.alcantara@ioc.fiocruz.br)

# etymologia

## *Anopheles culicifacies*

[‘ə’ nɒfɪli:z’ kyü-lə cifā-sh(ē)-ēz]

Gaurav Kumar

In 1901, George Michael James Giles, a lieutenant-colonel and physician in the Indian Medical Service, described *Anopheles culicifacies*, which he collected from his guest house in Hoshangabad, India. This mosquito mimicked *Culex* spp. in facial appearance and resting posture (body angled to the surface they are resting on), prompting Giles to name it *Anopheles culicifacies* because of its culex (culici)-like appearance (facies).



**Figure 1.** *Anopheles culicifacies* mosquito. Photograph taken by the author.

*An. culicifacies* is the principle vector of malaria in India, contributing to >60% of malaria cases in this country annually. Therefore, ≈80% of the budget for malaria control in India is spent on control of this mosquito. Adults can

be identified based on characteristic wing morphology (dark third vein) and palpi ornamentation (apical pale band is nearly equal to the pre-apical dark band).



**Figure 2.** Wing morphology of *Anopheles culicifacies* mosquito showing the dark third vein (arrow). The length of the wing on the right is 2.5 mm. Photograph taken by the author.

### Acknowledgment

I thank the Director of the National Institute of Malaria Research, Delhi, India, for providing encouragement to write this etymologia.

### Sources

1. Giles GM. Description of four new species of *Anopheles* from India. *Entomologist's Monthly Magazine*. 1901;37:196–8.
2. Ramachandra Rao T. The anophelines of India. New Delhi: Oxford; 1984. p. 365–419.
3. Sharma VP, Dev V. Biology and control of *Anopheles culicifacies* Giles 1901. *Indian J Med Res*. 2015;141:525–36.

Author affiliation: National Institute of Malaria Research, Delhi, India

DOI: <https://doi.org/10.3201/eid2808.211875>

Address for correspondence: Gaurav Kumar, India Council of Medical Research, National Institute of Malaria Research, Sector 8, Dwarka, Delhi, India; email: [gauravnimr@gmail.com](mailto:gauravnimr@gmail.com)

## Early SARS-CoV-2 Reinfections within 60 Days and Implications for Retesting Policies

Louis Nevejan, Lize Cuypers, Lies Laenen, Liselotte Van Loo, François Vermeulen, Elke Wollants, Ignace Van Hecke, Stefanie Desmet, Katrien Lagrou, Piet Maes, Emmanuel André

Author affiliations: University Hospitals Leuven, Leuven, Belgium (L. Nevejan, L. Cuypers, L. Laenen, L. Van Loo, F. Vermeulen, I. Van Hecke, S. Desmet, K. Lagrou, E. André); Rega Institute, Katholieke Universiteit Leuven, Leuven (E. Wollants, S. Desmet, K. Lagrou, P. Maes, E. André)

DOI: <https://doi.org/10.3201/eid2808.220617>

Illustrated by a clinical case supplemented by epidemiologic data, early reinfections with SARS-CoV-2 Omicron BA.1 after infection with Delta variant, and reinfection with Omicron BA.2 after Omicron BA.1 infection, can occur within 60 days, especially in young, unvaccinated persons. The case definition of reinfection, which influences retesting policies, should be reconsidered.

The sequential emergence of SARS-CoV-2 variants of concern (VOCs), characterized by an antigenic drift and higher transmissibility, has been observed in countries around the world at least 3 times during the past 13 months (1). Although the SARS-CoV-2 Delta variant showed a limited antigenic diversity with previous VOCs, Omicron differs more notably from other VOCs than any previous VOC did at the time it emerged (K. Van der Straten et al., unpub. data, <https://www.medrxiv.org/content/10.1101/2022.01.03.21268582v2>). The resulting decrease of antibody efficacy in both convalescent and vaccinees' serum samples drives the high number of reinfection and vaccine breakthrough cases observed with Omicron compared with observations made during previous waves (2,3).

To date, reinfections with SARS-CoV-2 are defined by the European Centre for Disease Prevention and Control as a positive PCR or rapid antigen test  $\geq 60$  days after previous positive PCR, rapid antigen test, or serologic test (4). This definition has influenced testing strategies in several countries, and many countries consider a person protected for 180 days after an initial positive test result (5). We suggest that this reinfection definition should be revised.

To illustrate our point, we report a case of an immunocompetent unvaccinated 10-year-old boy with

no noteworthy medical history who tested positive for SARS-CoV-2 Delta variant ( $\geq 7.0$  log copies/mL, sublineage AY.43) on December 3, 2021, concomitant with an outbreak at the patient's school. The patient's brother and mother, both vaccinated, were infected as well. All 3 persons experienced mild COVID-19 symptoms. Because of a sports-related trauma, the patient was admitted for surgery on January 11, 2022. Pre-procedural SARS-CoV-2 screening detected a strong positive result (5.1 log copies/mL) with Omicron BA.1 variant, only 39 days after the patient's infection with Delta. The patient remained pauci-symptomatic. High-risk contact screening of the patient's brother detected a low viral load; the mother tested SARS-CoV-2-negative (Appendix Table, <https://wwwnc.cdc.gov/EID/article/28/8/22-0617-App1.pdf>).

To put this clinical case into a wider epidemiologic context, we estimated the incidence of early reinfection with Omicron BA.1 after Delta infection and reinfection with Omicron BA.2 after BA.1 infection in a community setting (Flemish Brabant, Belgium). During December 1, 2021–February 7, 2022 ( $n = 9$  weeks), a period characterized by the full viral replacement of Delta by Omicron BA.1 (Appendix Figure 1) (6), a total of 59,515 ambulatory patients tested SARS-CoV-2-positive at the federal testing platform located in Leuven, Belgium (positivity rate 36.5%). Among these patients, the spike (S) gene was detected in a first sample in 0.15% (91/59,515 persons) by using the TaqPath PCR test (ThermoFisher Scientific, <https://www.thermofisher.com>), which suggests Delta infection. S gene target failure was reported in a second positive sample within this period (nucleocapsid gene cycle threshold  $< 27.8$ ), indicating a reinfection with Omicron BA.1 briefly after Delta infection (7).

Similarly, during January 1, 2022–March 10, 2022 ( $n = 9$  weeks), a period characterized by the emerging viral replacement of Omicron BA.1 by BA.2 but declining disease prevalence (Appendix Figure 1) (6), a total of 58,166 patients tested SARS-CoV-2-positive (positivity rate 48.3%). Among these, 0.01% (5/58,166) demonstrated S gene target failure in a first sample but an S gene was detected in a second positive sample, indicating a reinfection with Omicron BA.2 after BA.1 infection in these patients.

We noted the age and vaccination status of these 96 patients with documented early reinfection and compared that with the vaccination rate for the same age groups in the same geographic region (Flanders, Belgium) (Figure) (8). Early reinfections were most frequently observed among young unvaccinated patients ( $< 12$  years of age). Compared with the

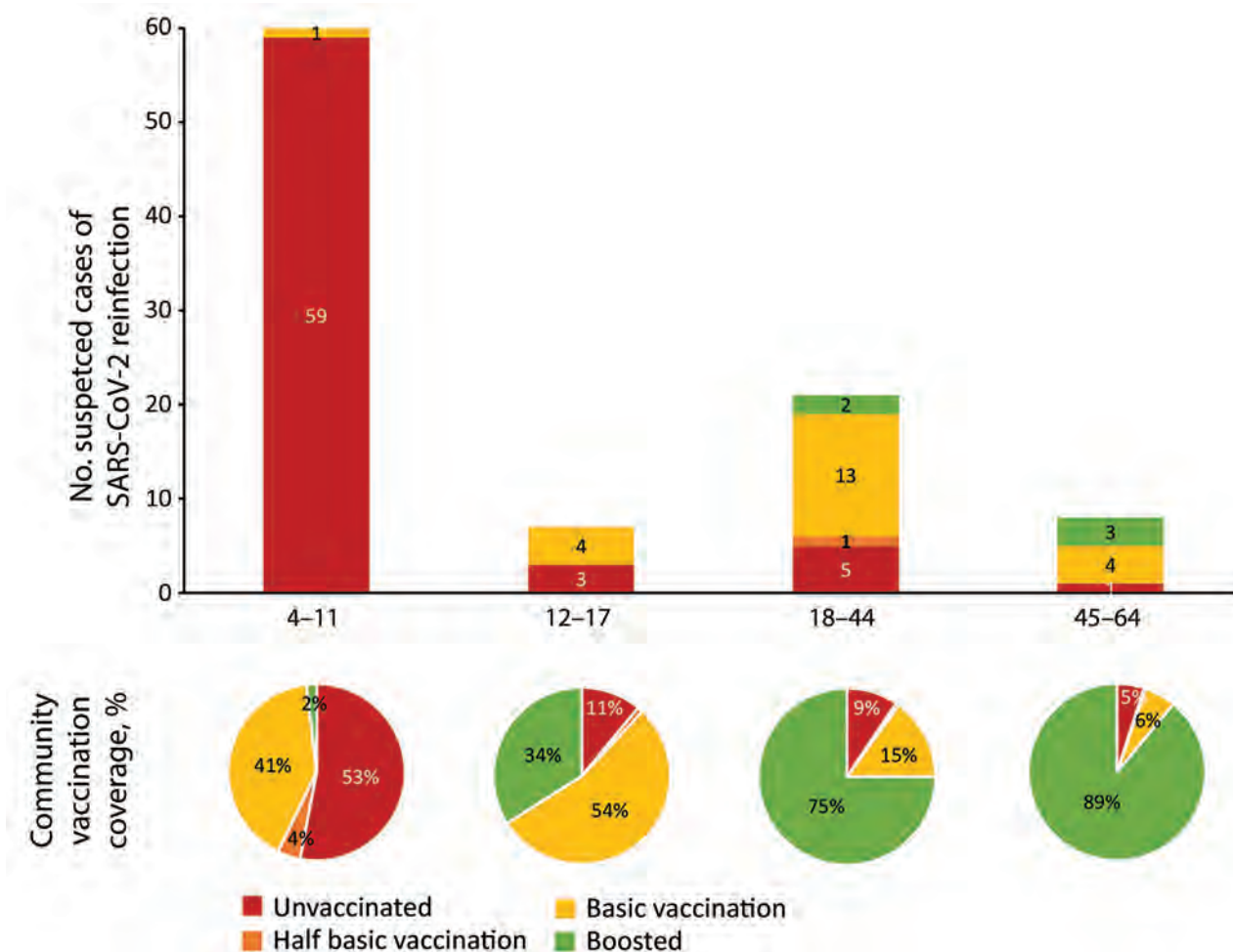


**Figure.** Number of patients with presumed SARS-CoV-2 reinfection including vaccination status compared with age-corresponding vaccination coverage in the community, Flanders, Belgium. Consecutive infections were detected during December 1, 2021–February 7, 2022 (reinfection with Omicron BA.1 shortly after Delta infection,  $n = 91$  patients) and during January 1–March 10, 2022 (reinfection with Omicron BA.2 shortly after Omicron BA.1 infection,  $n = 5$  patients). Half basic vaccination indicates 1 vaccine of ChAdOx1 nCoV-19 (AstraZeneca, <https://www.astrazeneca.com>), BNT162b2 (Pfizer-BioNTech, <https://www.pfizer.com>), or mRNA-1273 (Moderna, <https://www.modernatx.com>); basic vaccination indicates 2 vaccines of ChAdOx1, BNT162b2, or mRNA-1273 or 1 vaccine of Ad26.COVS.2 (Johnson & Johnson/Janssen, <https://www.janssen.com>); boosted indicates basic vaccination followed by 1 vaccine of BNT162b2 or mRNA-1273.

corresponding age groups in the general population, patients with early reinfections tended to be unvaccinated, partially vaccinated, or vaccinated but not boosted. Median time between the 2 positive samples with different VOCs was 47 days (range 17–65 days) (Appendix Figure 2).

Previous retrospective cohort studies (2) showing a prolonged maintenance of protection against reinfection should be questioned after the emergence of Omicron. Our data confirm that early Omicron BA.1 reinfection (<60 days) after Delta infection and BA.2 reinfection after BA.1 infection can occur, especially in young, unvaccinated persons. In older patient groups, unvaccinated persons and persons who had

received basic vaccination but no booster might be more vulnerable to reinfections than patients who received a first booster vaccine. Data from Denmark (M. Stegger et al., unpub. data, <https://www.medrxiv.org/content/10.1101/2022.02.19.22271112v1>) suggest reinfection usually results in mild disease not requiring hospitalization, as demonstrated by the case we report here.

The occurrence of a full viral replacement in a matter of weeks will continue to affect the duration and efficacy of immunity in the future. For this reason, in cases of sustained variant circulation, indications for retesting persons after a previous SARS-CoV-2 infection within 180 days are limited.

However, in cases of cocirculation or switch of VOC with antigenic drift within this period, this minimum retesting interval should be omitted to adequately detect SARS-CoV-2 reinfections.

This article was preprinted at <https://www.medrxiv.org/content/10.1101/2022.04.04.22273172v1>.

UZ Leuven, as the National Reference Center for Respiratory Pathogens, is supported by Sciensano, which is gratefully acknowledged.

### About the Author

Mr. Nevejan is a trainee in clinical biology at the Department of Laboratory Medicine of University Hospitals Leuven. His current research interest is the field of epidemiology and medical microbiology.

### References:

1. Mullen JL, Tsueng G, Abdel Latif A, Alkuzweny M, Cano M, Haag E, et al. Outbreak information. A standardized, open-source database of COVID-19 resources and epidemiology data [cited 2022 Feb 4]. <https://outbreak.info>
2. Kim P, Gordon SM, Sheehan MM, Rothberg MB. Duration of severe acute respiratory syndrome coronavirus 2 natural immunity and protection against the Delta variant: a retrospective cohort study. *Clin Infect Dis*. 2021 Dec 3 [Epub ahead of print]. <https://doi.org/10.1093/cid/ciab999>
3. Pulliam JRC, van Schalkwyk C, Govender N, von Gottberg A, Cohen C, Groome MJ, et al. Increased risk of SARS-CoV-2 reinfection associated with emergence of Omicron in South Africa. *Science*. 2022;376:eabn4947. <https://doi.org/10.1126/science.abn4947>
4. European Centre for Disease Prevention and Control. Reinfection with SARS-CoV-2: implementation of a surveillance case definition within the EU/EEA [cited 2022 Mar 21]. <https://www.ecdc.europa.eu/en/publications-data/reinfection-sars-cov-2-implementation-surveillance-case-definition-within-eueea>
5. European Commission. EU Digital COVID Certificate. 2022 [cited 2022 May 10]. [https://ec.europa.eu/info/live-work-travel-eu/coronavirus-response/safe-covid-19-vaccines-europeans/eu-digital-covid-certificate\\_en](https://ec.europa.eu/info/live-work-travel-eu/coronavirus-response/safe-covid-19-vaccines-europeans/eu-digital-covid-certificate_en)
6. Cuyppers L, Baele G, Dellicour S, Maes P, André E. Genomic surveillance of SARS-CoV-2 in Belgium. 2022 [cited 2022 May 10]. <https://www.uzleuven.be/nl/laboratoriumgeeneskunde/genomic-surveillance-sars-cov-2-belgium>
7. World Health Organization. Classification of Omicron (B.1.1.529): SARS-CoV-2 variant of concern. 2021 [cited 2022 May 10]. [https://www.who.int/news/item/26-11-2021-classification-of-omicron-\(b.1.1.529\)-sars-cov-2-variant-of-concern](https://www.who.int/news/item/26-11-2021-classification-of-omicron-(b.1.1.529)-sars-cov-2-variant-of-concern)
8. Vaesen J. Covid Vaccinaties België. 2022 [cited 2022 Mar 21]. <https://covid-vaccinatie.be/nl>

Address for correspondence: Louis Nevejan, Department of Laboratory Medicine, National Reference Center for Respiratory Pathogens, UZ Leuven–University Hospitals Leuven, Herestraat 49, 3000 Leuven, Belgium; email: [louis.nevejan@uzleuven.be](mailto:louis.nevejan@uzleuven.be)

## Household Secondary Attack Rates of SARS-CoV-2 Omicron Variant, South Korea, February 2022

Do Sang Lim,<sup>1</sup> Young June Choe,<sup>1</sup> Young Man Kim, Sang Eun Lee, Eun Jung Jang, Jia Kim, Young-Joon Park

Author affiliations: Korea Disease Control and Prevention Agency, Cheongju, South Korea (D.S. Lim, Y.M. Kim, S.E. Lee, E.J. Jang, J. Kim, Y.-J. Park); Korea University Anam Hospital, Seoul, South Korea (Y.J. Choe)

DOI: <http://doi.org/10.3201/eid2808.220384>

We studied the effect of booster vaccinations on reducing household transmission of SARS-CoV-2 B.1.1529 (Omicron) variant in a February 2022 sampling of contacts in South Korea. The secondary attack rate was lower for vaccinated versus unvaccinated contacts, and booster vaccination resulted in a lower incidence rate ratio.

Since its initial detection in November 2021, the SARS-CoV-2 B.1.1529 (Omicron) variant has become the dominant strain in South Korea. Its emergence led to a large increase in the number of COVID-19 cases, mainly through household transmission (1,2). In this study, we sought to estimate the effect of booster vaccinations on reducing the household transmission of COVID-19 to guide current COVID-19 mitigation strategy.

This national, retrospective cohort study included all residents in South Korea with laboratory-confirmed SARS-CoV-2 infection reported during February 1–10, 2022. The background population was estimated as 53 million persons according to the 2021 census. Booster vaccinations with mRNA vaccines were provided in October 2021, reaching ≈30 million doses (60% of the total population) by February 2022. We retrieved epidemiologic data, merged with the national immunization registry of household contacts of persons infected with SARS-CoV-2, to describe the difference in secondary attack rates (SARs) by vaccination status. Details of the surveillance system, vaccination program, and dataset employed in this study are described in a previous study (3). Persons who had household contact with laboratory-confirmed SARS-CoV-2-positive patients underwent mandatory PCR testing, regardless of the presence of symptoms, and were put under active surveillance for 10

<sup>1</sup>These first authors contributed equally to this article.

days. During the quarantine period, PCR testing was mandated when the household contact had symptoms, and testing was performed on day 9 or day 10 if the contact had no symptoms.

We defined an index case-patient as a person with a positive SARS-CoV-2 test result determined through epidemiologic investigation who was most likely not infected in the household, a household contact as a person living in the same home as an index case-patient, and a household-infected case-patient as a person living in the same home as an index case-patient who had a positive PCR test result for SARS-CoV-2. We defined partly vaccinated persons as those who had received the first dose of a 2-dose vaccination regimen  $\geq 14$  days and fully vaccinated persons as those who had completed a 2-dose regimen of Pfizer-BioNTech (<https://www.pfizer.com>), AstraZeneca (<https://www.astrazeneca.com>), Moderna (<https://www.moderna.com>), or mix-and-match vaccines (time since vaccination  $\geq 14$  days) or those who completed a 1-dose regimen of the Janssen/Johnson & Johnson (<https://www.janssen.com>) vaccine (time since vaccination  $\geq 28$  days). We defined a booster dose as a third vaccination dose ( $\geq 14$  days since administration) after 2 doses of a primary vaccination series.

Data from the period February 1–10, 2022, revealed 163,581 household contacts of index case-patients with PCR-confirmed SARS-CoV-2 (Table). Within 10 days of active monitoring, 59,982 household contacts were confirmed to have SARS-CoV-2

infection, resulting in an SAR of 36.7%. Children 0–11 years of age had the highest SAR (55.1%), followed by adolescents 12–17 years of age (44%) and adults 30–39 years of age (44%) ( $p < 0.001$ ). The SAR was highest in contacts who were unvaccinated (53%), followed by those who received the Janssen vaccine (49%) or the AstraZeneca vaccine (37.2%). The SAR was comparatively lower in contacts who received the Pfizer-BioNTech vaccine (34.1%), the Moderna vaccine (32.7%), or a mix-and-match vaccine series (30.4%) ( $p < 0.001$ ). In examining the incidence rate ratio of household contacts according to the vaccination status of the SARS-CoV-2 index case-patients (Figure), we found that booster vaccination in household contacts resulted in a lower incidence rate ratio, irrespective of vaccination status of the index case-patient.

Our findings offer evidence of improved protection against SARS-CoV-2 transmission when household contacts have received booster vaccinations. Transmission occurred in 36.7% (59,982/163,581) of the household contacts we studied, a percentage that falls within the range of results from similar studies in Denmark (29%–39%) and the United States (67.8%) (4,5). Another study demonstrated an association between booster vaccination with mRNA vaccines and protection against symptomatic Omicron infection (6). Consistent with these findings, our observations suggest that booster vaccination offers a higher level of protection against Omicron infection when household contacts are vaccinated and boosted.

**Table.** Household contacts, household infected cases, and secondary attack rate of SARS-CoV-2 Omicron variant, South Korea, February 1–10, 2022

| Characteristic             | No. household contacts | No. household infection cases | Secondary attack rate, % |
|----------------------------|------------------------|-------------------------------|--------------------------|
| Total                      | 163,581                | 59,982                        | 36.7                     |
| Sex                        |                        |                               |                          |
| M*                         | 80,145                 | 27,595                        | 34.4                     |
| F                          | 83,436                 | 32,387                        | 38.8                     |
| Age group, y               |                        |                               |                          |
| 0–11*                      | 18,456                 | 10,173                        | 55.1                     |
| 12–17                      | 13,266                 | 5,839                         | 44.0                     |
| 18–29                      | 26,243                 | 8,497                         | 32.4                     |
| 30–39                      | 15,920                 | 7,006                         | 44.0                     |
| 40–49                      | 31,477                 | 12,497                        | 39.7                     |
| 50–59                      | 33,920                 | 9,302                         | 27.4                     |
| 60–74                      | 18,037                 | 5,056                         | 28.0                     |
| $\geq 75$                  | 6,262                  | 1,612                         | 25.7                     |
| Vaccine type†              |                        |                               |                          |
| Comirnaty/Pfizer-BioNTech* | 87,296                 | 29,808                        | 34.1                     |
| Vaxzevria/AstraZeneca      | 1,638                  | 610                           | 37.2                     |
| Spikevax/Moderna           | 19,398                 | 6,335                         | 32.7                     |
| Jcovden/Janssen            | 261                    | 128                           | 49.0                     |
| Mix-and-match‡             | 26,780                 | 8,144                         | 30.4                     |
| Unvaccinated               | 28,208                 | 14,957                        | 53.0                     |

\* $p < 0.001$ .

†Pfizer-BioNTech, <https://www.pfizer.com>; AstraZeneca, <https://www.astrazeneca.com>; Moderna, <https://www.modernatx.com>; Janssen/Johnson & Johnson, <https://www.janssen.com>.

‡Heterologous (mix-and-match) vaccinations with mRNA vaccines were provided to AstraZeneca-primed and Janssen-primed persons.

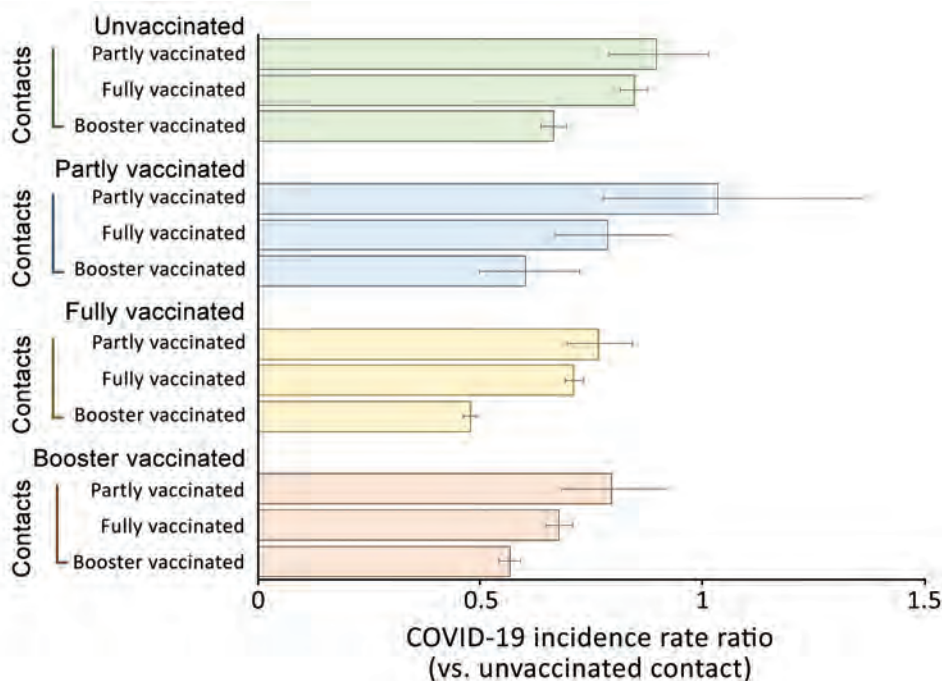


**Figure.** Vaccination status of household contacts relative to the vaccination status of SARS-CoV-2 Omicron variant index case-patients, South Korea, February 1–10, 2022. Header rows indicate vaccination status of index case-patients, and vaccination status categories for their contacts are displayed below. Error bars indicate 95% CIs.

The first limitation of our study is that surveillance did not clearly distinguish other potential sources of transmission within a household. Exposure outside the household might have led to some secondary cases. Second, difference in testing behavior based on vaccination status might have introduced bias into our findings. If unvaccinated persons have a different probability of getting tested compared with vaccinated persons, our results could be underestimating the true effectiveness of vaccines against household transmission; therefore, results of this study should be interpreted cautiously. Last, results based on such a large population might have produced statistical significance despite small effect size.

In summary, we provide real-world evidence to better understand the effect of booster vaccination in preventing household transmission of the Omicron variant of SARS-CoV-2. Additional studies are needed to determine the effectiveness of booster vaccination in regard to severe infections and deaths across different age groups. However, the higher SAR in younger household contacts we studied supports the need for public health initiatives to extend booster vaccination in younger age groups.

#### Acknowledgments

We thank the COVID-19 Vaccination Task Force and Division of National Immunization, Korea Disease Control and Prevention Agency; relevant ministries, including the Ministry of Interior and Safety, Si/Gu,

and Si/Gun/Gu; medical staff in health centers; and medical facilities for their efforts in responding to the COVID-19 outbreak.

This study is part of K-COVE (Korea COVID-19 Vaccine Effectiveness Study), which was initiated and operated by the Korea Disease Control and Prevention Agency.

The opinions expressed by the authors contributing to this journal do not necessarily reflect the opinions of the Korea Disease Control and Prevention Agency or the institutions with which the authors are affiliated.

#### About the Authors

Mr. Lim is a public health officer of the Korea Disease Control and Prevention Agency. His main research interests are epidemiologic investigations and surveillance measures for infectious diseases. Dr. Choe is a clinical associate professor of pediatrics at Korea University Anam Hospital. His main research addresses the quantification and understanding of the mechanisms by which immunization programs affect public health.

#### References

1. Kim EY, Choe YJ, Park H, Jeong H, Chung JH, Yu J, et al. Community transmission of SARS-CoV-2 Omicron variant, South Korea, 2021. *Emerg Infect Dis.* 2022; 28:898–900. <https://doi.org/10.3201/eid2804.220006>
2. Song JS, Lee J, Kim M, Jeong HS, Kim MS, Kim SG, et al. Serial intervals and household transmission of SARS-CoV-2 Omicron variant, South Korea, 2021. *Emerg Infect Dis.* 2022;28:756–9. <https://doi.org/10.3201/eid2803.212607>

3. Yi S, Choe YJ, Lim DS, Lee HR, Kim J, Kim YY, et al. Impact of national Covid-19 vaccination campaign, South Korea. *Vaccine*. 2022;40(36):3670–5. <https://doi.org/10.1016/j.vaccine.2022.05.002>
4. Madewell ZJ, Yang Y, Longini IM, Halloran ME, Dean NE. Household secondary attack rates of SARS-CoV-2 by variant and vaccination status: an updated systematic review and meta-analysis. *JAMA Netw Open*. 2022;5:e229317. <https://doi.org/10.1001/jamanetworkopen.2022.9317>
5. Baker JM, Nakayama JY, O'Hegarty M, McGowan A, Teran RA, Bart SM, et al. SARS-CoV-2 B.1.1.529 (Omicron) variant transmission within households—four U.S. jurisdictions, November 2021–February 2022. *MMWR Morb Mortal Wkly Rep*. 2022;71:341–6. <https://doi.org/10.15585/mmwr.mm7109e1>
6. Accorsi EK, Britton A, Fleming-Dutra KE, Smith ZR, Shang N, Derado G, et al. Association between 3 doses of mRNA COVID-19 vaccine and symptomatic infection caused by the SARS-CoV-2 Omicron and Delta variants. *JAMA*. 2022;327:639–51. <https://doi.org/10.1001/jama.2022.0470>

Address for correspondence: Young-Joon Park, (28159) Korea Disease Control and Prevention Agency, Osong Health Technology Administration Complex, 187, Osongsaengmyeong 2-ro, Osong-eup, Heungdeok-gu, Cheongju-si, Chungcheongbuk-do, South Korea; email: pahmun@korea.kr

## Estimating COVID-19 Vaccine Effectiveness for Skilled Nursing Facility Healthcare Personnel, California, USA

Monise Magro, Andrea Parriott, Tisha Mitsunaga, Erin Epton

Author affiliation: California Department of Public Health, Richmond, California, USA

DOI: <https://doi.org/10.3201/eid2808.220650>

We estimated real-world vaccine effectiveness among skilled nursing facility healthcare personnel who were regularly tested for SARS-CoV-2 infection in California, USA, during January–March 2021. Vaccine effectiveness for fully vaccinated healthcare personnel was 73.3% (95% CI 57.5%–83.3%). We observed high real-world vaccine effectiveness in this population.

The COVID-19 pandemic has severely affected skilled nursing facility (SNF) residents and healthcare personnel (HCP) (1,2). HCP are at high risk for SARS-CoV-2 exposure during patient care (3,4), and were among the earliest groups prioritized for COVID-19 vaccination starting in mid-December 2020 (5). Through June 2021, all SNF HCP in California, regardless of vaccination status or symptoms, were required to undergo at least weekly screening testing for SARS-CoV-2 infection (6). This system provided us with ideal conditions to assess vaccination effectiveness.

We estimated real-world effectiveness of COVID-19 vaccination against PCR-confirmed SARS-CoV-2 infections in SNF HCP in California by using a matched case-control study. We identified SNF HCP COVID-19 case-patients and controls from the statewide communicable disease reporting system (Appendix, <https://wwwnc.cdc.gov/EID/article/28/8/22-0650-App1.pdf>). We selected persons 18–54 years of age (Appendix) with specimen collection dates during January–March 2021. We obtained COVID-19 vaccination status from the California Immunization Registry (Appendix).

We defined partial vaccination as  $\geq 1$  vaccine dose received before specimen collection with a second dose (if received, for a 2-dose series vaccine)  $< 14$  days before collection, and full vaccination as the second dose (or 1 dose in a single-dose series) received  $\geq 14$  days before specimen collection. We matched case-patients to controls on specimen collection date and SNF county by using simple random sampling (without replacement) and a 1:1 ratio. We applied conditional logistic regression to estimate vaccine effectiveness for partial and full vaccination (compared with no vaccination).

Because of the density-based selection of the control series, in which controls are time-matched to case-patients, drawing from a risk set of persons who are at risk for becoming case-patients at the time the case is detected, the odds ratio approximates the incidence rate ratio without reliance on the rare disease assumption (7). We examined age, sex, and California Healthy Places Index (HPI) composite health score (8) by using HCP residential address and race and ethnicity (Appendix) as potential confounders.

We performed the analysis before and after excluding case-patients and controls who had previously confirmed positive test results within 90-day and 180-day windows (Table). We performed analyses by using SAS version 9.4 (<https://www.sas.com>). This study received an exempt determination from the California Committee for the Protection of Human Subjects.

**Table.** Estimated COVID-19 vaccine effectiveness among skilled nursing facility healthcare personnel, California, USA, January–March 2021\*

| Models   | Vaccination status† | No.           |          | Vaccine effectiveness (95% CI), % |
|--|---------------------|---------------|----------|-----------------------------------|
|  |                     | Case-patients | Controls |                                   |
| No removal of previous positive results (4,238 case–control participants; 2,119 matched pairs)           | Partial             | 465           | 629      | 37.5 (27.7–46.0)                  |
|  | Full                | 36            | 94       | 71.7 (55.9–81.8)                  |
| Removal of previous positive results within 90 d (3,742 case–control participants; 1,871 matched pairs)  | Partial             | 430           | 567      | 35.6 (24.8–44.8)                  |
|  | Full                | 32            | 89       | 73.3 (57.5–83.3)                  |
| Removal of previous positive results within 180 d (3,424 case–control participants; 1,712 matched pairs) | Partial             | 394           | 524      | 36.3 (25.1–45.8)                  |
|  | Full                | 25            | 70       | 72.7 (54.3–83.7)                  |

\*Unadjusted analysis results are presented. Adjustment for sex, age, and Healthy Places Index scores did not substantially alter these estimates.

†Partial vaccination:  $\geq 1$  dose before specimen collection date but final dose  $< 14$  d before specimen collection date; full vaccination: final dose  $\geq 14$  d before specimen collection date.

Of the 4,238 study participants, 28.9% (1,224) were partially or fully vaccinated; 71.1% (3,014) were classified as unvaccinated, including 47.8% (2,025) who did not have a California Immunization Registry COVID-19 vaccination record and 23.3% (989) who were vaccinated on or after specimen collection date. A higher proportion of controls than case-patients were partially or fully vaccinated (Table). Among the fully vaccinated, 91.5% received Pfizer-BioNTech vaccine (<https://www.pfizer.com>) and 8.5% received Moderna vaccine (<https://www.modernatx.com>). Among the partially vaccinated, 54% received Pfizer-BioNTech vaccine, 45% received Moderna vaccine, and  $< 1\%$  received a combination of 2 different vaccines (e.g., Pfizer-BioNTech and Moderna). All Johnson & Johnson/Janssen vaccine (<https://www.janssencovid19vaccine.com>) recipients, representing 1.7% of participants matched to a vaccination record, were classified as unvaccinated because the vaccination date was after the specimen collection date.

Vaccine effectiveness was 73.3% (95% CI 57.5%–83.3%) for full vaccination (Table). We observed no substantial change ( $< 10\%$ ) in vaccine effectiveness estimates produced by the models with or without removal of previous positive test results (Table). We assumed the model excluding previous positive test results within 90 days was the most appropriate because this model excludes persons with potential residual viral shedding and agrees with the national COVID-19 disease (new) case definition (9) that excludes persons who had previous positive test results within 90 days. Adjustment for age, sex, and HPI score did not change vaccine effectiveness estimates by  $> 10\%$ , and inclusion of race/ethnicity did not alter the full vaccination estimate by  $> 10\%$  (Appendix Tables 2–5).

A major strength of our study is that SNF HCP were tested regularly irrespective of symptoms or known exposure, enabling us to capture their infection status and estimate vaccine effectiveness for prevention of COVID-19, including asymptomatic infection. The unchanged vaccine effectiveness estimate after adjustment for HPI score reflects that COVID-19

vaccination efforts for SNF HCP engaged persons regardless of their residential community. One limitation is that the study period was before the Delta or Omicron virus variants became dominant. Because serial testing of vaccinated SNF HCP in California stopped during July 2021, the study period could not be expanded to examine effectiveness against later variants or changes in vaccine effectiveness over time since vaccination. In addition, a higher proportion of case-patients and controls were classified as partially vaccinated, rather than fully vaccinated, during the study period, and we did not have sufficient follow-up time to assess waning of vaccine effectiveness. Some residents could have been misclassified as HCP, but the age selection criteria limiting age group helped minimize this factor. Finally, misclassification of vaccination status is possible, but most likely is nondifferential, which we would expect to bias the odds ratio toward the null.

In conclusion, we observed high real-world effectiveness of COVID-19 vaccination in SNF HCP in California. Our methods can guide future studies evaluating vaccine effectiveness.

### Acknowledgments

The California Department of Public Health thanks all California healthcare personnel, laboratorians, and local health departments throughout the COVID-19 pandemic for their diligent work. We thank the California Department of Public Health COVID-19 Science Branch and Data teams and the Center for Health Care Quality Skilled Nursing Facilities Analytics team for their support and data resources provided to successfully complete this study.

### About the Author

Dr. Magro is a research scientist in the Healthcare-Associated Infections Program, Center for Health Care Quality, California Department of Public Health, Richmond, CA. Her primary research interests are healthcare-associated infections and antimicrobial drug resistance.

## References

1. AARP Public Policy Institute. Issues. Long-term services and supports and family caregiving. AARP Nursing Home Dashboard [cited 2022 Jan 11]. <https://www.aarp.org/ppi/issues/caregiving/info-2020/nursing-home-covid-dashboard.html>
2. Kaiser Family Foundation. Coronavirus (COVID-19). Nursing homes experienced steeper increase in COVID-19 cases and deaths in August 2021 than the rest of the country [cited 2022 Jan 11]. <https://www.kff.org/coronavirus-covid-19/issue-brief/nursing-homes-experienced-steeper-increase-in-covid-19-cases-and-deaths-in-august-2021-than-the-rest-of-the-country>
3. Roth A, Feller S, Ruhnau A, Plamp L, Viereck U, Weber K, et al. Characterization of COVID-19 outbreaks in three nursing homes during the first wave in Berlin, Germany. *Sci Rep*. 2021;11:24441. <https://doi.org/10.1038/s41598-021-04115-9>
4. Taylor J, Carter RJ, Lehnertz N, Kazazian L, Sullivan M, Wang X, et al.; Minnesota Long-Term Care COVID-19 Response Group. Serial testing for SARS-CoV-2 and virus whole genome sequencing inform infection risk at two skilled nursing facilities with COVID-19 outbreaks – Minnesota, April–June 2020. *MMWR Morb Mortal Wkly Rep*. 2020;69:1288–95. <https://doi.org/10.15585/mmwr.mm6937a3>
5. Dooling K, Marin M, Wallace M, McClung N, Chamberland M, Lee GM, et al. The Advisory Committee on Immunization Practices' updated interim recommendation for allocation of COVID-19 vaccine – United States, December 2020. *MMWR Morb Mortal Wkly Rep*. 2021;69:1657–60. <https://doi.org/10.15585/mmwr.mm695152e2>
6. California Department of Public Health. All facilities letter 20–53 [cited 2022 Jan 6]. <https://www.cdph.ca.gov/Programs/CHCQ/LCP/Pages/AFL-20-53.aspx>
7. Rothman KJ, Greenland S, Lash T. Case-control studies. In: Rothman KJ, Greenland S, Lash T. *Modern epidemiology*, 3rd ed. Philadelphia: Lippincott Williams and Wilkins; 2008. p. 124–5.
8. Public Health Alliance of Southern California. The California healthy places index (HPI) [cited 2022 Jan 11]. <https://healthyplacesindex.org>
9. Council of State and Territorial Epidemiologists (CSTE). Update to the standardized surveillance case definition and national notification for 2019 novel coronavirus disease (COVID-19). CSTE position statement 21-ID-01. 2021 Aug [cited 2022 Jan 20]. [https://cdn.ymaws.com/www.cste.org/resource/resmgr/21-ID-01\\_COVID-19\\_updated\\_Au.pdf](https://cdn.ymaws.com/www.cste.org/resource/resmgr/21-ID-01_COVID-19_updated_Au.pdf)

Address for correspondence: Monise Magro, Healthcare-Associated Infections Program, California Department of Public Health, 850 Marina Bay Pkwy, Richmond, CA 94804, USA; email: [monise.magro@cdph.ca.gov](mailto:monise.magro@cdph.ca.gov)

## COMMENT LETTERS

## Seroprevalence of Chikungunya Virus, Jamaica, and New Tools for Surveillance

Andre R.R. Freitas, Laura Pezzi, Luciano P.G. Cavalcanti, Fabrice Simon

Author affiliations: Faculdade São Leopoldo Mandic, Campinas, São Paulo, Brazil (A.R.R. Freitas); Unité des Virus Émergents, INSERM-IRD, Aix-Marseille Université, Marseille, France (L. Pezzi, F. Simon); Universidade Federal do Ceará, Fortaleza, Brazil (L.P.G. Cavalcanti)

DOI: <https://doi.org/10.3201/eid2808.220558>

**To the Editor:** We read with great interest the recent article by Anzinger et al. (1), who found a seroprevalence of 83.6% for chikungunya in pregnant women in the metropolitan region of Kingston, Jamaica. These data are similar to the seroprevalence found nationwide by the Jamaica Health and Lifestyle Survey III, 2016–2017 (Ministry of Health and Welfare, Jamaica), which was 82% among women, 78.5% among men, and 80.4% overall. These values enable estimating a total of 2,187,325 chikungunya infections in Jamaica during the 2014 epidemic. The government of Jamaica reported

1,420 cases of chikungunya to PAHO in 2014 and no deaths (2), even correcting for the proportion of unapparent infections, the proportion of cases captured by passive surveillance was <0.1%. Although there were no officially reported deaths in Jamaica, 2 cases of newborn deaths from chikungunya were reported (3), and 1 study found 2,499 excess deaths (2) during the epidemic period. The increase in mortality was greater for the extremes of age, but it occurred in several age groups (2).

Anzinger et al.'s results reinforce the findings of Sharp et al. (4), who showed the importance of active surveillance to assess chikungunya burden. Through active surveillance implemented in Puerto Rico, it was possible to verify that 8% of symptomatic cases of chikungunya identified were captured by passive surveillance. In addition, passive surveillance identified 7 deaths, whereas active surveillance was able to confirm 31 deaths from chikungunya. However, 1,310 excess deaths were reported during the Puerto Rico epidemic in 2014 (5).

The introduction of chikungunya in the Americas has brought greater complexity to surveillance in the region, which includes some low-resource countries. It is essential to establish active and viable surveillance tools and, perhaps, new case definitions in order to better assess the population burden of this disease and the complications of acute and chronic cases.

## References

1. Anzinger JJ, Mears CD, Ades AE, Francis K, Phillips Y, Leys YE, et al.; ZIKAction Consortium. Antenatal seroprevalence of Zika and chikungunya viruses, Kingston metropolitan area, Jamaica, 2017–2019. *Emerg Infect Dis.* 2022;28:473–5. <https://doi.org/10.3201/eid2802.211849>
2. Freitas ARR, Gérardin P, Kassir L, Donalisio MR. Excess deaths associated with the 2014 chikungunya epidemic in Jamaica. *Pathogens and Global Health.* 2019;113:27–31. <https://doi.org/10.1080/20477724.2019.1574111>
3. Evans-Gilbert T. Chikungunya and neonatal immunity: fatal vertically transmitted chikungunya infection. *Am J Trop Med Hyg.* 2017;96:913–5. <https://doi.org/10.4269/ajtmh.16-0491>
4. Sharp TM, Ryff KR, Alvarado L, Shieh W-J, Zaki SR, Margolis HS et al. Surveillance for chikungunya and dengue during the first year of chikungunya virus circulation in Puerto Rico. *J Infect Dis.* 2016;214(suppl\_5):S475–81. <https://doi.org/10.1093/infdis/jiw245>
5. Freitas ARR, Donalisio MR, Alarcón-Elbal PM. Excess mortality and causes associated with chikungunya, Puerto Rico, 2014–2015. *Emerg Infect Dis.* 2018;24:2352–5. <https://doi.org/10.3201/eid2412.170639>

---

Address for correspondence: Andre Ricardo Ribas Freitas, School of Medicine San Leopoldo Mandic – Department of Social Medicine, R. Dr. José Rocha Junqueira, 13 – Swift, Campinas, SP, São Paulo 13045-755, Brazil; email: andre.freitas@slmandic.edu.br

---

**In Response:** I thank the authors for their favorable commentary (1) related to our recently published article (2). In their commentary the authors note that the low number of chikungunya cases captured through passive surveillance underrepresents the true burden of disease in Jamaica, particularly fatal infections during the 2014 chikungunya epidemic year (3).

Underreporting of chikungunya cases in Jamaica has been acknowledged and has multiple factors (4). Most chikungunya cases are not captured through a passive clinic-based surveillance (5), and in Jamaica most case-patients likely did not seek care at the advanced public health center passive surveillance sites. In addition, real-time PCR, the most sensitive diagnostic test type during acute infection, was highly limited in Jamaica during the 2014 chikungunya epidemic. For these reasons, identification of chikungunya cases through passive surveillance was expected to represent only a small fraction of the population.

It is possible that many excess deaths in Jamaica during 2014 were the result of chikungunya virus infections escaping surveillance. Chikungunya fatalities may be difficult to capture with limited surveillance capacity.

Furthermore, chikungunya virus infections, particularly in the elderly, may exacerbate existing comorbidities and lead to extended hospitalization that could result in nosocomial infections; either event may prove fatal and ultimately be considered the cause of death (6).

During the COVID-19 pandemic in Jamaica, surveillance systems have been bolstered; the Ministry of Health and Wellness introduced broad community-based testing, many diagnostic laboratories have introduced real-time PCR testing, and the University of the West Indies has introduced next-generation techniques sequencing techniques for whole-genome sequencing of viruses. Further enhancing responses to emerging viruses, the University of the West Indies recently became a member of the Abbott Pandemic Defense Coalition that aims to increase virus surveillance and discovery (7). This increased infrastructure will likely improve surveillance for future viral epidemics in Jamaica.

## References

1. Freitas ARR, Pezzi L, Cavalcanti LPG, Simon F. The complexity of chikungunya and the importance of new tools for epidemiological surveillance. *Emerg Infect Dis.* 2022 Aug. <https://doi.org/10.3201/eid2808.220558>
2. Anzinger JJ, Mears CD, Ades AE, Francis K, Phillips Y, Leys YE, et al.; ZIKAction Consortium. Antenatal seroprevalence of Zika and chikungunya viruses, Kingston metropolitan area, Jamaica, 2017–2019. *Emerg Infect Dis.* 2022;28:473–5. <https://doi.org/10.3201/eid2802.211849>
3. Freitas ARR, Gérardin P, Kassir L, Donalisio MR. Excess deaths associated with the 2014 chikungunya epidemic in Jamaica. *Pathogens and Global Health.* 2019;113:27–31. <https://doi.org/10.1080/20477724.2019.1574111>
4. Duncan J, Gordon-Johnson KA, Tulloch-Reid MK, Cunningham-Myrie C, Ernst K, McMorris N, et al. Chikungunya: important lessons from the Jamaican experience. *Rev Panam Salud Publica.* 2017;41:e60. <https://doi.org/10.26633/RPSP.2017.60>
5. Paul KK, Salje H, Rahman MW, Rahman M, Gurley ES. Comparing insights from clinic-based versus community-based outbreak investigations: a case study of chikungunya in Bangladesh. *Int J Infect Dis.* 2020;97:306–12. <https://doi.org/10.1016/j.ijid.2020.05.111>
6. Lima Neto AS, Sousa GS, Nascimento OJ, Castro MC. Chikungunya-attributable deaths: A neglected outcome of a neglected disease. *PLoS Negl Trop Dis.* 2019;13:e0007575. <https://doi.org/10.1371/journal.pntd.0007575>
7. Averhoff F, Berg M, Rodgers M, Osmanov S, Luo X, Anderson M, et al. The Abbott Pandemic Defense Coalition: a unique multisector approach adds to global pandemic preparedness efforts. *Int J Infect Dis.* 2022;117:356–60. <https://doi.org/10.1016/j.ijid.2022.02.001>

Joshua J. Anzinger

DOI: <https://doi.org/10.3201/eid2808.221006>

Author affiliations: The University of the West Indies, Kingston, Jamaica; The Global Virus Network Jamaica Affiliate, Kingston, Jamaica

Address for correspondence: Joshua J. Anzinger, Department of Microbiology, The University of the West Indies, Kingston, Jamaica; email: [joshua.anzinger@uwimona.edu.jm](mailto:joshua.anzinger@uwimona.edu.jm)

## Imported Monkeypox from International Traveler, Maryland, USA, 2021

Faisal S. Minhaj, Agam K. Rao, Andrea M. McCollum

Author affiliation: Centers for Disease Control and Prevention, Atlanta, Georgia, USA

DOI: <https://doi.org/10.3201/eid2808.220726>

**To the Editor:** Costello et al. described a patient in Maryland, USA, with a diffuse vesicular rash initially diagnosed as disseminated varicella zoster virus (VZV) infection. Only after a biopsy revealed unexpected findings was monkeypox suspected (1). Monkeypox is commonly confused with VZV in countries where both infections are endemic. High fever, lymphadenopathy, and a deep-seated, well-circumscribed, umbilicated rash in the same stage of development (i.e., macule, papule, vesicle, or scab) in distinct anatomic locations are characteristic of monkeypox (2). Although the patient in Maryland experienced lymphadenopathy and rash with umbilicated lesions suggestive of monkeypox, he was afebrile, denied other prodromal signs and symptoms (e.g., headache and chills) that typically precede monkeypox rash, and improved while receiving intravenous acyclovir, features more consistent with VZV. However, the unusual clinical signs and symptoms experienced by this patient were similar to those observed in other patients in the evolving 2022 multinational monkeypox response.

Because differential diagnosis can be challenging, public health authorities should be consulted promptly when monkeypox is possible. US Laboratory Response Network laboratories (<https://emergency.cdc.gov/lrn>) can enable rapid testing of specimens (e.g., lesions swab), and pathogen-specific antiviral medications can be acquired through consultation with the Centers for Disease Control

and Prevention. Public health investigation for a single case of monkeypox can be intensive and complicated; case-patient contacts outside of the hospital must be identified, monitored, and potentially given 1 of the 2 orthopoxvirus vaccines offered for postexposure prophylaxis in the United States (3–5).

Factors that should raise suspicion for monkeypox in a patient with related signs and symptoms include history of travel outside of the United States to a country with confirmed cases or where monkeypox virus is endemic, contact with a person with a similar-appearing rash or who has received a diagnosis of confirmed or probable monkeypox, contact with Africa-endemic wild animal or pet species (living or dead), or use of a product derived from those animals (e.g., game meat, creams, lotions, powders). Monkeypox should also be considered in patients with close or intimate contact with persons in social networks experiencing high monkeypox activity, including men who have sex with men who meet partners through a website, digital application, or social event. Prompt consultation with public health authorities is essential for providing clinical guidance, expediting testing and treatment, and preventing secondary cases (3).

### References

1. Costello V, Sowash M, Gaur A, Cardis M, Pasiaka H, Wortmann G, et al. Imported monkeypox from international traveler, Maryland, USA, 2021. *Emerg Infect Dis.* 2022;28:1002–5. <https://doi.org/10.3201/eid2805.220292>
2. Osadebe L, Hughes CM, Shongo Lushima R, Kabamba J, Nguete B, Malekani J, et al. Enhancing case definitions for surveillance of human monkeypox in the Democratic Republic of Congo. *PLoS Negl Trop Dis.* 2017;11:e0005857. <https://doi.org/10.1371/journal.pntd.0005857>
3. Rao AK, Schulte J, Chen T-H, Hughes CM, Davidson W, Neff JM, et al.; July 2021 Monkeypox Response Team. Monkeypox in a traveler returning from Nigeria—Dallas, Texas, July 2021. *MMWR Morb Mortal Wkly Rep.* 2022;71:509–16. <https://doi.org/10.15585/mmwr.mm7114a1>
4. Petersen BW, Damon IK, Pertowski CA, Meaney-Delman D, Guarnizo JT, Beigi RH, et al. Clinical guidance for smallpox vaccine use in a postevent vaccination program. *MMWR Recomm Rep.* 2015;64(RR-02):1–26.
5. Rao AK, Petersen BW, Whitehill F, Razeq JH, Isaacs SN, Merch linsky MJ, et al. Use of JYNNEOS (smallpox and monkeypox vaccine, live, nonreplicating) for preexposure vaccination of persons at risk for occupational exposure to orthopoxviruses: recommendations of the Advisory Committee on Immunization Practices—United States, 2022. *MMWR Morb Mortal Wkly Rep.* 2022;71:734–42. <https://doi.org/10.15585/mmwr.mm7122e1>

Address for correspondence: Faisal Syed Minhaj, Centers for Disease Control and Prevention, 1600 Clifton Rd NE, Mailstop 24-12, Atlanta, GA 30327-4027, USA; email: [fminhaj@cdc.gov](mailto:fminhaj@cdc.gov)

**In Response:** We appreciate Minhaj et al. for their correspondence regarding our experience treating an imported case of monkeypox from an international traveler (1). Their letter reaffirms the instructive points of our case: monkeypox poses a diagnostic challenge because its clinical presentation shares features with a variety of additional infectious diseases, including varicella zoster virus (the infection we initially suspected), and prompt coordination with public health officials is critical for diagnosing, treating, and mitigating secondary spread.

Since our report of monkeypox in November 2021, there have been outbreaks of monkeypox throughout multiple countries (2), including one case identified in the United States (3). Monkeypox had never previously been diagnosed in several of these countries and, remarkably, in only 1 of these cases (4) was there a history of travel to a monkeypox-endemic country, in direct contrast to nearly all prior cases that have been reported outside of Africa (5–7), which were epidemiologically linked to a monkeypox-endemic region.

In our case report (8), we had concluded that monkeypox had become clinically relevant within the confines of a travel-related illness. However, the additional cases diagnosed since November 2021 strongly suggest that community transmission is now occurring, and a history of travel to a monkeypox-endemic country is no longer prerequisite to contracting this disease. Community prevalence rates remain unknown, so healthcare providers should consider monkeypox in any patient who manifests with fever and lymphadenopathy accompanied by a disseminated vesicular, pustular, or umbilicated rash. Under those conditions, the provider should immediately initiate infection control and contact public health authorities. Monkeypox is an emerging zoonotic disease with incompletely appreciated clinical features, and healthcare providers should be made aware of its increasingly widespread incidence.

## References

1. Minhaj FS, Rao AK, McCollum A. Imported monkeypox from international traveler, Maryland, USA, 2021. *Emerg Infect Dis.* 2022 Aug [date cited]. <https://doi.org/10.3201/eid2808.220726>
2. United Nations. Europe: WHO supporting countries affected by rare monkeypox outbreak [cited 2022 May 21]. <https://news.un.org/en/story/2022/05/1118712>
3. Centers for Disease Control and Prevention. Monkeypox virus infection in the United States and other non-endemic countries – 2022 [cited 2022 May 21] <https://emergency.cdc.gov/han/2022/han00466.asp>
4. World Health Organization. Monkeypox – United Kingdom of Great Britain and Northern Ireland [cited 2022 May 21]. <https://www.who.int/emergencies/disease-outbreak-news/item/2022-DON381>
5. Erez N, Achdout H, Milrot E, Schwartz Y, Wiener-Well Y, Paran N, et al. Diagnosis of imported monkeypox, Israel, 2018. *Emerg Infect Dis.* 2019;25:980–3. <https://doi.org/10.3201/eid2505.190076>
6. Yong SEF, Ng OT, Ho ZJM, Mak TM, Marimuthu K, Vasoo S, et al. Imported monkeypox, Singapore. *Emerg Infect Dis.* 2020;26:1826–30. <https://doi.org/10.3201/eid2608.191387>
7. Vaughan A, Aarons E, Astbury J, Balasegaram S, Beadsworth M, Beck CR, et al. Two cases of monkeypox imported to the United Kingdom, September 2018. *Euro Surveill.* 2018;23:1800509. <https://doi.org/10.2807/1560-7917.ES.2018.23.38.1800509>
8. Costello V, Sowash M, Gaur A, Cardis M, Pasiaka H, Wortmann G, et al. Imported monkeypox from international traveler, Maryland, USA, 2021. *Emerg Infect Dis.* 2022;28:1002–5.

---

Address for correspondence: Varea Costello, Walter Reed National Military Medical Center – Infectious Diseases, 8901 Rockville Pike, Bethesda, MD 20889, USA; email: [varea.h.costello2.mil@mail.mil](mailto:varea.h.costello2.mil@mail.mil)

---

Varea Costello, Madeleine Sowash, Aahana Gaur, Michael Cardis, Helena Pasiaka, Glenn Wortmann, Sheena Ramdeen

DOI: <https://doi.org/10.3201/eid2808.220830>

Author affiliations: Walter Reed National Military Medical Center, Bethesda, Maryland, USA (V. Costello); Medstar Washington Hospital Center, Washington, D.C., USA (M. Sowash, A. Gaur, M. Cardis, H. Pasiaka, G. Wortmann, S. Ramdeen)

## Karen Foster (1955–2022)

Byron Breedlove

**K**aren Lynn Foster, who worked as a technical writer-editor and subject matter expert for *Emerging Infectious Diseases* from 2009 until early 2022, died on March 10, 2022, at age 66. Throughout her time with the journal, Karen was known for her exemplary knowledge of language, editing, grammar, and science and for her ability to handle tough assignments and deadlines.

Born in Quonset Point, Rhode Island, USA, the oldest of 6 children, Karen graduated cum laude from Longwood College, Farmville, Virginia, USA, where she received a Bachelor of Arts in English. Karen earned a Master of Arts in Creative Writing from Hollins College, Roanoke, Virginia, and also completed postgraduate work in English at Vanderbilt University, Nashville, Tennessee, USA.

In 1982, she joined the Centers for Disease Control and Prevention as an assistant editor for the *Morbidity and Mortality Weekly Report*, followed by a stint as a writer-editor for what was then the Center for Infectious Diseases. During 1988–2000, Karen served as managing editor of *MMWR*. She worked another 5 years as a technical writer-editor in the National Center for Environmental Health/Agency for Toxic Substances & Disease Registry before retiring from CDC in 2005. During the next phase of her career, which also encompassed her time with *Emerging Infectious Diseases*, Karen worked as a freelance writer/editor and editorial consultant in public health and epidemiology. Karen is among the editors of the second edition of *Law in Public Health Practice* (2006) and served as one of the managing editors of the *CDC Field Epidemiology Manual* (2019).

Karen's career and accomplishments are all the more remarkable in that she overcame a serious visual handicap to excel in a profession that required close and careful reading. Her colleagues recall Karen not only for her exacting editorial skills and high standards but also for having a terrific sense of humor and formidable wit.

Apart from work, Karen's true passion was raising, showing, and breeding English Springer Spaniels. She was a charter member of the Chattahoochee English



**Figure.** Karen Foster (1955–2022). Image courtesy of the Foster family.

Springer Spaniel Club of Greater Atlanta and was also a member of English Springer Rescue America and the English Springer Spaniel Field Trial Association.

Karen leaves behind many colleagues who, during the course of 4 decades, worked with her, worked for her, and learned from her. Some may be interested to know that shortly before her passing, Karen finished writing her first novel, which her family hopes to have published in the near future. We offer our condolences to her surviving family members and friends.

---

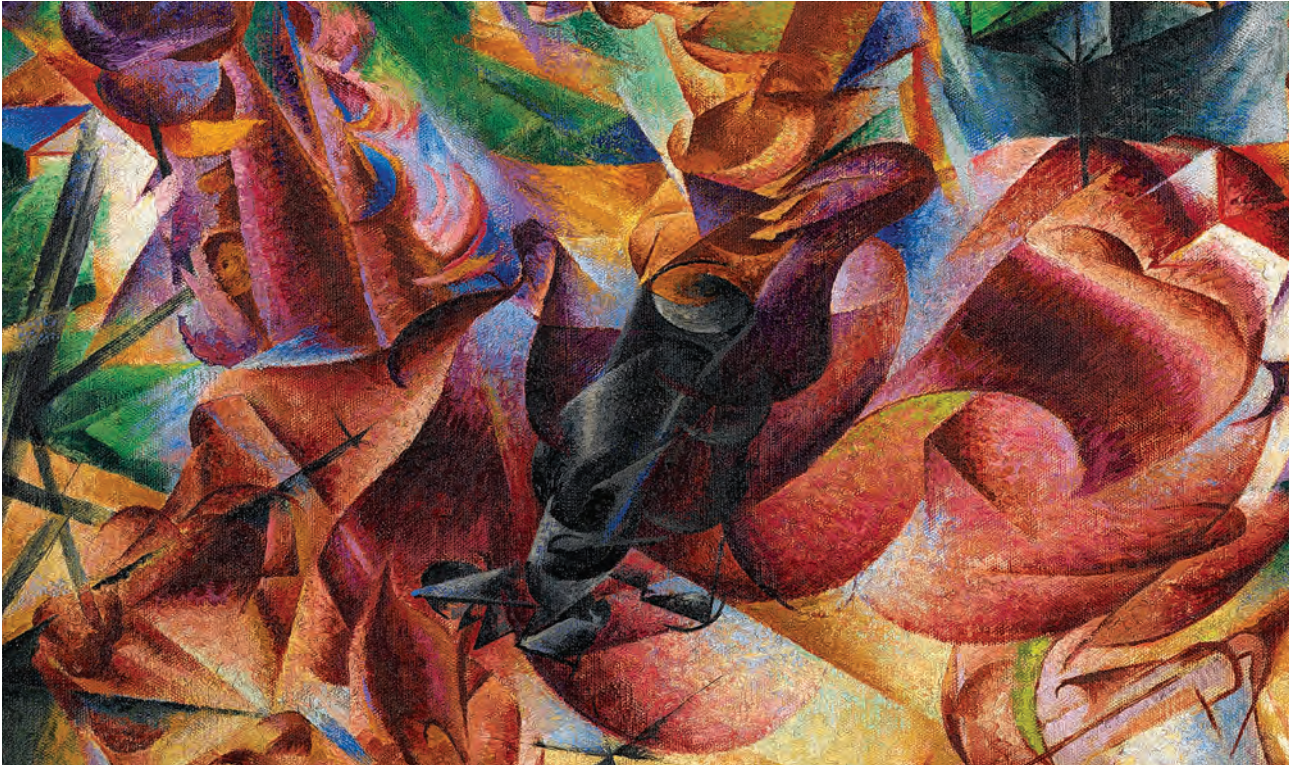
Author affiliation: Centers for Disease Control and Prevention, Atlanta, Georgia, USA

DOI: <https://doi.org/10.3201/eid2808.220746>

---

Address for correspondence: Byron Breedlove, EID Journal, Centers for Disease Control and Prevention, 1600 Clifton Rd NE, Mailstop H16-2, Atlanta, GA 30329-4027, USA; email: [wbb1@cdc.gov](mailto:wbb1@cdc.gov)

## ABOUT THE COVER



**Umberto Boccioni (1882–1916), *Elasticity*, 1912 (detail).** Oil on canvas 39.3 in x 39.3 in/100.06 cm x 100.06 cm. Museo del Novecento, Milano, Italy. Digital image from Art Resource, New York, New York, USA.

### “A Great Synthesis of Labor, Light, and Movement”

Byron Breedlove

“Let us not offend Boccioni with a funeral eulogy,” stated Italian writer Filippo Tommaso Marinetti, founder of the early 20th Century avant-garde Italian Futurist movement, at a retrospective exhibition for Italian painter and sculptor Umberto Boccioni. Despite a life cut short, Boccioni was one of the best known and most influential artists associated with early manifestations of Italian Futurism. Boccioni was born in the coastal Italy city of Reggio Calabria, but his family moved frequently during his childhood. After attending technical college in Catania, Sicily, in 1899 he studied drawing and painting in Rome. In 1906, Boccioni visited Paris to expand his artistic perspectives and then spent a portion of 1907 in Venice learning printmaking before relocating to Milan, where he met Marinetti.

Author affiliation: Centers for Disease Control and Prevention, Atlanta, Georgia, USA

DOI: <https://doi.org/10.3201/eid2808.AC2808>

Art historian Rosalind McKeever noted, “In February 1909, Marinetti published his famous manifesto in the French newspaper *Le Figaro*, demanding that Italian culture stop looking backward and embrace modernity.” Boccioni and his peers drafted a pair of related manifestos calling on other artists to discard traditional motifs and conventions and to find inspiration from science, technology, and modern urban life. In Boccioni’s words, this artistic response would be “a great synthesis of labor, light, and movement.” A 1911 trip to Paris opened his eyes to the artistic style known as Cubism, and as McKeever wrote, “Boccioni integrates the Cubist use of collage-like numerals and straight lines that divide spatial planes into his more expressionistic style... the dissected planes implied dynamism and the straight lines became ‘force-lines’ showing motion.”

Boccioni’s painting *Elasticity*, this month’s cover image, fuses stylistic elements from Cubism with themes from Futurism. Its fractured, chaotic elements

also may serve as a visual metaphor calling for collective, focused public health action in response to an array of emerging zoonotic diseases.

Art historian Kate Bryan wrote, “Boccioni’s subject matter was not still life, as had been largely the case with Cubism, to which the movement owed a clear stylistic debt, but rather the more impossible endeavour of depicting objects in motion.” Horse and rider frantically gallop across a landscape that is the antithesis of a bucolic, pastoral setting. Jutting electrical towers, rendered as fractured angular black lines and factory chimneys belching smoke, reveal a setting reshaped by human hands. Angular forms and planes representing glimpses of sky and artifacts of industry recede from the horse and rider they surround. The distorted, dynamic image of the horse with its flaring nostrils, sweeping forelock, and rippling muscles, and its forward-leaning rider, wearing a brimmed hat and black boots, trampling across a dusty road, transfixes the viewer’s attention toward the center of the painting. Artist and writer Marcus Bunyan commented that in *Elasticity*, Boccioni depicted “the pure energy of a horse, captured with intense chromaticism.”

As is already clear, Boccioni did not have a long career or life. In 1915, he volunteered for military service in the first World War. Although not a casualty of combat, Boccioni succumbed to severe injuries after being thrown from his horse startled by a passing lorry in August 1916. McKeever noted, “Throughout his career Boccioni had painted horses and it is a cruel irony that, having named his steed *Vermiglia* after the flaming red beast in the centre of *The City Rises* (1910), his fall would imitate the scene of what has become his most famous painting.” Many of Boccioni’s generation also died during World War I, including his Futurist colleague Antonio Sant’Elia and artists Henri Gaudier-Brzeska and Franz Marc.

Overlapping that global conflict was the 1918 influenza pandemic, caused by what would later be categorized as an H1N1 virus with genes of avian origin, which eventually infected one third of the world’s population. Of that pandemic, Taubenberger and Morens wrote, “Many questions about its origins, its unusual epidemiologic features, and the basis of its pathogenicity remain unanswered.” Among the human-mediated factors that drove the high rates of death and illness associated with that pandemic were wartime conditions, marshalling of military operations, mass transportation by ship and rail, and growing urbanization, which would have been celebrated by Futurists as transformative forces.

More than a century later, the web of inter-related factors contributing to the emergence and reemergence of zoonotic infectious diseases has become more complicated and intertwined. Efforts to mitigate this complex global problem, if fragmented like the myriad shapes and shards in Boccioni’s *Elasticity*, are unlikely to succeed. As Ghai et al. noted, “Effectively preventing and controlling zoonotic diseases requires a One Health approach that involves collaboration across human health, animal health, and environmental sectors, as well as other partners. This framework provides a structure for using a One Health approach in zoonotic disease programs and can help build capacity for preventing and controlling zoonotic diseases at the local, sub-national, national, regional, or international level.” The urgency encapsulated in Boccioni’s notion of “a great synthesis of labor, light, and movement” is needed to drive this unified public health framework to prevent, prepare for, and respond to emerging zoonotic diseases.

#### Bibliography

1. Beard L, Butler A, Cleave CV, Fortenberry D, Stirling S. The art book. London: Phaidon Press; 2014.
2. Bryan K. Bright stars: great artists who died too young. London: Francis Lincoln; 2021.
3. Bunyan M. Art Blart. Umberto Boccioni [cited 2022 Jun 29]. <https://artblart.com/tag/umberto-boccioni-elasticity>
4. Centers for Disease Control and Prevention. History of 1918 flu pandemic [cited 2022 Jun 23]. <https://www.cdc.gov/flu/pandemic-resources/1918-commemoration/1918-pandemic-history.htm>
5. Centers for Disease Control and Prevention. Zoonotic diseases [cited 2022 Jun 14]. <https://www.cdc.gov/onehealth/zoonotic-diseases.html>
6. Coen E. Umberto Boccioni: a retrospective. New York: Metropolitan Museum of Art; 1988.
7. Ghai RR, Wallace RM, Kile JC, Shoemaker TR, Vieira AR, Negron ME, et al. A generalizable One Health framework for the control of zoonotic diseases. *Sci Rep*. 2022;12:8588. <https://doi.org/10.1038/s41598-022-12619-1>
8. McKeever R. Harnessing the future: the art of Umberto Boccioni [cited 2022 Jun 4]. <https://www.apollo-magazine.com/harnessing-the-future-the-art-of-umberto-boccioni>
9. McKeever R. Umberto Boccioni (1882–1916) [cited 2022 Jun 14]. [https://www.metmuseum.org/toah/hd/umbo/hd\\_umbo.htm](https://www.metmuseum.org/toah/hd/umbo/hd_umbo.htm)
10. Short KR, Kedzierska K, van de Sandt CE. Back to the future: lessons learned from the 1918 influenza pandemic. *Front Cell Infect Microbiol*. 2018;8:343. <https://doi.org/10.3389/fcimb.2018.00343>
11. Taubenberger JK, Morens DM. 1918 Influenza: the mother of all pandemics. *Emerg Infect Dis*. 2006;12:15–22. <https://doi.org/10.3201/eid1209.05-0979>

Address for correspondence: Byron Breedlove, EID Journal, Centers for Disease Control and Prevention, 1600 Clifton Rd NE, Mailstop H16-2, Atlanta, GA 30329-4027, USA; email: wbb1@cdc.gov

# EMERGING INFECTIOUS DISEASES<sup>®</sup>

## Upcoming Issue • September 2022

- Fetal Loss and Preterm Birth Caused by Intraamniotic *Haemophilus influenzae* Infection
- Quantifying Population Burden and Effectiveness of Decentralized Surveillance Strategies for Skin-Presenting Neglected Tropical Diseases, Liberia
- Costs of Tuberculosis at Three Centers, Canada
- Emergence and Spread of SARS-CoV-2 Omicron Variant in Large and Small Communities Revealed by Wastewater Monitoring, Alberta, Canada
- Age-Dependent Effects of COVID-19 Vaccine and of Healthcare Burden on COVID-19 Deaths, Tokyo, Japan
- Longitudinal SARS-CoV-2 Nucleocapsid Antibody Kinetics, Seroreversion, and Implications for Seroepidemiologic Studies
- Epidemiology of Infections with SARS-CoV-2 Omicron BA.2 Variant, Hong Kong, January–March 2022
- Coccidioidomycosis Among Military Personnel, Naval Air Station Lemoore, San Joaquin Valley, California, USA
- Susceptibility of Wild Canids to SARS-CoV-2
- Epidemiologic Features and Control Measures during Monkeypox Outbreak, Spain, June 2022
- Sporadic Occurrence of Enteroaggregative Shiga Toxin–Producing *E. coli* O104:H4 Similar to 2011 Outbreak Strain
- Social and Behavioral Factors Associated with Lack of Intent to Receive COVID-19 Vaccine, Japan
- Fatal Triazole-Resistant *Aspergillus fumigatus* Infection, Pennsylvania, USA
- Pathogenesis and Transmissibility of North American Highly Pathogenic Avian Influenza A(H5N1) Virus in the Ferret Model
- *Tropheryma whipplei* Intestinal Colonization in Migrant Children, Greece
- Arthritis caused by *Nannizziopsis obscura*, Paris, France
- *Trichodysplasia Spinulosa* Polyomavirus Endothelial Infection, California, USA
- Correlation between Clinical and Wastewater SARS-CoV-2 Genomic Surveillance, Oregon, USA
- Impact of Frequent SARS-CoV-2 Testing on Weekly Case Rates in Long-Term Care Facilities, Florida, USA
- Highly Divergent SARS-CoV-2 Alpha Variant in Chronically Infected Immunocompromised Person
- Plagues Upon the Earth: Disease and the Course of Human History

Complete list of articles in the September issue at  
<https://wwwnc.cdc.gov/eid/#issue-291>

## Earning CME Credit

To obtain credit, you should first read the journal article. After reading the article, you should be able to answer the following, related, multiple-choice questions. To complete the questions (with a minimum 75% passing score) and earn continuing medical education (CME) credit, please go to <http://www.medscape.org/journal/eid>. Credit cannot be obtained for tests completed on paper, although you may use the worksheet below to keep a record of your answers.

You must be a registered user on <http://www.medscape.org>. If you are not registered on <http://www.medscape.org>, please click on the "Register" link on the right hand side of the website.

Only one answer is correct for each question. Once you successfully answer all post-test questions, you will be able to view and/or print your certificate. For questions regarding this activity, contact the accredited provider, [CME@medscape.net](mailto:CME@medscape.net). For technical assistance, contact [CME@medscape.net](mailto:CME@medscape.net). American Medical Association's Physician's Recognition Award (AMA PRA) credits are accepted in the US as evidence of participation in CME activities. For further information on this award, please go to <https://www.ama-assn.org>. The AMA has determined that physicians not licensed in the US who participate in this CME activity are eligible for *AMA PRA Category 1 Credits™*. Through agreements that the AMA has made with agencies in some countries, AMA PRA credit may be acceptable as evidence of participation in CME activities. If you are not licensed in the US, please complete the questions online, print the AMA PRA CME credit certificate, and present it to your national medical association for review.

### Article Title

## Evidence for Ribavirin Treatment of Lassa Fever in Systematic Review of Published and Unpublished Studies

### CME Questions

**1. You are advising a tropical medicine clinic regarding treatment of Lassa fever. According to the systematic review by Cheng and colleagues, which of the following statements about the overall effectiveness of ribavirin for treatment of Lassa fever is correct?**

- A. Ribavirin treatment was generally associated with lower mortality, but almost all results were rated as at critical risk for bias when appraised using the ROBINS-I tool
- B. In the McCormick et al study, ribavirin treatment was associated with lower overall mortality in patients with confirmed Lassa fever compared with no ribavirin treatment
- C. In IND 16666, after adjusting for confounding factors using logistic regression, ribavirin was associated with 36% lower overall mortality
- D. None of the studies identified evidence of immortal time bias

**2. According to the systematic review by Cheng and colleagues, which of the following statements about the effectiveness of ribavirin for treatment of Lassa fever in subgroups is correct?**

- A. In patients with aspartate aminotransferase (AST) <150 IU/L, ribavirin was associated with lower mortality

- B. In patients with measurable viremia, ribavirin was associated with higher mortality
- C. The association of ribavirin treatment with lower mortality did not differ for early vs late treatment onset
- D. The IND 16666 study reported separate results for pregnant women (odds ratio [OR] 2.06 [95% CI: 0.64, 6.6]) and nonpregnant women (OR 1.12 [95% CI: 0.71, 1.77])

**3. According to the systematic review by Cheng and colleagues, which of the following statements about clinical implications of the overall effectiveness of ribavirin for treatment of Lassa fever is correct?**

- A. This systemic review provided robust evidence supporting the use of ribavirin in Lassa fever
- B. Well-conducted randomized controlled clinical trials (RCTs) are needed to determine the effectiveness of ribavirin for Lassa fever
- C. Given the lost cost and good safety profile of ribavirin, empiric treatment is justified for Lassa fever
- D. This systemic review identified optimal ribavirin treatment regimens for Lassa fever

## Earning CME Credit

To obtain credit, you should first read the journal article. After reading the article, you should be able to answer the following, related, multiple-choice questions. To complete the questions (with a minimum 75% passing score) and earn continuing medical education (CME) credit, please go to <http://www.medscape.org/journal/eid>. Credit cannot be obtained for tests completed on paper, although you may use the worksheet below to keep a record of your answers.

You must be a registered user on <http://www.medscape.org>. If you are not registered on <http://www.medscape.org>, please click on the “Register” link on the right hand side of the website.

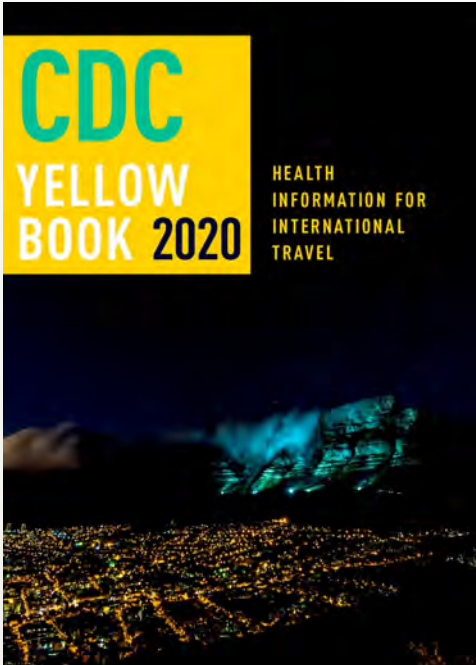
Only one answer is correct for each question. Once you successfully answer all post-test questions, you will be able to view and/or print your certificate. For questions regarding this activity, contact the accredited provider, [CME@medscape.net](mailto:CME@medscape.net). For technical assistance, contact [CME@medscape.net](mailto:CME@medscape.net). American Medical Association’s Physician’s Recognition Award (AMA PRA) credits are accepted in the US as evidence of participation in CME activities. For further information on this award, please go to <https://www.ama-assn.org>. The AMA has determined that physicians not licensed in the US who participate in this CME activity are eligible for *AMA PRA Category 1 Credits™*. Through agreements that the AMA has made with agencies in some countries, AMA PRA credit may be acceptable as evidence of participation in CME activities. If you are not licensed in the US, please complete the questions online, print the AMA PRA CME credit certificate, and present it to your national medical association for review.

### Article Title

## **Weighing Potential Benefits and Harms of *Mycoplasma genitalium* Testing and Treatment Approaches**

### CME Questions

- 1. Your patient is a 34-year-old female patient with pelvic inflammatory disease (PID). According to the updated systematic review by Manhart and colleagues, which of the following statements about associations of *Mycoplasma genitalium* with reproductive, urologic, and perinatal complications is correct?**
  - A. The association of *M. genitalium* with PID is well-established
  - B. *M. genitalium* is a documented cause of male infertility and proctitis
  - C. The bulk of evidence supports a link between *M. genitalium* and obstetric outcomes
  - D. Gaps in our understanding of *M. genitalium* must be filled to optimize testing and treatment strategies
- 2. According to the updated systematic review by Manhart and colleagues, which of the following statements about indications for *M. genitalium* testing is correct?**
  - A. Most diagnostic tests for *M. genitalium* include detection of antimicrobial resistance
  - B. Evidence to date allows weighing the benefits and harms of *M. genitalium* testing
  - C. Screening, diagnostic testing, and tests of cure each have different goals, and evidence to date for *M. genitalium* is insufficiently robust to inform clear recommendations
  - D. Culturing urine (for men) or vaginal swabs (for women) for *M. genitalium* is the preferred method of detection
- 3. According to the updated systematic review by Manhart and colleagues, which of the following statements about management of *M. genitalium* infections is correct?**
  - A. Although treatment approaches for *M. genitalium* infections have been identified, antimicrobial resistance has emerged and spread at an alarming rate
  - B. To limit spread, testing and treatment for *M. genitalium* infections should include asymptomatic contacts of known cases
  - C. Single-dose azithromycin (1 g) is currently preferred for treatment for *M. genitalium* infections
  - D. 2021 CDC guidelines recommend treating infected partners with a different antibiotic from that provided to the index person



# Available Now

## Yellow Book 2020

The fully revised and updated CDC Yellow Book 2020: Health Information for International Travel codifies the US government's most current health guidelines and information for clinicians advising international travelers, including pretravel vaccine recommendations, destination-specific health advice, and easy-to-reference maps, tables, and charts.

ISBN: 978-0-19-006597-3 | \$115.00 | May 2019 | Hardback | 720 pages

ISBN: 978-0-19-092893-3 | \$55.00 | May 2019 | Paperback | 687 pages



### Yellow Book 2020 includes important travel medicine updates

- The latest information on emerging infectious disease threats, such as Zika, Ebola, and henipaviruses
- Considerations for treating infectious diseases in the face of increasing antimicrobial resistance
- Legal issues facing clinicians who provide travel health care
- Special considerations for unique types of travel, such as wilderness expeditions, work-related travel, and study abroad

**OXFORD**  
UNIVERSITY PRESS

Order your copy at:  
[www.oup.com/academic](http://www.oup.com/academic)